Identification of novel antihormone-induced pro-survival genes in oestrogen receptor-positive breast cancer cells

---

Jessica Jane Davis

A thesis submitted for the degree of Doctor of Philosophy

Division of Cancer & Genetics

Department of Pharmacology, Therapeutics & Toxicology

School of Medicine

Cardiff University

2016

DECLARATION

This work has not been submitted in substance for any other degree or award at this or any other university or place of learning, nor is being submitted concurrently in candidature for any degree or other award.

Signed …… (candidate) Date ……

STATEMENT 1

This thesis is being submitted in partial fulfillment of the requirements for the degree of PhD.

Signed …… (candidate) Date ……

STATEMENT 2

This thesis is the result of my own independent work/investigation, except where otherwise stated. Other sources are acknowledged by explicit references. The views expressed are my own.

Signed …… (candidate) Date ……

STATEMENT 3

I hereby give consent for my thesis, if accepted, to be available online in the University's Open Access repository and for inter-library loan, and for the title and summary to be made available to outside organisations.

Signed …… (candidate) Date ……

In loving memory of Aunty Hilary
(1963-2013)

&

my best friend's mother, Marian
(1964-2011).

Summary

The growth inhibitory actions of antihormones in the treatment of oestrogen receptor-positive (ER+) breast cancer are compromised by the development of resistance. There is emerging evidence that antihormones can rapidly induce expression of genes that enable cells to survive the initial impact of these agents and ultimately aid the acquisition of resistance.

The aims of this thesis were to identify novel antihormone-induced pro-survival genes in a panel of ER+ breast cancer cell lines and to determine whether such genes contribute to the limited efficacy of antihormones during response and subsequently contribute to the emergence of resistant cell growth.

Microarray analysis, together with a stringent filtering process, identified 14 pro-survival genes significantly induced by at least one antihormone treatment (10 day tamoxifen, fulvestrant or oestrogen deprivation) in ER+ MCF-7 breast cancer cells, with increased expression maintained into cell models of antihormone-resistance. Of these 15 genes, 5 (GABBR2, CLU, CTNND2, BCL3 and TSC22D3) were significantly induced by all antihormone treatments. PCR and/or Western blotting demonstrated antihormone-induced expression of these 5 genes in T47D (ER+/HER2-), BT474 and MDA-MB-361 (ER+/HER2+) cell lines.

The role of BCL3 and CLU during antihormone response and resistance were next investigated. siRNA-mediated BCL3 knockdown had no effect on cell survival but reduced proliferation of tamoxifen-resistant (TAMR) and oestrogen deprivation-resistant (XR) cells. Immunoprecipitation and immunofluorescence studies revealed nuclear localisation and direct association of BCL3 and p50 in TAMR and XR cells. However, during response, BCL3 was located in the nucleus and p50 in the cytoplasm. In contrast, siRNA-mediated CLU knockdown reduced proliferation of fulvestrant-treated MCF-7 cells but was without effect on the growth of resistant cells.

To conclude, this thesis has identified one antihormone-induced gene (CLU), which appears to limit response, and a second (BCL3), which appears to promote the growth of antihormone-resistant cells, potentially via activation of NFκB-mediated gene transcription.

Publications

Burnley-Hall, N., Willis, G., Davis, J., Rees, D. & James, E. Nitrite-derived nitric oxide reduces hypoxia-inducible factor 1α-mediated extracellular vesicle production by endothelial cells. *Nitric Oxide* **63**, 1-12 (2017).

Davis, J., Knowlden, J., Pepper, C., Gee, J. & Hutcheson, I. Antihormone-induced expression of BCL3 in estrogen receptor-positive breast cancer drives resistant cell growth. In: Proceedings of the 107th Annual meeting of the American Association for Cancer Research; 2016 April 16-20; New Orleans, USA.

Davis, J., Francies, H., Farrow, L., Knowlden, J., Barrow, D., Routledge, P., Gee, J. & Hutcheson, I. Identification of novel antihormone-induced pro-survival genes in oestrogen receptor-positive breast cancer. NCRI Cancer Conference, Liverpool, UK 2013.

Acknowledgements

First and foremost, I would like to thank my supervisors, Dr Iain Hutcheson and Dr Julia Gee for their support, guidance and enthusiasm as well as providing me with the opportunity to undertake this PhD. I am extremely grateful to Dr Janice Knowlden who provided me with fantastic lab training, daily advice and support and was always on hand to troubleshoot the problems that go together with the lab experiments. Also, thanks to the staff at the Pharmacology department for their support and friendship. My warmest thanks to Dr Hayley Francies and Lynne Farrow for their knowledge of microarray gene expression profiling and without whom I would still be trying to interpret the data. I would also like to thank Professor Chris Pepper and Dr Kathryn Taylor for allowing me access to their facilities. A massive thank you to my parents for their continuous support, doing my washing and ironing and without whom this PhD would have been profoundly more difficult. A big thanks to Carl for supporting and encouraging me throughout this experience, for tolerating my miserable moods and for trying to show an interest in my work when really not understanding. Thanks to Katie for the many stimulating and constructive lab-related evening discussions and an exhaustive supply of delicious cakes – my star baker! Last but not least, I would like to thank Professor Philip Routledge (via the RD Leaker Memorial Fund, Cardiff and Vale University Health Board) and the Division of Cancer and Genetics, Cardiff University for providing the funding to carry out this work.

Contents

Abbreviations

AF	Activating function
AI	Aromatase inhibitor
AIB1	Nuclear receptor coactivator 3
AKT (1)	v-*akt* murine thymoma viral oncogene homolog 1
ALDH	Aldehyde dehydrogenase
ANOVA	Analysis of variance
AP-1	Activator protein 1
ATCC	American Type Cell Collections
BAG1	BCL2-Associated athanogene
BCL2	B-cell lymphoma 2
BCL2L1	BCL2-Like 1
BCL3	B-cell lymphoma 3
BCSCs	Breast cancer stem cells
BLAST	Basic Local Alignment Search Tool
BOLERO-2	Breast Cancer Trials of Oral Everolimus-2
bp	Base pairs
BRCA1	Breast cancer type 1 susceptibility protein
BRCA2	Breast cancer type 2 susceptibility protein
cAMP	Cyclic adenosine monophosphate
CBS	Cardiff University Central Biotechnology Services

CDKs	Cyclin-dependent kinases
CLU	Clusterin
CLU-S	Pro-survival cytoplasmic secretory CLU
CON	Control
CONFIRM	Comparison of Faslodex in Recurrent or Metastatic Breast Cancer
CSCs	Cancer stem cells
CTNND2	Catenin (Cadherin-Associated Protein), Delta 2
CXCR4	Chemokines (C-X-C motif) receptor 4
DBD	DNA binding domain
DDAH2	Dimethylarginine Dimethylaminohydrolase 2
DFS	Disease-free survival
DNTP	Deoxynucleotide triphosphates
DTT	Dithiothreitol
E2	17β-oestradiol
ED	Oestrogen deprivation
EGF	Epidermal growth factor
EGFR	Epidermal growth factor receptor
EMT	Epithelial-mesenchymal transition
ER	Oestrogen receptor
ERα	Oestrogen receptor alpha
ERβ	Oestrogen receptor beta
ERC1	ELKS/RAB6-Interacting/CAST Family Member 1

ERE	Oestrogen response element
ERK	Extracellular-signal-regulated kinases
FACT	Fulvestrant and Anastrozole Combination Therapy
FAS	Fulvestrant
FASR	Fulvestrant resistant
FCS	Foetal calf serum
FGFR	Fibroblast growth factor receptors
FIRST	Fulvestrant First-Line Study Comparing Endocrine Treatments
GABA	Gamma-aminobutyric acid
GABBR1	Gamma-aminobutyric acid (GABA) B receptor, 1
GABBR2	Gamma-aminobutyric acid (GABA) B receptor, 2
GAD1	Glutamate decarboxylase 1
GAD2	Glutamate decarboxylase 2
GOBO	Gene Expression-Based Outcome for Breast Cancer Online
GPCRs	G-protein coupled receptors
GRIP1	Glutamate receptor interacting protein 1
HBXIP	Late Endocomal/Lysosomal Adaptor, MAPK and MTOR Activator 5
HDAC	Histone deacetylases
HER2/ERBB2	Human epidermal growth factor receptor 2
HER3	Human epidermal growth factor receptor 3
HSP	Heat shock proteins
IκB	Inhibitor of NF-κB

IGF-1R	Insulin-like growth factor-I receptor
IGFBP5	Insulin-like growth factor binding protein 5
IL	Interleukin
INPP4B	Inositol polyphosphate-4-phosphatase type II
LBD	Ligand-binding domain
MAPK	Mitogen-activated protein kinases
MET	Mesenchymal-epithelial transition
MMP	Matrix metalloproteinase
MNAR	Modulator of Non-Genomic Activity of Estrogen Receptor
mRNA	Messenger RNA
mTOR	Mammalian target of rapamycin
NCOR	Nuclear receptor corepressor 1
NEWEST	Neoadjuvant Endocrine Therapy for Women with Estrogen-Sensitive Tumours
NF-κB	Nuclear factor kappa-light-chain enhancer of activated B cells
PCR	Polymerase chain reaction
PI3K	Phosphoinositide-3-kinase
PR	Progesterone receptor
p21	Cyclin-dependent kinase inhibitor 1A
PALB2	Partner and localiser of BRCA2
PH	Pleckstrin homology
PI	Propidium iodide

PIP_2	Phosphatidylinositol 4,5 bisphosphate
PIP_3	Phosphatidylinositol 3,4,4-triphosphate
PS	Phosphatidylserine
PSEN1	Presenilin 1
PTEN	Phosphate and tensin homology
RTK	Receptor tyrosine kinases
RT-PCR	Reverse-transcription PCR
SDS-PAGE	Sodium Dodceyl Sulphate-Polyacrylamide Gel Electrophoresis
SEM	Standard error of the mean
SERM	Selective oestrogen modulator
sFCS	Charcoal stripped FCS
siRNA	Small interfering RNA
SMRT	Nuclear receptor corepressor 2
SP1	Sp1 transcription factor
SRC1	Nuclear receptor coactivator 1
SRC	SRC proto-oncogene, non-receptor tyrosine kinase
SWOG	Southwest Oncology Group
TAE	Tris base, acetic acid and EDTA
TAM	Tamoxifen
TAMR	Tamoxifen resistant
TGF-α	Transforming growth factor alpha
TGF-β	Transforming growth factor beta

TNF-α	Tumour Necrosis Factor-alpha
TORC-1	mTOR-containing complex 1
TSC22D3	TSC22 Domain Family, Member 3
XR	Oestrogen deprivation resistant

1 Introduction

1.1 Incidence of breast cancer

Breast cancer is the most common female cancer in the UK and women have a 1 in 8 lifetime risk of developing the disease. The incidence of female breast cancer has increased since the 1970s. This increase has been attributed to earlier detection as a result of the introduction of national screening programmes in the late 1980s. However, despite the increase in incidence, female breast cancer mortality rates have decreased in the last 40 years with improved detection, increased awareness and more effective treatments resulting in almost 8 out of 10 women surviving the disease beyond 10 years (2012 statistics)[1]. Unfortunately, however, breast cancer is the second most common cause of cancer death among women in the UK (2012) with 32 women dying from the disease every single day[1]. Thus, further research and improved treatments are required to target breast cancer in patients whose disease progresses on current therapies.

1.2 Risk factors of breast cancer

The majority of breast cancers are sporadic and result from the accumulation of uncorrected mutations in somatic genes. However, there are several risk factors that are associated with the development of breast cancer, with increased concentrations of the female steroid hormone oestrogen being the most significant[2]. Additionally, in support of the endocrine status link, less than 1% of breast cancers are diagnosed in men (2012 statistics)[1]. Factors that increase lifetime exposure to oestrogen include increasing age, women who are younger at menarche and older at menopause[3]. Furthermore, exposure to exogenous oestrogens from the use of hormone replacement therapy and oral contraceptives are also associated with increased risk of developing breast cancer[4–6]. Interestingly, breast cancer incidence rates are highest in developed Western countries and significantly less in developing countries, particularly middle Africa[1]. This may be due to women in developing countries having more children and breastfeeding for longer[7] which suppresses ovulation, both contributing to a reduced exposure to oestrogen.

Furthermore, approximately a quarter of breast cancers are hereditary, characterised by a young age at diagnosis and/or first degree relatives affected by the disease[8]. In particular, it has been shown that women diagnosed before the age of 50, with a history of breast cancer in at least one first-degree relative, are associated with an approximately two-fold relative risk[9]. This risk has been attributed to the inheritance of autosomal dominant breast cancer susceptibility genes. Mutations in two breast cancer tumour suppressor genes, BRCA1 and BRCA2, have been identified and account for a substantial proportion of high risk families. Indeed, a meta-analysis has revealed an average cumulative lifetime risk of 65% to develop breast cancer in BRCA1 carriers compared to 45% in BRCA2 mutation carriers[10]. However, BRCA1 and BRCA2 genes are only involved in approximately 30% of breast cancer cases with a hereditary component[11]. Thus, with the rapid expansion of next generation DNA sequencing, more recent research is discovering new susceptibility genes. For example, the BRCA2-interacting protein PALB2 has emerged as a new breast cancer susceptibility gene. Indeed, a recent study has revealed an estimated cumulative risk of 35% to develop breast cancer in PALB2 mutation carriers[12].

1.3 Oestrogen and breast cancer

Oestrogen exposure has been long established as a cause of breast cancer and for maintaining its growth. Indeed, breast cancer growth appears to be dependent on oestrogens and in particular the predominant circulating oestrogen, 17β-oestradiol (E2), as demonstrated by an increase in breast cancer cell line growth in response to this hormone[13]. This dependency is reflected by the increased incidence of breast cancer in women who are exposed to increased endogenous and exogenous oestrogens (as previously described in section 1.2). Interestingly, the mitotic effects of oestrogens appear to accelerate the development of breast cancer at several stages along the progression from early mutation to tumour metastasis[14]. Additionally, increased cell division induced by oestrogen may increase the risk of DNA damage not being repaired, ultimately resulting in mutations[15].

The first recognition that the ovaries influence the development of the normal human female breast was in 1775 when Sir Percival Pott demonstrated that the

removal of the ovaries of a young woman resulted in breast atrophy[16]. Over a decade later in 1882, the first evidence of the relationship between ovarian function and breast cancer was discovered by Thomas William Nunn who reported the case of a perimenopausal woman whose breast cancer regressed 6 months after menopause. Later, in 1889, Albert Schinzinger first proposed the theory of surgical oophorectomy as a treatment for advanced disease and as prophylaxis against local recurrence[17]. This surgical procedure was later first performed by George Beatson in 1896 and led to the regression of mammary tumours of pre-menopausal women[18]. Importantly, removal of the ovaries was used as an effective treatment, together with surgical breast tumour excision, for much of the 20th century.

1.4 Oestrogen receptor

Oestrogen-induced cell proliferation and survival is mediated through its two receptors which are members of the nuclear receptor family of ligand-activated transcription factors[19]: oestrogen receptor alpha (ERα) and oestrogen receptor beta (ERβ). The oestrogen receptor (later denoted ERα) was first discovered by Elwood Jensen in 1958 and was later cloned and sequenced in 1986 by Green et al[20]. By the beginning of the 1970s, the theory had been established that breast cancers exhibiting a high expression of the receptor protein would respond to endocrine treatment; however, there was very little evidence supporting this hypothesis. In 1974, overwhelmingly supportive data was presented which revealed clinically important separation of endocrine therapy responders and non-responders according to the detection of the oestrogen receptor in the primary tumour, as summarised by McGuire[14]. More recently, a novel oestrogen receptor was discovered in 1996 and named ERβ[22]. The original oestrogen receptor is now commonly referred to as ERα.

Both ERα and ERβ consist of six functional domains (A-F) that serve specific roles (Figure 1). The A/B domain located at the N-terminus contains activation function 1 (AF1) which is responsible for regulating transcriptional activity in a hormone-independent manner[23]. The highly conserved C domain encompasses the DNA binding domain (DBD) which is responsible for binding oestrogen response elements (ERE) in the promoter regions of target oestrogen-responsive genes.

Domain E comprises the ligand-binding domain (LBD) which contains a hydrophobic 'pocket' that binds E2 inducing a conformational change, thus allowing helix 12 to seal the E2 within the pocket. Additionally, domain E contains activation function 2 (AF2) responsible for activating transcription in a ligand-dependent manner [24].

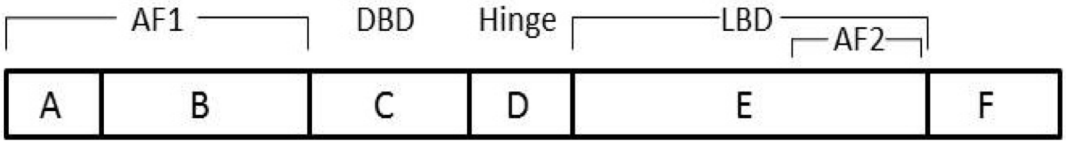

Figure 1 Schematic structure of the oestrogen receptor depicting six domains. The A and B domains at the N terminus contain the ligand-independent transcriptional activation function 1 (AF1), the C domain contains the DNA binding domain (DBD) responsible for binding to the oestrogen response elements in the promoters of target genes, the D domain corresponds to the hinge region, the E domain is the ligand binding domain (LBD) and also contains the ligand-dependent transcriptional activation factor 2 (AF2) and lastly the F domain at the C-terminus. Figure adapted from Fan et al.[456].

ERα and ERβ confer a high degree of homology between their DBD (more than 95%) and LBD (approximately 55%). However, the AF1 domain and hinge regions are the least conserved with 30% and 36% sequence similarity, respectively[25,26]. A significant functional difference between these receptors is related to the AF1 domain. Indeed, ERα contains a constitutive AF1 that functions to enhance transcriptional response of the receptor, whereas the equivalent region of ERβ exhibits negligible transcriptional activity and contains a repressor domain that decreases the transcriptional activity of the receptor[25]. These differences have been suggested to contribute to the varying responses of these receptors to various ligands. An additional difference between these receptors includes their tissue distribution. ERα is predominantly expressed in the breast and uterus, whereas high ERβ expression is apparent in the ovary, prostate and lung[27,28].

Both receptors are expressed at low levels in the normal breast[29]; however, ERα is the dominant subtype in breast cancer as detected by immunohistochemistry in breast cancer biopsies. Although ERβ expression has been detected in breast cancer, its function remains elusive with studies reporting contrasting roles, with some suggesting a role in cell proliferation and tumour progression and others suggesting a potential role in tumour suppression[30–33]. ERα is expressed in

approximately 70% of breast cancers and is a hallmark of hormone-dependent growth. Consequently, the growth inhibitory actions of antihormones for the treatment of breast cancer result from the blocking of ERα (termed ER for the remainder of this project) signalling and downstream cell growth and survival.

1.5 Oestrogen receptor signalling

1.5.1 Genomic ER signalling

1.5.1.1 Classical pathway

In the absence of E2, ERs are located in the nucleus and exist as inactive monomers bound to a multi-chaperone protein complex containing heat shock proteins (HSP)[34,35]. Upon E2 binding to the LBD of the ER, HSP complexes are released and the receptor undergoes a series of modifications, conformational changes, phosphorylations and dimerisation[36,37]. The ER dimer binds to a 13 base pair DNA consensus sequence, known as the ERE characteristic of oestrogen-regulated genes, in the promoter region of target genes to induce up regulation of pro-proliferative and pro-survival genes (e.g. cyclin D1 and survivin) and down regulation of anti-proliferative and pro-apoptotic genes (e.g. cyclin-dependent kinase inhibitor 1A (p21) and Bcl2-antagonist/killer 1)[38]. However, recruitment of E2:ER dimers to the promoter of target genes induces transcription providing that AF1 and/or AF2 are activated. In most cells AF1 and AF2 act synergistically, however certain gene promoters, possibly depending on the cellular milieu, can be independently transactivated by either activation function alone[34,39,40].

AF2 becomes active upon ligand binding. E2 binds within the hydrophobic 'pocket' of the LBD which is sealed by helix 12, thus exposing the AF2 region and generating binding surfaces for co-regulatory proteins, including coactivators and corepressors[41,42]. Coactivators contain histone acetyltransferase activity which targets histones bound to DNA, directing an allosteric change in the nucleosome conformation and destabilising higher-order structure to render the nucleosomal DNA more accessible to transcription factors[43–45]. Ultimately, histone acetylation allows transcription factors to gain access to the transcriptionally repressed chromatin, to modulate transactivation of target genes. The most characterised ER coactivators are the p160 protein family, comprised of SRC1, GRIP1 and AIB1[46–48].

In contrast, corepressors function through several mechanisms but appear to act most prominently through modification of chromatin[49]. Indeed, corepressors recruit histone deacetylase complexes which reverse the activity of histone acetyltransferases, promote chromatin condensation thus limiting the accessibility of the transcription machinery, to ultimately repress gene transcription. NCOR and SMRT are the best characterised corepressors of ER and function by recruiting histone deacetylase complexes[50,51]. Critically, AF1 is activated in the absence of E2 by phosphorylation following the activation of growth factor receptors (such as epidermal growth factor receptor (EGFR)) and downstream kinase signalling (e.g. mitogen-activated protein kinase (MAPK))[52]. Indeed, epidermal growth factor (EGF)-mediated activation of the Ras-Raf-MAPK cascade results in the phosphorylation of serine 118 of the ER[53]. Several serine phosphorylation sites have been identified on the ER, however, the major oestrogen-induced phosphorylation site is serine 167 mediated by casein kinase 2[54]. AF1 phosphorylation at specific serine residues recruits coactivators exclusive or identical to those recruited by AF2 to induce transcription of E2-regulated genes, thus inducing cell growth and survival in a ligand-independent manner[55].

1.5.1.2 Non-classical pathway

ERs can also regulate the transcription of genes lacking ERE sequences. This mechanism occurs independent of direct DNA binding of the ER and hence can be activated by ERs lacking a DBD. Instead, ERs bind via protein-protein interactions to other transcriptional factors such as activator protein-1 (AP-1) and nuclear factor kappa B (NF-κB), stabilising their direct binding to promoter regions of target genes, thus enhancing transcription[56–58]. Specifically, E2 induction of cyclin D1, which lacks ERE sites, is mediated by ER binding to transcription factors such as SP1 which are recruited to the regulatory regions of the target gene to induce transcription[59]. Additionally, SP1 is crucial for E2 activation of the insulin-like growth factor-I receptor (IGF-1R) via this non-classical pathway[60]. Alternatively, E2 also negatively regulates genes via this non-classical system. In particular, E2 represses interleukin 6 (IL-6) expression by direct interaction of the ER with NF-κB, inhibiting its binding to the IL-6 promoter thus preventing subsequent transcription[61]. Together, via this non-classical pathway, ER can function to either

stabilise transcription factor binding to response elements thus inducing transcription or alternatively can prevent binding of transcription factors to DNA to repress transcription.

Interestingly, several E2-responsive genes lacking an ERE site contain both half-ERE sites and non-classical sites. An example is the promoter of the progesterone receptor (PR) which contains an ERE-half site and SP1 binding sites. Thus, E2-induced PR expression can be mediated by direct binding of the ER to the half-site, indirectly by interaction of ER with proteins bound to the SP1 sites, or by both methods combined[62].

1.5.2 Non-genomic ER signalling

In addition to the nuclear transcriptional events, E2 also exerts rapid actions within minutes independent of gene transcription. These non-genomic events have been attributed to the presence of ER at the plasma membrane. Indeed, activated E2:ER complexes at the membrane have been shown to directly interact and activate tyrosine kinase receptors, including IGF-1R[63] and EGFR[64], resulting in enhanced signalling via MAPK and phosphoinositide-3-kinase (PI3K) pathways.

Moreover, additional functional domains of the ER provide docking stations for scaffold proteins and signalling molecules to promote further interactions with various proteins to modulate/enhance ER signalling cascades. For instance, the scaffold protein MNAR modulates the interaction of E2-activated ER with Src kinase, leading to an increase in Src activity and stimulation of the MAPK signalling pathway[65]. Similar to genomic actions, non-genomic activity is influenced by the presence of signal transduction molecules and downstream targets in the cell. Thus, responses are likely to be diverse and cell type specific[66].

1.5.3 Convergence of genomic and non-genomic ER signalling

The genomic and non-genomic actions of E2 are interconnected by signal transduction pathways. E2-activated membrane ER triggers protein kinase cascades, leading to the phosphorylation of target transcription factors; e.g. E2-mediated activation of MAPK signalling enhances DNA binding of AP-1 transcription factor complex, thus increasing its transcriptional activity[67,68]. Such MAPK and PI3K signalling pathways downstream of membrane ER may also

phosphorylate nuclear ER in a ligand-independent manner to promote the expression of E2-regulated genes[53].

Together, ERs can regulate genes expression by at least four mechanisms. These include the classical mechanism of direct E2:ER binding to EREs, the non-classical mechanism of nuclear E2:ER binding to transcription factors via protein-protein interactions to induce transcription of target genes, ligand-independent activation of nuclear ER following activation of growth factor pathways and finally, non-genomic membrane-associated ER activation of signal transduction pathways leading to activation of transcription factors and/or ER (Figure 2).

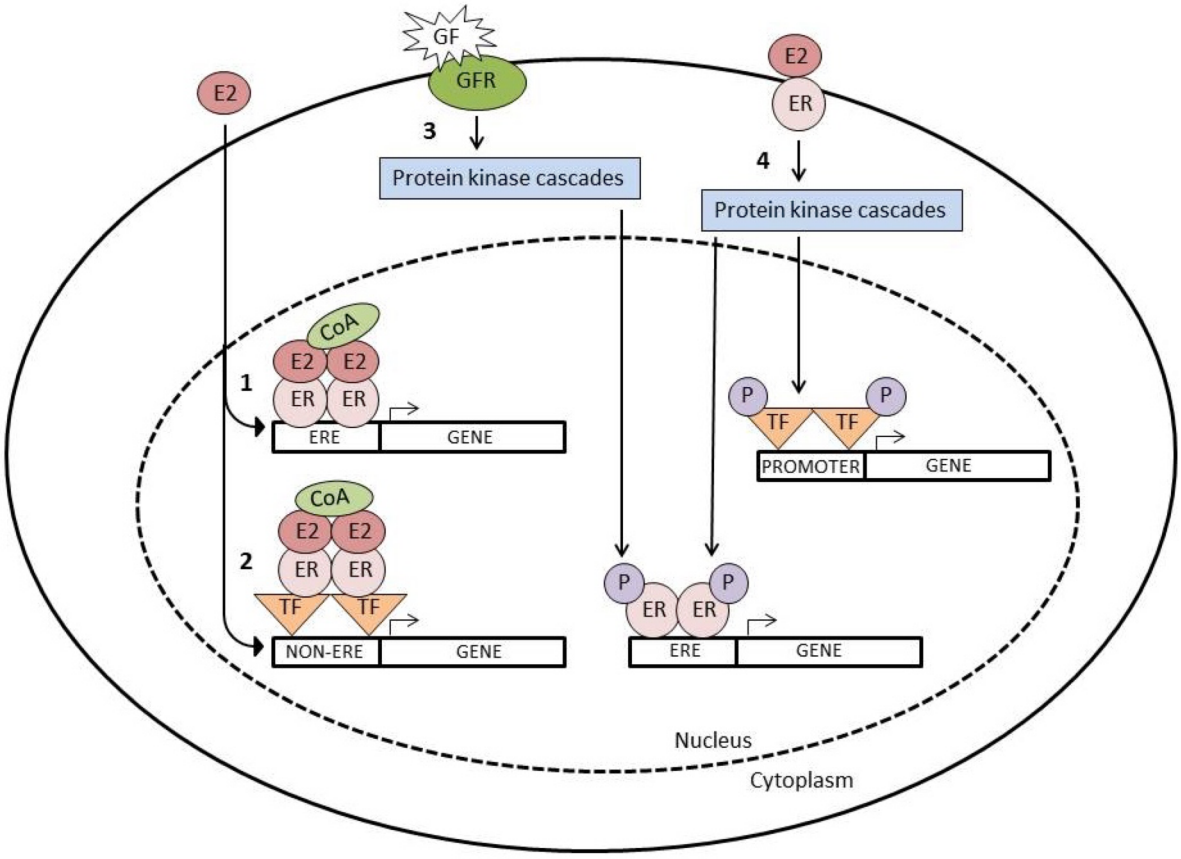

Figure 2 Schematic diagram of the pathways utilised by the oestrogen receptor (ER) to regulate gene expression. (1) Classical signalling: oestradiol (E2):ER complexed with coactivators (CoA) binds to oestrogen response elements (ERE) located in the promoter of target genes. (2) Non-classical signalling: E2:ER binds to transcription factors (TF) to induce transcription of genes lacking ERE sites. (3) Ligand-independent genomic activation: activation of protein kinases cascades downstream of growth factor receptor (GFR) activation results in the phosphorylation (P) of ER in the absence of E2. GF: growth factor. (4) Non-genomic signalling: membrane-associated E2:ER activates protein kinase cascades results in the activation of transcription factors and/or ER to induce transcription.

1.6 Therapeutic approaches to block E2 action and ER activity

Clinically, the hormone receptor (ER and/or PR) and human epidermal growth factor receptor 2 (HER2) status of breast cancers are prognostic and predictive factors used to select patients for treatments with antihormone or anti-HER2 therapies. The majority of breast cancers (70%) are ER positive (ER+), with 80% of which being ER+/HER2-negative (HER2-)[69] while the remainder overexpress HER2 (ER+/HER2-positive (HER2+))[70]. Antihormones which subvert E2/ER signalling and prevent downstream cell growth and survival are the mainstay therapy for ER+/HER2- disease. However, ER+/HER2+ tumours have a decreased benefit from antihormones but achieve a greater response to HER2-targetted therapies[71,72].

Antihormones can be broadly classified into two groups: firstly, the anti-oestrogens tamoxifen and fulvestrant which competitively inhibit E2 binding to the ER with the latter also inducing down regulation of the ER protein, and secondly the aromatase inhibitors (AIs) which block the conversion of androgens into biologically active oestrogens, to deprive the environment of oestrogen and consequently prevent E2 activation of the ER (Figure 3). Antihormones are invaluable adjuvant treatments for early ER+ breast cancer patients post-surgery to increase survival rates or potentially cure[73]. Furthermore, these agents are also used in advanced metastatic disease to limit tumour growth[74] and in the neoadjuvant setting to reduce the tumour volume to facilitate breast surgery[75].

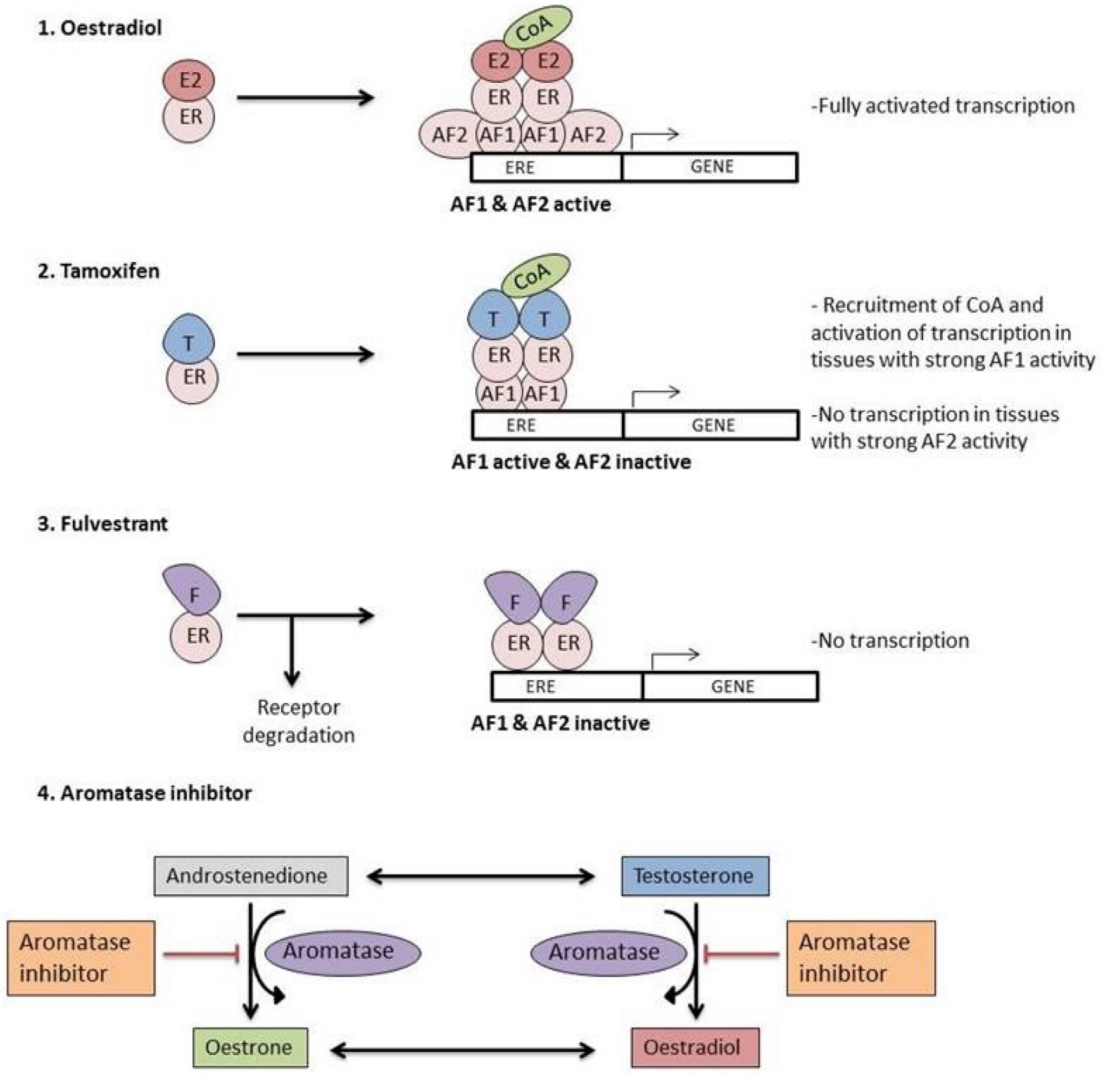

Figure 3 The mechanism of action of oestradiol (E2), tamoxifen (T), fulvestrant (F) and aromatase inhibitors. (1) E2-activated oestrogen receptor (ER) dimers bind to the oestrogen response elements (ERE) in the promoter region of target genes, activation function 1 (AF1) and 2 (AF2) are activated and recruit coactivators (CoA) to induce gene transcription. (2) Tamoxifen bound ER dimers bind to the ERE of target genes but only AF1 is active. In tissues with strong AF-1 activity, CoA are recruited and transcription of target genes is initiated. However, in tissues exhibiting strong AF-2 activity, tamoxifen inhibits transcription. (3) Fulvestrant causes rapid degradation of the ER and impairs both AF1 and AF2 domains resulting in complete inhibition of transcription. (4) Aromatase inhibitors prevent the synthesis of E2 from its androgenic precursors thus inhibiting E2-driven gene transcription (adapted from Johnston & Dowsett[92]).

1.6.1 Selective ER Modulator (SERM): Tamoxifen

The non-steroidal anti-oestrogen tamoxifen competitively inhibits E2 binding to the ER and consequently prevents transcription of oestrogen-regulated genes. Upon binding to the LBD of nuclear ER, tamoxifen induces receptor dimerisation similar to E2. Significantly, however, the bulky side chain of tamoxifen prevents helix 12 from sealing the binding pocket, thus preventing the exposure and formation of a transcriptionally competent AF2 conformation and hence inhibiting AF2-mediated transcription[76]. However, tamoxifen is without effect on AF1 transcriptional activity[77]. Critically, in tissues where AF1 activity is strong (e.g. uterus), tamoxifen exerts agonistic effects. The nature of AF1 activation by tamoxifen is largely undefined but it may involve ER phosphorylation and recruitment of coactivators[78]. The predominance of AF1 and AF2 in driving ER-mediated transcription within tissues has resulted in tissue selectivity of agonistic and antagonistic tamoxifen activity and the derivation of the abbreviation SERM to describe its mechanism of action. In the hormone responsive breast, ER activity is dominantly mediated by AF2-driven transcription and tamoxifen functions as an antagonist[79], whereas in the bone and uterus, ER-mediated transcription is driven by AF1 and consequently tamoxifen behaves as an agonist[39,80]. Furthermore, the tissue-dependent activity of tamoxifen is also regulated by the presence of coactivators and corepressors. Tamoxifen bound ER favours recruitment of corepressor molecules to the complex to inhibit its agonistic activity[81]. However, decreased availability of corepressors has been shown to cause a shift in tamoxifen function from antagonistic to agonistic[82]. Together, tamoxifen is an anti-oestrogen in tissues with strong AF2-mediated ER transcription, however, in tissues with predominantly AF1-mediated E2 activity and in the presence of reduced availability of corepressors and altered/increased growth factor signalling which phosphorylates AF1 in a ligand independent manner, tamoxifen behaves as a partial agonist and such events may ultimately contribute to tamoxifen resistance.

Since the early 2000s tamoxifen was the first line treatment for ER+ breast cancer patients. However, its agonistic activity in certain ER+ tissues results in toxic side effects, including greater risk of endometrial cancer and venous thromboembolisms, and has subsequently led to the development and increased

popularity of AIs. Over the past decade several clinical trials have demonstrated superiority of AIs over tamoxifen as a first line adjuvant treatment for postmenopausal women[83]. As such, tamoxifen is primarily used as first line therapy in ER+ premenopausal women (since ovarian function cannot be controlled by AIs). Tamoxifen is approved for use in both women (premenopausal and postmenopausal)[84] and men[85] in the adjuvant setting and with advanced ER+ disease. Five years of adjuvant tamoxifen treatment has been shown to significantly reduce recurrence rates and mortality rates throughout the first 10 years and 15 years from the start of treatment respectively[86]. Furthermore, alternating tamoxifen with an AI[87] and extending tamoxifen treatment from 5 to 10 years both produce a further reduction in mortality and recurrence[88]. More recently, tamoxifen has been approved as a preventive mechanism for women at high risk of developing ER+ disease[89].

1.6.2 AIs

In premenopausal women the ovaries represent the main supply of oestrogen. However, after the menopause, oestrogen production from the ovaries ceases but production persists in extra-ovarian tissues, particularly peripheral adipose tissue and indeed the breast tumour itself by the enzyme aromatase[90]. In postmenopausal women aromatase activity serves as the main supply of oestrogen production, hence stimulating the growth of breast cancer cells. Aromatase, a member of the cytochrome P450 family, converts androgens, such as testosterone and androstenedione, to oestrogens, such as E2 and oestrone. AIs block aromatase activity, thus depleting the environment of oestrogens and prevent E2 activation of the ER. Indeed, AIs have been shown to reduce oestrogen to an undetectable level in postmenopausal ER+ breast cancer patients[91].

AIs are classified as steroidal (Type 1) and non-steroidal (Type 2). Steroidal inhibitors mimic the structure of androstenedione (natural aromatase substrate) and bind to the substrate binding site of the aromatase enzyme. These agents are then converted into reactive intermediates which bind to the enzyme resulting in an irreversible inactivation of aromatase[92]. Exemestane is the only orally active steroidal AI used clinically[93]. In contrast, non-steroidal inhibitors non-covalently bind the heme moiety of aromatase, occupying the substrate binding site thus

preventing androgen binding[94]. This competitive antagonism is reversible as non-steroidal AIs can be displaced from the active site by endogenous ligands. The non-steroidal AIs in clinical use include anastrozole and letrozole.

AIs are only approved for use in postmenopausal women with ER+ disease. Specifically, anastrozole initially approved as the first line treatment for metastatic disease has recently become the gold standard therapy for postmenopausal women in the adjuvant setting, following the results from the ATAC (Arimidex, Tamoxifen, Alone or in Combination) trial where anastrozole was shown to be superior to tamoxifen[95]. Letrozole is also approved for first line adjuvant therapy, in addition to extended therapy following standard 5 year tamoxifen treatment. Exemestane is currently used in the adjuvant setting following 2-3 years of adjuvant tamoxifen therapy to complete 5 year endocrine treatment[96]. AIs are not effective in reducing oestrogen levels in premenopausal women without concurrent suppression of ovarian function. The initial transient reduction of oestrogen levels induced by AIs in premenopausal women triggers feedback stimulation to the ovaries resulting in a subsequent rise in oestrogen levels[97]. Furthermore, in perimenopausal women, AIs can induce reactivation of the ovaries which is unfavourable for breast cancer patients[93].

1.6.3 Selective ER Down-regulator (SERD): Fulvestrant

The intramuscularly administered steroidal ER antagonist fulvestrant (trade name faslodex) is a 7-alkylsulphinyl analogue of E2 and is structurally distinct from SERMs[98]. Accordingly, fulvestrant exhibits a higher affinity for the ER compared to tamoxifen[98]. Like E2 and tamoxifen, fulvestrant binds to the ER, however its long bulky side chain severely alters the conformation of the receptor, preventing receptor dimerisation and binding to DNA[99,100].

Furthermore, fulvestrant has been demonstrated to disrupt the shuttling of the ER between the nucleus and cytoplasm, thereby blocking nuclear localisation of the receptor[101]. Fulvestrant also induces degradation of the receptor protein without affecting its mRNA level, via the ubiquitin-proteasome pathway[102]. More recently, it has been suggested that even if any fulvestrant-ER complexes are present in the nucleus, fulvestrant mobilises the receptor into the nuclear matrix which is

necessary for its polyubiquitination via a mechanism involving the NEDD8 ubiquitin-like protein and the Uba3-containing NEDD8-activiating enzyme and subsequent degradation by the 26S proteasome[103,104]. Unlike tamoxifen, fulvestrant also impairs both the AF1 and AF2 domains of the ER, resulting in complete ER antagonist activity while showing no agonistic activity and as such fulvestrant is described as a 'pure antioestrogen'[105]. In summary, fulvestrant binds to, blocks and induces rapid degradation of ERs resulting in complete abrogation of oestrogen signalling and transcription of oestrogen-regulated genes.

Several phase III studies have shown that fulvestrant is as effective as anastrozole for postmenopausal women with advanced disease which had progressed on prior endocrine therapy, which subsequently led to the approval of 250 mg per month fulvestrant as second line treatment for such patients[106,107]. However, in the first line setting, 250 mg fulvestrant did not confer additional benefits over tamoxifen in postmenopausal women[108]. More recently, studies including the CONFIRM (Comparison of Faslodex in Recurrent or Metastatic Breast Cancer) trial have demonstrated a further benefit of fulvestrant at a higher-dose regimen (500 mg per month plus an additional 500 mg on day 14 of the first month only) for the treatment of advanced ER+ disease in postmenopausal women following prior endocrine failure[109]. Based on these data, fulvestrant is now approved at this higher dose.

The efficacy of fulvestrant at the higher dose has also been studied in the neoadjuvant and first line settings. The phase II NEWEST (Neoadjuvant Endocrine Therapy for Women with Estrogen-Sensitive Tumours) study comparing the biological and clinical activity of fulvestrant 250 mg and 500 mg in the neoadjuvant setting of postmenopausal women with ER+ locally advanced breast cancer, revealed that the higher dose of fulvestrant was superior, resulting in a significant decrease in protein expression of the proliferation marker Ki67, ER and ER-regulated PR[110]. In the first line setting, the FIRST (Fulvestrant First-Line Study Comparing Endocrine Treatments) trial compared the efficacy of 500 mg fulvestrant with anastrozole for advanced ER+ disease in postmenopausal women. Fulvestrant was as effective as anastrozole for clinical benefit rate and objective response rate[111]. Additionally, fulvestrant is associated with a significantly longer

time to progression compared with anastrozole and therefore may provide longer-lasting disease control if given first line to advanced disease postmenopausal patients[112].

Further studies including FACT (Fulvestrant and Anastrozole Combination Therapy) and SWOG (Southwest Oncology Group) trials are exploring the potential benefit of fulvestrant alongside anastrozole in postmenopausal women. Specifically, the FACT trial investigated whether fulvestrant (500 mg on day 1 followed by 250 mg on days 15 and 29 and thereafter every fourth week) combined with anastrozole was superior compared to anastrozole alone in ER+ breast cancer with relapse after/during primary treatment. The results revealed no advantage of the combined therapy versus the monotherapy in this population with two-thirds of which having been exposed to previous adjuvant antioestrogens[113]. Notably the dose of fulvestrant in this study was lower than that approved, thus a 500 mg per month dose may provide greater clinical benefit. In contrast, postmenopausal women with previously untreated metastatic ER+ disease have demonstrated a greater clinical benefit from a combination of fulvestrant and anastrozole therapy compared to anastrozole alone, exemplified by the SWOG trial[114].

1.7 Endocrine resistance

Antihormones have contributed to a substantial decrease in mortality over recent decades; however, their growth inhibitory actions are compromised by the development of resistance. Indeed, more than 40% of ER+ patients acquire resistance and virtually all advanced disease patients eventually relapse. In both instances, resistance is associated with accelerated tumour growth and increased aggressive behaviour, ultimately resulting in poorer patient outlook. Thus, it is imperative to understand the mechanisms of resistant growth to provide enhanced therapeutic options for such patients.

1.7.1 ER status

The growth inhibitory action of antihormones has been predominantly attributed to the ability of these agents to block the transcriptional activity of the ER and prevent activation of genes involved in cell proliferation and survival. Accordingly,

ER expression is the main predictor of antihormone response, thus alterations in its expression and activity have been extensively studied as a mechanism responsible for endocrine resistance. In fact, approximately 20% of antihormone-treated ER+ patients lose expression of the receptor and become insensitive to further therapy[115,116]. Several mechanisms have been described to cause such down-regulation or complete loss of the ER. At the epigenetic level, hypermethylation of CpG islands within the ER promoter have been demonstrated to contribute to the absence of ER gene expression in breast cancer cells[117,118]. Accordingly, treatment of ER negative (ER-) breast cancer cells with demethylating agents resulted in the re-expression of the ER gene[119]. However, further studies are required to decipher the mechanisms involved and elucidate whether methylation acts solely or partially to silence ER expression.

Moreover, ER- tumours frequently overexpress growth factor receptors, such as EGFR and HER2, suggesting that up regulation of these proteins may provide alternative growth signalling pathways. To further investigate the mechanisms underlying the role of up regulated growth factor signalling in oestrogen-independent growth, [120] previously constructed an ER+ MCF-7 in vitro model with constitutively active MAPK signalling. These genetically engineered cell lines exhibited oestrogen-independent growth, resistance to antihormone therapy and more surprisingly a complete loss of ER mRNA and protein. MAPK activity was demonstrated to be responsible for the down regulation of ER expression, since abrogation of such signalling resulted in rapid restoration of ER. Additionally, constitutive activation of HER2 and EGFR in ER+ breast cancer cells also promoted MAPK-induced down regulation of ER which was reversed by abrogation of MAPK activity[120]. Although the mechanisms involved in MAPK-induced ER down regulation are largely unknown, a subsequent study by the same group proposed a potential role for NF-κB in this process[121].

More recent research is addressing the role of microRNAs in regulating ER stability and representing a novel mechanism responsible for ER loss. MicroRNAs are small non-coding RNAs that negatively regulate gene expression by degrading mRNA or inhibiting translation[122]. Indeed, microRNA-221 and -222 have been shown to decrease ER protein expression in MCF-7 and T47D breast cancer cells[123].

Significantly, microRNA-221/222-transfected MCF-7 and T47D cells became resistant to tamoxifen, suggesting that these microRNAs may be potential targets for restoring ER expression and re-sensitising cells to antihormone therapy. Similarly, microRNA-206 has also been demonstrated to repress ER mRNA and protein expression in MCF-7 cells[124].

Moreover, expression of ER spliced variants have been associated with reduced endocrine response. In particular, a novel variant of ER termed ERα36 has been identified and cloned. This ERα36 differs from the original ER as it lacks both transcriptional activation function domains (AF1 and AF2) but retains the DBD and LBD[125]. ERα36 is predominantly located at the plasma membrane and in the cytoplasm and mediates membrane-initiated oestrogen signalling including activation of the MAPK/ERK pathway and stimulation of growth[126]. Significantly, ERα36-mediated activation of the MAPK/ERK pathway was shown to be unaffected by tamoxifen; instead tamoxifen promoted cell growth of ERα36-overexpressing cells. In support of this *in vitro* study, ERα36 expression has also been examined in clinical breast cancer specimens. Indeed, ER+ tumours expressing high levels of ERα36 were associated with poorer survival and achieved less benefit from tamoxifen therapy[127]. More recently, Zhang & Wang have revealed that short term tamoxifen treatment in fact up regulates ERα36 expression in MCF-7 cells, with increased ERα36 concentrations reported in a tamoxifen resistant MCF-7 cell model[128]. Accordingly, down regulation of ERα36 in the tamoxifen resistant cells restored tamoxifen sensitivity, thus suggesting that increased ERα36 expression contributes to the emergence of tamoxifen resistance.

Furthermore, ERα36 expression is highly correlated with HER2 expression and positive regulatory loops exist between ERα36 and EGFR as well as ERα36 and HER2. EGFR and HER2 signalling induces promoter activity of ERα36 which in turn stabilises the EGFR protein and downstream oestrogen-ERα36 signalling induces HER2 promoter activity[127,129,130]. Accordingly, ERα36 down regulation in HER2-overexpressing cells also resulted in the down regulation of EGFR and HER2, confirming the existence of these regulatory loops[131]. Disruption of these loops via the dual EGFR and HER2 tyrosine kinase inhibitor, lapatanib, successfully increased the sensitivity of stably transfected HER2+ MCF-7 cells and HER2-

overexpressing BT474 cells to tamoxifen. These findings suggest that one of the mechanisms by which ER+ breast cancer cells escape tamoxifen challenge may be via elevated expression of ERα36-HER2/EGFR regulatory loops.

As previously described (section 1.5.1.1), oestrogen-mediated tumour growth is controlled by interactions between the ER and co-regulatory proteins, including coactivators and corepressors. Coactivators function to enhance ER-mediated gene transcription, whereas corepressor proteins function to suppress transcription. E2 binding to the ER triggers the release of the corepressors and subsequently the recruitment of coactivators. In contrast, tamoxifen favours recruitment of corepressors to the ER to inhibit transcription (as described in section 1.1.1). However, a shift in the balance of coactivators and corepressors and overexpression of the former can directly influence the agonistic versus antagonistic properties of SERMs like tamoxifen, to enhance their agonistic activity leading to resistance. To this regard, the ER coactivator AIB1 has been identified and widely studied as a potential mechanism involved in promoting resistance. Indeed, breast cancer cells exhibit increased AIB1 levels compared with normal duct epithelial cells[48,132]. Increased AIB1 expression has been demonstrated to be a marker of tamoxifen resistance in HER2-overexpressing tumours and is associated with increased relapse and death of tamoxifen-treated patients with HER3-overexpressing tumours[133,134]. Patients with AIB1- and HER2-overexpressing tumours displayed 45% 10 year disease-free survival (DFS) on tamoxifen versus 75% 10 year DFS for all other patients. Moreover, patients with HER3- and AIB1-overexpressing tumours exhibited only 30% 10 year DFS on tamoxifen compared with 70% 10 year DFS on tamoxifen for all other patients. These findings are not surprising since AIB1 is phosphorylated and functionally activated by MAPK[135], thus it is likely that HER2/HER3-mediated MAPK activation triggers the activation of AIB1 in breast cancer cells, therefore contributing to the reduction of the antagonistic and enhanced agonistic effects of tamoxifen, leading to the emergence of resistance.

In the presence of antioestrogens, such as tamoxifen, corepressors are recruited to inhibit ER-mediated gene transcription. Studies have demonstrated that inhibition of the corepressor NCOR in tamoxifen-treated MCF-7 cells converted this

antihormone into an agonist, evidenced by an increase in ER activity[82]. In a MCF-7 mouse model system, NCOR levels were decreased in tumours that had acquired resistance to tamoxifen compared to those retaining a response to the drug[82]. Similarly, in ER+ breast cancer tissue samples, NCOR levels decreased during tumour progression and low levels were associated with significantly shorter relapse-free survival[136,137]. Together, these studies support the possibility that reductions in corepressor levels during tamoxifen therapy may enhance the agonist effects of the antihormone on the ER and promote resistance.

1.7.2 Breast cancer stem cells

Cancer stem cells (CSCs) are defined as a heterogeneous population of cancer cells that have the ability to seed new tumour growth. Breast CSCs (BCSCs) were first recognised by Al-Hajj et al.[138] who identified a subpopulation of breast cancer cells able to form tumours in immunocompromised mice. These cells were characterised by expression of the cell surface marker profile $CD44^+/CD22^-$. Following the identification of tumour-initiating $CD44^+/CD22^-$ BCSCs, Ginestier et al.[139] have more recently identified a second marker, the enzyme aldehyde dehydrogenase (ALDH), characteristic of BCSCs. Interestingly, in primary breast xenografts, $CD44^+/CD22^-$ and ALDH identified overlapping but non-identical cell populations, both capable of forming tumours in immunocompromised mice. Additionally, BCSCs possessing both CSC markers ($CD44^+/CD22^-$ and ALDH) displayed the greatest tumour-initiating capacity[139].

More recent studies have shown that BCSCs exist in distinct mesenchymal-like (epithelial-mesenchymal transition (EMT)) and epithelial-like (mesenchymal-epithelial transition (MET)) states characterised by expression of distinct CSC markers[140]. During EMT, epithelial cells lose cell-cell adhesion and acquire a mesenchymal phenotype, allowing them to detach from the primary tumour site and metastasise at distant sites[141]. MET, the reverse of EMT, is characterised by E-cadherin expression of the epithelial phenotype and has been proposed as a mechanism for establishment of the metastatic neoplasm[142]. Subsequent studies have revealed that mesenchymal-like CSCs are characterised as $CD44^+/CD22^-$, are primarily quiescent and are located at the tumour invasive front. In contrast, epithelial-like CSCs express ALDH, are proliferative and located centrally within

tumours[140]. Importantly, BCSCs display cellular plasticity that enables them to transition between EMT and MET states, likely regulated by the tumour microenvironment and potentially involved in allowing tumour cells to invade and form metastasis.

CSCs have been largely studied as key tumour-initiating cells that exhibit inherent resistance to chemotherapy (as reviewed by Abdullah & Chow[143]). Indeed, Li et al.[144] demonstrated enhanced expression of tumour-initiating $CD44^+/CD22^-$ cells in primary breast cancer biopsies following neoadjuvant chemotherapy treatment compared to biopsies obtained prior to treatment. This suggests that $CD44^+/CD22^-$ cells are more resistant to chemotherapy and therefore allow tumour regrowth and relapse. This is proposed to be due to mechanisms including more efficient DNA damage checkpoints and enhanced survival pathways in CSCs compared to the more differentiated tumour cell population[145,146].

There is now a large body of evidence suggesting a potential role for CSCs in the development of endocrine resistance. Of significance interest, normal breast tissue and breast carcinoma $CD44^+/CD22^-$ cells exhibit low or absent ER expression compared to more differentiated tumour cells[147,148]. Thus, BCSCs are highly likely to be endocrine resistant due to the lack of the target receptor. Moreover, increased EGFR signalling has been demonstrated in stem cells of the normal mammary gland and in malignant CSCs of the breast[149–151]. Accordingly, inhibition of EGFR significantly reduced the CSC population, evidenced by a decrease in self-renewal capacity[151]. Interestingly, as mentioned in section 1.7.4, endocrine resistant cells have enhanced growth factor tyrosine kinase signalling, including EGFR and HER2. Therefore, it is possible that acquisition of increased EGFR/HER2 signalling in ER+ antihormone resistant cells potentially results from the selection of CSC-like cells by endocrine therapies[152]. Accordingly, increased CSCs, demonstrated by the expression of stem cell surface markers and their self-renewal capacity, have been identified in tamoxifen-resistant cells compared to tamoxifen-treated wild type MCF-7 cells[153]. Similarly, *in vitro* and *in vivo* studies have demonstrated that tamoxifen treatment of ER+ breast cancer cells contributes to an increase in cells with self-renewing capacity that express lower levels of ER[154]. More recently, Karthik et al.[155] have revealed a potential

mechanism mediated by tamoxifen to enhance the CSC population. Indeed, the authors showed that tamoxifen induced mammalian target of rapamycin (mTOR) signalling in CSCs which was antagonised by mTOR inhibitors. The PI3K/AKT/mTOR pathway drives cell growth and survival and hyperactivation of this pathway is implicated in ER+ breast cancer and in resistance to antihormone therapy (as reviewed by Ciruelos Gil[156] and described in section 1.7.4). Thus, it is possible that tamoxifen-induced mTOR activation in BCSCs plays a role in expanding this resistant cell population.

1.7.3 Cell cycle regulators

The cell cycle functions as a tightly regulated process comprised of several distinct phases required for cell division and replication: G0 (quiescence), G1 (pre-DNA synthesis), S phase (DNA synthesis), G2 and M phase (mitosis). Disruption of the cell cycle regulation contributes to unrestrained growth, a hallmark of cancer. The progression from G1 to S phase is regulated by the interaction between cyclin-dependent kinases (CDKs) and cyclin proteins. CDKs are a group of serine/threonine kinases that cooperate with cyclins to regulate cell cycle checkpoints. CDK4 and CDK6 interact with cyclin D1 and CDK2 interacts with cyclin E1 during G1 and subsequently phosphorylate the retinoblastoma protein. This results in the inactivation of the retinoblastoma protein and release of transcription factors that allow progression to the S phase[157,158].

Several cell cycle regulators have been recognised as potential players in endocrine resistance. Of these, the nuclear transcription factor MYC and cyclins D1 and E1 have been the most comprehensively studied. These regulatory proteins promote progression and completion of the cell cycle by shortening arrest in the G1 phase. Indeed, oestrogens rapidly induce expression of MYC, cyclin D1, CDK4/6-cyclin D1 complexes, cyclin E1 and CDK2-cyclin E1 complexes to induce cell proliferation[159–163]. Conversely, antihormone therapy has an inhibitory effect, preventing cell cycle progression and promoting arrest in G1[164,165]. Paradoxically, however, the acquisition of antihormone resistance is associated with up regulation of these key cell cycle regulators[166,167]. Indeed, constitutive and inducible expression of MYC and cyclin D1 have been shown to rescue breast cancer cells from antihormone-induced growth arrest enabling them to complete

the cell cycle[161,168–170]. Furthermore, overexpression of these proteins, which occurs in approximately 30-45% of breast cancers, is associated with reduced antihormone response[171]. Studies have shown that overexpression of cyclins D1 and E1 are able to abrogate tamoxifen- and fulvestrant-mediated growth arrest[172–174].

In addition, cyclin D1 can bind and activate the ER in a ligand-independent manner with such an event not inhibited by antihormone treatment[175–177]. This suggests an additional mechanism by which overexpression of cyclin D1 contributes to endocrine resistance through sustaining ER transcriptional activity and activation of downstream proliferation and survival genes.

Furthermore, CDK4/6 inhibitors are currently in clinical development. Palbociclib, a highly selective CDK4/6 inhibitor, thus blocking retinoblastoma phosphorylation and thereby inducing G1 arrest, has been the most extensively studied. An *in vitro* study revealed that ER+ and HER2-overexpressed breast cancer cell lines were the most sensitive to growth inhibition by palbociclib while basal subtypes were the most resistant[178]. Additionally, palbociclib acted synergistically with tamoxifen in ER+ antihormone sensitive cell lines, and enhanced the sensitivity of tamoxifen-resistant cells to the antihormone. Based on these data, a clinical study was conducted to test the safety and efficacy of palbociclib in combination with antihormones in ER+ breast cancer. Initially, a phase I study confirmed the safety of palbociclib in combination with letrozole in patients with ER+ and HER2- advanced breast cancer and determined the optimal recommended dosage[179]. A large randomised phase II study was subsequently conducted to assess the safety and efficacy of palbociclib in combination with letrozole compared to letrozole alone in the first-line treatment of postmenopausal women with advanced ER+ HER2- breast cancer. The results from this study revealed that patients treated with the combination therapy had significantly longer progression-free survival (20.2 months) compared to letrozole treatment alone (10.2 months)[180]. Significantly, following the results of this study, in February 2015 the US Food and Drug Administration granted accelerated approval of palbociclib in combination with letrozole for the treatment of postmenopausal women with ER+ HER2- advanced breast cancer as initial endocrine-based therapy for their metastatic

disease[181]. A double-blinded phase III, placebo-controlled study (NCT01740427) in a similar patient population, with the aim of confirming the phase II findings, is currently underway. Additionally, a phase III study of palbociclib in combination with fulvestrant in ER+ HER2- metastatic breast cancer patients previously treated with endocrine therapy (NCT01942135) is ongoing.

1.7.4 Growth factor signalling

The majority of patients who acquire resistance to tamoxifen continue to express the ER[182]. Indeed, up to 20% of such patients respond to second line antihormone therapy including AIs and fulvestrant, suggesting that the ER continues to regulate growth during resistance[106,107].

Hyperactivation of growth factor signalling has been heavily implicated in driving resistance. Such signalling circumvents the inhibitory effects of antihormones via bidirectional cross-talk and modulation of the ER to promote growth despite the presence of endocrine therapy. When extreme, growth factor pathways drive tumour growth and survival in an ER-independent manner evidenced by a significant number of patients who fail to respond to second line antihormone therapy, indicating a loss of reliance on ER-mediated growth[121,183].

1.7.4.1 ER-dependent

This phenomenon has been widely documented for the receptor tyrosine kinases (RTK) EGFR, HER2 and IGF-1R. Activation of these receptors stimulates cell growth via downstream MAPK and PI3K pathways. Studies in antihormone-resistant breast cancer cell lines, like their clinical counterparts, have shown increased expression of these receptors, their ligands and associated downstream kinases compared to that observed in the parental cell lines[184–188]. Critically, besides the capacity to promote cell growth in their own right, such signalling can phosphorylate the ER and its co-regulatory proteins, altering the receptor transcriptional activity and ultimately contributing to antihormone-resistant proliferation. Specifically, MAPK and PI3K signalling can phosphorylate key residues within the AF1 region of the ER (serine 118 and serine 167) thus allowing persistent activation of nuclear ER[53,189]. Such activation of the ER promotes re-expression of oestrogen regulated genes in a ligand-independent manner and in

the presence of antihormone[190,191]. Indeed, tamoxifen-resistant and long term oestrogen deprived breast cancer cells exhibit increased levels of phosphorylated ER at serine 118 and 167 with consequent re-expression of oestrogen-regulated genes[192–196]. Significantly, EGFR/MAPK-mediated ER phosphorylation at serine 118 and subsequent continued activation of the ER in tamoxifen-resistant cells results in the re-expression of the EGFR ligand amphiregulin[196], thus generating a self-propagating EGFR-driven autocrine growth-regulatory loop in these cells in which amphiregulin expression is induced by ligand-independent serine 118 ER phosphorylation.

Moreover, despite reduced expression of IGF-1R signalling in MCF-7 cells during antihormone response, EGFR-activated ER in tamoxifen resistant cells promotes the expression of insulin-like growth factor (IGF)-II and consequently re-activates IGF-1R signalling[197]. Importantly, there is considerable evidence implicating EGFR and IGF-1R cross-talk in breast cancer cells. Besides its effects on cell proliferation and survival, IGF-II-induced activation of IGF-1R in tamoxifen resistant cells has also been shown to phosphorylate and thus activate EGFR signalling via a c-src dependent mechanism[198]. Additionally, this pathway also contributes to increased ER phosphorylation on serine 118 in tamoxifen-resistant cells[197]. This cross-talk is however unidirectional with EGF failing to induce phosphorylation of IGF-1R. Complementing these cell lines studies, IGF-1R expression and activity have also been detected in ER+/EGFR+ tamoxifen-resistant clinical samples supporting the role for such signalling in promoting the growth of acquired tamoxifen-resistant tumours[198].

Furthermore, there is increasing evidence implicating aberrant fibroblast growth factor receptor (FGFR) signalling in breast cancer cells, capable of promoting endocrine resistance. The FGFR family comprises of four members, all of which have been implicated in breast cancer: FGFR1, FGFR2, FGFR3 and FGFR4[199]. Similarly to the abovementioned RTKs, activation of FGFRs promotes cell proliferation via downstream MAPK and PI3K/AKT signalling pathways. FGFR1 amplification, observed in approximately 10% of breast cancers[200], has been demonstrated to promote endocrine resistance. Turner et al.[201] revealed that FGFR1-amplified breast cancer cell lines are resistant to tamoxifen therapy, which

is reversed by small interfering (si)RNA targeting FGFR1. This *in vitro* data strongly suggests that FGFR1 overexpression drives endocrine therapy resistance, and this observation is supported by the poor-prognosis exhibited by FGFR1-overexpressing tumours treated with adjuvant tamoxifen therapy. Similarly, increased FGFR3 expression has been demonstrated in tamoxifen-resistant tumours compared to tamoxifen-sensitive tumours[202]. *In vitro,* FGFR3 activation in MCF-7 cells stimulated MAPK and PI3K signalling pathways concurrent with decreasing the sensitivity of these cells to tamoxifen and fulvestrant treatment. Interestingly, although activation of FGFR and EGFR stimulate similar downstream pathways (i.e. MAPK and PI3K), unlike EGFR, FGFR signalling did not influence ER activity but instead appeared to override ER activity[202]. Furthermore, in a tamoxifen-resistant breast cancer cell model, FGFR3 activation induced cell proliferation independent of ER activation. Furthermore, increased FGFR4 expression has been associated with endocrine resistance. In tamoxifen treated patients with recurrent disease, increased FGFR4 expression predicts antihormone failure together with decreased progression-free survival[203]. Together, these studies suggest that activation of FGFRs might be an important mechanism by which breast cancer cells escape antihormone challenge, subsequently contributing to the resistant phenotype.

As mentioned above, growth factor signalling can also phosphorylate ER co-regulatory proteins to activate ER-mediated gene transcription. The most widely studied is the coactivator AIB1. Indeed, HER2-driven MAPK signalling not only induces ligand-independent activation of the ER but has also been shown to phosphorylate and activate AIB1. Thus, tumours with high expression of both HER2 and AIB1 are less responsive to tamoxifen therapy due to an increase in ER coactivator activity mediated by HER2 signalling, subsequently increasing the agonistic activity of tamoxifen[133]. The level of AIB1 expression in HER2+ breast cancer may provide an important predictive marker for tamoxifen resistance[195]. Interestingly, AIs are more effective than tamoxifen therapy for HER2+ tumours[204]. However, this was not confirmed in a larger study that followed. This more recent study demonstrated that although letrozole is more effective than tamoxixen therapy for ER+ disease, it is irrespective of HER2 expression[205]. It is possible that

the correlation between HER2 and AIB1 and the consequent activation of the coactivator is less important for potent oestrogen deprivation therapy, compared to tamoxifen therapy which exhibits agonistic and antagonistic properties greatly influenced by the equilibrium of coactivator and corepressor proteins.

1.7.4.2 ER-independent

Although growth factor signalling contributes to increased ER phosphorylation and transcriptional activation, paradoxically, sustained hyperactivation of such signalling has also been associated with reducing ER expression. These antihormone resistant tumours are comprised of ER- and growth factor receptor-overexpressing cells that are no longer reliant on ER signalling for cell growth and as such are not growth inhibited by further antihormone therapy[121]. Indeed, several studies have demonstrated that exposure of ER+ cells to growth factors, such as EGF, can down-regulate ER protein expression[206]. Similarly, transfection of constitutively active HER2, MEK1 and Raf1 into breast cancer cells results in a decrease in ER protein expression[120,207–209]. More recent findings have identified the transcription factor NF-κB as an intermediary in hyperactivated MAPK-induced ER down-regulation[121]. Interestingly, NF-κB is also elevated in *de novo* ER-breast cancer exhibiting increased EGFR and HER2 activity[210,211] and has also been associated with increased AKT activity in tamoxifen resistance[212]. To this regard, it is conceivable that sustained hyperactivation of growth factor pathways contributes to an ER- and endocrine-independent phenotype.

1.7.4.3 Combination of ER-dependent and ER-independent growth factor signalling mechanisms implicated in driving antihormone-resistance

Together, hyperactivation of EGFR, HER2 and IGF-1R in endocrine resistance induces a vicious circle between these signalling pathways and the ER to promote cell proliferation and survival via ER genomic and non-genomic activities (Figure 4). Accordingly, potent targeting of these ER activities by oestrogen deprivation and ER down regulation (fulvestrant) therapy are effective in ER+ HER2+ patients[204]. Sadly, however, growth factor signalling pathways develop the ability to drive tumour growth and survival in an ER-independent manner, thus tumours also become resistant to AIs and fulvestrant. Such pathways include growth factor-activation of MAPK and PI3K which in turn activates transcription factors such as

NF-κB[213] to induce expression of proliferation and survival genes (e.g. cyclins D1 and E1 and MYC) in an ER-independent manner[214].

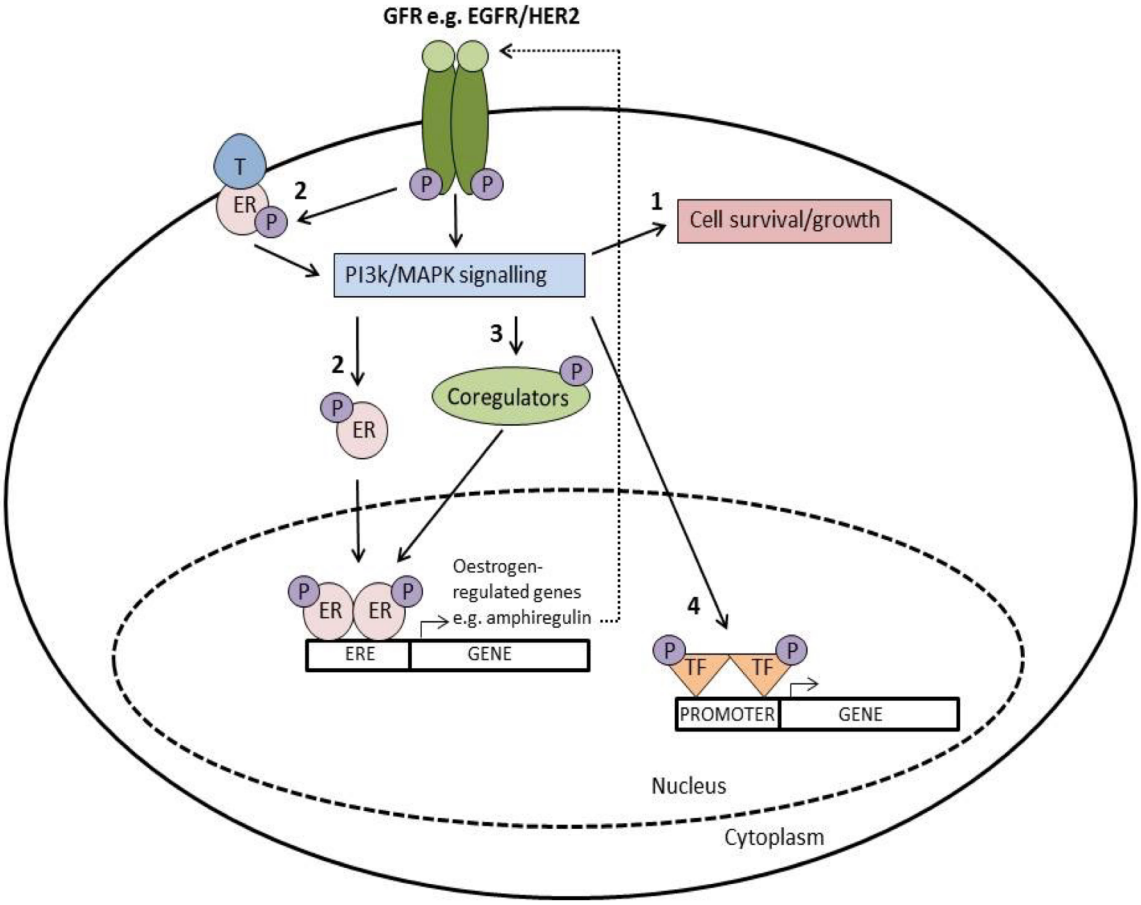

Figure 4 Cross-talk between oestrogen receptor (ER) and growth factor receptor (GFR) signalling pathways. Besides cell survival and growth (1), activation of GFRs such as epidermal growth factor receptor (EGFR) and human epidermal growth factor receptor 2 (HER2) can phosphorylate the ER in a ligand-independent manner and in the presence of antihormones (e.g. tamoxifen (T)) to induce transcription of oestrogen-regulated genes (such as the EGFR ligand amphiregulin) to generate an autocrine-driven growth regulatory loop (2). GFR signalling can also phosphorylate co-regulatory proteins to activate ER-mediated gene transcription (3) in addition to activating transcription factors (TF) to induce transcription (4). ERE: oestrogen response elements.

1.7.4.4 Therapeutic targeting of growth factor signalling in resistance

Several pre-clinical studies have targeted these up regulated growth factor signalling pathways. Indeed, the EGFR inhibitor gefitinib and the HER2 monoclonal antibody trastuzumab have both been studied as a monotherapy to inhibit

resistant cell growth and also as a combination therapy alongside antihormones during response to delay or prevent the emergence of resistant growth. As previously mentioned, tamoxifen- and fulvestrant-resistant MCF-7 cells exhibit increased EGFR and HER2 activity. Thus, blockade of EGFR and HER2 in these resistant cell models using gefitinib and trastuzumab, respectively, has been shown to inhibit cell growth[184,185]. Additionally, targeted therapy of the downstream kinases, including MAPK and PI3K/AKT, has also been shown to inhibit resistant cell growth[184,185]. More recent findings have shown that gefitinib treatment of tamoxifen resistant breast cancer cells which have developed an ER- phenotype (likely due to sustained MAPK signalling and NF-κB activity) results in a decrease in expression of MAPK signalling proteins with a parallel increase in ER protein expression, thus re-sensitising the resistant cells to tamoxifen[215]. However, functional E2/ER signalling in wild type MCF-7 cells represses EGFR and HER2 expression and as such are unaffected by gefitinib and trastuzumab treatment[184,185]. Interestingly, blockade of ER signalling by antihormones during response contributes to an induction of EGFR expression. Thus, a combination of gefitinib and tamoxifen or fulvestrant therapy during antihormone response has been shown to induce greater inhibition of proliferation and promotion of apoptosis compared to either therapy alone[216]. This combination therapy prevented early induction of EGFR/MAPK signalling during response and significantly delayed the development of resistance. In support of this study in cell lines, gefitinib has also been shown to improve the growth inhibitory actions of tamoxifen and delay the emergence of resistant growth *in vivo*[217].

Based on the pre-clinical rationale for enhanced benefit, there have been a number of phase II studies of gefitinib/trastuzumab in combination with endocrine therapy[218–221]. Specifically, patients with ER+ newly diagnosed metastases or disease that had recurred after adjuvant tamoxifen therapy demonstrated increased progression-free survival from gefitinib plus tamoxifen therapy compared to gefitinib plus placebo[219]. Similarly, anastrozole and gefitinib and anastrozole/letrozole and trastuzumab combination therapies also resulted in increased clinical benefit in ER+ metastatic breast cancer patients[218,220,221]. However, the benefit of such combination therapies is short-lived with the

emergence of aggressive resistance growth which remains a significant clinical problem[222–224]. Indeed, studies have revealed that gefitinib- and trastuzumab-resistant growth is dominated by IGF-1R signalling, indicating an ability of the tumour cells to switch to an alternative growth factor pathway in the presence of the drug[222,225,226]. Importantly, further studies are clearly required to decipher and prevent the emergence of resistant cell growth.

1.7.5 PI3K and AKT signalling

The PI3K/AKT/mTOR pathway plays a crucial role in cell proliferation, growth and survival. Dysregulation of this signal transduction pathway occurs in several tumour types, including breast cancer, and has been implicated in tumour progression and antihormone resistance[227]. Following activation by growth factor RTKs or G-protein-coupled receptors[228,229], PI3K phosphorylates phosphatidylinositol 4,5 bisphosphate (PIP_2) to produce phosphatidylinositol 3,4,4-triphosphate (PIP_3), which subsequently recruits proteins containing pleckstrin homology (PH) domains to the plasma membrane. Such PH domain-containing proteins include AKT and its activating kinase PDK1[230]. PDK1 binds PIP_3 at the plasma membrane and phosphorylates AKT, which in turn regulates downstream proteins to promote cell cycle progression and survival[231]. Activated AKT stimulates mTOR-containing complex 1 (TORC1) activity to positively regulate protein translation and synthesis[232,233]. Additionally, AKT promotes cell survival through phosphorylation of Mdm2, a protein that binds to and inhibits the activation of the p53 tumour suppressor protein[234], and through inactivation of pro-apoptotic BCL-2 family members including BAD[235]. PI3K activity is antagonised by the negative regulatory proteins, phosphatase and tensin homolog (PTEN) and inositol polyphosphate-4-phosphatase type II (INPP4B), which catalyse the dephosphorylation of PIP_3 and PIP_2, respectively[236,237].

The PI3K/AKT/mTOR pathway is frequently altered early in ER+ breast cancer to promote cell proliferation and survival, ultimately contributing to the progression of the disease[238]. Such alterations include activating mutations or amplifications of the genes encoding PI3K (p110α)[239,240], PDK1[241], AKT1[239], and loss of function or reduced expression of the genes encoding PTEN[242–244] and INPP4B[237,245]. Furthermore, significant cross-talk between the PI3K/AKT/mTOR pathway and

the ER has been demonstrated. Indeed, as mentioned elsewhere (sections 1.7.4.1, 1.7.6.1 and 1.7.6.2), signalling through the PI3K/AKT/mTOR pathway activates ER transcriptional activity in a ligand-independent manner via direct phosphorylation of the ER at serine 167 by AKT[246]. Additionally, vice versa, the ER promotes the transcription of genes upstream of the PI3K/AKT/mTOR pathway, such as RTKs and their ligands. As previously discussed (section 1.5.2), E2-activated ER at the plasma membrane stimulates PI3K signalling via activation of RTKs, including IGF-1R and EGFR[63,64], ultimately enhancing tumour cell proliferation and survival.

Unsurprisingly, the increased growth factor RTK signalling present in endocrine resistance (as discussed in section 1.7.4) results in hyperactivated downstream PI3K/AKT/mTOR signalling and consequently resistant cell growth and survival. Additionally, reduction of PTEN expression has been shown to enhance PI3K signalling, reduce antihormone sensitivity and ultimately promote endocrine resistance in ER+/HER2- breast cancer cells *in vitro* and *in vivo*[247]. Accordingly, combined treatment with an AKT inhibitor or mTOR inhibitor plus fulvestrant was shown to inhibit PI3K downstream signalling, induce apoptosis and accelerate regression of reduced-PTEN-expressing xenograft tumours. Interestingly, a correlation between increased PI3K activity and decreased ER expression has been documented in ER+ breast cancer. Indeed, Creighton et al.[248] have reported a negative correlation between ER level and PI3K activity in ER+ tumours. Additionally, the authors demonstrated increased PI3K activity in the more aggressive luminal B tumours, compared to those of the less aggressive luminal A subtype. This increase in PI3K activity in the luminal B tumours was associated with lower ER levels. Notably, PI3K inhibition in ER+ cell lines resulted in an increase in ER expression and ER target genes and increased the sensitivity of the cells to tamoxifen. Together, hyperactivated PI3K signalling in ER+ breast cancer may reduce ER expression, which is a hallmark of endocrine resistance (as previously discussed in section 1.7.1). Accordingly, targeting of PI3K in these tumours, may increase ER expression and subsequently re-sensitise the cells to antihormone therapy.

Several clinical trials targeting the PI3K/AKT/mTOR pathway have been conducted. One key study in the advanced setting evaluated everolimus (inhibits

mTOR via allosteric binding to the mTORC1) in combination with exemestane in patients who had progressed on aromatase inhibitor treatment. The Breast Cancer Trials of Oral Everolimus-2 (BOLERO-2) is an on going randomised phase III study of postmenopausal women with ER+/HER2- disease. The interim results showed that the combination therapy prolonged progression-free survival compared to exemestane treatment alone (6.9 versus 2.8 months), providing support for this combination therapy in hormone-resistant, advanced disease [249].

1.7.6 Antihormone-induced compensatory signalling

Classically, oestrogen induces expression of target genes bearing EREs in their promoter region, as previously described in section 1.5.1.1. Surprisingly, however, it has been shown that transcriptional repression of oestrogen-regulated genes comprises the bulk (70%) of expression changes present in ER+ breast cancer cells upon E2 challenge (Frasor et al. 2003). The underlying mechanisms involved in E2-mediated transcriptional repression are beginning to emerge. One proposed mechanism is competition for coactivators by E2-repressed gene promoters. This mechanism has been suggested to be responsible for oestrogen-suppression and antihormone-induction of HER2 in ER+ breast cancer cells. A region within the first intron of the HER2 gene has been shown to act as an oestrogen suppressible enhancer in ER+ breast cancer cells and appears to mediate ER-dependent suppression of HER2 expression[250]. Subsequent studies by Newman et al.[251] revealed that the ER and AP-2 transcription factor compete for the limiting coactivator, SRC-1. SRC-1-mediated activation of the AP-2 transcription factor results in activation of the HER2 promoter and subsequently increases HER2 expression[252]. However, in the presence of oestrogen and subsequent ER activation, the AF2 domain of the receptor provides a strong binding site for SRC-1 and sequesters the coactivator, thus preventing AP-2 activation and downstream HER2 expression[251]. In contrast, following antihormone treatment, SRC-1 is released from the ER and available to bind and activate AP-2, thus promoting HER2 expression.

A second mechanism involved in E2-mediated transcriptional repression comprises the recruitment of corepressor proteins by the E2:ER complex to some gene promoters. This has been demonstrated for several genes. For example, Stossi

et al.[253] have shown that E2-bound ER is able to repress expression of the negative regulator of the cell cycle, cyclin G2, by recruitment of the corepressor NCOR and histone deacetylase complexes, leading to chromatin condensation and transcriptional repression (as previosuly described in section 1.5.1.1). E2-mediated repression of E-cadherin expression in ER+ breast cancer cells has also been attributed to the recruitment of the corepressor, scaffold attachment factor B, to the ER[254]. This E2-induced suppression of E-cadherin was reversed by tamoxifen treatment. Furthermore, E2-activated ER has been shown to recruit DEAD box RNA helicase 97 (DP97) corepressor to the promoter of the HER2 gene, subsequently suppressing its expression. Accordingly, silencing of DP97 enhanced HER2 expression[255].

A third mechanism proposed for E2-mediated gene repression includes E2:ER protein/protein interactions with, and subsequent sequestering of, additional transcription factors to prevent their activity. Such interactions have been implicated between the ER and two distinct transcription factor families, NF-κB and C/EBP, and shown to be involved in E2-mediated IL-6 repression in human osteoblast and MCF-7 cell lines[61]. IL-6, secreted by osteoblasts, plays a role in the regulation of bone metabolism by activating osteoclast cells which mediate bone resorption. NF-κB and C/EBPβ are strong activators of the IL-6 promoter; however, in the presence of E2, activated ER directly interacts with both transcription factors, suppressing their transcriptional activity at the IL-6 promoter and downstream bone resorption. Thus, by inhibiting IL-6 promoter activity, E2 inhibits bone resorption and consequently disrupts bone metabolism[61]. Accordingly, this study supports the development of osteoporosis commonly observed in post-menopausal women and provides a mechanism of prevention mediated by oestrogen treatment. Further examples of protein/protein interactions between transcription factors and the E2:ER complex includes E2-mediated repression of transforming growth factor (TGF)-β in MCF-7 cells via an association between activated ER and the transcription factor SMAD3[256]. TGF-β has been considered as a tumour suppressor in early breast cancer disease but at later stages, TGF-β evolves into a promoter of tumour progression and invasion[257,258].

Many of the oestrogen-suppressed genes are anti-proliferative and pro-apoptotic[259], thus the benefit of antihormone therapy is achieved by counteracting the repressive events induced by oestrogen, triggering re-expression of these growth repressors. However, it is also plausible that oestrogens suppress and antihormones induce genes involved in cell proliferation and survival, with emerging evidence supporting this hypothesis (as described for the pro-proliferative/pro-survival genes EGFR, AKT, BCL-2 and 14-3-3ζ in sections 1.7.6.1 and 1.7.6.2 below)[197,216,259]. Such events may potentially limit the anti-tumour activity of antihormones, providing survival mechanisms to a cohort of tumour cells early during response and ultimately aid the emergence of resistant growth. Such genes may provide targets for novel therapies to reverse or prevent the development of resistance. Indeed, the growth inhibitory actions of antihormones are incomplete, with some cells evading the initial impact of these agents, resulting in limited anti-tumour responses. Studies in ER+ MCF-7 cells have shown that tamoxifen exerts significant anti-proliferative effects as early as week 2 post-treatment. However, only a modest increase in apoptosis was observed in parallel with partial suppression of the cell survival protein, BCL-2. Additionally, the emergence of highly proliferative tamoxifen-resistant cells was apparent as early as week 5 post-treatment [216].

1.7.6.1 Proof of principle: oestrogens suppress and antihormones induce EGFR expression

As briefly described in section 1.7.4.4, oestrogen challenge has been shown to suppress EGFR at the transcriptional level in several ER+ breast cancer cell models[260,261]. In turn, EGFR expression is up regulated by antihormones during response, with induction occurring from as early as one week with tamoxifen in MCF-7 cells[216]. The tamoxifen-induced EGFR maintained residual activity through downstream MAPK and AKT, cross-talked with the ER maintaining phosphorylation of serine 118/serine 167 with some expression of the ER-regulated pro-survival gene BCL-2. Consequently, the anti-tumour effects of tamoxifen were incomplete, with only partial inhibitory effects on proliferation and minimal induction of apoptosis[216]. By three months, the majority of tamoxifen-treated cells exhibited increased EGFR expression with substantial downstream

kinase activity. Interestingly, these events were paralleled with the emergence of tamoxifen resistance, coincident with restoration of ER activity and expression of ER-regulated growth factor ligands, particularly amphiregulin, completing an EGFR-driven autocrine growth-regulatory loop facilitated by IGF-1R[185,196]. Together, these studies provide proof of principle that antihormone-induced signalling genes have substantial potential to limit the initial anti-tumour response of ER+ cells, providing early protective mechanisms to a cohort of cells from which resistance subsequently emerges.

1.7.6.2 Antihormone-induced pro-survival genes

There is now considerable evidence implicating the role of antihormone-induced pro-proliferative genes in endocrine resistance. However, the role played by antihormone-induced pro-survival genes remains largely unexplored. Since these agents are weak promoters of apoptosis, this may reflect a significant capacity for induction of pro-survival mechanisms by such drugs during response. Indeed, antihormones have been shown to induce activation of the pro-survival gene AKT in the ER+ breast cancer cell line MCF-7[262,263] with such activation of AKT associated with a decreased sensitivity of MCF-7 cells to the growth inhibitory actions of endocrine agents[246,264]. Furthermore, increased activity of AKT is maintained through to the development of tamoxifen-resistance suggesting that the AKT signalling pathway may play a role in the acquisition of resistance[263]. Immunohistochemical analysis of antihormone-treated tumour specimens identified a correlation between shorter disease free survival and activated AKT, suggesting that there is a link between the AKT pathway and antihormone therapy failure in patients[265]. Several studies have now indicated that one significant mechanism by which AKT contributes to antihormone failure and resistance is through aberrant activation of the ER. AKT has been shown to phosphorylate key serine residues on the AF1 domain of the ER resulting in transcriptional activation of the receptor in a ligand-independent manner[246]. Interestingly, the previously mentioned cross-talk between the RTKs EGFR and IGF-R1 with the ER has been shown to involve AKT[266]. Indeed, treatment of MCF-7 cells with EGF or IGF-I results in rapid phosphorylation and thus activation of AKT with a concurrent increase in ER activity via the AF1 domain[266]. Similarly, in tamoxifen resistant cells

derived from MCF-7 cells, the growth factor ligands EGF and TGFα have been shown to induce phosphorylation of AKT[263].

Furthermore, tamoxifen has also been shown to induce up regulation of the anti-apoptotic proteins BCL-2 and BCL-XL thus decreasing the anti-tumour response to tamoxifen[267,268]. Additionally, the survival of ER+ breast cancer cells treated with oestrogen deprivation (to mimic AI therapy) is supported by increased activity of BCL-2[269]. More recently, increased expression of the pro-survival gene 14-3-3ζ has been shown to promote endocrine resistance. In turn, down-regulation of 14-3-3ζ in antihormone-resistant cells reversed resistance and restored antihormone sensitivity, paralleled with reduced expression of signature genes involved in cell proliferation and survival[270].

Taken together, these limited studies reveal promising results for the role of pro-survival genes in the development of endocrine resistance, particularly those promoted by antihormone treatment. Importantly however, further studies are clearly required to identify novel pro-survival genes induced by antihormones during response that may play a role in the development of endocrine resistance. Such findings may provide novel therapeutic strategies to reverse or prevent the development of resistance.

1.7.6.3 Antihormone-induced autophagy

Autophagy is an evolutionary conserved process responsible for the degradation of proteins and the turnover of organelles to maintain homeostasis. Autophagy is characterised by the segregation of cytoplasm and/or intracellular organelles into double membrane-bound vesicles, referred to as autophagosomes. The autophagosomes next fuse with lysosomes where the vesicle content is degraded and essential proteins/amino acids are recycled and provided back to the cell in order to preserve energy[271,272]. Both pro-survival and pro-apoptotic functions have been attributed to autophagy, however the latter remains controversial and less well-defined. With regard to a pro-survival role, a deficiency in nutrients stimulates the activation of autophagy to produce amino acids essential for metabolism and survival[273]. Similarly, in cancer cells, autophagy is stimulated to

protect cells from low nutrient supply (e.g. the cells comprising the inner part of a solid tumour that have limited access to a blood supply) and therapeutic insult[274].

In breast cancer, emerging evidence is supporting a pro-survival role for autophagy in the development of endocrine resistance as demonstrated by studies in antihormone responsive and resistant cell lines. Significantly, short term tamoxifen treatment induced autophagy in the antihormone-responsive MCF-7 and T47D cells and in a tamoxifen-resistant MCF-7, HER2-overexpressing cell line[275]. Indeed, following combination treatment of tamoxifen and autophagy knockdown in MCF-7 and T47D cells, cell viability was significantly reduced compared to either treatment alone[275]. Additionally, in tamoxifen resistant MCF-7-HER2 cells, autophagy knockdown and tamoxifen treatment dramatically reduced cell viability, suggesting that autophagy down-regulation was able to re-sensitise the cells to the antihormone. Additionally, a similar study by Samaddar et al.[276] also revealed that tamoxifen and fulvestrant induced autophagy in MCF-7 cells. Furthermore, the antihormone-induced autophagy was demonstrated to play a critical role in cell survival and facilitated the development of acquired endocrine resistance. Accordingly, inhibition of autophagy in the tamoxifen resistant cells led to the restoration of tamoxifen sensitivity, evidenced by an increase in cell death. Together, these studies suggest that autophagy is induced early during antihormone response and may represent a protective mechanism to allow the cells to escape the growth inhibitory actions of these agents and allow cell survival during antihormone challenge, consequently facilitating the development of antihormone resistance.

1.8 Gene expression profiling

Following the completion of the sequencing of the human genome came the emergence of microarray technologies. Such technologies allow thousands of genes in a tumour sample to be analysed simultaneously, creating a genome-wide gene expression profile. Indeed, microarray gene expression profiling studies have enhanced our understanding of the complexity and heterogeneity of breast cancer and have confirmed that it is by no means a single disease. Early microarray studies by Perou and colleagues[277] revealed that ER+ and ER- breast cancers are fundamentally distinct at the transcriptomic level and can further be divided into

four molecular subtypes, including luminal A, luminal B, basal and HER2[277–279]. Several studies have now demonstrated that breast cancer comprises a collection of diseases, expressing different transcriptional profiles, have distinct risk factors, clinical presentation, histological features, response to therapy and outcome[280–282]. These studies have also shown that treatment response is governed by the underlying molecular characteristics of the tumours and indeed have identified an obvious potential role for microarray profiling as a means of predicting prognosis and treatment response.

Several groups have developed gene signatures aiming to predict prognosis. The first gene signature consisted of 70 genes shown to identify patients with good prognosis characterised by a 5-year minimum risk of developing distant metastasis in systemic therapy-naïve patients[283]. Subsequent studies have demonstrated that the 70-gene signature classifies the majority of ER- breast cancers as poor prognosis with a high histological grade[284–286]. Further studies have led to the development of several additional prognostic signatures, including Oncotype DX. This genetic test analyses 21 genes to determine the 10-year distant recurrence risk of ER+, node negative breast cancers treated with tamoxifen and subsequently identifies high-risk patients that would benefit from the addition of chemotherapy to their endocrine treatment[287]. However, such genetic tests/gene signatures provide only prognostic data and fail to identify therapeutic targets that may improve response. Furthermore, several patients present with de novo resistance while all advanced disease patients eventually acquire resistance.

Several studies have employed microarrays to explore oestrogen response genes, and in turn have evaluated the effectiveness of the different classes of antihormones in reversing these profiles[38]. However, these studies have predominantly focused on the growth-inhibitory effects induced by antihormones, as opposed to exploring the increases in oestrogen-repressed, antihormone-induced signalling genes that may serve to limit antihormone response.

1.9 Aims and objectives

Antihormones are the mainstay therapy for ER+ breast cancer and have contributed to a substantial decrease in mortality over recent decades. However,

their growth inhibitory actions are limited by *de novo* and acquired resistance resulting in increased metastatic capacity, disease progression and poorer patient outlook. To delay, prevent or ultimately treat resistance, it is imperative that we understand the complexities of the underlying signalling mechanisms that limit antihormone response. The identification of novel antihormone-induced pro-survival genes/proteins will further our understanding of the multitude of mechanisms that together determine antihormone response in ER+ breast cancer and confirm the concept of drug-induced events contributing substantially to the emergence of resistance.

To this regard, the work in this thesis focuses on pro-survival genes induced by antihormone treatment during initial response whose expression may contribute substantially to the emergence of resistance. Four antihormone-sensitive cell lines are to be used to reflect the heterogeneity present in clinical ER+ breast cancer (ER+/HER2-: MCF-7 and T47D, ER+/HER2+: BT474 and MDA-MB-361). Microarray technology will be utilised to identify novel pro-survival genes induced following short-term antihormone treatment in each cell model. These studies will further extend into cell models of antihormone-resistant breast cancer to determine whether expression of such genes are maintained and hence play a role in the emergence of resistance. Such studies may identify these pro-survival genes as potential novel therapeutic targets both in the antihormone-responsive and –resistant settings and the overexpression of these proteins could be utilised as potential novel biomarkers indicative of endocrine resistance. Thus, the objectives of this thesis are:

- To identify, via Affymetrix gene expression profiling, novel pro-survival genes induced by a range of currently-used endocrine therapies (tamoxifen, fulvestrant and oestrogen deprivation) in a panel of ER+ human breast cancer cell lines. Subsequently, a robust filtering procedure, including ontological investigation and polymerase chain reaction (PCR) verification of the array profiles, will be used to prioritise candidate genes.
- To investigate the protein expression of the candidate pro-survival genes identified, to further verify the microarray profile.

- To determine whether these genes/proteins persist into, and hence play a significant role in, antihormone resistance.
- To address the targeting potential of these proteins in model systems. siRNA will be used to target these proteins in antihormone resistance to determine whether this strategy can promote apoptosis and also in combination with antihormone therapy to determine whether this strategy can improve the anti-tumour response of these agents.

2 Materials and Methods

Tissue culture medium and constituents were purchased from Life Technologies, UK. Tissue culture plastics were purchased from Nunc, Roskilde, Denmark supplied by Fisher Scientific, Loughborough, UK. All chemicals and reagents were purchased from Sigma-Aldrich (Poole, UK) unless stated otherwise.

2.1 Cell culture

2.1.1 Routine maintenance of cell lines

All four ER+ human breast cancer cell lines, obtained from American Type Culture Collection (ATCC; Manassa, VA, USA), were grown *in vitro* in phenol-red RPMI medium supplemented with foetal calf serum (FCS; 5% in MCF-7 and T47D and 10% in BT474 and MDA-MB-361), penicillin-streptomycin (10 IU/ml to 10 µg/ml) and fungizone (2.5 µg/ml) in a 37°C/5% CO_2 incubator (NuAire NU-5510E incubator, Triplered, UK). The characteristics of each of the cell lines used are shown in Table 1. The cell medium was changed every 3 days until approximately 70% confluency was reached and subsequent passaging was required. Cell growth was assessed visually by a phase-contrast microscope (Inverso TC100 inverted microscope, Fisher Scientific, UK).

The cells were passaged by discarding the medium and replacing it with trypsin (0.05% w/v) and EDTA (0.02% w/v). The proteolytic enzyme trypsin detaches adherent cells from the flask and the chelating agent EDTA binds calcium and magnesium ions present in the medium that may potentially inhibit trypsin activity. Once the cells had completely detached from the flask (approximately 3 to 5 minutes in the 37°C/5% CO_2 incubator), they were transferred to a sterile universal tube and an equal volume of growth medium was added to neutralise the trypsin/EDTA solution. The cells were collected and the trypsin/EDTA was removed by centrifugation (Mistral 2000 centrifuge, Fisher Scientific, UK) at 1000 rpm for 5 minutes. The supernatant was discarded and the cell pellet was re-suspended in an appropriate volume of growth medium (between 5 and 10 ml) and mixed by gentle pipetting to dissociate cell clumps into single cells. A

proportion of the cell suspension was diluted in growth medium (1:10 dilution) and added to a new flask which was incubated at 37°C/5% CO_2 until required for experimentation or further passaging.

Table 1 Molecular classification of the human breast cancer cell models used in this project.

Cell Line	Classification	ER	PR	HER2	TP53	Source	Tumour Type
BT474	Luminal B	+	+	+	+	Primary breast tumour	Invasive ductal carcinoma
MDA-MB-361	Luminal B	+	-	+	-	Metastatic site: brain	Adenocarcinoma
MCF-7	Luminal A	+	+	-	+/-	Pleural effusion	Invasive ductal carcinoma
T47D	Luminal A	+	+	-	M	Pleural effusion	Invasive ductal carcinoma

ER: oestrogen receptor; PR: progesterone receptor; HER2: human epidermal growth factor receptor 2; TP53: tumour protein p53; M: mutant. Adapted from Neve et al.[288] and Holliday & Speirs[289].

2.1.2 Experimental cell culture

The cells were trypsinised and re-suspended in phenol-red-free RPMI medium (to remove the unwanted oestrogenic properties of phenol-red[290,291]) supplemented with 5% or 10% FCS or charcoal stripped FCS (sFCS) (dependent on the cell line), penicillin-streptomycin (10 IU/ml to 10 µg/ml), fungizone (2.5 µg/ml) and glutamine (4 mM). The cell suspension was dispersed in to single cells by passing through a 25G syringe and needle and the cell number of 100 µl of this solution was measured by an automatic cell counter (Scepter 2.0 automatic cell counter, Merck Millipore, UK) according to manufacturer's

instructions. Cells (0.5 x 10^6) were seeded onto 60 mm culture dishes and allowed to adhere overnight prior to the addition of antihormone treatments and the appropriate controls (E2 or untreated medium). Table 2 lists the treatments used throughout the study, their concentration and source. The cells were maintained at 37°C/5% CO_2 and the medium (± treatment) were renewed every 3 days. The cells were harvested following 10 day treatment (unless stated otherwise).

Table 2 Treatments used in this study, their concentration, diluent and source.

Treatment	Concentration	Diluent	Source
Oestradiol	10^{-9} M	Ethanol	AstraZeneca, UK
Tamoxifen	10^{-7} M	Ethanol	T5648, (Sigma-Aldrich, UK)
Fulvestrant	10^{-7} M	Ethanol	AstraZeneca, UK
Charcoal stripped FCS			In-house (see below)

2.1.3 Charcoal Stripped FCS (sFCS)

FCS was stripped of steroids to mimic the oestrogen depriving actions of aromatase inhibitor therapies. FCS was adjusted to pH 4.2 by the addition of 5 M HCl and allowed to equilibrate for 30 minutes at 4°C. A charcoal solution (11.1 % activated charcoal, 0.06 % dextran T 70 in distilled water) was prepared and stirred vigorously for 1 hour. To every 100 ml of FCS, 5 ml of charcoal solution was added and stirred gently at 4°C for 16 hours. To remove the charcoal, the solution was centrifuged (Labofuge 400R centrifuge, Heraeus, Germany) at 12,000 rpm for 40 minutes and the supernatant was coarse filtered through Whatman filter paper No. 4 several times. The solution was adjusted to pH 7.2 using 5 M NaOH and filter sterilised through a 0.2 µM Supor Vacucap membrane to remove any contaminating microorganisms. The sFCS was stored at -20°C.

2.1.4 Generation of resistant cell lines

In vitro cell models of acquired resistance to antihormones were previously generated by the Breast Cancer Molecular Pharmacology Group. The tamoxifen-resistant cell lines were developed by culturing MCF-7 and T47D cells in phenol-red-free RPMI supplemented with 5% sFCS, antibiotics (fungizone (2.5 µg/ml) and penicillin-streptomycin (10 IU/ml to 10 µg/ml)),

glutamine (4 mM) and tamoxifen (100 nM) for 6 months. Tamoxifen-resistant MCF-7 cells were denoted TAMR and the T47D cells denoted T47D TAMR. Likewise, the fulvestrant-resistant cell model (FASR) was generated by culturing MCF-7 cells in phenol-red-free RPMI plus 5% sFCS, antibiotics, glutamine (4 mM) and fulvestrant (100 nM) for 6 months[184]. The model of acquired resistance to severe oestrogen deprivation (denoted XR), was generated by the long term culture of MCF-7 cells in phenol-red-free RPMI supplemented with 5% heat inactivated (65°C for 30 minutes) sFCS, antibiotics and glutamine (4 mM)[292]. The medium was changed every 3-4 days and the cells were passaged when necessary by trypsinisation (section 2.1.1). Upon acquisition of resistance, as determined by the ability of these cells to grow in the presence of antihormone/severe oestrogen deprivation, with growth rates mirroring those observed in the wild-type parental cells, the resistant cells were cultured for several months to achieve a stable resistant phenotype prior to the commencement of any experimental work. These TAMR, T47D TAMR, FASR and XR cell models, developed by exposure to antihormones for 6 months are referred to as short-term resistant cell models throughout this thesis.

Long-term resistant cell models, derived from the four ER+ cell lines, were also generated by the Breast Cancer Molecular Pharmacology Group. TAMR and FASR cells were developed by culturing MCF-7, T47D, BT474 and MDA-MB-361 cells in phenol-red-free RPMI supplemented with FCS (5% for MCF-7 and T47D, 10% for BT474 and MDA-MB-361), antibiotics and glutamine (4 mM) plus tamoxifen (100 nM) or fulvestrant (100 nM), respectively for 3 years. XR cells were developed by culturing MCF-7, T47D and BT474 cells in phenol-red-free RPMI supplemented with heat inactivated (65°C for 30 minutes) sFCS (5% for MCF-7 and T47D, 10% for BT474), antibiotics and glutamine (4 mM) for 3 years. The medium was changed every 3-4 days and the cells were passaged when necessary by trypsinisation (section 2.1.1). Similarly to the short-term resistant cell models, the long-term resistant cells were cultured for several months to achieve a stable resistant phenotype prior to the commencement of any experimental work. These cell models are referred to long-term resistant cell models throughout this thesis.

2.2 Microarray gene expression

Prior to the commencement of this project, triplicate mRNA samples from MCF-7 cells treated with E2, tamoxifen, fulvestrant and oestrogen deprived conditions (and fulvestrant treated BT474, MDA-MB-361 and T47D), routinely prepared by the tissue culture staff of the breast cancer group, were microarrayed by Cardiff University Central Biotechnology Services (CBS) at Cardiff University. Additionally, the resistant cell models (with the exception of short-term T47D TAMR cells) and wild-type controls were also microarrayed. The analysis of the gene expression data generated during antihormone response and short-term resistance was the initial focus point of this project. The cell culture preparation and the microarray procedure are described below:

2.2.1 Cell lysis

MCF-7 cells were seeded at 3 x 10^6 cells per 150 mm diameter dish in phenol-red-free RPMI medium plus 5% sFCS and allowed to adhere for 24 hours prior to the addition of E2-control and antihormone treatments for 10 days. Similarly, the untreated control and the resistant cell models were grown in 150 mm dishes in phenol-red-free RPMI and 5% or 10% sFCS or FCS and supplemented with the respective treatments (section 2.1.4).

The cell medium was removed and the cells were washed with 10 ml of tissue culture grade PBS for 10 seconds. The PBS was removed and the wash was repeated two times. After the final wash, the PBS was thoroughly removed and 1.5 ml of Tri-Reagent (Sigma-Aldrich, UK) was rocked over the plate for 1 minute to ensure complete coverage of cells with reagent. The lysate was scraped using a disposable cell scraper, collected and divided equally in to two 1.5 ml micro-centrifuge tubes. The tubes were gently inverted twice and placed on dry ice. This was repeated for every sample. Once complete, the frozen tubes were stored at -80°C prior to RNA isolation.

2.2.2 RNA isolation

The cell lysates were removed from the -80°C freezer and thawed on ice. The volume of each sample was adjusted to 1 ml by addition of extra Tri-Reagent. The tubes were gently inverted and allowed to equilibrate to room temperature

for 5 minutes. Chloroform (200 µl) was added to the samples and mixed thoroughly by vortexing for 20 seconds and then left to stand at room temperature for 10 minutes. The tubes were spun at 16,000 g for 10 minutes in a precooled centrifuge (4°C; Labofuge 400R centrifuge, Heraeus, Germany). The samples separated in to three phases: the RNA is contained within the upper aqueous phase, the mid phase contains DNA and the lower phenolic phase contains protein. The upper RNA phase was carefully removed avoiding DNA contamination from the mid phase, and transferred to a clean micro-centrifuge tube. Room temperature isopropanol (500 µl) was added to the RNA to precipitate it. The samples were briefly vortexed and allowed to stand at room temperature for 10 minutes before spun again for 10 minutes at 16,000 g in a precooled centrifuge (4°C). The RNA pelleted at the base of the tube. The supernatant was carefully removed and 500 µl of 70% ethanol made up in sterile RNase/DNase-free water was added to wash the pellet and the tubes were spun again for 10 minutes in a precooled centrifuge (4°C) at 16,000 g. The ethanol was discarded and the tubes were inverted to drain away any excess ethanol. The pellet was air dried for 5 minutes before being re-suspended in 50 µl of RNase-free water.

2.2.3 RNA concentration and purity

The purity and concentration of the RNA was determined by spectrophotometry (Jenway 7315 spectrophotometer, Fisher Scientific, UK). The RNA was diluted 1/1000 in sterile water and the absorbance was measured at 260 nm and 280 nm wavelengths. The concentration was calculated as follows:

RNA concentration (µg/ml) = (absorbance at 260 nm) X (dilution factor i.e. 1000) X (extinction coefficient of single stranded RNA i.e. 40 µg/ml).

The purity of the RNA was calculated by the A260/A280 ratio. A ratio of between 1.8 and 2 (of the spectrophotometric readings at 260 nm and 280 nm) indicated that the RNA was pure.

2.2.4 Agarose gel electrophoresis

The integrity of each sample was assessed by gel electrophoresis. A 2% agarose gel was prepared in 1 X Tris-acetate-EDTA buffer (TAE; pH8) supplemented

with RedSafe nucleic acid stain (1:20,000; Chembio Ltd, UK). Once solidified the gel was placed in an electrophoretic tank (Gel unit MH-1510, Fischer, UK) and immersed in 1 X TAE buffer. The wells were loaded with 1 µg of RNA made up to 5 µl with sterile water and mixed with 5 µl of loading buffer (40% sucrose and 0.25% w/v bromophenol blue made up in sterile water and filter sterilised). The gel was run at 100V for 30 minutes and visualised on a UV transilluminator (G:BOX chemi XR5, Syngene, Fisher, UK) and analysed with GeneSys software (Syngene, Fisher, UK). Two strong clean bands representing the 18s and 28s ribosomal RNA confirmed that the RNA was pure and intact. This was evident for all RNA samples examined in this project. The RNA samples were stored at -80°C.

2.2.5 DNase treatment of isolated RNA

The isolated RNA from each sample was DNase treated to remove any genomic contamination. RNase-free DNase reagents provided with the Qiagen RNeasy Micro Kit were used for this protocol. In a sterile micro-centrifuge tube 45 µg of RNA adjusted to 87.5 µl by the addition of RNase-free water, 10 µl of kit buffer and 2.5 µl of kit DNase I solution were mixed and incubated at room temperature for 10 minutes. To each of the 100 µl RNA solutions, 350 µl of RLT buffer from the kit (supplemented with β-mercaptoethanol according to manufactures instructions) was added and mixed thoroughly before the addition of 250 µl 100% ethanol which was again mixed thoroughly. RNeasy MinElute spin columns were inserted into 2 ml kit collection tubes and the entire contents (700 µl) of each micro-centrifuge were transferred into the spin column. The lids were closed and the tubes were spun at 10,000 g for 15 seconds in a benchtop microcentrigue (Biofuge, Heraeus, Germany). The flow through was discarded and the membrane-bound RNA was washed by the addition of 700 µl of RW1 buffer to the column. The tubes were spun again for 15 seconds at 10,000 g and the flow through and collection tubes were discarded. The columns were placed into clean 2 ml collection tubes and 500 µl of RPE buffer was added to the column to wash the membrane-bound RNA again. The lids were closed and the tubes were spun for 15 seconds at 10,000 g. The flow through was discarded and 500 µl of 80% ethanol was added to the

columns before being spun for 2 minutes at 10,000 g. The flow through and collection tubes were discarded. The columns were placed in to clean 2 ml collection tubes and spun, with the lids open, for 5 minutes at 10,000 g to thoroughly dry the columns and remove any excess ethanol. The columns were transferred into sterile 1.5 ml micro-centrifuge tube and 14 µl of RNase-free sterile water was added to the centre of the column membrane. The lids were closed and the tubes were spun for 1 minute at 13,000 g to elute the RNA. The columns were discarded and the micro-centrifuge tubes containing 12 µl of eluted RNA were placed on ice. The RNA concentration and integrity were determined (as described 2.2.3 and 2.2.4) and the samples were aliquoted and stored at -80°C.

2.2.6 Affymetrix microarray

Triplicate RNA preparations of 10 day control and antihormone-treated cells and resistant cell models (with the exception of short-term resistant T47D TAMR cells) were sent to CBS. Initially, the quality of the RNA was assessed to ensure no contamination or degradation and once considered suitable these samples were ran on Affymetrix Human Genome U133Aplus2 gene chips (containing approximately 23,000 gene probes representing approximately 14,500 genes) following standard Affymetrix procedures. Briefly, the RNA was reverse transcribed and the resulting complimentary (c)DNA underwent an *in vitro* transcription reaction with the incorporation of a biotin label which was then hybridised to the gene chip (as shown in Figure 5). The gene chip was then stained with a fluorescent molecule that binds biotin and scanned to determine the relative expression levels of all genes. The Affymetrix Microarray Suite 5.0 software determined and subtracted background and non-specific hybridisation, in addition to generating appropriate output files for uploading onto the online bioinformatics software GeneSifter (https://login.genesifter.net/).

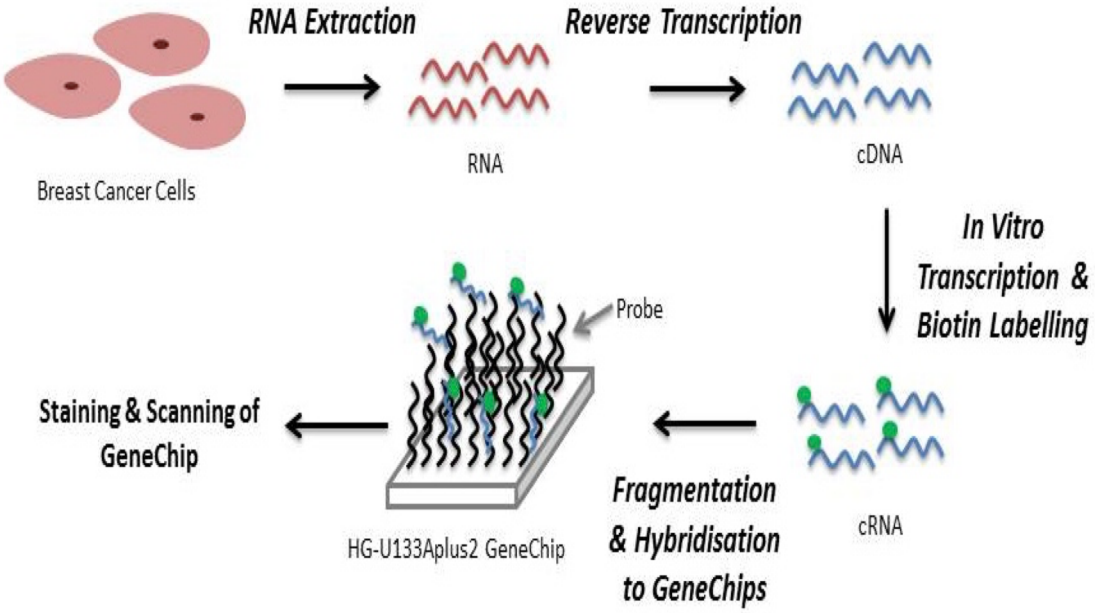

Figure 5 Diagram of Affymetrix microarray procedure. RNA extracted from cells was reverse transcribed and the resulting complimentary (c)DNA underwent *an vitro* transcription (back to RNA known as cRNA) with the incorporation of a biotin label. The labelled sample was hybridised to Human Genome (HG)-U133Aplus2 gene chips which contain approximately 23,000 gene probes. The gene chip was then stained and scanned to determine the expression level of genes.

2.2.7 GeneSifter analysis of microarray data

Triplicate raw data uploaded to GeneSifter was first log transformed and median normalised prior to analysis. Initial array analysis was performed on MCF-7 cells treated for 10 days with tamoxifen, fulvestrant and oestrogen deprivation. This project interrogated this GeneSifter-assembled array resource to identify up regulated expression of a pre-defined list of pro-survival genes (n=248; assembled using ontology and website resources; Appendix Table 15) with antihormone treatment versus E2-treated control. Heatmaps and log2 intensity plots generated by GeneSifter were utilised to visualise the level of gene expression. In the majority of cases, the Affymetrix gene chip contained more than one probe for each gene. All of the available probes for the genes of interest were analysed to determine whether a consistent profile was achieved across all probes for a given gene, providing further confidence that any antihormone-induced change in expression was robust. Particular importance

was placed on the 'jetset' probe for each gene of interest. The 'jetset' probe characterises the optimal probe to represent a gene that is detected by multiple probes which may deliver inconsistent or even contradictory measurements. Jetset in an online tool created by the Technical University of Denmark and gives each Affymetrix probe a score based on three factors: i) specificity of the probe to the target gene, ii) ability of the probe to detect as many splice isoforms of the target gene as possible to estimate the overall gene expression and iii) probe targeting the gene at a position near the 3' end of the corresponding transcript, as it has been shown that probes too far from the 3' end are likely to have a reduced signal intensity and are susceptible to false signal changes[293]. Together, each probe is scored according to specificity, coverage and robustness against transcript degradation. The probe with the highest overall score for a given gene represents the optimal probe and is termed the 'jetset' probe.

GeneSifter also generates detection call results for each gene. These detection call algorithms indicate whether the expression of a transcript is reliably measured, reduces the number of false positive findings, thus providing further confidence that a change in gene expression is robust[294]. An 'absent' detection call indicated unreliable detection of gene expression, a 'marginal' call represented partial detection of expression and a 'present' detection call signified reliable detection of gene expression. These detection calls were utilised to remove data that was not reliably detected before further analysis. Specifically, probes with a 'marginal' or 'present' detection call in at least one antihormone treatment were selected. Next, the microarray profiles of these genes of interest were examined in MCF-7 short-term antihormone-resistant models. Again, expression of probes with a 'marginal' or 'present' detection call maintained from antihormone-response into the appropriate resistance setting were selected (e.g. 'marginal'/'present' call in tamoxifen-treated MCF-7 cells and in the TAMR cells). The genes of interest filtered based on common profile and detection calls underwent further analysis to identify the most robustly up regulated genes. This included ANOVA with Tukey post-hoc testing to identify significant ($p < 0.05$) genes, in additional to examination of the fold change in

gene expression to identify gene probes up regulated by greater than 1.5 fold change in at least one antihormone treatment.

2.3 Ontological investigation of the genes of interest identified by microarray analysis

Ontological studies were performed on the genes of interest identified by microarray analysis to aid prioritisation of these genes for further investigation. Specifically, the multiple names/aliases of the genes of interest (obtained from GeneCards (http://www.genecards.org/)) along with several key words (e.g. 'breast cancer' 'cancer' 'antihormone' 'resistance' 'survival') were searched in PubMed (http://www.ncbi.nlm.nih.gov/pubmed) to identify any reported associations with cancer, antihormone-response and –resistance in the literature. For one gene in particular, the ontological studies revealed genes/proteins essential for/implicated in its function (e.g. genes involved in the synthesis of the ligand where the gene of interest was a receptor) and subsequently, heatmaps and log2 profiles were generated to examine the profile of such genes in our cell models.

2.4 Reverse transcription–PCR verification of the genes of interest identified by microarray analysis

Following the identification by microarray and ontological analysis of pro-survival genes significantly induced by 10 day antihormone treatment with significant induction maintained in to antihormone-resistance, reverse transcription (RT) and subsequent PCR was performed to verify this data and to determine the high priority/expressing genes. Independent triplicate MCF-7 cells treated for 10 days with antihormones and the short-term MCF-7 TAMR and XR cells were prepared, lysed and the RNA was isolated equivalent to the microarray samples (as described in sections 2.2.1-2.2.4). RT-PCR was performed on these samples to verify the microarray profile. RT-PCR was also performed on additional ER+ cell lines (T47D, BT474 and MDA-MB-361) treated for 10 days with antihormones and the T47D-TAMR short-term resistant cell line to determine whether the increase in expression of the genes of interest was evident for more than one cell line to consider the heterogeneity of breast cancer.

2.4.1 RT

RT is the synthesis of complementary DNA (cDNA) from a RNA template. The cDNA generated is necessary for PCR amplification. A mastermix solution was prepared with the following reagents: 10 µl of deoxynucleotide triphosphates (dNTPs; 2.5 mM, Invitrogen, UK) consisting of all four bases: dATP, dTTP, dGTP and dCTP, 4 µl 5 X RT buffer (Tetro reverse transcriptase kit, Bioline Ltd, UK) and 2 µl of random hexamers (100 µM, Fisher Scientific, UK) which contain short single stranded random hexanucleotides that act as primers for DNA synthesis. The volumes described are for one RNA sample.

To the 11.5 µl of mastermix solution, 1 µg of RNA in 7.5 µl of sterile water was added. This reaction mix was denatured at 95°C for 5 minutes (Prime V Techne thermal cycler, Fisher Scientific, UK) and then cooled rapidly on ice for 5 minutes. The sample was pulse spun in a microcentrifuge (Heraeus Fresco 17 microcentrifuge, Thermo Scientific, UK) and returned back to the ice. The reverse transcriptase enzyme MMLV (1 µl; Tetro reverse transcriptase kit, Bioline Ltd, UK) and an RNAse inhibitor (0.5 µ; RiboSafe RNase inhibitor, Bioline Ltd, UK) were added to give a final volume of 20 µl. The sample was reverse transcribed in the thermal cycler using the following parameters:

1. Annealing: 22°C for 10 minutes
2. RT extension: 42°C for 40 minutes
3. Denaturing: 95°C for 5 minutes

The cDNA samples generated were stored at -20°C until required.

2.4.2 PCR

PCR is a technique used to amplify a specific region of DNA that lies between two regions of known DNA sequence. A pair of short DNA fragments known as oligonucleotide primers are synthesised to be complementary to the DNA sequences on both strands of the DNA, flanking the target sequence/region that is to be amplified. In the presence of dNTPs (comprising the four bases dATP, dTTP, dGTP and dCTP), the thermal stable DNA polymerase, Taq, synthesises a new strand of DNA from the end of one primer using the target sequence as a template. The reaction involves repeated cycles of heat denaturation to separate

the double stranded DNA, followed by cooling to allow annealing of the primers to their complementary sequences and extension of the annealed primers with the DNA polymerase. DNA synthesis proceeds across the target region, between the two primers. The products formed from the first cycle of the reaction serve as DNA templates for subsequent cycles. Thus, with each cycle, the amount of DNA synthesised doubles to that of the previous cycle, resulting in exponential accumulation of the PCR product.

2.4.3 Primer Design

The oligonucleotide primers used were designed using ThermoFisher Scientific OligoPerfect™Designer (https://tools.thermofisher.com/content.cfm?pageid=9716_&icid=fr-oligo-6?CID=fl-oligoperfect) using gene sequences obtained from the National Center for Biotechnology Information (NCBI) database (http://www.ncbi.nlm.nih.gov/nuccore) for the genes of interest. From these sequences, the OligoPerfect™ Designer identified potential primer pairs and also allowed consideration of product size, melting temperature and percentage of guanine and cytosine bases which is indicative of the formation of undesirable primer-dimer formation. Once selected, the primer pairs were inputted into the online programme Basic Local Alignment Search Tool (BLAST; http://blast.ncbi.nlm.nih.gov/). BLAST compares nucleotide sequences across the human genome and identifies regions of similarity between sequences. The primer sequences used within this project were inputted into BLAST to ensure that they were specific to the gene of interest.

Table 3 Oligonucleotide sequences, product size, optimised cycle number and annealing temperature.

Gene	Forward Primer Sequence (5'→3')	Reverse Primer Sequence (5'→3')	Product Size (bp)	Cycle Number	Annealing Temperature (°C)
β-Actin	GGAGCAATGATCTTGATCTT	CCTTCCTGGGCATGGAGTCCT	202	25	55
BAG1	GCTCCTATCTGTTTTCTCCT	CCTTCTCTTTGCCCTTCCT	570	36	60
BCL2L1	GCTATGATCCTGTCCCTCCA	TGGCTTCTCACTGGTCTCCT	340	38	60
BCL3	CTGGCTGTGATCACCACATT	TCGTTGTGGCAGTTCTTGAG	497	30	55
CLU	CGACTCACCCACAGACAAGA	GAGTCACCTGAGCCTGGAAG	298	36	57
CLU*	ACAGGGTGCCGCTGACC	TTCAGGCAGGGCTTACACTCT	400		55
CXCR4	TTCTACCCCAAT GACTTGTG	ATGTAGTAAGGC AGCCAACA	206	39	55
CTNND2	TGGCACCCATCAATAGTCAA	AATCACTTGGTGCAGTGTGC	390	34	55
DDAH2	GATCTGGCCAAAGCTCAAAG	TCGCGTTCTCGTCTCCTATT	259	30	55
ERC1	ACAGCTCTCAGCAGCTACAG	CTGCTGTACCAGACGATCCT	445	36	55
GABBR2	ACAACAGAGCCCTCTCGAAC	GAGACCATGACTCGGAAGGA	180	39	58
HBXIP	GCAGCACTTGGAAGACACAA	GTGATGCCATCGTGTTTCTG	231	36	55
IGFBP5	CCCTTTATCCCTGCACTCTC	GGCTTCTCCTCGTCCTGCCG	330	40	55
PSEN1	TGAGTTGGGGAAAAGTGAC	CATAAGAAGAACAGGGTGG	316	40	57
TSC22D3	CCCTGACAAGAGCAGGTCTC	GCCTTCACGAAACAGAGGAG	301	34	55

bp: base pairs. *CLU primer sequence designed according to Prochnow et al.[295].

2.4.4 PCR Procedure

All reagents and samples were kept on ice. A mastermix was prepared in a sterile eppendorf tube using the following reagents:

- 18 µl sterile RNA/DNAse free water
- 2.5 µl PCR 10 X NH_4 buffer (BIOTAQ DNA polymerase kit, Bioline Ltd, UK)
- 0.75 µl $MgCl_2$ (50 mM; BIOTAQ DNA polymerase kit, Bioline Ltd, UK)
- 2 µl dNTPs (2.5 mM)
- 0.625 µl of each primer of gene of interest (20 µM; Invitrogen, ThermoFisher Scientific, UK)
- 0.2 µl TAQ DNA polymerase (5 units/µl; BIOTAQ DNA polymerase kit, Bioline Ltd, UK).

The volumes described are per individual cDNA sample. The mastermix was thoroughly mixed and 0.5 µl (equal to 0.05 µg RNA) of cDNA was added to give a final volume of 25 µl. A drop of mineral oil was added on top of each sample to prevent evaporation during the PCR reaction. The sample was amplified in a thermal cycler using the parameters shown in Table 4. The PCR products (10 µl) were mixed with 5 µl of loading buffer and loaded on to a 2% agarose gel for visualisation (as detailed in 2.2.4). A DNA marker (5 µl, 100 bp DNA ladder, Fisher, UK) was mixed with 5 µl loading buffer and loaded alongside the samples to allow the product size to be determined. To ensure equal loading on such gels and to allow for normalisation, the housekeeping gene β-actin was amplified in parallel following the same parameters shown in Table 4 for 25 cycles. The gel was visualised on a UV transilluminator (G:BOX). Densitometry analysis was performed using GeneSys software. Raw densitometry values were normalised to β-actin loading control.

Table 4 Polymerase chain reaction programme. Shown is the standard PCR programme.

Stage	Number of Cycles	Temperature (°C)	Duration (seconds)
1	1	Denaturing: 95	120
		Annealing: 55	60
		Extension: 72	300
2	25-39	Denaturing: 94	30
		Annealing: 55-60*	60
		Extension: 72	60
3	1	Denaturing: 94	60
		Annealing: 55	60
		Extension: 60	300
		Finish: 4	∞

***The number of cycles and annealing temperature were optimised for each gene of interest.**

2.5 Sodium dodceyl sulphate-polyacrylamide gel electrophoresis and Western blotting to verify the genes of interest identified by microarray analysis

Following the initial identification by microarray analysis and subsequent RT-PCR verification of pro-survival genes significantly induced by 10 day antihormone treatment with induction maintained in to antihormone-resistance, sodium dodecyl sulphate-polyacrylamide gel electrophoresis (SDS-PAGE) and Western blotting was performed to confirm expression of these genes at the protein level. This was important to ensure that the mRNA of target proteins was translated in to protein to perform its function.

Western blot is a method used to identify and analyse specific proteins within a complex protein mixture, such as cell lysate. Briefly, proteins are denatured and

separated according to their molecular weight by gel electrophoresis. The proteins are then transferred to a nitrocellulose membrane which is incubated with primary antibodies specific to the protein of interest. The unbound antibody is washed off, and the membrane is probed with a horseradish peroxidase (HRP)-labelled secondary antibody which binds to the already bound primary antibody. The unbound antibody is washed off and the specific protein of interest is detected on the membrane. The membrane is incubated with an enhanced chemiluminiescent (ECL) substrate which reacts with the HRP bound to the secondary antibody and subsequently produces a signal. The signal produced represents the protein of interest and the thickness of the band corresponds to the amount of protein present.

2.5.1 Protein isolation

MCF-7, T47D, BT474 and MDA-MB-361 cells (0.5 x 10^6) were seeded onto 60 mm dishes and treated with antihormones for 10 days as described in section 2.1.2. Similarly, the resistant cell models and wild type control were seeded onto 60 mm dishes.

The cell medium was removed and the cells were washed with 2 ml of tissue culture grade PBS. The PBS was removed and the wash was repeated two times. After the final wash, the PBS was removed by aspiration and 250 µl of ice cold lysis buffer (50 mM Trizma base, 150 mM NaCl, 5 mM EGTA and 1% v/v TritonX 100, distilled water, pH 7.6) supplemented with a protease and phosphatase inhibitors (HALT protease and phosphatase inhibitor cocktail (100X), ThermoFisher Scientific, UK) was added to each cell dish. The dishes were incubated on ice and the cell lysates were collected using a disposable cell scraper and then transferred into a 1.5 ml microcentrifuge tubes. The tubes were spun at 14,000 x g for 15 minutes at 4°C. The supernatant was aliquoted and stored at -20°C until required.

2.5.2 Protein isolation of nuclear and cytoplasmic cell fractions

Antihormone-resistant and wild type control cells were grown in 60 mm dishes. The cell medium was removed, the dishes were placed on ice and the cells were washed two times with tissue culture grade PBS. After the final wash, 200 µl of

PBS was added to the cells and they were collected using a disposable cell scraper and then transferred into a 1.5 ml microcentrifuge tubes. The tubes were centrifuged at 1000 rpm for 5 minutes at 4°C. The pellet was re-suspended in 5 pellet volumes of cytoplasmic extract buffer (10 mM HEPES, 60 mM KCl, 1 mM EDTA, 1 mM phenylmethylsulfonyl fluoride (PMSF; ThermoFisher Scientific, UK) and 1 mM DTT, distilled water, pH 7.6) supplemented with NP40 (0.075%) and incubated on ice for 5 minutes. The tubes were centrifuged again at 1000 rpm for 5 minutes at 4°C and the supernatant containing the cytoplasmic fraction was added to a fresh eppendorf tube and kept on ice. Cytoplasmic extract buffer (100 µl) without NP40 was added to the pellet which contained the cell nuclei, and mixed gently by pipetting prior to centrifugation at 1000 rpm for 5 minutes at 4°C. The supernatant was discarded and the pellet was re-suspended in 2 pellet volumes of nuclear extract buffer (20 mM Tris-HCl, 420 mM NaCl, 1.5 mM $MgCl_2$, 0.2 mM EDTA, 1 mM PMSF, 1 mM DTT and 25% v/v glycerol, distilled water, pH 8) and incubated on ice for 10 minutes with intermittent vortexing to disperse the pellet. The cytoplasmic and nuclear extract were centrifuged at 14,000 rpm for 10 minutes at 4°C. The supernatants were transferred to fresh eppendorf tubes and stored at -20°C until required for SDS-PAGE and Western blotting.

2.5.3 Protein assay

A protein assay adapted from the Bradford assay was used to determine the protein concentration of each cell lysate. A standard curve of known concentrations (0, 5, 10, 15, 20 and 25 µg/ml) of bovine serum albumin (BSA) diluted in distilled H_20 were prepared in 1.5 ml microcentrifuge tubes. The cell lysates of unknown protein concentration were diluted in distilled H_2O (1/200). Bio-Rad Dye Concentrate (100 µl; Bio-Rad Laboratories Ltd, UK) was added to 400 µl of the standard and test samples. The reaction mixtures were vortexed and left to stand for 10 minutes before being transferred in triplicate (3 x 130 µl) to a 96 well plate. The absorbance was measured at 595 nm (OD_{595}) in a plate reader (Multiscan EX 355, Thermo Scientific, UK). A standard curve of the known protein concentrations was generated and the concentration of the cell lysate samples was calculated from this.

2.5.4 Protein sample preparation

Prior to separation by electrophoresis, the proteins were first denatured. Proteins (20 µg) were diluted in an equal volume (1:1) of 2 X Lamelli sample loading buffer (4% w/v SDS, 20 % v/v glycerol, 120 mM TRIS pH 6.8, 1.54 % w/v DTT, 0.01% w/v bromophenol blue and distilled water) and heated at 95°C for 5 minutes. SDS is an anionic detergent which causes complex secondary, tertiary and quaternary proteins to be denatured in addition to applying a negative charge to the proteins in proportion to their mass. Consequently, when an electrical field is applied each protein will migrate towards the anode. DTT further denatures the proteins by reducing the disulphide bonds. Glycerol increases the density of each sample making it easier to load in to the wells and bromophenol blue is a coloured tracking dye which allows the migration of the proteins through the polyacrylamide gel during electrophoresis to be visualised.

2.5.5 SDS-PAGE

SDS-PAGE is a method used to separate proteins according to their size. All SDS-PAGE gels were prepared in a gel casting apparatus (Bio-Rad Laboratories Ltd, UK). SDS-PAGE uses two polyacrylamide gels: a resolving gel and a stacking gel. The resolving gel is basic (pH 8.8) and has a higher percentage of acrylamide, thus making the pores in the gel smaller and consequently proteins are separated based on their size as the smaller proteins travel more easily and rapidly through the gel. The percentage of acrylamide in the resolving gel is dependent on the molecular weight of the protein of interest; as the percentage of acrylamide increases, the pore size decreases and consequently smaller proteins are resolved better. The upper stacking gel is acidic (pH 6.8) with a lower percentage of acrylamide and consequently larger pores, and functions to allow the proteins to stack in to one band at the interface between the two gels allowing proteins to migrate in to the resolving gel at the same time.

2.5.6 Polyacrylamide gel preparation

A resolving gel between 7.5% and 15% acrylamide was prepared to separate proteins between 8 and 200 kDa. Once prepared (Table 5), the gel was poured and 100 µl of isopropanol was added on top to remove any air bubbles and to level the surface. Once set, the isopropanol was poured off and the stacking gel

(Table 5) was prepared and added on top of the resolving gel. A 10 well comb was inserted into the stacking gel and the gel was left to set for 20 minutes.

Table 5 Components of the polyacrylamide resolving and stacking gels.

Component	7.5% Resolving gel	10% Resolving gel	15% Resolving gel	4% Stacking gel
Molecular weight of protein	40-200 kDa	20-100 kDa	8-50 kDa	
dH_2O	4.8 ml	4 ml	2.3 ml	6.1 ml
30 % Acrylamide	2.5 ml	3.3 ml	5 ml	1.3 ml
1.5 M TRIS pH 8.8	2.5 ml	2.5 ml	2.5 ml	
0.5 M TRIS pH 6.8				2.5 ml
10% SDS	100 µl	100 µl	100 µl	100 µl
10% APS	100 µl	100 µl	100 µl	50 µl
TEMED	6 µl	6 µl	6 µl	10 µl

SDS: sodium dodecyl sulphate; APS: ammonium persulphate; TEMED: tetramethylethylenediamine. Percentages are w/v.

2.5.7 Gel electrophoresis

The comb was removed and the gel was placed into an electrophoresis tank (Mini-PROTEAN, Bio-Rad Laboratories, UK) and submerged in running buffer (25 mM TRIS Base, 192 mM Glycine, 0.1% w/v SDS, pH 8.3). Protein molecular weight marker (3 µl; Spectra multicolour broad range protein ladder, ThermoFisher Scientific, UK) was loaded into the first well of each gel and 20 µg of prepared protein sample (section 2.5.4) was loaded into the remaining wells. An electrical field was applied to the gel causing the negative charged proteins to migrate towards the anode. The gel was run for approximately 45 minutes at 180V or until the dye front had reached the bottom of the gel.

2.5.8 Transfer of proteins to nitrocellulose membrane

Once separated, the proteins were transferred on to a nitrocellulose membrane. The gel was carefully removed from the glass plates, the stacking gel was discarded and the resolving gel was placed into a transfer cassette. The cassette was composed of foam pads, filter paper and membrane which had all been pre-soaked in transfer buffer (25 mM TRIS Base, 192 mM Glycine, 20% v/v methanol, pH 8). The cassette was placed into a wet electroblotting tank (Mini-PROTEAN, Bio-Rad Laboratories, UK) with the membrane located between the gel and positive electrode, thus when an electrical field is applied the negative charged proteins transfer from the gel to the membrane, as shown in Figure 6. An ice block was added to the tank which was filled with transfer buffer. The proteins were transferred for 1 hour at 100V. Once transferred, the membrane was removed from the cassette and submerged in 0.1 % w/v Ponceau S (made up in 5 % v/v acetic acid in distilled water) stain to visualise the protein bands, ensure efficient transfer and equal protein loading. The Ponceau S was washed off with tris buffered saline (TBS)-Tween (0.05 % v/v) comprised of Trizma base (10 mM), NaCl (100mM) and Tween 20 (0.05 % v/v) and the membrane was blocked in 5% non-fat dried milk (Marvel) in TBS-Tween (0.05 % v/v) for 1 hour with agitation at room temperature. Blocking prevents antibodies from binding non-specifically to the membrane.

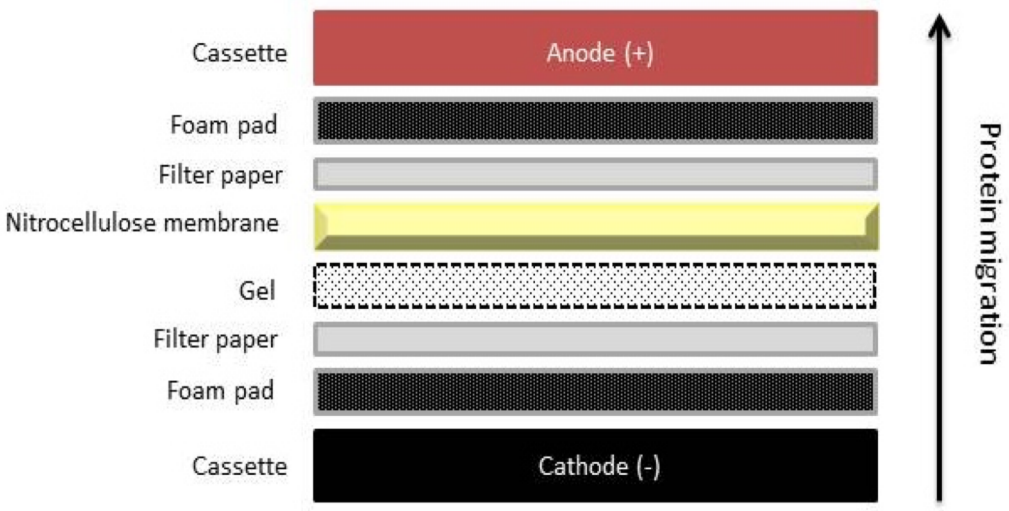

Figure 6 Assembly of Western blot transfer apparatus. The membrane is placed between the gel and the positive anode to allow the negative charged proteins to transfer from the gel to the membrane towards the anode as indicated.

2.5.9 Incubation with antibodies

The membrane was removed from the blocking solution and incubated in 5 ml of primary antibody (Table 6) (diluted in 1% Marvel/TBS-Tween) overnight at room temperature on a roller mixer. The membrane was washed in TBS-Tween (3 X 5 minutes) to remove any unbound antibody before being incubated in 5 ml of horseradish peroxidase (HRP)-conjugated secondary antibody (Table 6) (diluted in 1% Marvel/TBS-Tween) for 1 hour at room temperature on a roller mixer (MX-T6-S, Camlab, UK). The membrane was washed in TBS-Tween (5 X 5 minutes) to remove any unbound antibody before protein detection.

Table 6 Primary antibodies used for Western blotting along with their corresponding dilution, source, product number, host species, secondary antibody and predicted molecular weight.

Target	Dilution	Species	Product Number	Source	Secondary Antibody	Protein Size
BCL3	1:1000	Rabbit (pAb)	sc-185	SCBT	HRP-conjugated anti-Rabbit diluted 1:5000	60 kDa
CLU	1:1000	Mouse	sc-5289	SCBT	HRP-conjugated anti-Mouse diluted 1:10000	70 kDa & 40 kDa
GABBR2	1:1000	Rabbit (mAb)	ab75838	Abcam	HRP-conjugated anti-Rabbit diluted 1:5000	106 kDa *
GILZ/ TSC22D3	1:1000	Mouse (mAb)	sc-133215	SCBT	HRP-conjugated anti-Mouse diluted 1:10000	18 kDa
GRB2¶	1:1000	Mouse		SCBT	HRP-conjugated anti-Mouse diluted 1:10000	30 kDa
p50	1:1000	Rabbit (pAb)	sc-7178	SCBT	HRP-conjugated anti-Rabbit diluted 1:5000	50 kDa & 100 kDa
p52	1:1000	Rabbit (pAb)	sc-298	SCBT	HRP-conjugated anti-Rabbit diluted 1:5000	52 kDa & 100 kDa
p105/ p50	1:1000	Mouse (mAb)	NBP2-22178	NB	HRP-conjugated anti-Mouse diluted 1:10000	50 kDa & 100 kDa

Target	Dilution	Species	Product Number	Source	Secondary Antibody	Protein Size
SP-1¶	1:1000	Rabbit		SCBT	HRP-conjugated anti-Rabbit diluted 1:5000	100 kDa
β-actin	1:2000	Rabbit (mAb)	A5060	Sigma-Aldrich, UK	HRP-conjugated anti-Rabbit diluted 1:5000	40 kDA
δ-catenin	1:1000	Mouse (mAb)	sc-81793	SCBT	HRP-conjugated anti-Mouse diluted 1:10000	133 kDa

SCBT: Santa Cruz Biotechnology, Inc. NB: Novus Biologicals, UK, pAb: Polyclonal antibody, mAb: Monoclonal antibody, HRP: Horseradish peroxidase. *GABBR2 predicted molecular weight is 106 kDa, but the observed protein weight in this project is 80 kDa supporting the findings from Kuriyama et al.[296]. ¶ Kindly provided by Dr Glorianne Lazaro, School of Pharmacy and Pharmaceutical Sciences, Cardiff University.

2.5.10 Protein detection

The appropriate ECL reagent (100 µl; SuperSignal West Dura or SuperSignal West Femto chemiluminescent detection reagent, ThermoFisher Scientific, UK) was applied to the membrane following the manufactures instructions, before being placed into the G:BOX for detection. Densitometry analysis was performed using GeneSys software. Raw densitometry values were normalised to β-actin loading control.

2.6 Functional studies of high priority genes

2.6.1 siRNA transfection

siRNA is a sequence-specific, short double-stranded RNA able to destruct complementary mRNA, to induce knockdown of target gene expression. siRNA is transported into the cell via lipid carriers and once in the cytoplasm, the siRNA is incorporated into a protein complex called RNA-induced silencing complex (RISC) as shown in Figure 7[297]. Subsequently, RISC unwinds the double-stranded siRNA and cleaves the sense strand to generate an activated RISC complex containing the antisense strand of the siRNA[298]. The antisense strand directs the RISC to complementary mRNA and once bound, the antisense-RISC complex cleaves the target mRNA resulting in gene silencing[299]. The activated RISC-siRNA complex is then recycled for continued destruction of identical mRNA targets to further propagate gene silencing[300]. However, this gene silencing is transient, only lasting approximately 4 days in rapidly dividing cells. siRNA becomes diluted due to cell division and thus requires repeated administration to achieve a persistent knockdown effect[301].

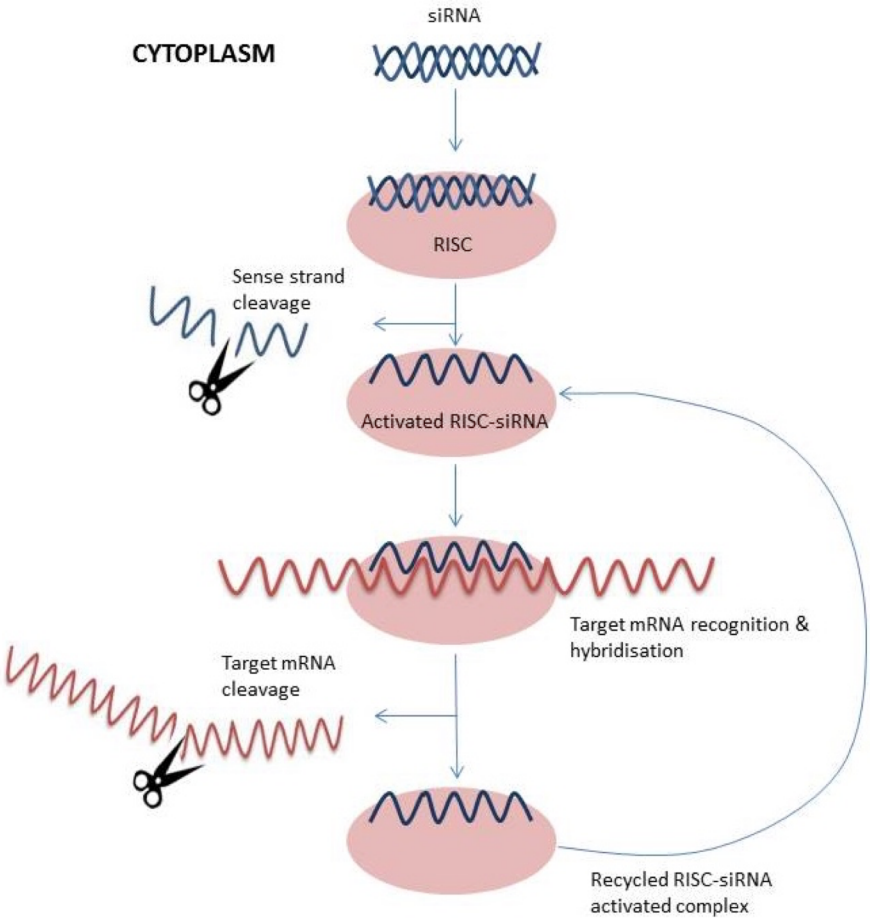

Figure 7 Mechanism of siRNA-mediated gene silencing. Once in the cytoplasm, double stranded small interfering RNA (siRNA) is incorporated into the RNA-induced silencing complex (RISC). The sense strand is cleaved, resulting in an activated RISC-siRNA complex containing the antisense strand. The activated RISC complex seeks out, binds to and cleaves the complementary RNA, leading to the knockdown of the target gene. The activated RISC complex is then recycled for continued destruction of identical mRNA targets. Adapted from Whitehead et al.[457].

In vitro siRNA transfection was utilised in this study to transiently suppress the high priority genes BCL3 and CLU to allow investigation of cell growth, cell cycle distribution and apoptosis to determine whether such knockdown promoted the survival of antihormone-responsive and –resistant cells and ultimately contributed to the development of resistance. Cells were seeded into 60 mm dishes (3×10^5 cells) in experimental media (see section 2.1.2) and grown until approximately 60% confluency was reached before being transferred into antibiotic-free experimental medium for 1 hour prior to siRNA transfection. Transfections were performed according to the manufacturer's instructions

(Dharmacon RNA Technologies, Lafayette, CO, USA). siRNA (Table 7) were diluted to a working stock concentration of 20 µM in sterile Dharmacon RNase free 1 x siRNA buffer. The siRNA were then mixed with DharmaFECT 1 transfection reagent (Dharmacon, GE Healthcare, UK) at a ratio of 20 µl siRNA: 1 µl transfection reagent and incubated at room temperature for 20 minutes, allowing the formation of siRNA-containing micelles. The cell medium was discarded and replaced with fresh antibiotic-free experimental medium to which the siRNA transfection reagent mix was added to give a final siRNA concentration of 100 nM per dish. Control experiments comprised of medium only, DharmaFECT 1 transfection reagent only and transfection with a non-targeting scrambled control siRNA (100 nM per dish). Cells were incubated for 4 days prior (unless stated otherwise) to RNA and protein lysis for subsequent RT-PCR and Western blot analysis (as described in sections 2.2, 2.4 and 2.5). Fulvestrant (100 nM) was added to MCF-7 and T47D cells 48 hours post siRNA transfection for the remaining 2 day incubation period.

Table 7 Target siRNA, source and product number.

Target siRNA	Source	Product Number
ON-TARGETplus Human BCL3	Dharmacon, GE Healthcare, UK	L-003874-00-0020
ON-TARGETplus Human CLU	Dharmacon, GE Healthcare, UK	L-019513-00-0010
ON-TARGETplus Non-targeting (control)	Dharmacon, GE Healthcare, UK	D-001810-10-20

2.6.2 Flow cytometry

Flow cytometry is a laser-based technique that allows rapid analysis of multiple characteristics of single cells, including cell size, DNA or RNA content and a wide range of membrane-bound and intracellular proteins. Briefly, a cell suspension (containing fluorochrome-labelled target proteins) is injected into the flow cell and drawn into a stream of single cells created by the surrounding sheath of isotonic fluid (as shown in Figure 8). Upon arrival at the interrogation point, a laser beam intersects each cell individually. Scattered laser light and fluorescent emissions are collected by several detectors. The forward scatter channel collects light scattered in a forward direction and is indicative of cell size and the side scatter light, detected by the side scatter channel, relates to the internal structure (granularity) of the cell. Fluorescent emissions (of known wavelength from excited fluorochromes) are directed through a series of filters according to their wavelength towards the appropriate detector. The detectors generate an electrical signal that is sent to the computer for analysis.

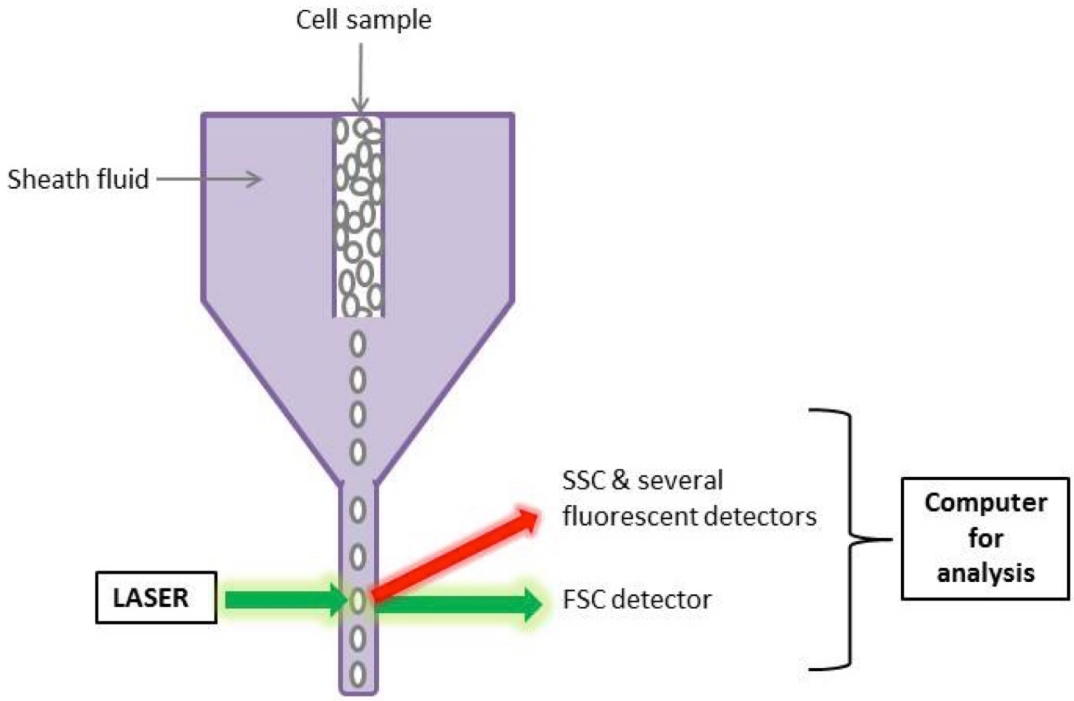

Figure 8 Flow cytometer. Cells injected into the flow cell are hydrodynamically focussed by the surrounding sheath fluid to generate a stream of single cells. The laser beam interrogates each cell individually and a series of detectors collect the scattered light and fluorescence emissions to generate an electrical signal which is sent to the computer for analysis. FSC; forward scatter channel, SSC: side scatter channel.

2.6.2.1 Apoptosis assay

An Annexin V-FITC and propidium iodide (PI) apoptosis detection kit (eBioscience Ltd, UK) was used to examine apoptosis. Briefly, upon the acquisition of apoptosis, cells lose membrane phospholipid asymmetry and phosphatidylserine (PS) is translocated from the inner to the outer surface of the plasma membrane. Annexin V is a calcium-dependent phospholipid-binding protein that has a high affinity for PS. Thus, annexin V labelled with a fluorochrome (e.g. FITC) binds PS exposed on the outer surface of the plasma membrane which can be detected by flow cytometry. Counterstaining with the nucleic acid binding dye PI allows the discrimination of early apoptotic and late apoptotic/dead cells. PI is impermeant to viable cells, however during late stage apoptosis the loss of membrane integrity allows the uptake of PI which binds to the nucleic acids and stains dead cells with red fluorescence which is detected by flow cytometry.

The adherent cells were collected by trypsinisation (see section 2.1.1) and combined with the non-adherent cells present in the medium prior to centrifugation for 5 minutes at 1000 rpm. The cell pellet (containing approximately 5 x 10^5 cells) was re-suspended in 1 ml of binding buffer (Annexin V-FITC apoptosis detection kit, eBioscience Ltd, UK) and passed through a 25G needle and syringe to ensure a single cell suspension. The cells were centrifuged for 5 minutes at 1000 rpm prior to a second wash in binding buffer to remove any residual trypsin that may inhibit annexin V staining. The cell pellet was re-suspended in 200 µl of binding buffer. Annexin V-FITC (5 µl; Annexin V-FITC apoptosis detection kit, eBioscience Ltd, UK) was added to 185 µl of the cell suspension and incubated for 10 minutes at room temperature prior to the addition of 10 µl of PI (20 µg/ml; Annexin V-FITC apoptosis detection kit, eBioscience Ltd, UK). The samples (20,000 events) were analysed by an Accuri C6 flow cytometer and CFlow Plus software (BD, UK). Forward and side scatter plots were used for gating cells, excluding debris and identifying any changes in the scatter properties of the cells (as shown in Figure 9A). This gate was applied to PI versus annexin V-FITC plots with quadrant gates to determine the populations corresponding to viable (annexin V^-/PI^-), early

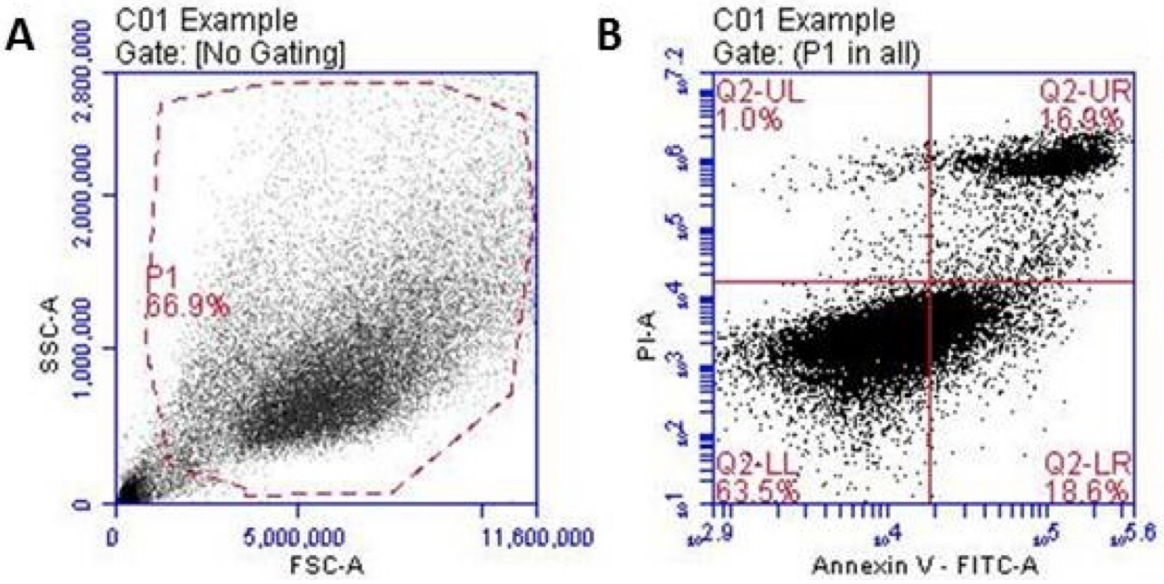

Figure 9 Cytometry gating for apoptosis. Forward scatter channel – area (FSC-A) versus side scatter channel – area (SSC-A) plots were used to gate the cells and exclude debris (A). This gate was applied to annexin V-FITC – area (annexin V-FITC-A) versus propidium iodide – area (PI-A) plots (B). The quadrant gates show the populations of cells corresponding to viable (Annexin V^-/PI^-; Q2-LL), early apoptotic (annexin V^+/PI^-; Q2-LR) and late apoptotic/dead (annexin V^+/PI^+; Q2-UR) cells. Annexin V^-/PI^+ cells are also gated (Q2-UL).

apoptotic (Annexin V^+/PI^-) and late apoptotic/dead (Annexin V^+/PI^+) cells (Figure 9B).

Positive control cells were treated with the apoptosis inducer thapsigargin (1 μM diluted in dimethyl sulfoxide) 48 hours prior to analysis. Thapsigargin is an inhibitor of the sarcoendoplasmic reticulum calcium ATPase and as such blocks the ability of these pumps to transfer calcium from the cytoplasm into the endoplasmic reticulum. The endoplasmic reticulum calcium stores become depleted and in turn induces endoplasmic reticulum stress which ultimately leads to cell death.

2.6.2.2 Cell cycle distribution

Cell cycle was monitored by measuring DNA content using the DNA-binding fluorescent dye PI which is detected by flow cytometry. Analysis of DNA content reveals the percentage of cells in the G1, S and G2/M phases of the cell cycle (as detailed in Figure 10). Initially, cells are fixed/permeabilised with ethanol to allow entry of PI. However, since PI also stains double stranded RNA, the cells are pre-treated with RNase for optimal DNA resolution before staining with PI. The cell medium was removed and the cells (approximately 1 x 10^6) were harvested by trypsination (detailed in 2.1.1). The cell pellet was washed by re-suspending in 5 ml of PBS followed by centrifugation for 5 minutes at 1000 rpm. The supernatant was discarded and the cell pellet was washed a further two times. The cell pellet was re-suspended in 1ml of PBS and transferred to a 5 ml polypropylene tube. Cold absolute ethanol (1 ml) was added to the cells which were then passed through a 25G needle and syringe to ensure a single cell suspension and prevent cell clumping. The cells were fixed for at least 24 hours at -20°C. The cells were then washed twice in 5 ml of PBS followed by centrifugation at 2000 rpm for 5 minutes. The cell pellet was re-suspended in 50 μl of RNase A stock solution (10 μg/ml) and incubated at 37°C for 45 minutes. PI staining solution (300 μl of 50 μg/ml PI in PBS) was next added and the samples (50,000 events) were analysed by an Accuri C6 flow cytometer and CFlow Plus software (BD, UK). Cell gating to exclude cell doublets and debris was applied to the PI histogram plot (Figure 11). The percentage of cells in each cell cycle phase was determined by gating each phase individually.

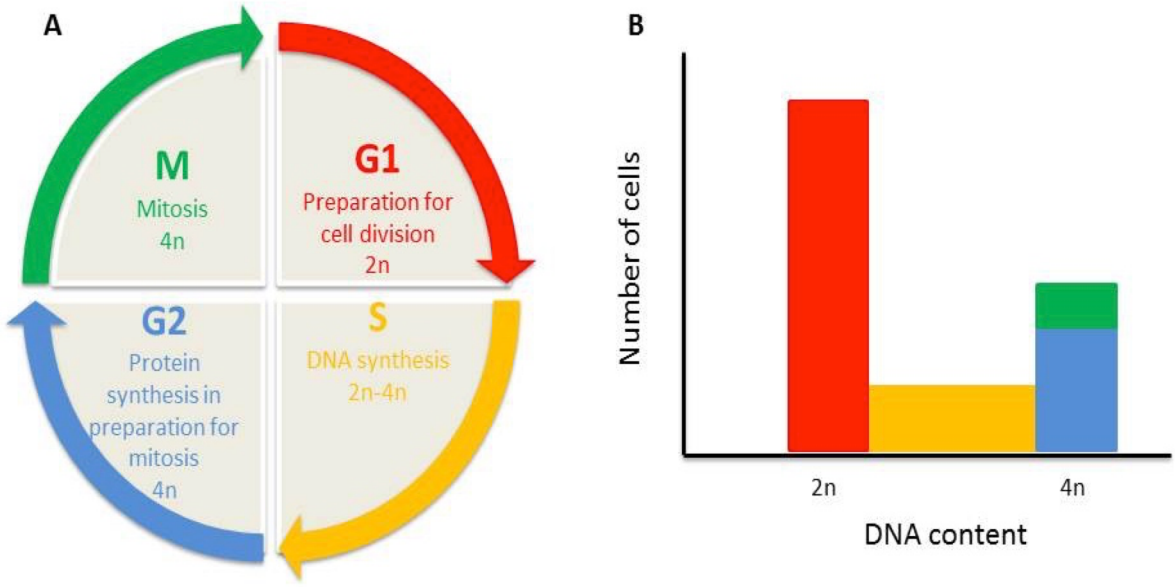

Figure 10 Relationship between the cell cycle and the DNA content represented by a histogram. (A) Phases of the cell cycle: at G1, the interval between mitosis and initiation of DNA replication, the cells are diploid (2n). As the cells enter the S phase, DNA replication begins and the DNA content increases from 2n to 4n. DNA content remains at 4n in the G2 and M phase decreasing to 2n after cytokinesis. (B) Demonstrative histogram of cell number versus DNA content. DNA content is determined by the fluorescence intensity of propidium iodide-labelled DNA detected by flow cytometry. The distribution shows two peaks equivalent to cells with DNA contents of 2n and 4n; these cells are in G1 and G2/M phase of the cycle, respectively. The cells in S phase have DNA contents between 2n and 4n and are distributed between these two peaks.

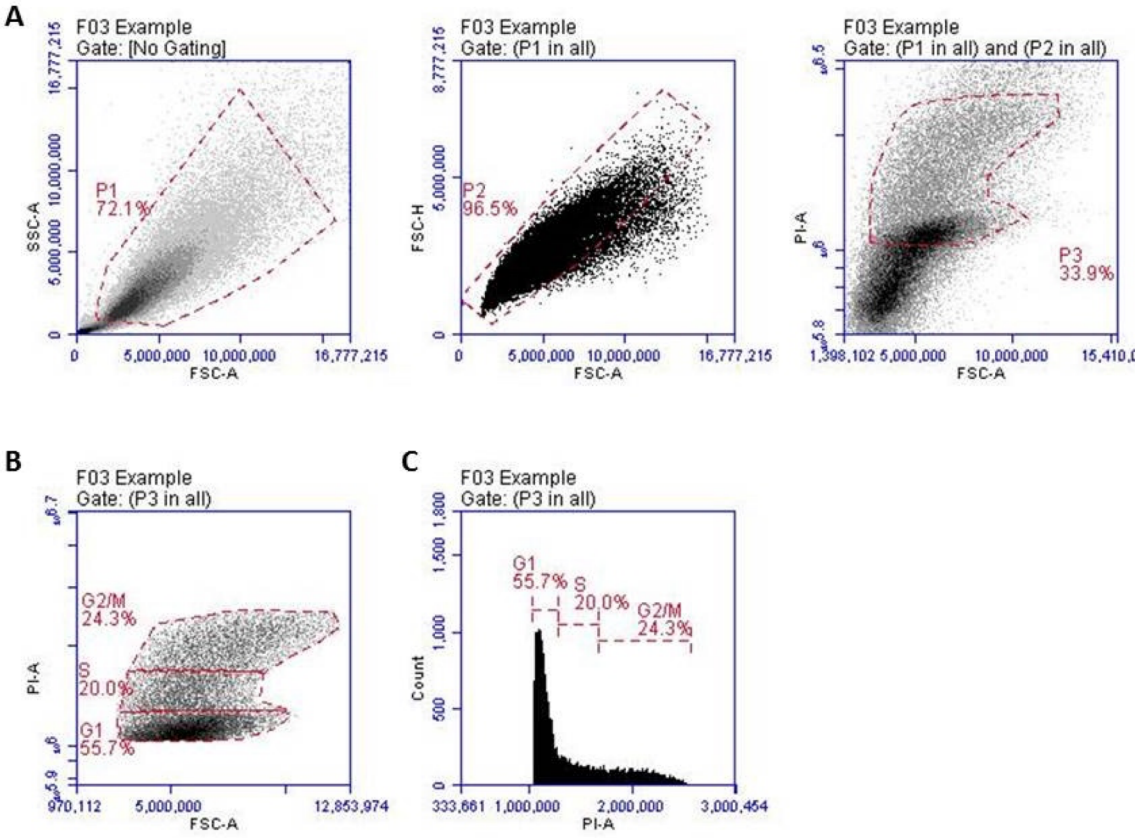

Figure 11 Cytometry gating for cell cycle phases. Side scatter channel – area (SSC-A) versus forward scatter channel – area (FSC-A), FSC-height (FSC-H) versus FSC-A and propidium iodide – area (PI-A) versus FSC-A plots were used to gate the cells and exclude debris and cell doublets (A). Histogram plot of cell count versus PI-A (C) from the gated cells shows the population of cells in each stage of the cell cycle. The percentage of cells in each cell cycle phase was determined by gating each phase individually (B).

2.6.3 Cell counting

Cells were seeded into 24 well plates at a density of 3 x 10^4 cells per well in 1 ml of experimental media (detailed in 2.1.2). Once approximately 60% confluencey was reached, siRNA (100 nM) ± fulvestrant (100 nM) (as detailed in 2.6.1) were added in triplicate to antihormone responsive and resistant cell lines. The cells were counted following four days of incubation. The medium was removed and the cells were washed three times with 1 ml of tissue culture grade PBS. Trypsin/EDTA (250 µl) was added to each well and once the cells had completely detached (approximately 3 to 5 minutes in the 37°C/5% CO_2 incubator), 750 µl of appropriate medium was added to each well to neutralise the trypsin/EDTA solution. The cells were passed through a sterile 25G syringe

needle twice to ensure a single cell suspension. The cell number was measured by an automated cell counter (see section 2.1.2).

2.6.4 Immunofluorescence

Cells were seeded into 6 well plates containing 0.13-0.17 mm thick glass coverslips (VWR microscope cover glasses 22 x 22 mm, No.1, VWR International Ltd, UK) at a density between 1.5 – 2 x 10^5 / well in 1.5 ml media (detailed in 2.1.2). MCF-7 and T47D cells were allowed to adhere to the coverslips for 24 hours prior to the addition of control and antihormone treatments for 7 days. The resistant and wild-type control cells were allowed to grow until they reached approximately 60-70% confluency. After incubation, the media was removed and the cells were fixed with 3.7% formaldehyde (diluted in PBS) for 15 minutes. Cells were then washed with PBS two times before being permeabilised by incubation in PBS containing 1% BSA and 0.4% saponin for 15 minutes. Cells were blocked in 10% normal goat serum (Dako normal goat serum X0907, Dako UK Ltd) (diluted in 1% BSA and 0.4% saponin in PBS) for 15 minutes to prevent non-specific antibody binding. The cells were then incubated in two primary antibodies simultaneously, one from mouse and the other from rabbit host species, (diluted in PBS containing 1% BSA and 0.4% saponin; Table 8) for 1 hour. Cells were washed three times with PBS prior to 30 minute incubation in the dark with fluorophore-conjugated secondary antibodies (Table 8) diluted 1:1000 in PBS containing 1% BSA and 0.4% saponin. Coverslips were drained and mounted onto glass slides (SuperFrost Plus glass microscope slides, Menzel-Gläser, Germany supplied by Thermo Fisher, UK) using Vectashield mounting medium containing DAPI (4', 6-diamidino-2-phenylindole) nuclear counterstain. The cells were viewed on a Leica fluorescent microscope (Leica DMil, Leica Microsystemt Ltd, Milton Keynes, UK) at x63 magnification under an oil immersion (Zeiss immersion oil, Thermofisher Scientific, UK) and analysed by OpenLab software (PerkinElmer, UK).

Table 8 Primary and secondary antibodies used for immunofluorescence with their corresponding dilution, conjugate where applicable, species, source and product number

Target	Dilution	Conjugate	Species	Source	Product Number
BCL3	1:250		Rabbit	SCBT	sc-185
CLU	1:250		Mouse	SCBT	sc-5289
p50	1:250		Rabbit	SCBT	sc-7178
p50	1:500		Mouse	NB	NBP2-22178
Anti-rabbit IgG	1:1000	Alexa Fluor 488	Goat	Thermofisher Scientific, UK	A-11034
Anti-mouse IgG	1:1000	Alexa Fluor 594	Goat	Thermofisher Scientific, UK	A-11032

SCBT: Santa Cruz Biotechnology, NB: Novus Biologicals.

2.6.5 Immunoprecipitation

Immunoprecipitation is a method used to purify a protein of interest or group of proteins from a complex mixture using a specific antibody immobilised to a solid support. Within this project, immunoprecipitation was used to investigate proteins interacting with the protein of interest. Briefly, an antibody is incubated with protein cell lysate to allow an immune complex to form with the antigen it recognises. The antibody/antigen complex is then captured on a solid support (e.g. agarose) with immobilised Protein A (IgG binding protein). Any proteins not bound by the Protein A are washed away and the antigen along with any proteins bound to it is eluted. This protein complex can then be analysed by SDS-PAGE and Western blotting.

Protein lysates (500 µg) were diluted in 500 µl of ice cold lysis buffer (see section 2.5.1) containing cocktail protease inhibitor and 1 mM of PMSF diluted in isopropanol and incubated with 1 µg of primary antibody for 1 hour with rotation at 4°C to allow formation of antibody/antigen complexes. Meanwhile, protein A agarose beads were washed and prepared for immunoprecipitation. The beads (30 µl) were aliquoted into eppendorf tubes and resuspended in 750 µl of ice cold lysis buffer then centrifuged for 1 minute at 10,000 rpm at 4°C. The

supernatant was decanted and this wash step was repeated two more times. After the final wash the supernatant was removed and the bead pellet kept on ice.

The antibody/antigen complexes were added to 30 µl of the prepared beads and incubated for 2 hours with rotation at 4°C, to allow the complexes to bind to the beads via Protein A, prior to storage overnight at -20°C. The samples were then centrifuged at 10,000 rpm for 2 minutes at 4°C and the supernatant was carefully removed. The bead pellet was washed three times by adding 750 µl of ice cold lysis buffer, vortexed briefly, allowed to stand for 5 minutes on ice, followed by centrifugation as above. After the final wash, the supernatant was removed and the pellet was resuspended in 60 µl of 2 X Lamelli sample loading buffer (see section 2.5.4, except supplemented with 3.08 % w/v DTT) and vortexed prior to incubation at 70°C for 15 minutes to release the immune complexes from the beads. The samples were vortexed again and centrifuged at 13,000 rpm for 2 minutes. The supernatant containing the immunoprecipitated proteins was collected and separated by SDS-PAGE followed by Western blotting.

2.6.6 Statistical analysis

Data were analysed using GraphPad Prism (GraphPad Software, Inc. USA). The specific statistical analyses utilised are detailed in each results Chapter. Data are expressed as mean ± SEM and a p value <0.05 was considered statistically significant.

3 Results I: Identification and validation of antihormone-induced pro-survival genes in MCF-7 cells

3.1 Introduction

Antihormones are the mainstay therapy for ER+ breast cancer and have contributed to a substantial decrease in mortality over recent decades. However, resistance remains a significant clinical problem, with 40% of such tumours in the adjuvant setting and virtually all patients with advanced disease, acquiring resistance to these therapies. Surprisingly, the majority of oestrogen-regulated genes in human breast cancer cells are repressed and many of these genes act as growth and/or transcriptional repressors[38]. Thus, the benefit of antihormone therapy arises from their ability to induce the expression of these negative regulators of cell proliferation. Indeed, the main mechanism of action of antihormones is to inhibit cell proliferation, however they are unable to promote significant levels of cell death[216]. Paradoxically, more recent research has revealed that oestrogens can suppress, and antihormones induce, genes that promote cell proliferation and survival[197,216,259]. Furthermore, antihormones have the ability to rapidly induce "compensatory" signal transduction pathways to promote cell survival[302]. Critically, such "reprogramming" of intracellular signalling networks, induced by antihormones, may allow a cohort of cells to escape the initial growth inhibitory actions of these agents and ultimately drive acquired resistant cell growth.

Clearly, the ultimate marker of antihormone resistance is the loss of the drug target i.e. ER[303]. However, there are currently very few markers predicting the degree and duration of patient response and the acquisition of resistance. Such markers have been identified by comparing endocrine resistant cell models to their wild type counterparts. For example, increased expression of EGFR and HER2 receptors has been demonstrated in tamoxifen-resistant cells versus tamoxifen-responsive wild type MCF-7 cells[185]. Furthermore, increased EGFR/HER2 heterodimerisation and receptor phosphorylation and consequently increased

activation of downstream kinases ERK 1/2 MAP kinase and AKT, previously implicated in cell proliferation and survival, has been reported in these tamoxifen-resistant cells compared to wild type[185,263]. In support of these findings, Miller et al. have also reported increased activity of AKT signalling in oestrogen deprivation-resistant cell lines versus wild type[296].

Although several studies have identified alterations in signalling pathways utilised by endocrine resistant cell models compared to endocrine sensitive wild type counterparts, more recent studies addressing the temporal changes in the genotype/phenotype directly associated with the acquisition of resistance are emerging. Indeed, the pro-proliferative genes, EGFR and HER2, have been established as oestrogen-suppressed and antihormone-induced in a panel of ER+ breast cancer cell lines. Short-term tamoxifen treatment has been shown to increase EGFR and HER2 expression *in vitro* and *in vivo* MCF-7 cell models of ER+ breast cancer, with subsequent downstream activity of cell survival and proliferation pathways[216,217]. Such signalling may allow cells to escape inhibition, thus supporting the partial inhibitory effects on proliferation and minimal cell death promoted by this antihormone. Indeed, targeting of these receptors in conjunction with tamoxifen suppressed downstream residual kinase signalling activity, greatly enhanced the anti-tumour activity of this antihormone and delayed the acquisition of resistance[216,217]. Furthermore, increased expression of EGFR and HER2 and substantial downstream kinase activity was maintained through to the emergence of resistance[216,217], suggesting that early tamoxifen-induced EGFR and HER2 expression limits the anti-tumour response and provides protective mechanisms to a cohort of cells from which resistance subsequently emerges. In addition to the well-characterised EGFR and HER2 genes, antihormones have been shown to induce expression of pro-invasive genes (RhoE and δ-catenin), with expression maintained through to the acquisition of resistance[304]. Such genes may contribute to the small inductive effect of invasiveness observed in MCF-7 cells in the presence of antioestrogens[305].

There is now considerable evidence implicating the role of antihormone-induced pro-proliferative genes in endocrine resistance, however the role played by antihormone-induced pro-survival genes remains largely unexplored. Importantly,

identification of early antihormone-induced pro-survival genes may reveal novel biomarkers predictive of response and underlying mechanisms involved in resistance, which may lead to the identification of potential therapeutic targets to improve antihormone response and prevent the establishment of the resistant phenotype. Thus, the purpose of the work described in this thesis is to identify and characterise antihormone-induced pro-survival genes involved in limiting response and promoting the acquisition of resistance. Tamoxifen, fulvestrant and oestrogen deprivation treatments were examined to determine whether common resistant-promoting genes are induced by all three clinically used treatments. Furthermore, 4 ER+ breast cancer cell lines (HER2-: MCF-7 and T47D; HER2+: BT474 and MDA-MB-361) were utilised to consider an aspect of heterogeneity that exists in ER+ breast cancer and also to determine whether antihormone-induced mechanisms of acquired hormone-independent growth are common across several cell lines and molecular subtypes including HER2- and HER2+ disease.

In this Chapter, microarray gene expression profiling has been utilised to identify antihormone-induced pro-survival genes in MCF-7 cells during response with increased expression maintained in to cell models of endocrine resistance. It was hypothesised that antihormone-induced expression of these pro-survival genes early during response may limit the pro-apoptotic actions of antihormones and allow a cohort of cells to evade the growth inhibitory actions of these agents, resulting in anti-tumour responses of finite duration and ultimately the development of resistance. Microarray technologies allow thousands of mRNA transcripts to be examined simultaneously, creating a genome-wide gene expression profile. Such profiling has proved very successful in breast cancer research. Indeed, microarray studies identified the heterogeneity that exists in breast cancer and demonstrated that breast cancer is a collection of distinct diseases affecting the same anatomical site[277]. Furthermore, microarray gene expression profiling has been utilised in breast cancer studies to investigate overexpressed genes that may be involved in disease progression[306], gene signatures predictive of clinical outcome[283,307] and tumour aggressiveness[308]. Such studies have led to the development of commercially available genomic assays to predict clinical outcome in breast cancer patients. For example, the OncotypeDX

assay measures the expression of a 21-gene panel, consisting of ER, HER2, ER-regulated genes and several proliferative genes, to estimate the probability of recurrence at 10 years and to stratify patients into low-, intermediate- and high-risk cohorts[280]. Furthermore, studies have demonstrated that patients in the high-risk category are likely to respond to adjuvant chemotherapy combined with endocrine treatment. Since the majority of patients with early breast cancer receive adjuvant chemotherapy, this assay would prevent those patients who are likely to obtain low/no benefit from receiving unnecessary treatment and critically being affected by its toxicity[281].

However, such assays provide only prognostic data and fail to identify therapeutic targets that may improve response. Furthermore, there are no gene signatures to distinguish endocrine sensitive from resistant patients or signatures predictive of antihormone response. A limited number of studies have employed global gene expression profiling combined with antihormone therapy during response to potentially identify drug-induced molecular signatures that serve to limit response and ultimately are involved in the acquisition of resistance. Cappelletti et al. utilised microarrays to define a gene expression profile associated with toremifene response in ER+ breast cancer patients and to identify potential genes modulated by neo-adjuvant toremifene treatment which may be involved in antihormone resistance mechanisms[309]. Indeed, this study identified a 53-gene signature significantly related to treatment response and more importantly identified genes (including MAPK6 and MMP2) modulated by toremifene treatment in non-responding patients which are likely to be involved in resistance.

The aims of this Chapter were to (i) recapitulate in part the study by Cappelletti et al. and utilise microarray gene expression profiling to examine whether any genes with known pro-survival ontology are induced in response to a range of antihormones in ER+ MCF-7 cell lines, (ii) identify those genes that are common to all antihormones and (iii) examine whether these genes are also expressed at increased levels in endocrine-resistant MCF-7 cell lines to potentially implicate such genes in the development of resistance. It was hoped that novel drug-induced genes that may subsequently limit response and contribute to the adverse

resistant phenotype could be revealed and ultimately lead to the identification of novel therapeutic options for such patients.

3.2 Methods

3.2.1 Microarray analysis

Microarray gene expression profiling, as described in section 2.2, was completed for 10 day antihormone-treated (tamoxifen, falsodex and oestrogen deprivation) MCF-7 cells, in addition to the associated MCF-7 cell models of acquired (short-term) endocrine resistance (TAMR, FASR and XR), versus E2-treated and wild type control, respectively. The cell culture methods and the generation of the resistant cell lines are detailed in section 2.1.

The resultant triplicate data were uploaded on to the online bioinformatics software GeneSifter where the data were first median normalised and log transformed prior to analysis. Heatmaps and log2-expression intensity plots were constructed to allow individual gene expression changes to be investigated. This GeneSifter-assembled array resource was interrogated to identify robust antihormone-induced expression of pro-survival genes (n=248; assembled using ontology and website resources; Appendix Table 15) during drug response and was extended into cell models of antihormone-resistance to determine whether expression of such genes was maintained and hence may contribute substantially to the emergence of resistance. In the majority of cases, each gene was represented by more than one probe on the Affymetrix gene chip. All of the probes for the genes of interest were analysed to determine whether a consistent expression profile was achieved across all probes for a given gene, providing further confidence that any antihormone-induced change in expression was robust. Particular importance was placed on the optimal 'jetset' probe (detailed in section 2.2.7). ANOVA and post-hoc Tukey tests were used to analyse the differences between means. A p value <0.05 was considered statistically significant.

3.2.2 RT-PCR

RT-PCR (as described in section 2.4) was performed on triplicate RNA from 10 day E2- and antihormone-treated MCF-7 cells (cultured under the same conditions as

those used to generate the samples for microarray gene expression profiling), to verify the Affymetrix expression profiles of the genes of interest.

3.2.3 Ontological investigation of the genes of interest identified by microarray analysis

Ontological studies were performed on the genes of interest to identify any reported associations with cancer, antihormone-response and –resistance in the literature. Searches in Pubmed using the gene name/acronym combined with keywords such as 'breast cancer,' 'antihormone,' 'resistance' and 'survival' were performed to generate the ontological information for each gene. For one gene in particular, such studies identified genes/proteins essential for the function of this gene and subsequently, heatmaps and log2 profiles were generated to examine the profile of these essential genes in antihormone-treated MCF-7 cells and the resistant cell models.

3.2.4 Western blotting

The expression of the genes of interest was examined at the protein level by Western blotting. Western blotting (as described in section 2.5) was performed on triplicate protein samples from 10 day E2- and antihormone-treated MCF-7 cells (cultured under the same conditions as those used to generate the samples for microarray gene expression profiling and subsequent RT-PCR).

3.3 Results

3.3.1 Validation of antihormone-induced repression of E2-regulated genes and subsequent decrease in MCF-7 cell proliferation following short-term treatment

The short-term effects of antihormones on E2-regulated genes and the proliferation of hormone-responsive MCF-7 cells have previously been examined within the group. Indeed, 10 day oestrogen deprivation, tamoxifen and fulvestrant treatment of MCF-7 cells, cultured under the same conditions as those used to generate the gene expression profiles in this thesis, resulted in a depletion of the E2-regulated genes, pS2 and amphiregulin[310]; thus verifying the cells as hormone responsive. Moreover, the group has previously shown that short-term antihormone treatment exerts significant anti-proliferative effects, but promotes only minimal cell death. Indeed, tamoxifen has been demonstrated to decrease MCF-7 cell growth from as early as week one, which reached statistical significance (reducing by 55%) by week two[216]. Concomitant decreases in the Ki67/MIB1 proliferation marker and the percentage of cells in the S phase of the cell cycle, with an increase in G0/G1 arrest were observed. A modest increase in apoptosis with partial suppression of the cell survival protein, BCL-2, was apparent at week four of tamoxifen treatment[216]. In support of our studies, others have also demonstrated tamoxifen-induced anti-proliferative effects in MCF-7 cells from as early as 24 hours, together with marked accumulation of cells in G1 and a depletion of cells in the S phase of the cell cycle[311,312].

Similarly, our group have previously demonstrated a statistically significant decrease in MCF-7 cell growth following seven days of fulvestrant treatment, parallel with a decrease in ER protein expression and associated reductions in PR mRNA and cyclin D1 protein expression, indicative of a reduction in ER transcriptional activity[262]. A statistically significant decrease in MCF-7 cell growth following fulvestrant treatment has been reported from as early as day three[313]. Likewise, oestrogen deprived cells express lower protein levels of cyclin D1 compared to E2-treated cells, coincident with a decrease in cell proliferation from as early as 30 hours of treatment[314]. Together, these findings confirm

antihormone-induced repression of E2-regulated genes in MCF-7 cells and downstream repression of cell proliferation and regulation of cell cycle kinetics, following short-term treatment.

3.3.2 Confirmation of antihormone-induced HER2 expression using the microarray datasets

Initially, to validate and assess the quality of the array data, expression of known antihormone-induced gene, HER2, was examined. As predicted, the heatmap presented in Figure 12A shows that HER2 expression was statistically significantly ($p < 0.05$) induced by fulvestrant and oestrogen deprivation treatments, with fold changes >1.5, versus E2-treated control (Figure 12A, B & C). Tamoxifen induced a small, non-significant, increase in HER2 expression compared to E2-treated control (Figure 12A, B & C).

A

B

C

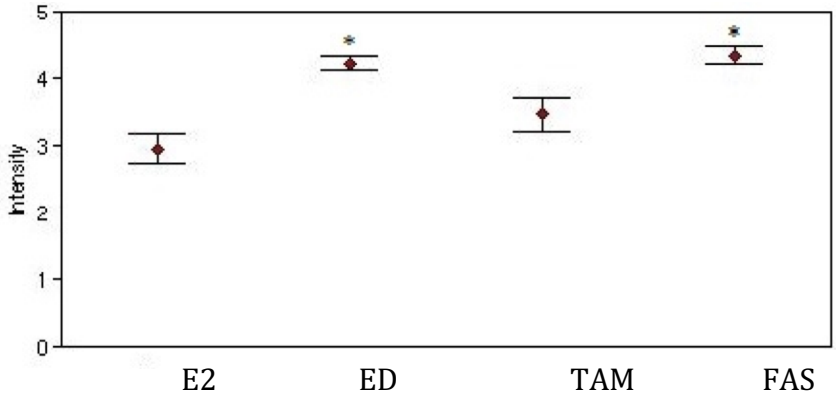

	E2-control	ED	TAM	FAS
Fold change		2.44	1.44	2.64

Figure 12 Heatmap (A) and log2 intensity plot (B) displaying the normalised (mean of three independent replicates ± SEM) gene expression of HER2 (jetset probe ID: 216836_s_at) in MCF-7 cells treated for 10 days with oestradiol (E2 control; 10^{-9} M), oestrogen deprivation (ED), tamoxifen (TAM; 10^{-7} M) and fulvestrant (FAS; 10^{-7} M). Red denotes an increase in gene expression compared to control (shown in black). (C) Table displaying the corresponding fold change in gene expression from the triplicate samples. * p <0.05 compared to E2-control.

3.3.3 Identification of pro-survival genes up regulated with antihormone treatment and maintained into the development of resistance

Following the validation of the quality of the array expression data and confirmation that antihormones were deregulating known oestrogen-suppressed genes in MCF-7 cells, the expression data were further interrogated to determine whether pro-survival genes were induced by antihormones during response, with expression maintained into the acquisition of resistance. The pro-survival genes (n=248) were subjected to a stringent filtering process to maximise identification of the most robust antihormone-induced proteins (Figure 13). Firstly, the heatmap tool was utilised to identify genes up regulated by at least one antihormone treatment during response, with increased expression also reported in at least one antihormone-resistant cell model (Appendix Table 16). Additionally, all of the probes representing each gene were examined to ensure a consistent expression profile was displayed. To filter the genes further, the detection calls were next studied. The detection call algorithms indicate whether the expression of a gene transcript is reliably detected (as described in section 2.2.7). Genes with a 'marginal' or 'present' detection call (signifying partial and reliable detection of gene expression respectively) in at least one antihormone treatment and resistant cell line were selected for further study. Genes exhibiting an 'absent' detection call, indicating unreliable detection of expression, were dismissed from further study.

Next, the heatmaps of the remaining genes were considered to ensure that the up regulation induced by antihormones was maintained into the associated resistant model (e.g. induced by tamoxifen during response with maintained expression in TAMR cells). The remaining 92 genes (Appendix Table 17) were exposed to an ANOVA and post-hoc tukey statistical test to identify those significantly ($p < 0.05$) up regulated by at least one antihormone treatment during response, to further maximise the chances of determining robust induced expression changes with antihormone treatment (n=17, Appendix Table 18). Finally, the fold change tool in GeneSifter was utilised to identify genes with a greater than 1.5 fold change induction during antihormone treatment versus E2-treated control. Together, this stringent filtering process identified 14 genes significantly up regulated by at least one antihormone treatment during response, with expression maintained into

antihormone resistance. The magnitude of antihormone-induced expression during response and expression in resistant cell models versus wild-type is illustrated by the heatmaps shown in Figure 14 and Figure 15. Figure 16 to Figure 30 further illustrate the corresponding intensity profiles, associated detection calls and fold change inductions for each of the 14 genes identified. The optimal 'jetset' probe was used to generate the heatmap and intensity profiles.

The Affymetrix expression profiles of the 14 high priority genes identified, and hypothesised to contribute to the development of antihormone resistance, were verified in MCF-7 cells during antihormone response by RT-PCR. The PCR results are illustrated alongside the intensity profiles in Figure 16 to Figure 30.

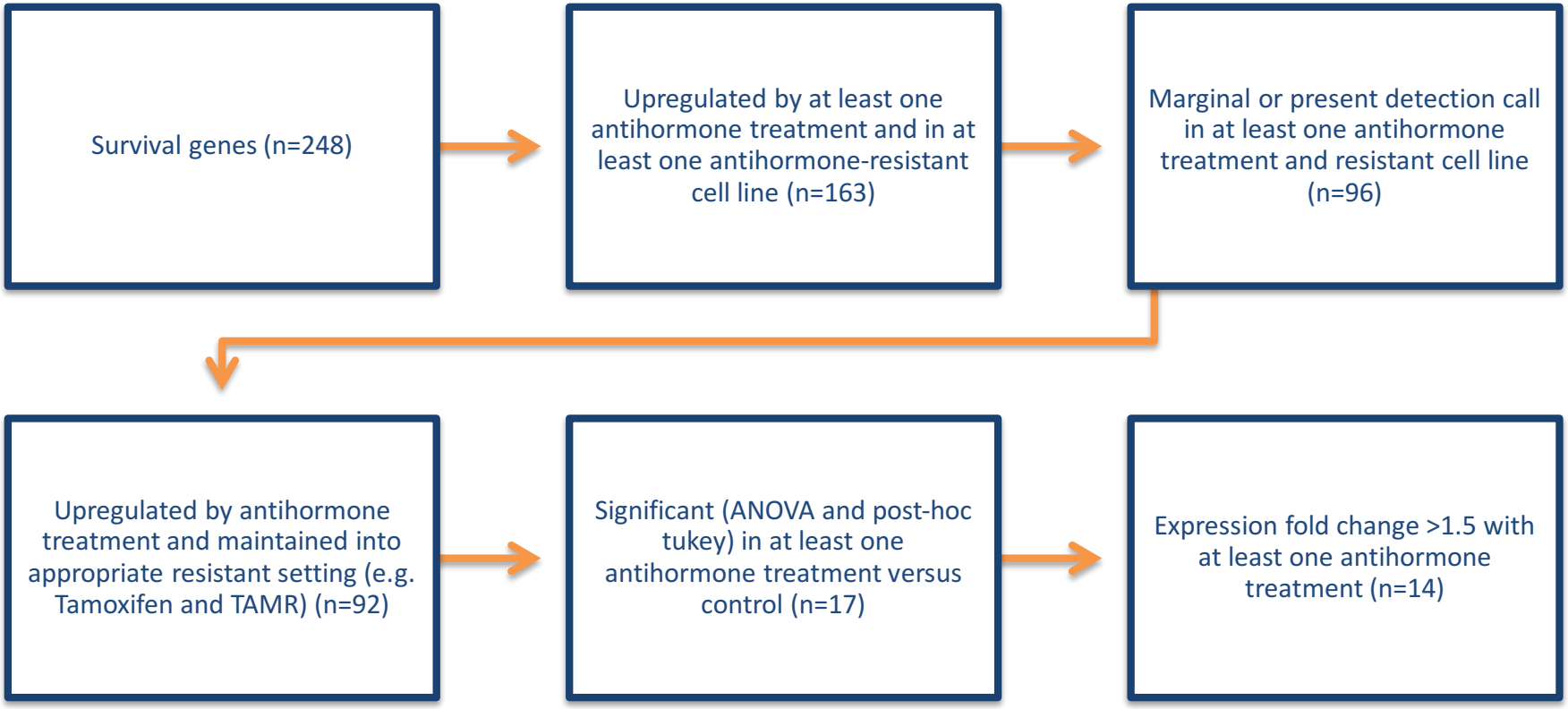

Figure 13 Flow diagram illustrating the filtering stages used within this project to identify the high priority genes to take forward for further investigation.

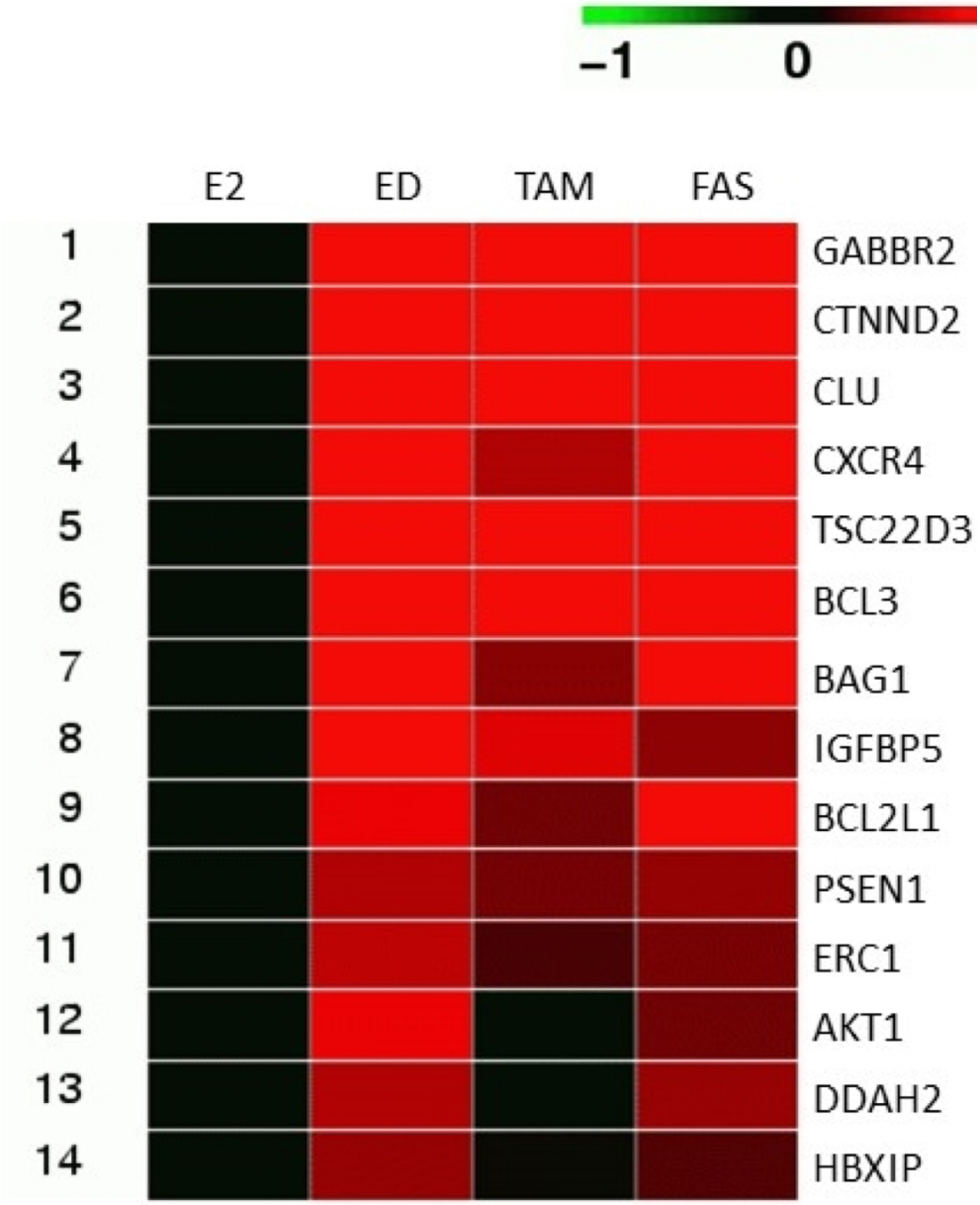

Figure 14 Heatmap displaying the change in expression of the 14 genes of interest following 10 day oestradiol (E2 control; 10^{-9} M), oestrogen deprivation (ED), tamoxifen (TAM; 10^{-7} M) and fulvestrant (FAS; 10^{-7} M) treatment in MCF-7 cells. Red denotes an increase in gene expression compared to control (shown in black).

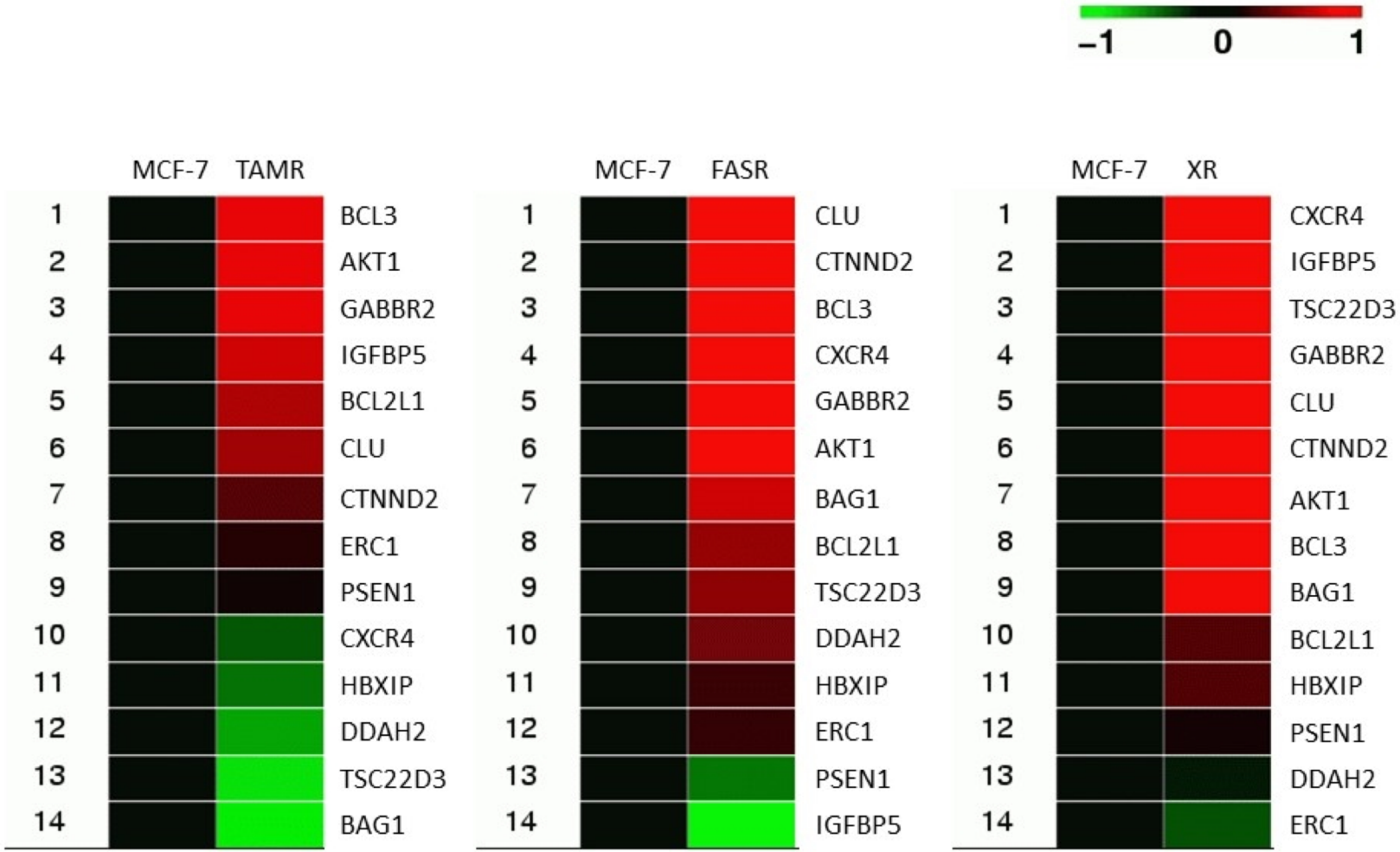

Figure 15 Heatmaps displaying the change in expression of the 14 genes of interest in tamoxifen-resistant (TAMR), fulvestrant-resistant (FASR) and oestrogen deprivation-resistant (XR) cells versus MCF-7 cells. Red denotes an increase, and green denotes a decrease, in gene expression compared to control (shown in black).

3.3.3.1 Gamma-aminobutyric acid B receptor, 2 (GABBR2)

The G-protein-coupled GABBR2 was identified as the gene with the greatest fold change induced by all antihormones compared to E2-treated control as illustrated in Figure 16A. Following 10 day antihormone treatment, GABBR2 expression was significantly ($p < 0.05$) up regulated by all treatments, with the greatest induction mediated by fulvestrant, which showed almost a 95 fold induction (Figure 16A). The detection calls were present following antihormone treatment, indicative of reliable gene expression whereas the log2 expression of E2-treated MCF-7 cells was below 0, suggesting extremely low/no gene expression (Figure 16B).

GABBR2 expression was maintained through to resistance, demonstrated by the present detection calls in the TAMR, FASR and XR cells (Figure 16C). GABBR2 expression was also significantly ($p < 0.05$) up regulated in the three resistant cell models versus MCF-7 control, with the greatest induction apparent in the XR cells, which showed almost a 6 fold induction (Figure 16C).

The Affymetrix profile of GABBR2 during antihormone response was next verified by RT-PCR. In agreement with the microarray data, GABBR2 RNA expression was induced by tamoxifen, fulvestrant and oestrogen deprivation treatments compared to E2-treated control and actin levels remained constant (Figure 16D). Fulvestrant induced the greatest up regulation of GABBR2 expression (Figure 16D), mimicking the log2 expression intensity plot and fold change reported from the microarray data (Figure 16A and B). Furthermore, the microarray detection calls reported 'absent' for E2- and 'present' for antihormone-treated cells, which were mirrored by the absent and present mRNA expression of GABBR2 detected by PCR.

A

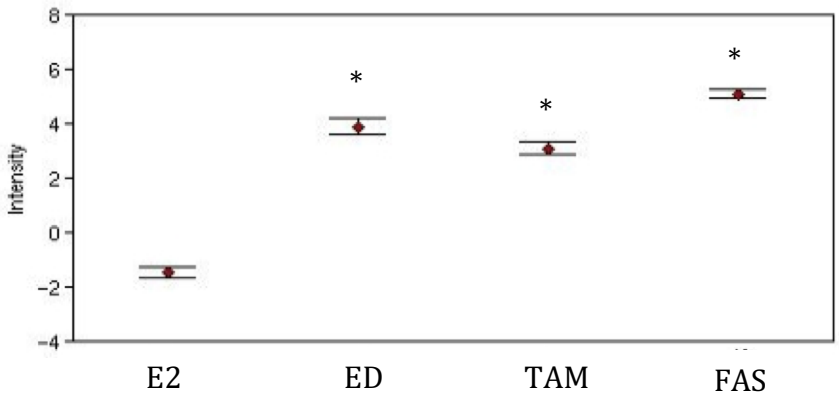

B

	E2-control	ED	TAM	FAS
Fold change		40.95	23.27	94.04
Detection call	AAA	PPP	PPP	PPP

C

	TAMR	FASR	XR
Fold change	2.55	2.70	5.88
Detection call	PPP	PPP	PPP
P <0.05	✓	✓	✓

Continued on next page

D

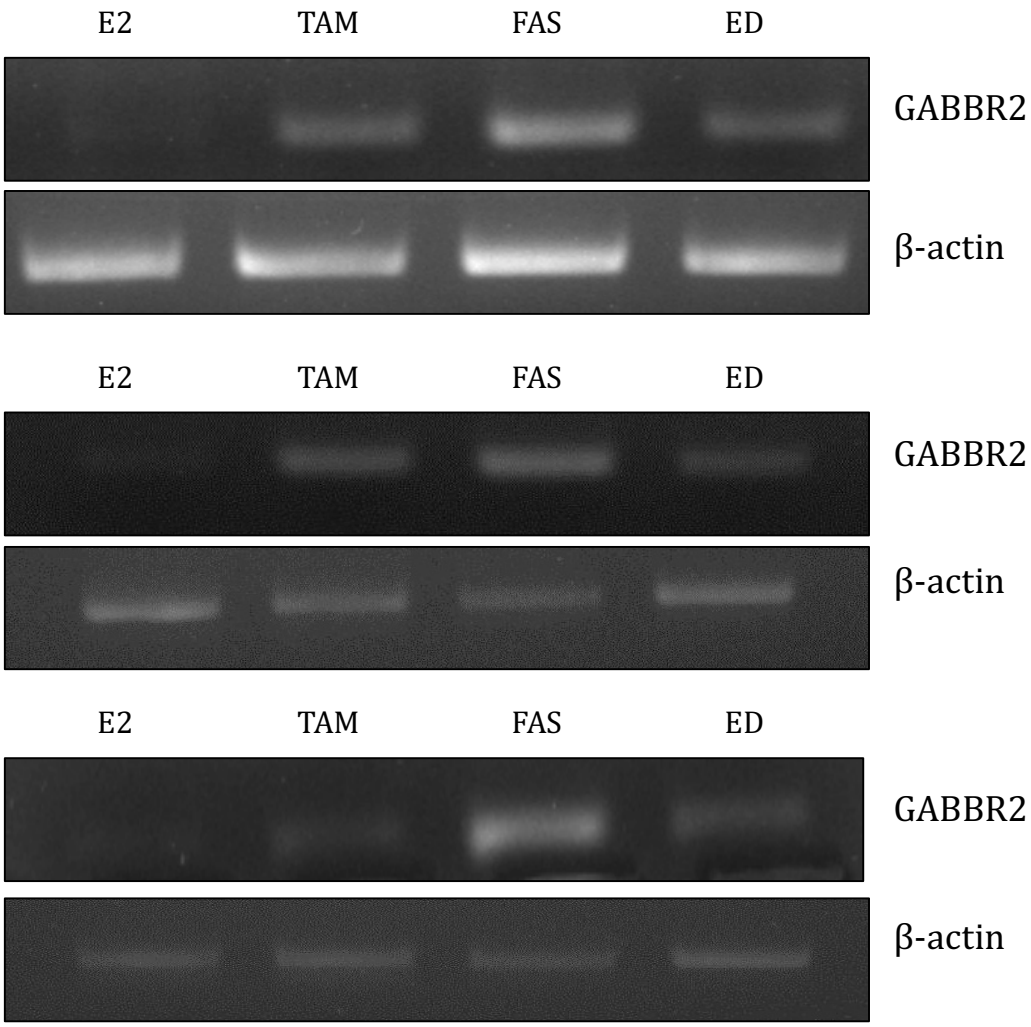

Figure 16 (A) Log2 intensity plot displaying the normalised (mean of three independent replicates ± SEM) gene expression of GABBR2 (jetset probe ID: 209990_s_at) in MCF-7 cells treated for 10 days with oestradiol (E2 control; 10^{-9} M), oestrogen deprivation (ED), tamoxifen (TAM; 10^{-7} M) and fulvestrant (FAS; 10^{-7} M). (B) Table displaying the corresponding fold change in gene expression and detection calls from the triplicate samples. (C) Table displaying the fold change increase in GABBR2 gene expression, detection calls and displaying whether the change in expression is statistically significant in tamoxifen-resistant (TAMR), fulvestrant-resistant (FASR) and oestrogen deprivation-resistant (XR) cell models compared to MCF-7 control. (D) PCR images from three independent experiments showing GABBR2 and β-actin mRNA expression in MCF-7 cells treated with E2, TAM, FAS and ED for 10 days. P: present; A: absent; * p <0.05 compared to E2-control; ✓: p <0.05 compared to MCF-7 control.

3.3.3.2 Catenin (Cadherin-associated protein), delta 2 (CTNND2)

The log2 intensity plot and corresponding fold change and detection calls (Figure 17A and B) revealed significant ($p < 0.05$) up regulation of δ-catenin, CTNND2, gene expression (greater than 1.5 fold change) by all three antihormone treatments compared to E2-treated control. Fulvestrant promoted the greatest up regulation of CTNND2 expression, showing approximately 9 fold induction in expression (Figure 17B). This profile was mirrored by absent expression of CTNND2 in E2-treated cells versus present detection calls in tamoxifen- and fulvestrant-treated cells and predominantly absent calls in the oestrogen deprived cells (Figure 17B).

CTNND2 expression was maintained through to antihormone resistance. Specifically, CTNND2 expression was significantly ($p < 0.05$) increased, together with present detection calls, in FASR cells versus MCF-7 control (Figure 17C). Similarly, CTNND2 expression was up regulated in TAMR and XR cells versus control. Predominantly absent detection calls were recorded in the TAMR and XR cell lines (Figure 17C).

PCR verification revealed induction of CTNND2 mRNA expression by all three antihormone treatments compared to E2-treated control (Figure 17D). Actin levels remained constant following all treatments. This again nicely paralleled the microarray profile.

A

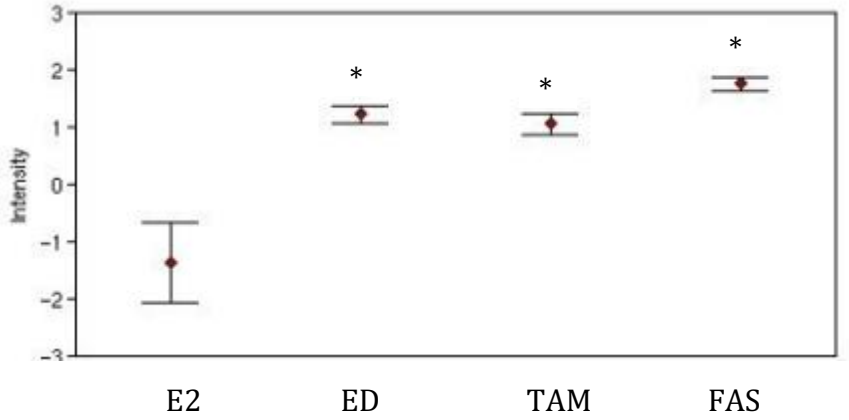

B

	E2-control	ED	TAM	FAS
Fold change		5.99	5.33	8.70
Detection call	AAA	PAA	PPP	PPP

C

	TAMR	FASR	XR
Fold change	1.26	4.70	3.40
Detection call	AAA	PPP	AAP
P <0.05		✓	

Continued on next page

D

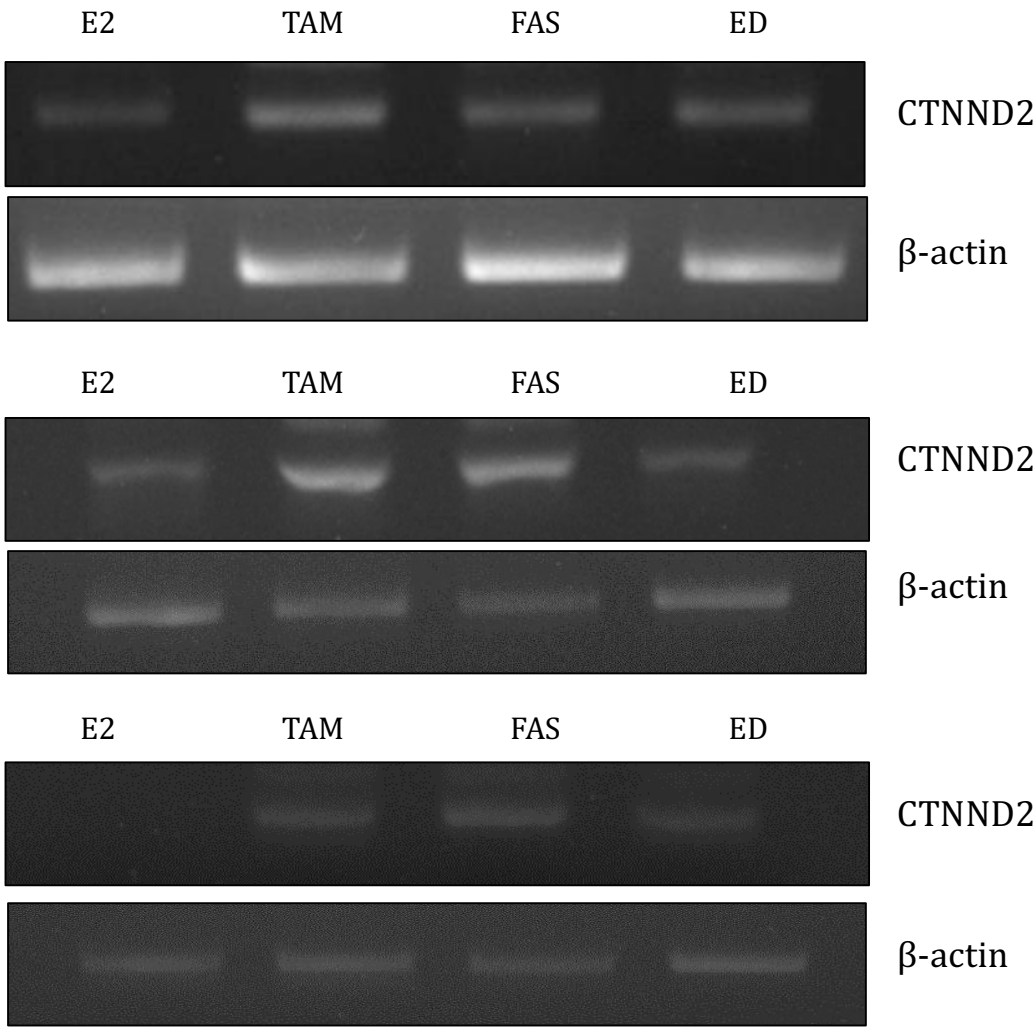

Figure 17 (A) Log2 intensity plot displaying the normalised (mean of three independent replicates ± SEM) gene expression of CTNND2 (jetset probe ID: 209618_at) in MCF-7 cells treated for 10 days with oestradiol (E2 control; 10^{-9} M), oestrogen deprivation (ED), tamoxifen (TAM; 10^{-7} M) and fulvestrant (FAS; 10^{-7} M). (B) Table displaying the corresponding fold change in gene expression and detection calls from the triplicate samples. (C) Table displaying the fold change increase in CTNND2 gene expression, detection calls and displaying whether the change in expression is statistically significant in tamoxifen-resistant (TAMR), fulvestrant-resistant (FASR) and oestrogen deprivation-resistant (XR) cell models compared to MCF-7 control. (D) PCR images from three independent experiments showing CTNND2 and β-actin mRNA expression in MCF-7 cells treated with E2, TAM, FAS and ED for 10 days. P: present; A: absent; * p <0.05 compared to E2-control; ✓: p <0.05 compared to MCF-7 control.

3.3.3.3 Clusterin (CLU)

The log2 expression plot revealed significant ($p < 0.05$) up regulation of CLU (a multifunctional glycoprotein) expression by all three antihormone treatments versus E2-treated control (Figure 18A). Predominantly present detection calls were reported in the antihormone-treated cells, indicating reliable detection of CLU gene expression (Figure 18B). However, an absent call was recorded in the E2-treated control cells, together with a negative log2 expression value, suggesting relatively low/no expression of this gene following this treatment (Figure 18A and B).

Similarly, CLU expression was up regulated in the three antihormone-resistant cell lines (fold change > 1.5), with significant up regulation in FASR cells, compared to MCF-7 control cells (Figure 18C). Predominantly, present detection calls were reported in the FASR and XR cells, with absent calls reported in the TAMR cells (Figure 18C).

Although the microarray data indicated up regulation of CLU expression by all three antihormone treatments, PCR was only able to validate gene induction by tamoxifen and fulvestrant. CLU mRNA expression following oestrogen deprivation treatment was comparable to the expression observed following E2 treatment (Figure 18D). Actin levels remained constant following each treatment.

A

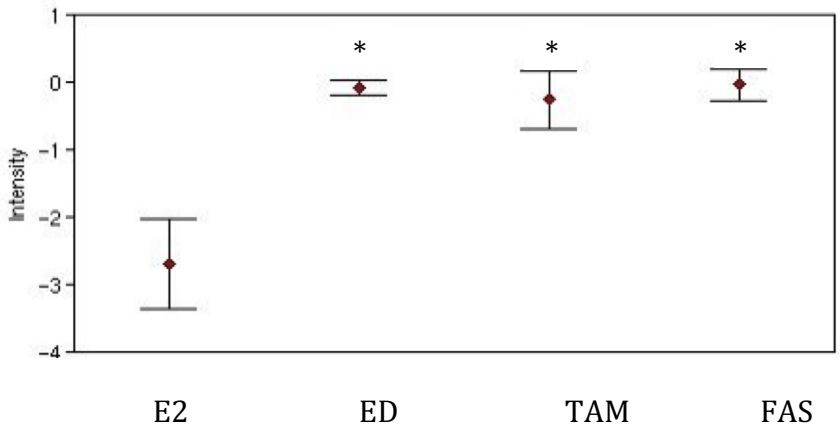

B

	E2-control	ED	TAM	FAS
Fold change		6.12	5.39	6.31
Detection call	AAA	PPP	APP	PPP

C

	TAMR	FASR	XR
Fold change	1.56	15.79	3.70
Detection call	AAA	PPP	PAP
P <0.05		✓	

Continued on next page

D

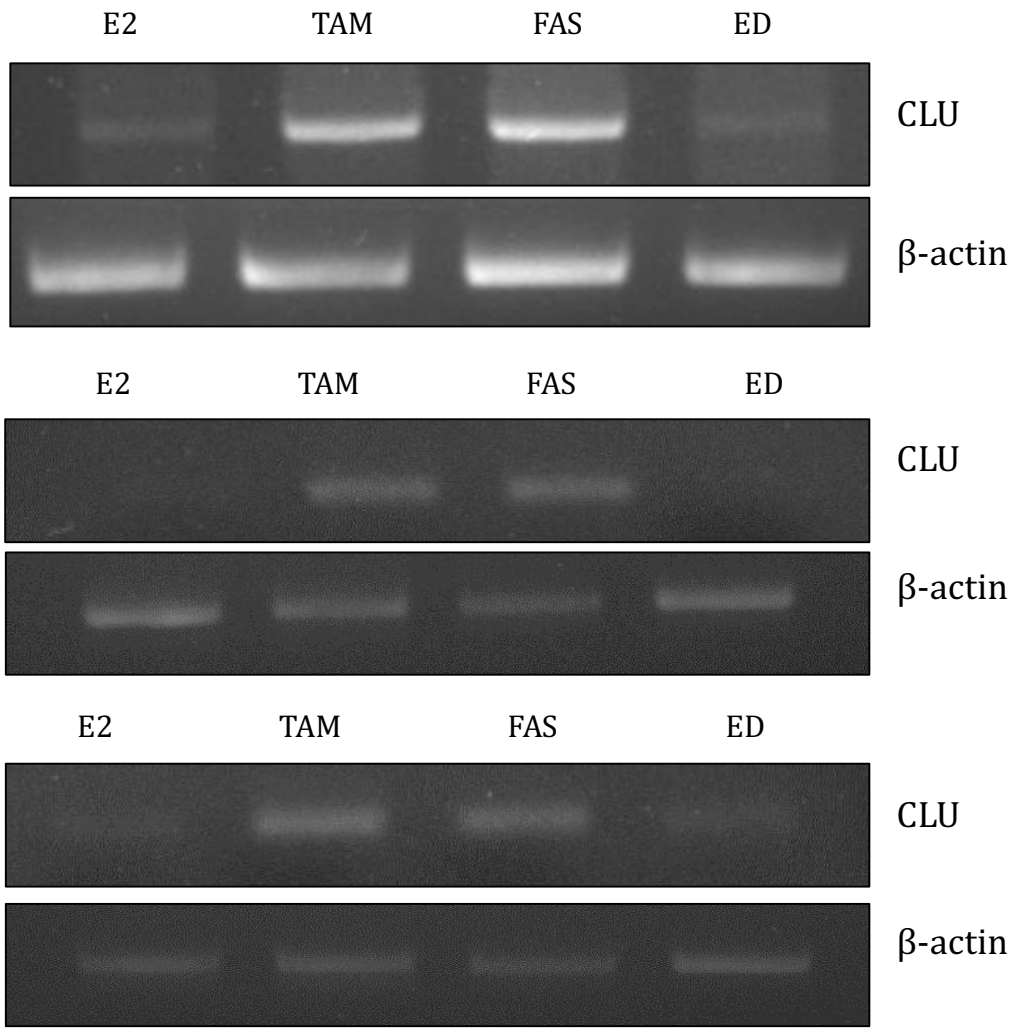

Figure 18 (A) Log2 intensity plot displaying the normalised (mean of three independent replicates ± SEM) gene expression of CLU (jetset probe ID: 222043_at) in MCF-7 cells treated for 10 days with oestradiol (E2 control; 10^{-9} M), oestrogen deprivation (ED), tamoxifen (TAM; 10^{-7} M) and fulvestrant (FAS; 10^{-7} M). (B) Table displaying the corresponding fold change in gene expression and detection calls from the triplicate samples. (C) Table displaying the fold change increase in CLU gene expression, detection calls and displaying whether the change in expression is statistically significant in tamoxifen-resistant (TAMR), fulvestrant-resistant (FASR) and oestrogen deprivation-resistant (XR) cell models compared to MCF-7 control. (D) PCR images from three independent experiments showing CLU and β-actin mRNA expression in MCF-7 cells treated with E2, TAM, FAS and ED for 10 days. P: present; A: absent; * p <0.05 compared to E2-control; ✓: p <0.05 compared to MCF-7 control.

3.3.3.4 Chemokine receptor 4 (CXCR4)

All three antihormones induced up regulation of the chemokine receptor, CXCR4 (fold change greater than 1.5), which was significant ($p < 0.05$) with fulvestrant and oestrogen deprivation treatments, versus E2-treated control (Figure 19A and B). Present detection calls were recorded in the antihormone- and E2-treated cells (Figure 19B).

In the antihormone-resistant cells, CXCR4 expression was significantly ($p < 0.05$) up regulated in XR and FASR cells (by 41 and 3 fold, respectively) versus MCF-7 control cells (Figure 19C). Present detection calls were also reported in these cell lines. However, CXCR4 expression was down regulated in TAMR cells, together with predominantly absent detection calls, compared to MCF-7 control cells (Figure 19C).

In response to all three antihormones, CXCR4 mRNA expression was clearly induced (Figure 19D) which is in agreement with the microarray profile (Figure 19). Actin levels remained relatively constant following each treatment.

A

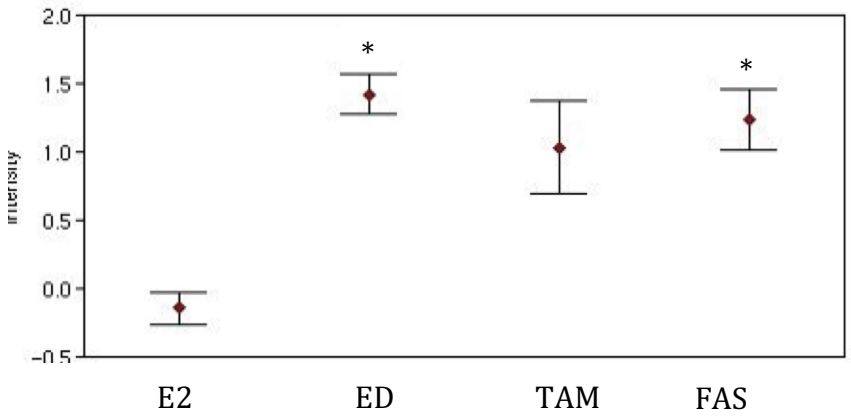

B

	E2-control	ED	TAM	FAS
Fold change		4.10	1.62	6.13
Detection call	PPP	PPP	PPP	PPP

C

	TAMR	FASR	XR
Fold change	1.27***	3.37	41.22
Detection call	APA	PPP	PPP
P <0.05		✓	✓

Continued on next page

D

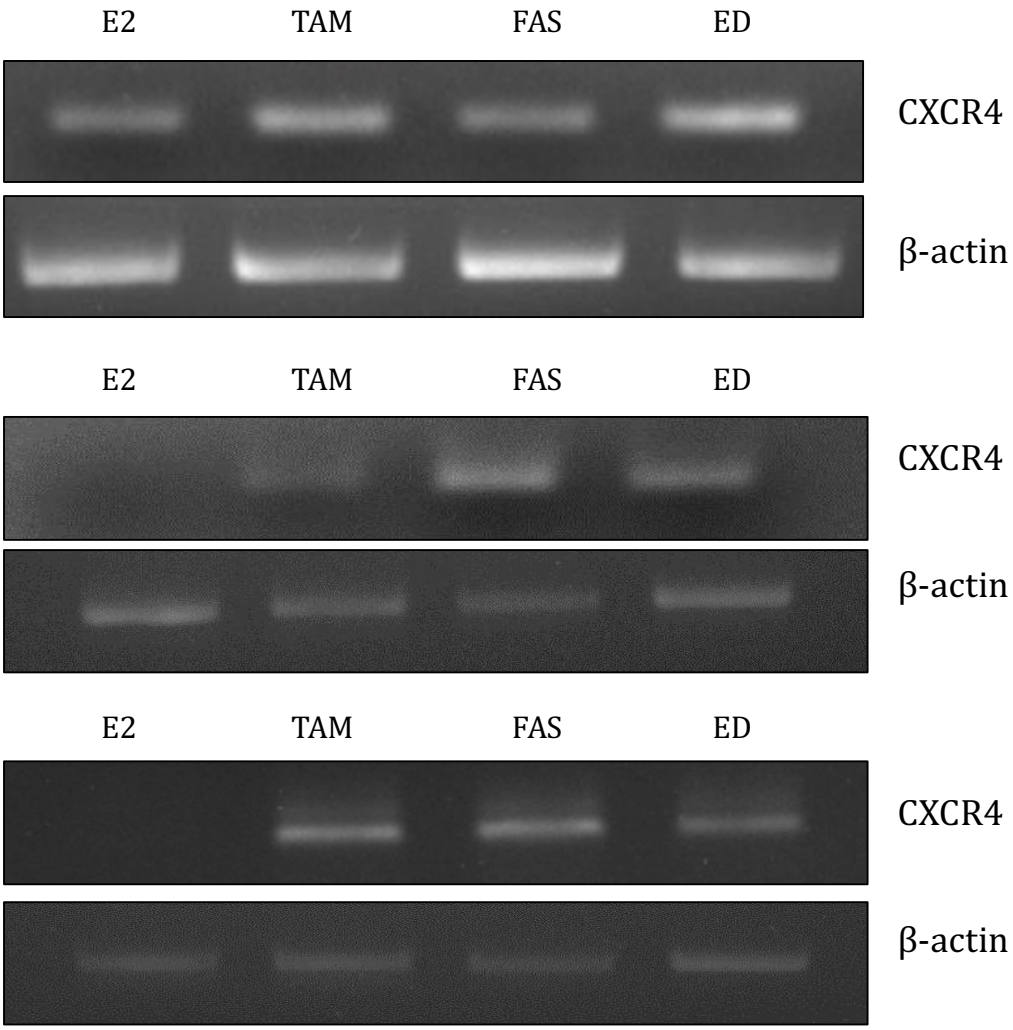

Figure 19 (A) Log2 intensity plot displaying the normalised (mean of three independent replicates ± SEM) gene expression of CXCR4 (jetset probe ID: 217028_at) in MCF-7 cells treated for 10 days with oestradiol (E2 control; 10^{-9} M), oestrogen deprivation (ED), tamoxifen (TAM; 10^{-7} M) and fulvestrant (FAS; 10^{-7} M). (B) Table displaying the corresponding fold change in gene expression and detection calls from the triplicate samples. (C) Table displaying the fold change increase in CXCR4 gene expression, detection calls and displaying whether the change in expression is statistically significant in tamoxifen-resistant (TAMR), fulvestrant-resistant (FASR) and oestrogen deprivation-resistant (XR) cell models compared to MCF-7 control. (D) PCR images from three independent experiments showing CXCR4 and β-actin mRNA expression in MCF-7 cells treated with E2, TAM, FAS and ED for 10 days. P: present; A: absent; * p <0.05 compared to E2-control; * suppressed versus control; ✓: p <0.05 compared to MCF-7 control.**

3.3.3.5 TSC22 domain family, member 3 (TSC22D3)

The log2 intensity plot revealed significant ($p < 0.05$) induction in expression of a gene encoding a glucocorticoid-induced leucine zipper protein, TSC22D3, following 10 day oestrogen deprivation, tamoxifen and fulvestrant treatment compared to E2-treated control (Figure 20A). This profile was parallel to the log2 expression values that showed predominantly absent expression of TSC22D3 in E2-treated control cells and present expression calls in antihormone-treated cells implying reliable detection of gene expression (Figure 20B).

TSC22D3 was also up regulated in FASR and XR cells, which was significant ($p < 0.05$) in the latter, compared to MCF-7 control (Figure 20C). Additionally, present detection calls were reported in these cell lines. Similar to CXCR4 expression, TSC22D3 was also down regulated in TAMR cells, with absent detection calls reported, compared to MCF-7 control (Figure 20C).

In agreement with the microarray profile, the PCR data demonstrated up regulation of TSC22D3 expression by all three antihormone treatments compared to E2-treated control (Figure 20D). Actin levels remained relatively constant following each treatment.

A

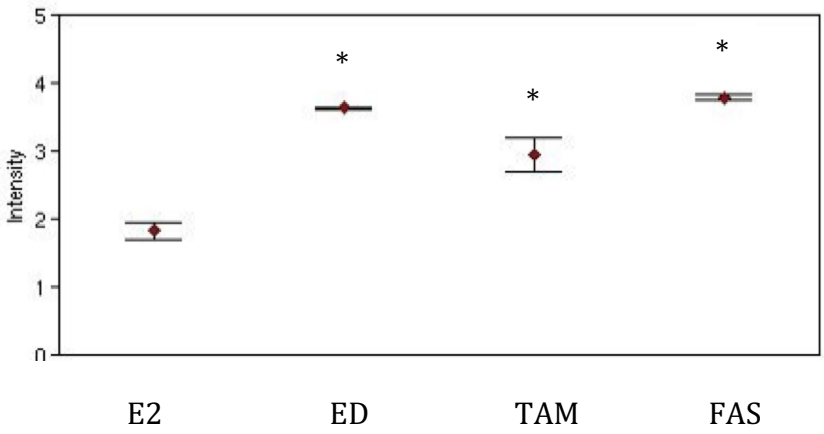

B

	E2-control	ED	TAM	FAS
Fold change		3.49	2.16	3.90
Detection call	AAP	PPP	PPP	PPP

C

	TAMR	FASR	XR
Fold change	1.84***	1.48	6.70
Detection call	AAA	PPP	PPP
P <0.05			✓

Continued on next page

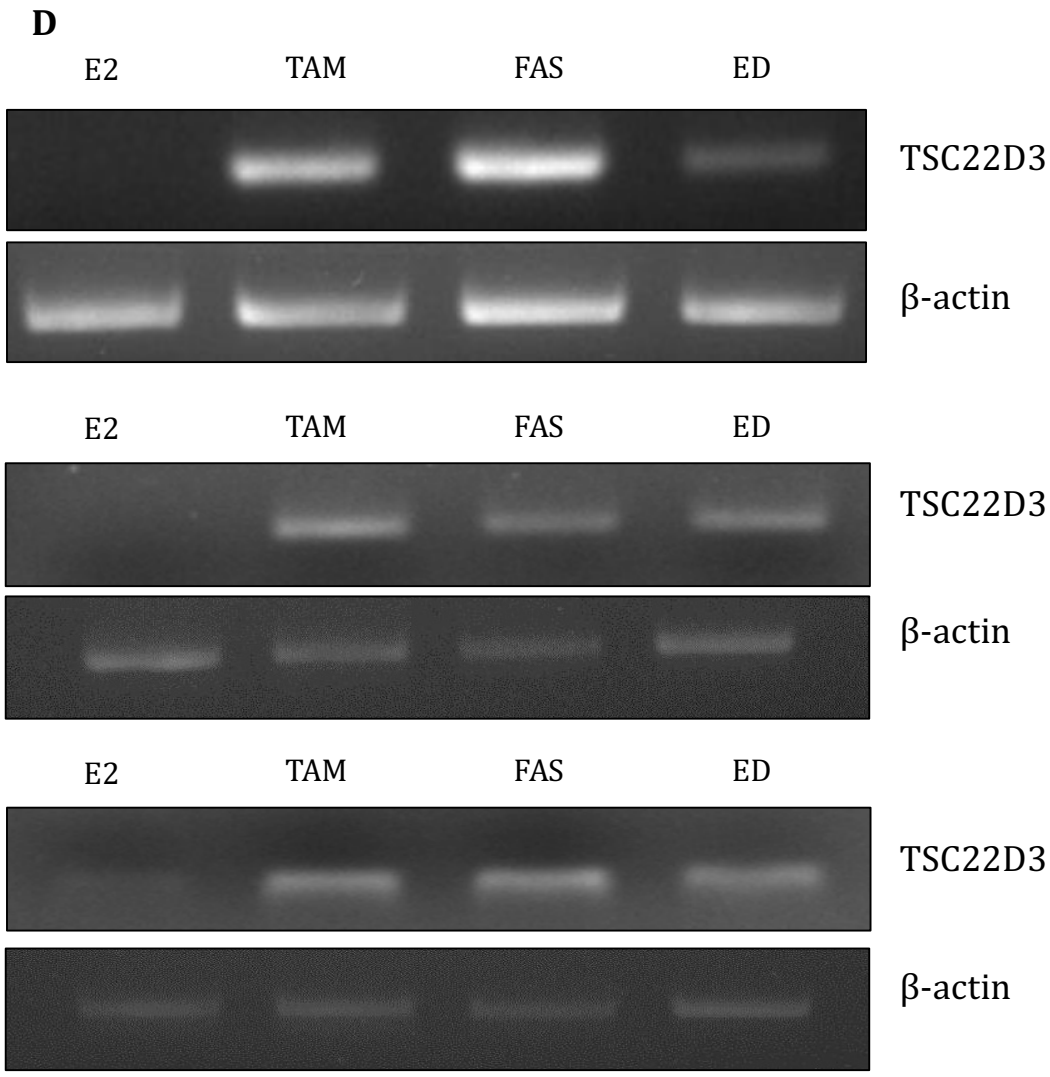

Figure 20 (A) Log2 intensity plot displaying the normalised (mean of three independent replicates ± SEM) gene expression of TSC22D3 (jetset probe ID: 208763_s_at) in MCF-7 cells treated for 10 days with oestradiol (E2 control; 10^{-9} M), oestrogen deprivation (ED), tamoxifen (TAM; 10^{-7} M) and fulvestrant (FAS; 10^{-7} M). (B) Table displaying the corresponding fold change in gene expression and detection calls from the triplicate samples. (C) Table displaying the fold change increase in TSC22D3 gene expression, detection calls and displaying whether the change in expression is statistically significant in tamoxifen-resistant (TAMR), fulvestrant-resistant (FASR) and oestrogen deprivation-resistant (XR) cell models compared to MCF-7 control. (D) PCR images from three independent experiments showing TSC22D3 and β-actin mRNA expression in MCF-7 cells treated with E2, TAM, FAS and ED for 10 days. P: present; A: absent; * p <0.05 compared to E2-control; * suppressed versus control; ✓: p <0.05 compared to MCF-7 control.**

3.3.3.6 B cell lymphoma 3 (BCL3)

Similar to TSC22D3 expression, BCL3 gene expression, which transcribes a protein involved in the regulation of NF-κB activity, was also significantly ($p < 0.05$) induced by all three antihormone treatments (Figure 21A). All detection calls identified the gene as being present in antihormone-treated cells indicating reliable detection of BCL3 gene expression. However, the log2 expression values of BCL3 in E2-treated cells failed to rise above 0 and a predominantly absent call was recorded suggesting relatively low/no expression of this gene following this treatment (Figure 21B). In resistance, BCL3 expression was significantly ($p < 0.05$) up regulated in all three antihormone-resistant cell lines, together with present detection calls recorded, versus MCF-7 control cells (Figure 21C).

In agreement with the log2-expression intensity plot generated from the microarray data, PCR revealed up regulation of BCL3 expression across all antihormone treatments with little expression detected in the E2-treated control cells while actin levels remained constant (Figure 21D). This profile mimicked the detection calls from the microarray analysis (Figure 21B).

A

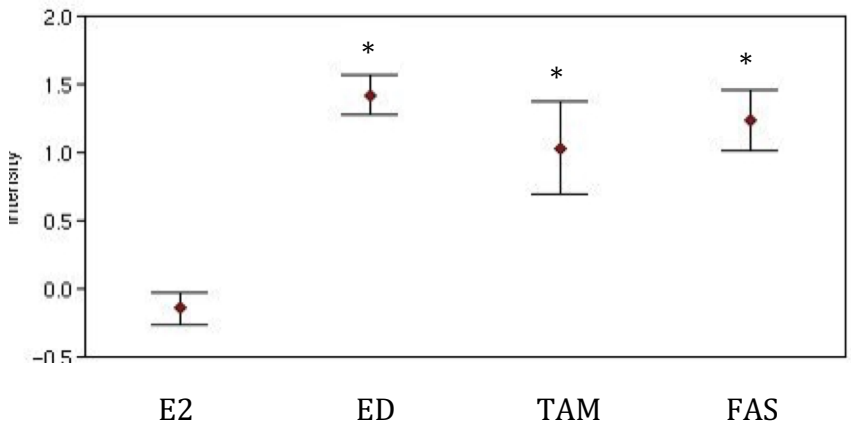

B

	E2-control	ED	TAM	FAS
Fold change		2.96	2.26	2.61
Detection call	AAP	PPP	PPP	PPP

C

	TAMR	FASR	XR
Fold change	3.23	3.63	2.43
Detection call	PPP	PPP	PPP
P <0.05	✓	✓	✓

Continued on next page

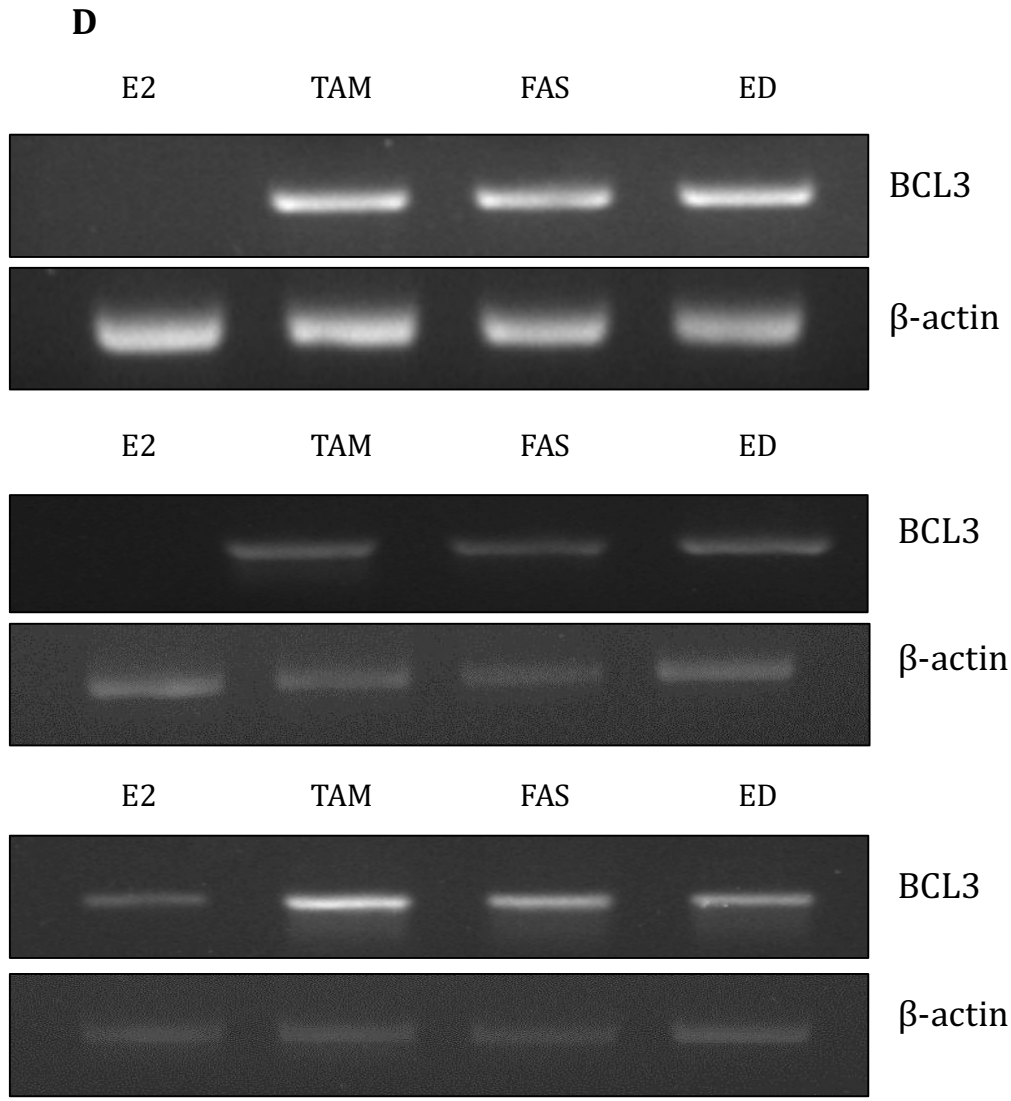

Figure 21 (A) Log2 intensity plot displaying the normalised (mean of three independent replicates ± SEM) gene expression of BCL3 (jetset probe ID: 204908_s_at) in MCF-7 cells treated for 10 days with oestradiol (E2 control; 10^{-9} M), oestrogen deprivation (ED), tamoxifen (TAM; 10^{-7} M) and fulvestrant (FAS; 10^{-7} M). (B) Table displaying the corresponding fold change in gene expression and detection calls from the triplicate samples. (C) Table displaying the fold change increase in BCL3 gene expression, detection calls and displaying whether the change in expression is statistically significant in tamoxifen-resistant (TAMR), fulvestrant-resistant (FASR) and oestrogen deprivation-resistant (XR) cell models compared to MCF-7 control. (D) PCR images from three independent experiments showing BCL3 and β-actin mRNA expression in MCF-7 cells treated with E2, TAM, FAS and ED for 10 days. P: present; A: absent; * p <0.05 compared to E2-control; ✓: p <0.05 compared to MCF-7 control.

3.3.3.7 BCL2-associated anthanogene (BAG1)

The log2 intensity profile demonstrated significant ($p < 0.05$) induction of BAG1 gene expression following oestrogen deprivation and fulvestrant treatment with slightly less induction mediated by tamoxifen treatment (Figure 22A). All detection calls indicated that the gene was present following the four treatments and the error bars were small (with the exception of tamoxifen), implying reproducible detection of gene expression in all samples (Figure 22B).

BAG1 expression was maintained through to resistance, represented by present detection calls in the three antihormone-resistant cells (Figure 22C). In the FASR and XR cell lines, BAG1 expression was significantly up regulated, whereas in the TAMR cells BAG1 expression was decreased, versus MCF-7 control (Figure 22C).

Antihormone-induced up regulation of BAG1 expression reported by the microarray data, was not successfully verified by PCR (Figure 22D). Indeed, similar to actin expression, BAG1 mRNA expression was relatively equal following all four treatments.

A

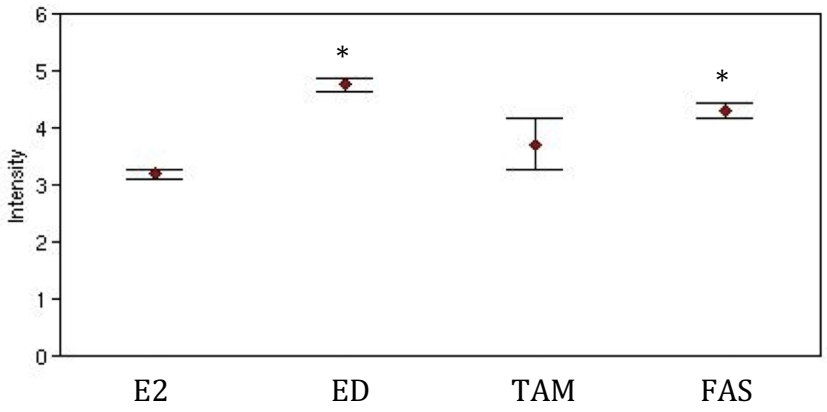

B

	E2-control	ED	TAM	FAS
Fold change		2.96	1.45	2.16
Detection call	PPP	PPP	PPP	PPP

C

	TAMR	FASR	XR
Fold change	1.91***	1.75	1.98
Detection call	PPP	PPP	PPP
P <0.05		✓	✓

Continued on next page

D

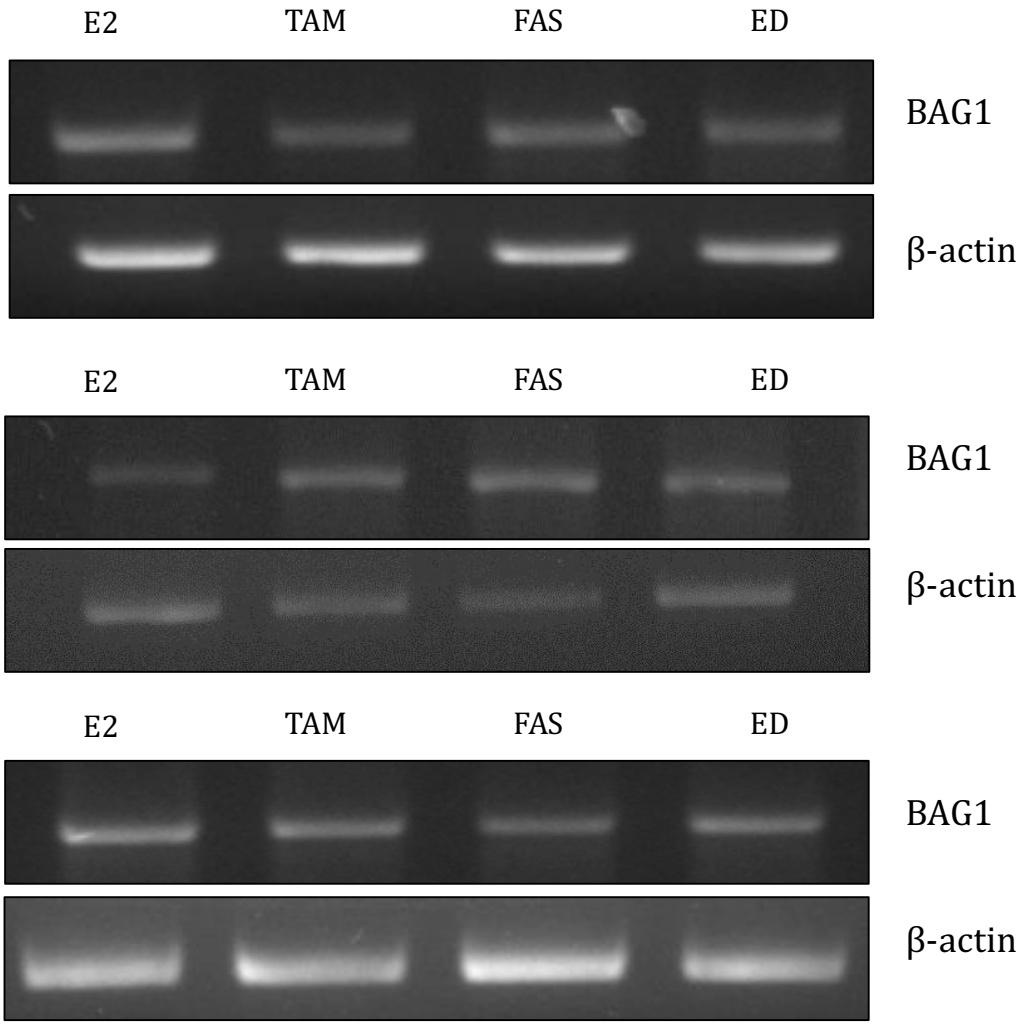

Figure 22 (A) Log2 intensity plot displaying the normalised (mean of three independent replicates ± SEM) gene expression of BAG1 (jetset probe ID: 202387_at) in MCF-7 cells treated for 10 days with oestradiol (E2 control; 10^{-9} M), oestrogen deprivation (ED), tamoxifen (TAM; 10^{-7} M) and fulvestrant (FAS; 10^{-7} M). (B) Table displaying the corresponding fold change in gene expression and detection calls from the triplicate samples. (C) Table displaying the fold change increase in BCL3 gene expression, detection calls and displaying whether the change in expression is statistically significant in tamoxifen-resistant (TAMR), fulvestrant-resistant (FASR) and oestrogen deprivation-resistant (XR) cell models compared to MCF-7 control. (D) PCR images from three independent experiments showing BAG1 and β-actin mRNA expression in MCF-7 cells treated with E2, TAM, FAS and ED for 10 days. P: present; * p <0.05 compared to E2-control; * suppressed versus control; ✓: p <0.05 compared to MCF-7 control.**

3.3.3.8 Insulin-like growth factor binding protein 5 (IGFBP5)

Although all antihormone treatments promoted up regulation of IGFBP5 gene expression, which encodes an IGFR binding protein, only tamoxifen and oestrogen deprivation treatments induced up regulation with a fold change greater than 1.5, with the latter additionally reaching significance ($p < 0.05$) (Figure 23A). Present detection calls across all four treatments were also reported, thus indicating reliable gene expression (Figure 23B).

IGFBP5 expression was maintained through to the acquisition of resistance, as demonstrated by the present detection calls reported in the three antihormone-resistant cells (Figure 23C). In the TAMR and XR cell lines, IGFBP5 was up regulated with a fold change greater than 1.5, with the latter also reaching significance ($p < 0.05$) (Figure 23C). In the FASR cells, IGFBP5 expression was down regulated compared to MCF-7 control (Figure 23C).

Subsequent PCR verification of IGFBP5 expression during antihormone response continued to fail, with no mRNA detected in MCF-7 cells irrespective of treatment (Figure 23D). Equal mRNA expression of actin was demonstrated following the four treatments.

A

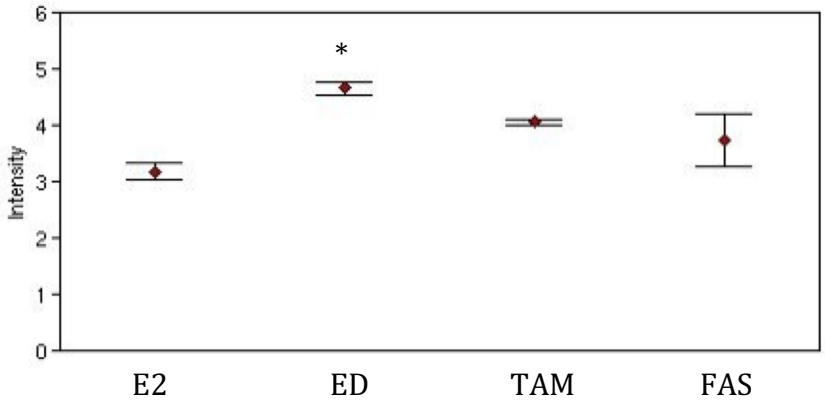

B

	E2-control	ED	TAM	FAS
Fold change		2.78	1.84	1.48
Detection call	PPP	PPP	PPP	PPP

C

	TAMR	FASR	XR
Fold change	1.76	2.06***	10.83
Detection call	PPP	PPP	PPP
P <0.05			✓

Continued on next page

D

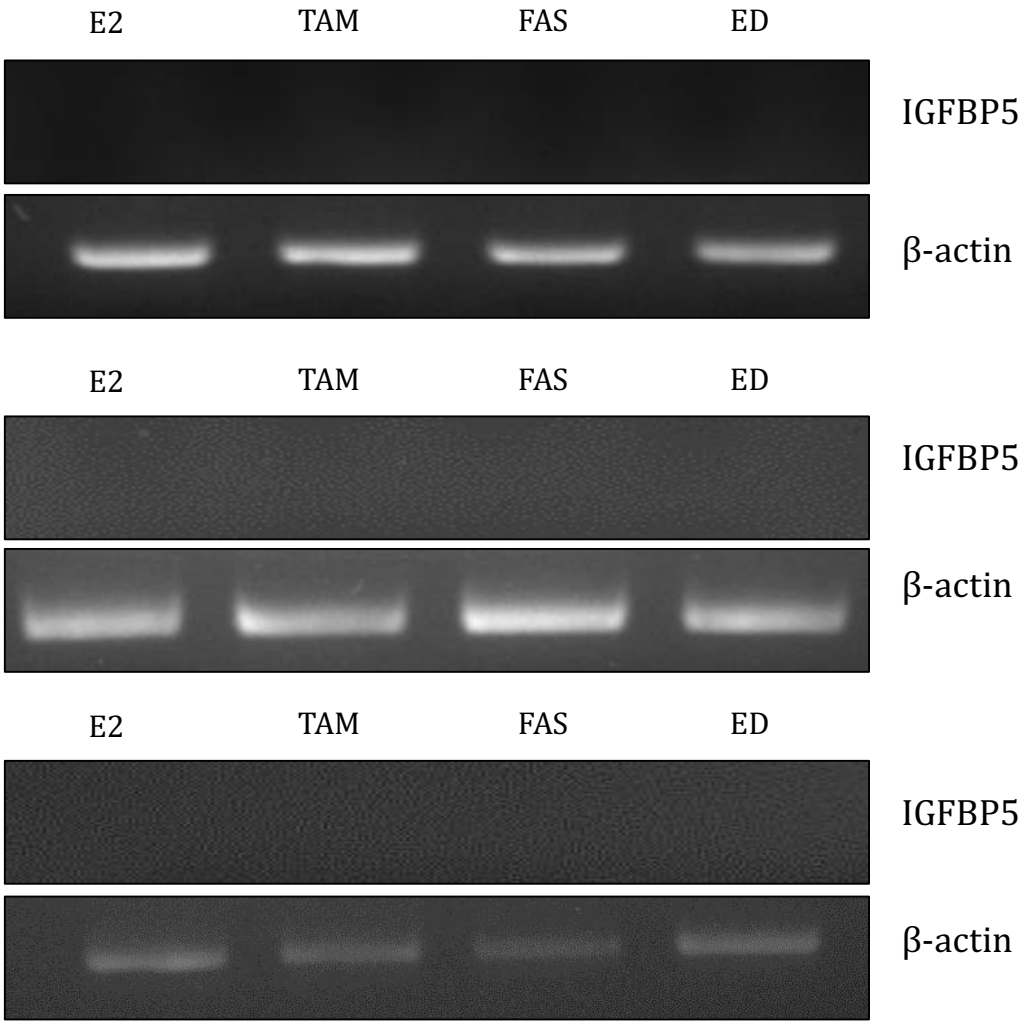

Figure 23 (A) Log2 intensity plot displaying the normalised (mean of three independent replicates ± SEM) gene expression of IGFBP5 (jetset probe ID: 211959_at) in MCF-7 cells treated for 10 days with oestradiol (E2 control; 10^{-9} M), oestrogen deprivation (ED), tamoxifen (TAM; 10^{-7} M) and fulvestrant (FAS; 10^{-7} M). (B) Table displaying the corresponding fold change in gene expression and detection calls from the triplicate samples. (C) Table displaying the fold change increase in IGFBP5 gene expression, detection calls and displaying whether the change in expression is statistically significant in tamoxifen-resistant (TAMR), fulvestrant-resistant (FASR) and oestrogen deprivation-resistant (XR) cell models compared to MCF-7 control. (D) PCR images from three independent experiments showing IGFBP5 and β-actin mRNA expression in MCF-7 cells treated with E2, TAM, FAS and ED for 10 days. P: present; * p <0.05 compared to E2-control; * suppressed versus control; ✓: p <0.05 compared to MCF-7 control.**

3.3.3.9 BCL2 like 1 (BCL2L1)

The log2 intensity profile demonstrated that all three antihormone treatments induced up regulation of BCL2L1 expression compared to E2-treated control (Figure 24A). BCL2L1 encodes a protein belonging to the BCL2 protein family. Oestrogen deprivation and fulvestrant treatments promoted the greatest induction of gene expression (fold change greater than 1.5) with the latter also reaching significance ($p < 0.05$). Tamoxifen promoted a lesser degree of up regulation of gene expression compared to the other antihormonal treatments, characterised by a 1.36 fold induction. The log2 expression values were all above 0 and present detection calls were reported for all four treatments (Figure 24B).

BCL2L1 was also up regulated in the three antihormone-resistant cell models, together with present detection calls reported, versus MCF-7 control (Figure 24C). The greatest up regulation was apparent in the FASR cells, characterised by a 2.51 fold induction.

In agreement with the microarray profile, tamoxifen, fulvestrant and oestrogen deprivation treatments induced up regulation of BCL2L1 mRNA expression compared to E2-treated control as determined by PCR (Figure 24D and E). Actin levels remained constant following the four treatments. Furthermore, fulvestrant induced the greatest up regulation of expression, which mimicked the microarray profile. Additionally, the microarray data reported 'present' detection calls (suggesting reliable detection of gene expression) across all four treatments. The PCR profile mirrored the detection calls, with mRNA expression detected in all treatments, although BCL2L1 expression was minimal in E2-treated cells (Figure 24D).

A

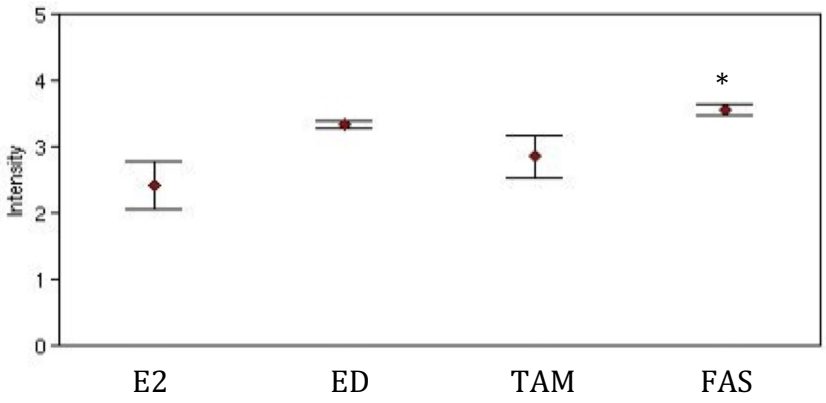

B

	E2-control	ED	TAM	FAS
Fold change		1.90	1.36	2.20
Detection call	PPP	PPP	PPP	PPP

C

	TAMR	FASR	XR
Fold change	1.61	2.51	1.25
Detection call	PPP	PPP	PPP
P <0.05			

Continued on next page

D

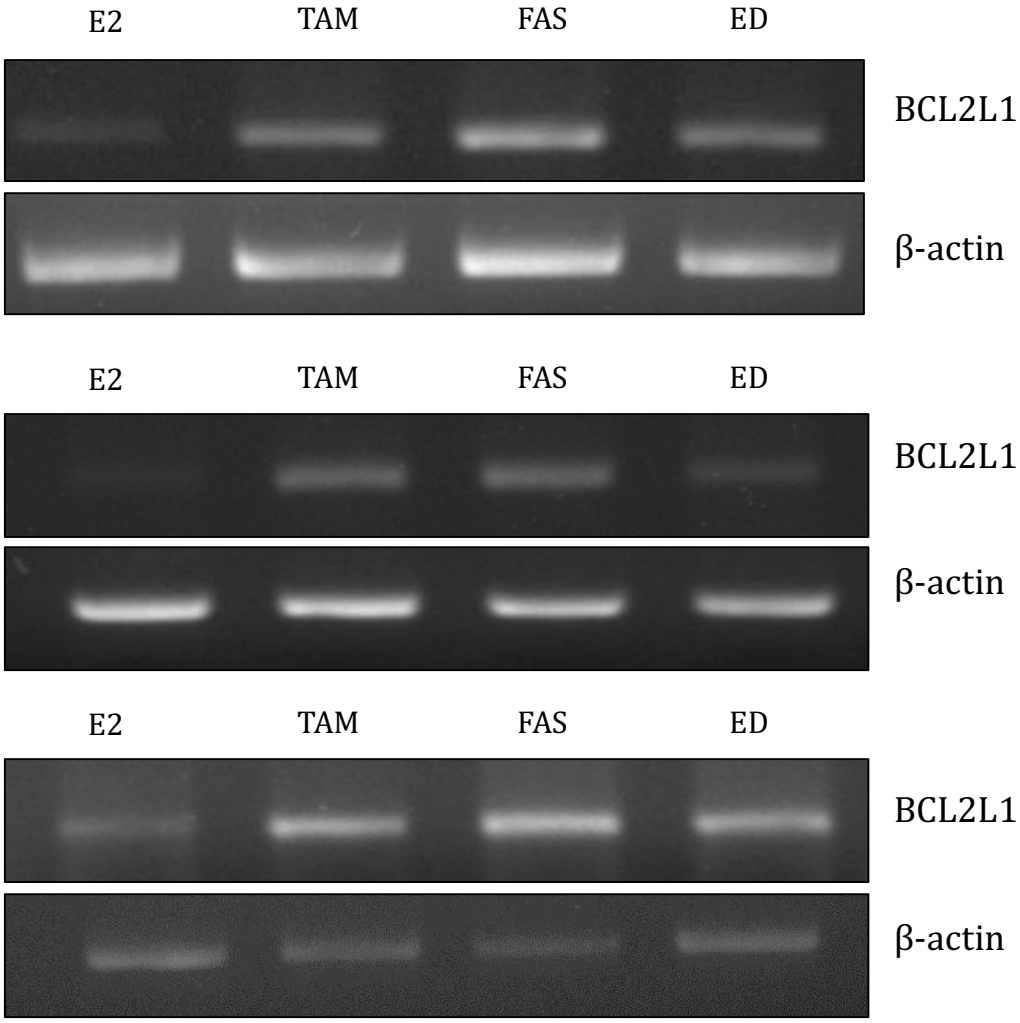

Figure 24 (A) Log2 intensity plot displaying the normalised (mean of three independent replicates ± SEM) gene expression of BCL2L1 (jetset probe ID: 212312_at) in MCF-7 cells treated for 10 days with oestradiol (E2 control; 10^{-9} M), oestrogen deprivation (ED), tamoxifen (TAM; 10^{-7} M) and fulvestrant (FAS; 10^{-7} M). (B) Table displaying the corresponding fold change in gene expression and detection calls from the triplicate samples. (C) Table displaying the fold change increase in BCL2L1 gene expression, detection calls and displaying whether the change in expression is statistically significant in tamoxifen-resistant (TAMR), fulvestrant-resistant (FASR) and oestrogen deprivation-resistant (XR) cell models compared to MCF-7 control. (D) PCR images from three independent experiments showing BCL2L1 and β-actin mRNA expression in MCF-7 cells treated with E2, TAM, FAS and ED for 10 days. P: present; * p <0.05 compared to E2-control.

3.3.3.10 Presenilin 1 (PSEN1)

The log2 intensity plot and associated fold changes showed antihormone-induced up regulation of PSEN1 expression, which encodes a presenilin protein, compared to E2-treated control (Figure 25A). Oestrogen deprivation and fulvestrant promoted significant ($p < 0.05$) up regulation of gene expression, whilst tamoxifen promoted only minimal induction represented by a 1.38 fold change. The error bars were small and present detection calls were reported in all treatments, implying reproducible detection of expression in all samples (Figure 25B).

PSEN1 expression was maintained through to the acquisition of resistance, represented by the present detection calls reported (Figure 25C). PSEN1 was up regulated in the TAMR and XR cell lines, and down regulated in the FASR cell line, versus MCF-7 control (Figure 25C).

The PCR of PSEN1 revealed antihormone-induced up regulation of expression compared to E2-control (Figure 25D), which is in agreement with the microarray data. In accordance with the 'present' detection calls identified in the microarray data, mRNA expression of PSEN1 was apparent following all four treatments (Figure 25D). Actin expression remained constant following all four treatments.

A

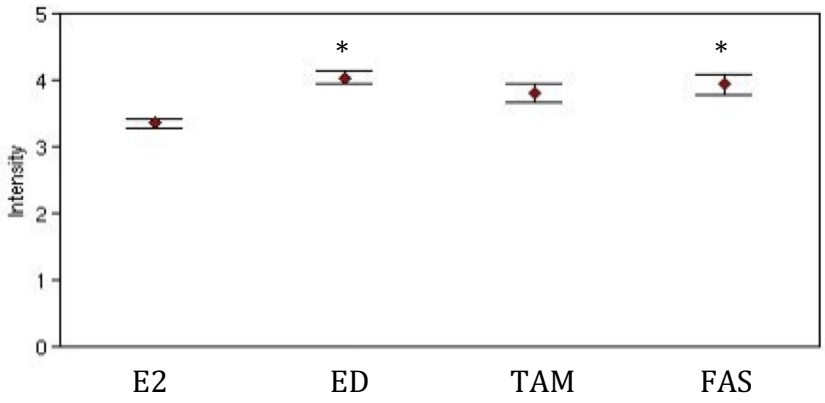

B

	E2-control	ED	TAM	FAS
Fold change		1.61	1.38	1.50
Detection call	PPP	PPP	PPP	PPP

C

	TAMR	FASR	XR
Fold change	1.05	1.38***	1.06
Detection call	PPP	PPP	PPP
P <0.05			

Continued on next page

D

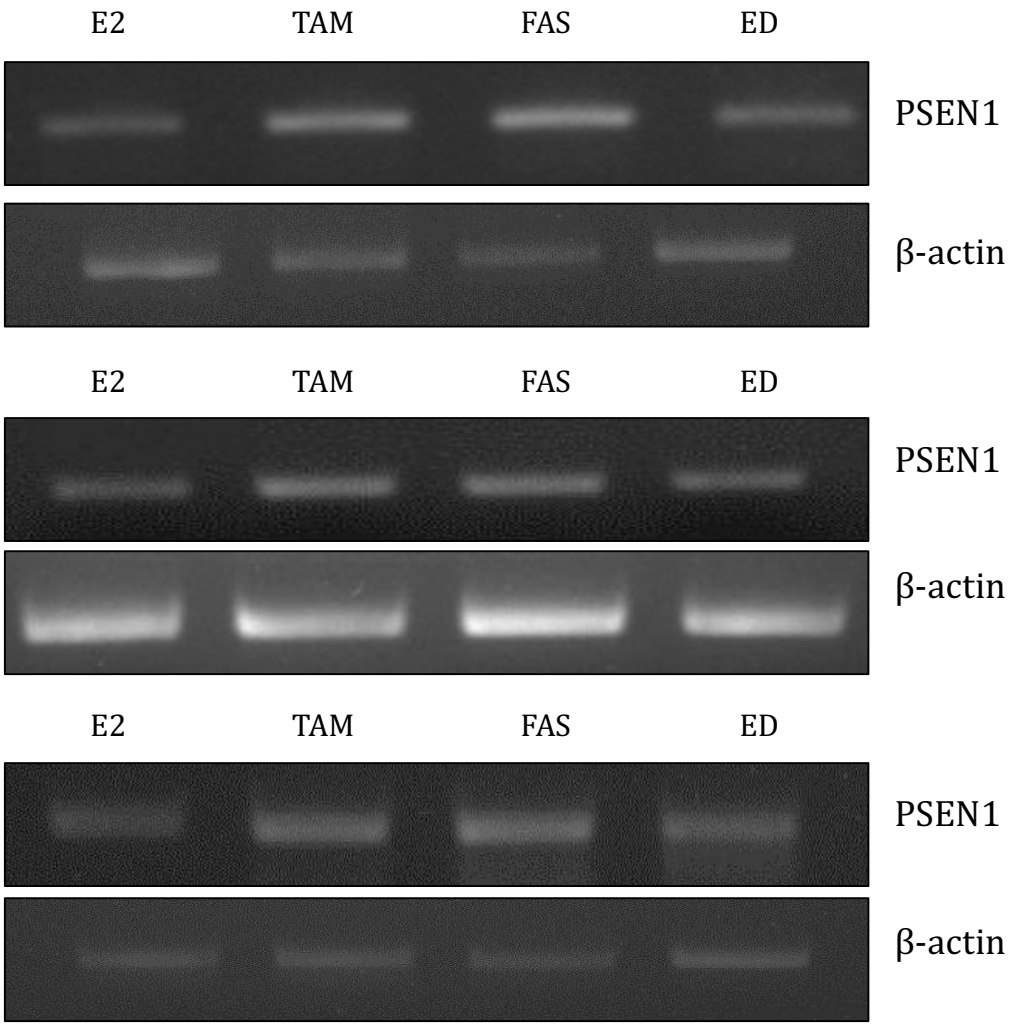

Figure 25 (A) Log2 intensity plot displaying the normalised (mean of three independent replicates ± SEM) gene expression of PSEN1 (jetset probe ID: 203460_s_at) in MCF-7 cells treated for 10 days with oestradiol (E2 control; 10^{-9} M), oestrogen deprivation (ED), tamoxifen (TAM; 10^{-7} M) and fulvestrant (FAS; 10^{-7} M). (B) Table displaying the corresponding fold change in gene expression and detection calls from the triplicate samples. (C) Table displaying the fold change increase in PSEN1 gene expression, detection calls and displaying whether the change in expression is statistically significant in tamoxifen-resistant (TAMR), fulvestrant-resistant (FASR) and oestrogen deprivation-resistant (XR) cell models compared to MCF-7 control. (D) PCR images from three independent experiments showing PSEN1 and β-actin mRNA expression in MCF-7 cells treated with E2, TAM, FAS and ED for 10 days. P: present; * p <0.05 compared to E2-control; * suppressed versus control.**

3.3.3.11 ELKS/RAB6-interacting/CAST family member 1 (ERC1)

The log2 intensity plot demonstrated significant ($p < 0.05$) up regulation of ERC1 gene expression (which encodes a protein belonging to the family of RIM-binding proteins) by fulvestrant and oestrogen deprivation treatments versus control, with the latter promoting the greatest induction represented by an almost 1.7 fold change (Figure 26A). Tamoxifen promoted up regulation of gene expression but this induction did not reach statistical significance. The log2 expression values were all above 0 and present detection calls were reported for all four treatments (Figure 26B).

ERC1 expression was up regulated in TAMR and FASR cells and down regulated in XR cells versus MCF-7 control (Figure 26C). Predominantly absent detection calls were reported in the TAMR and XR cell lines, whereas predominantly marginal calls were reported in the FASR cells (Figure 26C).

According to the PCR data, tamoxifen and fulvestrant induced up regulation of ERC1 expression compared to control (Figure 26D). However, oestrogen deprivation- and E2-treated cells exhibited comparable ERC1 expression. This was in partial disagreement with the microarray profile, which demonstrated that all three antihormones promoted up regulation of ERC1 gene expression, with the greatest induction mediated by oestrogen deprivation treatment (Figure 26A and B). Actin levels remained constant following all four treatments.

A

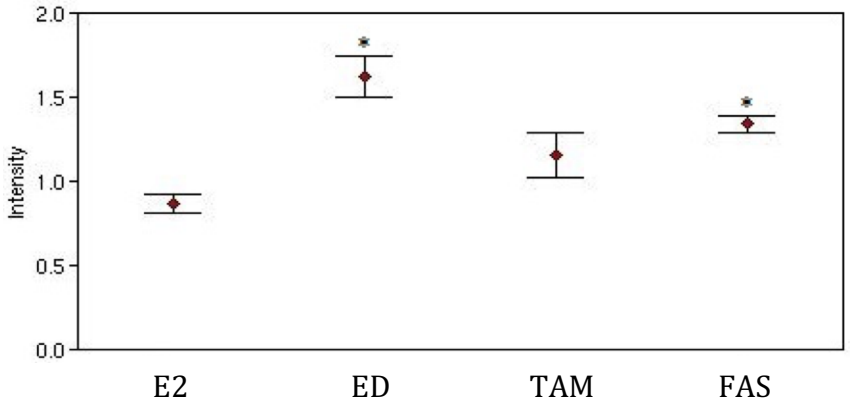

B

	E2-control	ED	TAM	FAS
Fold change		1.69	1.22	1.39
Detection call	PPP	PPP	PPP	PPP

C

	TAMR	FASR	XR
Fold change	1.10	1.15	1.24***
Detection call	APA	AMM	AAA
P <0.05			

Continued on next page

D

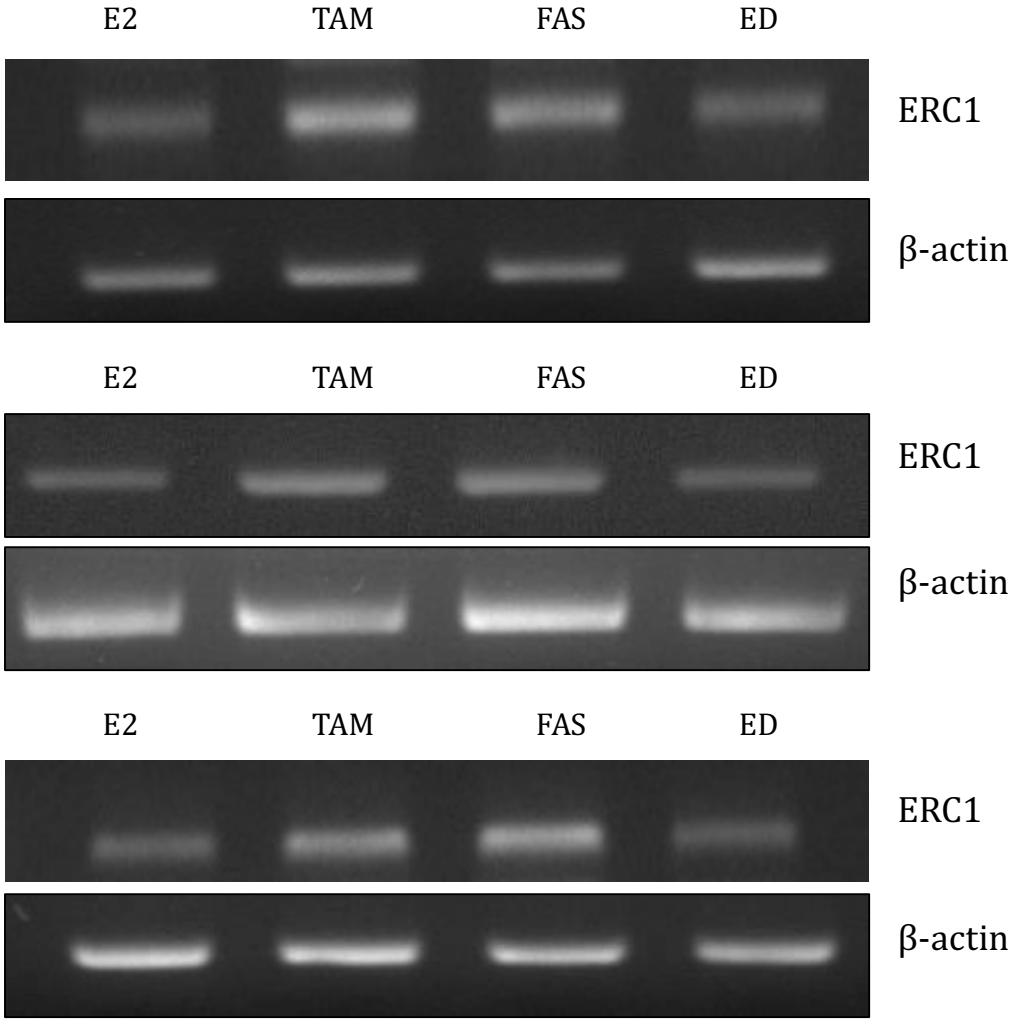

Figure 26 (A) Log2 intensity plot displaying the normalised (mean of three independent replicates ± SEM) gene expression of ERC1 (jetset probe ID: 215606_s_at) in MCF-7 cells treated for 10 days with oestradiol (E2 control; 10^{-9} M), oestrogen deprivation (ED), tamoxifen (TAM; 10^{-7} M) and fulvestrant (FAS; 10^{-7} M). (B) Table displaying the corresponding fold change in gene expression and detection calls from the triplicate samples. (C) Table displaying the fold change increase in ERC1 gene expression, detection calls and displaying whether the change in expression is statistically significant in tamoxifen-resistant (TAMR), fulvestrant-resistant (FASR) and oestrogen deprivation-resistant (XR) cell models compared to MCF-7 control. (D) PCR images from three independent experiments showing ERC1 and β-actin mRNA expression in MCF-7 cells treated with E2, TAM, FAS and ED for 10 days. P: present; M: marginal; A: absent; * p <0.05 and ** p <0.01 compared to E2-control; * suppressed versus control.**

3.3.3.12 Dimethylarginine dimethylaminohydrolase 2 (DDAH2)

The log2 intensity profile demonstrated up regulation of DDAH2 gene expression following 10 day oestrogen deprivation and fulvestrant treatment compared to E2-treated control with fold change inductions greater than 1.5 (Figure 27A). DDAH2 encodes a dimethylarginine dimethylaminohydrolase, which functions in nitric oxide generation[315]. Tamoxifen promoted only minimal induction of gene expression. All detection calls were reported as present, implying reliable detection of gene expression (Figure 27B). DDAH2 expression was maintained through to the development of resistance, as demonstrated by the present detection calls reported in the three antihormone-resistant cell lines (Figure 27C). DDAH2 was up regulated in the FASR cells and down regulated in the TAMR and XR cells versus MCF-7 control.

However, it is apparent that the jetset probe did not detect significant up regulation of DDAH2 by any antihormone treatment. In accordance with the initial filtering stages applied to the microarray data (i.e. significant induction of gene expression by at least one antihormone treatment; Figure 13), identification of DDAH2 arose from a non-jetset gene probe (215537_x_at). Indeed, this gene probe exhibited a very similar antihormone-induced profile to the jetset probe, with significant ($p < 0.05$) induction of DDAH2 expression following oestrogen deprivation treatment (Figure 28A). Additionally, in agreement with the jetset probe, predominantly present detection calls were reported following E2 and antihormone treatments (Figure 28B). In resistance, DDAH2 expression was significantly ($p < 0.05$) up regulated in FASR cells, together with present detection calls, versus MCF-7 control (Figure 28C). In XR cells, DDAH2 was also up regulated yet to a lesser degree than in FASR cells, along with present detection calls reported (Figure 28C). In TAMR cells, DDAH2 was significantly ($p < 0.05$) down regulated, with absent calls reported, compared to MCF-7 control (Figure 28C).

Although the microarray data revealed antihormone-induced up regulation of DDAH2 gene expression, particularly following oestrogen deprivation and fulvestrant treatments, this profile was not verified by PCR (Figure 28D). Indeed, PCR revealed comparable expression of DDAH2 following all four treatments and actin levels remained constant. In accordance with the 'present' detection calls

reported from the microarray data, DDAH2 mRNA expression was apparent following all four treatments (Figure 28D).

A

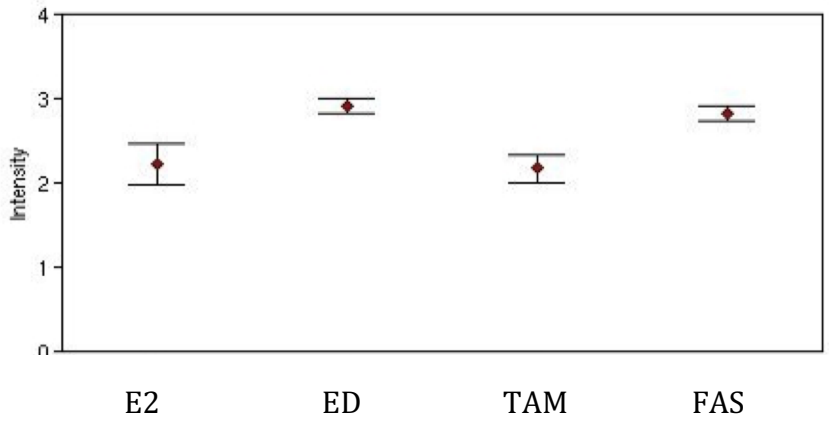

B

	E2-control	ED	TAM	FAS
Fold change		1.61	1.04	1.51
Detection call	PPP	PPP	PPP	PPP

C

	TAMR	FASR	XR
Fold change	1.57***	1.37	1.07***
Detection call	PPP	PPP	PPP
P <0.05			

Figure 27 (A) Log2 intensity plot displaying the normalised (mean of three independent replicates ± SEM) gene expression of DDAH2 (jetset probe ID: 214909_s_at) in MCF-7 cells treated for 10 days with oestradiol (E2 control; 10^{-9} M), oestrogen deprivation (ED), tamoxifen (TAM; 10^{-7} M) and fulvestrant (FAS; 10^{-7} M). (B) Table displaying the corresponding fold change in gene expression and detection calls from the triplicate samples. (C) Table displaying the fold change increase in DDAH2 gene expression, detection calls and displaying whether the change in expression is statistically significant in tamoxifen-resistant (TAMR), fulvestrant-resistant (FASR) and oestrogen deprivation-resistant (XR) cell models compared to MCF-7 control. P: present; * suppressed versus control.**

A

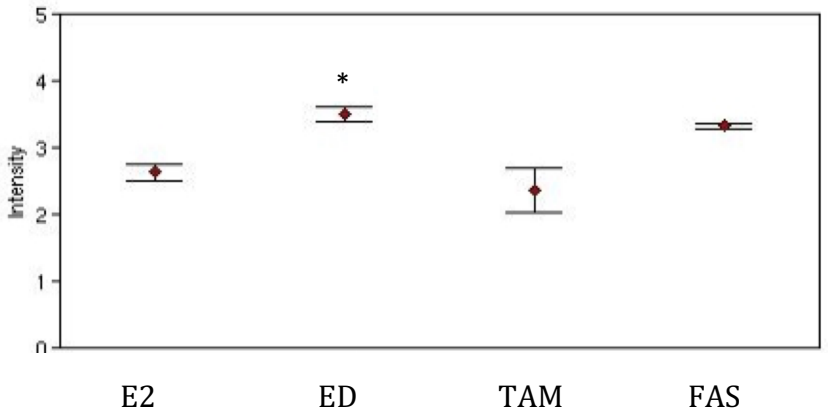

B

	E2-control	ED	TAM	FAS
Fold change		1.83	1.20	1.62
Detection call	APP	PPP	MPP	PPP

C

	TAMR	FASR	XR
Fold change	2.11***	1.63	1.07
Detection call	AAA	PPP	PPP
P <0.05	✓	✓	

Continued on next page

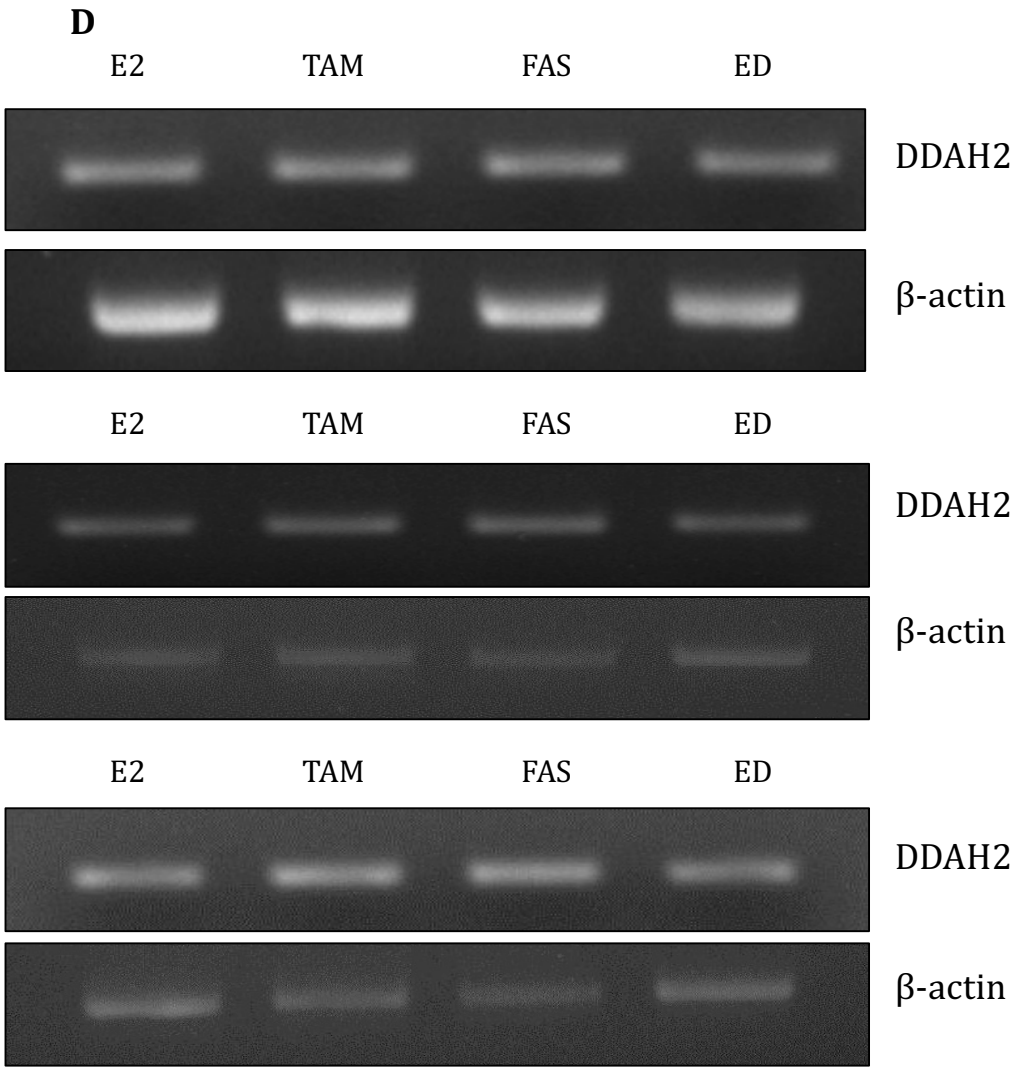

Figure 28 (A) Log2 intensity plot displaying the normalised (mean of three independent replicates ± SEM) gene expression of DDAH2 (probe ID: 215537_x_at) in MCF-7 cells treated for 10 days with oestradiol (E2 control; 10^{-9} M), oestrogen deprivation (ED), tamoxifen (TAM; 10^{-7} M) and fulvestrant (FAS; 10^{-7} M). (B) Table displaying the corresponding fold change in gene expression and detection calls from the triplicate samples. (C) Table displaying the fold change increase in DDAH2 gene expression, detection calls and displaying whether the change in expression is statistically significant in tamoxifen-resistant (TAMR), fulvestrant-resistant (FASR) and oestrogen deprivation-resistant (XR) cell models compared to MCF-7 control. (D) PCR images from three independent experiments showing DDAH2 and β-actin mRNA expression in MCF-7 cells treated with E2, TAM, FAS and ED for 10 days. P: present; M: marginal; A: absent; * $p < 0.05$ compared to E2-control; * suppressed versus control; ✓: $p < 0.05$ compared to MCF-7 control.**

3.3.3.13 AKT1

The log2 intensity plot demonstrated significant ($p < 0.05$) induction of AKT1 expression, which encodes a serine-threonine protein kinase, following oestrogen deprivation therapy compared to E2-treated control (Figure 29A). Fulvestrant promoted some induction of gene expression (fold change less than 1.5) whilst tamoxifen promoted very little, if any, induction compared to E2-treated control. All detection calls were recorded as present, suggesting reliable detection of expression (Figure 29B). In resistance, AKT1 expression was significantly ($p < 0.05$) up regulated in all three antihormone-resistant cell lines, together with present detection calls reported, versus MCF-7 control (Figure 29C).

The PCR data revealed a small induction of AKT1 expression following fulvestrant and tamoxifen treatment (Figure 29D). Oestrogen deprivation failed to induce up regulation of AKT1 expression compared to E2-treated control. Indeed the mRNA expression of AKT1 was comparable in these two samples (Figure 29D). Actin levels remained constant. However, the AKT1 mRNA profile was in disagreement with the microarray profile, where oestrogen deprivation treatment was shown to induce the greatest and significant induction of AKT1 gene expression compared to E2-treated control (Figure 29A).

A

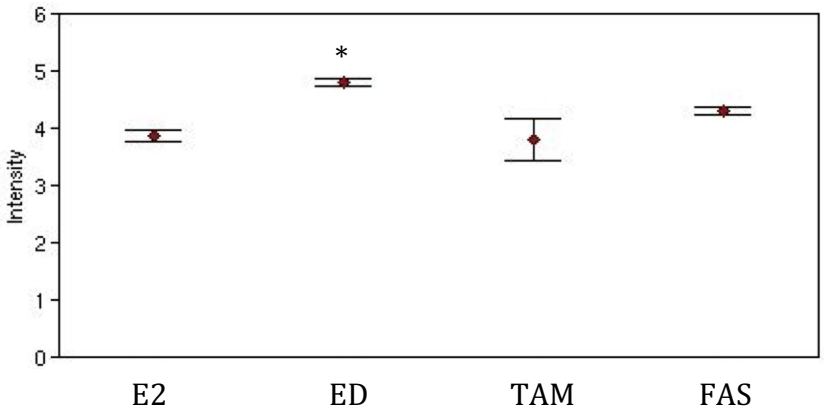

B

	E2-control	ED	TAM	FAS
Fold change		1.90	1.04	1.36
Detection call	PPP	PPP	PPP	PPP

C

	TAMR	FASR	XR
Fold change	2.76	2.12	2.67
Detection call	PPP	PPP	PPP
P <0.05	✓	✓	✓

Continued on next page

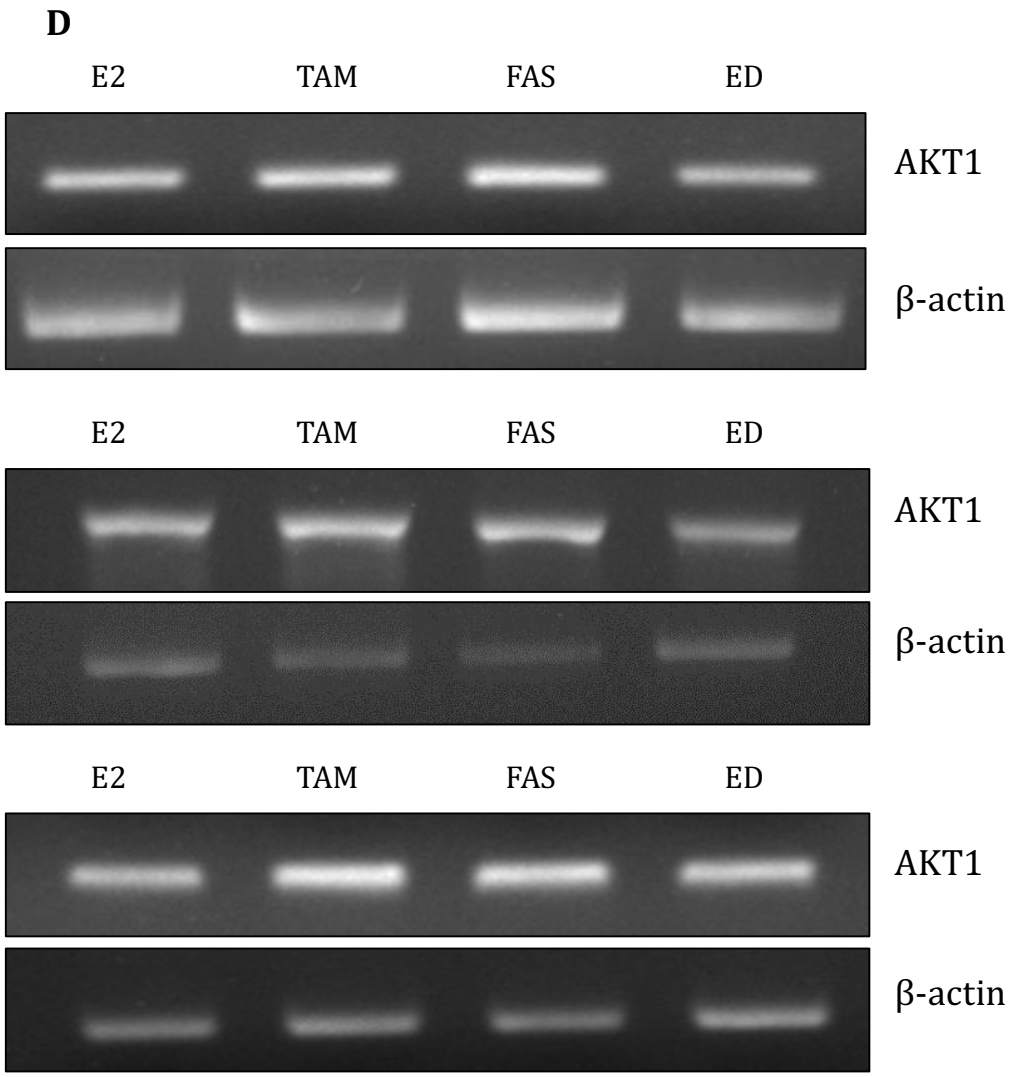

Figure 29 (A) Log2 intensity plot displaying the normalised (mean of three independent replicates ± SEM) gene expression of AKT1 (jetset probe ID: 207163_s_at) in MCF-7 cells treated for 10 days with oestradiol (E2 control; 10^{-9} M), oestrogen deprivation (ED), tamoxifen (TAM; 10^{-7} M) and fulvestrant (FAS; 10^{-7} M). (B) Table displaying the corresponding fold change in gene expression and detection calls from the triplicate samples. (C) Table displaying the fold change increase in AKT1 gene expression, detection calls and displaying whether the change in expression is statistically significant in tamoxifen-resistant (TAMR), fulvestrant-resistant (FASR) and oestrogen deprivation-resistant (XR) cell models compared to MCF-7 control. (D) PCR images from three independent experiments showing AKT1 and β-actin mRNA expression in MCF-7 cells treated with E2, TAM, FAS and ED for 10 days. P: present; * p <0.05 compared to E2-control; ✓: p <0.05 compared to MCF-7 control.

3.3.3.14 Hepatitis B virus X-interacting protein (HBXIP)

Oestrogen deprivation induced significant ($p < 0.05$) up regulation of HBXIP gene expression as demonstrated by the log2 intensity plot versus E2-treated control (Figure 30A). HBXIP was originally identified through its interaction with hepatitis B virus X protein[316]. Fulvestrant induced some expression of HBXIP, whilst tamoxifen promoted very little, if any, expression compared to E2-treated control. HBXIP expression was present in all treatments, including the control, as demonstrated by the present detection calls (Figure 30B). Present detection calls were maintained through to the acquisition of resistance to all three antihormones (Figure 30C). HBXIP expression was up regulated in FASR and XR cells, and down regulated in TAMR cells, compared to MCF-7 control (Figure 30C).

Although the microarray data revealed antihormone-induced up regulation of HBXIP gene expression, particularly by oestrogen deprivation and fulvestrant treatments, this profile was not verified by PCR (Figure 30D). Indeed, PCR revealed comparable expression of HBXIP following E2 and the three antihormone treatments (Figure 30D). Actin levels remained constant.

A

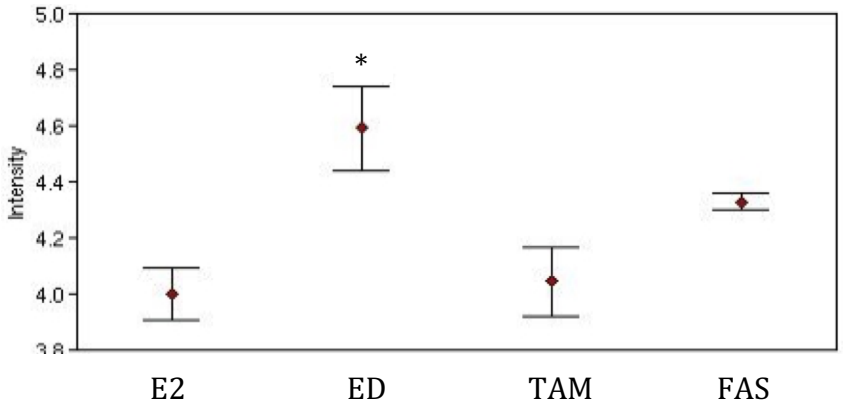

B

	E2-control	ED	TAM	FAS
Fold change		1.51	1.03	1.26
Detection call	PPP	PPP	PPP	PPP

C

	TAMR	FASR	XR
Fold change	1.37***	1.17	1.25
Detection call	PPP	PPP	PPP
P <0.05			

Continued on next page

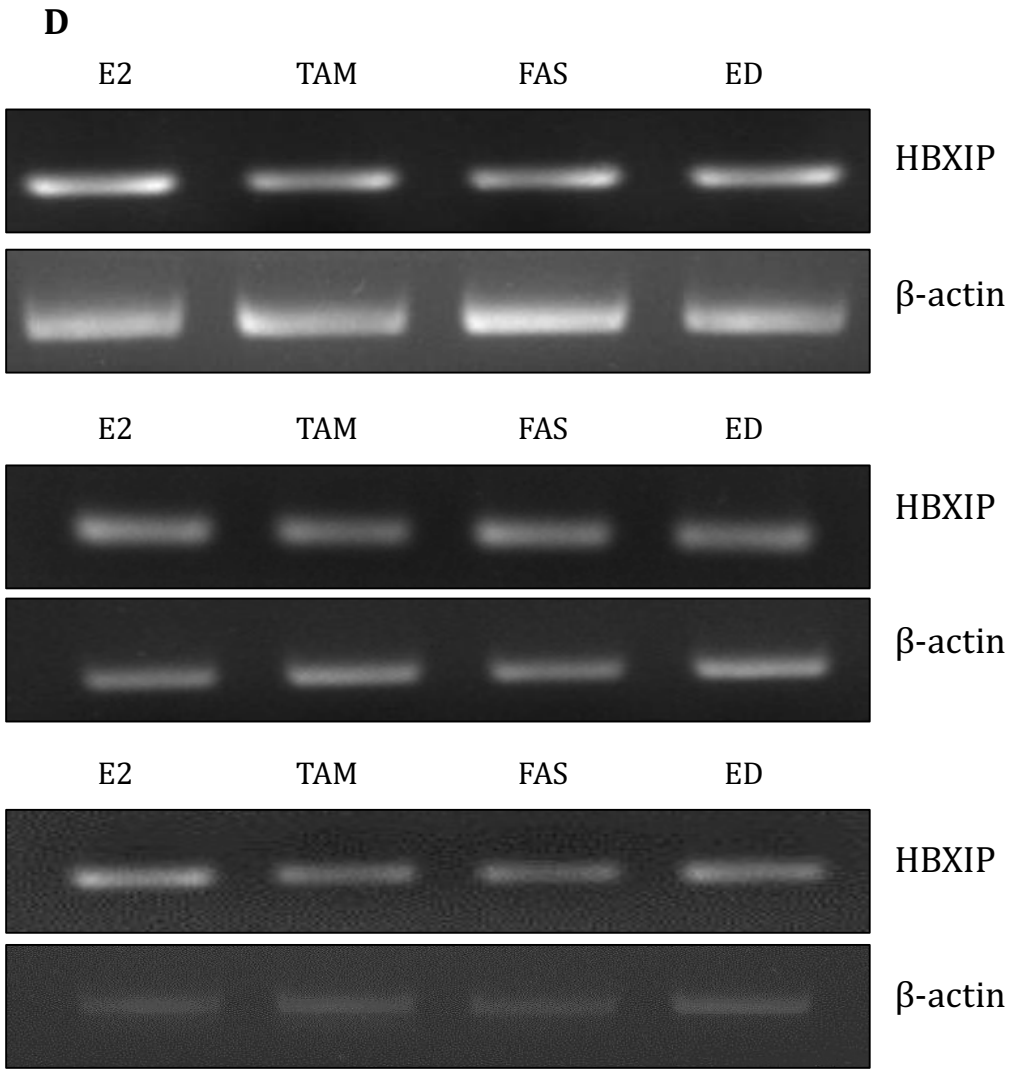

Figure 30 (A) Log2 intensity plot displaying the normalised (mean of three independent replicates ± SEM) gene expression of HBXIP (jetset probe ID: 202299_s_at) in MCF-7 cells treated for 10 days with oestradiol (E2 control; 10^{-9} M), oestrogen deprivation (ED), tamoxifen (TAM; 10^{-7} M) and fulvestrant (FAS; 10^{-7} M). (B) Table displaying the corresponding fold change in gene expression and detection calls from the triplicate samples. (C) Table displaying the fold change increase in HBXIP gene expression, detection calls and displaying whether the change in expression is statistically significant in tamoxifen-resistant (TAMR), fulvestrant-resistant (FASR) and oestrogen deprivation-resistant (XR) cell models compared to MCF-7 control. (D) PCR images from three independent experiments showing HBXIP and β-actin mRNA expressio in MCF-7 cells treated with E2, TAM, FAS and ED for 10 days. P: present; * p <0.05 compared to E2-control; * suppressed versus control.**

3.3.4 Identification of genes significantly induced by all three antihormone treatments versus control

Following extensive analysis of microarray gene expression profiles combined with a stringent filtering strategy, supported by PCR verification, 14 antihormone-induced genes were identified with increased expression maintained into resistance. It was hypothesised that these genes could allow a cohort of breast cancer cells to survive the growth inhibitory actions of antihormones and ultimately contribute substantially to the development of resistance. To prioritise these genes further, those identified by the microarray data to be significantly induced by all three antihormone treatments were considered for further investigation. The Venn diagram shown in Figure 31, constructed from the microarray data, identifies 5 genes (GABBR2, CTNND2, CLU, TSC22D3 and BCL3), which were significantly induced by all three antihormone treatments. The rationale was that continued study of these genes may ultimately lead to the identification of a resistance mechanism common to three antihormone therapies used clinically. Furthermore, such studies may identify a potential therapeutic target or novel biomarker of resistance exhibited by a large cohort of patients. Interestingly, as illustrated in the Venn diagram, not one gene was significantly induced by tamoxifen only.

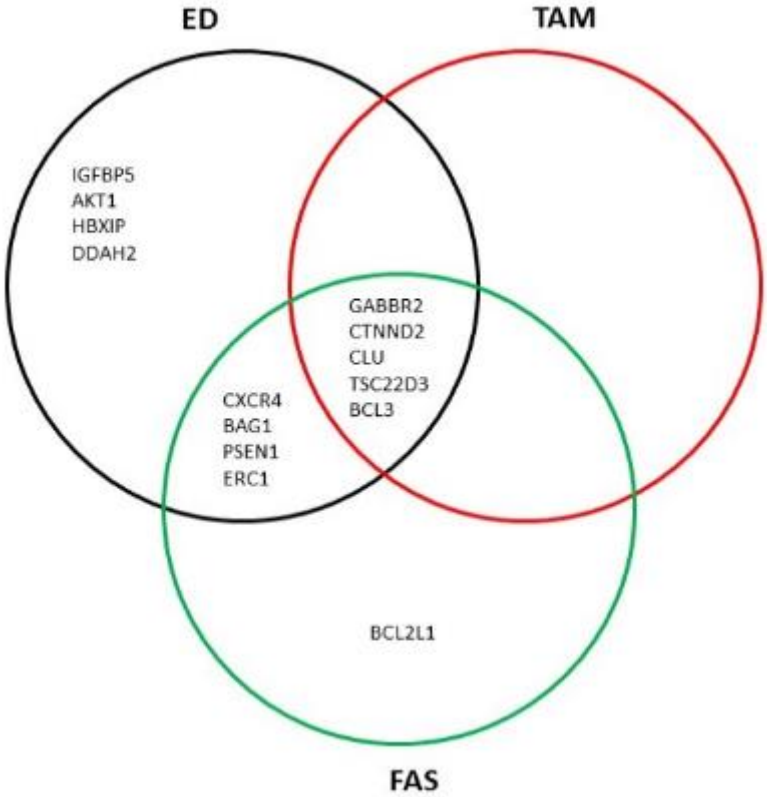

Figure 31 Venn diagram of the 14 genes significantly upregulated by 10 day antihormone treatment versus E2-treated control. ED: oestrogen deprivation; TAM: tamoxifen; FAS: fulvestrant.

3.3.5 Ontological investigation of the potential antihormone-induced pro-survival genes

Ontological studies were also performed on the 5 genes of interest to determine their:

1. Function
2. Association with breast cancer and antihormone response and resistance
3. Association with other cancers
4. Known or potential pro-survival role which may ultimately contribute to the emergence of antihormone resistance

This information is collated in Table 9 to Table 13.

3.3.5.1 GABBR2

Table 9 Summary of the function of GABBR2 including its previously reported association with breast and other cancers and potential pro-survival role.

Gene name	Gamma-aminobutyeic acid type B receptor, 2
Function	Gamma-aminobutyric acid (GABA) B receptors belong to the C family of G-protein coupled receptors (GPCRs). GABA-mediated activation of these receptors inhibits neuronal activity by activating G proteins and their downstream effectors. GABA B receptors are heterodimers composed of GABBR1 and GABBR2 subunits, both of which are believed to be required for normal receptor function[317].
Associations with breast cancer	GABA is synthesised predominantly from glutamate by glutamate decarboxylase (GAD). Both GABA content and GAD activity are increased in breast tumour tissue compared to normal tissue[318]. Furthermore, activation of GABA B receptors has been shown to promote breast cancer cell invasion and metastasis by promoting phosphorylation of ERK 1/2 and subsequently increasing the expression of matrix metalloproteinase-2 (MMP-2)[319]. MMP-2 positivity is associated with progression of breast cancer and poorer patient outlook[320].
Associations with other cancers	Increased GABA content and GAD activity have also been shown in colon[321], stomach[322], thyroid[323] and ovarian cancers[324]. In prostate cancer, activation of GABA B receptors has been shown to increase the invasive ability of tumour cells by promoting MMP-3 production[325].
Pro-survival role	GABA B receptors in neuronal cells have been shown to transactivate IGF-1R to induce AKT phosphorylation and downstream survival signalling to protect neurons from apoptosis[326].

As described in Table 9, GABA B receptors are heterodimers comprised of GABBR1 and GABBR2 subunits and both of which are reported to be required for normal receptor function. Thus, expression of GABBR1 in parallel with GABBR2 may indirectly suggest receptor dimerisation and normal function. Using the jetset gene probe (205890_s_at) for GABBR1, the microarray expression level of this gene was analysed in MCF-7 cells following antihormone treatment and in the antihormone-resistant cell models. The heatmap shown in Figure 32A suggests that 10 day fulvestrant treatment down regulated GABBR1 expression, whereas oestrogen deprivation and tamoxifen had no effect on gene expression compared to E2-treated control. The log2 expression values failed to reach 0, indicative of very low gene expression (Figure 32B). In antihormone-resistance, the heatmaps shown in Figure 33A suggests that GABBR1 expression is up regulated in TAMR cells, with very little change in expression apparent in the XR and FASR cells, compared to MCF-7 control. However, the log2 expression values failed to reach 0, indicative of very low gene expression (Figure 33B).

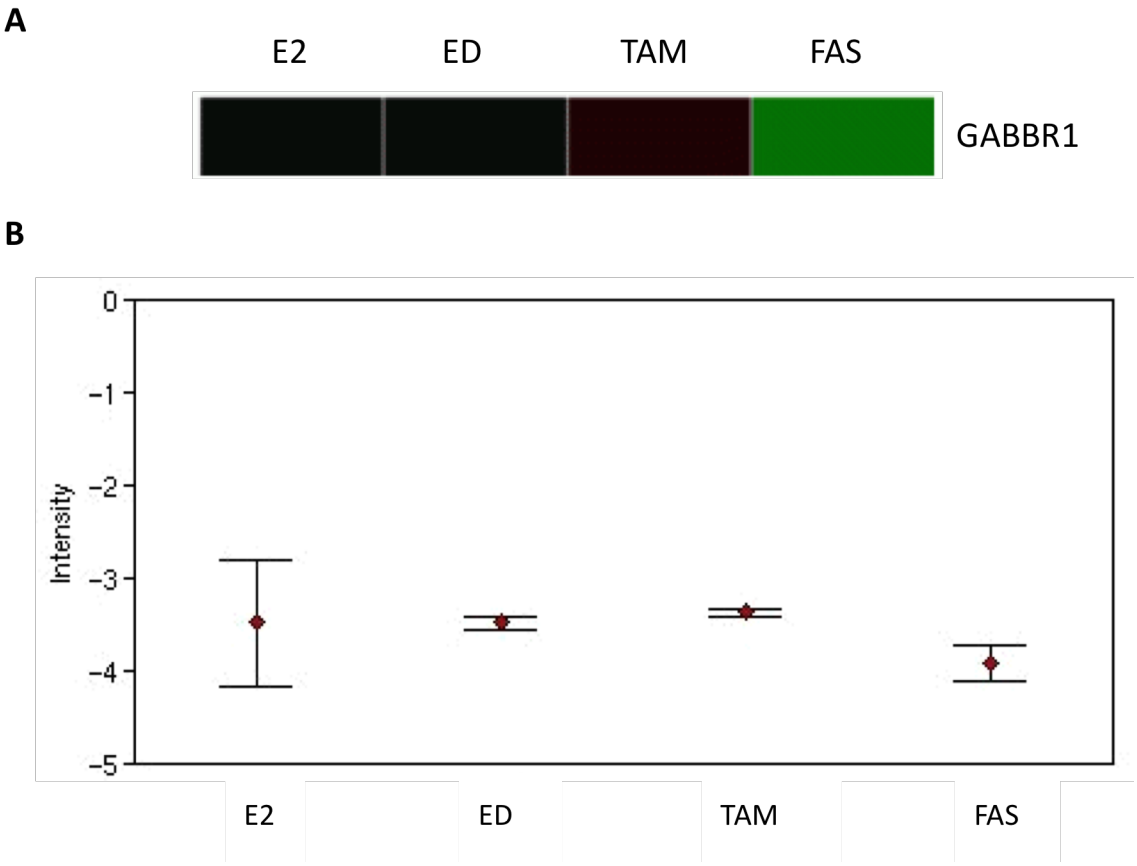

Figure 32 (A) Heatmap displaying the change in expression of GABBR1 (jetset probe ID: 205890_s_at) following 10 day oestradiol (E2 control; 10^{-9} M), oestrogen deprivation (ED), tamoxifen (TAM; 10^{-7} M) and fulvestrant (FAS; 10^{-7} M) treatment in MCF-7 cells. Red denotes an increase, and green denotes a decrease, in gene expression compared to control (shown in black). (B) Corresponding log2 intensity plot displaying the normalised (mean of three independent replicates ± SEM) gene expression of GABBR1.

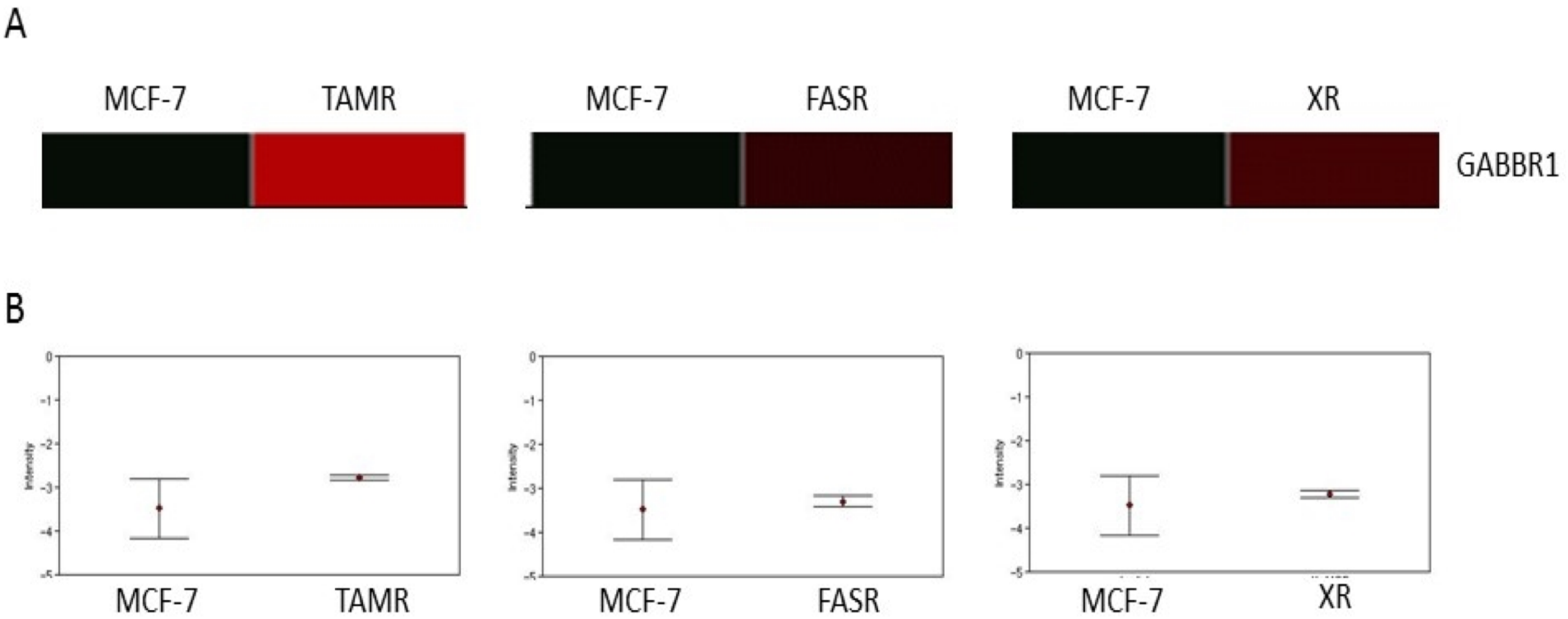

Figure 33 (A) Heatmaps displaying the change in expression of GABBR1 (jetset probe ID: 205890_s_at) in tamoxifen-resistant (TAMR), fulvestrant-resistant (FASR) and oestrogen deprivation-resistant (XR) cells versus MCF-7 cells. Red denotes an increase in gene expression compared to control (shown in black). (B) Corresponding log2 intensity plot displaying the normalised (mean of three independent replicates ± SEM) gene expression of GABBR1.

Furthermore, GABA, the ligand for the receptor must be produced by the cells to promote receptor activation. GABA is synthesised from glutamate by GAD enzyme. Thus it was hypothesised that increased GAD expression may indirectly suggest increased GABA levels. The expression of the two isoforms of GAD, GAD1 and GAD2, (using the jetset probes 206669_at and 216651_s_at, respectively) were next analysed in antihormone-treated MCF-7 cells. The heatmaps shown in Figure 34A reveal that oestrogen deprivation treatment induced up regulation of GAD2 expression, whereas tamoxifen and fulvestrant promoted down regulation of the gene compared to E2-treated control. GAD1 expression was down regulated by all three antihormone treatments, with the greatest down regulation induced by oestrogen deprivation and fulvestrant treatments compared to the control. The log2 intensity profiles (Figure 34B and C) mirror the heatmaps. However, the majority of log2 expression values did not reach above 0 suggesting very little gene expression.

Following the acquisition of resistance, GAD1 and, to a lesser degree, GAD2 expression were up regulated in TAMR cells versus MCF-7 control (Figure 35A). Furthermore, the log2 intensity plot revealed expression values above 0, suggesting reliable gene expression (Figure 35B & C). In contrast, GAD1 expression was down regulated in FASR and XR cells, with very little change in GAD2 expression apparent, compared to MCF-7 control (Figure 35A). Additionally, the log2 intensity plots demonstrated expression levels below 0, indicative of very little gene expression (Figure 35B & C).

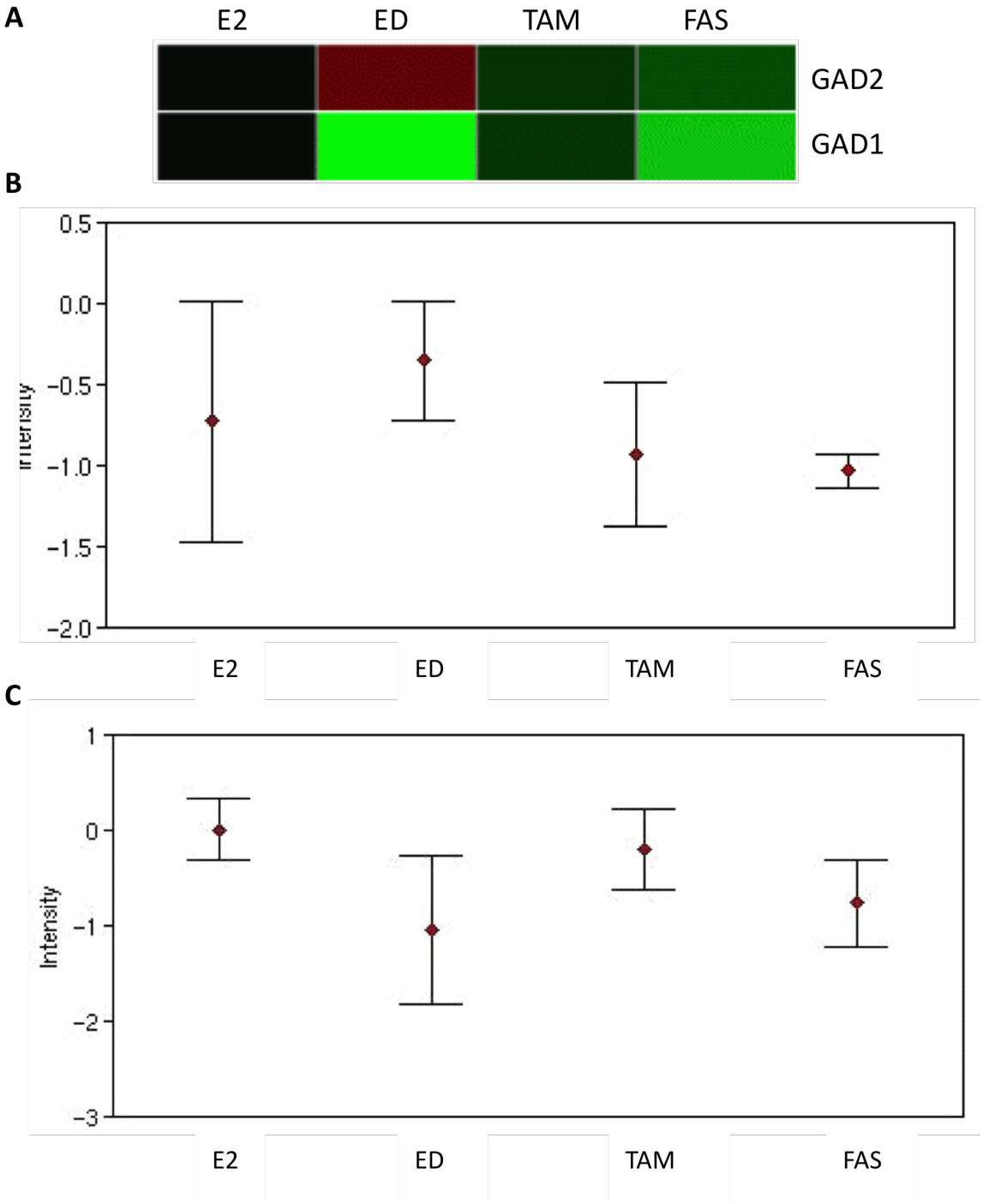

Figure 34 (A) Heatmap displaying the change in expression of GAD2 (jetset probe ID: 216651_s_at) and GAD1 (jetset probe ID: 206669_at) following 10 day oestradiol (E2 control; 10^{-9} M), oestrogen deprivation (ED), tamoxifen (TAM; 10^{-7} M) and fulvestrant (FAS; 10^{-7} M) treatment in MCF-7 cells. Red denotes an increase, and green denotes a decrease, in gene expression compared to control (shown in black). Corresponding log2 intensity plot displaying the normalised (mean of three independent replicates ± SEM) gene expression of GAD2 (B) and GAD1 (C).

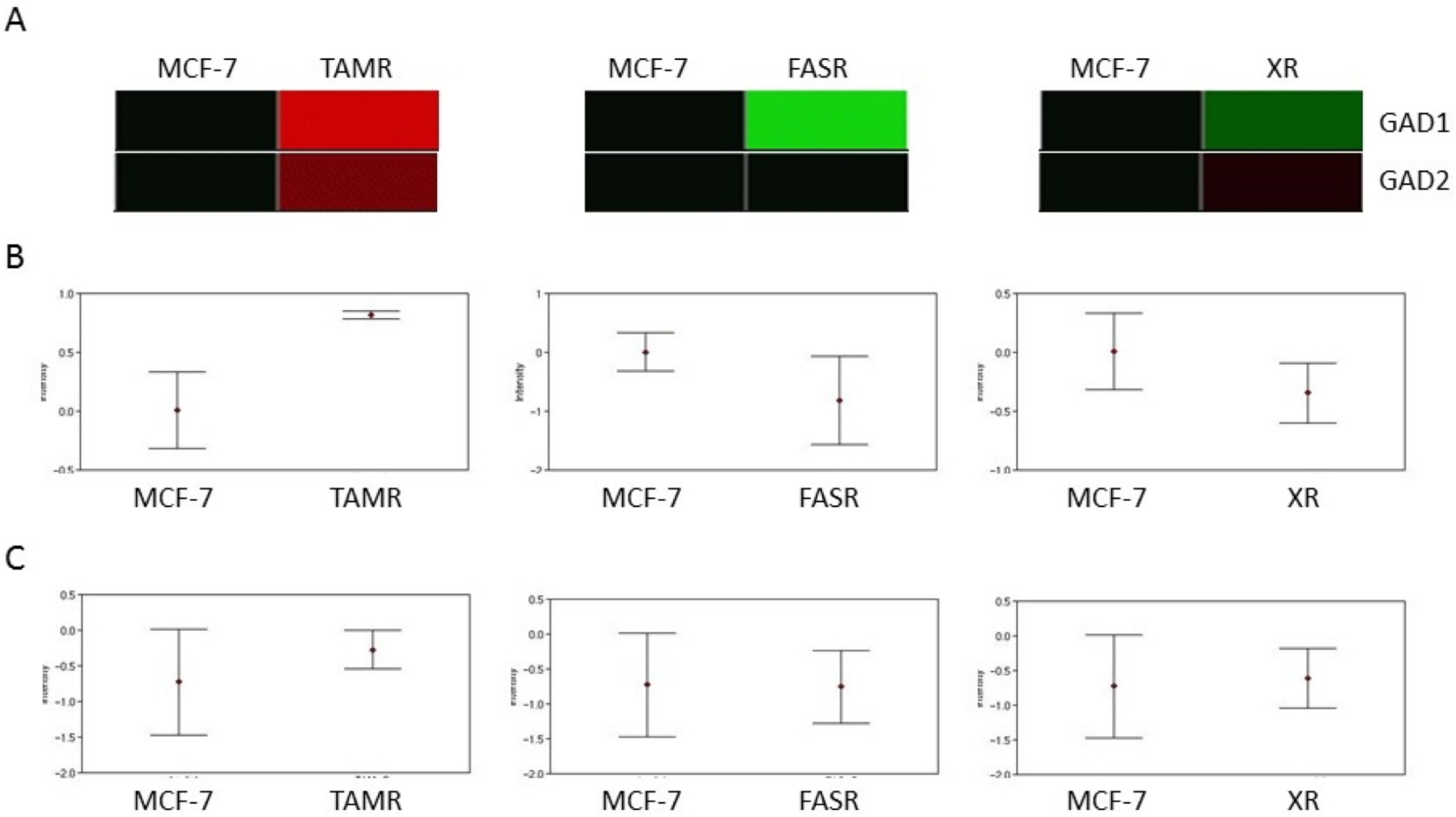

Figure 35 (A) Heatmap displaying the change in expression of GAD2 (jetset probe ID: 216651_s_at) and GAD1 (jetset probe ID: 206669_at) in tamoxifen-resistant (TAMR), fulvestrant-resistant (FASR) and oestrogen deprivation-resistant (XR) cells versus MCF-7 cells. Red denotes an increase, and green denotes a decrease, in gene expression compared to control (shown in black). Corresponding Log2 intensity plot displaying the normalised (mean of three independent replicates ± SEM) gene expression of GAD1 (B) and GAD2 (C).

3.3.5.2 CTNND2

Table 10 Summary of the function of CTNND2, including previous associations of CTNND2 with breast and other cancers and its potential pro-survival role.

Gene name	Catenin (Cadherin-associated protein), delta 2
Function	CTNND2 is an adhesive junction protein of the β-catenin/armadillo superfamily, abundantly expressed in neuronal cells. It plays a role in promoting disruption of E-cadherin based adherens junctions to promote cell spreading.
Associations with breast cancer	Until a recent study by Zhang et al.[327] CTNND2 expression had not been previously reported in breast cancer. Zhang et al. reported increased expression of CTNND2 in breast cancer tissues which was associated with increased malignancy and poor prognosis[327]. In breast cancer cell lines, CTNDD2 expression promoted invasion and cell cycle progression[327].
Associations with other cancers	CTNND2 is strongly expressed in several cancers, including lung, ovarian, prostate and oesophageal[328–331]. Increased expression of CTNND2 in prostate cancer promotes cell growth and survival by up regulating expression of cyclin D1 and BCL2L1 genes which are involved in promoting cell cycle progression and protecting cells from apoptosis, respectively[332]. Furthermore, CTNND2-induced E-cadherin processing in prostate cancer cells has been shown to be mediated by PSEN1[333].
Pro-survival role	CTNND2 has been shown to up regulate survival proteins in prostate cancer cells to provide protection from apoptosis[332].

Interestingly, as described in Table 10, CTNND2-induced E-cadherin processing and anti-apoptotic functions in prostate cancer cells has been shown to be mediated by PSEN1 and BCL2L1 genes, respectively. In support of this, microarray studies and subsequent PCR verification performed previously within this project identified increased expression of both PSEN1 and BCL2L1 in MCF-7 cells treated with antihormones and expression was maintained into the development of resistance.

3.3.5.3 CLU

Table 11 Summary of CLU function, including its reported association with breast and other cancers and pro-survival role.

Gene name	Clusterin
Function	CLU is a ubiquitously expressed glycoprotein involved in several physiological processes including lipid transportation, complement regulation and apoptosis. CLU has also been implicated in pathological disorders such as neurodegenerative diseases, ischemia and cancer[334]. As a result of alternative splicing, CLU has two main isoforms with distinct biologic activities. The cytoplasmic secreted form promotes cell survival whereas the nuclear form is associated with cell death.
Associations with breast cancer	CLU has been largely explored in breast cancer where its elevated expression is associated with invasion, metastasis, cell survival and ultimately poor patient survival[335,336]. Indeed, secretory CLU (CLU-S) expression in breast cancer cells plays a significant role in promoting tumour growth by inhibiting apoptosis, resulting in cell survival whilst also allowing the cells to survive the multiple stages of metastasis [337]. More recent research is focusing on a possible role for CLU during antihormone response and resistance. Indeed, tamoxifen treatment has been shown to increase CLU expression in MCF-7 cells correlated with an increase in cell viability[338,339]. Furthermore, tamoxifen combined with antibodies targeting CLU produced a greater and significant effect on cytotoxicity compared to tamoxifen alone. Moreover, CLU has also been shown to promote the growth of antihormone-resistant cells and CLU down regulation restored the sensitivity of these cells to the antioestrogen toremifene[338].
Associations with other cancers	Increased expression of the CLU-S has been reported in several cancers, including lung, bladder and kidney, where it is found to play a significant role in disease progression.

	In hormone-dependent prostate cancer, CLU-S expression increases with androgen withdrawal therapy, thus identifying CLU-S as a potential anticancer target. Antisense-induced down regulation of secretory CLU expression in prostate cancer enhances tumour regression and the cytotoxicity of several chemotherapeutic agents (reviewed by Miyake et al.[340]). Consistent with prostate cancer, inhibition of CLU expression also chemosensitises several other cancers including bladder and lung. An antisense inhibitor of CLU, OGX-011, is currently in clinical development. Phase I and II trials in prostate cancer patients demonstrated that OGX-011 is well tolerated and produces significant suppression of CLU in tumour tissues. In advanced lung and breast cancers, phase II trials of OGX-011 combined with chemotherapy produced positive results in terms of overall survival[341,342]. Several Phase III trials evaluating OGX-011 in combination with chemotherapy in prostate cancer patients are underway (reviewed by Zielinski & Chi[343]).
Pro-survival role	The anti-apoptotic/pro-survival actions of CLU have been described to function through a variety of mechanisms. CLU has been reported to bind to the pro-apoptotic protein Bax thus interfering with its activation in the mitochondria and preventing apoptosis[344]. Moreover, CLU-S has been shown to regulate ERK1/2 activity in several cancers, including pancreatic, lung and osteosarcoma[345–347]. ERK1/2 signalling has been identified as a potential survival pathway in cancer. Furthermore, in prostate cancer cells, CLU-S has been shown to up regulate AKT phosphorylation and downstream survival signalling, as well as promote nuclear translocation of NF-κB, thus increasing its transcriptional activation of genes implicated in cell survival and proliferation[348,349].

3.3.5.4 TSC22D3

Table 12 Summary of TSC22D3 function including previously reported associations with breast and other cancers and potential pro-survival role.

Gene name	TSC22 domain family, member 3
Function	TSC22D3 is a ubiquitous glucocorticoid-induced leucine zipper protein, which mediates several anti-inflammatory and immunomodulatory functions of glucocorticoids. TSC22D3 has been largely studied in T lymphocytes where it mediates a number of glucocorticoid effects, such as T cell activation, apoptosis and proliferation (as reviewed by Ayroldi & Riccardi[350]).
Associations with breast cancer	There is only one study demonstrating an association between TSC22D3 and breast cancer whereby tamoxifen up regulated TSC22D3 expression in MCF-7 cells, which was reversed with oestrogen treatment[351]. In contrast, oestrogen has been shown to up regulate TSC22D3 expression in HeLa cervical cancer cells indicating that cell type specific factors are likely to be involved in the oestrogen regulation of the gene and its functions are likely to differ according to the cellular milieu[351]. However, its function in breast cancer remains unexplored.
Associations with other cancers	TSC22D3 has been reported in multiple myeloma, lymphoblastic leukaemia and ovarian cancer[352–354]. In ovarian cancer, TSC22D3 activates AKT signalling, enhances cyclin D1 expression and down regulates p21 expression to promote tumour progression[354].
Pro-survival role	TSC22D3 has been shown to promote apoptosis in neutrophils and chronic myeloid leukaemia cells but protects T cells from activation-induced cell death[355–357]. The pro-survival role of TSC22D3 is likely to differ according to cell type. There are no studies describing a pro-survival role of this protein in breast cancer.

3.3.5.5 BCL3

Table 13 Summary of BCL3 function including previously reported associations with breast and other cancers and potential pro-survival role.

Gene name	B cell lymphoma 3
Function	BCL3 is an atypical member of the inhibitor of κB (IκB) family of proteins. Typically, IκB proteins function by binding and sequestering NF-κB dimers in the cytoplasm, blocking nuclear translocations, thus preventing transcription of a large number of genes involved in cell survival and proliferation[358]. However, BCL3 is a nuclear protein with both transactivation and transrepressor functions mediated by its association with NF-κB p50 and p52 homodimers[359]. Physiologically, BCL3 is required for T-cell dependent immunity and B cell survival.
Associations with breast cancer	BCL3 is overexpressed in breast cancer tissue and cell lines, however its precise function in tumourigenesis is largely unknown[360]. Studies in cell lines suggest that BCL3 stimulates cell proliferation and survival. Indeed, Westerheide et al. demonstrated in breast cancer cell lines that BCL3, acting as a coactivator of p50 dimers, stimulates transcription of the cyclin D1 gene thus potentiating G1 to S phase cell cycle transition[361] . Furthermore, BCL3 has been shown to promote metastasis of HER2+ breast tumours without effect on cell growth[362]. Regarding a role for BCL3 in antihormone failure and promoting endocrine resistance, Pratt et al. have shown that oestrogen withdrawal increases BCL3 expression and NF-κB activity in MCF-7 cells in parallel with enhanced tumour growth[363]. Furthermore, BCL3 expression and NF-κB activity (dominantly p50 dimers) was enhanced further in ER+, oestrogen-independent cells (model of resistance) derived from MCF-7 cells, suggesting that both BCL3 and NF-κB activities may allow a cohort of cells to grow and survive oestrogen withdrawal, thus establishing a hormone-independent phenotype.

Associations with other cancers	BCL3 was first identified in chronic lymphocytic leukaemia but has since been shown to be overexpressed in several cancers, including nasopharyngeal, endometrial and colorectal[364–366]. In nasopharyngeal carcinomas, BCL3 and p50 homodimers are complexed in the nucleus and these complexes are reported to bind to the promoter of EGFR, potentially inducing transcriptional up regulation of this oncogene and playing a crucial role in its overexpression[364]. Similarly, in metastatic colorectal cancer, nuclear expression of BCL3 together with p50 was negatively associated with patient survival[366].
Pro-survival role	Several studies have reported a survival role for BCL3 in a variety of cell types. Interestingly, in response to DNA damage, BCL3 up regulation has been shown to inhibit activation of the tumour suppressor p53 in breast cancer cells, consequently suppressing cell cycle arrest and apoptosis, ultimately promoting cell growth and survival. The major proposed mechanism in this circuit is the ability of BCL3 to induce up regulation of HDM2, the main negative regulator of p53[367]. Furthermore, BCL3 has been shown to bind CtBP1 and prevent its apoptotic responses, ultimately resulting in survival[368].

Interestingly, CLU and BCL3 may work together to promote cell survival. As mentioned in Table 11, CLU has been shown to promote nuclear translocation of NF-κB[349], which may include p50 dimers. Nuclear BCL3 may activate these dimers to promote downstream transcription of genes involved in cell survival.

Together, as demonstrated in Table 9-Table 13, increased expression of GABBR2, CTNND2, CLU, TSC22D3 and BCL3 in breast cancer has been previously reported to be involved in disease progression and poorer patient outlook. Furthermore, with regard to a role in limiting antihormone response and promoting resistance, the ontological studies (Table 9 to Table 13) revealed that tamoxifen has been shown to induce TSC2DD3 and CLU expression and oestrogen deprivation treatment has been shown to promote BCL3 expression[338,351,363].

3.3.6 Verification of the 5 genes of interest at the protein level by Western blotting

The expression of GABBR2, CTNND2, CLU, TSC22D3 and BCL3 was next examined at the protein level by Western blotting (shown in Figure 36 to Figure 40).

3.3.6.1 GABBR2

In agreement with previous microarray and PCR data, Western blotting analysis revealed up regulation of GABBR2 expression following tamoxifen, fulvestrant and oestrogen deprivation treatments compared to E2-treated control (Figure 36). GABBR2 expression was relatively consistent with all antihormone treatments and very little protein expression was apparent in the E2-treated control. Actin levels were similar following all treatments.

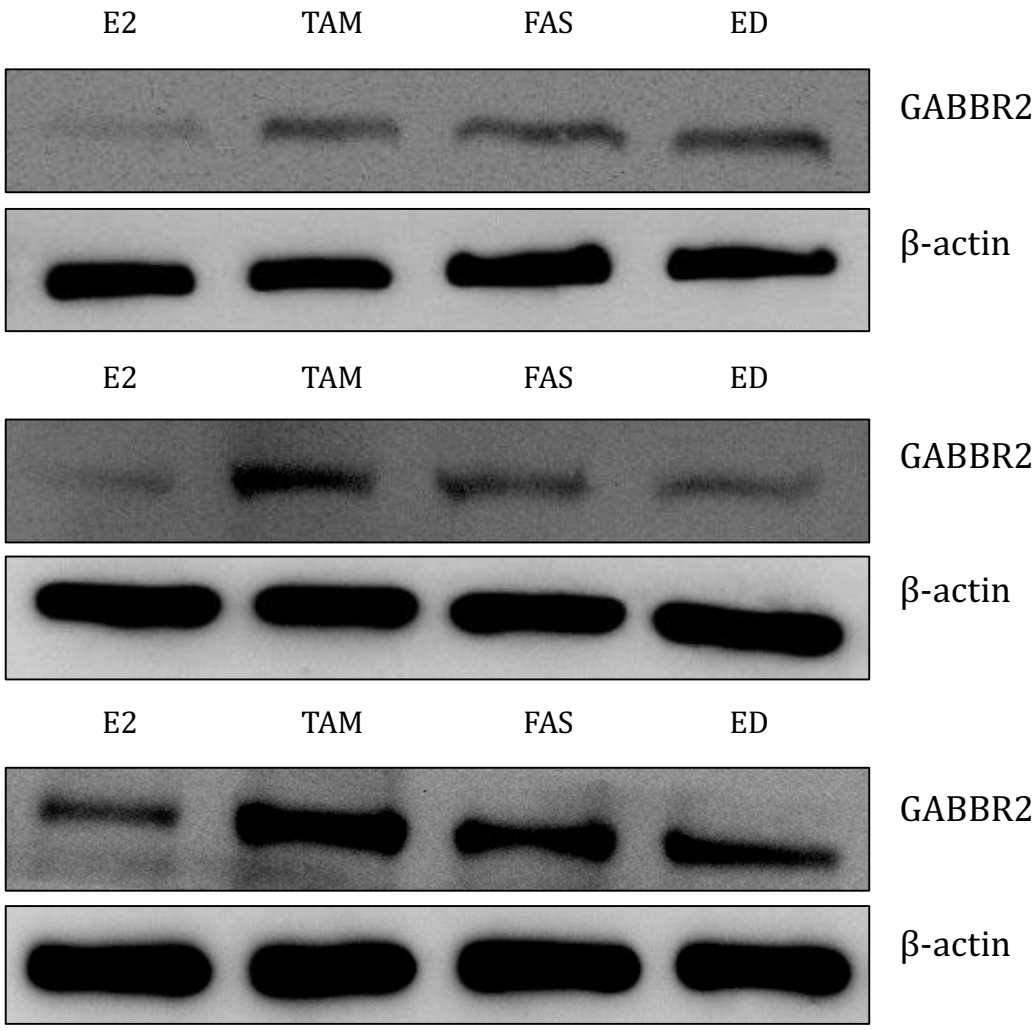

Figure 36 Western blot images from three independent experiments showing GABBR2 and β-actin protein expression in MCF-7 cells treated with oestradiol (E2 control; 10^{-9} M), tamoxifen (TAM; 10^{-7} M), fulvestrant (FAS; 10^{-7} M) and oestrogen deprivation (ED) for 10 days.

3.3.6.2 CTNND2

Unfortunately, CTNND2 expression could not be verified at the protein level (Figure 37). This was likely due to the poor specificity of the antibody and the lack of available antibodies.

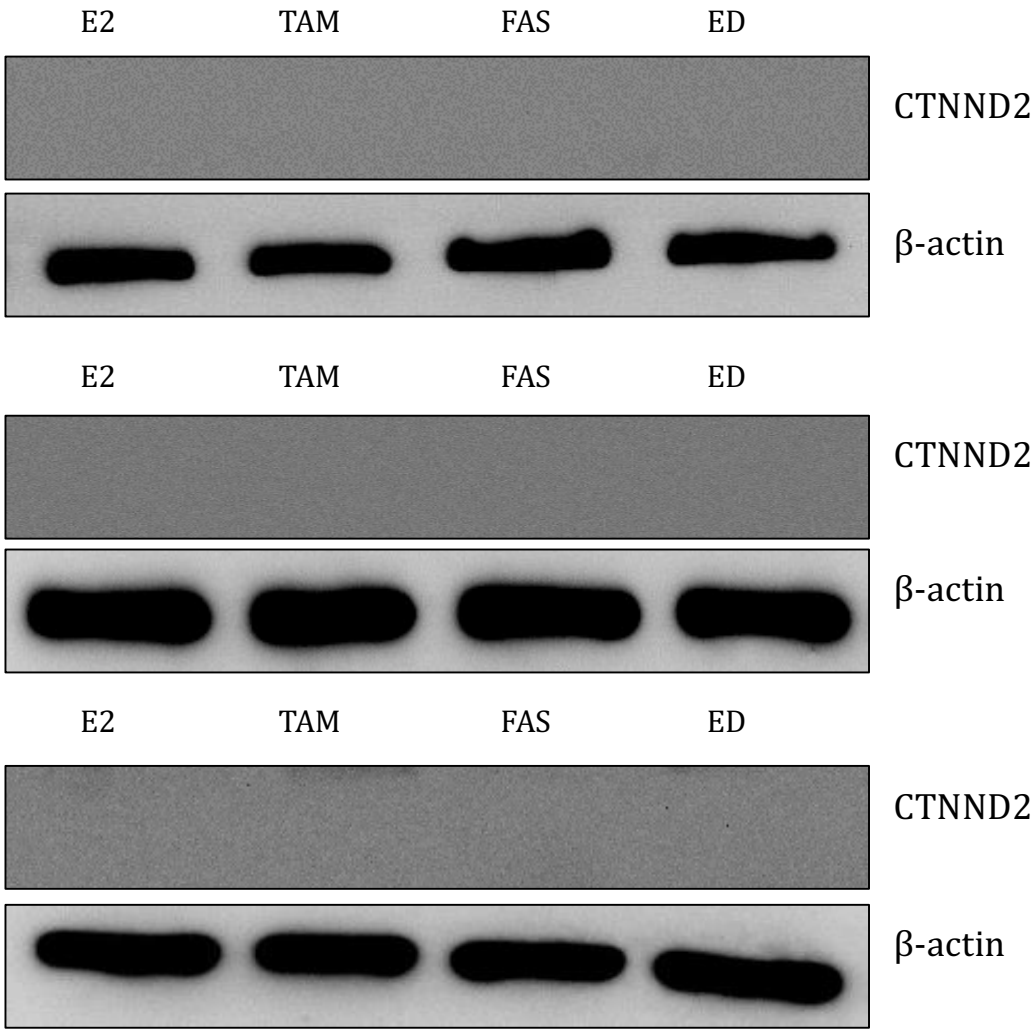

Figure 37 Western blot images from three independent experiments showing CTNND2 and β-actin protein expression in MCF-7 cells treated with oestradiol (E2 control; 10^{-9} M), tamoxifen (TAM; 10^{-7} M), fulvestrant (FAS; 10^{-7} M) and oestrogen deprivation (ED) for 10 days.

3.3.6.3 CLU

As determined from the ontological studies (Table 11), two isoforms of CLU exist. The nuclear isoform is associated with promoting cell death whereas the CLU-S form is associated with cell survival[369,370]. Since this project is interested in the survival role of CLU, CLU-S was analysed by Western blotting. CLU-S exists as a precursor (approximately 60 kDa) which is cleaved into α- and β-subunits that dimerise to form the mature secretory CLU form, with an apparent molecular weight of 75-80 kDa[371]. However, under reducing SDS-PAGE conditions, the α- and β-subunits appear as 36-39 kDa and 34-36 kDa bands, respectively.

Western analysis (specific for CLUα) revealed up regulation of CLU-S following tamoxifen, fulvestrant and oestrogen deprivation treatment (Figure 38). Two bands appeared on the blot at 60 kDa and 40 kDa representing the CLU precursor and α-subunit, respectively. All three antihormone treatments induced protein expression of CLU precursor and CLUα, which mimics the microarray profile. Protein expression was minimal following E2 treatment (Figure 38). Actin levels remained constant following all treatments.

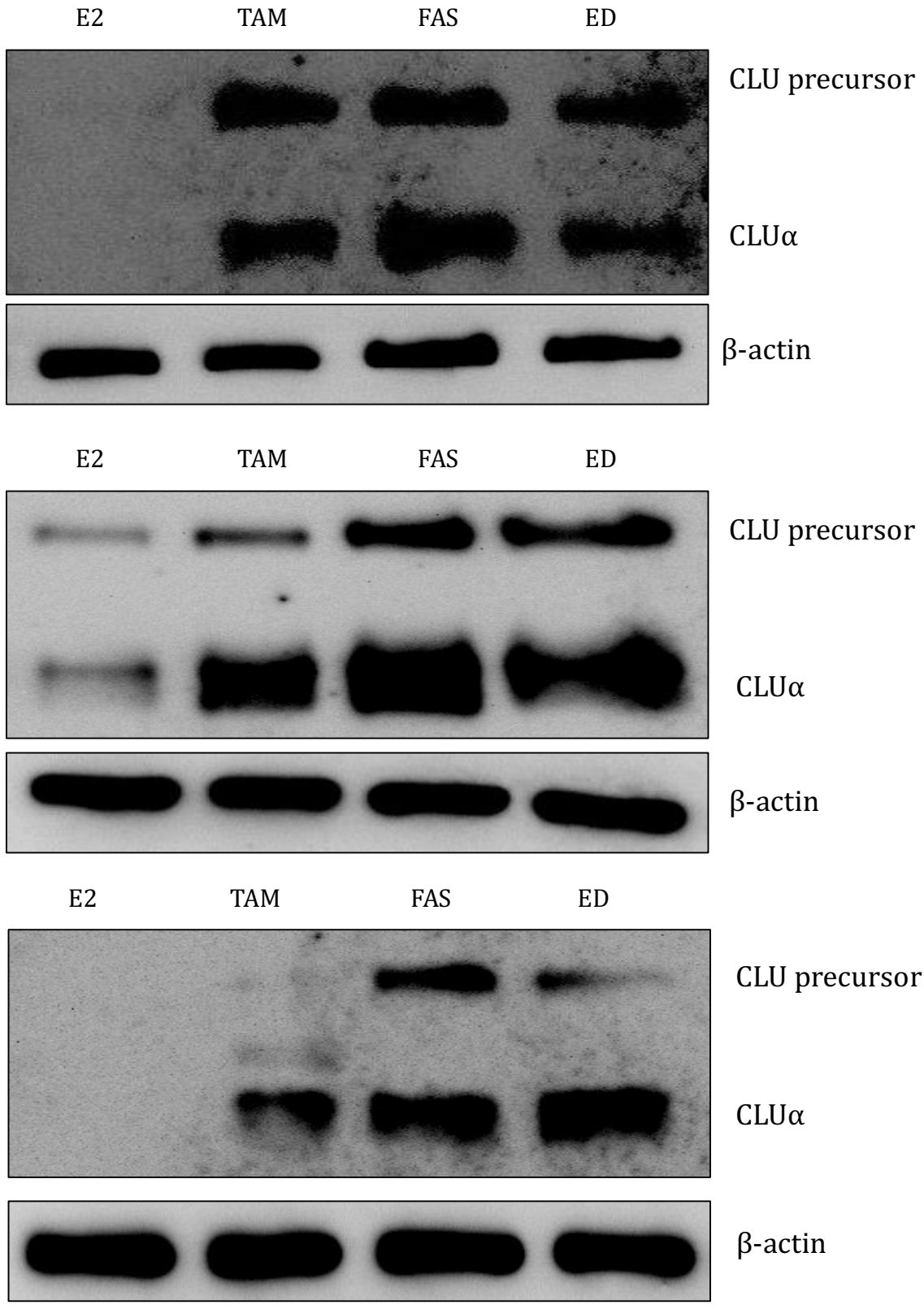

Figure 38 Western blot images from three independent experiments showing CLU precursor, CLUα and β-actin protein expression in MCF-7 cells treated with oestradiol (E2 control; 10^{-9} M), tamoxifen (TAM; 10^{-7} M), fulvestrant (FAS; 10^{-7} M) and oestrogen deprivation (ED) for 10 days.

3.3.6.4 TSC22D3

In agreement with previous microarray and PCR data, Western blot analysis demonstrated up regulation of TSC22D3 expression by all three antihormone treatments (Figure 39). Actin levels remained constant following all four treatments.

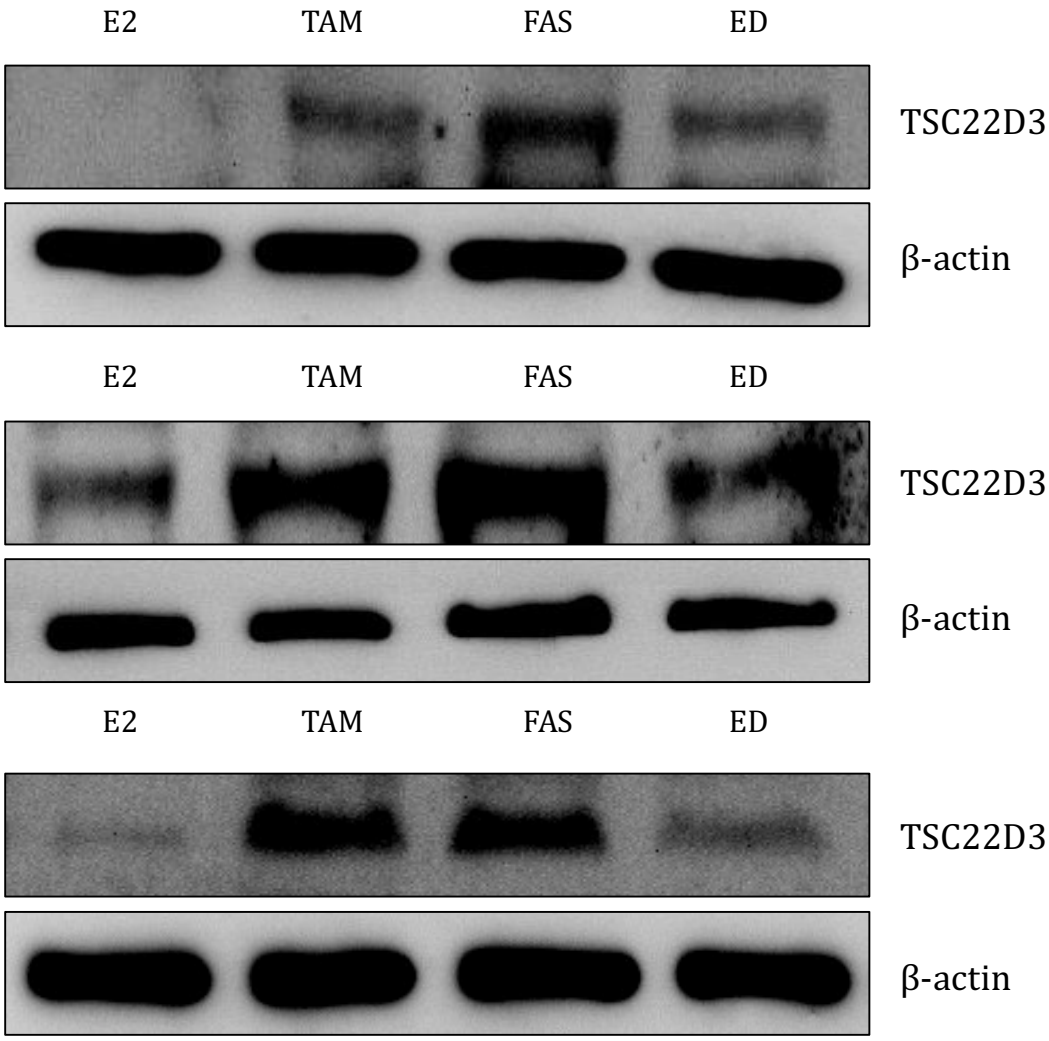

Figure 39 Western blot images from three independent experiments showing TSC22D3 and β-actin protein expression in MCF-7 cells treated with oestradiol (E2 control; 10^{-9} M), tamoxifen (TAM; 10^{-7} M), fulvestrant (FAS; 10^{-7} M) and oestrogen deprivation (ED) for 10 days.

3.3.6.5 BCL3

In agreement with the microarray and subsequent PCR data, BCL3 protein expression was up regulated by all three antihormone treatments compared to E2-treated control (Figure 40). BCL3 was expressed at low levels in E2-treated control cells and actin levels remained constant following all four treatments.

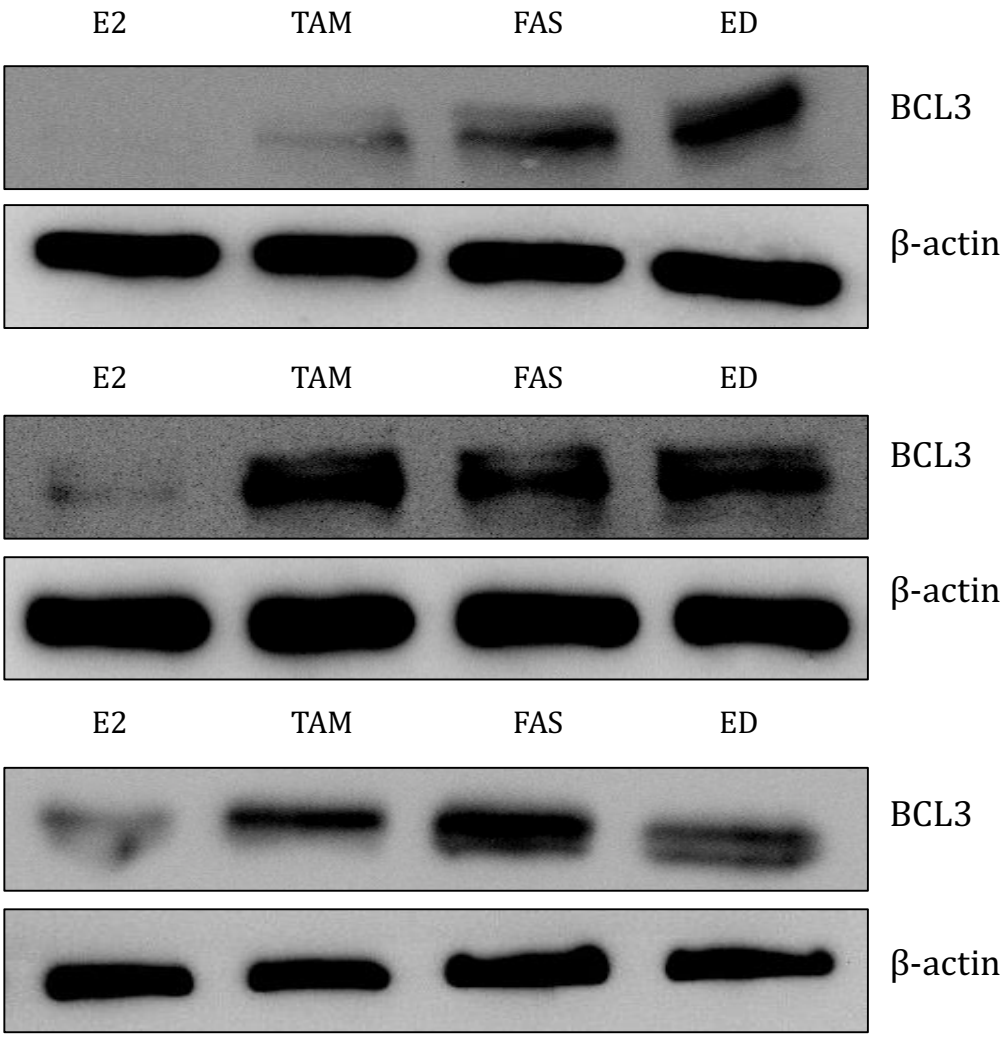

Figure 40 Western blot images from three independent experiments showing BCL3 and β-actin protein expression in MCF-7 cells treated with oestradiol (E2 control; 10^{-9} M), tamoxifen (TAM; 10^{-7} M), fulvestrant (FAS; 10^{-7} M) and oestrogen deprivation (ED) for 10 days.

3.4 Discussion

In this Chapter a filtering process was performed to identify pro-survival genes significantly induced by 10 day antihormone treatment (fold change greater than 1.5, combined with present detection calls) in MCF-7 cells, with expression maintained into the acquisition of resistance. Following extensive analysis of the microarray gene expression data, 14 genes were identified as being significantly induced by at least one antihormone treatment during response, with expression maintained into the development of resistance. It was hypothesised that these antihormone-induced pro-survival genes could allow a cohort of breast cancer cells to evade the growth inhibitory actions of these agents early during response, ultimately driving acquired resistant growth, thus resulting in poorer patient outcome. Furthermore, targeting of these genes alongside antihormones during response may enhance the anti-proliferative actions exerted by these therapies and prevent or delay the development of resistance. Additionally, targeting of these genes during resistance may potentially reverse this adverse phenotype and re-sensitise the cells to antihormone treatments. Alternatively, expression of these pro-survival genes during initial antihormone response may provide early predictive markers of limited response and subsequently the acquisition of resistance.

The majority of the microarray profiles of the 14 genes were successfully verified by RT-PCR, with the exception of BAG1, DDAH2 and HBXIP, which showed similar levels of mRNA expression following E2-control and antihormone treatments. Additionally, RT-PCR verification of IGFBP5 continued to fail, with no mRNA expression detected. This was likely due to the PCR primers recognising an alternative region of mRNA to that recognised by the probes on the Affymetrix gene chip.

To prioritise the genes further, those identified by microarray gene expression profiling to be significantly induced by all three antihormone treatments, with PCR verification, were considered for further investigation. These genes included BCL3, GABBR2, CTNND2, CLU and TSC22D3. It was hoped that a common mechanism of resistance to all three clinically-used antihormone treatments could be identified. Such genes may ultimately provide a novel biomarker indicative of treatment

response or a therapeutic target common to resistance to all three antihormones and thus offering a therapeutic option to a significant cohort of breast cancer patients. Ontological investigation confirmed tumour-promoting functions for these genes and Western blot analysis (except for CTNND2) revealed antihormone-induced expression at the protein level in MCF-7 cells as well as absent expression following E2-control treatment.

Increased expression of BCL3 has been demonstrated in breast cancer tissue and cell lines, however its precise role remains largely unknown[360]. BCL3 is an atypical member of the IκB family of proteins and its function as a transactivator and transrepressor of NF-κB p50 and p52 homodimers has been well established. Indeed, the majority of studies exploring the role of BCL3 in cancer have examined its association with p50 and p52 and consequently the activation of downstream NF-κB-regulated genes. NF-κB regulates a wide variety of genes involved in inflammation, immunity, cell growth and apoptosis[372]. In breast cancer cell lines, BCL3 has been shown to act as a coactivator of p50 dimers to stimulate transcription of the cyclin D1 gene, subsequently promoting G1 to S phase cell cycle transition and cell cycle progression[361].

Short-term tamoxifen, fulvestrant and oestrogen deprivation treatments have been shown in this study to induce up regulation of BCL3 mRNA and protein expression in MCF-7 cells, with increased expression maintained into the emergence of resistant growth. In agreement with these findings, Pratt et al. demonstrated increased expression of BCL3 in MCF-7 cells following oestrogen withdrawal, with parallel increases in NF-κB activity (consisting primarily of p50 homodimers) and enhanced tumour growth[363]. These actions may be due in part to the reported ability of BCL3-p50/p52 complexes to induce cyclin D1[361,373] expression as well as promote AP-1-mediated transactivation and cell proliferation[374]. Moreover, BCL3 and NF-κB activity was enhanced further in ER+ oestrogen-independent cells derived from MCF-7 cells. The findings presented in the current study, as well as those reported previously, strongly suggest that early induction of BCL3 by antihormones during response likely contributes to the ability of cells exhibiting increase BCL3-p50/p52 complexes to grow and survive the antihormone challenge to establish the hormone-independent cohort.

Several studies have reported a pro-survival for BCL3. In MCF-7 cells, BCL3 expression has been reported to increase following DNA damage, with constitutive expression of BCL3 promoting suppression of DNA-damage-induced cell death via inhibiting the expression of the tumour suppressor gene p53[367]. Consequently, such inhibition results in the suppression of apoptosis and ultimately stimulates cell survival. The dominant mechanism reported by which this inhibition occurs is via the ability of BCL3 to induce up regulation of the p53 inhibitor Hdm2[367]. Furthermore, BCL3 has been shown to bind to the anti-apoptotic protein CtBP1 to promote cell survival[368]. CtBP1 exerts its anti-apoptotic function by transcriptionally repressing pro-apoptotic genes. In response to apoptotic stimuli, CtBP1 is degraded which results in derepression of pro-apoptotic genes to allow apoptosis to proceed[375]. However, BCL3 has been shown to bind to CtBP1, blocking its ubiquitination thus leading to its stabilisation. Consequently, CtBP1-mediated repression of pro-apoptotic genes is sustained and cells become resistant to apoptotic stimuli, ultimately promoting cell survival[368]. Moreover, a positive correlation between increased BCL3 and CtBP1 proteins levels has been demonstrated in breast cancer cell lines and tissues[368].

Of the 5 pro-survival genes identified, CLU has been explored the most with regard to breast cancer and endocrine resistance. CLU is a ubiquitously expressed glycoprotein implicated in several physiological processes, including lipid transport, complement cascade and programmed cell death. As a result of alternative splicing, CLU has two main isoforms, both exhibiting opposing biological functions. The CLU-S form starts as an approximately 60 kDa precursor peptide which is cleaved and glycosylated to generate an α and β chain, each approximately 40 kDa, which heterodimerise and ultimately become the secreted form[370]. CLU-S is believed to be cytoprotective and involved in the clearance of cellular debris and promotion of phagocytosis[376,377]. In contrast, the nuclear form is first translated into an inactive 49 kDa form which is post-translationally modified to an active 55 kDa form which accumulates in the nucleus and promotes cell death[369,378,379].

Increased expression of CLU-S has been reported in several cancers, including gastric, ovarian and breast where it is found to play a significant role in metastasis,

invasion and cell survival, ultimately contributing to poor patient outlook[336,337,380,381]. Furthermore, short-term tamoxifen, fulvestrant and oestrogen deprivation treatments have been shown here to significantly up regulate CLU expression in MCF-7 cells during response, with expression maintained into the acquisition of resistance. Although the microarray gene probes and PCR primers did not specifically target CLU-S, the antibody used in the Western analysis was CLU-S-specific and a previous study has identified CLU-S as the most abundant form in MCF-7 cells[295]. Together this strongly suggests that the anti-apoptotic CLU-S form is induced by antihormones. In agreement with these findings, Toffanin et al. have demonstrated increased expression of CLU-S following 3 day treatment with the SERMs tamoxifen and toremifene in ER+ breast cancer cell lines, including MCF-7 cells[338]. Moreover, Redondo et al. demonstrated increased CLU expression as early as 24 hours post-tamoxifen treatment in MCF-7 cells[339]. Additionally, a combination of tamoxifen and antibodies targeting CLU inhibited CLU expression together with inducing a decrease in cell viability. This combination treatment had a greater effect on cytotoxicity compared to tamoxifen alone[339]. These findings strongly suggest a cytoprotective role for CLU in breast cancer cells which may limit the anti-tumour actions of antihormones to promote resistant growth, and also illustrates the potential for anti-CLU therapy in the treatment of breast cancer. Furthermore, increased levels of CLU have been shown in T47D cells deemed resistant to antihormones, with CLU expression involved in promoting resistant cell growth. Down regulation of CLU re-sensitised these cells to toremifene[338]. However there are no studies showing an association between CLU expression and limited response to fulvestrant and oestrogen deprivation/AIs.

Several studies have reported a pro-survival role for CLU-S via interacting with, and modulating, several key signalling pathways involved in carcinogenesis. In prostate cancer cells, CLU-S has been demonstrated to increase AKT phosphorylation and promote downstream survival signalling[348]. Additionally, also in prostate cancer, CLU-S has been shown to enhance nuclear translocation of NF-κB subsequently increasing transactivation of NF-κB–regulated genes implicated in cell survival and proliferation[349]. Furthermore, several studies have shown that ERK 1/2 (members of the MAPK super family, involved in cell

proliferation and apoptosis) is regulated by CLU-S in several cancers, including pancreatic, lung and osteosarcoma[345–347]. These pathways have all been heavily implicated in breast cancer and indeed endocrine resistance, thus it is strongly possible that antihormone-induced CLU-S interacts and regulates these pathways to establish a mechanism to combat antihormone challenge and promote resistant cell growth. An antisense inhibitor of CLU, OGX-011, is currently in clinical development. Phase I and II clinical trials have demonstrated that OGX-011 is well tolerated and is successfully delivered to malignant tissues with significant inhibition of CLU expression. A phase II study demonstrated a survival advantage of OGX-011 combined with docetaxel in patients with advanced prostate cancer[382]. This led to the development of phase III trials which are currently underway, examining OGX-011 in combination with chemotherapy in patients with metastatic prostate cancer. If successful, these studies will validate OGX-011 as a new option for metastatic prostate cancer patients[343]. These studies may endorse a new class of targets and targeted therapy approach for cancer. In breast cancer, combination of OGX-011 and antihormone therapy may delay/prevent the development of resistance or in endocrine resistant tumours OGX-011 may reverse the resistant phenotype and re-sensitise breast cancer cells to antihormones.

Increased GABA B receptor expression has been reported in several cancers, including gastric, thyroid and breast[317]. However, the role of this receptor and in particular the GABBR2 subunit in cancer remains largely unexplored. Increased expression of GABA B receptor and the GABA synthesising enzymes, GAD1 and GAD2, in breast cancer cells has been demonstrated suggesting the existence of GABAergic signalling within these cells[318]. Furthermore, activation of GABA B receptors promotes breast cancer cell invasion and metastasis by increasing phosphorylated ERK 1/2 levels and subsequently increasing the expression of MMP-2[319]. Similarly, increased GABA B receptor signalling in prostate cancer cells has been shown to enhance the metastatic and invasive capacity of the cells, again by promoting expression of MMPs, in particular MMP-3[325]. MMPs play vital roles in degrading the extracellular matrix, thus enabling tumour cells to penetrate the basement membrane, enter the circulation and invade target organs[319]. MMP-2 has been shown to play a role in metastasis of breast cancer to the brain and as such its

expression is associated with disease progression and poorer patient outlook[320,383]. In contrast, studies in pancreatic and lung cancer have implicated a growth inhibitory role for GABA B receptor activation[384,385].

However, GABBR2 has never previously been associated with limiting antihormone response in breast cancer and promoting the development of resistance. GABBR2 expression increases in MCF-7 cells treated short-term with tamoxifen, fulvestrant and oestrogen deprivation (to mimic the actions of AIs) and its expression is maintained into the resistant setting as shown in TAMR, FASR and XR cells. These findings demonstrate that antihormones induce the expression of GABBR2 early during response, with increased expression maintained through to the acquisition of resistance, and together with the above-mentioned tumour-promoting functions reported for GABA B receptor, suggest that this gene may contribute substantially to the emergence of endocrine resistance.

GABA B receptors are heterodimeric GPCRs comprised of GABBR1 (which contains the ligand-binding domain) and GABBR2 (which is coupled to G proteins to regulate activity) subunits, both of which are required for normal receptor function. Therefore, the expression of GABBR1 was also investigated during antihormone response and resistance to determine whether it is present together with GABBR2, thus rendering the receptor fully active. GABBR1 expression was analysed in the microarray gene expression dataset of MCF-7 cells treated for 10 days with antihormones and in the endocrine-resistant cell models. The data suggested absent expression of this protein following E2-control and antihormone treatments in MCF-7 cells, characterised by log2 intensity values below 0 and down regulation of expression mediated by fulvestrant treatment. Following the acquisition of resistance, the microarray data demonstrated up regulation of GABBR1 in TAMR cells, with no change in gene expression apparent in the FASR and XR cells compared to MCF-7 control. However, the log2 intensity values were below 0 in the three antihormone-resistant cell lines, indicative of very low gene expression.

Moreover, GAD1 and GAD2 are the key enzymes involved in the synthesis of the ligand, GABA. Thus, their expression was next investigated to determine whether

GABA is produced by the cells and therefore able to activate GABA B receptor signalling. Analysis of GAD1 and GAD2 in the microarray dataset revealed absent expression in MCF-7 cells regardless of treatment, characterised by log2 expression values below 0. Furthermore, antihormones induced down regulation of GAD1 expression compared to E2-control. Similarly, tamoxifen and fulvestrant promoted down regulation of GAD2 expression whilst oestrogen deprivation increased its expression compared to control. In contrast, GAD1 and GAD2 expression were up regulated in TAMR cells versus MCF-7 control, together with log2 intensity values above 0, strongly suggesting reliable gene expression. However, in the FASR and XR cell models, GAD1 was down regulated, and GAD2 expression was unchanged, compared to MCF-7 control, together with log2 expression values below 0, representative of very low gene expression.

The microarray data suggested very low expression of GABBR1 in MCF-7 cells during antihormone response, with low expression maintained through to the acquisition of resistance. Similarly, low expression of GAD1 and GAD2 were reported in antihormone-treated MCF-7 cells and antihormone-resistant FASR and XR cells. Together, these findings imply no GABBR2 activation during antihormone response and following the development of resistance to fulvestrant and oestrogen deprivation. However, the microarray data suggest that the ligand, GABA, is synthesised in TAMR cells, characterised by the presence of GAD1 and GAD2 genes. Even though the microarray findings suggest low expression of GABBR1 during antihormone-response and –resistance (necessary for normal GABA B receptor function), antihormone-induced expression of GABBR2 at the mRNA and protein level, with expression detected in resistance by microarray, plus ontology strongly suggesting a role in disease progression, warrants further study of GABBR2.

However, in contrast to the microarray data reported in this study, Zhang et al. have demonstrated expression of GABBR1 and GAD1/2 proteins in breast cancer cell lines, including MCF-7 cells, and in normal and cancerous breast tissue[319]. Additionally, the GABA B receptor agonist baclofen promoted cell invasion and migration *in vitro* and metastasis *in vivo,* mediated via enhanced ERK 1/2 signalling and MMP-2 production. This suggests that GABAB receptors (comprising

GABBR1 and GABBR2 subunits) are functional and activated in breast cancer, with such activation involved in promoting disease progression.

The function of GABBR2 in breast cancer is largely unknown and a pro-survival role is particularly unreported. However, GABBR2 activation has been shown to promote survival of neuronal cells and to inhibit apoptosis by transactivating IGF-1R[326]. The importance of IGF-1R signalling in promoting breast cancer cell survival is well established with increased signalling also playing a role in drug resistance (as previously discussed in section 1.7.4.1)[198]. Specifically, increased signalling via the IGF-1R pathway has been associated with the acquisition of resistance to gefitinib (EGFR inhibitor), herceptin (HER2 inhibitor) and tamoxifen[198,222,386].

Increased expression of CTNND2 has been observed in several human cancers including ovarian, prostate and oesophageal, and is associated with enhanced malignancy and poor prognosis[329,331,332]. The role of CTNND2 has been largely studied in prostate cancer. Indeed, CTNND2 disrupts E-cadherin-based cell-cell junctions (which are pivotal in maintaining epithelial tissue integrity) to promote cell migration, increases the expression of cyclin D1 to promote cell cycle progression and increases the expression of the anti-apoptotic protein BCL2L1 to promote cell survival[332,333]. Similarly, overexpression of CTNND2 in ovarian cancer cells promotes invasion and cell proliferation and accelerated cell cycle progression by up regulating cyclin D1 expression[329]. Until recently, CTNND2 expression in breast cancer had not been reported. Zhang et al. showed increased expression of CTNND2 in breast cancer tissue compared to normal breast, again with increased expression associated with a higher degree of malignancy and poor prognosis[327]. Furthermore, in breast cancer cell lines (including ER+ MCF-7 cells) CTNND2 has been shown to promote cell cycle progression by accelerating G1 to S phase transition and has also been shown to enhance cell invasion[327].

Apart from array studies within the group showing antihormone-induced expression of CTNND2 with increased expression maintained into TAMR/FASR cells[304], there are no other studies reporting an association between CTNND2 and antihormone failure and consequently the development of resistance. In support of

the previous findings, CTNND2 expression increases in MCF-7 cells treated for 10 days with tamoxifen, fulvestrant and oestrogen deprivation with expression maintained into TAMR, FASR and XR cell models. Although this was demonstrated at the mRNA level, it could not be confirmed at the protein level due to the poor specificity/failure of the antibody and indeed the lack of available antibodies.

Regarding a pro-survival role, previous studies in prostate cancer cell lines have shown that increased CTNND2 expression up regulates expression of anti-apoptotic proteins, BCL2L1 and survivin, to promote cell survival and protection from apoptosis[332]. Interestingly, initial extensive analysis of the microarray data in this study identified both BCL2L1 and survivn/BIRC5 as antihormone-induced genes, with expression maintained into the acquisition of resistance. BCL2L1 expression was subsequently verified by PCR which demonstrated up regulation of expression following 10 day tamoxifen, fulvestrant and oestrogen deprivation treatments compared to E2-control in MCF-7 cells. It is possible from these results, supported by those from the study by Zeng et al. in prostate cancer cells[332], that antihormone induced CTNND2 may promote breast cancer cell survival by up regulating the expression of BCL2L1. The anti-apoptotic protein BCL2L1, also known as BCL-X_L, belongs to the family of BCL-2 proteins, and its expression has been associated with the progression of breast cancer and the development of advanced metastatic disease[387,388]. In MCF-7 cells, overexpression of HER2 has been shown to promote increased expression of BCL-X_L resulting in suppression of tamoxifen-induced apoptosis[267]. Thus, since antihormones induce HER2 expression early during response as reported here and in previous studies[217], it is possible that such induction contributes to cell survival by promoting expression of CTNND2 which subsequently increases the anti-apoptotic protein BCL2L1, resulting in de-regulation of apoptotic pathways and consequently constituting a potential mechanism of resistance to antihormones.

However, although BIRC5 expression was induced by antihormones with expression maintained into cell models of resistance, together with marginal or present detection calls recorded, this induction did not reach significance and BIRC5 was therefore dismissed from further study during the initial filtering stages of the microarray data. However, this does not rule out a role for BIRC5 in limiting

the efficacy of antihormones and promoting resistance. Survivin/BIRC5 is a member of the inhibitor of apoptosis protein family. These proteins block apoptotic cell death primarily by preventing the activation and activity of several caspases. Increased expression of BIRC5 has been reported in breast cancer[389,390]. Interestingly, HBXIP is a co-factor for BIRC5 and when complexed they bind and suppress activation of pro-caspase-9 to prevent downstream apoptosis[391]. In support of this, HBXIP was identified in the microarray data of the present study as an antihormone-induced gene with expression maintained through to the acquisition of resistance. Short-term antihormone-induced expression of HBXIP was also verified at the mRNA level by PCR. Thus it is possible, that HBXIP and BIRC5 proteins complex following antihormone therapy to inhibit apoptosis and consequently contribute to the emergence of resistant growth.

Interestingly, in prostate cancer cells Kim et al. have shown that CTNND2-induced E-cadherin processing is mediated by PSEN1[333]. In turn, E-cadherin-based cell-cell junctions, pivotal in maintaining epithelial tissue integrity, are disrupted resulting in tumour proliferation and progression. In support of this, microarray studies and RT-PCR performed in this study confirm increased expression of PSEN1 in MCF-7 cells treated with antihormones with expression maintained into the resistance setting, mirroring CTNND2 expression. Thus, an alternative mechanism by which CTNND2 potentially promotes breast cancer progression early during antihormone response may be through recruitment of PSEN1 to induce E-cadherin processing, ultimately stimulating aggressive malignant behaviour.

The ubiquitously expressed small leucine zipper protein TSC22D3 has been largely studied in T lymphocytes where it mediates several glucocorticoid functions such as T lymphocyte activation, apoptosis and cell proliferation[350]. These actions in T cells are accomplished by TSC22D3 interacting with and modulating key signalling pathways important for tumorigenesis. For example, TSC22D3 binds and traps NF-κB in the cytosol, preventing its nuclear localisation and activation of target genes involved in cell proliferation and survival[392]. Furthermore, TSC22D3 binds Raf and Ras to inhibit activation of downstream targets including ERK 1/2, AKT and cyclin D1, thus resulting in inhibition of cell proliferation[393]. TSC22D3 expression has been demonstrated in multiple myeloma, leukaemia and ovarian

cancer, however its role in tumorigenesis remains elusive[352–354]. In ovarian cancer TSC22D3 has been shown to enhance phosphorylated AKT content and activity to promote cell proliferation. This is in contrast to the roles reported in T lymphocytes, where TSC22D3 inhibits downstream AKT signalling cascades resulting in an anti-proliferative effect in these cells[393,394]. These opposing roles of TSC22D3 are likely due to the differing cell types and the associated cellular milieus. Furthermore, TSC22D3 promotes cell cycle progression in ovarian cancer cells by up regulating cyclin D1 and down regulating p21 expression, thus promoting S phase entry[354], again in contrast to that observed in T lymphocytes.

In the present study, TSC22D3 expression was induced by 10 day tamoxifen, fulvestrant and oestrogen deprivation in MCF-7 cells, with increased expression maintained into resistance. In support of these findings, tamoxifen and fulvestrant have been shown to induce TSC22D3 expression in MCF-7 and uterine epithelial cells, respectively, which was reversed by oestrogen[351,395]. Tynan et al. is the only study demonstrating an association between TSC22D3 and breast cancer[351]. In contrast, oestrogen has been shown to up regulate TSC22D3 expression in cervical cancer and human embryonic kidney cells, suggesting that cell specific factors are involved in oestrogen regulation of TSC22D3 which is not surprising [351]. However, there are no previous reports associating TSC22D3 expression and function with antihormone resistance.

Furthermore, there are no studies describing a pro-survival role for TSC22D3 in breast cancer. TSC22D3 has been shown to promote apoptosis in neutrophils (by inhibiting AKT phosphorylation)[355] and chronic myeloid leukaemia cells expressing BCR-ABL oncogene[356]. However, in T cells TSC22D3 has been shown to be protective against activation-induced cell death, but not from apoptosis induced by other apoptotic stimuli[357]. Furthermore, in solid tumours, particularly ovarian cancer, TSC22D3 has been shown to promote AKT signalling (as previously mentioned)[354] which is implicated in cell survival, although this was not directly examined in this study. Together, these findings support the suggestion that the role of TSC22D3 is likely to be multifaceted and dependent on the cellular milieu. Thus, further studies are clearly required to determine whether this protein promotes cell survival in breast cancer, to allow the cells to overcome the

antihormone challenge and ultimately contribute to the emergence of resistant growth and poor clinical outcome.

In summary, this Chapter has identified a panel of antihormone-induced pro-survival genes via extensive analysis of microarray gene expression data combined with a robust filtering strategy and subsequent PCR and Western blot analysis, whose ontology strongly suggests a role in limiting drug response and promoting the emergence of resistance: GABBR2, CTNND2, CLU, TSC22D3 and BCL3. However, additional experimental repeats to increase the n numbers are required to increase the reliability of the data. In the following Chapter, the expression of these 5 genes has been examined in additional cell lines with differing HER2 status to consider an aspect of heterogeneity that exists in ER+ breast cancer and also to determine whether antihormone-induced up regulation of these genes is common across several cell lines and molecular subtypes. It is feasible that these studies could identify an antihormone-induced mechanism of limiting drug response and promoting acquisition of hormone-independent growth, common to 4 ER+ breast cancer cell lines with differing HER2 expression.

4 Results II: Analysis of genes of interest in MCF-7, T47D, BT474 and MDA-MB-361 cell lines

4.1 Introduction

The research field relies heavily on single cancer cell lines and with regard to hormone-dependent breast cancer the MCF-7 cell line is predominantly used due to its high ER expression and subsequent exquisite hormone sensitivity, making it an ideal model to study hormone response[396]. Significant advances have been derived from MCF-7 cell studies, in particular the recognition that tamoxifen regulates oestrogen-stimulated tumour cell proliferation[397,398] which steered the way for the ultimate development and subsequent clinical trials of fulvestrant, that is now in clinical use for recurrent ER+ advanced disease in postmenopausal women[399,400]. Although significant information has been generated from the use of individual cancer cell lines, breast cancer has been long established as a heterogeneous disease and it is becoming increasingly recognised that the use of the MCF-7 cell line to represent all ER+ breast cancer is insufficient. As reviewed by Holliday & Speirs, it was concluded that studies must move on from 'the one marker, one cell line' approach[289].

Genomic studies have established four major subtypes of breast cancer (shown in Table 14) with each subtype exhibiting a disparate prognosis and treatment response partly due to inherent genetic differences between the subtypes[277,278]. ER+ tumours occur most frequently and comprise two molecular classifications: luminal A and luminal B. The former is the most common, representing 28-31% of breast cancers[277]. Luminal B breast cancers occur less frequently, representing approximately 20% of patients, and are characterised by HER2 over expression together with ER expression. The HER2 gene encodes a transmembrane RTK that belongs to the EGFR family. Activation of this receptor stimulates cell growth via downstream MAPK and PI3K pathways (detailed in sections 1.7.4 and 1.7.5), thereby serving as an oncogenic driver in breast cancer. Hyperactivation of HER2 signalling has been heavily implicated in driving endocrine resistance as

previously discussed in section 1.7.4. ER+ and HER2+ luminal B tumours have a greater proliferative index, characterised by high Ki67 (proliferation marker) expression, a more aggressive phenotype and worse prognosis compared to the luminal A subtype[401,402].

Table 14 Major molecular subtypes of breast cancer.

Classification	Immunoprofile
Luminal A	ER+, PR+, HER2-, Ki67-
Luminal B	ER+, PR+/-, HER2+, Ki67+
Basal	ER-, PR-, HER2-, Ki67+
HER2	ER-, PR-, HER2+, Ki67+

ER: oestrogen receptor; PR: progesterone receptor; HER2: human epidermal growth factor receptor 2; Ki67: proliferation marker. Adapted from Holliday & Speirs[289].

The basal-like subtype lacks expression of the ER, PR and HER2 (triple negative) and represents approximately 15% of all breast cancers. These cancers are highly aggressive and currently lack any form of standard targeted systemic therapy and are therefore difficult to treat and thus have extremely poor clinical outcomes[403]. These cancers are associated with distinct risk factors, including earlier menarche, younger age at first full-term pregnancy, high parity together with lack of breast feeding, and abdominal adiposity[403,404]. HER2+ cancer represents approximately 17% of all breast cancers. As well as HER2, these tumours are characterised by high expression of genes associated with the HER2 pathway e.g. GRB7 (growth factor receptor-bound protein 7)[403]. Morphologically HER2+ breast cancers are highly proliferative and typically ER-. Therapies for these cancers include HER2-targeted therapy (e.g. trastuzumab) in combination with cytotoxic chemotherapy. However, HER2+ tumours are associated with poor clinical outcomes[404]. Other molecular subtypes such as normal-like have also been identified in some studies, but are less well characterised. They tend to cluster closely with normal breast epithelium in microarray studies and as such there are doubts regarding their existence with some researches believing that they could be

a technical artefact from high contamination with normal tissue during microarray studies[401,404].

In the previous Chapter, extensive microarray analysis combined with verification by PCR and Western blot analysis, in addition to ontological investigation, identified GABBR2, CTNND2, CLU, TSC22D3 and BCL3 as the most robust proteins up regulated by all three antihormones in MCF-7 cells with expression maintained into the acquisition of resistance. It is hypothesised that induction of these pro-survival genes early during antihormone response allows a cohort of cells to survive the initial growth inhibitory actions of these therapies and ultimately contributes substantially to the emergence of resistant growth.

The aim of this Chapter was to consider the heterogeneity that exists in ER+ breast cancer and to build on the data presented in Chapter 3 to determine whether antihormone-induced expression of these 5 genes is common across additional models of ER+ disease, encompassing luminal A and luminal B subtypes. Microarray data obtained from four ER+ breast cancer cell lines (HER2-: MCF-7 and T47D and HER2+: BT474 and MDA-MB-361; characteristics detailed in section 2.1.1) treated for 10 days with fulvestrant compared to untreated control was utilised, with subsequent PCR and Western blot verification alongside tamoxifen, oestrogen deprivation and E2 treatments. Ultimately, such studies may identify a novel biomarker of endocrine failure or a potential therapeutic target for resistance, common to several subtypes of breast cancer and thus representing a large cohort of patients.

4.2 Methods

4.2.1 Microarray analysis

Microarray gene expression profiling, as described in section 2.2, was completed for 10 day fulvestrant-treated BT474, MDA-MB-361, MCF-7 and T47D cells versus untreated control. The four cell lines were cultured in medium supplemented with FCS ± fulvestrant. The resultant triplicate data were uploaded on to the online bioinformatics software GeneSifter where the data was first median normalised and log transformed prior to analysis. This GeneSifter-assembled array resource was interrogated using the gene probes representing GABBR2, CTNND2, CLU,

TSC22D3 and BCL3 as identified in Chapter 3 to be robustly induced by antihormones in MCF-7 cells, to determine whether fulvestrant promoted their expression in additional cell models of ER+ breast cancer, thus encompassing HER2+ and HER2- disease. ANOVA and post-hoc Tukey tests were used to analyse the differences between means. A p value <0.05 was considered statistically significant.

4.2.2 RT-PCR

RT-PCR was performed, as described in section 2.4, to verify the Affymetrix expression profiles of GABBR2, CTNND2, CLU, TSC22D3 and BCL3 in the HER2+ BT474 and MDA-MB-361 and HER2- MCF-7 and T47D cell lines. Triplicate RNA from 10 day untreated control and fulvestrant-treated cells (cultured under the same conditions as those used to generate the samples for microarray gene profiling), in addition to 10 day E2-, tamoxifen- and oestrogen deprivation-treated cells were analysed. Densitometry analysis was performed and the raw densitometry values of the genes of interest were normalised to β-actin loading control. The data were analysed using GraphPad prism. ANOVA and Tukey's multiple comparisons post-hoc tests were used to compare the means. A p value <0.05 was considered statistically significant.

4.2.3 Western blotting

The expression of GABBR2, CTNND2, CLU, TSC22D3 and BCL3 were examined at the protein level by Western blotting. Western blotting was performed on triplicate protein samples from 10 day untreated control, E2-, tamoxifen-, fulvestrant- and oestrogen deprivation-treated MCF-7, T47D, BT474 and MDA-MB-361 cells as described in section 2.5. The data were analysed using GraphPad prism. ANOVA and post-hoc Tukey's multiple comparisons tests were used to compare the means. A p value <0.05 was considered statistically significant.

4.3 Results

4.3.1 Microarray analysis of the 5 genes of interest in fulvestrant-treated BT474, MDA-MB-361, MCF-7 and T47D cell lines

The heatmap shown in Figure 41, generated from the jetset Affymetix gene probes, demonstrated up regulation (denoted in red) of GABBR2, CTNND2, CLU, TSC22D3 and BCL3 expression in all four cell lines following 10 day fulvestrant treatment compared to untreated control. In the MDA-MB-361 and T47D cell lines, TSC22D3 and CLU expression, respectively, were similar pre- and post-fulvestrant treatment as illustrated by the heatmap. The corresponding log2 intensity profiles, fold change in gene induction and detection calls for the 5 genes are illustrated in Figure 42-Figure 46.

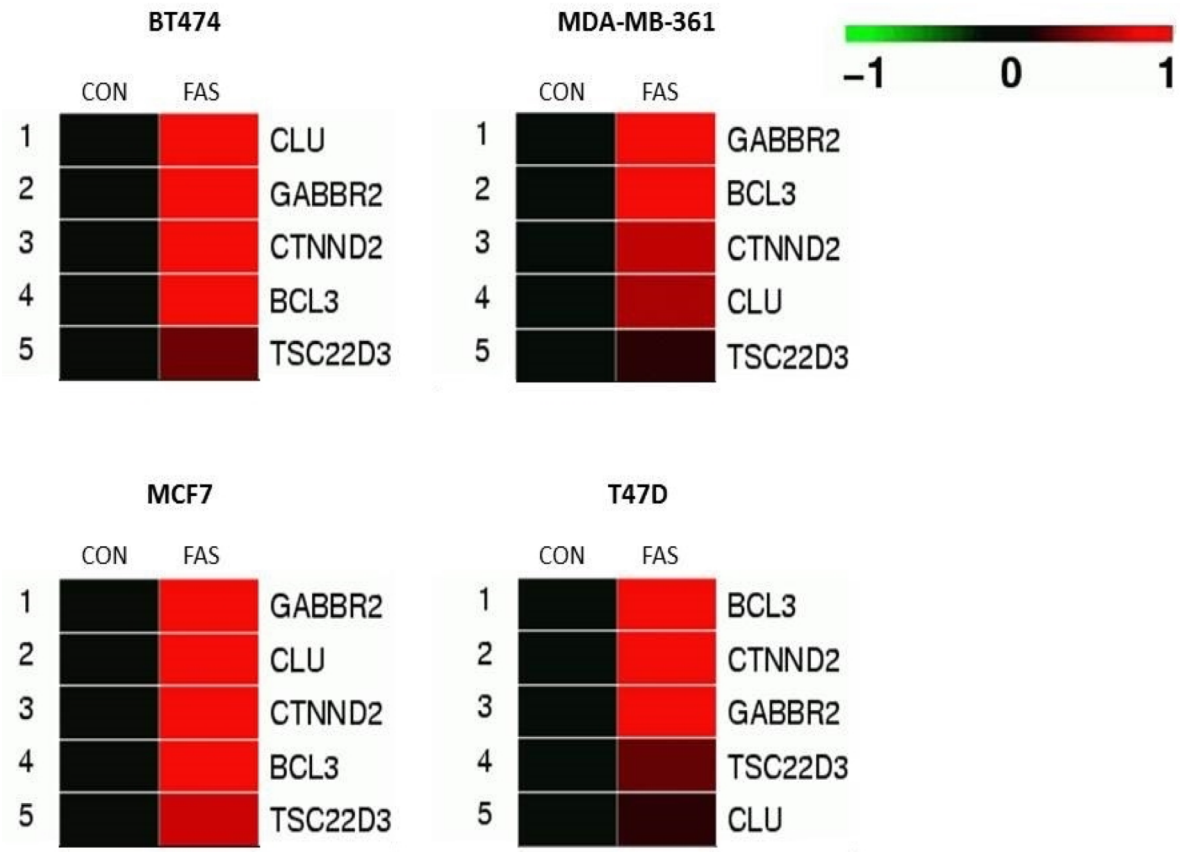

Figure 41 Heatmaps displaying change in expression of the 5 genes of interest following 10 day fulvestrant (FAS; 10^{-7} M) treatment versus untreated control (CON) in all four oestrogen receptor positive cell lines. Red denotes an increase in gene expression compared to control (shown in black).

4.3.1.1 BCL3

The log2 intensity profile showed significant ($p < 0.05$, $n=3$) induction of BCL3 expression (greater than 1.5 fold change) following fulvestrant treatment in all four cell lines (Figure 42A and B). The greatest up regulation was observed in the T47D cell lines, with a fold change of 3.29. Present detection calls were recorded in all four cell models irrespective of treatment, indicative of reliable detection of expression (Figure 42C).

A

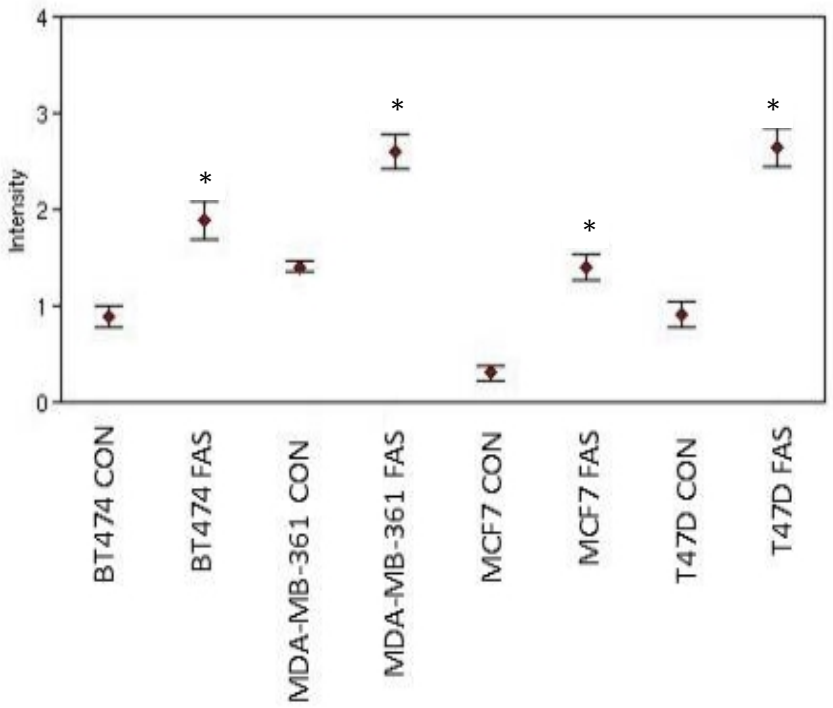

B

Fold change of gene expression following fulvestrant treatment			
BT474	**MDA-MB-361**	**MCF7**	**T47D**
2.00	2.28	2.15	3.29

C

	BT474 CON	**BT474 FAS**	**361 CON**	**361 FAS**	**MCF7 CON**	**MCF7 FAS**	**T47D CON**	**T47D FAS**
Detection call	PPP	PPP	PPP	PPP	PPP	PPP	PPP	PPP

Figure 42 (A) Log2 intensity plot displaying the normalised (mean of three independent replicates ± SEM) gene expression of BCL3 (jetset probe ID: 204908_s_at) in BT474, MDA-MB-361, MCF-7 and T47D cells treated for 10 days with fulvestrant (FAS; 10^{-7} M) versus untreated control (CON). (B) Table displaying the corresponding fold change in gene expression following fulvestrant treatment and (C) detection calls from the triplicate samples. * p <0.05 compared to control treatment of the equivalent cell line. 361: MDA-MB-361; P: present.

4.3.1.2 CLU

Fulvestrant promoted up regulation of CLU expression in the HER2+ and MCF-7 cell lines with a fold change greater than 1.5 (Figure 43A and B). Significant ($p < 0.05$, $n=3$) up regulation was observed in the MCF-7 and BT474 cell lines combined with present detection calls (Figure 43A and C). However, the log2 expression of the untreated controls (BT474 and MCF-7) failed to reach 0, which was mirrored by absent detection calls, suggestive of extremely low/no expression (Figure 43C). Interestingly, the T47D cell line demonstrated the greatest basal level of CLU expression with a predominantly present call reported. A small induction of CLU was apparent in the MDA-MB-361 (1.59 fold changed) and T47D (1.13 fold change) cell lines with present detection calls reported pre- and post-treatment, indicative of gene expression.

A

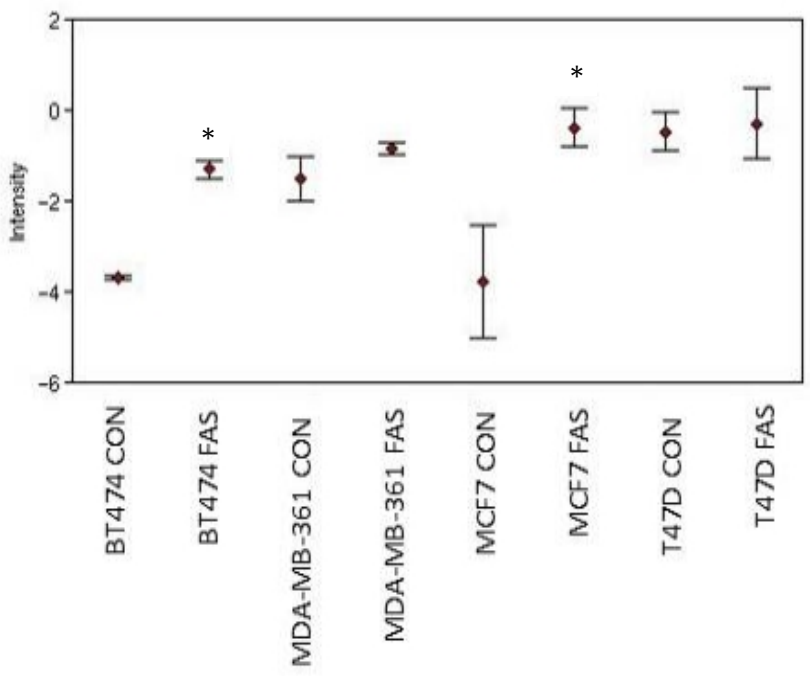

B

Fold change of gene expression following fulvestrant treatment			
BT474	**MDA-MB-361**	**MCF7**	**T47D**
5.22	1.59	10.54	1.13

C

	BT474 CON	**BT474 FAS**	**361 CON**	**361 FAS**	**MCF7 CON**	**MCF7 FAS**	**T47D CON**	**T47D FAS**
Detection call	AAA	PPP	PAP	PPP	AAA	PPP	PPA	PPP

Figure 43 (A) Log2 intensity plot displaying the normalised (mean of three independent replicates ± SEM) gene expression of CLU (jetset probe ID: 222043_at) in BT474, MDA-MB-361, MCF-7 and T47D cells treated for 10 days with fulvestrant (FAS; 10^{-7} M) versus untreated control (CON). (B) Table displaying the corresponding fold change in gene expression following fulvestrant treatment and (C) detection calls from the triplicate samples. * p <0.05 compared to control treatment of the equivalent cell line. 361: MDA-MB-361; P: present; A: absent.

4.3.1.3 GABBR2

The log2 intensity plot revealed up regulation of GABBR2 expression by 10 day fulvestrant treatment in all four ER+ cell lines versus untreated control (Figure 44A). The greatest induction was observed in the MCF-7 cells, with almost 190 fold change (Figure 44B). In the MDA-MB-361 and MCF-7 cells, the log2 expression values were below 0 and the detection calls were absent in the untreated control cells whereas present calls were reported following fulvestrant treatment (Figure 44A & C). In the BT474 cell line, present detection calls were reported in the control and fulvestrant-treated cells (Figure 44C) Furthermore, fulvestrant-induced up regulation of GABBR2 in the BT474, MDA-MB-361 and MCF-7 cells was statistically significant ($p < 0.05$, $n=3$). Although fulvestrant promoted induction of GABBR2 gene expression in the T47D cell, this induction failed to reach statistical significance. Additionally, the detection calls pre- and post-treatment were absent in this cell line, suggesting very low gene expression (Figure 44C).

A

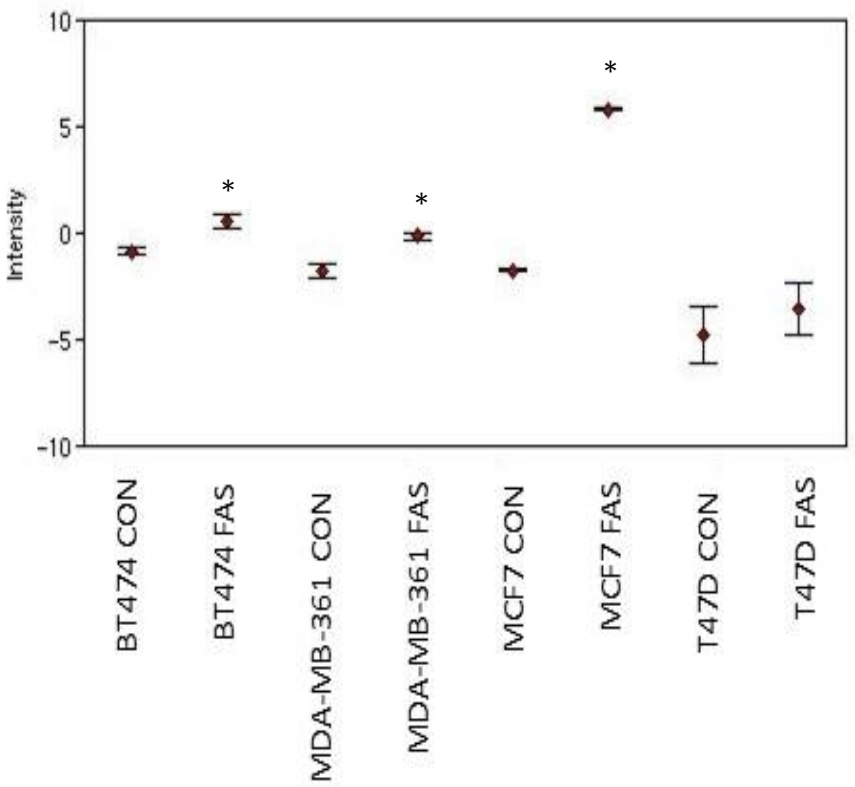

B

Fold change of gene expression following fulvestrant treatment			
BT474	**MDA-MB-361**	**MCF7**	**T47D**
2.59	3.11	187.37	2.40

C

	BT474 CON	**BT474 FAS**	**361 CON**	**361 FAS**	**MCF7 CON**	**MCF7 FAS**	**T47D CON**	**T47D FAS**
Detection call	PPP	PPP	AAP	PPP	APA	PPP	AAA	AAA

Figure 44 (A) Log2 intensity plot displaying the normalised (mean of three independent replicates ± SEM) gene expression of GABBR2 (jetset probe ID: 209990_s_at) in BT474, MDA-MB-361, MCF-7 and T47D cells treated for 10 days with fulvestrant (FAS; 10^{-7} M) versus untreated control (CON). (B) Table displaying the corresponding fold change in gene expression following fulvestrant treatment and (C) detection calls from the triplicate samples. * p <0.05 compared to control treatment of the equivalent cell line. 361: MDA-MB-361; P: present; A: absent.

4.3.1.4 CTNND2

The log2 intensity plot showed up regulation (greater than 1.5 fold change) of CTNND2 expression following fulvestrant treatment in all four cell lines (Figure 45A and B). However, although fulvestrant promoted up regulation in the T47D cell line, the induced levels remained lower than in the other 3 cell lines and absent calls were recorded (Figure 45C). Present detection calls were reported in the BT474, MDA-MB-361 and MCF-7 cells pre- and post-treatment (Figure 45C). Furthermore, this was mirrored by a significant ($p < 0.05$) induction by fulvestrant in the HER2+ and MCF-7 cell lines compared to control, however, the small induction induced by fulvestrant failed to reach significance in the T47D cell line (Figure 45A).

A

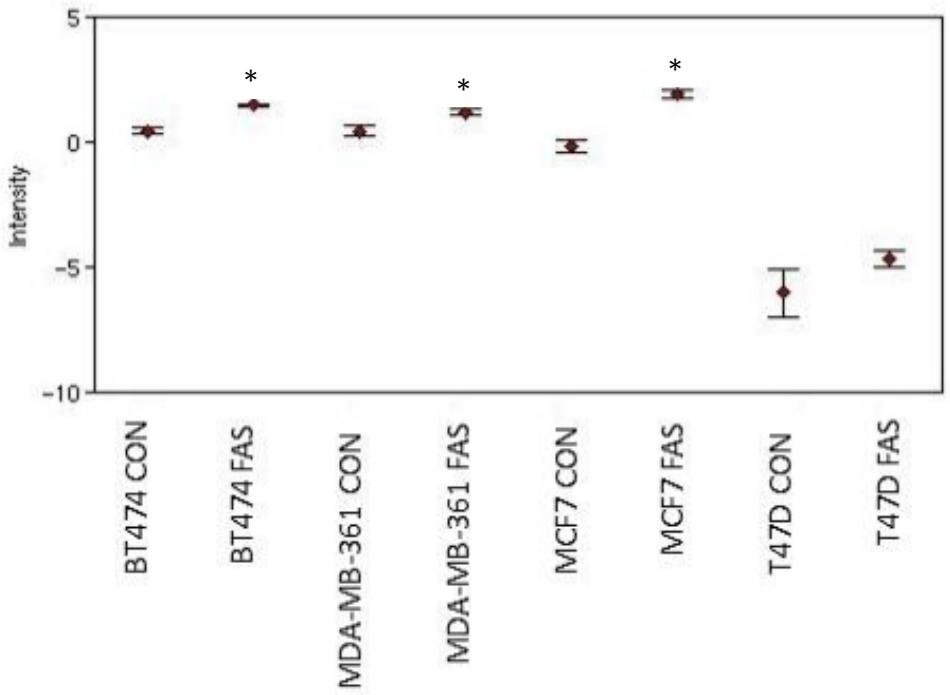

B

Fold change of gene expression following fulvestrant treatment			
BT474	**MDA-MB-361**	**MCF7**	**T47D**
2.05	1.69	4.29	2.59

C

	BT474 CON	BT474 FAS	361 CON	361 FAS	MCF7 CON	MCF7 FAS	T47D CON	T47D FAS
Detection call	PPP	PPP	PPP	PPP	PPP	PPP	AAA	AAA

Figure 45 (A) Log2 intensity plot displaying the normalised (mean of three independent replicates ± SEM) gene expression of CTNND2 (jetset probe ID: 209618_at) in BT474, MDA-MB-361, MCF-7 and T47D cells treated for 10 days with fulvestrant (FAS; 10^{-7} M) versus untreated control (CON). (B) Table displaying the corresponding fold change in gene expression following fulvestrant treatment and (C) detection calls from the triplicate samples. * p <0.05 compared to control treatment of the equivalent cell line. 361: MDA-MB-361; P: present; A: absent.

4.3.1.5 TSC22D3

The log2 intensity plot revealed greater basal expression of TSC22D3 in the HER2+ cell lines compared to the HER2- models (Figure 46A). Fulvestrant promoted up regulation of TSC22D3 expression in all four cell lines. However, this induction was only significant ($p < 0.05$, $n=3$) in the BT474 and MCF-7 cell lines, with the latter also displaying a fold change greater than 1.5 (Figure 46B). Present detection calls and log2 expression values greater than 0 were apparent in all four cell lines irrespective of treatment, suggesting reliable detection of expression (Figure 46C).

A

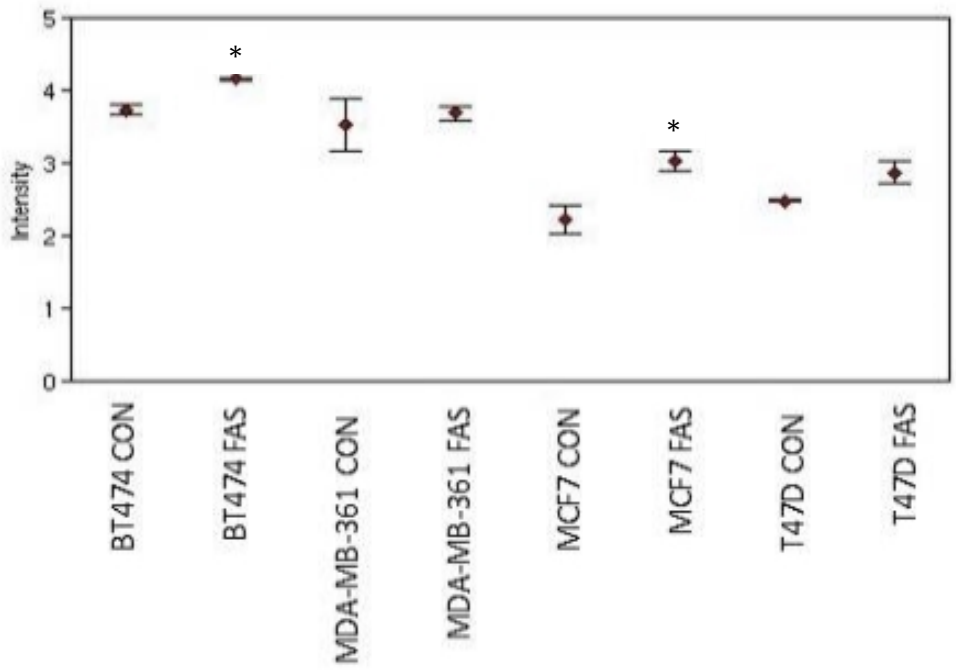

B

Fold change of gene expression following fulvestrant treatment			
BT474	**MDA-MB-361**	**MCF7**	**T47D**
1.34	1.12	1.74	1.31

C

	BT474 CON	**BT474 FAS**	**361 CON**	**361 FAS**	**MCF7 CON**	**MCF7 FAS**	**T47D CON**	**T47D FAS**
Detection call	PPP	PPP	PPP	PPP	PPP	PPP	PPP	PPP

Figure 46 (A) Log2 intensity plot displaying the normalised (mean of three independent replicates ± SEM) gene expression of TSC22D3 (jetset probe ID: 208763_s_at) in BT474, MDA-MB-361, MCF-7 and T47D cells treated for 10 days with fulvestrant (FAS; 10^{-7} M) versus untreated control (CON). (B) Table displaying the corresponding fold change in gene expression following fulvestrant treatment and (C) detection calls from the triplicate samples. * p <0.05 compared to control treatment of the equivalent cell line. 361: MDA-MB-361; P: present.

4.3.2 Verification of the microarray data by RT-PCR and Western blotting

The Affymetrix expression profiles of GABBR2, CTNND2, CLU, TSC22D3 and BCL3 in the HER2+ BT474 and MDA-MB-361 and HER2- MCF-7 and T47D cell lines were verified by RT-PCR and Western blotting. In agreement with the findings of the previous Chapter, the CTNND2 antibody continued to fail in all four cell lines, with no protein expression detected. RT-PCR and Western blotting were performed on triplicate RNA and protein samples from 10 day untreated control and fulvestrant-treated cells (under the same conditions as those used to generate the samples for microarray gene profiling). Although there are no microarray gene expression data for these cell lines following E2, tamoxifen and oestrogen deprivation treatments, and since this project is interested in all three antihormone treatments, the four cell lines were exposed to these treatments and analysed by RT-PCR and Western Blotting. The results are illustrated in Figure 47 to Figure 55

4.3.2.1 BCL3

In agreement with the microarray data, fulvestrant promoted increased expression of BCL3 mRNA and protein compared to untreated control in both the HER2+ and HER2- cell lines (Figure 47 and Figure 48). Furthermore, BCL3 mRNA and protein up regulation was also induced by tamoxifen and oestrogen deprivation treatments in all four cell lines (Figure 47 and Figure 48). Densitometry analysis revealed that tamoxifen promoted the greatest induction of BCL3 mRNA in the BT474, MCF-7 and T47D cell lines, with a statistically significant ($p < 0.05$) up regulation observed in the BT474 and T47D cell lines compared to control (Figure 47A and D). Tamoxifen also statistically significantly increased BCL3 mRNA expression versus E2 treatment in the BT474 ($p < 0.01$), MCF-7 ($p < 0.05$) and T47D ($p < 0.05$) cell lines (Figure 47A, C and D). In contrast, oestrogen deprivation treatment was shown to induce the greatest up regulation, although not significant, of BCL3 mRNA in the MDA-MB-361 cell line (Figure 47B). In the BT474 cell line, oestrogen deprivation treatment induced significant ($p < 0.05$) up regulation of BCL3 mRNA compared to E2 treatment (Figure 47A). Fulvestrant significantly ($p < 0.05$) increased BCL3 expression in the T47D cell line versus E2 treatment (Figure 47D). There was very little expression of BCL3 mRNA apparent in the four

cell lines following E2 treatment and in the untreated control cells (Figure 47). For each cell line, actin levels were similar following all treatments (Figure 47).

At the protein level, densitometry analysis and β-actin normalisation demonstrated that oestrogen deprivation treatment promoted the greatest expression of BCL3 in the BT474 and MCF-7 cell lines, which was statistically significant ($p < 0.01$) in the former cell line versus E2 treatment and control (Figure 48A and C). In the MDA-MB-361 cell line, tamoxifen was shown to induce the greatest expression (although not significant) of BCL3 compared to control and E2 treatment, whereas fulvestrant and oestrogen deprivation treatments were shown to significantly ($p < 0.001$) induce the greatest expression of BCL3 in the T47D cell line (Figure 48B and C). Minimal BCL3 expression was observed at baseline (control) and following E2 treatment in the four cell lines (Figure 48). For each cell line, actin levels were similar following all treatments (Figure 48).

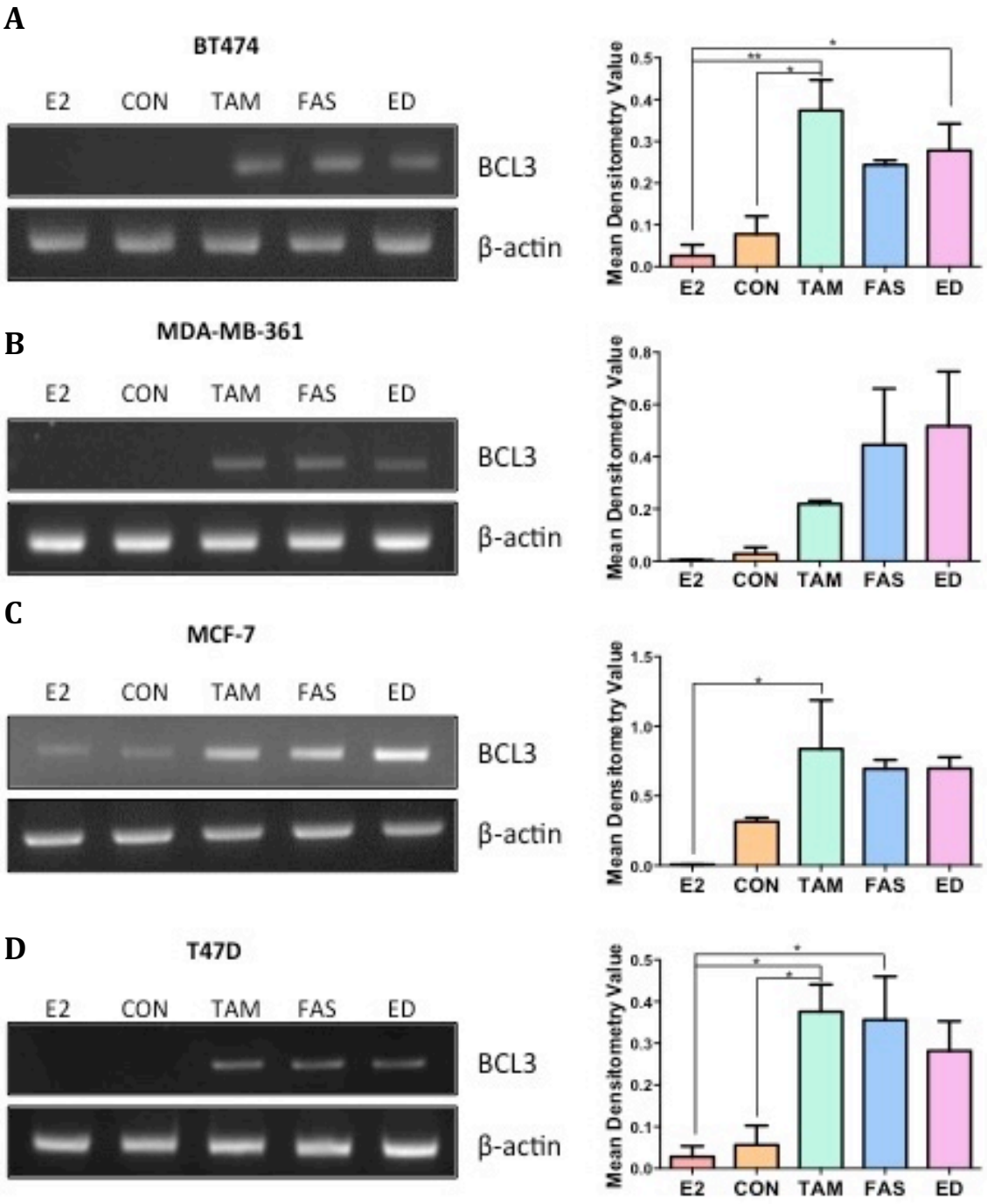

Figure 47 Representative PCR images and corresponding β-actin normalised densitometry graphs from three independent experiments showing BCL3 mRNA expression in BT474 (A), MDA-MB-361 (B), MCF-7 (C) and T47D (D) cells treated with oestradiol (E2; 10-9 M), untreated control (CON), tamoxifen (TAM; 10-7 M), fulvestrant (FAS; 10-7 M) and oestrogen deprivation (ED) for 10 days. The results are expressed as means ± SEM and the data were analysed by an ANOVA and post-hoc Tukey's multiple comparisons test. * p <0.05; ** p <0.01.

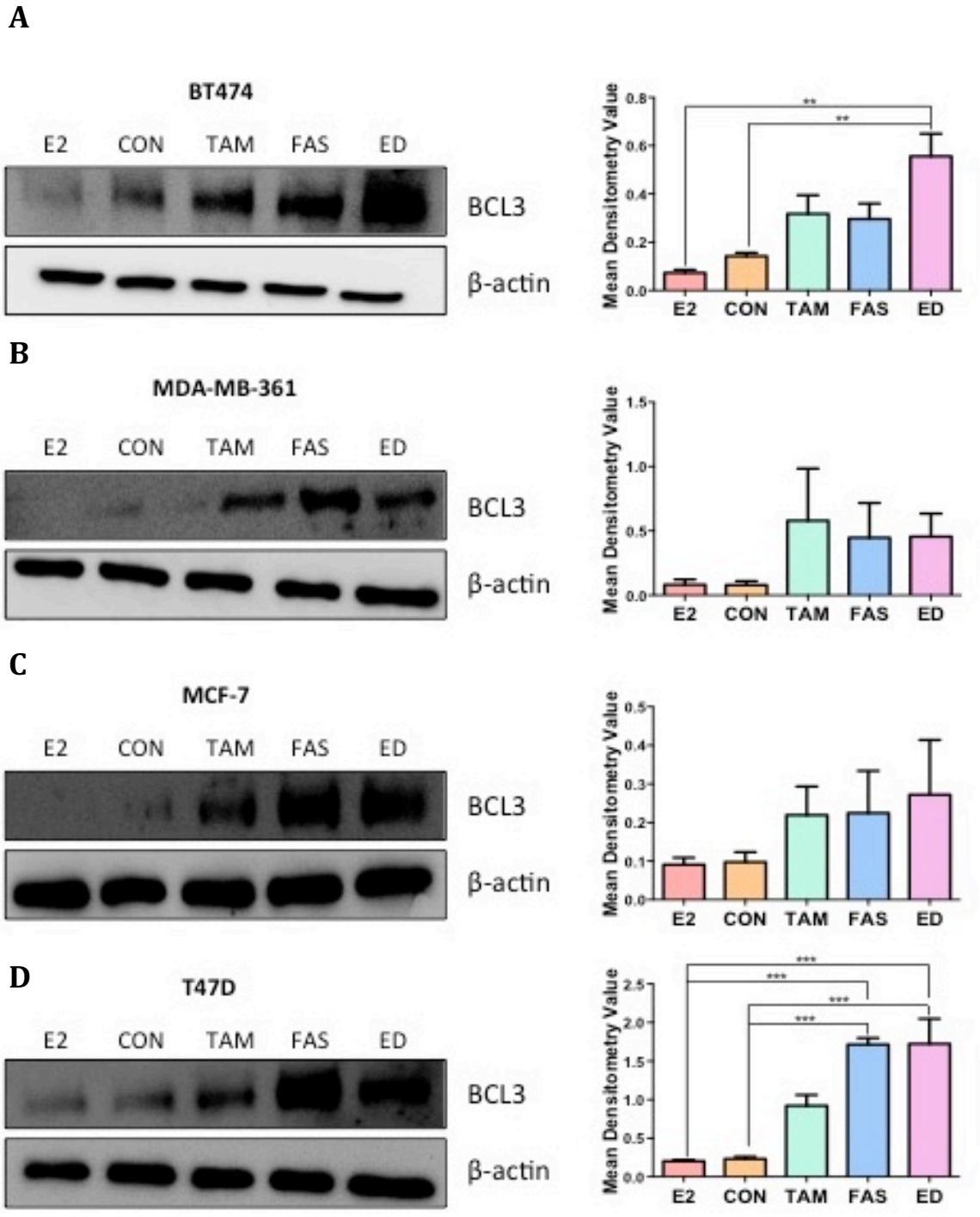

Figure 48 Representative Western blot images and corresponding β-actin normalised densitometry graphs from three independent experiments showing BCL3 protein expression in BT474 (A), MDA-MB-361 (B), MCF-7 (C) and T47D (D) cells treated with oestradiol (E2; 10-9 M), untreated control (CON), tamoxifen (TAM; 10-7 M), fulvestrant (FAS; 10-7 M) and oestrogen deprivation (ED) for 10 days. The results are expressed as means ± SEM and the data were analysed by an ANOVA and post-hoc Tukey's multiple comparisons test. ** p <0.01; *** p <0.001.

4.3.2.2 CLU

PCR and subsequent densitometry analysis revealed that tamoxifen, fulvestrant and oestrogen deprivation treatments induced up regulation of CLU mRNA expression in MCF-7 cell lines compared to E2 treatment and control (Figure 49C). However, this up regulation was not significant. Similarly, tamoxifen and fulvestrant induced up regulation, although not significant, of CLU mRNA expression in the BT474 cell line, compared to E2 treatment and control, however CLU expression was similar in oestrogen deprivation-treated and control cells (Figure 49A). These data are in agreement with the microarray data, which showed that fulvestrant promoted CLU gene up regulation in these cell lines. In the MDA-MB-361 cell line, although tamoxifen induced increased expression of CLU mRNA expression which was not significant, the expression levels of CLU following E2, control, fulvestrant and oestrogen deprivation treatments were comparable (Figure 49B). There was no obvious up regulation of CLU expression in this cell line following fulvestrant treatment compared to control, which is in disagreement with the microarray data. From the PCR gel, the baseline expression of CLU (untreated control) was greatest in the MDA-MB-361 cells compared to the BT474 and MCF-7 cells. This profile mimicked the detection calls reported from the microarray data which were present in MDA-MB-361 control cells and absent in BT474 and MCF-7 controls. Although present detection calls were recorded from the microarray data for CLU expression in the T47D cell lines pre- and post-fulvestrant treatment, CLU mRNA expression could not be detected by PCR in this cell line following E2, control, tamoxifen, fulvestrant and oestrogen deprivation treatments (Figure 49D). For each cell line, actin mRNA levels were constant following all treatments (Figure 49).

As previously revealed in Chapter 3, the pro-survival isoform of CLU (known as CLU-S) exists as a precursor and a mature form composed of α- and β-subunits. The CLU-S antibody used within this project recognises the 60 kDa precursor and 40 kDa CLUα subunit. Western analysis revealed up regulation of the CLUα subunit following tamoxifen, fulvestrant and oestrogen deprivation compared to E2 and control treatments in BT474, MDA-MB-361, MCF-7 and T47D cell lines (Figure 50). The CLU precursor subunit was up regulated by all three antihormones in the

MDA-MB-361 and MCF-7 cell lines, was up regulated by fulvestrant and oestrogen deprivation treatments in the T47D cell line, and tamoxifen and oestrogen deprivation in the BT474 cell line, compared to E2 treatment and control (Figure 50). In agreement with the PCR data, tamoxifen promoted the greatest induction of CLUα protein expression in the BT474 cell line versus control, which was statistically significant ($p < 0.05$) compared to E2 treatment, with less expression induced by fulvestrant and oestrogen deprivation treatments (Figure 50A). In the MDA-MB-361 cell line, oestrogen deprivation treatment promoted the greatest up regulation of CLU precursor and CLUα expression followed by fulvestrant and tamoxifen treatments, respectively (Figure 50B). In fact, oestrogen deprivation and fulvestrant treatment promoted a statistically significant ($p < 0.01$ and $p < 0.05$, respectively) increase in CLUα expression compared to E2 treatment and control (Figure 50B). In MCF-7 cells, similar expression of the CLU precursor was observed following antihormone treatment. However, CLUα expression was up regulated by all three antihormones, although it was not significant (Figure 50C). In the T47D cell line, oestrogen deprivation treatment statistically significantly induced CLUα expression versus control ($p < 0.05$) and E2 treatment ($p < 0.01$) (Figure 50D). Tamoxifen and fulvestrant treatments also induced CLUα expression however this was only significant ($p < 0.05$) following tamoxifen treatment compared to E2 treatment (Figure 50D). CLU precursor protein was statistically significantly ($p < 0.05$) up regulated by fulvestrant and oestrogen deprivation treatments compared to control and E2 treatment (Figure 50D). However, less expression was induced by tamoxifen treatment (Figure 50D). For each cell line, actin protein levels were constant following all treatments (Figure 50).

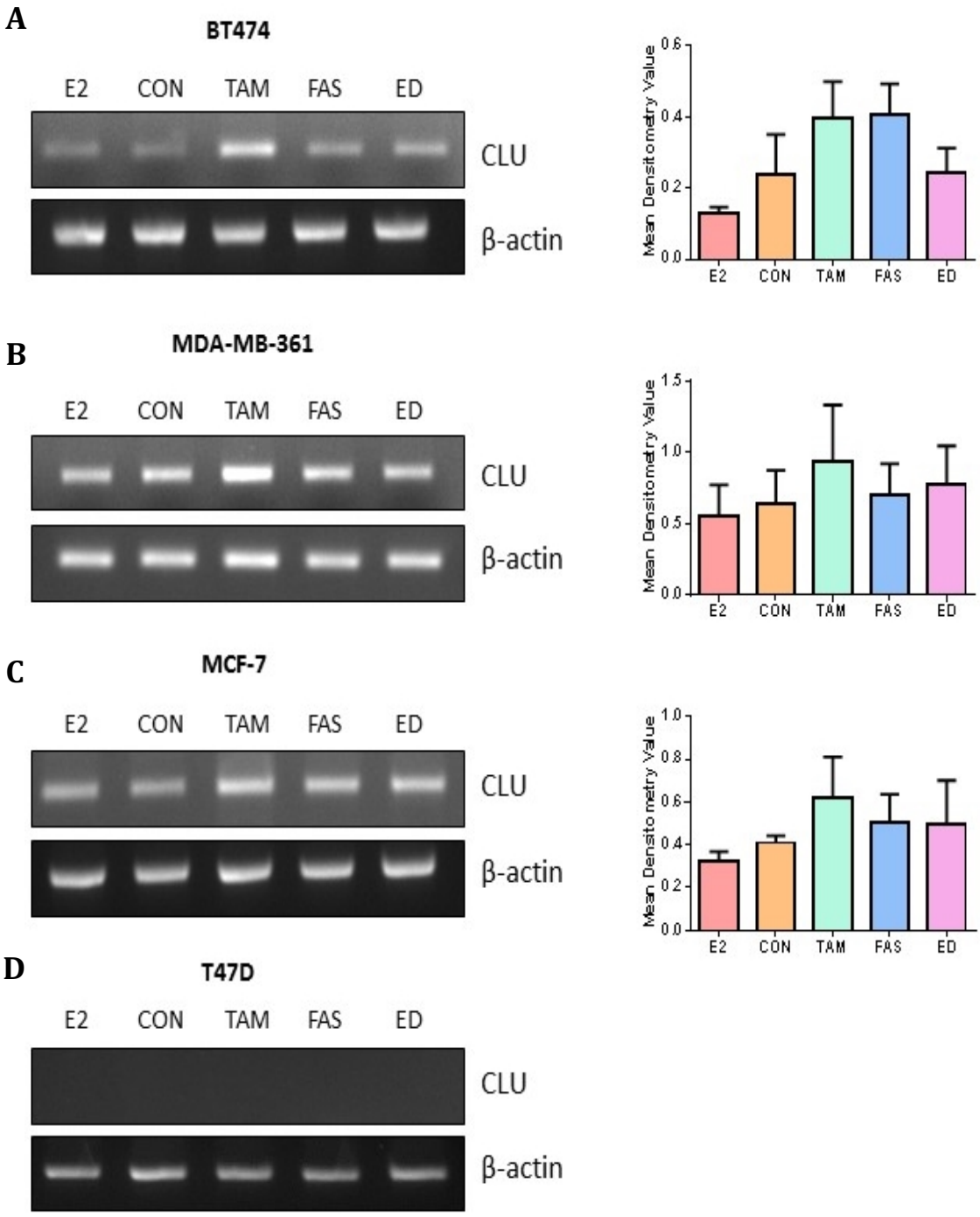

Figure 49 Representative PCR images and corresponding β-actin normalised densitometry graphs from three independent experiments showing CLU mRNA expression in BT474 (A), MDA-MB-361 (B), MCF-7 (C) AND T47D (D) cells treated with oestradiol (E2; 10-9 M), untreated control (CON), tamoxifen (TAM; 10-7 M), fulvestrant (FAS; 10-7 M) and oestrogen deprivation (ED) for 10 days. The results are expressed as means ± SEM and the data were analysed by an ANOVA and post-hoc Tukey's multiple comparisons test.

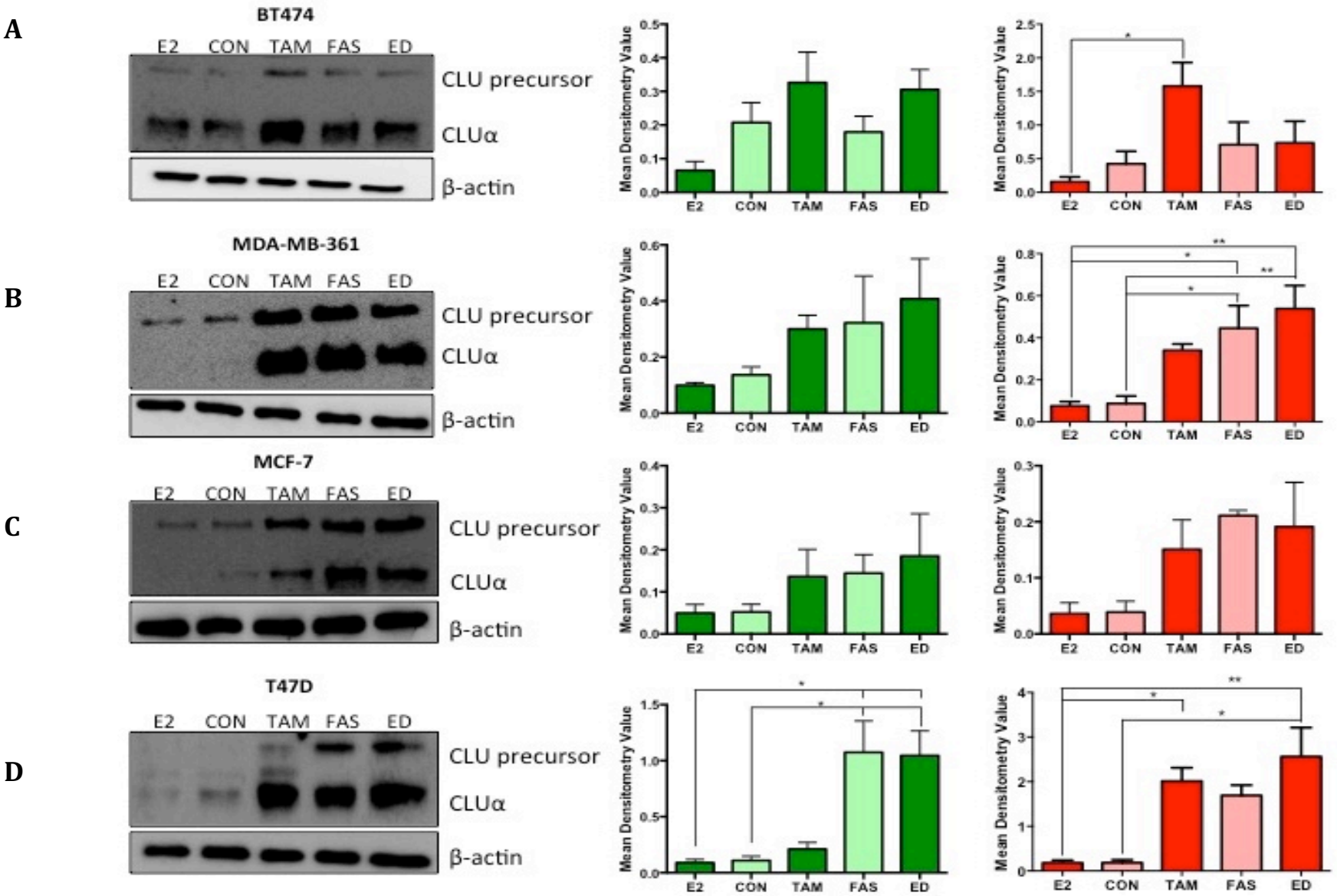

Figure 50 Representative Western blot images and corresponding β-actin normalised densitometry graphs from three independent experiments showing CLU precursor (green graphs) and CLUα (red graphs) protein expression in BT474 (A), MDA-MB-361 (B), MCF-7 (C) AND T47D (D) cells treated with oestradiol (E2; 10-9 M), untreated control (CON), tamoxifen (TAM; 10-7 M), fulvestrant (FAS; 10-7 M) and oestrogen deprivation (ED) for 10 days. The results are expressed as means ± SEM and the data were analysed by an ANOVA and post-hoc Tukey's multiple comparisons test. * p <0.05; ** p <0.01.

4.3.2.3 GABBR2

In agreement with the microarray profile, 10 day fulvestrant treatment promoted up regulation of GABBR2 mRNA and protein expression in BT474, MDA-MB-361 and MCF-7 cells compared to untreated control (Figure 51 and Figure 52). However, this up regulation was not significant in the three cell lines at the mRNA and protein level compared to control. At the mRNA level in the MCF-7 cell line, fulvestrant induced significant ($p < 0.01$) up regulation of GABBR2 expression compared to E2 treatment (Figure 51C). Additionally, in accordance with the absent detection calls reported from the microarray data, GABBR2 mRNA and protein expression was not detected in T47D cells pre- or post-fulvestrant treatment (Figure 51D and Figure 52D). Furthermore, in addition to fulvestrant, 10 day tamoxifen and oestrogen deprivation treatments induced up regulation of GABBR2 mRNA and protein expression in BT474, MDA-MB-361 and MCF-7 cells, and actin levels remained constant, compared to E2 treatment and untreated control (Figure 51 and Figure 52).

At the mRNA level, oestrogen deprivation and fulvestrant treatment statistically significantly ($p < 0.05$ and $p < 0.01$, respectively) induced GABBR2 expression compared to E2 treatment in the MCF-7 cell line (Figure 51C). At the protein level, in the BT474 and MDA-MB-361 cell lines, oestrogen deprivation treatment induced significant up regulation of GABBR2 expression compared to control ($p < 0.05$ and $p < 0.001$, respectively) and E2 treatment ($p < 0.01$ and $p < 0.001$, respectively) (Figure 52A and B). Additionally, fulvestrant promoted significant ($p < 0.05$) up regulation of GABBR2 protein expression in the BT474 cell line versus E2 treatment (Figure 52A). Despite relatively similar actin mRNA and protein levels shown in the T47D cell line following antihormone, E2 and control treatments, GABBR2 mRNA and protein expression was not detected (Figure 51D and Figure 52D). For each cell line (not including T47D), GABBR2 mRNA and protein was expressed at low levels in the control, and at lower levels following E2 treatment (Figure 51 and Figure 52).

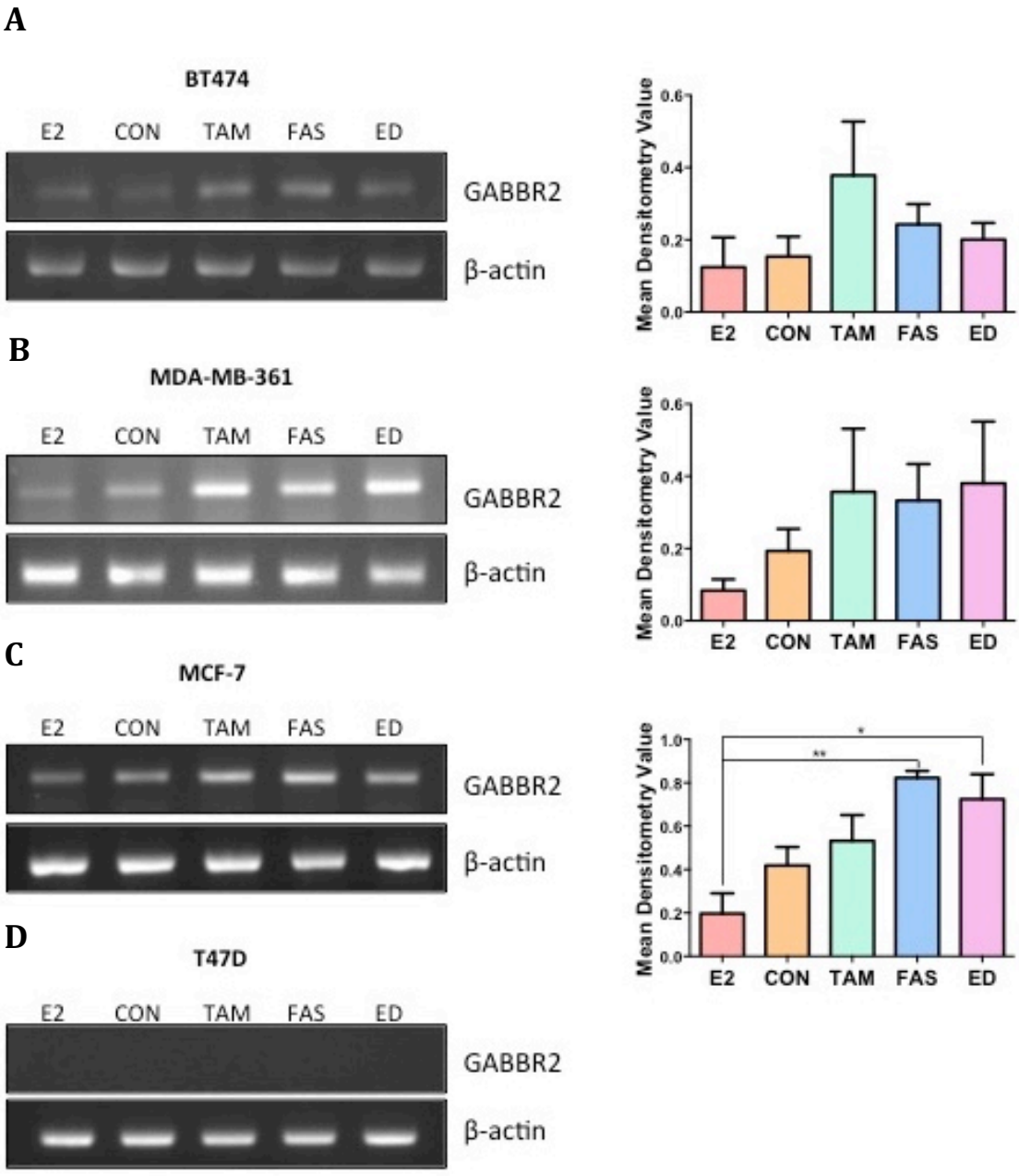

Figure 51 Representative PCR images and corresponding β-actin normalised densitometry graphs from three independent experiments showing GABBR2 mRNA expression in BT474 (A), MDA-MB-361 (B) MCF-7 (C) and T47D (D) cells treated with oestradiol (E2; 10-9 M), untreated control (CON), tamoxifen (TAM; 10-7 M), fulvestrant (FAS; 10-7 M) and oestrogen deprivation (ED) for 10 days. The results are expressed as means ± SEM and the data were analysed by an ANOVA and post-hoc Tukey's multiple comparisons test. * p <0.05; ** p <0.01.

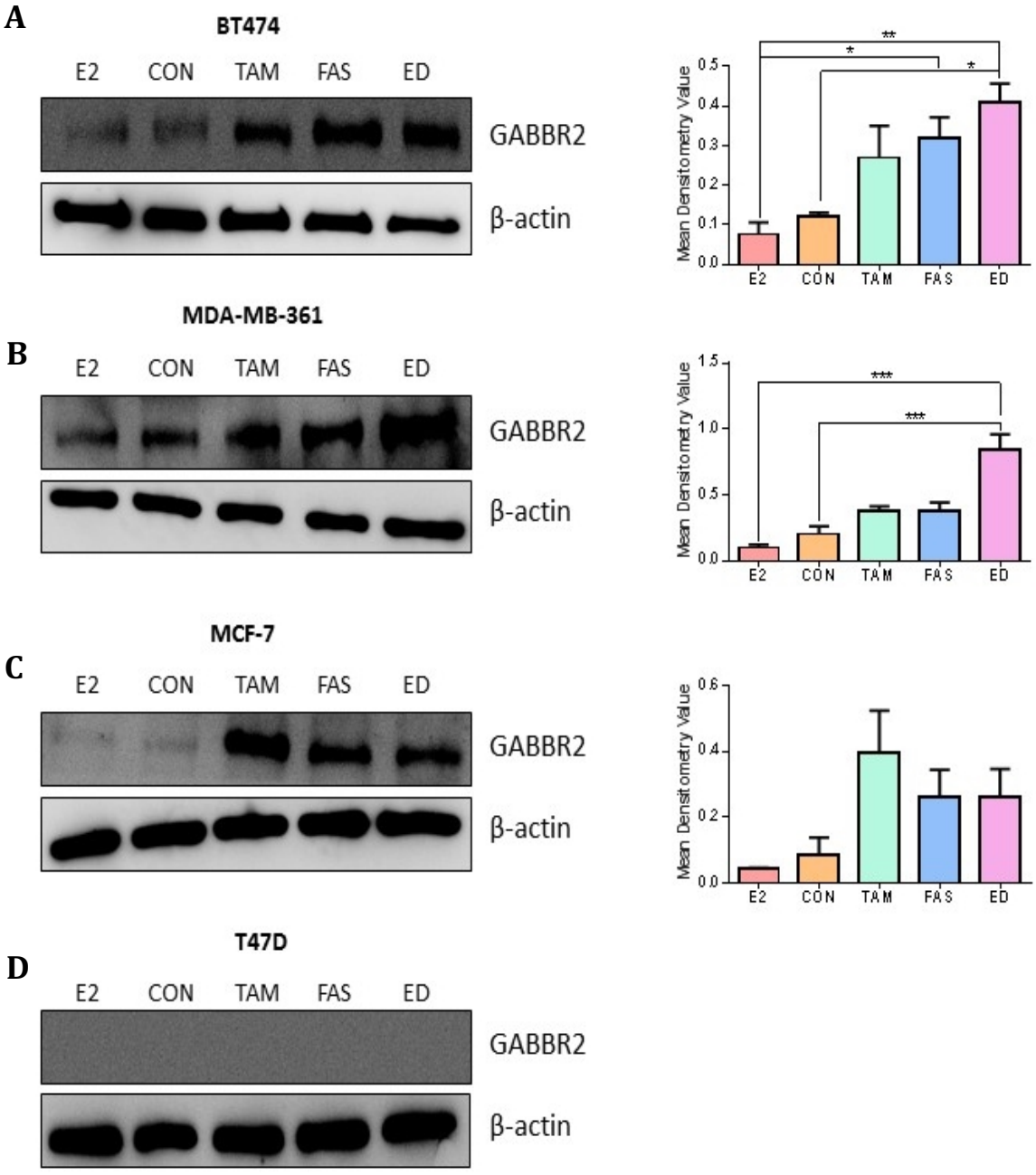

Figure 52 Representative Western blot images and corresponding β-actin normalised densitometry graphs from three independent experiments showing GABBR2 protein expression in BT474 (A), MDA-MB-361 (B), MCF-7 (C) and T47D (D) cells treated with oestradiol (E2; 10-9 M), untreated control (CON), tamoxifen (TAM; 10-7 M), fulvestrant (FAS; 10-7 M) and oestrogen deprivation (ED) for 10 days. The results are expressed as means ± SEM and the data were analysed by an ANOVA and post-hoc Tukey's multiple comparisons test. * p <0.05; ** p <0.01; *** p <0.001.

4.3.2.4 CTNND2

In contrast to the microarray profile, there was no apparent up regulation of CTNND2 mRNA expression in BT474, MDA-MB-361 and MCF-7 cells following 10 day fulvestrant treatment compared to untreated control (Figure 53). A non-specific band, of a higher molecular weight, was detected by the CTNND2 primers in the three cell lines. Furthermore, CTNND2 mRNA expression could not be detected in T47D cells irrespective of treatment (Figure 53D). This supports the absent detection calls and low log2 expression values observed in this cell line during analysis of the microarray data. Moreover, in the BT474, MDA-MB-361 and MCF-7 cell lines, CTNND2 mRNA expression following tamoxifen and oestrogen deprivation treatments were relatively similar to untreated control and fulvestrant treatments (Figure 53A, B and C). In all three cell lines, CTNND2 mRNA expression was slightly down regulated by 10 day E2 treatment compared to control. For each cell line, actin mRNA levels were constant following all treatments (Figure 53). As mentioned above, the CTNND2 antibody continued to fail in all four cell lines, with no protein expression detected.

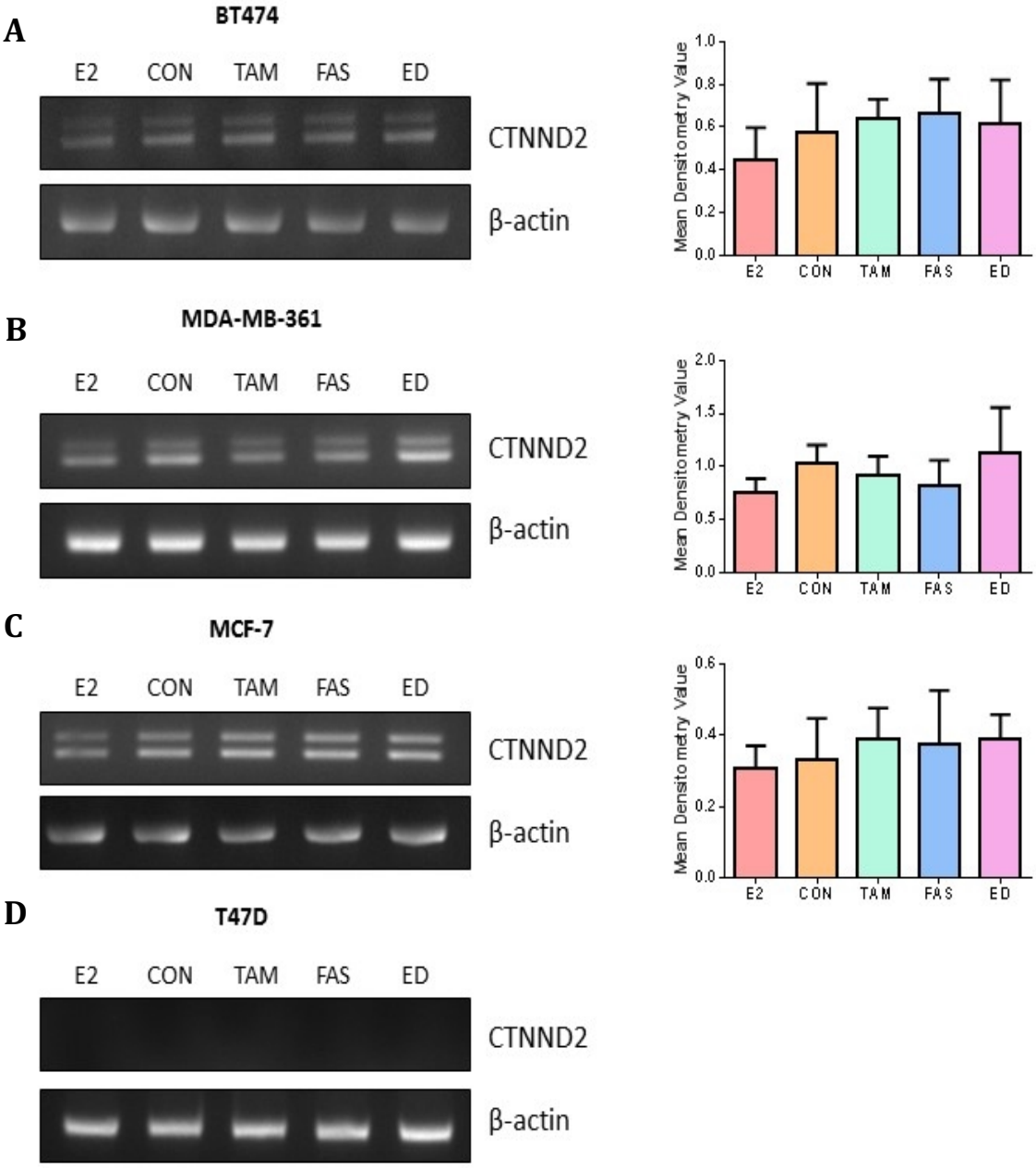

Figure 53 Representative PCR images and corresponding β-actin normalised densitometry graphs from 3 independent experiments showing CTNND2 mRNA expression in BT474 (A), MDA-MB-361 (B), MCF-7 (C) and T47D (D) cells treated with oestradiol (E2; 10-9 M), untreated control (CON), tamoxifen (TAM; 10-7 M), fulvestrant (FAS; 10-7 M) and oestrogen deprivation (ED) for 10 days. The results are expressed as means ± SEM and the data were analysed by an ANOVA and post-hoc Tukey's multiple comparisons test.

4.3.2.5 TSC22D3

The PCR and Western blotting data demonstrated up regulation of TSC22D3 expression by tamoxifen, fulvestrant and oestrogen deprivation treatments in MDA-MB-361 and MCF-7 cells compared to E2 treatment and control (Figure 54B and C, Figure 55B and C). However, a statistically significant ($p < 0.05$) induction was only observed at the protein level in the MDA-MB-361 cell line. Fulvestrant induced significant up regulation of TSC22D3 protein expression compared to control ($p < 0.001$) and E2 treatment ($p < 0.0001$) in the MDA-MB-361 cell line (Figure 55B). TSC22D3 protein expression was also significantly up regulated by tamoxifen treatment compared to control ($p < 0.05$) and E2 treatment ($p < 0.001$), and also by oestrogen deprivation treatment versus E2 treatment ($p < 0.05$) in this cell line (Figure 55B). These profiles are in agreement with the microarray data which revealed that fulvestrant promoted TSC22D3 expression in these two cell lines compared to control. However, in the BT474 and T47D cells lines, TSC22D3 mRNA expression was similar following antihormone-, E2- and control-treatments (Figure 54A and Figure 54D), whereas at the protein level, TSC22D3 expression was induced by all three antihormones versus E2 treatment and control (Figure 55A and Figure 55D). However, this up regulation was only significant ($p < 0.05$) in oestrogen deprivation-treated BT474 cells versus E2 treatment (Figure 55A). These profiles are in agreement with the microarray data which suggested that fulvestrant promoted up regulation of TSC22D3 expression in these cell lines. Actin mRNA and protein levels remained constant following all treatments for each cell line (Figure 54 and Figure 55). Moreover, at the protein level, very little TSC22D3 expression was detected following E2 and control treatments (Figure 55).

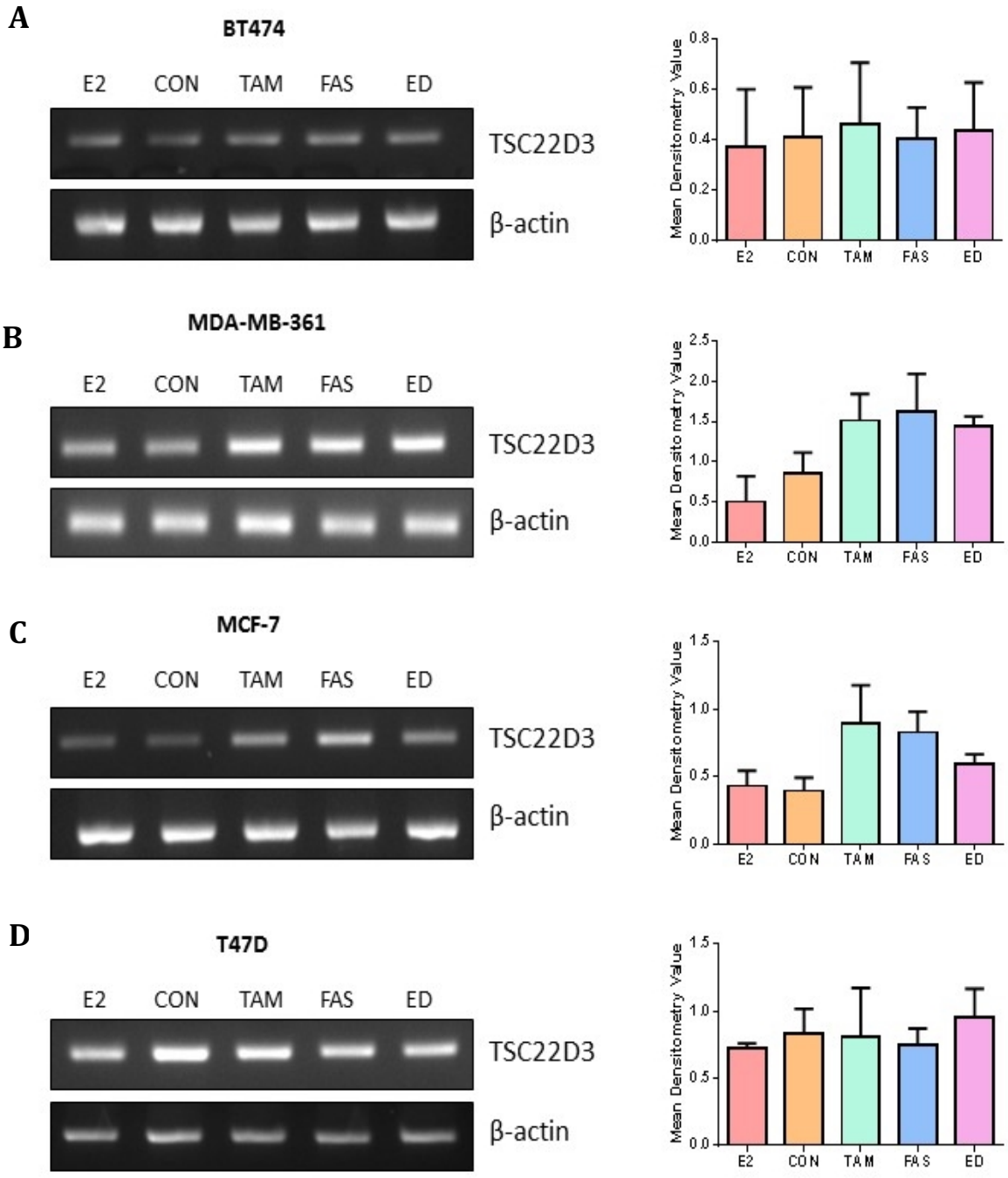

Figure 54 Representative PCR images and corresponding β-actin normalised densitometry graphs from three independent experiments showing TSC22D3 mRNA expression in BT474 (A), MDA-MB-361 (B), MCF-7 (C) AND T47D (D) cells treated with oestradiol (E2; 10-9 M), untreated control (CON), tamoxifen (TAM; 10-7 M), fulvestrant (FAS; 10-7 M) and oestrogen deprivation (ED) for 10 days. The results are expressed as means ± SEM and the data were analysed by an ANOVA and post-hoc Tukey's multiple comparisons test.

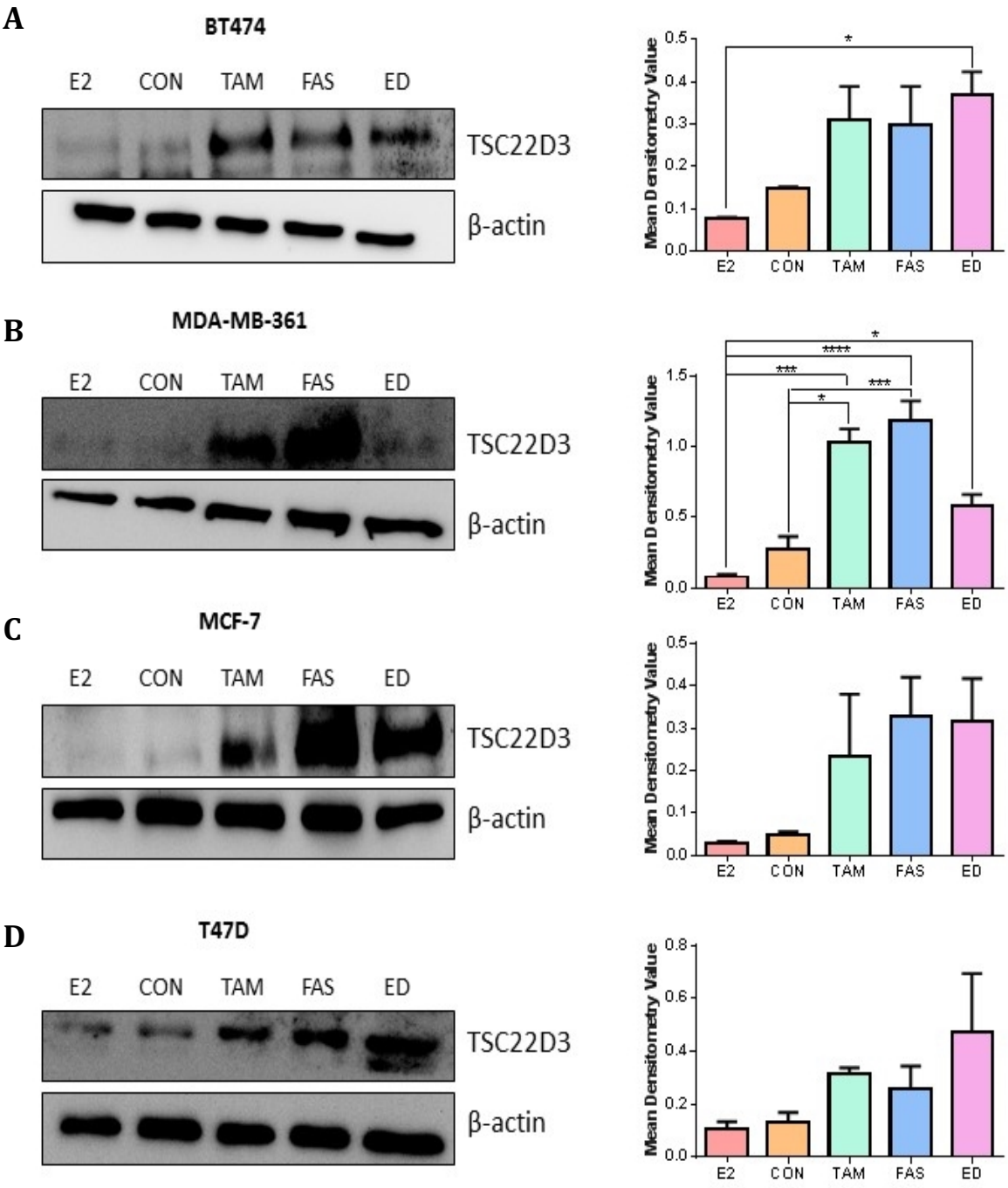

Figure 55 Representative Western blot images and corresponding β-actin normalised densitometry graphs from three independent experiments showing TSC22D3 protein expression in BT474 (A), MDA-MB-361 (B), MCF-7 (C) AND T47D (D) cells treated with oestradiol (E2; 10-9 M), untreated control (CON), tamoxifen (TAM; 10-7 M), fulvestrant (FAS; 10-7 M) and oestrogen deprivation (ED) for 10 days. The results are expressed as means ± SEM and the data were analysed by an ANOVA and post-hoc Tukey's multiple comparisons test. * p <0.05; *** p <0.001; **** p <0.0001.

4.4 Discussion

Breast cancer is a highly heterogeneous disease and has been classified into at least five subtypes, with each demonstrating a different prognosis and response to treatment[277,278]. However, the majority of studies have utilised the MCF-7 cell line to represent ER+ breast cancer. It is becoming increasingly clear that such studies are inadequate and equivalent investigations in additional cell lines are required to better reflect this heterogeneity. Therefore, in this Chapter, a panel of four ER+ breast cancer cell lines with differing HER2 status were employed to examine antihormone-induced expression of GABBR2, CTNND2, CLU, TSC22D3 and BCL3, previously identified in Chapter 3 by microarray analysis to be significantly up regulated by short term tamoxifen, fulvestrant and oestrogen deprivation treatments in MCF-7 cells with expression maintained into the acquisition of resistance. It was hypothesised that rapid antihormone-induced up regulation of these pro-survival genes during initial drug response may allow a cohort of tumour cells to evade the antihormone challenge and promote the development of resistant growth, ultimately resulting in poorer patient outlook.

Initially, microarray gene expression data derived from HER2- MCF-7 and T47D cells and HER2+ BT474 and MDA-MB-361 cells were interrogated to examine the expression of the 5 genes following 10 day fulvestrant treatment versus untreated control in the panel of cell lines. Importantly, however, the HER2+ cell lines do not proliferate very well in stripped serum therefore the microarray data utilised in this Chapter was generated from the four cell lines cultured in medium supplemented with FCS ± fulvestrant for 10 days. This is in contrast to the previous Chapter, whereby MCF-7 cells were cultured for 10 days in medium supplemented with sFCS plus antihormone or E2-control treatments. For all subsequent experiments all cell lines were cultured in FCS. The microarray data was verified by subsequent PCR and Western blot analysis. Additionally, PCR and Western blotting were performed to examine the expression of the 5 genes following 10 day E2, tamoxifen and oestrogen deprivation treatments in the four cell lines (cultured in FCS) for which there was no microarray gene expression data. Such studies were performed to consider an aspect of heterogeneity and to determine whether all three clinically used antihormone treatments (tamoxifen,

fulvestrant and oestrogen deprivation) induce expression of the 5 genes, whose ontology strongly suggests a potential role in limiting response and promoting resistance, in four ER+ breast cancer cell lines representing HER2- and HER2+ disease. Ultimately such studies may potentially identify an antihormone-induced resistant mechanism common to several antihormone therapies and breast cancer disease subtypes.

Interestingly, from the microarray gene expression data BCL3 was the only gene identified to be significantly induced by fulvestrant in the four cell lines versus untreated control, including the T47D cell line, which was not observed with any of the other 4 genes. This profile was verified by RT-PCR and Western blotting, with concurrent increases in BCL3 mRNA and protein expression following tamoxifen and oestrogen deprivation treatments, with down regulation induced by E2, versus untreated control. At the mRNA level, such antihormone-induced expression of BCL3 was significant versus control in the BT474 and T47D cell lines following tamoxifen treatment. At the protein level, oestrogen deprivation treatment induced significant up regulation of BCL3 expression in the BT474 and T47D cell lines versus control, in addition to fulvestrant treatment, which also induced significant up regulation of BCL3 expression in the latter cell line. Together, these studies identify BCL3 as a protein induced rapidly by three clinically used antihormones in a panel of four ER+ breast cancer cell models, hypothesised to play a significant role in limiting the efficacy of such agents during response and ultimately contributing to the emergence of resistant growth.

As concluded from the ontological investigations performed in Chapter 3, BCL3 is a co-activator of NF-κB transcriptional activity, comprised of p50 and p52 homodimers, which regulates several genes involved in immune response, cell growth and survival[372]. The role of NF-κB in oncogenesis and indeed breast cancer has been extensively studied. However, the potential role of BCL3 in activating aberrant NF-κB signalling to induce cell proliferation and survival in ER+ breast cancer and particularly in limiting antihormone efficacy and promoting the resistant phenotype, is largely unexplored. Cogswell et al. demonstrated increased expression of BCL3 in breast cancer tissues representing a range of tumour types (including ER+) and grades[360]. BCL3 expression has also been observed in a range

of breast cancer cell lines comprising ER+/ER- and HER2+/HER2- disease, including the MCF-7 cell line[368]. However, the precise role of BCL3 remains to be elucidated. In response to oestrogen withdrawal in MCF-7 cells and in ER+ oestrogen-independent MCF-7 cells (model of hormone independence), BCL3 expression has been shown to increase versus control, thus supporting the data presented here, with concurrent increases in NF-κB activity (predominantly p50 dimers) and cell growth, suggesting the ability of BCL3 to co-activate p50 to allow a cohort of cells to grow and survive oestrogen withdrawal to establish a hormone-independent phenotype[363]. However, studies examining BCL3 expression in ER+ breast cancer and exploring a potential role in antihormone response and resistance have focussed on the individual ER+ MCF-7 cell line. As previously mentioned, the use of MCF-7 cells to represent heterogeneous ER+ disease is insufficient. The data presented in this Chapter are the first to our knowledge investigating the expression of BCL3 and its induction in response to antihormone treatment in multiple ER+ breast cancer cell lines comprising HER2+ and HER2- disease, thus better reflecting the heterogeneity that exists.

The microarray data identified significant fulvestrant-induced CLU expression in the BT474 and MCF-7 cell lines, with a small induction observed in the MDA-MB-361 and T47D cell lines versus untreated control. Subsequent RT-PCR partially verified the microarray gene expression profiles of CLU, with increased mRNA expression observed in the BT474 and MCF-7 cell lines following fulvestrant treatment, which was also apparent following 10 day tamoxifen treatment in both cell lines and oestrogen deprivation treatment in the MCF-7 cell line, compared to E2-treated and untreated control cells. However, such antihormone-induced increases in CLU expression were not significant. Conversely, fulvestrant and oestrogen deprivation treatments induced relatively similar CLU mRNA expression in the MDA-MB-361 cells to untreated control and E2-treated cells, while tamoxifen promoted a slight increase in gene expression. Furthermore, CLU mRNA could not be detected in the T47D cell line, irrespective of treatment, which is in disagreement with the present detection calls reported from the microarray data. However, the differences in the microarray and PCR profiles may be due to the different regions of mRNA recognised by the PCR primers to

those recognised by the Affymetrix gene chip. Additionally, a splice variant of CLU (not recognised by the designed CLU primers) may be present in the T47D cell line, potentially explaining the lack of CLU mRNA detected in this cell line.

As previously described, CLU exists as two main forms with contrasting functions as a result of alternative splicing. The cytoplasmic secreted (CLU-S) form promotes cell survival and the nuclear form promotes apoptosis. This project is interested in the pro-survival role and therefore the CLU-S form. Prochnow et al. have shown that CLU-S represents the most abundant (> 99%) CLU form in several cell lines, including MCF-7 cells[295]. Although the microarray gene probes and PCR primers did not specifically target CLU-S, the antibody used for Western analysis was CLU-S-specific. In contrast to the mRNA profile, at the protein level, the secretory CLUα subunit was increased by all antihormone treatments in all four ER+ cell lines compared to E2-treated and untreated control cells. Such increases reached statistical significance following oestrogen deprivation treatment in the T47D and MDA-MB-361 cell lines as well as fulvestrant treatment in the latter compared to control. Additionally, statistically significant antihormone-induced CLUα expression was observed versus E2 treatment following tamoxifen treatment in the T47D and BT474 cells, fulvestrant treatment in the MDA-MB-361 cell line and oestrogen deprivation treatment in the latter cell line and T47D cell line. The CLU precursor subunit was up regulated by all three antihormone treatments in the four cell lines versus control, with the exception of fulvestrant treatment in the BT474 cell line and tamoxifen treatment in the T47D cell line, which expressed similar CLU precursor treatment to control. Statistically significant increases in CLU precursor expression were demonstrated versus E2 treatment and control in the T47D cell line. In summary, these studies identify secretory CLU as a protein induced early during response to three clinically used antihormones in multiple ER+ breast cancer cell models, whose expression may contribute substantially to the limited efficacy of these agents and ultimately the development of resistance.

As identified from the ontological studies in Chapter 3, CLU is a ubiquitously expressed glycoprotein implicated in several physiological processes such as lipid transport and complement regulation. Increased CLU expression has been reported in breast cancer tissues representing a range of tumour types (including

ER+) and grades, as well as breast cancer cell lines, including the MCF-7 cell line[335,336]. Increased CLU expression in breast cancer has been associated with cell survival, invasion and metastasis. More recent research is emerging focussing on the potential role of CLU in limiting antihormone response and promoting resistance. In agreement with the data presented in this study, short term tamoxifen (and toremifene) treatment has been shown to increase CLU expression in MCF-7 and T47D cells[338,339]. Furthermore, the combination of antibody targeting CLU plus tamoxifen in MCF-7 cells has been shown to increase the sensitivity of these cells to the antihormone, evidenced by a decrease in cell viability, compared to tamoxifen treatment alone[339]. However, 3 day tamoxifen (100 nM) and toremifene (100 nM) treatment were shown to increase T47D cell growth and consequently this cell line was deemed antihormone resistant[338]. Surprisingly, this observation is in contrast to the literature, where T47D cells are shown to be antihormone sensitive (in particular, 100 nM tamoxifen has been shown to inhibit T47D cell growth as early as 48 hours[405]). It has been long established that classically, E2 stimulates T47D cell proliferation which is inhibited with tamoxifen[406,407]. Furthermore, down regulation of CLU in the T47D cells deemed antihormone resistant, re-sensitised these cells to toremifene[338]. Together, these findings suggest that CLU up regulation in response to antihormone treatment triggers an adaptive survival mechanism to counteract the growth inhibitory effects of these agents, which may ultimately result in the development of resistance.

However, the majority of studies examining the expression of CLU in ER+ breast cancer and exploring a possible role in antihormone response and resistance have predominantly utilised the MCF-7 cell line, with the exception of Toffanin et al. who performed equivalent studies in the T47D cell line although these cells was considered antihormone resistant[338]. To represent the heterogeneity of ER+ breast cancer, it is necessary to utilise a panel of cell lines to better reflect the variety of molecular subtypes. As such, this Chapter has utilised multiple ER+ cell lines to demonstrate antihormone-induced CLU expression in HER2+ and HER2- disease. Interestingly, although there are no studies examining the association between antihormones and CLU in HER2+ breast cancer, Biroccio et al. have identified a

strong link between HER2-signalling and CLU expression[408]. Similarly to antihormones, the HER2-monoclonal antibody trastuzumab down regulates receptor expression and inhibits cell growth but promotes very little apoptosis in BT474 cells. Short-term trastuzumab treatment of these cells was shown to increase CLU expression. Accordingly, trastuzumab therapy combined with the antisense inhibitor of CLU, OGX-011 (currently in clinical development), significantly enhanced the sensitivity of BT474 cells to trastuzumab, evidenced by an increase in apoptosis and reduction in cell proliferation, compared to either treatment alone. This study identifies CLU as a survival protein that may play a role in trastuzumab resistance through inhibition of apoptosis, and combined targeting of HER2 and CLU may provide a novel approach to breast cancer therapy. Additionally, combination of OGX-011 with antihormones may similarly improve the anti-tumour activity of these agents and notably enhance cell kill, to prevent or delay the emergence of resistant growth.

The microarray gene expression data revealed that fulvestrant induced up regulation of GABBR2 and CTNND2 expression in the four ER+ cell lines, which was significant in the HER2+ and MCF-7 cell lines. The microarray profile of GABBR2 was successfully verified by RT-PCR, although no mRNA expression was detected in the T47D cell line, irrespective of treatment, which is in agreement with the microarray data which revealed absent detection calls in this cell line. Additionally, 10 day tamoxifen and oestrogen deprivation treatments induced up regulation, while E2 induced down regulation, of GABBR2 expression in the HER2+ and MCF-7 cell lines, again with no expression detected in the T47D cell line. However, antihormone-induced expression of GABBR2 mRNA did not reach significance versus control in any of the cell lines. Statistically significant antihormone-induced GABBR2 mRNA expression was observed following fulvestrant and oestrogen deprivation treatment compared to E2 treatment in the MCF-7 cell line. At the protein level, this profile was mirrored with increased GABBR2 expression observed following the three antihormone treatments in the HER2+ and MCF-7 cell lines. Oestrogen deprivation treatment induced significant up regulation of GABBR2 protein expression versus control and E2 treatment in the HER2+ cell lines. Fulvestrant treatment also induced significant up regulation

of GABBR2 protein expression in BT474 cells versus E2 treatment. Together, short-term tamoxifen, fulvestrant and oestrogen deprivation treatments induced up regulation of GABBR2 expression in the HER2+ and MCF-7 cell lines, with no expression detected in the T47D cell line.

Although MCF-7 and T47D cell lines are both luminal A and derived from a metastatic site of pleural effusion, proteomic analyses have identified more than 164 proteins differentially expressed between both cell lines[409]. In the T47D cells, proteins involved in cell growth, anti-apoptosis and tumourigenesis were more strongly expressed. In contrast, proteins implicated in transcription repression and apoptosis regulation were more strongly expressed in MCF-7 cells. Furthermore, the apoptotic mechanisms of both cell lines differ, involving activation of different caspases and mitochondrial changes[410]. Additionally, of significant interest is the differential expression of p53 in these cell lines. Indeed, in contrast to MCF-7 cells, the tumour suppressor protein p53 is mutated on one allele of the gene in T47D cells[411]. Thus, it is possible that GABBR2 expression in MCF-7 cells during antihormone response regulates p53 activity, to induce anti-apoptotic functions; a mechanism not observed in the p53 mutant T47D cells.

As revealed from the ontological studies in Chapter 3, GABA B receptors (composed of GABBR1 and GABBR2 subunits) are involved in mediating GABA-induced inhibition of neuronal activity. GABA is synthesised from glutamate by GAD enzyme, of which there are two isoforms (GAD1 and GAD2). Increased GABA B receptor expression has been reported in several cancers, however the role of this receptor and particularly the GABBR2 subunit in cancer remains elusive. With regard to breast cancer, increased GABA content and GAD activity has been observed in tumour tissue compared to normal breast[318], suggesting abundant expression and synthesis of the ligand, GABA, and the existence of GABAergic signalling within these cells. Furthermore, GABBR1 (required to heterodimerise with GABBR2 for normal receptor function) and GAD proteins have been demonstrated in breast cancer cell lines, including MCF-7 cells[319]. Moreover, in triple negative disease, GABA B receptor activation has been shown to promote cell invasion, migration and metastasis via enhanced ERK 1/2 signalling and MMP-2 production[319]. However, GABBR2 expression has never previously been

observed in ER+ breast cancer and its association with limiting antihormone response and contributing to the emergence of resistance remains unexplored. In this Chapter, GABBR2 expression has been shown to be induced by three clinically used antihormones in a panel of ER+ breast cancer cell lines, reflecting HER2+ and HER2- disease. These findings suggest that GABBR2 may provide a common resistant mechanism early during response to all three antihormones in several ER+ disease molecular subtypes. However, further studies are required to determine whether GABBR1 subunit and GAD enzymes are expressed together with GABBR2, signifying functional GABA B receptor and production of the ligand, respectively, and ultimately receptor activation.

Conversely, the microarray profile of CTNND2 expression could not be verified by RT-PCR. Indeed, CTNND2 mRNA expression was similar following fulvestrant and untreated control treatments in the three cell lines, with no expression detected in the T47D cell line which supports the absent detection calls reported from the microarray gene expression profiles. Furthermore, tamoxifen and oestrogen deprivation treatments induced similar CTNND2 expression to the control in the three cell lines, with no expression detected in the T47D cell line. It is possible that the above-mentioned differences in protein expression and in particular p53 expression between the T47D cells and MCF-7 cells contribute to the lack of CTNND2 expression in the former cell line. Furthermore, it is possible that the microarray profile could not be verified by RT-PCR due to the different regions of mRNA recognised by the PCR primers to that recognised by the Affymetrix gene chip. Moreover, it was noticed throughout this Chapter that present detection calls in the untreated control and fulvestrant treated cells recorded from the microarray data were more difficult to verify an antihormone-induced up regulation by PCR as opposed to absent calls in the control and present in fulvestrant-treated. As previously described in Chapter 3, the CTNND2 antibody continued to fail in all cell lines, with no protein expression detected.

Increased CTNND2 expression has been reported in several cancers including lung, ovarian and prostate[328–330]. In the latter, CTNND2 has been shown to up regulate cyclin D1 and the anti-apoptotic gene BCL2L1 to promote cell proliferation and survival[332]. However, the expression and function of CTNND2 in breast cancer is

largely unexplored. A recent study by Zhang et al. demonstrated increased CTNND2 expression in breast cancer tissue compared to normal breast, with increased expression associated with a higher degree of malignancy and poor prognosis[327]. Furthermore, in ER+ MCF-7 and ER- MDA-MB-231 cells, increased CTNND2 expression was shown to promote cell proliferation and invasion[327]. In support of the microarray data from the MCF-7 cells reported in this Chapter (as well as Chapter 3), previous studies within the group have reported up regulation of CTNND2 expression following short-term tamoxifen, fulvestrant and oestrogen deprivation treatment in MCF-7 cells, with expression retained at increased levels in our TAMR and/or FASR cell lines[304,412]. However, the precise function of CTNND2 remains to be deciphered. The very few studies examining CTNND2 expression in ER+ breast cancer and its potential role in antihormone failure or resistance have utilised the single ER+ cell line, MCF-7. To better reflect the heterogeneity of ER+ disease, equivalent studies are necessary in additional cell models. In light of this, this study is the first to our knowledge investigating antihormone-induced expression of CTNND2 in a panel of ER+ breast cancer cell lines, encompassing HER2+ and HER2- disease. Although the results from the microarray data in this Chapter and Chapter 3, strongly suggest that antihormones induce up regulation of CTNND2 in HER2+ and MCF-7 cell lines with expression maintained into resistance, combined with strong ontology identifying CTNND2 as a potential significant player in limiting antihormone efficacy and promoting resistance; the failure to verify these profiles by RT-PCR in addition to the limited availability of antibodies necessary for further evaluation of the role of CTNND2, led to the elimination of this protein from further study.

The microarray data identified significant fulvestrant-induced TSC22D3 expression in the BT474 and MCF-7 cell lines, with a small induction observed in the MDA-MB-361 and T47D cell lines versus untreated control. However, the microarray gene expression profiles of TSC22D3 were only partly verified by RT-PCR. Indeed, in agreement with the microarray profile, TSC22D3 expression was up regulated, although not significantly, by fulvestrant, along with tamoxifen and oestrogen deprivation treatments versus E2 and untreated control treatments in the MCF-7 and MDA-MB-361 cells. However, there was no apparent change in

TSC22D3 mRNA expression following antihormone or E2 treatments versus control in the BT474 and T47D cell lines, which is in disagreement with the microarray data. Perhaps the PCR cycle number was not optimal in the BT474 and T47D cell lines, and a greater difference between TSC22D3 mRNA expression following antihormone treatment may be observed with a lower cycle number. Conversely, Western blot analysis revealed antihormone-induced expression of TSC22D3 protein in all four cell lines versus E2 and untreated control treatments. Such increases were significant following tamoxifen and fulvestrant treatments versus control in the MDA-MB-361 cell line. Statistically significant increases in TSC22D3 protein expression were observed following all three antihormones in the MDA-MB-361 cell line and oestrogen deprivation in the BT474 cell line compared to E2 treatment.

As revealed from the ontological studies in Chapter 3, TSC22D3 is an ubiquitously expressed protein involved in mediating several glucocorticoid functions, including T cell activation, apoptosis and cell proliferation[350]. TSC22D3 expression has been reported in leukaemia and ovarian cancer, however its precise function in tumourigenesis remains undefined[353,354]. From the ontological investigation, it was strongly evident that TSC22D3 exhibits opposing roles dependent on the cell type and associated cellular milieu. Indeed, in ovarian cancer, TSC22D3 has been shown to enhance phosphorylated AKT content and activity to promote cell proliferation, whereas in T lymphocytes, TSC22D3 inhibits AKT signalling resulting in an anti-proliferative effect in these cells[354,393,394]. Similarly, in ovarian cancer, TSC22D3 up regulates cyclin D1 expression to promote cell cycle progression, which is again in contrast to T lymphocytes where cyclin D1 activation is inhibited to prevent cell proliferation[354,393]. To our knowledge, there is only one study examining TSC22D3 expression in ER+ breast cancer, where 24 hour tamoxifen treatment has been shown to increase, and E2 treatment decrease, TSC22D3 expression in MCF-7 cells, which supports the data presented here[351]. However, Tynan et al. utilised the single ER+ MCF-7 cell line, whereas the data presented here was extended into additional ER+ cell lines and also included fulvestrant and oestrogen deprivation treatments, thus encompassing HER2+ and HER2- disease, to better reflect the heterogeneity present in breast cancer. Indeed, 10 day

tamoxifen, fulvestrant and oestrogen deprivation treatments were shown to increase TSC22D3 protein expression in HER2- MCF-7 and T47D cells and HER2+ BT474 and MDA-MB-361 cells compared to E2-treated and untreated control cells, thus identifying drug-induced expression of TSC22D3 common to three antihormones and four ER+ cell models, whose expression is hypothesised to limit the anti-tumour activity of these agents and ultimately promote the emergence of resistant growth.

In contrast, oestrogen has been shown to up regulate TSC22D3 expression in cervical cancer and human embryonic kidney cells[351], suggesting that cell specific factors are involved in oestrogen regulation of TSC22D3 expression, again supporting the concept that the role of TSC22D3 is multifaceted and dependent on the cellular milieu. Importantly, with regard to a pro-survival role to ultimately support our hypothesis and identify TSC22D3 as a potential significant protein involved in limiting antihormone efficacy and promoting endocrine resistance, the ontological studies in Chapter 3 identified pro-apoptotic and pro-survival roles of TSC22D3 in chronic myeloid leukaemia and ovarian cancer cells, respectively[354,356]. However, there are no studies identifying a pro-survival role for TSC22D3 in breast cancer, where its role remains elusive. Clearly, further studies are required to decipher the role of TSC22D3 in breast cancer and particularly in response to antihormones, to determine whether it promotes survival signalling to overcome antihormone challenge or alternatively it may exhibit pro-apoptotic functions and be a mechanism utilised by antihormones to induce their anti-proliferative and weak pro-apoptotic effects. Taken together, TSC22D3 is a ubiquitously expressed protein, abundant in several cell types where it is involved in either promoting or inhibiting cell proliferation and survival dependent on the cell type. The complexity of TSC22D3 combined with its ubiquitous and abundant expression and ability to interact with a variety of cellular proteins, with limited literature supporting a pro-survival role in breast cancer, led to the decision to dismiss TSC22D3 from further study.

Together, in support of the hypothesis and building on the data generated from Chapter 3, this Chapter has revealed that the expression of 4 pro-survival genes (GABBR2, CLU, TSC22D3 and BCL3) potentially involved in antihormone failure

and promoting the emergence of resistant growth, is induced following short-term tamoxifen, fulvestrant and oestrogen deprivation treatments in four cell lines (except GABBR2, which was not detected in the T47D cell line) representing HER2+ and HER2- disease, suggesting that a common resistant mechanism may be induced by all three antihormone therapies in several ER+ disease subtypes. However, such antihormone-induced gene expression did not always reach significance compared to control at the mRNA and protein level likely due to the low number of experimental repeats, and the limitations in quantifying end-point PCR. Indeed, additional experimental repeats are required to increase the reliability of the data. This is one of a few studies that have utilised multiple cell lines to examine antihormone response and resistance mechanisms in breast cancer. In the following Chapters, the most promising genes, BCL3 and CLU, which were induced by all three clinically used antihormones in the four cell lines, were further examined to determine their role during antihormone response and resistance Further studies may identify these proteins as a novel therapeutic target, which during antihormone response could markedly improve the anti-tumour activity of these therapies and furthermore in resistance may reverse this phenotype and re-sensitise cells to endocrine treatments.

5 Results III: Further investigation of BCL3 function during antihormone-response and -resistance

5.1 Introduction

BCL3 is a nuclear protein and belongs to the family of IκB proteins that function to inhibit the activity of NF-κB transcription factors[358]. The family of NF-κB transcription factors consists of five members: p65 (RelA), RelB, cRel, p50/NFKB1 and p52/NFKB2. p50/NFKB1 and p52/NFKB2 are synthesised as large precursors (p105 and p100, respectively), which upon activation are partially degraded to their mature forms (p50/NFKB1 and p52/NFKB2, respectively)[413]. The NF-κB family members exist as hetero- or homodimers, although the most abundant form is generally the p65/p50 heterodimer[414].

In unstimulated cells, IκB proteins sequester NF-κB in the cytoplasm, thus blocking their nuclear translocation, thereby maintaining NF-κB in an inactive state preventing transcription of a large number of genes involved in cell survival and proliferation[358]. Upon activation induced by various stimuli, including inflammatory cytokines and growth factors, IκB is phosphorylated by IκB kinase and degraded by the proteasome[213]. The dissociation of IκB unmasks the nuclear localisation sequence of NF-κB, allowing translocation of NF-κB into the nucleus where it binds to DNA at specific NF-κB response elements to activate transcription of genes involved in cell proliferation, survival and the inflammatory response[414,415]. RelA, RelB and cRel proteins contain a transactivation domain at the C-terminus, which facilitates the recruitment of coactivators and the displacement of repressors, necessary for transactivation by these proteins. However, p50/NFKB1 and p52/NFKB2 homodimers lack transactivation domains and thus are inactive and unable to drive transcription. In fact, nuclear translocation of p50/NFKB1 and p52/NFKB2 homodimers and binding to κB sites results in the repression of NF-κB-dependent genes[414]. However, BCL3 functions to provide transactivating domains to these otherwise inactive homodimers to activate transcription of cell growth and survival genes[372]. Initial studies suggested

that BCL3 binds and removes repressive p50/NFKB1 and p52/NFKB2 homodimers from κB sites, to allow the engagement of transcriptionally active dimers (e.g. p65/p50) to drive transcription[416,417]. However, subsequent studies have suggested that BCL3 forms transcriptionally active complexes with p50/NFKB1and p52/NFKB2 homodimers to activate transcription[418,419].

The general consensus surrounding antihormone therapy is that they exert significant anti-proliferative actions but are unable to promote significant cell death. Antihormones exert their anti-proliferative activity through suppression of growth promoting genes and also through induction of negative regulators of cell proliferation. However, this inductive capacity is likely to be a double-edged sword since it has also been demonstrated that oestrogens can suppress, and antihormones induce, pro-proliferative and pro-survival genes. Thus, the weak pro-apoptotic activity of antihormones may be reflected by a significant capacity for induction of pro-survival mechanisms alongside their weak pro-apoptotic actions.

It was hypothesised that antihormones induce expression of pro-survival genes early during response, allowing a cohort of cells to evade the therapeutic challenge resulting in anti-tumour responses of finite duration and ultimately the development of resistant growth. Microarray analysis in Chapters 3 and 4 examined 10 day antihormone-treated ER+ breast cancer cell lines and corresponding resistant cell models and aimed to identify antihormone-induced pro-survival genes that may subsequently limit the efficacy of such agents and contribute towards the emergence of resistance. Further study of the most robust candidate genes could prove significant in identifying biomarkers of limited response or targets for novel therapeutic strategies to enhance antihormone response and significantly delay or prevent the development of resistance.

To this regard, the microarray gene expression profiling data identified BCL3 as the only gene significantly induced by fulvestrant treatment in 4 ER+ breast cancer cell lines, encompassing both HER2+ and HER2- disease. The microarray data were verified by RT-PCR and Western blotting and equivalent increases in BCL3 expression was apparent following tamoxifen and oestrogen deprivation

treatments in all 4 cell lines which was reversed by E2 treatment. Additionally, ontological investigations strongly suggested a role for BCL3 in disease progression by promoting cell growth and survival potentially via activation of NF-κB-mediated transcription of pro-proliferative and pro-survival genes. Together, this suggests that all three antihormone therapies rapidly induce BCL3 expression during response in several subtypes of breast cancer, possibly activating a common survival mechanism to promote resistance. Indeed, initial microarray studies (Chapter 3) in models of endocrine resistance derived from MCF-7 cells revealed increased BCL3 expression maintained through to the acquisition of resistance to tamoxifen, fulvestrant and oestrogen deprivation.

In this Chapter, several experimental approaches have thus been performed to further determine the role of BCL3 during antihormone response and resistance and whether its induction early during response contributes to the limited efficacy of these agents and ultimately promotes the development of the hormone-independent phenotype. Initially, the microarray profile of BCL3 in TAMR and XR cells (Chapter 3) was verified by RT-PCR and Western blotting, to determine whether BCL3 expression was maintained at increased levels through to the acquisition of resistance. Studies with BCL3 siRNA were subsequently performed to determine whether BCL3 knockdown combined with antihormone treatment improves the growth-inhibitory actions of these agents and as such identifies BCL3 as a gene involved in promoting cell growth and survival, as examined by cell growth and apoptosis assays. Additionally, similar BCL3 siRNA studies were performed in antihormone-resistant cell models to determine whether such knockdown can inhibit cell growth and promote apoptosis in resistance.

To investigate whether antihormone-induced BCL3 expression contributes to limited antihormone response and the development of resistance by activating NF-κB-mediated transcription of pro-survival and/or pro-proliferative genes, Western blotting studies were first performed to determine whether p50/NFKB1 and p52/NFKB2 proteins were expressed in ER+ breast cancer cell lines during antihormone-response and following the acquisition of resistance. Subsequent studies, including immunofluorescence and immunoprecipitation, examined the

potential association between BCL3 and p50/NFKB1 and p52/NFKB2 during antihormone-response and-resistance to further support the hypothesis.

5.2 Methods

5.2.1 Cell Culture

Antihormone-treated MCF-7 and T47D cells were re-suspended in phenol-red-free RPMI medium supplemented with 5% FCS, penicillin-streptomycin (10 IU/ml to 10 μg/ml), fungizone (2.5 μg/ml) and glutamine (4 mM) and allowed to adhere overnight prior to the addition of antihormone, E2 and control (untreated medium) treatments, as described in Chapter 2, section 2.1.2.

The (short-term) TAMR, FASR, XR and T47D TAMR cell models and wild type control cells were cultured in phenol-red-free RPMI medium supplemented with 5% sFCS, penicillin-streptomycin (10 IU/ml to 10 μg/ml), fungizone (2.5 μg/ml), glutamine (4 mM) and respective antihormone treatment, as described in Chapter 2, section 2.1.2. The long-term antihormone resistant cell models, derived from MCF-7, T47D, BT474 and MDA-MB-361 cells, and the wild type control cells were cultured in phenol-red-free RPMI medium supplemented with FCS (5%: MCF-7 and T47D, 10%: BT474 and MDA-MB-361), penicillin-streptomycin (10 IU/ml to 10 μg/ml), fungizone (2.5 μg/ml), glutamine (4 mM) and the respective antihormone treatment, as detailed in Chapter 2, section 2.1.2.

5.2.2 RT-PCR

Antihormone-treated cells and antihormone-resistant cells were prepared for RNA analysis as described above (section 5.2.1). RT-PCR was performed, as described in section 2.4, to determine RNA expression of BCL3. Densitometry analysis was performed and the raw densitometry values of BCL3 were normalised to β-actin loading control.

5.2.3 Western blotting

Antihormone-treated and resistant cells were prepared for Western blotting as described above (section 5.2.1). Twenty micrograms of protein was loaded and separated by SDS-PAGE and probed for BCL3, total and phosphorylated forms of ERBB2, AKT, ERK and EGFR, NFKB1 and NFKB2 antigens, as described in section

2.5. Densitometry analysis was performed and the raw densitometry values of the proteins of interest were normalised to β-actin loading control.

5.2.4 Microarray analysis

Triplicate mRNA preparations of resistant cell models were hybridised to Affymetrix Human Genome U133Aplus2 gene chips, as described in section 2.2. These data were analysed to identify expression of BCL3, p50/NFKB1 and p52/NFKB2 during antihormone-resistance, using the 'jetset' probes: 204908_s_at, 209239_at and 209636_at, respectively.

5.2.5 BCL3 knockdown

To decipher the role of BCL3 during antihormone response and resistance, BCL3 knockdown studies were performed utilising siRNA as described in section 2.6.1. Briefly, cells were grown until approximately 60% confluency prior to the addition of the siRNA tranfection reagent mix. Cells were incubated for 4 days (unless stated otherwise) prior to RNA and protein lysis for subsequent RT-PCR and Western blot analysis (as described above). Since BCL3 is expressed at low levels in wild type MCF-7 and T47D cells, fulvestrant was added to the medium 48 hours post siRNA transfection to induce BCL3 expression.

5.2.6 Apoptosis assay

An Annexin V-FITC and PI apoptosis detection kit was utilised with subsequent flow cytometery analysis, as described in section 2.6.2.1, to determine whether BCL3 plays a pro-survival role during antihormone response and resistance. Positive control cells were treated with the apoptosis inducer thapsigargin 48 hours prior to analysis, as detailed in section 2.6.2.1.

5.2.7 Cell counting

Cell counting studies were performed to determine the effect of BCL3 knockdown on cell growth during antihormone response and resistance. Cells were transfected with BCL3 siRNA (as described above) in triplicate and incubated for 4 days prior to the measurement of cell number, as described in section 2.6.3.

5.2.8 Cell cycle distribution

The effect of BCL3 on the cell cycle of antihormone-treated and –resistant cells was investigated by PI stain and flow cytometry analysis, as described in section 2.6.2.2.

5.2.9 Immunofluorescence

The cellular localisation of BCL3 and p50/NFKB1 during antihormone response and resistance was examined by immunofluorescence studies as described in section 2.6.4. Briefly, cells were grown on glass coverslips, incubated with BCL3 and p50/NFKB1 primary antibodies, followed by appropriate fluorphore-conjugated secondary antibodies prior to examination on a fluorescent microscope.

5.2.10 Immunoprecipitation

Immunoprecipitation studies were performed to determine whether BCL3 is associated with p50/NFKB1 during antihormone response and resistance. Briefly, protein cell lysates were incubated with an antibody (e.g. p50/NFKB1) to form an antibody/antigen complex. This complex was captured on a solid support, separated by SDS-PAGE and Western blotting and probed for the protein of interest (e.g. BCL3), as described in section 2.6.5.

5.2.11 Statistical analysis

The data were analysed using GraphPad prism. An unpaired t-test or an ANOVA (with a Tukey's multiple comparisons post-hoc test) were used to compare the means. A p value <0.05 was considered statistically significant.

5.3 Results

Initial microarray studies (Chapter 3) revealed increased BCL3 expression maintained through to the acquisition of resistance. Indeed, BCL3 expression was significantly up regulated (fold change > 1.5) in (short-term) TAMR, XR and FASR cells versus E2-treated control MCF-7 cells (as demonstrated in Chapter 3, section 3.3.2.6). Additionally, present detection calls were reported in the three resistant cell models, implying reliable gene expression, whereas predominantly absent calls were recorded in the untreated control, suggesting very low gene expression.

5.3.1 Verification of the microarray data by RT-PCR

The microarray expression profiles of BCL3 in (short-term) TAMR and XR cell lines were next verified by RT-PCR. To consider the heterogeneity of breast cancer, BCL3 RNA expression was also examined in a tamoxifen-resistant cell model derived from T47D cells (T47D TAMR). This project eliminated FASR cells from further study since we wished to focus on the first-line therapies (i.e. tamoxifen and AIs) and the resistance that develops from such agents. RT-PCR was performed on triplicate RNA from wild type control cells (i.e. MCF-7 and T47D) and (short-term) TAMR, XR and T47D TAMR cells (cultured under the same conditions as those used to generate the samples for microarray gene expression profiling). In agreement with the microarray profiles, BCL3 RNA expression was up regulated in the TAMR and XR cells models, with parallel up regulation also observed in the T47D TAMR cell line compared to control (Figure 56).

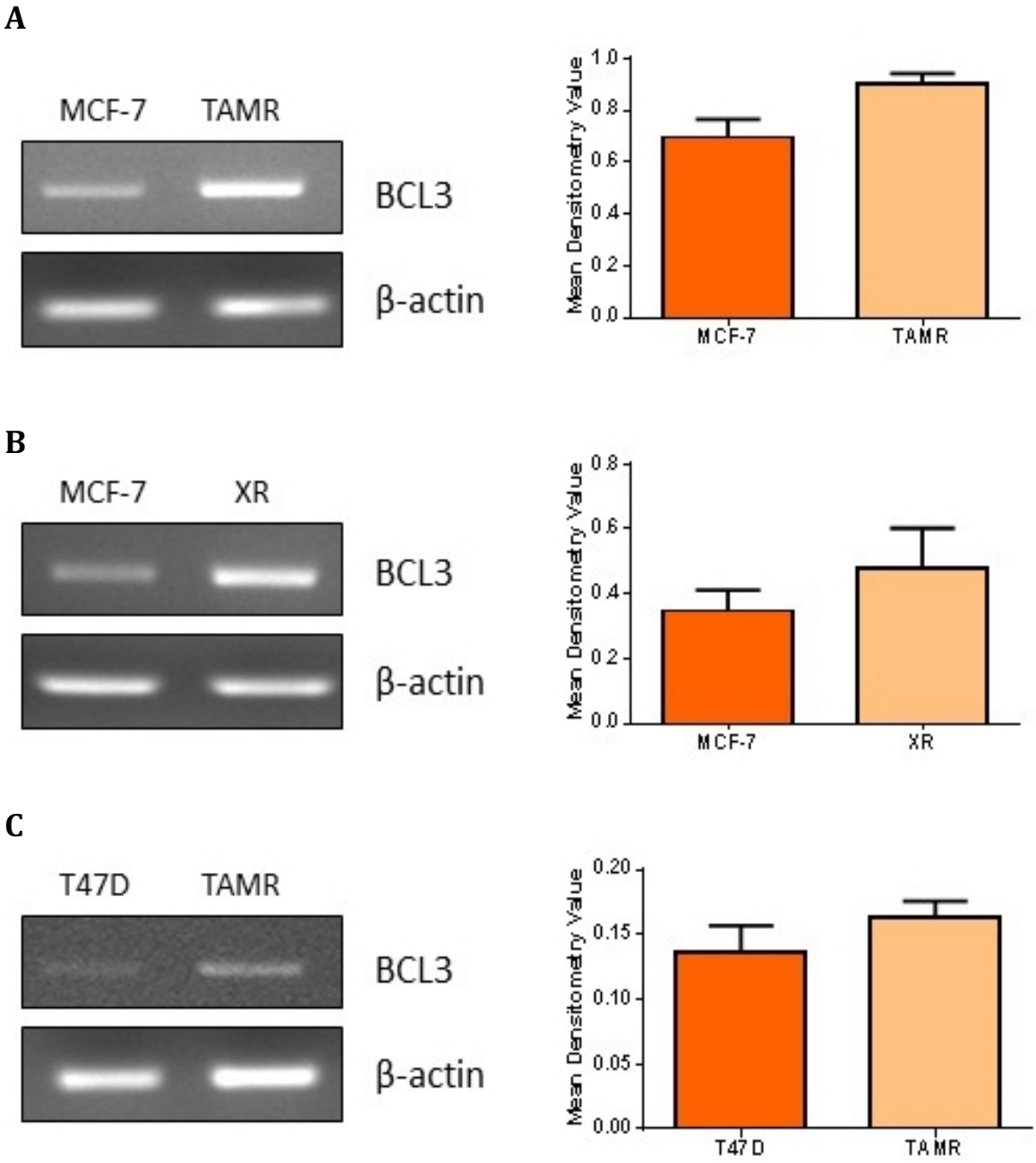

Figure 56 Representative PCR images and corresponding β-actin normalised densitometry graphs from three independent experiments showing BCL3 mRNA expression in tamoxifen resistant (TAMR) (A) and oestrogen deprived-resistant (XR) (B) MCF-7 cells versus wild type control cells and TAMR T47D cells (C) versus wild type control cells. The results are expressed as means ± SEM and the data were analysed by an unpaired T-test.

5.3.2 BCL3 protein expression in resistance

BCL3 expression was next examined at the protein level by Western blotting. Western blotting was performed on triplicate protein samples from wild type control cells and (short-term) TAMR, XR and T47D TAMR cells. In agreement with the previous microarray and PCR data, Western analysis revealed increased BCL3 expression in the TAMR and XR cell lines compared to parental MCF-7 cells (Figure 57A and B). However, BCL3 protein expression was not detected in the T47D TAMR cell line (Figure 57C).

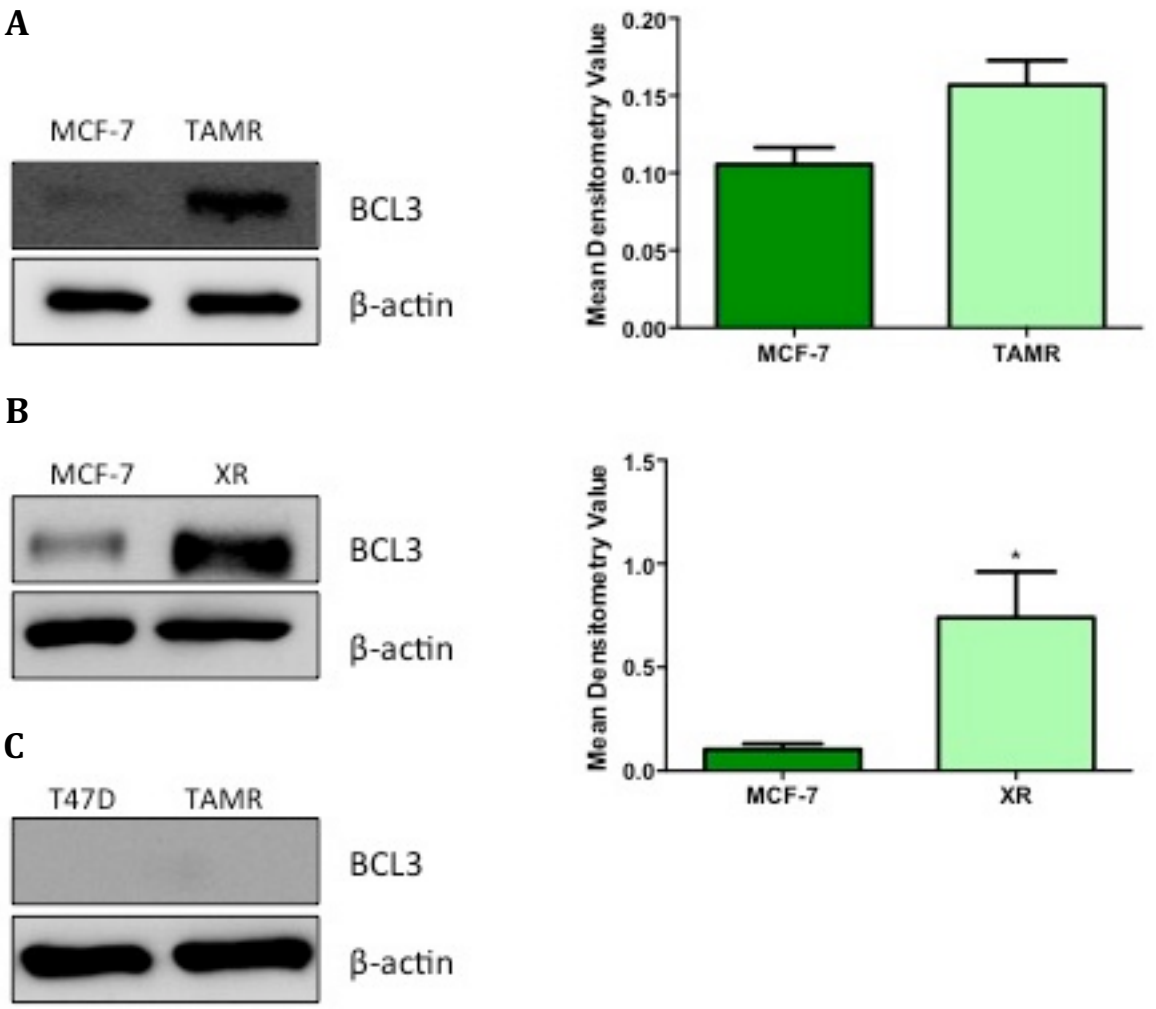

Figure 57 Representative Western blot images and corresponding β-actin normalised densitometry graphs from three independent experiments showing BCL3 protein expression in tamoxifen resistant (TAMR) (A) and oestrogen deprived-resistant (XR) (B) MCF-7 cells versus wild type control cells and TAMR T47D cells (C) versus wild type control cells. The results are expressed as means ± SEM and the data were analysed by an unpaired T-test. * p <0.05.

5.3.3 Microarray profile of BCL3 and RT-PCR verification in long-term antihormone-resistant cell models

Towards the end of this project, microarray gene expression profiling was completed on a panel of long-term (3 year) antihormone-resistant cell models. To determine whether increased BCL3 expression was maintained through to long-term resistance, the expression of BCL3 was next examined in this panel of resistant cell lines: TAMR, XR and FASR cell models derived from MCF-7, T47D, BT474 and MDA-MB-361 cells. The microarray log2 intensity plot (Figure 58A) demonstrated increased expression of BCL3 in the TAMR and XR models derived from MCF-7 and T47D cells, versus wild type control. However, in the FASR cells derived from T47D and MCF-7 cells, similar levels of BCL3 expression were observed to the control. In the BT474 cell line, decreased levels of BCL3 expression were apparent in TAMR and FASR cells, with an increase in the XR cells compared to control. In the MDA-MB-361 cells a statistically significant ($p < 0.05$) increase in BCL3 expression was demonstrated in the TAMR cells versus control, however BCL3 expression was similar in the FASR and control cells. Microarray gene expression profiling of the long term XR cell model derived from MDA-MB-361 cells is yet to be completed.

The microarray profile was subsequently verified by RT-PCR. RT-PCR was performed on triplicate RNA from wild type, TAMR and XR cells derived from MCF-7, T47D, BT474 and MDA-MB-361 cells, cultured under the same conditions as those used to generate the samples for microarray gene expression profiling. As previously mentioned above, FASR cells were eliminated from further study and thus their microarray profile was not verified by RT-PCR. In agreement with the microarray profiles, BCL3 mRNA expression was up regulated in the TAMR and XR cells derived from T47D cells, in the XR cells derived from BT474 cells and the TAMR cells derived from MDA-MB-361 cells (Figure 58B). However, in the MCF-7 cell lines, increased BCL3 mRNA expression was demonstrated in the TAMR cells, but could not be verified in the XR cells (Figure 58B).

A

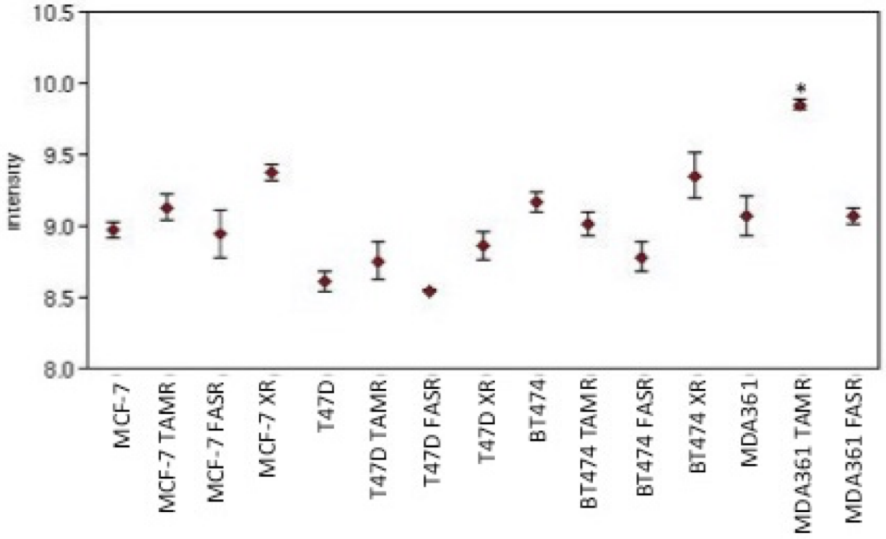

B

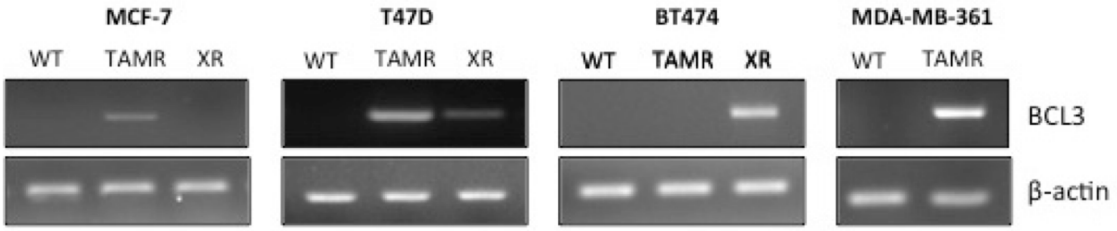

Figure 58 (A) Log2 intensity plot displaying the normalised (mean of three independent replicates ± SEM) gene expression of BCL3 (jetset probe ID: 204908_s_at) in long-term resistnat tamoxifen resistant (TAMR), fulvestrant resistant (FASR), oestrogen deprivation resistant (XR) cells and wild type (WT) control, derived from MCF-7, T47D, BT474 and MDA-MB-361 (MDA361) cells. (B) Representative PCR images from three independent experiments showing BCL3 and β-actin RNA expression in the resistant cell lines. * p <0.05.

5.3.4 BCL3 knockdown

BCL3 knockdown studies, utilising siRNA, were performed to determine whether BCL3 plays a pro-survival/pro-proliferative role during antihormone-response and –resistance and to determine whether such knockdown can improve the growth-inhibitory actions of antihormones during response and promote cell death in resistance.

5.3.4.1 BCL3 knockdown optimisation

Initially, optimisation studies were conducted to determine the optimum siRNA incubation conditions for the best gene knockdown.

5.3.4.1.1 BCL3 knockdown in antihormone-responsive MCF-7 and T47D cells

Since BCL3 is expressed at low levels in wild type/untreated MCF-7 and T47D cells particularly at the protein level (as previously demonstrated in Chapter 4, section 4.3.2.1), it was necessary to combine the siRNA with an antihormone to induce BCL3 expression. The pure antioestrogen fulvestrant was chosen to be combined with siRNA since it exhibits the greatest affinity for the ER and in addition to inhibiting E2 binding, fulvestrant also promotes degradation of the receptor. To increase the efficiency of siRNA transfection, siRNA was added to rapidly dividing cells prior to the addition of the growth-inhibitor fulvestrant.

Initially, a fulvestrant time point experiment was performed to determine how early post-fulvestrant treatment BCL3 is induced and ultimately determine the necessary incubation of siRNA with fulvestrant to induce BCL3 expression. As illustrated in Figure 59A and Figure 60A, BCL3 mRNA and protein expression was up regulated by fulvestrant as early as day 1 treatment in MCF-7 cells with this increased level of expression maintained through to day 2. However, mRNA and more substantially protein expression of BCL3 decreased at day 4 together with a corresponding decrease in actin expression indicative of mRNA and protein loading errors. At the mRNA level, BCL3 expression was consistent from day 4 to day 7, with a small increase at day 10. At the protein level, BCL3 expression remained low at day 5 and increased at day 7 and 10 fulvestrant treatment, together with an increase in actin expression. As illustrated in Figure 59B and Figure 60B, 1 day fulvestrant treatment induced up regulation of BCL3 mRNA and

protein in T47D cells compared to untreated control. BCL3 and actin expression remained relatively consistent at the mRNA and protein level during day 1 to day 10 treatment.

PCR and Western analysis revealed fulvestrant-induced BCL3 expression as early as day 2 in MCF-7 and T47D cells (Figure 59 and Figure 60). Subsequently, a siRNA time point experiment (including initial 2, 3 and 4 day siRNA incubation prior to the addition of 2 day fulvestrant treatment) was performed in MCF-7 cells to determine optimum siRNA and fulvestrant incubation for best BCL3 knockdown. Western analysis revealed similar levels of gene knockdown following all three incubation periods (Figure 61). Thus, since siRNA silencing is transient and only lasts approximately 4 days in rapidly dividing cells, to minimise the expense of additional administration of siRNA required to maintain knockdown, 2 day siRNA plus 2 day fulvestrant treatment (total 4 day) incubation was chosen as the optimum conditions for best gene knockdown and utilised for the remainder of this project.

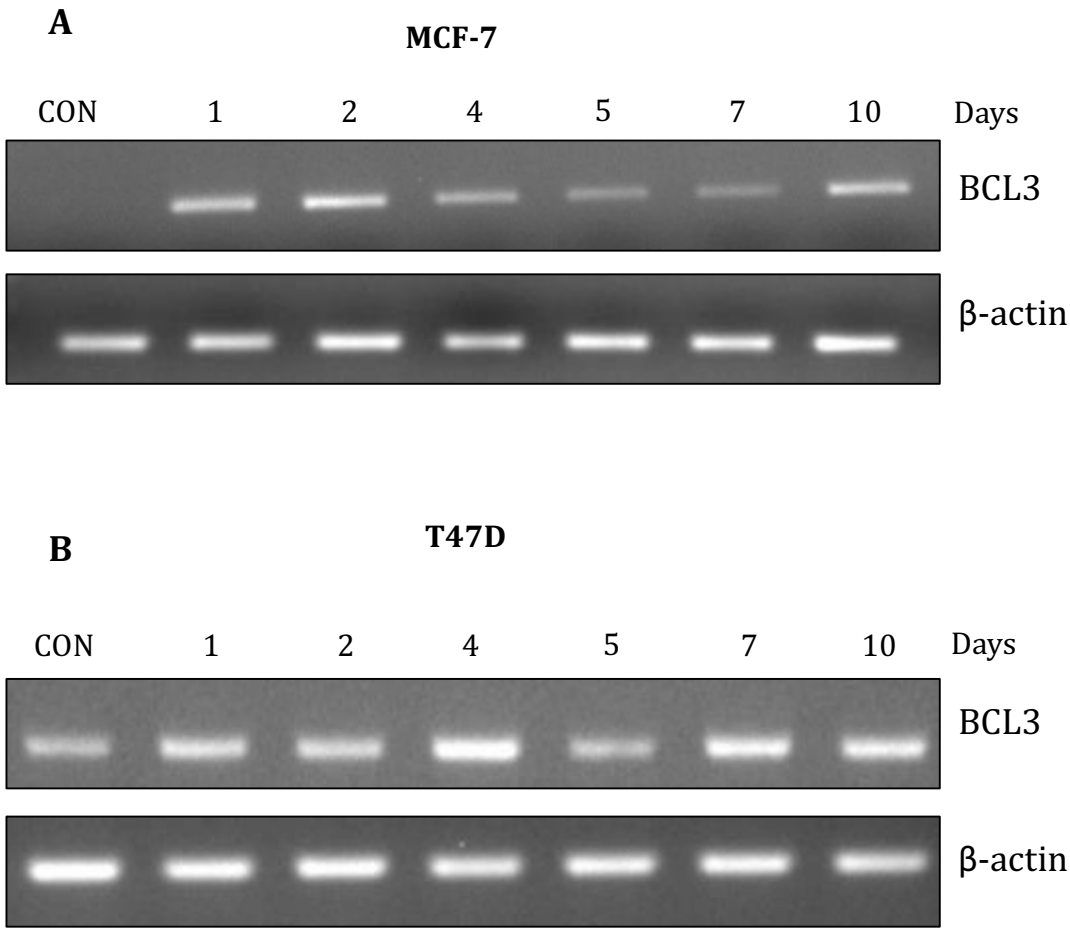

Figure 59 Representative PCR images from two independent experiments showing BCL3 mRNA expression and β-actin loading control in (A) MCF-7 and (B) T47D cells treated with fulvestrant (FAS; 10^{-7} M) for up to 10 days versus untreated control (CON).

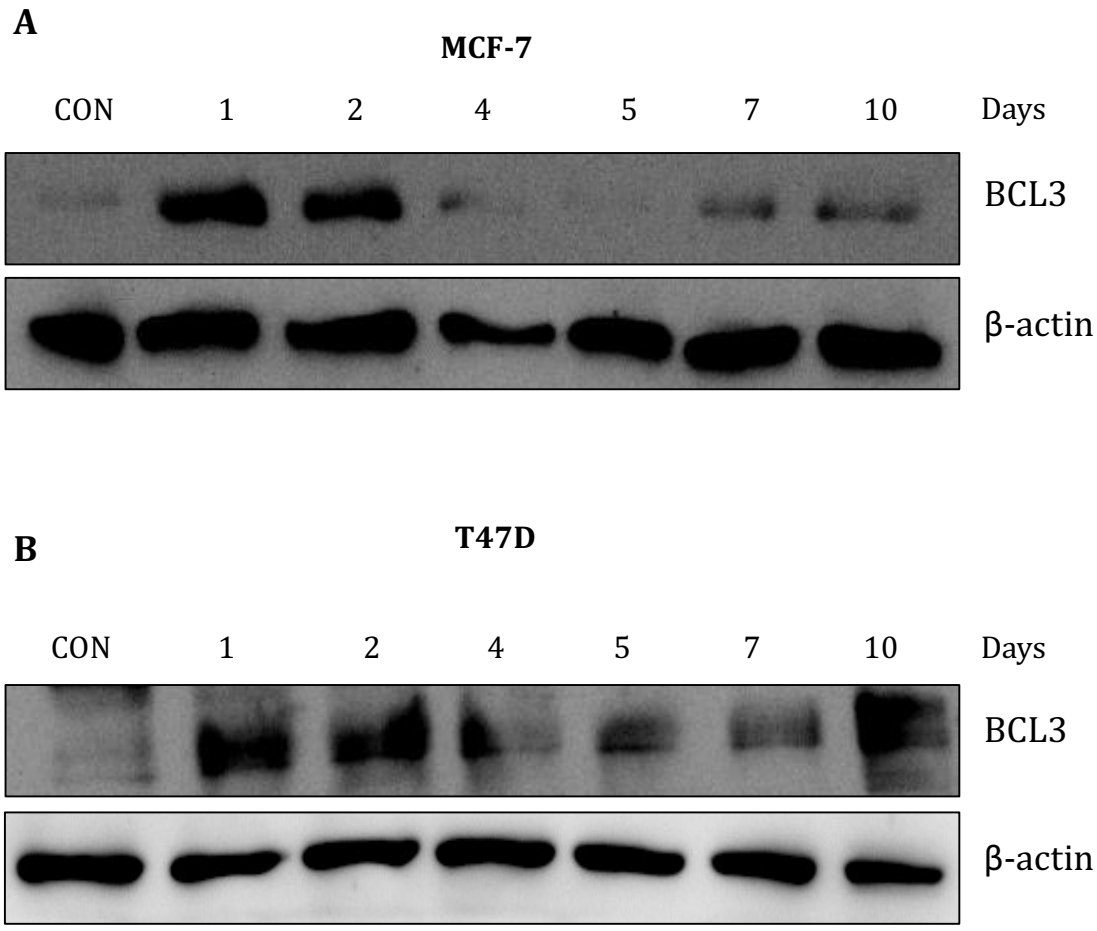

Figure 60 Representative Western blot images from two independent experiments showing BCL3 protein expression and β-actin loading control in (A) MCF-7 and (B) T47D cells treated with fulvestrant (FAS; 10^{-7} M) for up to 10 days versus untreated control (CON).

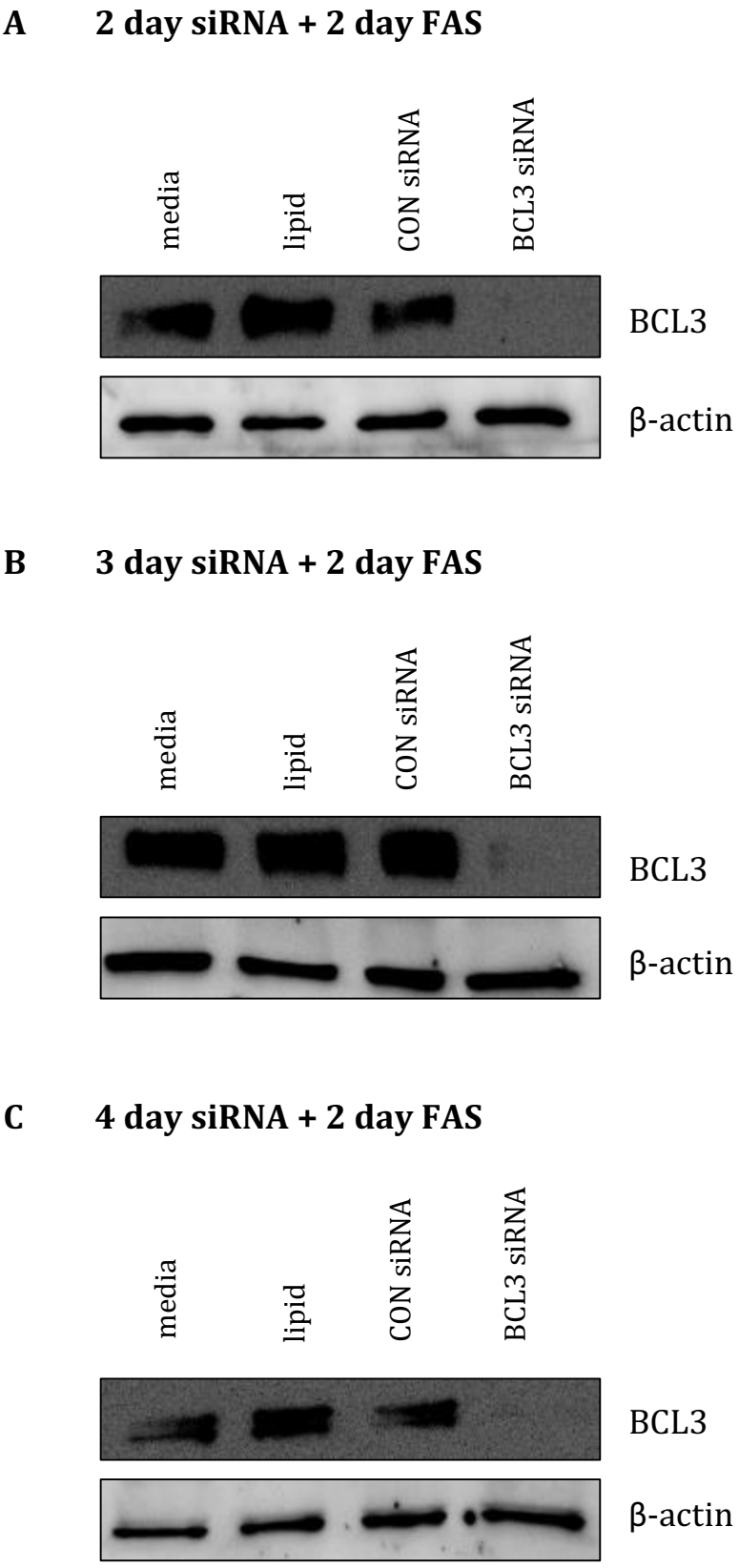

Figure 61 Western blot images (n=1) showing BCL3 protein expression and β-actin loading control in MCF-7 cells treated with media only, lipid only, unscrambled control small interfering RNA (CON siRNA) and BCL3 siRNA for (A) 2, (B) 3 and (C) 4 days prior to the addition of fulvestrant (FAS; 10^{-7} M) for a further 2 days.

Following the identification of the optimum BCL3 knockdown conditions by Western analysis in MCF-7 cells, PCR studies were performed on MCF-7 and T47D cells to examine the magnitude of knockdown at the mRNA level. As illustrated in Figure 62, 2 day fulvestrant treatment induced up regulation of BCL3 mRNA expression in MCF-7 and T47D cells (depicted by the 'media' treatment arm) compared to untreated control. Similarly, 2 day lipid and control siRNA treatment which was combined with a further 2 day treatment with fulvestrant induced similar BCL3 expression to fulvestrant alone ('media' arm), implying that lipid and control siRNA had no effect on BCL3 expression. BCL3 siRNA treatment (which was combined with fulvestrant to induce BCL3 expression) successfully reduced BCL3 mRNA expression in the MCF-7 and T47D cell lines.

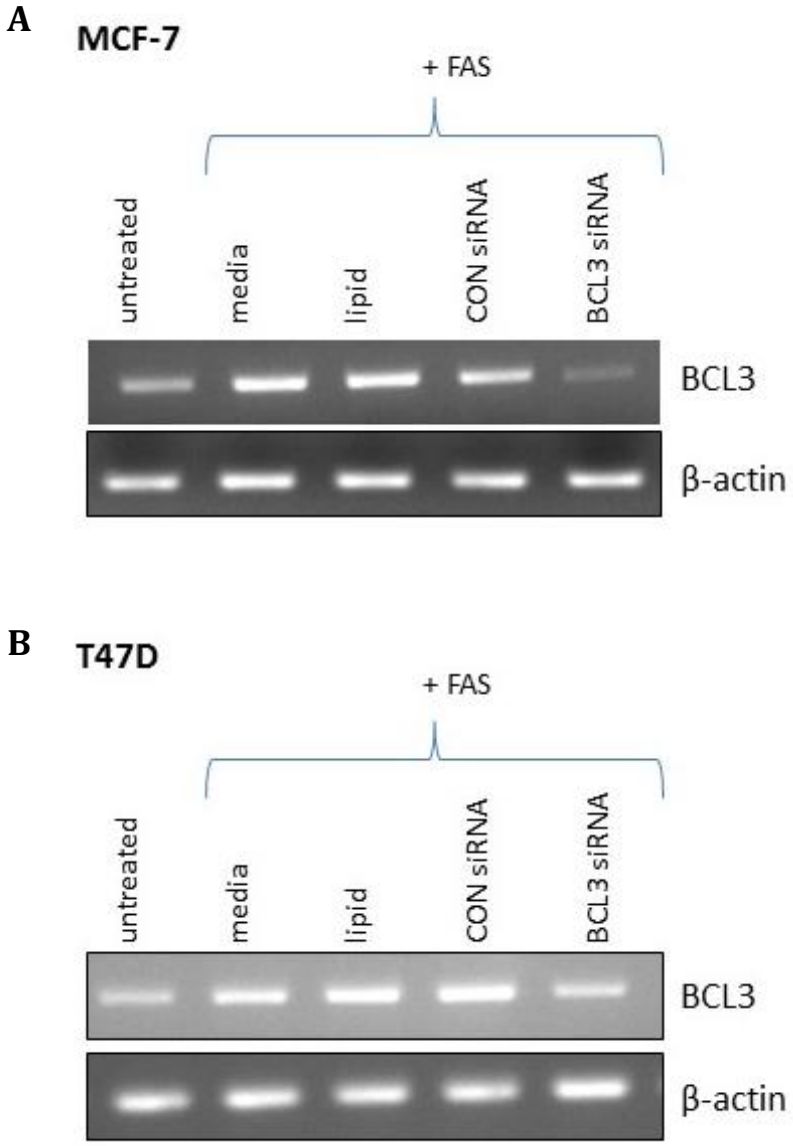

Figure 62 Representative PCR images from three independent experiments showing BCL3 mRNA expression and β-actin loading control in (A) MCF-7 and (B) T47D cells treated with media only, lipid only, unscrambled control small interfering RNA (CON siRNA) and BCL3 siRNA for 2 days prior to the addition of fulvestrant (FAS; 10^{-7} M) for a further 2 days. Untreated control is also shown.

In agreement with the PCR data, Western analysis revealed fulvestrant-induced (2 day treatment) up regulation of BCL3 protein expression in MCF-7 and T47D cells versus untreated control (Figure 63). Similarly, lipid and control siRNA treatment had no effect on BCL3 protein expression. BCL3 siRNA treatment induced a substantial knockdown of BCL3 expression demonstrated by the minimal BCL3 expression detected in the T47D cell line, and even less, if any at all, in the MCF-7 cells.

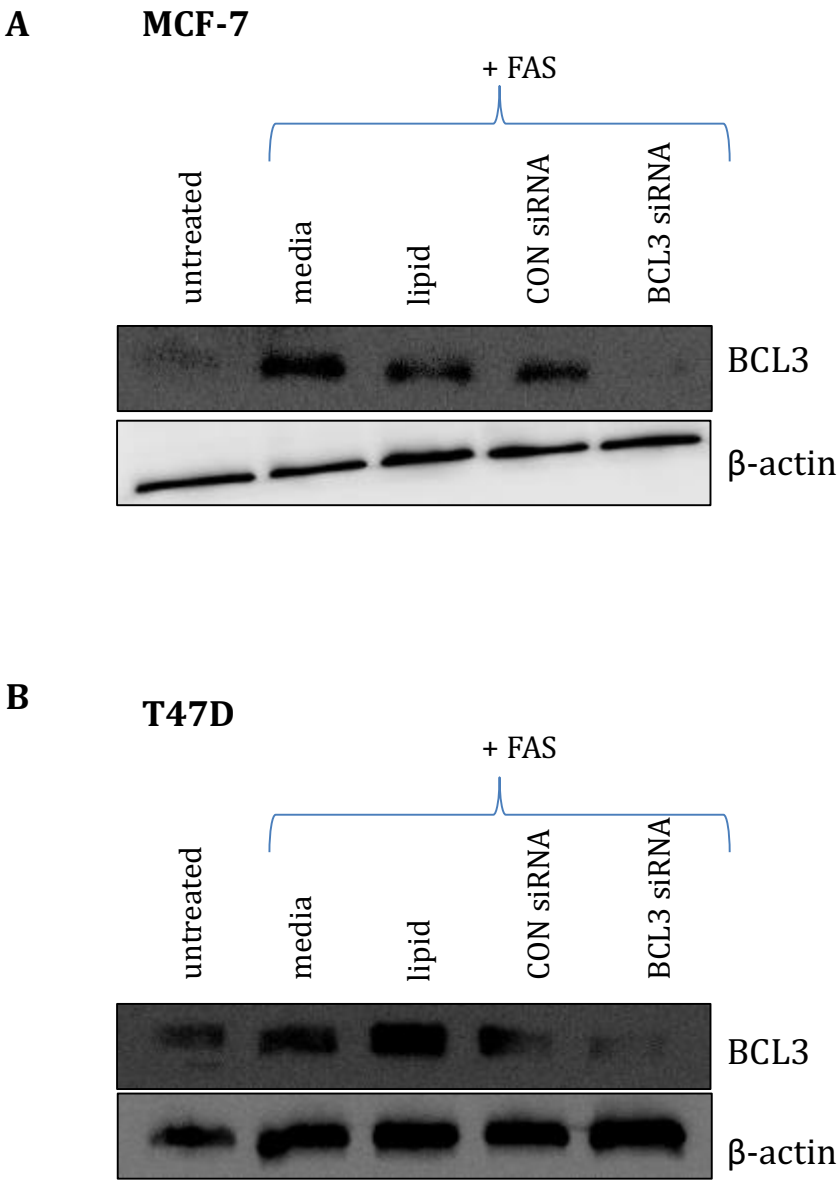

Figure 63 Representative Western blot images from three independent experiments showing BCL3 protein expression and β-actin loading control in (A) MCF-7 and (B) T47D cells treated with media only, lipid only, unscrambled control small interfering RNA (CON siRNA) and BCL3 siRNA for 2 days prior to the addition of fulvestrant (FAS; 10^{-7} M) for a further 2 days. Untreated control is also shown.

5.3.4.1.2 BCL3 knockdown in antihormone-resistant cell lines

In contrast to the antihormone responsive cells, the antihormone-resistant cell models (short-term TAMR, XR and T47D TAMR) constitutively express BCL3, as previously demonstrated (section 5.3.1 and 5.3.2). Therefore, unlike the antihormone responsive cells, it is not necessary to induce BCL3 expression in the antihormone resistant cell lines for subsequent knockdown via siRNA, to ultimately decipher the role of BCL3. Simply, BCL3 knockdown was achieved in the resistant cell models by 4 day incubation with BCL3 siRNA. As illustrated in Figure 64, TAMR, XR and T47D TAMR cells express BCL3 at the messenger level, which is not affected by lipid and control siRNA treatments. Four day BCL3 siRNA incubation induced down regulation of BCL3 mRNA expression in the three antihormone resistant cell models, with the greatest magnitude of knockdown observed in the MCF-7-derived models (i.e. TAMR and XR, Figure 64A and Figure 64B).

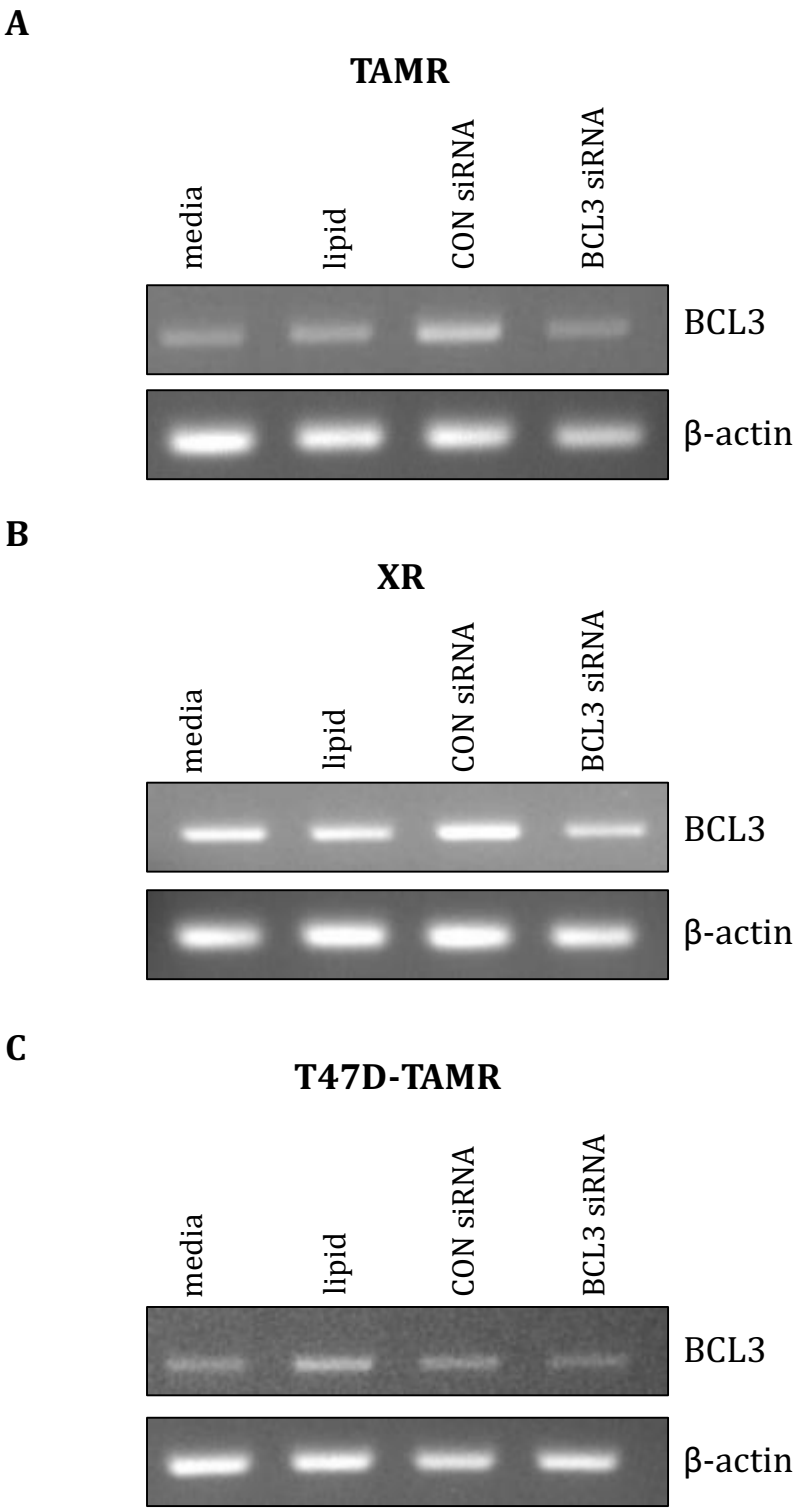

Figure 64 Representative PCR images from three independent experiments showing BCL3 mRNA expression and β-actin loading control in (A) tamoxifen-resistant (TAMR), (B) oestrogen deprivation-resistant (XR) and (C) TAMR cells derived from T47D cells (T47D TAMR) treated with media only, lipid only, unscrambled control small interfering RNA (CON siRNA) and BCL3 siRNA for 4 days.

In agreement with the PCR data, Western analysis demonstrated a substantial decrease in BCL3 protein expression mediated by 4 day incubation with BCL3 siRNA in the TAMR and XR cell models (Figure 65A and B). Lipid and control siRNA treatments had no effect on BCL3 protein expression in both cell lines. As previously reported in section 5.3.2, BCL3 expression could not be detected in the T47D TAMR cell line and thus BCL3 knockdown in this cell line at the protein level could not be examined (Figure 65C).

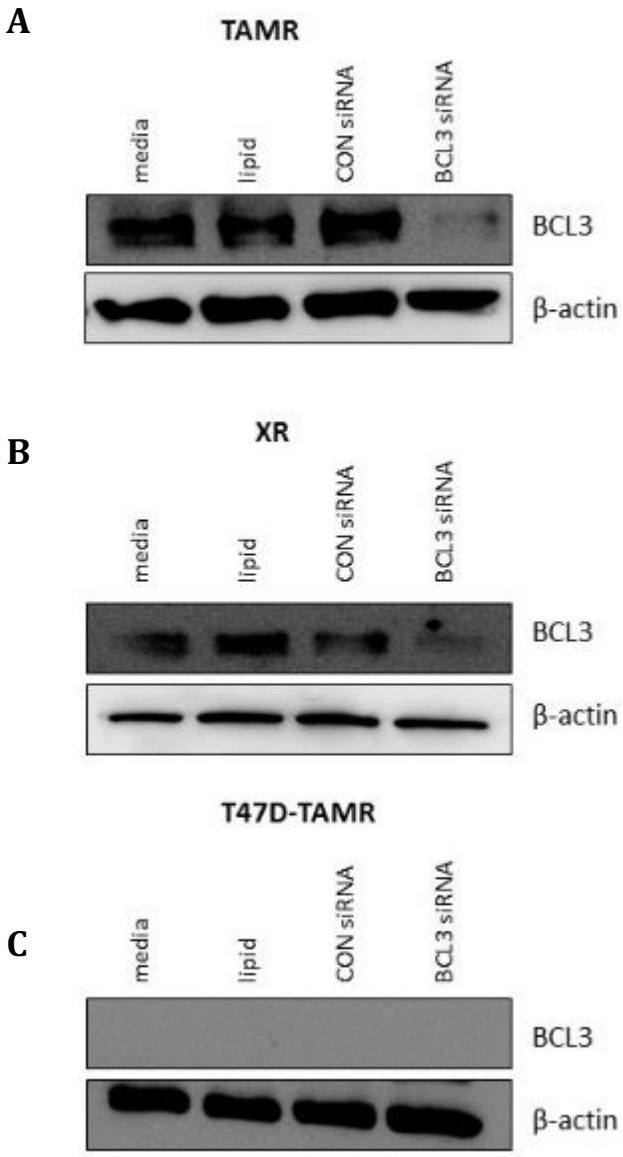

Figure 65 Representative Western blot images from three independent experiments showing BCL3 protein expression and β-actin loading control in (A) tamoxifen-resistant (TAMR), (B) oestrogen deprivation-resistant (XR) and (C) TAMR cells derived from T47D cells (T47D TAMR) treated with media only, lipid only, unscrambled control small interfering RNA (CON siRNA) and BCL3 siRNA for 4 days.

5.3.5 Effect of BCL3 knockdown on survival of antihormone-responsive and –resistant cells

Following the accomplishment of substantial BCL3 knockdown in the antihormone-responsive and -resistant cell lines, cell survival studies were performed to determine whether BCL3 is a pro-survival gene and ultimately plays a role in the survival of breast cancer cells in response to antihormone challenge and the emergence and maintenance of resistant cell growth. An Annexin V and PI stain was utilised with subsequent flow cytometery analysis.

5.3.5.1 Effect of antihormones on the survival of MCF-7 and T47D cells

Initially, baseline studies were performed on 7 day antihormone-treated MCF-7 cells. Seven day treatment was selected over the usual 10 day treatment used throughout this project because the 10 day untreated control cells became over confluent and thus gave rise to false positive data. The breast cancer cell lines used throughout this study were adherent and the dead/apoptotic cells floated in the medium. Typically, the cell medium was removed and replaced with fresh medium every 4 days. Thus, we first wanted to determine whether changing the medium at day 4 influenced the apoptotic data, since any dead floating cells would be discarded. As illustrated in Figure 66, 7 day antihormone treatment (including the removal of the medium comprising any dead floating cells at day 4 which was replaced with fresh medium) had no effect on the percentage of apoptotic cells.

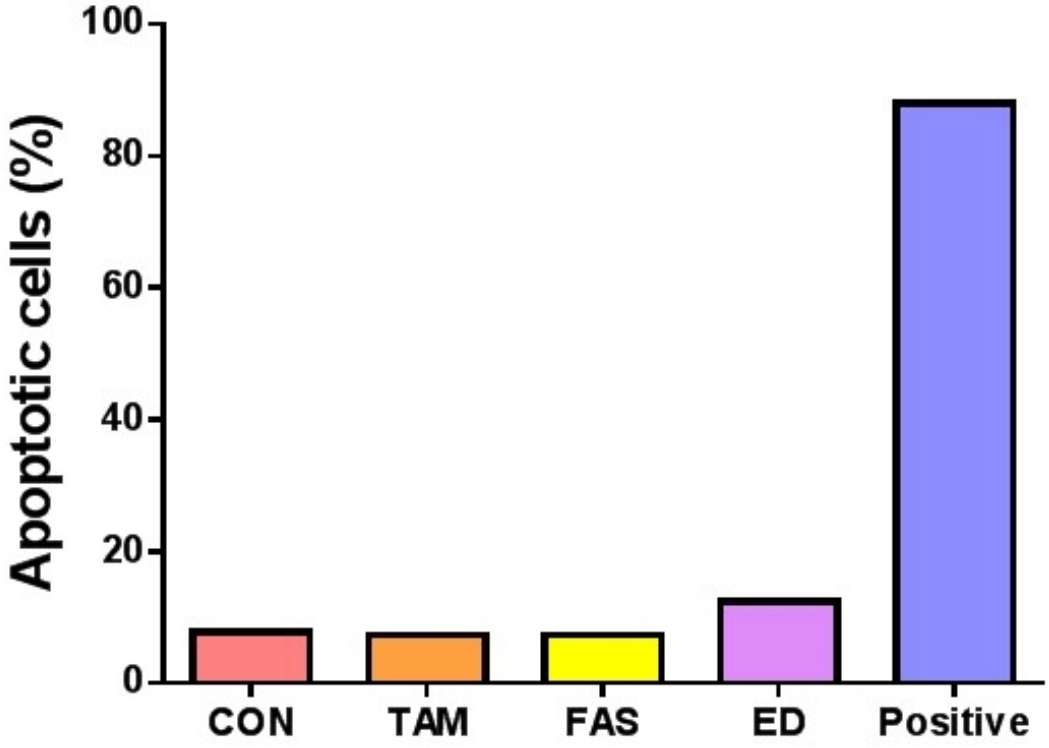

Figure 66 Graph displaying the percentage of apoptotic cells in MCF-7 cells treated with untreated control (CON) medium, tamoxifen (TAM; 10^{-7} M), fulvestrant (FAS; 10^{-7} M) and oestrogen deprivation (ED) for 7 days alongside the positive control thapsigargin (1 µM for 48 hours; n=1). The medium was removed and replaced with fresh medium at day 3.

To determine whether removing the cell medium affected the apoptotic data, survival assays were next performed on 7 day antihormone-treated MCF-7 cells, with fresh medium added on day 4 without the removal of the old medium, thus not discarding any apoptotic cells floating in the medium. As illustrated in Figure 67, tamoxifen and oestrogen deprivation treatments promoted a small increase in apoptosis, reflected by a small increase in the percentage of apoptotic cells versus untreated control, whereas a similar percentage of apoptotic cells were present following control and fulvestrant treatment. However, the small tamoxifen and oestrogen deprivation-induced apoptosis was not statistically significant compared to untreated control and the levels of apoptosis were much lower than the positive control. The levels of apoptotic cells were statistically significantly ($p < 0.05$) greater in the positive control compared to the untreated control. Together, it was concluded that changing the medium at day 4 influenced the apoptotic data, likely due to the removal and loss of apoptotic cells. Therefore, it

was decided that for subsequent cell survival studies requiring greater than 4 days incubation, fresh medium would be added without removing the old medium containing apoptotic cells.

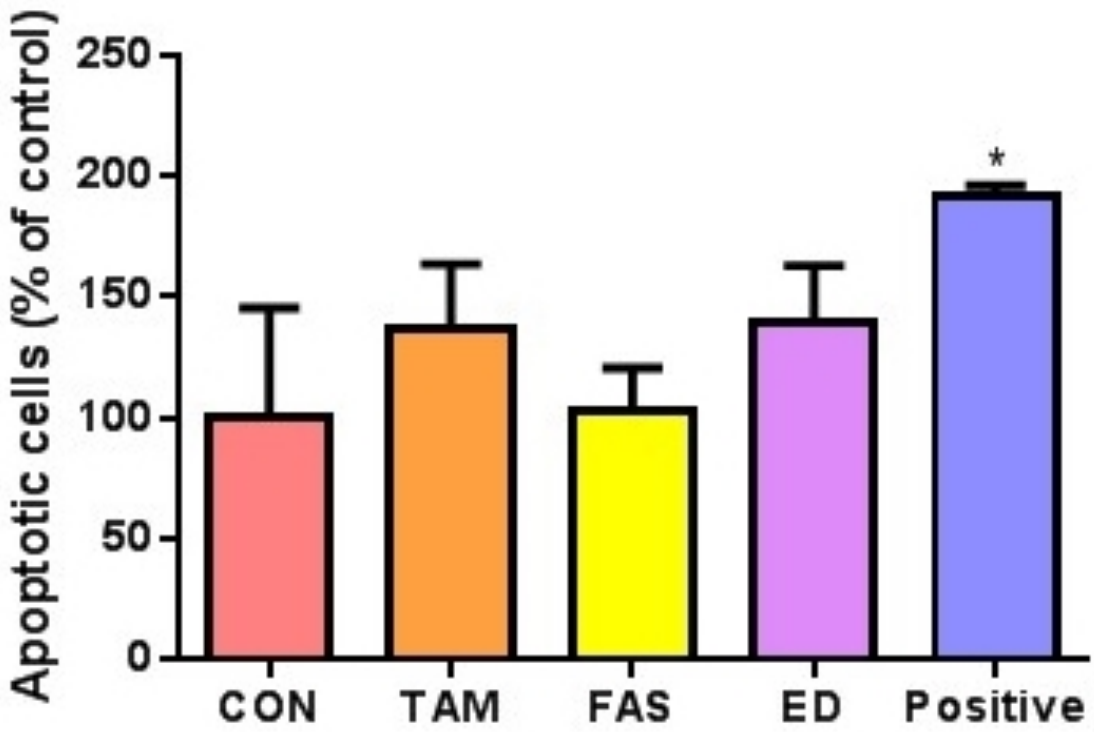

Figure 67 Graph displaying the percentage of apoptotic cells in MCF-7 cells treated with untreated control (CON) medium, tamoxifen (TAM; 10^{-7} M), fulvestrant (FAS; 10^{-7} M) and oestrogen deprivation (ED) for 7 days alongside the positive control thapsigargin (1 µM for 48 hours). Fresh medium was added at day 3. The results are expressed as the means ± SEM of three independent experiments and presented as the % of the control. The data were analysed by an ANOVA and post-hoc Tukey's multiple comparisons test * p <0.05 compared to control.

Subsequently, cell survival assays were performed to determine the baseline apoptotic levels of 7 day antihormone treated T47D cells. As shown in Figure 68, tamoxifen and fulvestrant treatments promoted a small and non-significant increase in apoptosis compared to control. Oestrogen deprivation treatment induced a statistically significant ($p < 0.05$) increase in apoptosis compared to untreated control. However, the levels of apoptosis observed following antihormone treatments were less than the levels induced by the positive control. Indeed, the positive control promoted a statistically significant ($p < 0.01$) increase in apoptosis compared to untreated control.

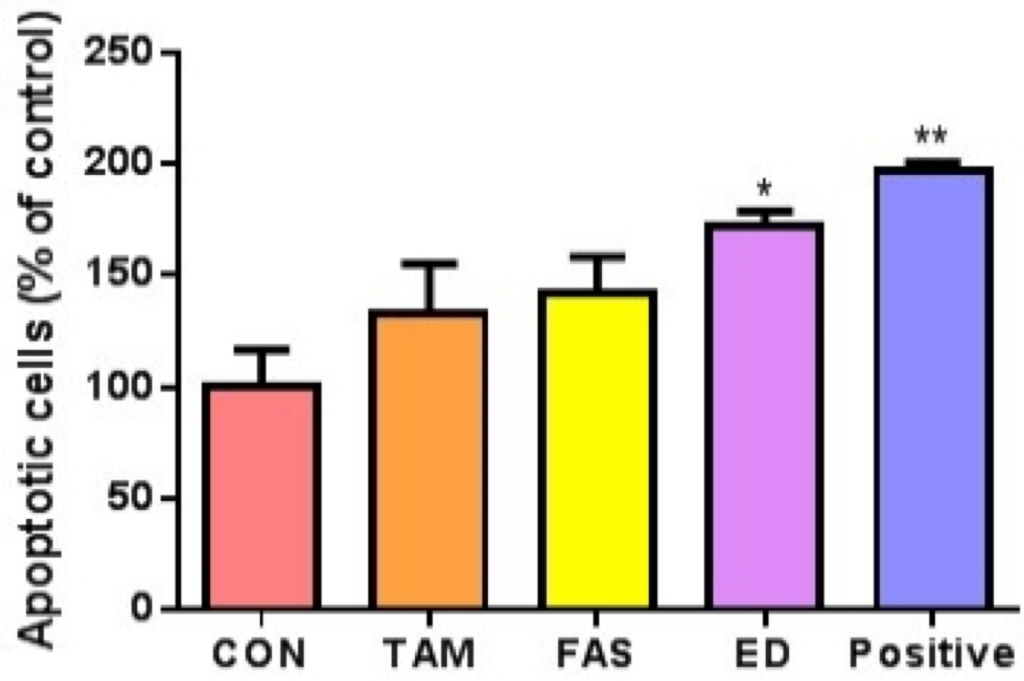

Figure 68 Graph displaying the percentage of apoptotic cells in T47D cells treated with untreated control (CON) medium, tamoxifen (TAM; 10^{-7} M), fulvestrant (FAS; 10^{-7} M) and oestrogen deprivation (ED) for 7 days alongside the positive control thapsigargin (1 µM for 48 hours). Fresh medium was added at day 3. The results are expressed as the means ± SEM of three independent experiments and presented as the % of the control. The data were analysed by an ANOVA and post-hoc Tukey's multiple comparisons test. * $p < 0.05$ and ** $p < 0.01$ compared to control.

5.3.5.2 Effect of BCL3 knockdown on the survival of antihormone-responsive MCF-7 cells

Following the optimisation of the cell survival experiment and the determination of baseline apoptosis in antihormone treated MCF-7- and T47D cells, the effect of BCL3 knockdown on the survival of fulvestrant-treated MCF-7 cells was investigated to determine whether BCL3 plays a pro-survival role during antihormone response and to determine whether targeting this protein alongside antihormone treatment enhances the apoptotic action of these agents. As revealed in Figure 69, targeted down regulation of BCL3 via siRNA had very little effect on the apoptosis of fulvestrant-treated MCF-7 cells versus control siRNA. Both the control and BCL3 siRNA treatments induced a slight increase in apoptosis, although not significant, compared to the untreated control and fulvestrant treatment alone (Figure 69). The levels of apoptotic cells were statistically significantly greater in the positive control arm compared to untreated control, fulvestrant ($p < 0.0001$, for both), control siRNA and BCL3 siRNA ($p < 0.001$, for both) (Figure 69).

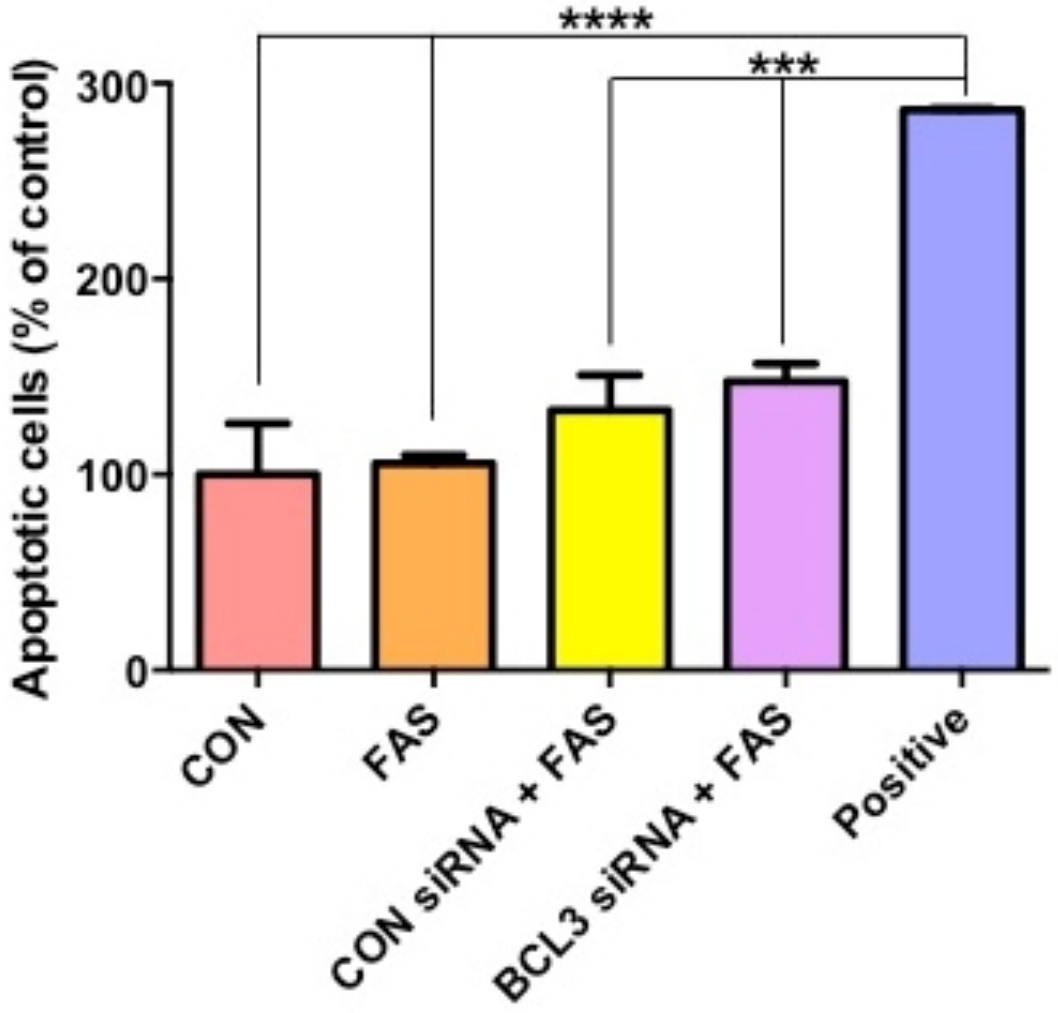

Figure 69 Graph displaying the percentage of apoptotic cells in MCF-7 cells treated with untreated control (CON) medium, fulvestrant (FAS; 10^{-7} M), CON siRNA plus FAS (2 day siRNA followed by 2 day FAS) and BCL3 siRNA plus FAS alongside thapsigargin positive control (1 µM for 48 hours). The results are expressed as the means ± SEM of three independent experiments and presented as the % of the control. The data were analysed by an ANOVA and post-hoc Tukey's multiple comparisons test. *** p <0.001; **** p <0.0001.

5.3.5.3 Effect of BCL3 knockdown on the survival of TAMR and XR cells

To determine whether BCL3 plays a pro survival role during resistance, cell survival assays were next performed on TAMR and XR cells. As shown in Figure 70, targeted down regulation of BCL3 by siRNA in TAMR and XR cell lines had very little effect on the percentage of apoptotic cells versus control, suggesting that BCL3 is not involved in the survival of resistant cells. In the XR cells, 4 day incubation with control and BCL3 siRNA resulted in the production of an equal percentage of apoptotic cells (Figure 70B); whereas BCL3 knockdown in the TAMR cell line appeared to result in a slightly lower production of apoptotic cells versus control (Figure 70A), possibly suggesting a pro-apoptotic role of BCL3 in this cell line. However, this observation in the TAMR cell line was marginal and not statistically significant. In this cell line, the levels of apoptotic cells were statistically significantly greater in the positive control arm compared to untreated control, control siRNA ($p < 0.05$, for both) and BCL3 siRNA ($p < 0.01$) (Figure 70A).

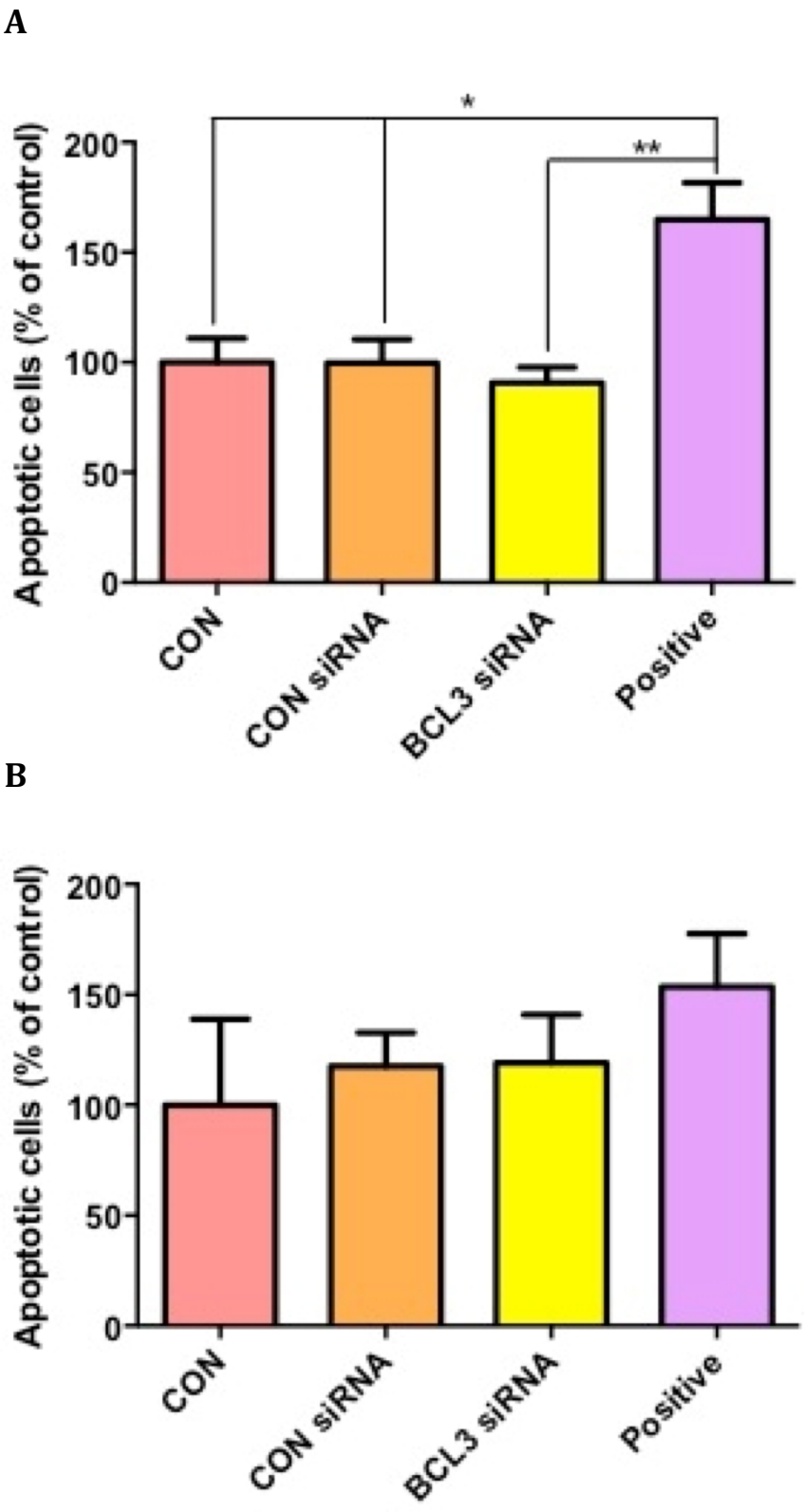

Figure 70 Graph displaying the percentage of apoptotic cells in (A) tamoxifen-resistant (TAMR) and (B) oestrogen deprivation-resistant (XR) cells treated with control (CON) medium only, CON siRNA plus fulvestrant (FAS; 10^{-7} M) (2 day siRNA followed by 2 day FAS) and BCL3 siRNA plus FAS alongside thapsigargin positive control (1 µM for 48 hours). The results are expressed as the means ± SEM of three independent experiments and presented as the % of the control. The data were analysed by an ANOVA and post-hoc Tukey's multiple comparisons test. * $p < 0.05$; ** $p < 0.01$.

5.3.6 Effect of BCL3 knockdown on cell growth during antihormone response and resistance

To further investigate the role of BCL3 during antihormone response and resistance cell counting experiments were next performed to determine whether BCL3 expression has any effect on the cell growth. The rationale was that a decrease in cell number/cell growth mediated by BCL3 siRNA versus control, suggests that BCL3 plays a role in promoting cell growth potentially via increasing cell proliferation.

5.3.6.1 Antihormone response

As illustrated in Figure 71, BCL3 knockdown (2 day BCL3 siRNA incubation followed by a further 2 day combined incubation with fulvestrant) had no effect on the growth of fulvestrant-treated MCF-7 cells, but promoted a small, yet non-significant, decrease in T47D cell growth versus control.

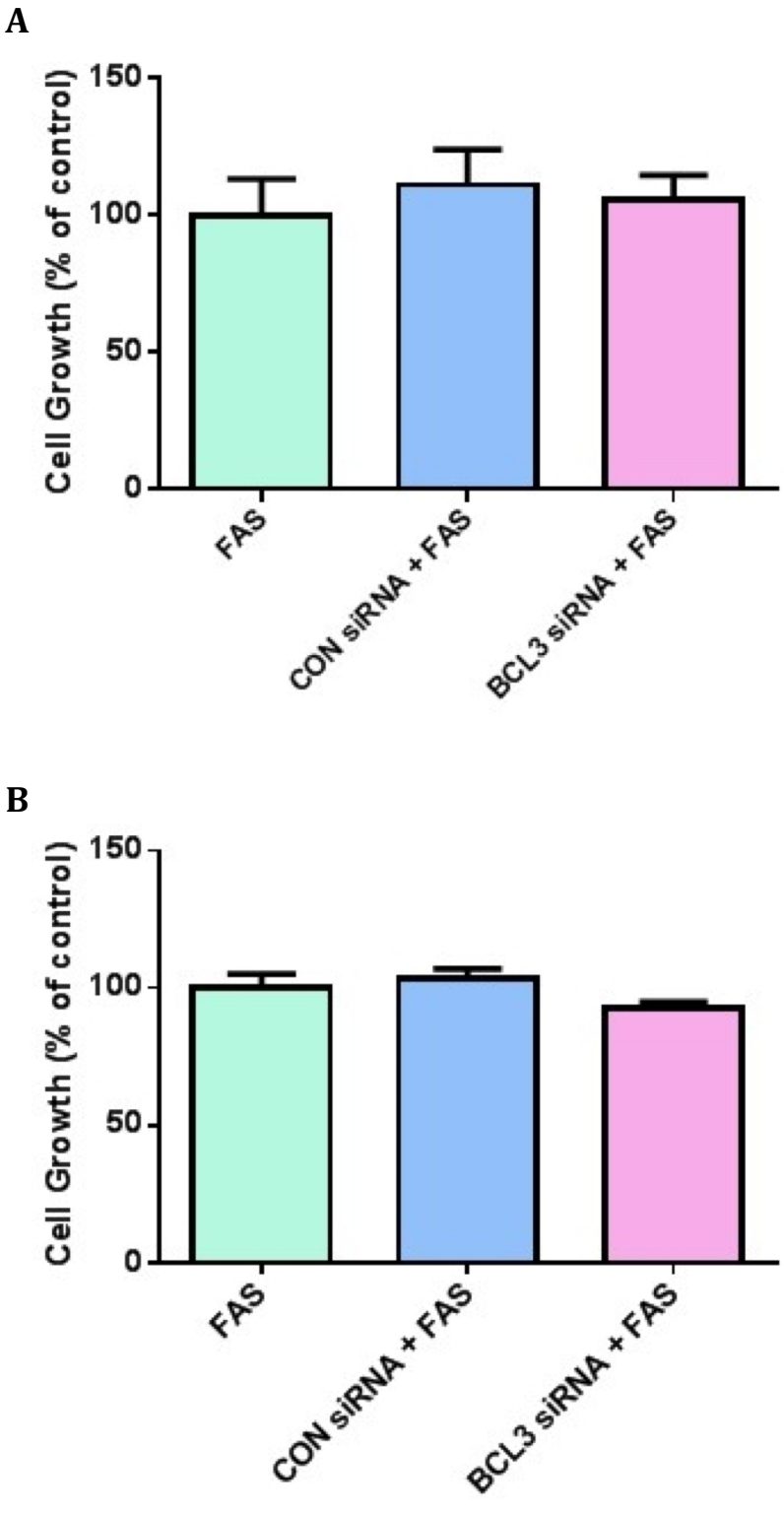

Figure 71 Effect of BCL3 knockdown (with 2 day BCL3 siRNA followed by 2 day fulvestrant (FAS; 10^{-7} M)) compared to control (CON; 2 day control siRNA followed by 2 day fulvestrant) and FAS alone on the growth of (A) MCF-7 and (B) T47D cells. The results are expressed as the means ± SEM of three independent experiments (n=3) and presented as the % of the control. The data were analysed by an ANOVA and post-hoc Tukey's multiple comparisons test.

5.3.6.2 Antihormone resistance

In contrast, targeted down regulation of BCL3 using siRNA in the antihormone resistant TAMR and XR cell lines reduced cell growth by approximately 40% and 20%, respectively, versus control siRNA (Figure 72A and B). However, such effects on the growth of TAMR and XR cells did not reach significance. BCL3 knockdown was without effect on the growth of T47D TAMR cells (Figure 72C).

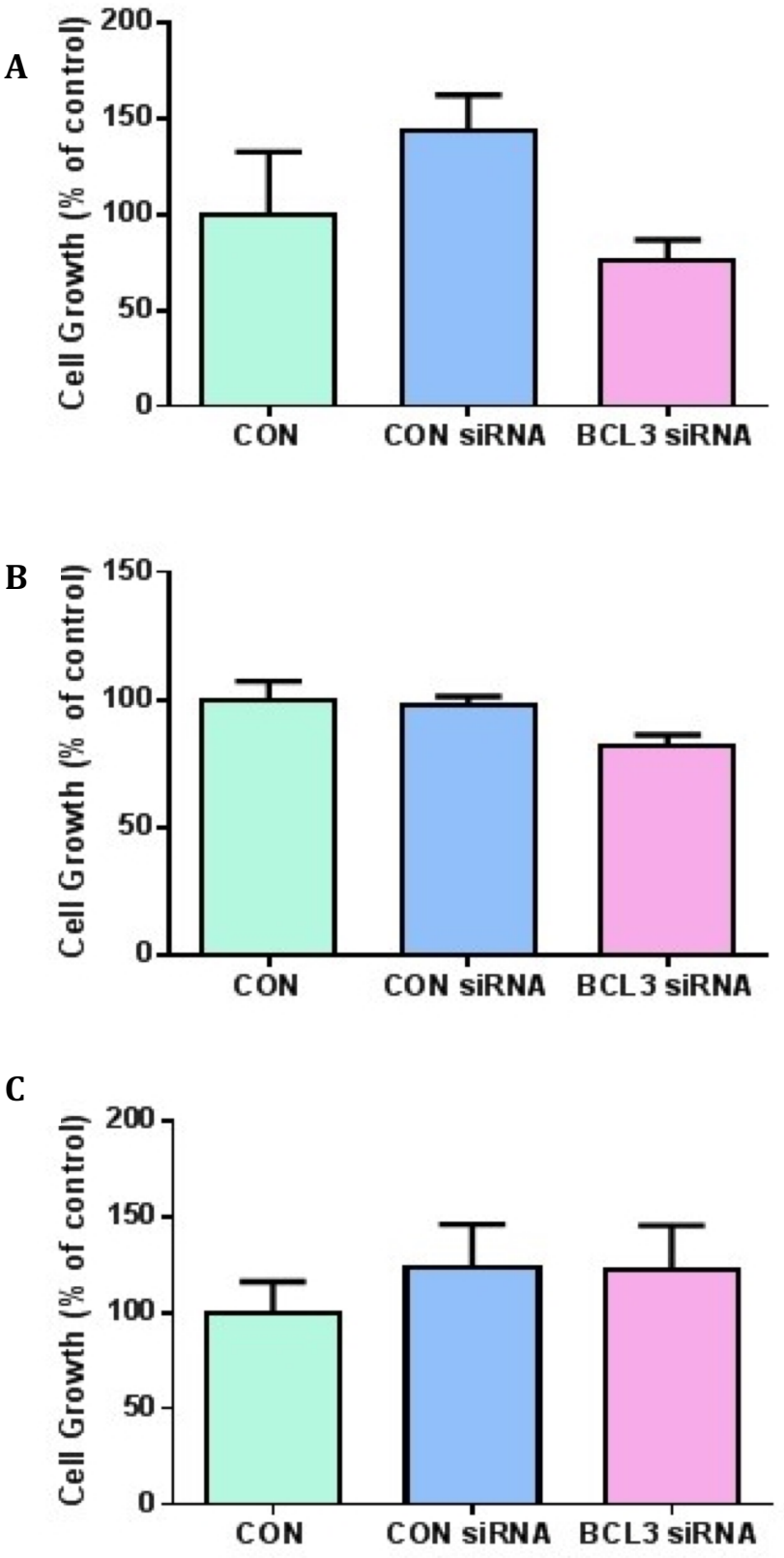

Figure 72 Effect of BCL3 knockdown (with 4 day BCL3 siRNA) compared to control (CON; 4 day control siRNA) and untreated CON on the growth of (A) tamoxifen-resistant (TAMR) (n=3), (B) oestrogen deprivation-resistant (XR) (n=6) and (C) TAMR cells derived from T47D cells (T47D-TAMR) (n=3). The results are expressed as the means ± SEM and presented as the % of the control. The data were analysed by an ANOVA and post-hoc Tukey's multiple comparisons test.

5.3.6.3 Effect of BCL3 knockdown on EGFR/HER2/MAPK signalling

The group has previously reported that TAMR cell growth is regulated by EGFR/HER2 driven MAPK and AKT signalling pathways[185]. To verify that the siRNA used in the present study specifically targeted BCL3 and not elements of these signalling pathways, Western blot analysis of these proteins was performed in the TAMR cell line following incubation with either BCL3 or control siRNA. As shown in Figure 73, BCL3 siRNA had no effect on total and phosphorylated forms of ERBB2, AKT, ERK and EGFR.

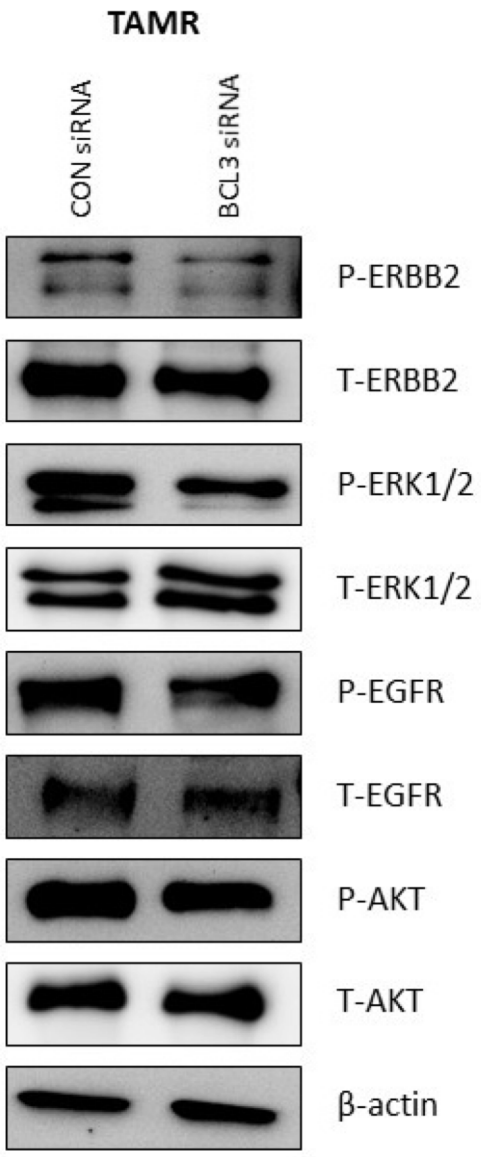

Figure 73 Representative Western blot images from three independent experiments showing protein expression of phosphorylated (P) and total (T) ERBB2, ERK1/2, EGFR and AKT in tamoxifen-resistant (TAMR) cells incubated for 4 days with unscrambled control (CON) and BCL3 siRNA.

5.3.7 Effect of BCL3 knockdown on cell cycle distribution during antihormone-response and –resistance

Cell cycle studies, utilising a PI stain and subsequent flow cytometry analysis, were next performed to investigate whether BCL3 plays a role in regulating progression of cells through the cell cycle during antihormone-response and in resistance.

5.3.7.1 Effect of antihormones on the cell cycle distribution of MCF-7 and T47D cells

Initially, the effect of 7 day antihormone treatment on the cell cycle distribution of MCF-7 and T47D cells was examined. Figure 74 displays the percentage of cells in each phase of the cell cycle following antihormone, E2 and control treatments. All three antihomrones induced G1 arrest of MCF-7 cells compared to control, with the greatest arrest induced by fulvestrant treatment (Figure 74A). However, such effects did not reach significance. E2- and control-treated cells had a relatively equal percentage of cells in each stage of the cell cycle (i.e. G1, S and G2/M phases) in MCF-7 cells. Following antihormone treatment, the percentage of cells in S phase decreased, although not significant, versus E2- and control-treated cells (Figure 74A). The percentage of cells in G2/M phase was relatively similar following antihormone, E2 and control treatments, with a small and non-significant decrease apparent following fulvestrant treatment (Figure 74A).

Similarly, tamoxifen and fulvestrant induced G1 arrest (although not significant) of T47D cells versus control (Figure 74B). Surprisingly, however, oestrogen deprivation treatment induced a decrease in the percentage of cells in G1 compared to control, with a statistically significant ($p < 0.05$) decrease observed versus E2 treatment (Figure 74B). The percentage of cells in S phase was relatively similar following tamoxifen, fulvestrant, E2 and control treatments. However, oestrogen deprivation treatment induced a statistically significant ($p < 0.05$) increase in the percentage of cells in S phase, indicative of increased DNA replication, compared to control and E2 treatment (Figure 74B). Tamoxifen and fulvestrant treated cells had a slightly lower, whereas oestrogen deprivation treated cells had a slightly higher, percentage of cells in the G2/M phase compared to control (Figure 74B). However, such effects were not significant. A similar

distribution of cells in each phase of the cell cycle was apparent following E2 and control treatments.

A

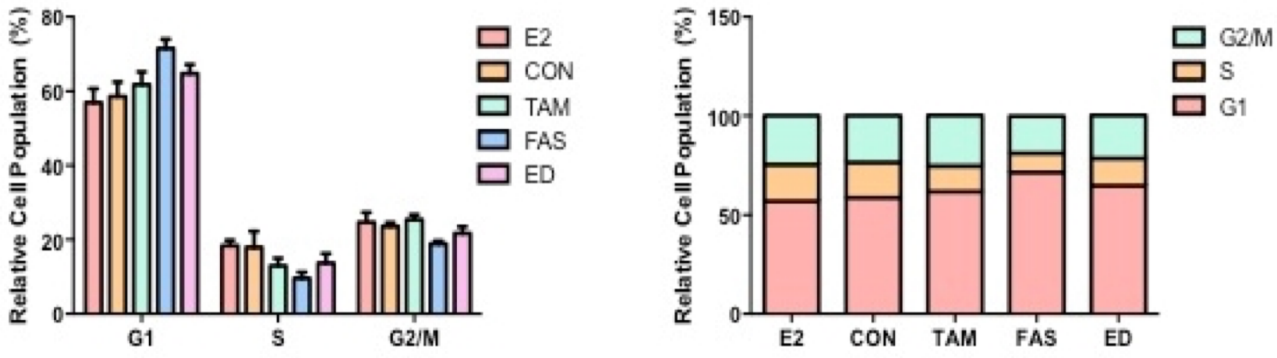

B

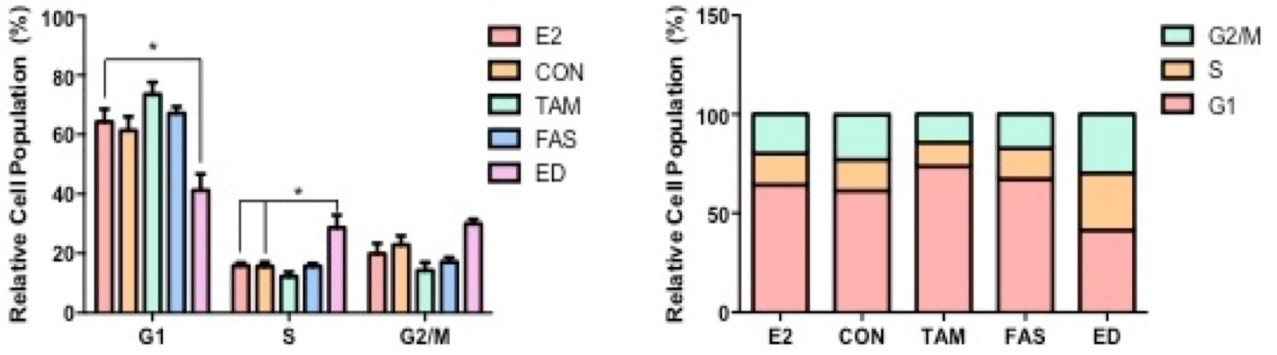

Figure 74 Effect of 7 day oestradiol (E2; 10^{-9} M), tamoxifen (TAM; 10^{-7} M), fulvestrant (FAS; 10^{-7} M) and oestrogen deprivation (ED) treatment on cell cycle distribution versus untreated control (CON) in MCF-7 (A) and T47D (B) cells. The results are expressed as the means ± SEM of three independent experiments. * $p < 0.05$. The data were analysed by a one-way ANOVA and post-hoc Tukey's multiple comparisons test

Tamoxifen has been widely recognised as a strong inducer of G1 arrest in MCF-7 cells[311,420], although such effects were not observed in the current study. However, the majority of studies examined short term antihormone treatment, ranging from 24 to 96 hours. Thus, it is highly likely that such antihormone-induced dysregulation of the cell cycle was missed following 7 day treatment. Therefore, a time course study was performed, comprising day 1 to day 4 antihormone treatments. As illustrated in Figure 75, tamoxifen induced G1 arrest of MCF-7 cells compared to control as early as day 2 treatment, which was maintained through to day 4 (n=1). However, as these experiments were only performed once, statistical analysis could not be applied. Concurrently, the percentage of tamoxifen-treated cells decreased in S and G2/M phases, compared to control, from day 2 to day 4 treatment. Following 24 hours of tamoxifen treatment, there was very little, if any, difference in the percentage of cells in each phase of the cycle, compared to control (Figure 75A). Fulvestrant promoted G1 arrest, together with a small decrease in the percentage of cells entering S and G2/M phases, compared to control, following 3 and 4 day treatment (Figure 75C and D). However, following day 1 and 2 treatment, fulvestrant had very little effect on the cell cycle compared to control (Figure 75A and B). Interestingly, oestrogen deprivation treatment induced marked G1 arrest following 1 day treatment with concurrent decreases in the percentage of cells in S phase and G2/M phase versus control (Figure 75A). Following 2 day oestrogen deprivation treatment, the percentage of MCF-7 cells in G1 was similar to control, whereas the percentage in S phase and G2/M phase were decreased and increased, respectively, versus control (Figure 75B). Following 3 and 4 day oestrogen deprivation treatment, the percentage of cells in each phase of the cell cycle was relatively similar to control (Figure 75C and D). Unsurprisingly, the percentage of cells arrested in G1 was lower following day 1 to day 4 E2 treatment compared to control (Figure 75). Additionally, the percentage of cells in S phase was slightly greater following E2 treatment compared to control, with the greatest induction apparent at day 1 (Figure 75A). Interestingly, the percentage of E2 treated cells in G2/M phase was marginally less at day 1, but greater at day 2 to day 4, compared to control.

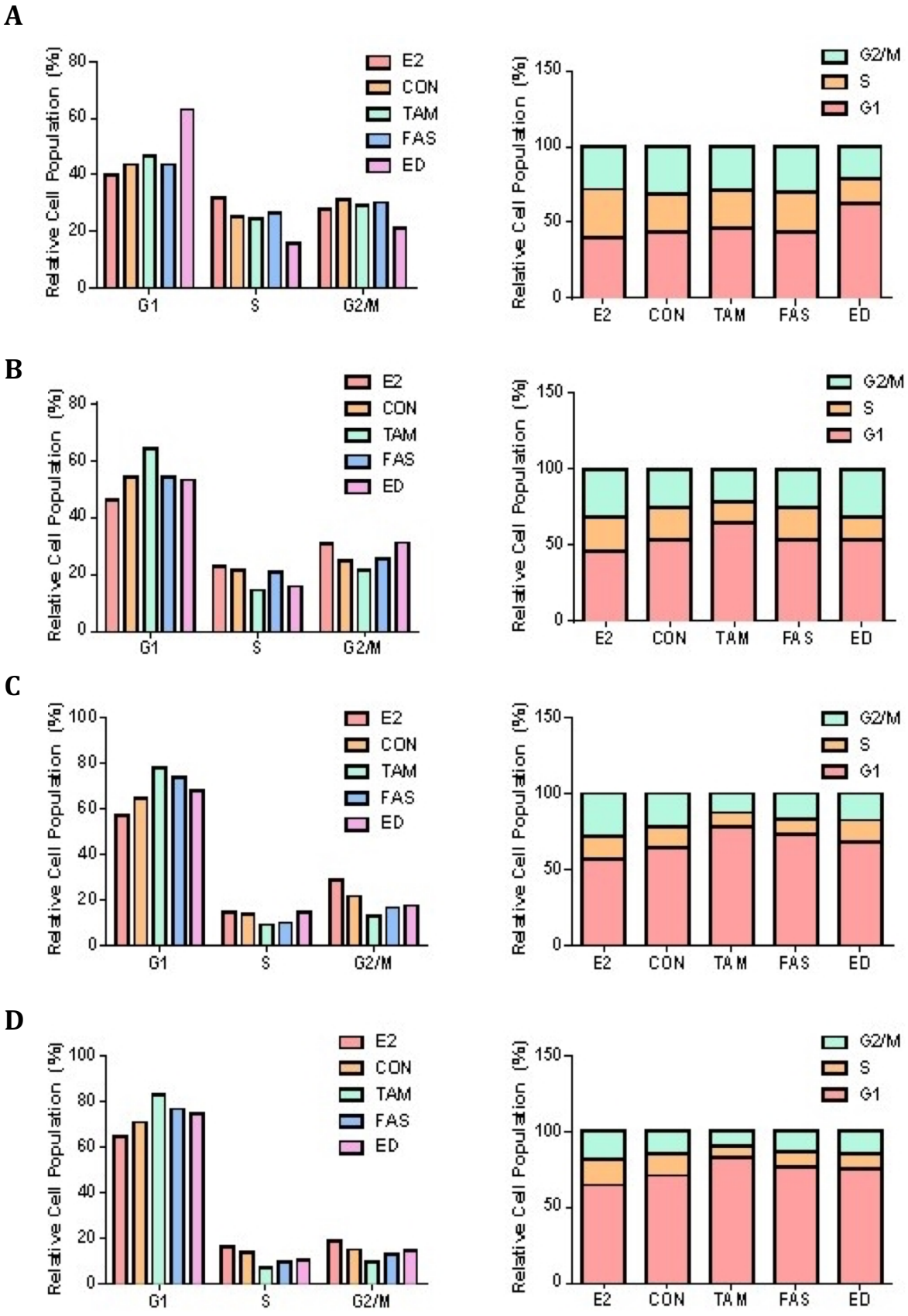

Figure 75 Effect of oestradiol (E2; 10^{-9} M), tamoxifen (TAM; 10^{-7} M), fulvestrant (FAS; 10^{-7} M) and oestrogen deprivation (ED) on cell cycle distribution versus untreated control (CON) in MCF-7 cells following 1 (A), 2 (B), 3 (C) and 4 (D) days treatment (n=1).

5.3.7.2 Effect of BCL3 knockdown on the cell cycle distribution of antihormone-responsive MCF-7 and T47D cells

The effect of BCL3 knockdown on the cell cycle of MCF-7 and T47D cells during antihormone response was next investigated to determine whether BCL3 plays a role in promoting cell cycle progression and to determine whether targeting this protein alongside antihormone treatment enhances the growth inhibitory action of these agents. MCF-7 and T47D cells were incubated with BCL3 or control siRNA for 2 days prior to the addition of fulvestrant for a further 2 days. As illustrated in Figure 76, BCL3 knockdown had no effect on the cell cycle of fulvestrant-treated MCF-7 and T47D cells compared to control siRNA. To a certain degree, this is in agreement with the cell growth data (Figure 71) which demonstrated no effect of targeted BCL3 down regulation on the growth of fulvestrant-treated MCF-7 and T47D cells, indirectly suggesting that BCL3 is not involved in cell proliferation or survival during antihormone response. Similarly, 2 day fulvestrant treatment had very little effect on the cell cycle of MCF-7 and T47D cells compared to media alone (Figure 76). This is in agreement with the data presented in Figure 75, which demonstrated that 2 day fulvestrant treatment had no effect on the cell cycle of MCF-7 cells.

A

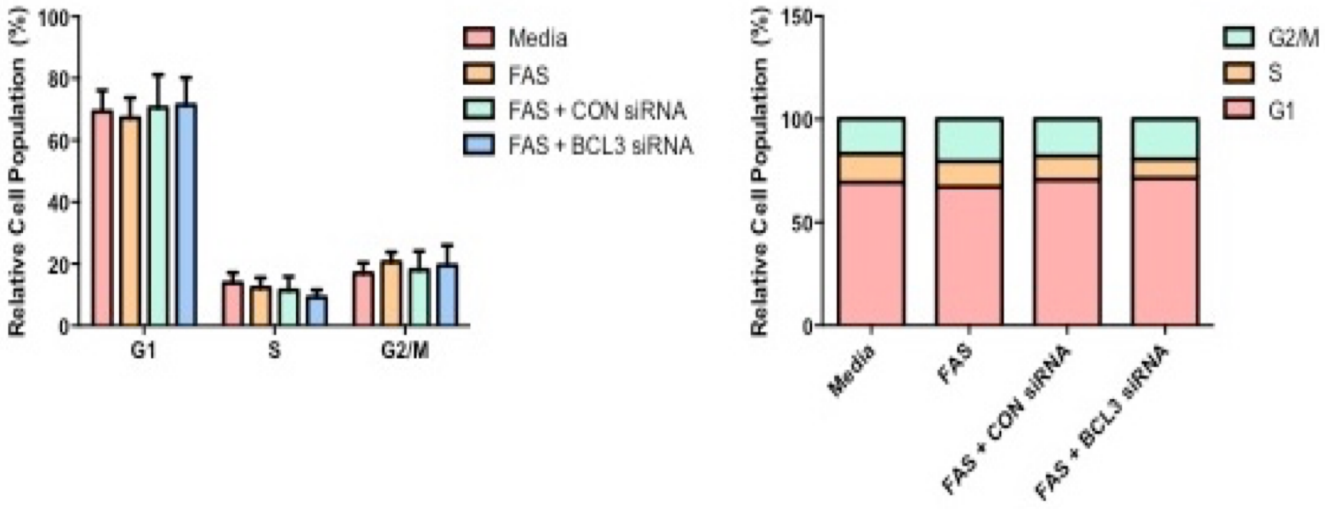

B

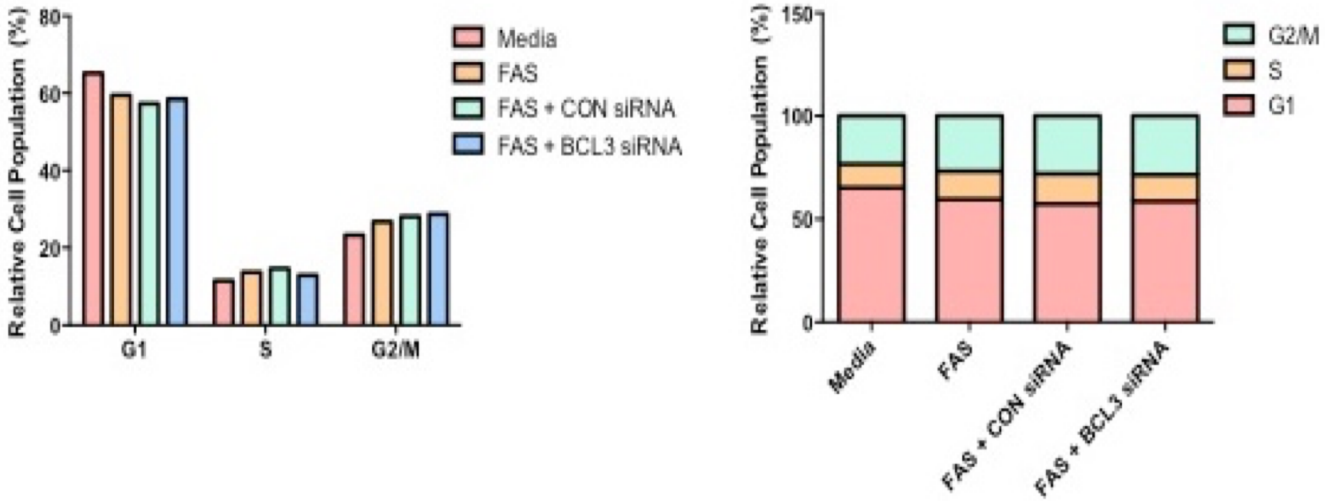

Figure 76 Effect of BCL3 knockdown (with 2 day BCL3 siRNA followed by 2 day fulvestrant (FAS; 10^{-7} M)) compared to control (CON; 2 day control siRNA followed by 2 day FAS) on the cell cycle distribution of MCF-7 (A; n=2; expressed as the means ± SEM) and T47D (n=1) cells. The cell cycle distributions of untreated control (CON) and 2 day FAS-treated cells are also shown.

5.3.7.3 Effect of BCL3 knockdown on the cell cycle distribution of TAMR and XR cells

As previously demonstrated in Figure 72, BCL3 knockdown in TAMR and XR cells led to a substantial decrease in cell growth. To determine whether BCL3 promotes cell cycle progression in these resistant cell models, thus potentially explaining the decrease in cell growth observed following targeted knockdown of this protein, cell cycle assays were next performed on TAMR and XR cells. As illustrated in Figure 77, BCL3 knockdown by siRNA in TAMR and XR cell lines had very little effect on the cell cycle compared to control siRNA, suggesting that BCL3 does not regulate the cell cycle. Media only-treated TAMR and XR cells exhibited a similar percentage of cells in each phase of the cell cycle compared to control and BCL3 siRNA-treated cells, with the exception of XR cells in S phase and G2/M phase. A lower percentage of XR cells were in S phase, whereas a slightly higher percentage were in G2/M phase following control siRNA and BCL3 siRNA treatment versus control (Figure 77). However, such effects were not significant.

Subsequently, BCL3 knockdown comprised of 2 and 3 day siRNA incubation was performed on TAMR cells and the cell cycle was assessed to determine whether shorter BCL3 knockdown disrupted the cell cycle. As revealed in Figure 78, 2 and 3 day BCL3 knockdown had very little effect on the cell cycle compared to control siRNA.

A

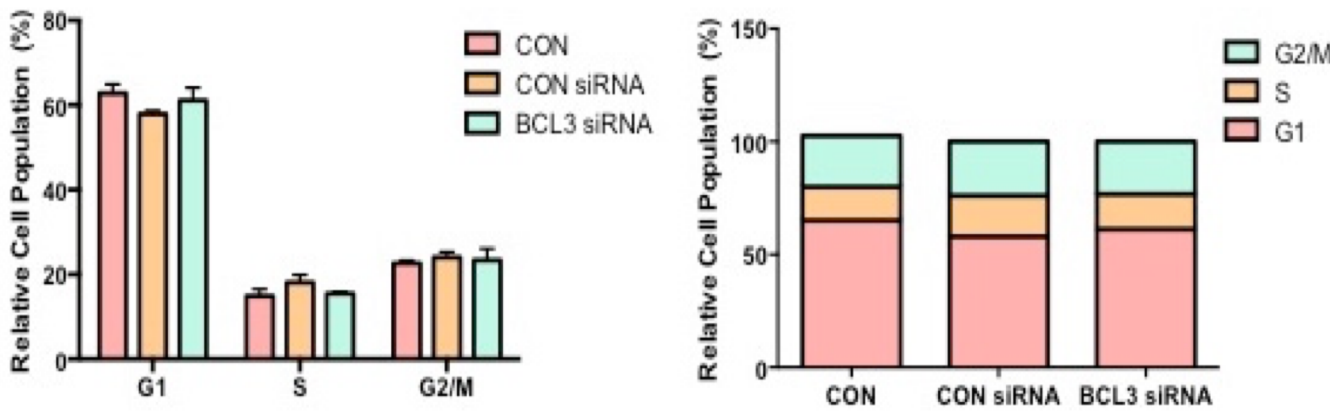

B

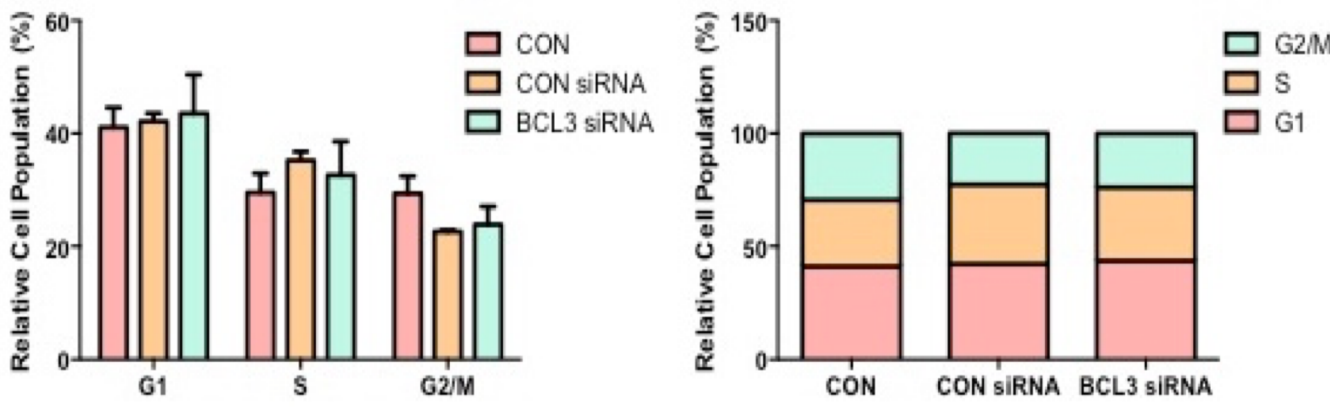

Figure 77 Effect of BCL3 knockdown (with 4 day BCL3 siRNA) compared to control (CON siRNA; 4 day control siRNA) on the cell cycle distribution of tamoxifen-resistant (TAMR) (A) and oestrogen deprivation-resistant (XR) (B) cells. The cell cycle distribution of untreated control (CON) cells is also shown. The results are expressed as the means ± SEM of three independent experiments. The data were analysed by an ANOVA and post-hoc Tukey's multiple comparisons test.

A

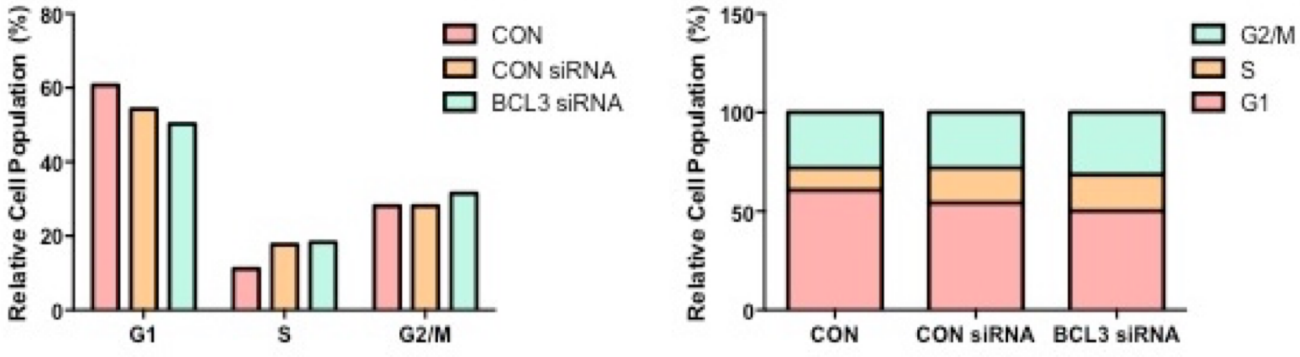

B

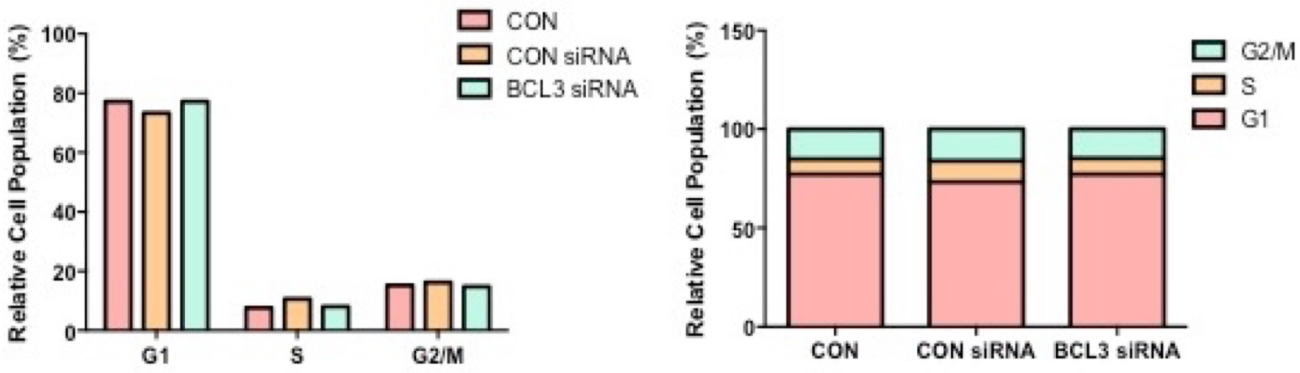

Figure 78 Effect of 2 (A; n=1) and 3 (B; n=1) day BCL3 siRNA incubation on the cell cycle distribution of tamoxifen-resistant (TAMR) cells versus control (CON siRNA). The cell cycle distribution of untreated control (CON) cells is also shown.

5.3.8 Investigation of potential mechanisms mediated by BCL3 to promote proliferation of antihormone-resistant MCF-7 cells

As determined from the ontological studies reported in Chapter 3, BCL3 is a nuclear protein with both transactivation and transrepressor functions, which are mediated by its association with the NF-κB homodimers, p50/NFKB1 and p52/NFKB2[359]. Furthermore, increased BCL3 expression and NF-κB activity (comprised predominantly of p50/NFKB1 dimers) have been reported in MCF-7 cells following oestrogen deprivation treatment, with BCL3 expression and NF-κB activity enhanced further in a ER+ MCF-7 cell model of oestrogen independence[363], strongly suggesting a positive correlation and association between both BCL3 and NF-κB activity, culminating in the activation of downstream NF-κB-regulated genes involved in tumourigenesis. In support of the BCL3 and NF-κB connection, BCL3 has been shown to coactivate p52/NFKB2 dimers in normal breast cell lines, resulting in the transcription of the cyclin D1 gene ultimately promoting G1 to S phase cell cycle transition and cell cycle progression[361].

To further explore the relationship between BCL3 and NF-κB, this project next aimed to determine whether p50/NFKB1 and p52/NFKB2 proteins are expressed alongside BCL3 during antihormone-response and -resistance and ultimately investigate whether they interact with BCL3 and thus play a role in BCL3-mediated cell growth observed particularly during resistance.

5.3.8.1 Microarray analysis of p50/NFKB1 and p52/NFKB2 expression during antihormone response

Initially, the microarray data utilised in Chapter 3 was interrogated to determine whether p50/NFKB1 and p52/NFKB2 are expressed together with BCL3 in MCF-7 cells during antihormone response and hence may contribute to aberrant cell growth. Microarray gene expression profiling was completed for 10 day antihormone-treated (tamoxifen, fulvestrant and oestrogen deprivation) MCF-7 cells cultured in sFCS versus E2-treated control. The resultant triplicate data were uploaded on to the bioinformatics software GeneSifter and first median normalised and log transformed prior to analysis. This GeneSifter-assembled array resource was interrogated using the 'jetset' probes representing p50/NFKB1 and p52/NFKB2: 209239_at and 209636_at respectively.

The log2 intensity plot and corresponding fold change revealed a small, non-significant increase in p50/NFKB1 expression following oestrogen deprivation versus E2-treated control (Figure 79). Ten day tamoxifen and fulvestrant treatment induced similar p50/NFKB1 expression to E2-treated control. Present detection calls were recorded in the antihormone- and E2-treated cells, implying reliable detection of gene expression (Figure 79B).

A

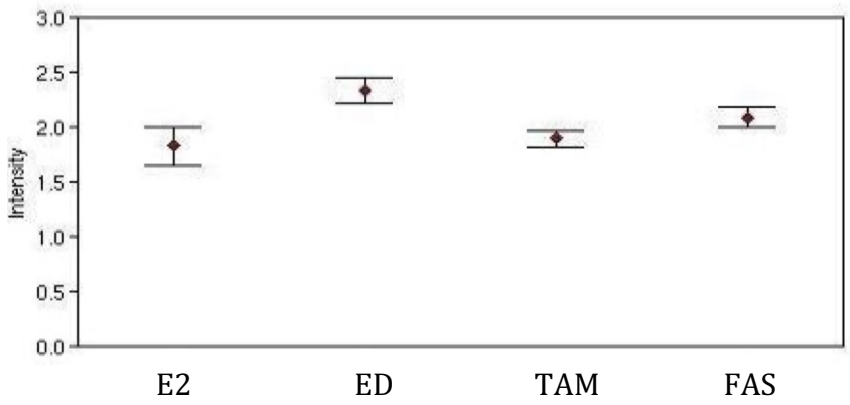

B

	E2-control	ED	TAM	FAS
Fold change		1.42	1.05	1.20
Detection call	PPP	PPP	PPP	PPP

Figure 79 (A) Log2 intensity plot displaying the normalised (mean of three independent replicates ± SEM) gene expression of p50/NFKB1 (jetset probe ID: 209239_at) in MCF-7 cells treated for 10 days with oestradiol (E2 control; 10^{-9} M), oestrogen deprivation (ED), tamoxifen (TAM; 10^{-7} M) and fulvestrant (FAS; 10^{-7} M). (B) Table displaying the corresponding fold change in gene expression and detection calls from the triplicate samples. P: present.

The log2 intensity plot revealed a small and a non-significant down regulation of p52/NFKB2 expression following all three antihormone treatments compared to E2-treated control (Figure 80). Tamoxifen induced the greatest down regulation of p52/NFKB2 expression (fold change > 1.5) followed by fasldox and oestrogen deprivation. The log2 expression values in antihormone- and control- treated cells failed to rise above 0 and absent calls were recorded suggesting relatively low/no gene expression.

A

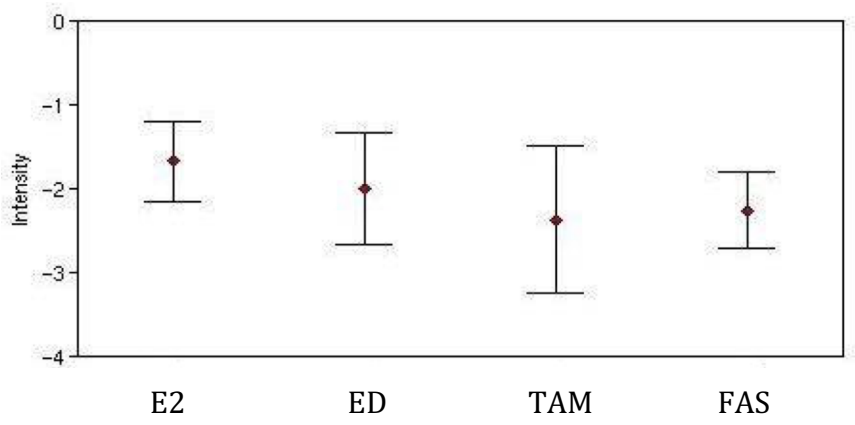

B

	E2-control	ED	TAM	FAS
Fold change		1.25	1.62	1.50
Detection call	AAA	AAA	AAA	MAA

Figure 80 (A) Log2 intensity plot displaying the normalised (mean of three independent replicates ± SEM) gene expression of p52/NFKB2 (jetset probe ID: 209636_at) in MCF-7 cells treated for 10 days with oestradiol (E2 control; 10^{-9} M), oestrogen deprivation (ED), tamoxifen (TAM; 10^{-7} M) and fulvestrant (FAS; 10^{-7} M). (B) Table displaying the corresponding fold change in gene expression and detection calls from the triplicate samples. M: marginal; A: absent.

5.3.8.2 Microarray analysis of p50/NFKB1 and p52/NFKB2 expression during antihormone resistance

p50/NFKB1 and p52/NFKB2 expression were next examined in the antihormone resistant cell models. The microarray gene expression profiling for TAMR and XR models of acquired (short-term) resistance derived from MCF-7 cells versus wild type control, utilised in Chapter 3, was interrogated using the 'jetset' probes representing p50/NFKB1 and p52/NFKB2.

5.3.8.2.1 TAMR

The log2 intensity plot shown in Figure 81 revealed a small, non-significant increase in p50/NFKB1 expression in the TAMR cell line compared to wild type MCF-7 cells. Present detection calls were recorded in the TAMR and wild type cells, indicative of reliable gene expression.

A

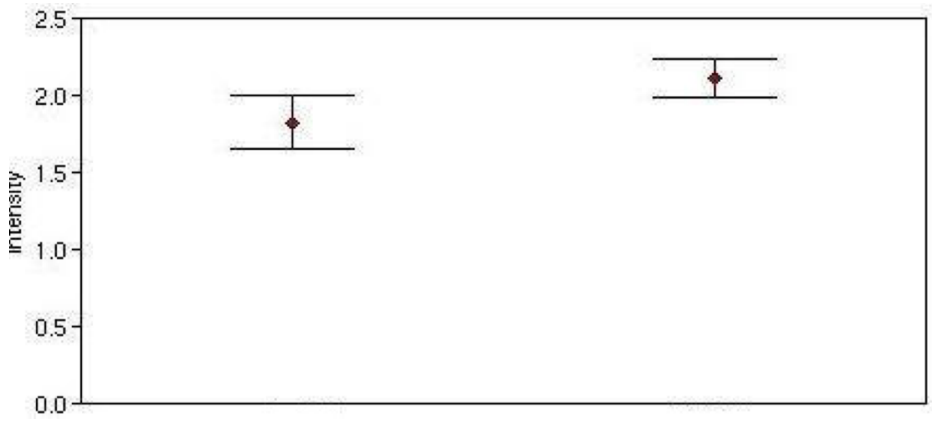

B

	MCF-7	TAMR
Fold change		1.22
Detection call	PPP	PPP

Figure 81 (A) Log2 intensity plot displaying the normalised (mean of three independent replicates ± SEM) gene expression of p50/NFKB1 (jetset probe ID: 209239_at) in tamoxifen-resistant MCF-7 cells (TAMR) versus wild type MCF-7 cells. (B) Table displaying the corresponding fold change in gene expression and detection calls from the triplicate samples. P: present.

In contrast, the log2 intensity plot demonstrated a non-significant down regulation (fold change > 1.5) of p52/NFKB2 expression in TAMR cells compared to MCF-7 control (Figure 82). Additionally absent detection calls were recorded in both the control and TAMR cells, implying relatively low/no gene expression.

A

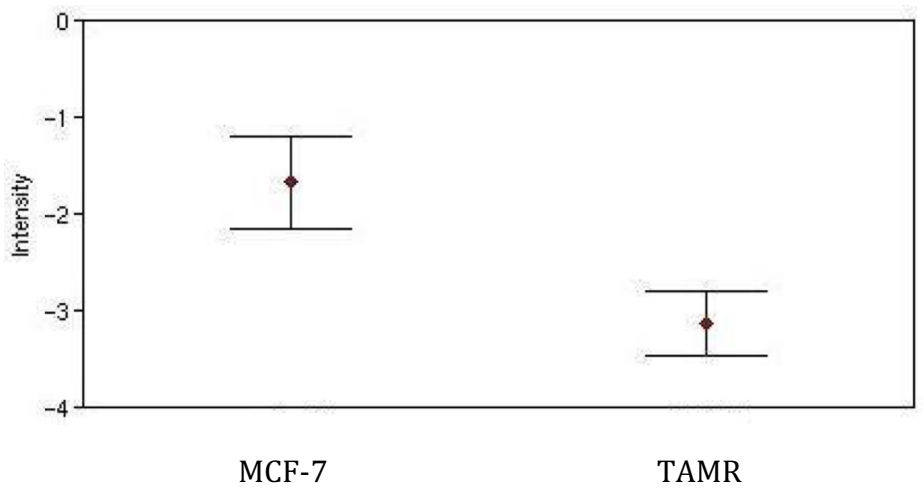

B

	MCF-7	TAMR
Fold change		2.74
Detection call	AAA	AAA

Figure 82 (A) Log2 intensity plot displaying the normalised (mean of three independent replicates ± SEM) gene expression of p52/NFKB2 (jetset probe ID: 209636_at) in tamoxifen-resistant MCF-7 cells (TAMR) versus wild type MCF-7 cells. (B) Table displaying the corresponding fold change in gene expression and detection calls from the triplicate samples. A: absent.

5.3.8.2.2 XR

The log2 intensity plot revealed a significant increase in p50/NFKB1 expression in XR cells versus wild type MCF-7 control (Figure 83). Present detection calls were reported in the XR and control cells implying reliable detection of gene expression.

A

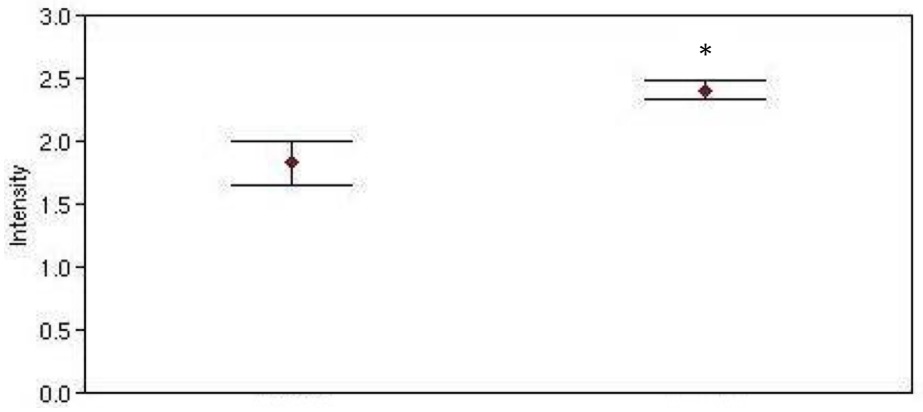

B

	MCF-7	XR
Fold change		1.50
Detection call	PPP	PPP

Figure 83 (A) Log2 intensity plot displaying the normalised (mean of three independent replicates ± SEM) gene expression of p50/NFKB1 (jetset probe ID: 209239_at) in oestrogen deprived-resistant MCF-7 cells (XR) versus wild type MCF-7 cells. (B) Table displaying the corresponding fold change in gene expression and detection calls from the triplicate samples. * p <0.05 compared to control. P: present

p52/NFKB2 expression was also marginally (non-significantly) increased in XR cells versus MCF-7 cells as demonstrated by the log2 intensity plot shown in Figure 84. However, the log2 expression levels failed to rise above 0 and absent detection calls were recorded in the control and XR cells, indicative of very low, if any, gene expression.

A

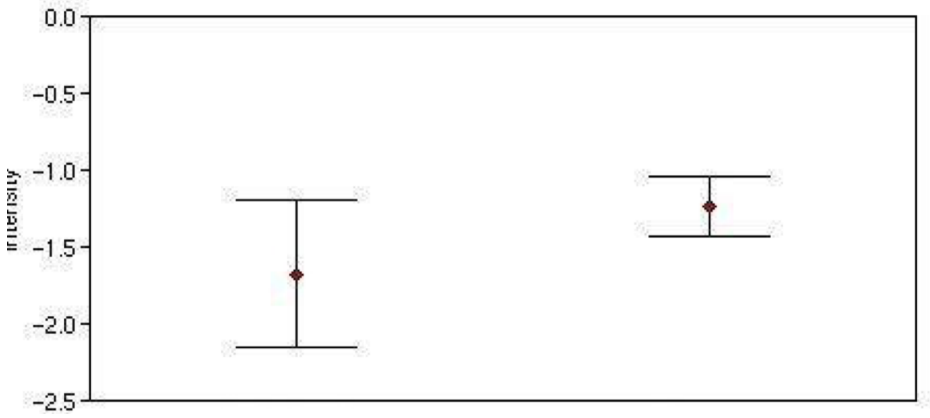

B

	MCF-7	XR
Fold change		1.36
Detection call	AAA	AAA

Figure 84 (A) Log2 intensity plot displaying the normalised (mean of three independent replicates ± SEM) gene expression of p52/NFKB2 (jetset probe ID: 209636_at) in oestrogen deprived-resistant MCF-7 cells (XR) versus wild type MCF-7 cells. (B) Table displaying the corresponding fold change in gene expression and detection calls from the triplicate samples. A: absent.

5.3.8.3 Protein expression of p50/NFKB1 and p52/NFKB2 during antihormone-response and -resistance

The Affymetrix expression profiles of p50/NFKB1 and p52/NFKB2 were subsequently verified at the protein level by Western analysis. Additionally, p50/NFKB1 and p52/NFKB2 protein expression was examined in antihormone-treated T47D cells and T47D TAMR cells for which there was no microarray data. Importantly however, the microarray data of the antihormone-treated MCF-7 cells was generated from 10 day culture of these cells in medium supplemented with sFCS comprising tamoxifen, fulvestrant, oestrogen deprivation or E2-control treatments; whereas Western blotting was performed on triplicate protein from 10 day antihormone-treated (tamoxifen, fulvestrant and oestrogen deprivation) MCF-7 (and T47D) cells cultured in FCS alongside E2 treatment and untreated control. As previously revealed in Chapter 4, the HER2+ cell lines do not proliferate well in stripped serum, therefore it was concluded to culture all cell lines in FCS for subsequent experiments. Western analysis was also performed on triplicate protein from antihormone resistant cell models versus E2-treated control, cultured under the same conditions as those used to generate the samples for microarray gene profiling.

In agreement with the absent detection calls reported from the microarray data for p52/NFKB2 during antihormone response and in the endocrine resistant cell models, p52/NFKB2 protein expression could not be detected by Western blotting (Figure 85 and Figure 86). In contrast, as illustrated in Figure 87A p50/NFKB1 protein expression was observed in untreated MCF-7 cells and was unaffected by E2 and antihormone treatments. Additionally, expression of the precursor protein, p105, was also expressed in untreated control, E2- and antihormone-treated MCF-7 cells, with the greatest expression induced by oestrogen deprivation treatment. However, p50/NFKB1 expression was markedly stronger than p105 in the MCF-7 cells, regardless of treatment. Similarly, comparable p50/NFKB1 expression was detected in untreated, E2-, tamoxifen- and fulvestrant-treated T47D cells, with slightly less detected following oestrogen deprivation treatment (Figure 87B). However, the lower expression of p50/NFKB1 observed in the oestrogen deprived T47D cells may be explained by the marginally lower protein

expression of the housekeeping gene, actin, observed following this treatment. Additionally, in contrast to the MCF-7 cell line, p105 protein expression was not detected in the T47D cells, irrespective of treatment.

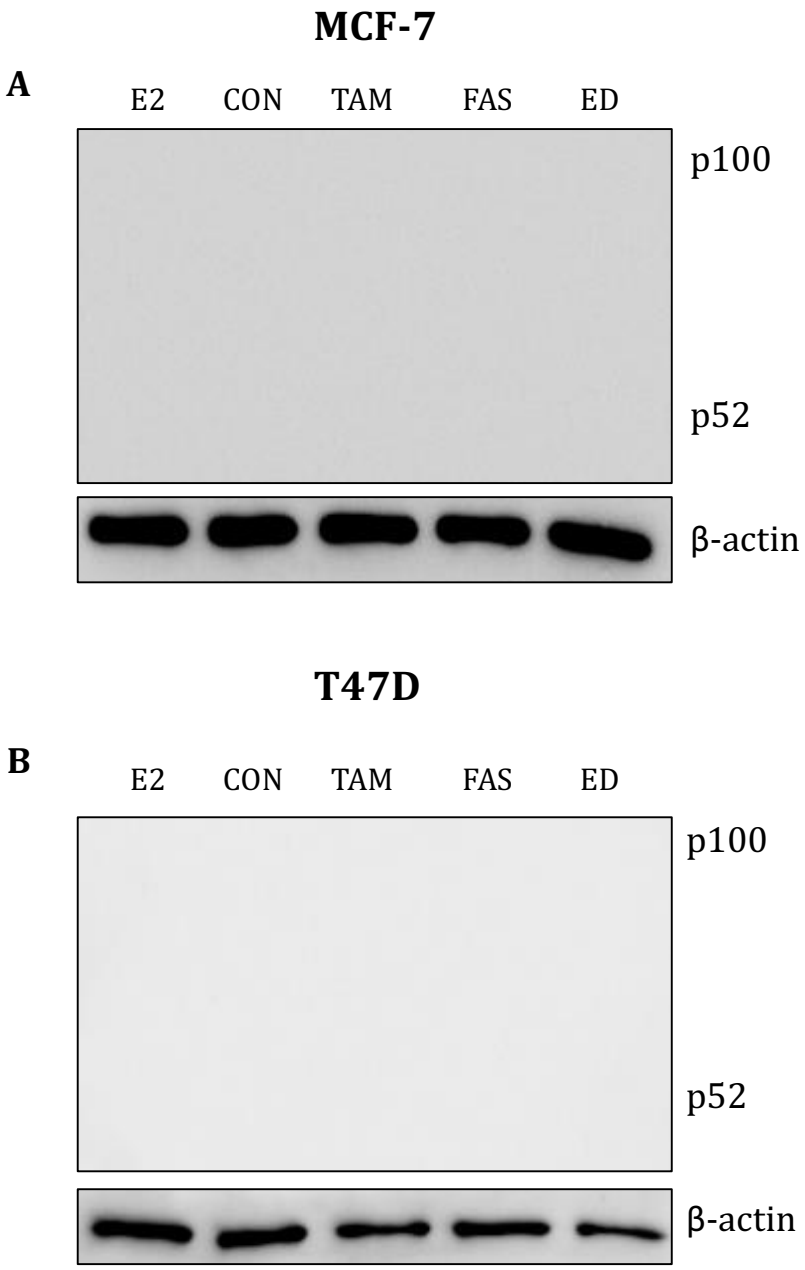

Figure 85 Representative Western blot images from three independent experiments showing p52/NFKB2 and p100 protein expression and β-actin loading control in MCF-7 (A) and T47D (B) cells treated with oestradiol (E2; 10-9 M), untreated control (CON), tamoxifen (TAM; 10-7 M), fulvestrant (FAS; 10-7 M) and oestrogen deprivation (ED) for 10 days.

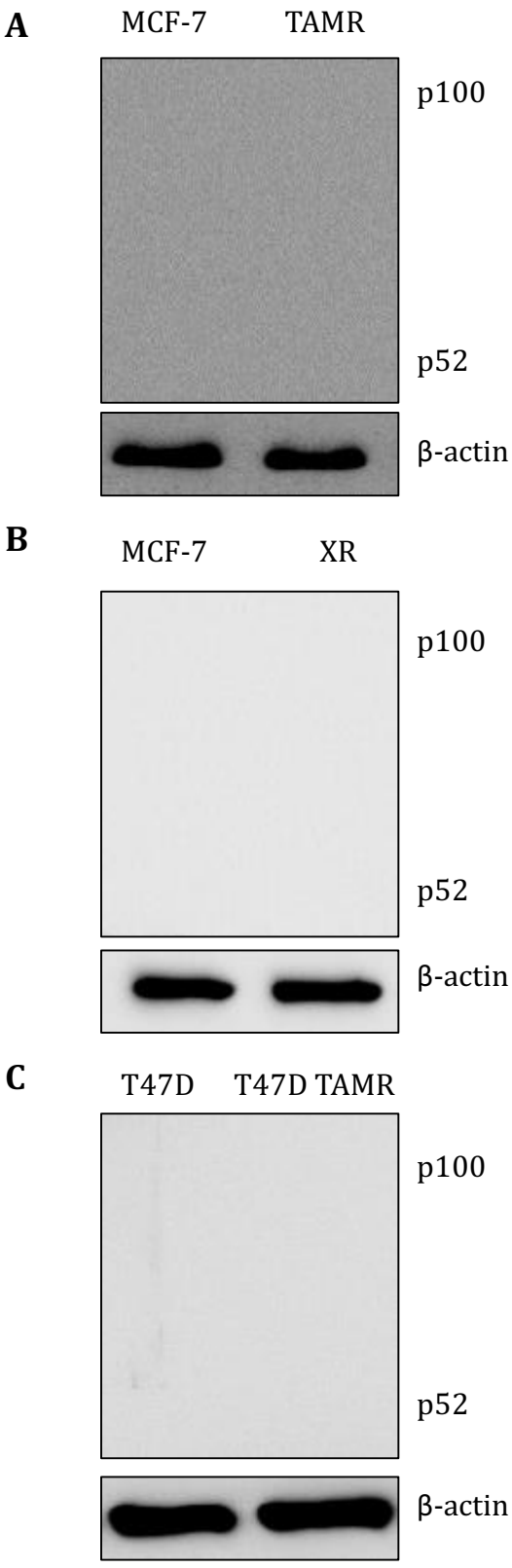

Figure 86 Representative Western blot mages from three independent experiments showing p52/NFKB2 and p100 protein expression and β-actin loading control in tamoxifen resistant (TAMR) (A) and oestrogen deprived-resistant (XR) (B) MCF-7 cells versus wild type MCF-7 cells and T47D TAMR cells (C) versus wild type T47D cells.

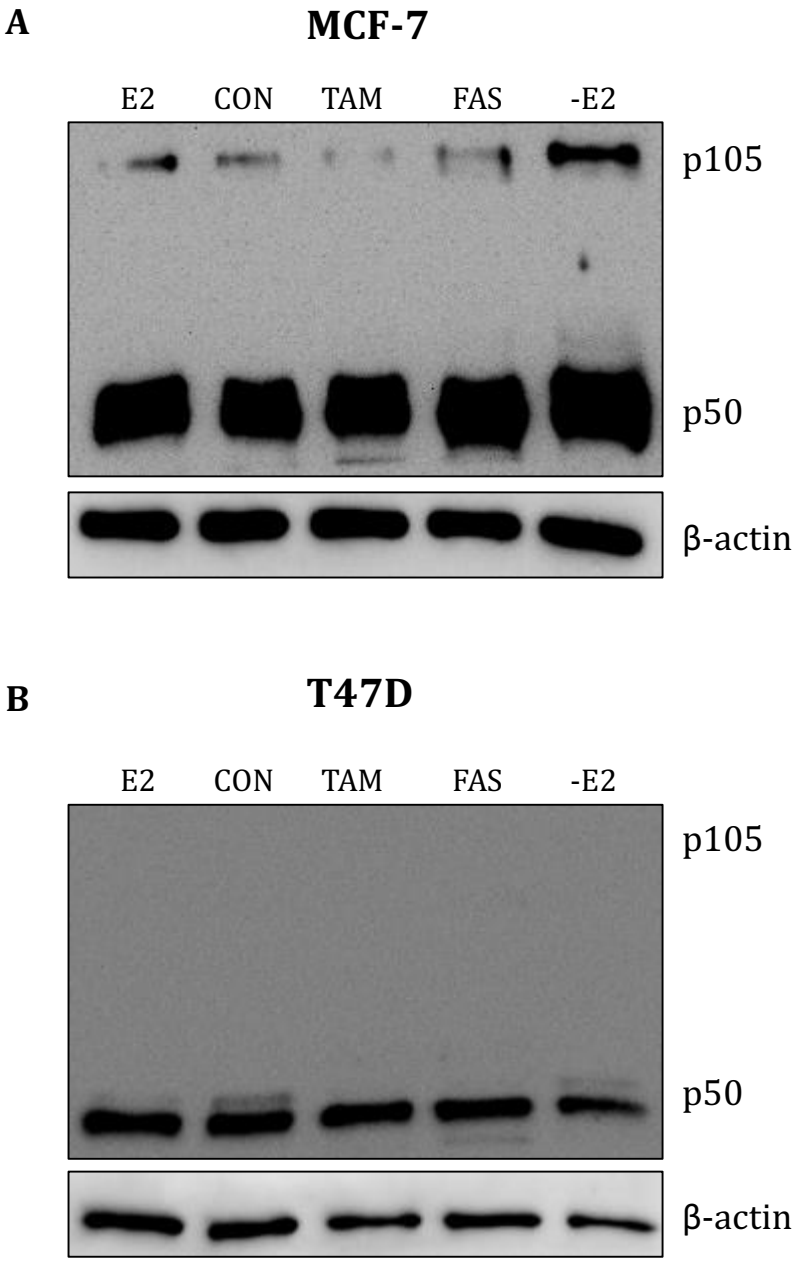

Figure 87 Representative Western blot images from three independent experiments showing p50/NFKB1and p105 protein expression and β-actin loading control in MCF-7 (A) and T47D (B) cells treated with oestradiol (E2; 10-9 M), untreated control (CON), tamoxifen (TAM; 10-7 M), fulvestrant (FAS; 10-7 M) and oestrogen deprivation (ED) for 10 days.

In the endocrine resistant cell models, similar p50/NFKB1 protein expression was observed in the TAMR and MCF-7 control cells (Figure 88A). Additionally, p105 was equally expressed in the TAMR and control cells; however, p50/NFKB1 expression was marginally greater than p105 in both the TAMR and control cells. Interestingly, p105 and p50/NFKB1 expression was up regulated in the XR cell line versus MCF-7 control cells, and both proteins were equally expressed in the resistant and control cells (Figure 88B). Likewise, p105 and p50/NFKB1 expression was up regulated in T47D TAMR cells compared to T47D control cells (Figure 88C). Additionally, greater expression of p50/NFKB1 than p105 was observed in the control and resistant cells, with minimal p105 detected in wild type control cells.

Together, p50/NFKB1 is expressed during antihormone response in MCF-7 and T47D cells and is maintained in cell models of acquired endocrine resistance (TAMR, XR and T47D TAMR), which is in parallel to BCL3 expression (previously shown in Chapter 4, Figure 48 and Figure 57 of the present Chapter), with the exception of T47D TAMR cells.

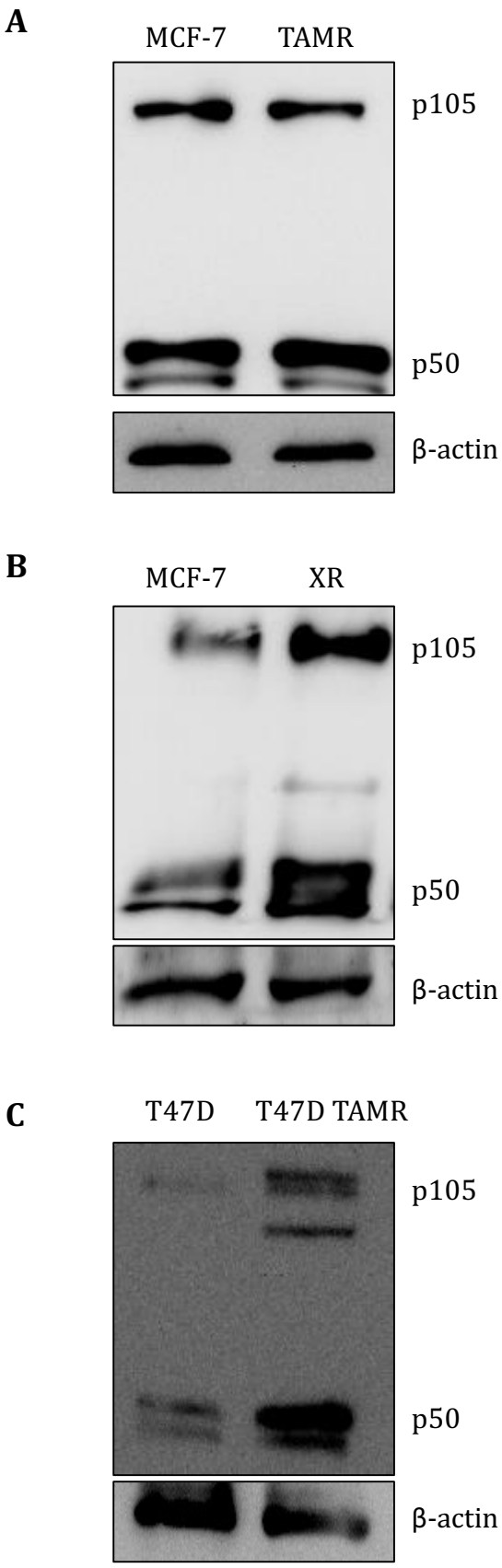

Figure 88 Representative Western blot mages from three independent experiments showing p50/NFKB1 and p105 protein expression and β-actin loading control in tamoxifen resistant (TAMR) (A) and oestrogen deprived-resistant (XR) (B) MCF-7 cells versus MCF-7 parental cells and TAMR T47D cells (C) versus T47D parental cells.

5.3.8.4 Cellular localisation of BCL3 during antihormone-response and -resistance

As previously described, BCL3 is a predominantly nuclear protein and is a co-activator of otherwise inactive p50/NFKB1 homodimers, and subsequently promotes NF-κB-mediated transcription of genes involved in cell survival and proliferation. Thus, to be co-activated by BCL3 and consequently bind to κB sites on target DNA, p50/NFKB1 must be located in the nucleus. Therefore, cellular localisation studies, via immunofluorescence, were next performed to determine whether BCL3 and p50/NFKB1 are co-located in the nucleus, thus suggesting active p50/NFKB1-mediated gene transcription.

Immunofluorescence staining revealed very little, if any, BCL3 in untreated control and 7 day E2-treated MCF-7 cells with a marked increase in expression following tamoxifen, fulvestrant and oestrogen deprivation treatments (Figure 89). This is in agreement with the Western blotting data, which showed antihormone-induced BCL3 expression in the MCF-7 cells (Chapter 4, Figure 48). Immunofluorescence staining revealed relatively equal p50/NFKB1 expression in the control, E2- and antihormone-treated cells (Figure 89), which is again in parallel with the Western blotting data (Figure 87A). BCL3 was located in the nucleus of fulvestrant- and oestrogen deprivation-treated cells, whereas p50/NFKB1 was predominantly located in the cytoplasm. Interestingly, BCL3 and p50/NFKB1 were similarly expressed in the cytoplasm and nucleus of tamoxifen-treated MCF-7 cells.

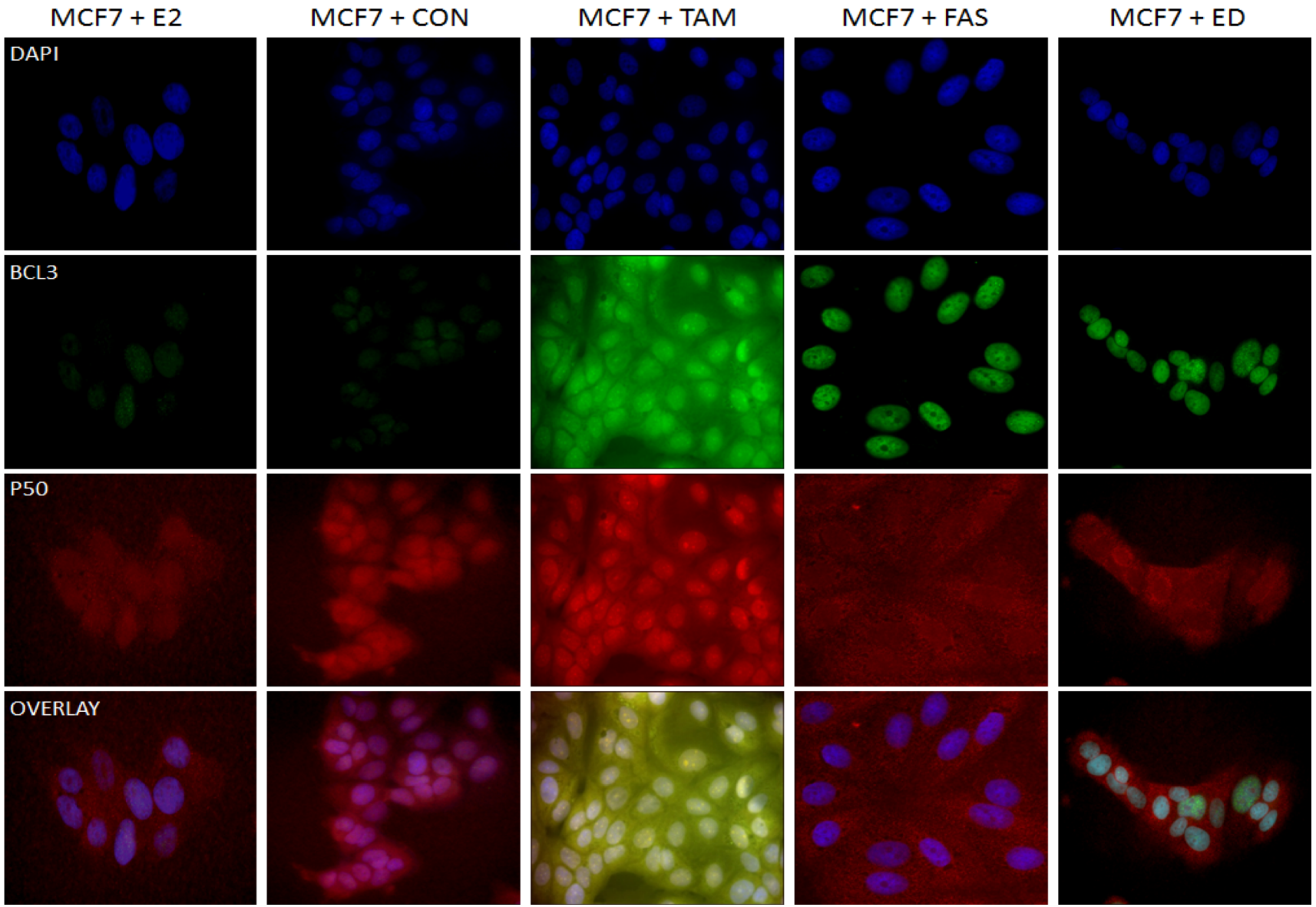

Figure 89 Immunofluorescence images of MCF-7 cells treated with oestradiol (E2; 10-9 M), untreated control (CON), tamoxifen (TAM; 10-7 M), fulvestrant (FAS; 10-7 M) and oestrogen deprivation (ED) for 7 days. Cells were stained for primary antibodies: BCL3 (green) and p50/NFKB1 (red), followed by staining with appropriate Alexa-fluor 488/594-conjugated secondary antibodies and counterstained with the nuclear dye DAPI (blue). Magnification: x63.

In the T47D cell line, immunofluorescence studies demonstrated very low, if any, BCL3 expression in the control and E2-treated cells, with a marked up regulation of expression in the antihormone-treated cells (Figure 90). This expression profile mirrored the Western blotting data, which also showed antihormone-induced BCL3 expression in T47D cells (Chapter 4, Figure 48). Again, in agreement with the Western blot data (Figure 87B), immunofluorescence studies revealed relatively consistent p50/NFKB1 expression in control, E2- and antihormone-treated T47D cells (Figure 90). BCL3 was predominantly located in the nucleus of antihormone-treated T47D cells, with some cytoplasmic BCL3 observed in tamoxifen-treated cells; however, in contrast to MCF-7 cells, some BCL3 was also located in the cytoplasm of fulvestrant- and oestrogen deprivation-treated T47D cells, with greater cytoplasmic staining apparent in the latter. p50/NFKB1 was predominantly expressed in the nucleus of untreated control T47D cells, with both nuclear and cytoplasmic staining observed in the E2- and antihormone-treated cells.

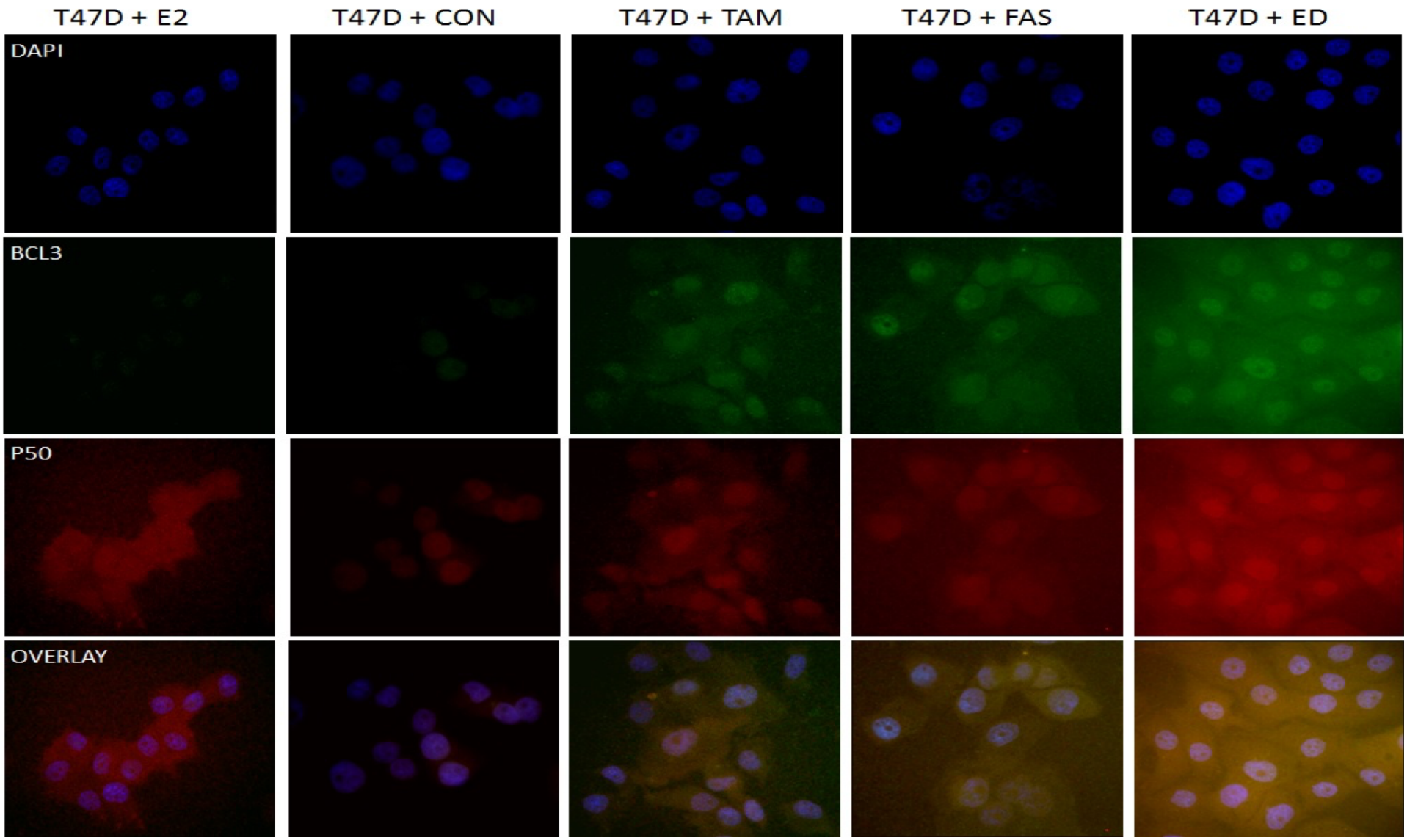

Figure 90 Immunofluorescence images of T47D cells treated with oestradiol (E2; 10-9 M), untreated control (CON), tamoxifen (TAM; 10-7 M), fulvestrant (FAS; 10-7 M) and oestrogen deprivation (ED) for 7 days. Cells were stained for primary antibodies: BCL3 (green) and p50/NFKB1 (red), followed by staining with appropriate Alexa-fluor 488/594- conjugated secondary antibodies and counterstained with the nuclear dye DAPI (blue). Magnification: x63.

In the (short-term) endocrine resistant cell models, immunofluorescence staining identified BCL3 and p50/NFKB1 expression in TAMR, XR and T47D TAMR (Figure 91). This is in agreement with the Western blotting data, which also showed expression of both proteins in the three cell lines, with the exception of T47D TAMR cells in which BCL3 protein expression could not be identified (Figure 57 and Figure 88). Interestingly, in the TAMR and XR cell lines, both BCL3 and p50/NFKB1 were predominantly located together in the nucleus, whereas both proteins were primarily located in the cytoplasm of T47D TAMR cells (Figure 91).

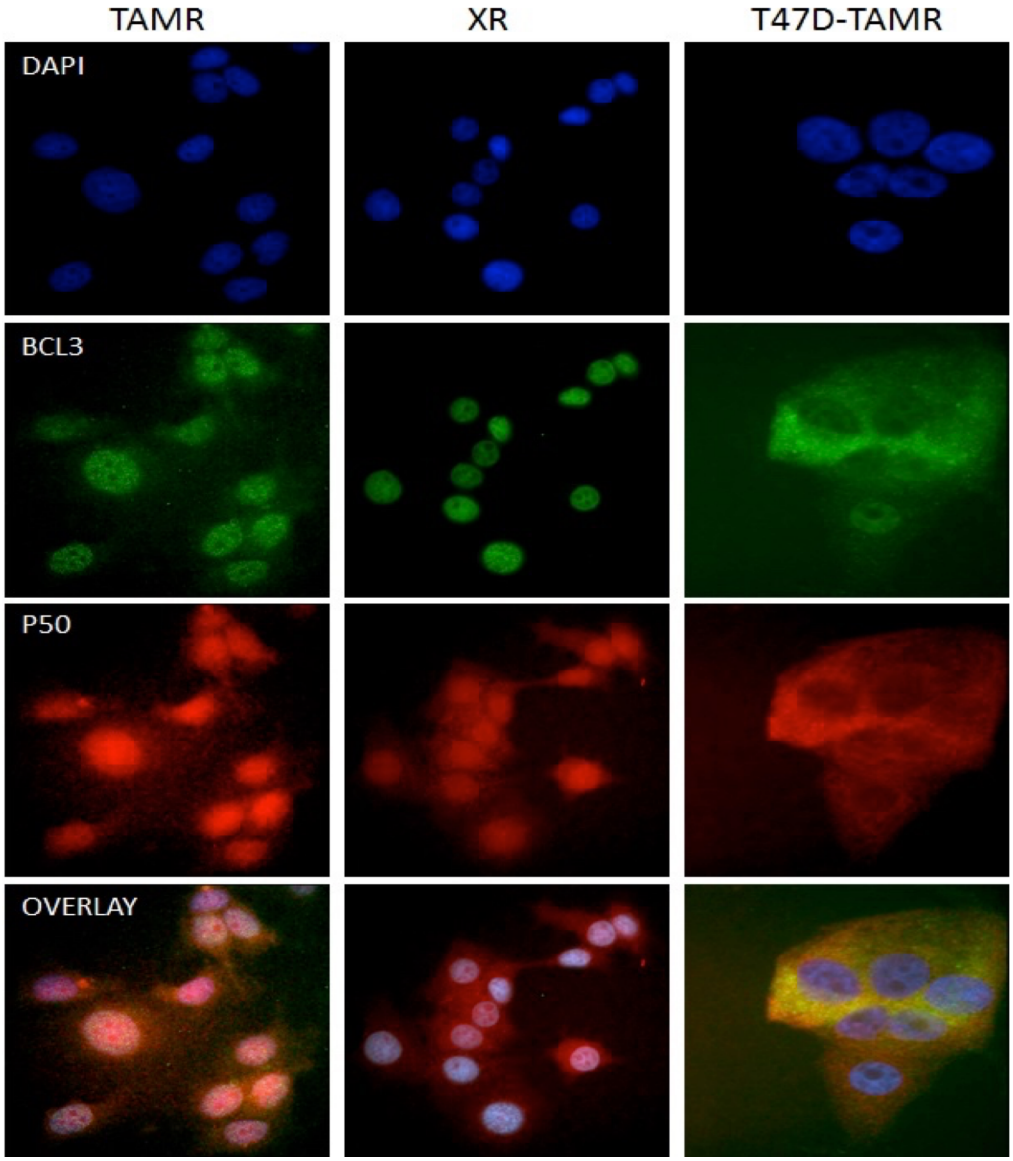

Figure 91 Immunofluorescence images of tamoxifen-resistant MCF-7 (TAMR), oestrogen deprivation-resistant MCF-7 (XR) and T47D TAMR cells. Cells were stained for primary antibodies: BCL3 (green) and P50/NFKB1 (red), followed by staining with appropriate Alexa-fluor 488/594-conjugated secondary antibodies and counterstained with the nuclear dye DAPI (blue). Magnification: x63.

Together, the immunofluorescence studies revealed co-expression of BCL3 and p50/NFKB1 in the cytoplasm and nucleus of antihormone-treated T47D cells and tamoxifen-treated MCF-7 cells, with contrasting cellular locations observed in the falsodex- and oestrogen deprivation-treated MCF-7 cells (BCL3 was located in the nucleus and p50/NFKB1 located in the cytoplasm). Interestingly, in the (short-term) antihormone-resistant cell lines, BCL3 and p50/NFKB1 were co-expressed either in the nucleus (TAMR and XR) or cytoplasm (T47D TAMR).

5.3.8.5 Immunoprecipitation

To determine whether BCL3 and p50/NFKB1 are complexed together when they are co-located in the nucleus, cytoplasm or both, with particular interest on the co-expression and binding of both proteins in the nucleus to support the hypothesis that BCL3 coactivates p50/NFKB1 to promote NF-κB-mediated gene transcription, immunoprecipitation experiments were next performed during antihormone-response and in resistance.

Since BCL3 is expressed at low levels in untreated and E2-treated MCF-7 and T47D cells (as demonstrated by the Western blots shown in Chapter 4, Figure 48), 10 day antihormone-treated MCF-7 and T47D cells alongside untreated control and E2 treatment were immunoprecipitated with p50/NFKB1 antibody and probed by Western blotting for BCL3. As illustrated in Figure 92, no association was observed between the two proteins in MCF-7 and T47D cells, irrespective of treatment. Following immunoprecipitation, p50/NFKB1 levels remained unchanged suggesting equivalent protein loading on the gel, with the exception of untreated control MCF-7 cells, in which the protein loading was likely to be less.

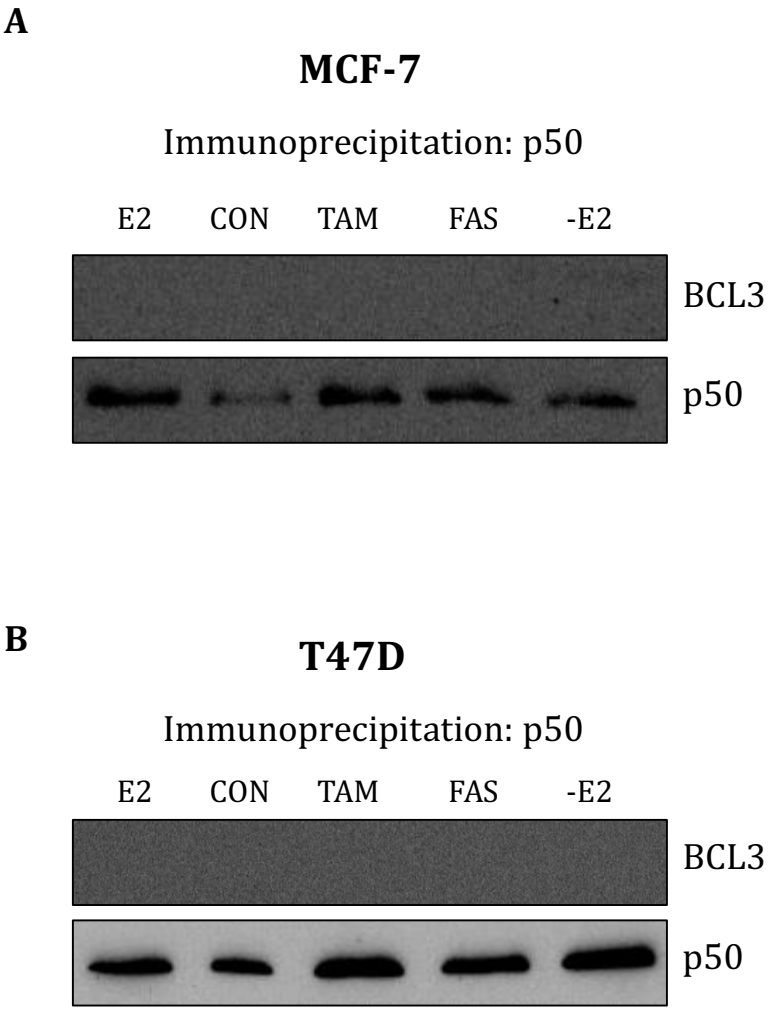

Figure 92 Co-immunoprecipitation of BCL3 with p50/NFKB1 in antihormone-treated MCF-7 (A) and T47D (B) cells. MCF-7 and T47D cells were treated with oestradiol (E2; 10-9 M), untreated control (CON), tamoxifen (TAM; 10-7 M), fulvestrant (FAS; 10-7 M) and oestrogen deprivation (ED) for 7 days. Following cell lysis, protein expression was assessed by Western blot analysis (n=1) for BCL3 and p50/NFKB1 following p50/NFKB1 immunoprecipitation.

Similarly, endocrine resistant cell models (short-term TAMR, XR and T47D TAMR) and wild type parental cells were immunoprecipitated with p50/NFKB1 antibody and probed by Western blotting for BCL3. In contrast to the antihormone-responsive cells, a strong direct physical association was apparent between BCL3 and p50/NFKB1 in the endocrine resistant (TAMR, XR and T47D TAMR) cells compared to a very weak association in the parental cells (Figure 93). p50/NFKB1 expression remained unchanged indicative of equivalent protein loading on the gel. Since the p50/NFKB1 antibody also binds to and recognises the p105 precursor protein (as illustrated in Figure 88), the endocrine resistant and respective control cells were immunoprecipitated with BCL3 and probed for p50/NFKB1 to determine whether the association was indeed between BCL3-p50 and/or BCL3-p105. As shown in Figure 93A and Figure 93B, Western analysis of TAMR and XR cells immunoprecipitated with BCL3 antibody and probed for p50 revealed strong expression of p50, thus indicative of a strong association between BCL3 and p50. However, p105 expression was not detected in BCL3-immunoprecipitated TAMR and XR cells, suggesting no presence of BCL3-p105 complexes. BCL3 immunoprecipitation in T47D TAMR cells was inconclusive.

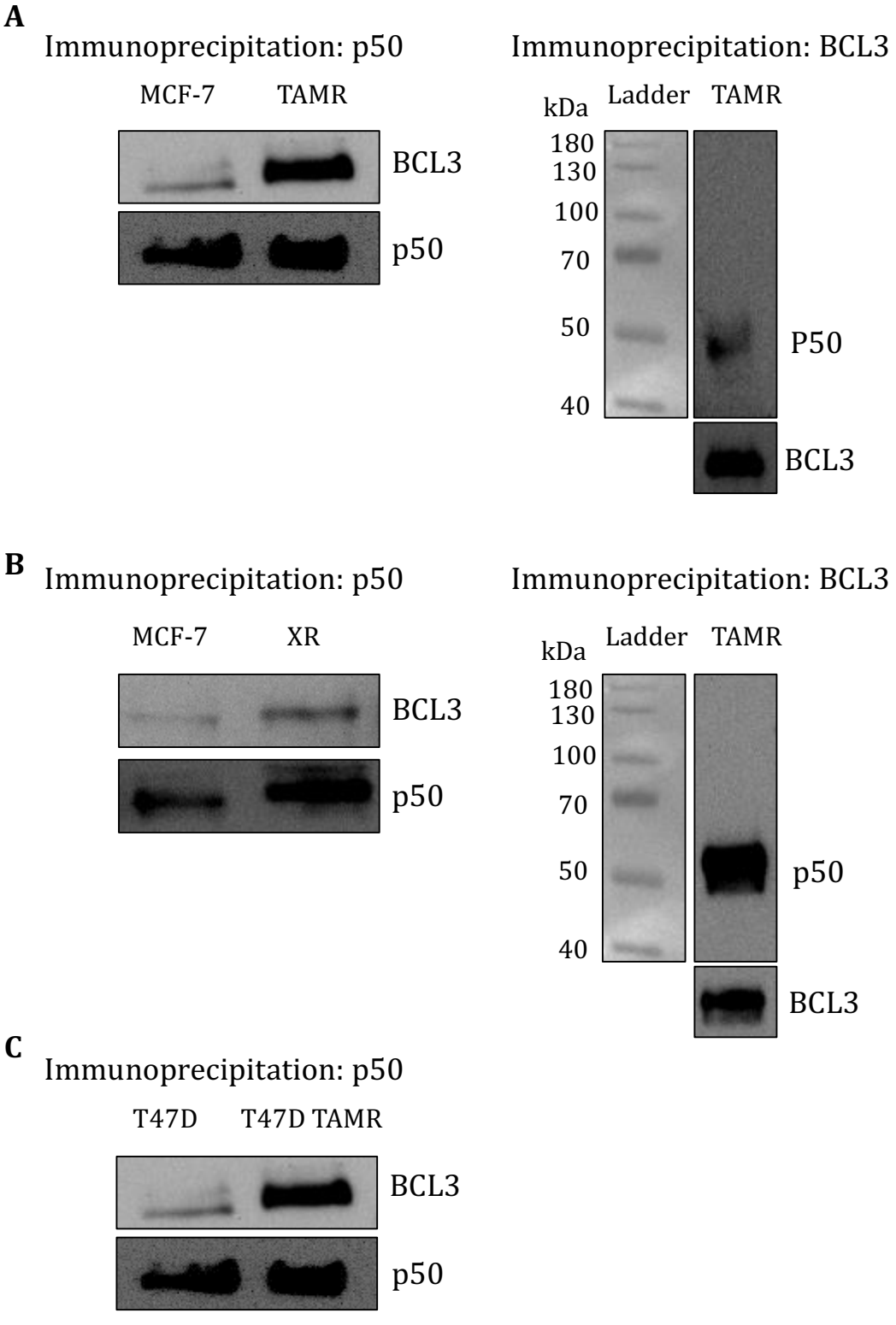

Figure 93 Co-immunoprecipitation of BCL3 with p50/NFKB1 in tamoxifen-resistant MCF-7 (TAMR) (A), oestrogen deprivation-resistant MCF-7 (XR) (B) and T47D TAMR (C) cells versus wild type control cells. Following cell lysis, protein expression was assessed by Western blot analysis (n=1) for BCL3 and p50/NFKB1 following p50/NFKB1 and/or BCL3 immunoprecipitation.

5.3.8.6 Effect of BCL3 knockdown on p50/NFKB1 expression

Although BCL3 is predominantly a nuclear protein, some cytoplasmic expression was detected by immunofluorescence during antihormone-response and in the T47D-TAMR cells, with less detected in the TAMR and XR cells (Figure 89-Figure 91). A cytoplasmic form of BCL3 has previously been detected in 293T (human embryonic kidney) cells[421]. This study reported that cytoplasmic BCL3 promotes release of p50 from the p50-p105 cytoplasmic pool and subsequently translocates the homodimer into the nucleus without effect on the proteolytic processing of p105 to p50. We were interested to investigate whether BCL3 is involved in the proteolytic processing of p105 to p50 in our cells.

To determine whether BCL3 regulates p50/NFKB1 expression in resistance, Western analysis was performed on TAMR cells incubated with control or BCL3 siRNA. As illustrated in Figure 94, BCL3 knockdown in TAMR cells results in a decrease in p50 expression but up regulates p105 expression compared to control.

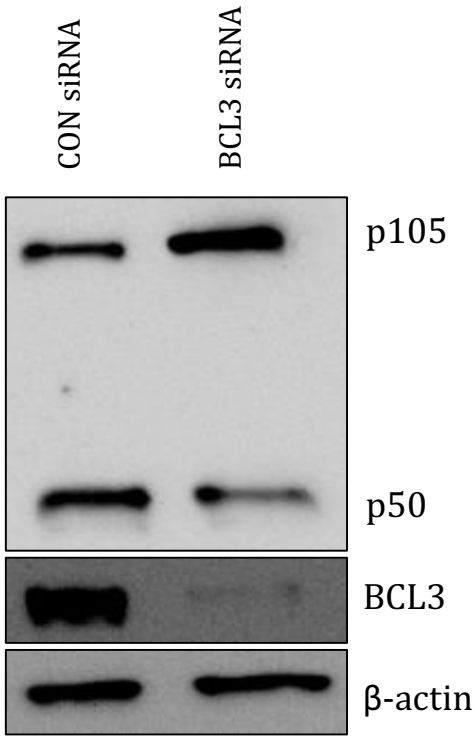

Figure 94 Representative Western blot mages from three independent experiments showing p50/NFKB1 and p105, BCL3 and β-actin loading control protein expression in tamoxifen resistant cells incubated for 4 days with unscrambled control (CON) or BCL3 siRNA.

5.4 Discussion

Extensive microarray gene profiling studies performed in Chapters 3 and 4 identified BCL3 as the most robust antihormone-induced gene in four ER+ breast cancer cell lines, encompassing HER2+ and HER2- disease, with increased expression maintained through to the acquisition of resistance. Therefore, in this Chapter the role of BCL3 was further examined to explore the hypothesis that BCL3 is a pro-survival gene, induced early during response and subsequently allows a cohort of breast cancer cells to escape antihormone challenge, resulting in a limited efficacy of these agents and ultimately the development of resistant growth.

Initially, microarray gene expression data examining BCL3 expression in (short-term) antihormone-resistant TAMR and XR cells (Chapter 3) was verified at the mRNA and protein levels and confirmed an increase in BCL3 expression during resistance versus wild type MCF-7 cells. In agreement with these findings, Pratt et al. previously demonstrated increased BCL3 expression in ER+, E2-independent MCF-7 cells compared with the parental cell line[363]. To consider the heterogeneity that exists in breast cancer, BCL3 expression was also examined in a model of (short-term) tamoxifen resistance derived from T47D cells. Similarly, BCL3 mRNA expression was increased in these resistant cells compared to wild type T47D cells. However, BCL3 protein expression could not be detected. It is possible that BCL3 mRNA was not translated into protein in the T47D-TAMR cells or that the protein was rapidly degraded. Furthermore, towards the end of this project, microarray gene expression profiling was completed for a panel of long-term (3 year) antihormone-resistant cell models. Thus, to determine whether increased expression of BCL3 is maintained during antihormone resistance, its expression was examined and verified by RT-PCR in these cell models. Indeed, increased mRNA expression of BCL3 was demonstrated in long term TAMR cells derived from MCF-7 and MDA-MB-361 cells, TAMR and XR cells derived from T47D cells, and XR cells derived from BT474 cells versus wild type control. This suggests that increased BCL3 expression is maintained into long term resistance. Due to these models becoming available for characterisation and further study at the end of this

project, additional examination of BCL3 expression and function in these resistant models could not be performed.

Following the identification of up regulated BCL3 expression in antihormone resistance (as well as during response as demonstrated in the previous Chapters), subsequent studies aimed to establish whether BCL3 expression correlated with, and ultimately contributed to, the limited efficacy of antihormones and the consequent development of resistance. Transient BCL3 knockdown studies using siRNA were conducted to determine the importance of BCL3 expression, particularly its potential role in promoting cell survival and proliferation, during antihormone-response and -resistance. Since BCL3 is antihormone-induced in MCF-7 and T47D cells, with very little expression present in untreated cells; fulvestrant combined with siRNA incubation was required to increase BCL3 expression and to determine what effect subsequent BCL3 knockdown had on cell growth and survival and whether such knockdown enhanced the growth-inhibitory actions of fulvestrant. Optimisation studies were first performed to determine the optimum siRNA plus fulvestrant incubation conditions for the best knockdown. Interestingly, a fulvestrant time course study from day 1 to day 10 in MCF-7 and T47D cells revealed the greatest BCL3 mRNA and protein expression as early as day 1 and day 2 post-fulvestrant treatment. BCL3 expression remained relatively consistent during the 10 day treatment of T47D cells. However, BCL3 protein expression decreased at day 4 and day 5 fulvestrant treatment in the MCF-7 cells, which was mirrored by a marked decrease in actin expression at day 4, suggesting unequal protein loading. Similarly, at the protein level it is likely that a loading error occurred at day 5, since at the mRNA level BCL3 was expressed; yet at the protein level very little BCL3 was apparent. BCL3 protein expression increased following day 7 and day 10 treatment, together with an increase in actin expression compared to day 4. Two day fulvestrant treatment was decided as the optimal treatment time for sufficient BCL3 up regulation necessary for subsequent knockdown.

Subsequently, a time course study examining the optimal siRNA incubation periods was performed. For the greatest transfection efficiency, siRNA is added to rapidly dividing cells. However, since fulvestrant treatment inhibits cell growth, siRNA was

first added and allowed to be incorporated into the cells prior to fulvestrant treatment. A time point study comprising day 2 to day 4 siRNA incubation prior to 48 hours fulvestrant treatment was performed to determine the optimal siRNA incubation period. Indeed, day 2, 3 and 4 siRNA incubation followed by 2 day fulvestrant treatment induced similar levels of BCL3 protein knockdown. Thus, to minimise the expense of re-administrating siRNA, which is necessary for incubations longer than a total of 4 days, 2 day siRNA followed by 2 day fulvestrant treatment was chosen as the optimal conditions for BCL3 knockdown and was employed for subsequent studies. With regard to the antihormone-resistant cell models, BCL3 is constitutively expressed, thus targeted BCL3 knockdown was induced by 4 day incubation with the siRNA. BCL3 knockdown was confirmed at the mRNA and protein level by RT-PCR and Western blotting, respectively, in the TAMR and XR cell models. However, BCL3 knockdown was only observed at the mRNA level in the T47D TAMR cells, with BCL3 protein expression not detected (as previously discussed above).

Cell survival studies were performed to determine whether BCL3 plays a pro-survival role, thus supporting the hypothesis that BCL3 is an antihormone-induced pro-survival gene. Baseline antihormone-induced apoptosis was first examined during response to 7 day treatment. The cell lines used throughout this project are adherent and the dead/apoptotic cells float in the medium. Thus, optimisation studies were initially performed to determine whether removing the medium (and the floating dead cells) at day 4 during 7 day treatment and replacing with fresh antihormone-treated medium had any effect on the number of apoptotic cells. Indeed, as expected, the removal of the cell medium at day 4 resulted in a decrease in the percentage of apoptotic cells compared to adding fresh medium without removing the old medium. Therefore, for subsequent studies the medium was not removed and fresh medium was added on top. Seven day antihormone treatment induced very little apoptosis in MCF-7 and T47D cells. This is in agreement with the initial rationale that antihormones exert significant anti-proliferative effects but promote only modest cell kill. Indeed, Gee et al. previously demonstrated that tamoxifen promotes significant growth inhibition but minimal apoptosis in MCF-7 cells[216].

To determine whether BCL3 is indeed a pro-survival gene, BCL3 knockdown studies were performed and the impact on cell survival/apoptosis was assessed. BCL3 had no effect on the survival of MCF-7 and T47D cells during antihormone response. In contrast to these findings, a pro-survival effect of BCL3 in breast cancer has been reported. Indeed, Choi et al. have demonstrated a novel link between BCL3 and the anti-apoptotic protein CtBP1 in several breast cancer cell lines, including MCF-7 cells and also in human clinical breast cancer samples[368]. CtBP1 promotes cell survival by transcriptionally repressing pro-apoptotic genes. In response to apoptotic stimuli, CtBP1 is degraded by ubiquitination which results in the derepression of pro-apoptotic genes to allow apoptosis to proceed[375]. BCL3 has been shown to increase the stability of CtbP1, thus preventing its degradation by ubiquitination. Consequently, CtBP1-mediated repression of pro-apoptotic genes is sustained and cells become resistant to apoptotic stimuli, subsequently promoting cell survival[368]. Together, this evidence suggests that stabilisation of CtBP1 by BCL3 may provide a potential molecular mechanism underlying the pro-survival role of BCL3. However, although this study strongly indicates a pro-survival role for BCL3, such an effect was only indirectly examined by measurement of the expression of two CtBP1-target pro-apoptotic genes[368]. Additional studies, including apoptosis assays would further confirm a pro-survival role.

Moreover, an alternative proposed mechanism by which BCL3 promotes cell survival is via inhibition of the expression of the tumour suppressor gene, p53[367]. In MCF-7 cells, UV-induced DNA damage has been shown to increase BCL3 expression. Additionally, constitutive BCL3 expression in MCF-7 cells has been shown to inhibit p53 expression and consequently prevent the induction of pro-apoptotic p53-target genes to prevent the activation of DNA-damage-induced cell death. The dominant proposed mechanism in this regulatory circuit is the ability of BCL3 to induce up regulation of the p53 inhibitor Hdm2. However, it is possible that BCL3-mediated p53 suppression and consequent cell survival was not observed in our study since, in addition to inducing BCL3 expression, fulvestrant also potentiates p53 activity[422]. Thus, it is plausible that fulvestrant-induced p53 activity outweighs BCL3 mediated p53 inhibition.

Additionally as previously discussed in Chapter 4, p53 is mutated on one allele of the gene in T47D cells, thus such BCL3-mediated regulation of this gene in the T47D cell line would not be observed.

Disappointingly, BCL3 had no effect on the survival of TAMR and XR cells. However, cell survival was assessed by an Annexin V/PI apoptosis assay on TAMR and XR cells following 4 day incubation with BCL3 siRNA. Thus, it is possible that such transient BCL3 knockdown is insufficient to promote significant apoptosis, which would perhaps be apparent with stable BCL3 knockdown. Thus with the elimination of a pro-survival role, subsequent studies aimed to further elucidate the role of BCL3 during antihormone response and resistance. The effect of BCL3 on cell growth was next examined.

The targeted down regulation of BCL3 correlated with a substantial decrease in the cell growth of TAMR and to a lesser degree XR cells, but was without effect on T47D TAMR cells. However, the decrease in cell growth observed in the TAMR and XR cells following BCL3 knockdown did not reach significance. Undoubtedly, additional experimental repeats are required to increase the reliability of the data. These findings suggests that BCL3 may play a role in promoting TAMR and XR cell growth with no such effect apparent in the T47D TAMR cells. However, BCL3 knockdown in the T47D TAMR cells could not be verified at the protein level. Therefore, it is possible that such knockdown was not translated to the protein level, thus explaining why no effect on cell growth was observed. Alternatively, as previously discussed in Chapter 4, more than 150 proteins are differentially expressed between the MCF-7 and T47D cell lines, of particular significance is the p53 tumour suppressor gene[409,411]. As discussed above, in contrast to the MCF-7 cell line, p53 is mutated on one allele of the gene in T47D cells. Thus, it is possible that BCL3-induced growth of MCF-7-derived resistant cell models is mediated via negative regulation of the p53 gene; a mechanism not observed in the p53 mutant T47D cells. To our knowledge, these are the first studies to date that demonstrate a role for BCL3 in antihormone-resistant breast cancer cell growth.

Interestingly, BCL3 knockdown had no effect on the cell growth of MCF-7 cells, but a very small, yet non-significant, effect on the growth of T47D cells during

antihormone response. Similarly, BCL3 has been previously shown to have no effect on the growth of HER2+ mammary tumour cells *in vivo*[362]. The magnitude of BCL3 knockdown was greater in the TAMR and XR cells compared to the antihormone-responsive MCF-7 and T47D cells, possibly due to fulvestrant inhibiting MCF-7 and T47D cell proliferation, thus leading to a reduced transfection efficiency of the siRNA. Together, these studies suggest that during antihormone resistance BCL3 may play a role in promoting cell growth with no such effect apparent early during response. In contrast to these studies, Pratt et al. have previously shown that BCL3 augments MCF-7 tumour cell growth[363]. Ovariectomised mice injected with MCF-7 cells ectopically expressing BCL3 displayed a markedly higher tumour growth rate compared to control. However, there are significant experimental differences between Pratt et al. and the current study, likely contributing to the contrasting results. Indeed, in Pratt et al.'s study, MCF-7 cells were transfected with BCL3 (MCF-7-BCL3) and injected into mice whereas in the current study MCF-7 cells were treated with the growth inhibitor fulvestrant to induce BCL3 expression in two dimension. Pratt et al.'s study was performed *in vivo* and therefore likely influenced by the stroma and tumour microenvironment, whereas the present study was conducted *in vitro* thus lacking the complex inter-relationships that exist between cells *in vivo.* Another opposing variable is the exposure period of MCF-7 cells to increased BCL3 expression. A stable BCL3 expressing system was used *in vivo* and the MCF-7-BCL3 cells were allowed to form tumours over a period of 4-6 weeks, whereas in the present study MCF-7 cells were exposed to a transient increase in BCL3 expression for 2 days. It is possible that long term BCL3 expression contributes to the reorganisation of the cellular networks to promote cell growth, which would not be possible following short term BCL3 exposure. Thus, it is conceivable that longer BCL3 expression in MCF-7 cells, either via fulvestrant treatment or more preferably via transfection, would result in enhanced cell growth.

The growth of our TAMR cell model has previously been reported to be regulated via EGFR/HER2 driven MAPK and AKT signalling pathways[185]. BCL3 knockdown in this cell line had no effect on these key signalling proteins confirming that the siRNA used was specific to BCL3. Additionally, these findings suggest that

BCL3-mediated cell growth apparent in the resistant cell model does not exploit the dominant MAPK and AKT growth signalling pathways.

Cell cycle studies were next performed to investigate whether BCL3 induces cell proliferation via dysregulation of the cell cycle. Baseline studies were first performed to examine the distribution of MCF-7 and T47D cells within each phase of the cell cycle following 7 day antihormone treatment. Tamoxifen has been widely reported to induce significant G1 arrest of MCF-7 cells with concurrent decreases of cells in S and G2/M phases compared to untreated control[311,420]. However, such tamoxifen-induced G1 arrest of MCF-7 cells was not apparent following 7 day treatment. Similarly, although tamoxifen induced a small increase in the percentage of T47D cells in G1 compared to control, this effect was not significant. However, there are substantial differences between the experimental design of this study and those of Osborne et al. and Sutherland et al[311,420]. Of particular significance is the shorter duration of tamoxifen treatment and increased drug concentration. Indeed, Osborne et al. demonstrated a marked accumulation of MCF-7 cells in G1 with a reduction of cells from S and G2/M phases following 3 day tamoxifen (10^{-6} M) treatment[311] Similarly, Sutherland et al. demonstrated a marked increase in the percentage of MCF-7 cells arrested in G1 together with a decrease in S phase from day 1 to day 3 tamoxifen (10^{-5} M)[420]. Thus, it is possible that 7 day treatment may promote growth inhibition in a density-dependent manner as the monolayer of cells neared confluence. To eliminate this possibility, a time course experiment was subsequently conducted including day 1 to day 4 antihormone treatment of MCF-7 cells. An increase in G1 arrest, together with a small depletion of cells from S phase and G2/M phase was apparent following day 2 to day 4 tamoxifen (10^{-7} M) treatment. These findings are in agreement with Sutherland et al.'s study, which demonstrated a small increase in G1 arrest, induced by tamoxifen (of equivalent concentration i.e. 10^{-7} M) from day 1 to day 3 treatment, together with a decrease in the percentage of cells in S phase[420]. However, this experiment was only completed once (n=1) and more experimental repeats are necessary to perform statistical analysis, which may prove significant. Additionally, it is highly likely that a higher concentration of

tamoxifen (in line with Osborne et al. and Sutherland et al. studies[311,420]) would enhance G1 arrest.

With regard to fulvestrant and oestrogen deprivation treatment, a similar cell cycle distribution profile to tamoxifen treatment (i.e. increase in G1 arrest with a decrease in S and G2/M phases), although to a lesser degree, was observed following 3 and 4 day treatment in MCF-7 cells compared to untreated control. In agreement with this data, Watts et al. have previously demonstrated an increase in the proportion of fulvestrant-treated MCF-7 cells in G1 arrest mirrored by a decrease of cells in S phase during 24–28 hour treatment compared to untreated control[165]. Following 7 day treatment, fulvestrant and oestrogen deprivation treatments promoted a small increase in G1 arrest of MCF-7 cells, with a small decrease in the percentage of cells in S and G2/M phases compared to control. However, such effects were not significant. In the T47D cell line, 7 day oestrogen deprivation treatment induced significant depletion of cells from G1 together with a significant accumulation of cells in S phase, suggesting enhanced DNA replication, compared to control. Interestingly, the percentage of cells in S phase, irrespective of treatment, decreased from day 1 to day 4 possibly due to depletion of nutrients from the medium in addition to density-dependent growth inhibition as the cells became confluent.

To determine whether BCL3 dysregulates the cell cycle to promote cycle progression and growth, BCL3 knockdown studies were performed and the impact on the cell cycle was assessed. In agreement with the cell growth data, BCL3 had no effect on the cell cycle distribution of fulvestrant-treated MCF-7 and T47D cells during response. However, these studies comprised of a n=2 and n=1, respectively, thus further repeats are necessary to clarify this data and to allow statistical analysis to be performed. In human breast epithelial cells, Westerheide et al. have previously demonstrated that BCL3 stimulates cyclin D1 expression and phosphorylation of the retinoblastoma protein and consequent G1 to S phase progression[361]. However, such events did not promote enhanced cell proliferation, suggesting that despite BCL3 promoting G1 to S transition, it has no effect on the proliferation of human breast epithelial cells. It is possible that additional oncogenic events are required to promote BCL3-mediated cell growth. In

antihormone-responsive breast cancer cells, we have shown that BCL3 down regulation has no effect on the cell cycle and ultimately no effect on cell growth/proliferation. However, such effects were only examined following transient BCL3 knockdown, which may be insufficient to promote significant alterations in the cell cycle. In addition to stable BCL3 gene knockdown, further studies examining the protein expression of cell cycle regulators, such as cyclin D1 and phosphorylation of the retinoblastoma protein, are necessary to support the cell cycle analysis data.

In the antihormone-resistant cell lines (TAMR and XR), BCL3 was shown to promote substantial (although not significant) cell growth. However, such effects were not mediated via dysregulation of the cell cycle. Indeed, incubation of TAMR and XR cells with BCL3 siRNA for 4 days had no effect on the cell cycle distribution. Interestingly, a substantial increase in the proportion of XR cells in S phase, mirrored by a slight increase in G2/M phase and a decrease in G1 phase irrespective of treatment, was observed compared to TAMR cells, suggesting increased DNA replication in the former cell line. The cell cycle of TAMR cells was also examined following 2 and 3 day incubation with BCL3 siRNA. Equally, such transient knockdown had no effect on the cell cycle. Stable BCL3 knockdown is unquestionably required in order to more effectively examine the effects of BCL3 on the cell cycle. Additionally, examination of the cell cycle regulators, as mentioned above, would further support the cell cycle analysis data.

As previously discussed above, BCL3 is a co-activator of the otherwise inactive p50 and p52 homodimers of the NF-κB family, and as a result activates transcription of genes involved in cell proliferation and survival[372]. Thus, the remainder of this Chapter focussed on the potential activation of NF-κB signalling by BCL3 and the transcription of target genes involved in cell growth/survival. Initially, the expression of p50/NFKB1 and p52/NFKB2 were examined in the microarray gene expression data of 10 day antihormone-treated MCF-7 cells and in the resistant TAMR and XR cell models, to determine whether such an association between these proteins and BCL3 is likely. Interestingly, p50/NFKB1 expression was present in E2-treated MCF-7 cells, with similar expression observed following antihormone treatment. In resistance, p50/NFKB1 expression was up regulated in

TAMR and significantly in XR cells compared to wild type control cells. In contrast, absent detection calls were reported for p52/NFKB2 expression during antihormone response in MCF-7 cells and also in the resistant cell models. Subsequent studies verified p50/NFKB1 and p52/NFKB2 expression at the protein level. In agreement with the microarray data, p52/NFKB2 protein expression was not detected in antihormone-responsive or –resistant cell models. However, protein expression of p50/NFKB1 and its precursor p105 (which is also detected by the p50/NFKB1 antibody) were apparent in control-, antihormone- and E2-treated MCF-7 cells and also in the TAMR and XR cell lines. In accordance with the microarray profile, p50/NFKB1 protein expression was unaffected by antihormone treatment. In support of this data, Yde et al. demonstrated consistent protein expression of p50/NFKB1 in untreated MCF-7 cells and those treated for 48 hours with tamoxifen and fulvestrant[358]. The precursor protein, p105, was weakly expressed in E2-, control-, tamoxifen and fulvestrant-treated MCF-7 cells but markedly increased following oestrogen deprivation treatment. To consider the heterogeneity of breast cancer, p50/NFKB1 and p105 protein expression were subsequently examined in T47D cells. In agreement with the MCF-7 cell line, p50/NFKB1 was similarly expressed in untreated control and 10 day E2- and antihormone-treated T47D cells. However, p105 expression was not observed. It is possible that p105 is weakly expressed in T47D cells compared to p50/NFKB1. Thus, with extended development of the Western blot, p105 expression may have been detected. In agreement with these studies, Cogswell et al. have demonstrated protein expression of p50/NFKB1 in nuclear extracts of MCF-7 and T47D cells, but failed to identify p52/NFKB2 expression[360]. Additionally, Yde et al. failed to detect expression of p52/NFKB2 in MCF-7 and TAMR cells[358]. Furthermore, parallel increases in p50/NFKB1 and BCL3 expression have been reported in clinical human breast tumours compared to adjacent normal breast tissue[360].

In the endocrine resistant cell lines, p50/NFKB1 and p105 were equally expressed in the TAMR and MCF-7 control cells, but were markedly increased in the XR cell line versus control. In support of these findings, Zhou et al. have demonstrated equal protein expression of p50/NFKB1 in untreated MCF-7 and tamoxifen-resistant MCF-7 cells, in concert with increased DNA binding and NF-κB

transcriptional activity in the resistant cell line[423]. Furthermore, Pratt et al. have reported increased NF-κB activity, comprised predominantly of p50/NFKB1 homodimers, in parallel with increased BCL3 expression in ER+, E2-independent MCF-7 cells compared with the parental cell line[363]. Similarly, in the T47D TAMR cell line, p50/NFKB1 and p105 were up regulated compared to control. Together, these studies demonstrate that p50/NFKB1 is expressed alongside BCL3 during antihormone-response and –resistance (with the exception of only mRNA and not protein expression of BCL3 in T47D TAMR detected), strongly supporting the hypothesis that BCL3 coactivates p50/NFKB1 homodimers to promote transcription of target genes.

NF-κB signalling has been shown to play a significant role in the growth of antihormone-resistant breast cancer cells. Indeed, Yde et al. demonstrated growth inhibition of tamoxifen-resistant and fulvestrant-resistant MCF-7 cells via abrogation of NF-κB signalling utilising and IκB kinase inhibitor[358]. Further investigation of the tamoxifen-resistant cell line demonstrated that p65 contributes to the resistant phenotype since down regulation of this protein re-sensitised the cells to tamoxifen. However, such cells did not regain complete sensitivity towards tamoxifen, suggesting that additional signalling molecules contribute to resistant cell growth. Since p50/NFKB1 is expressed in antihormone-resistant cells, perhaps this protein plays a role in their growth. Similarly, during antihormone response, IκB kinase inhibition hypersensitised MCF-7 cells to fulvestrant, highlighting a possible avenue for combined therapy including fulvestrant and NF-κB inhibition for hormone responsive breast cancer.

To further support the hypothesis that BCL3 coactivates p50/NFKB1 homodimers during antihormone-response and particularly during resistance, with such events contributing to the growth-regulatory effects of BCL3 observed during resistance, localisation studies were next performed to determine whether both BCL3 and p50/NFKB1 are co-located in the nucleus, thus suggesting activation of NF-κB and transcription of target genes. However, a major limitation of the immunofluorescence studies was the inability to distinguish between p50 and p105 isoforms, since the NFKB1 antibody recognised both. It is strongly likely that nuclear p50/NFKB1 expression represents the p50 isoform, whereas cytoplasmic

expressions represent both isoforms since p105 behaves as an IκB protein and sequesters p50 in an inactive form in the cytoplasm[424].

In agreement with BCL3 being a nuclear protein, immunofluorescence studies revealed that during antihormone response BCL3 was indeed predominantly located in the nucleus of MCF-7 cells. However, in the tamoxifen-treated cells, BCL3 was also located in the cytoplasm. Although BCL3 is predominantly a nuclear protein, an apparent cytoplasmic form has been previously detected in 293T (human embryonic kidney) cells[421]. This study reported that cytoplasmic BCL3 promotes release of p50 from the p50-p105 cytoplasmic pool and subsequently translocates the homodimer into the nucleus. Thus, cytoplasmic expression of BCL3 is likely to be transient since the release of p50 occurs rapidly. A similar mechanism for BCL3 has been reported in COS-1 cells whereby BCL3 promotes release of cytoplasmic p50 homodimers from IκB[425]. Therefore, it is possible that cytoplasmic expression of BCL3 in tamoxifen-treated MCF-7 cells functions to promote dissociation of p50 from p105/IκB in the cytoplasm and promote subsequent nuclear translocation of the homodimer. Accordingly, in parallel with BCL3 expression, immunofluorescence studies revealed both cytoplasmic and nuclear expression of NFKB1 in tamoxifen-treated MCF-7 cells. Moreover, nuclear BCL3 expression in fulvestrant- and oestrogen deprivation-treated MCF-7 cells was mirrored by cytoplasmic NFKB1 expression, with very little, if any expression detected in the nucleus. This supports the concept that cytoplasmic BCL3 promotes nuclear expression of p50/NFKB1.

In line with the Western analysis data, very little, if any, BCL3 was detected by immunofluorescence in the control and E2-treated MCF-7 cells. Interestingly, in these cells, p50/NFKB1 was predominantly located in the nucleus with little expression in the cytoplasm. This is in agreement with the Western blotting data which showed very little p105 expression in control and E2-treated MCF-7 cells. Very little BCL3 is expressed in these cells and therefore unlikely to promote the release of p50 from the p50-p105/IκB cytoplasmic pool. In these cells it is possible that various stimuli, including growth factors, activate IκB kinase which in turn phosphorylates and subsequently degrades IκB, to release p50 homodimers into the nucleus[213]. Additionally, activation of IκB kinases has been shown to

phosphorylate p105 and subsequently promote degradation by the 26S proteasome and release of p50/NFKB1[426,427]. The 20S proteasome has also been reported to constitutively process p105 to p50[427]. It is possible that such mechanisms are regulated by the ER and therefore inhibited by antihormones, thus potentially explaining the cytoplasmic localisation of p50/NFKB1 in the antihormone-treated cells. Additionally, the ER agonist activities exhibited by tamoxifen may explain the presence of some p50/NFKB1 in the nucleus of these cells. However, further studies are undoubtedly required to investigate the possible E2/ER-regulation of IκB kinase activation.

Interestingly, previous studies have reported very little NF-κB activity in ER+ breast cancer cell lines and human samples compared to constitutive activation in ER- disease[428]. Equal p65 expression was demonstrated in ER+ and ER- breast cancer cell lines; however, p105 to p50/NFKB1 processing was more efficient in the ER+ cell lines. In the absence of a transactivation domain (e.g. provided by co-activator BCL3 or p65 subunit), p50/NFKB1 homodimers function to inhibit NF-κB activity[414]. Thus, it is possible that in E2-treated and untreated MCF-7 cells, nuclear p50/NFKB1 homodimers bind DNA and repress transcriptional activation of NF-κB-target genes. Furthermore, Cogswell et al. have reported absent p65 nuclear expression, but present nuclear p50/NFKB1 expression in human breast tumours, further supporting the hypothesis that inactive p50/NFKB1 homodimers exist in the nucleus of MCF-7 cells[360]. Together, this data suggests that despite an increase in nuclear BCL3 expression during antihormone response, it is unlikely that BCL3 co-activates p50/NFKB1 homodimers (reported to be its principal mechanism) to subsequently promote transcription of target genes.

The cellular localisation of p50/NFKB1 was next examined in T47D cells. Similar to the MCF-7 cells, p50/NFKB1 was predominantly located in the nucleus of control and E2-treated T47D cells, with some cytoplasmic staining in the latter. However, in contrast to the MCF-7 cells, during antihormone-response p50/NFKB1 was located in the nucleus and cytoplasm, with the greatest cytoplasmic staining apparent in the oestrogen deprived T47D cells. As previously mentioned above, cytoplasmic staining of p50/NFKB1 is likely characteristic of p50/NFKB1 and p105 expression. Surprisingly, Western analysis failed to detect any p105 expression in

the T47D cells irrespective of antihormone treatment. However, the antibody concentration was markedly increased for immunofluorescence compared to Western blotting. Thus, it is possible that Western blotting performed with a higher concentration of p50/NFKB1 antibody would result in the detection of p105 in these cells. In agreement with the Western blotting data, immunofluorescence studies failed to identify BCL3 in the E2-treated and control T47D cells. However, during antihormone response, BCL3 was located in both the nucleus and cytoplasm of T47D cells, with the greatest cytoplasmic staining of BCL3 apparent in the oestrogen deprived cells. This profile strongly mirrors the expression profile of p50/NFKB1 in this cell line during antihormone-response, possibly supporting the hypothesis that cytoplasmic BCL3 regulates dissociation of p50/NFKB1 from p105 in the cytoplasm and consequently promotes nuclear localisation of p50/NFKB1.

The localisation of p50/NFKB1 and BCL3 are markedly different in the MCF-7 and T47D cell lines, highlighting the heterogeneity of breast cancer; in the former, during antihormone response, BCL3 and p50/NFKB1 are not co-located, whereas in the T47D cells, BCL3 and p50/NFKB1 are both expressed in the cytoplasm and nucleus. This suggests that there may be some BCL3-mediated p50/NFKB1 homodimer activation in the T47D cells during antihormone response, which is not apparent in the MCF-7 cells. However, as previously discussed above, ER+ breast cancer cells are reported to have very little NF-κB activity. Thus, it is likely that, rather than co-activating p50/NFKB1 homodimers in T47D cells, BCL3 functions to repress NF-κB activation by facilitating the binding of inactive p50/NFKB1 homodimers to the κB sites on DNA, to prevent the binding of transactivating dimers[429,430]. Moreover, further studies are required to determine whether BCL3 and p50/NFKB1 are indeed bound in the nucleus of T47D cells during antihormone response.

Interestingly, following the acquisition of resistance, immunofluorescence studies revealed strong expression and co-localisation of p50/NFKB1 and BCL3 in the nucleus of TAMR and XR cell models, thus suggesting transcriptional activation of p50/NFKB1 homodimers. In the TAMR cells, there was also some cytoplasmic staining of BCL3 and p50/NFKB1, with stronger cytoplasmic staining of

p50/NFKB1 apparent in the XR cells but exclusively nuclear expression of BCL3. Interestingly, immunofluorescence studies of the T47D TAMR cell line revealed co-localisation of BCL3 and p50/NFKB1 in the cytoplasm, with very little, if any, staining of each protein observed in the nucleus. The identification of BCL3 protein in T47D TAMR cells by immunofluorescence is surprising, since Western blotting failed to detect protein expression of BCL3 in this cell line. Therefore, it is possible that experimental errors in the Western blotting contributed to the lack of BCL3 protein detection, rather than the absence of BCL3 protein in these cells. In the T47D-TAMR cells, it is possible that IκB proteins are strongly expressed compared to resistant-MCF-7 cells, together with minimal IκB kinase-mediated IκB degradation, thus sequestering p50/NFKB1 in the cytoplasm and preventing/outweighing cytoplasmic BCL3-mediated p50/NFKB1 nuclear translocation. In contrast to the MCF-7-derived resistant cell models, these findings suggest the absence of BCL3-mediated p50/NFKB1 homodimer transcriptional activity in the T47D TAMR cell lines.

Remarkably, such studies may have identified a potential mechanism responsible for the previously demonstrated growth regulatory role of BCL3 in the TAMR and XR cell lines via BCL3-mediated co-activation of p50/NFKB1 transcriptional activity characterised by the co-localisation of both proteins in the nucleus. Accordingly, BCL3 was previously shown to have no effect on the growth of the T47D TAMR cells possibly due to the co-localisation of both proteins in the cytoplasm and subsequently no activation of NF-κB and transcription of growth regulatory proteins. Similarly, despite an increase in BCL3 expression during antihormone response of MCF-7 and T47D cells, BCL3 played no role in the growth of these cells. With regard to the MCF-7 cells, the immunofluorescence studies concluded no co-localisation of BCL3 and p50/NFKB1 in the nucleus, thus suggesting no activation of NF-κB and the downstream transcription of growth regulatory proteins. Surprisingly, during antihormone response in the T47D cells, the immunofluorescence studies suggested a possible co-localisation of BCL3 and p50/NFKB1 in the nucleus. However, in contrast to the resistant cell models, such nuclear co-localisation had no effect on the growth regulatory role of BCL3 during antihormone response in the T47D cells. Thus, it is possible that additional

oncogenic events, present in resistance (TAMR and XR) but not during response, are required to drive BCL3-mediated p50/NFKB1 activation and downstream growth regulation.

To further confirm the co-localisation data, immunoprecipitation studies were performed to examine whether BCL3 and p50/NFKB1 are complexed, particularly in the TAMR and XR cell lines, to support the hypothesis that BCL3 coactivates p50/NFKB1 to promote NF-κB-mediated gene transcription. In support of the Western analysis and immunofluorescence data, BCL3 expression was not detected in E2-treated and control MCF-7 and T47D cells immunoprecipitated with p50/NFKB1. Additionally, according to the nuclear and cytoplasmic expression of BCL3 and p50/NFKB1, respectively, in fulvestrant- and oestrogen deprivation-treated MCF-7 cells, immunoprecipitation studies demonstrated no interaction between both proteins. Surprisingly, BCL3 and p50/NFKB1 were not complexed in tamoxifen-treated MCF-7 cells and antihormone-treated T47D cells. This is surprising since immunofluorescence studies revealed a co-localisation of both proteins in the nucleus and cytoplasm. Further studies including nuclear and cytoplasmic fractionation of these cells followed by Western blotting to detect BCL3 and p50/NFKB1 would confirm the immunofluorescene data. Thus, cytoplasmic BCL3-mediated p50/NFKB1 translocation is likely to occur via an intermediary protein and not via direct association between BCL3 and p105/p50. In the nucleus of tamoxifen-treated MCF-7 and antihormone-treated T47D cells, p50/NFKB1 possibly exists as an inactive homodimer. However, further studies are clearly required to rule out the possible existence of p50/NFKB1 heterodimers with alternative NF-κB subunits, which contain a transactivation domain (e.g. p65) to subsequently activate NF-κB-mediated gene transcription. Furthermore, the role of BCL3 during antihormone-response remains to be elucidated.

In antihormone resistance, BCL3 expression was strongly apparent in TAMR, XR and T47D-TAMR cells immunoprecipitated with p50/NFKB1. The identification of BCL3 protein expression in these T47D TAMR cells strongly suggests (as previously mentioned above) that experimental errors in the Western blotting experiments of wild type versus T47D TAMR cells led to the failure of BCL3 detection. These findings are in agreement with the immunofluorescence data,

which demonstrated co-localisation of both proteins in the nucleus of TAMR and XR cells, and in the cytoplasm of T47D-TAMR cells. To further distinguish whether BCL3 was bound to p50 or p105, TAMR and XR cells were immunoprecipitated with BCL3 and probed with the p50/NFKB1 antibody. As predicted, BCL3 was associated with p50/NFKB1 in the nucleus of TAMR and XR cell lines. However, such studies were not performed in the T47D TAMR cell line. It is possible that, since p50/NFKB1 and BCL3 are co-located in the cytoplasm of T47D TAMR cells, BCL3 is bound to both p50/NFKB1 and p105 isoforms. To further confirm BCL3 and p50 and/or p105 interactions in the nucleus of TAMR and XR or cytoplasm of T47D-TAMR cells, immunoprecipitation could be performed on nuclear and cytoplasmic extracts individually. Interestingly, a weak association between p50/NFKB1 and BCL3 was observed in wild type control cells cultured in sFCS (i.e. MCF-7 and T47D), with such an association not apparent in the wild type MCF-7 and T47D cells cultured in FCS. These differences may be due to growth factors present in FCS cross-talking with the ER to facilitate BCL3 down regulation, which is incomplete following incubation with growth factor-depleted sFCS. Importantly, all immunoprecipitation studies were performed only once (n=1). Thus, further experiments are clearly necessary to clarify this data.

As previously discussed, Watanabe et al. have demonstrated that cytoplasmic BCL3 promotes release of p50 from the p50-p105 cytoplasmic pool and subsequently translocates the homodimer into the nucleus[421]. They also reported that such events were without effect on the proteolytic processing of p105 to p50. We were interested to investigate whether BCL3 effects the proteolytic processing of p105 to p50 in our cells. The protein expression of p105 and p50/NFKB1 was examined in BL3 knockdown TAMR cells. Interestingly, BCL3 down regulation resulted in an increase in p105 expression and a decrease in p50 expression. This suggests that BCL3 may play a role in promoting p105 processing to p50, subsequently increasing the levels of p50 produced and translocated into the nucleus ultimately increasing NF-κB activity and transcription of genes involved in cell growth and survival. To our knowledge, these are the first experiments to demonstrate a role for BCL3 in p105 to p50 processing. Certainly, additional experiments are required

to further explore this idea, including similar knockdown studies in XR and T47D TAMR cells as well as during antihormone response.

In summary, this Chapter has revealed a role for BCL3 in promoting resistant cell growth; however in contrast to what was first hypothesised, there was no evidence to suggest a role for BCL3 in limiting antihormone response. Indeed, BCL3 promoted growth (although not significant) of TAMR and XR MCF-7-derived resistant cells together with nuclear localisation and direct binding of BCL3 with p50 in the nucleus. Although BCL3 knockdown failed to significantly decrease cell growth in the resistant cells, it is possible that with more experimental repeats, such effects may prove significant. Such nuclear localisation of both proteins and their direct association suggests that BCL3 co-activates p50/NFKB1 homodimers to promote NF-κB-mediated gene transcription and ultimately cell growth. However, further studies, such as a NF-κB reporter gene assay or a DNA-binding ELISA are required to confirm p50/NFKB1 homodimer activation. Furthermore, it would be interesting to examine the expression of other NF-κB subunits, particularly those that contain a transactivation domain (e.g. p65, RelB and cRel) to determine whether they contribute to the predicted NF-κB activity apparent in TAMR and XR cells. Additionally chromatin immunoprecipitation (ChIP) sequencing would identify the potential pro-proliferative and pro-survival genes regulated by BCL3-activated p50/NFKB1 homodimers.

To consider the heterogeneity of breast cancer, the role of BCL3 in an additional tamoxifen resistance ER+ cell line (i.e. T47D-TAMR) was assessed. Interestingly, BCL3 did not promote the growth of T47D-TAMR cells. Although immunoprecipitation studies revealed an association between BCL3 and p50/NFKB1 in the T47D TAMR cell line, both proteins were sequestered in the cytoplasm together with p105 and therefore unable to promote gene transcription. The role of BCL3 in the cytoplasm remains largely unexplored. There are only a couple of studies which have demonstrated cytoplasmic expression of BCL3, with both suggesting that in the cytoplasm, BCL3 plays a role in the nuclear translocation of p50/NFKB1 from p105 and IκB proteins in the cytoplasm[421,425]. However, the exact mechanisms of such BCL3-mediated p50/NFKB1 nuclear translocation are unclear. It is possible that IκB protein expression is increased in

the T47D-TAMR cells compared to TAMR and XR cells (which could be examined by Western blotting), therefore retaining p50/NFKB1 in the cytoplasm and preventing BCL3-mediated p50/NFKB1 nuclear translocation. Alternatively, it is possible that additional proteins required to promote/facilitate BCL3-mediated p50/NFKB1 translocation are absent in the T47D cell line versus the MCF-7 cell line.

Similarly, during antihormone response, BCL3 had no effect on the growth of fulvestrant-treated MCF-7 and T47D cells. In the MCF-7 cells, BCL3 was located in the nucleus and p105/p50 was located in the cytoplasm. Unsurprisingly, immunoprecipitation studies failed to identify an association between both proteins. In the T47D cell line, although both proteins were located in the nucleus, immunoprecipitation studies failed to demonstrate a direct physical association between these proteins. Therefore, these findings suggest that BCL3 does not co-activate p50/NFKB1 homodimers during antihormone response to promote downstream transcription of genes involved in cell proliferation and survival, and in the antihormone-treated MCF-7 cells, p50/NFKB1 is not translocated from the cytoplasm to the nucleus.

However, cell survival and cell cycle assays failed to identify a role for BCL3 in either promoting cell survival or dysregulating the cell cycle during antihormone response and resistance. However, it is possible that such studies were insufficient to fully determine a role for BCL3 and the mechanisms by which BCL3 promotes cell growth in the TAMR and XR cell lines requires further study. Such studies could include examination of cell cycle regulators to determine whether nuclear BCL3:p50 complexes alter their expression, alongside examination of PARP cleavage, characteristic of apoptosis. Moreover, it is possible that transient BCL3 knockdown is insufficient to promote significant apoptosis and/or dysregulation of the cell cycle, which may be apparent following stable gene knockdown.

Furthermore, preliminary studies suggest that BCL3 may play a role in p105 to p50 processing in TAMR cells. However, further studies are required to determine whether BCL3 plays an equivalent role in additional models of endocrine resistance and also during response. Together, these are the first studies to our

knowledge that demonstrate that BCL3 promotes growth of antihormone resistant cells (derived from MCF-7 cells) by potentially enhancing p105 to p50 processing and promoting nuclear localisation of p50, to facilitate BCL3-mediated p50 homodimer activation and subsequent transcription of NF-κB-regulated genes. However, although BCL3 expression is up regulated during antihormone response, its role remains to be elucidated.

6 Results IV: Further investigation of CLU function during antihormone-response and -resistance

6.1 Introduction

CLU is a ubiquitously expressed glycoprotein implicated in several physiological processes important for carcinogenesis and tumour progression, including apoptosis, cell cycle regulation and DNA repair[371,431,432]. Deciphering the role of CLU has been challenging due to the existence of two main, functionally diverse, isoforms, as a result of alternative splicing. The cytoplasmic secretory isoform, CLU-S, functions to promote cell survival, whereas the nuclear isoform promotes cell death. Prochnow et al. have extensively studied the different CLU isoforms in non-cancer and cancer cell lines (including MCF-7 cells)[295]. They identified that the CLU gene encodes at least three different mRNA variants which are transcribed as pre-mRNAs, each comprising 9 exons and 8 introns (Figure 95). Each pre-mRNA variant contained a unique exon 1 sequence. Variant 1 encodes CLU-S, which is translated from a start codon located upstream of the signal sequence coding region (SSCR) on exon 2. An alternative spliced mRNA of variant 1 is translated from a start codon which resides on exon 3 and thus lacks exon 2 and the SSCR. Consequently, this protein lacks the signal sequence, yielding an intracellular CLU isoform known as the nuclear CLU protein. Translation of the other two pre-mRNAs gives rise to Variant 2 and Variant 3 CLU. However, RT-PCR using variant-specific primers in MCF-7 cells revealed that Variant 1 (CLU-S) represented the most abundant mRNA, whereas Variant 1 excluding exon 2 (nuclear CLU) represented approximately 0.01% of total CLU mRNA, with even less represented by Variant 2 and 3[295].

CLU-S is synthesised as a pre-pro-protein comprised of 449 amino acids, where the first 22 amino acids represent the secretory signal sequence. The primary translation molecule is converted to a high-mannose 60 kDa form, located in the endoplasmic reticulum. Subsequently, the protein is glycosylated and cleaved in the Golgi to α- and β-chains (34-36 kDa and 37-39 kDa, respectively) which

heterodimerise (70-80 kDa) yielding the mature secreted CLU protein[371]. Nuclear CLU (~55 kDa) protein is translated from the alternatively spliced Variant 1 CLU transcript, lacking exon 2.

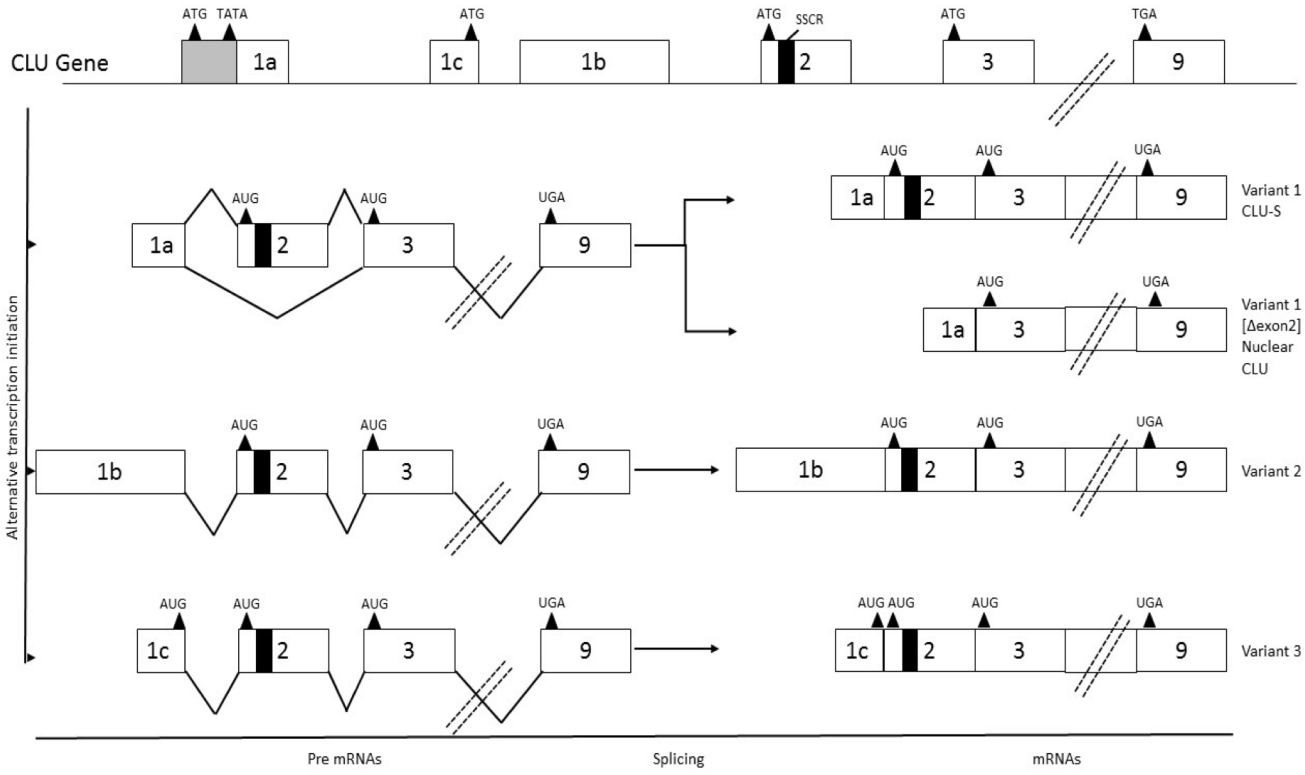

Figure 95 Structure of CLU gene and transcription products. The human CLU gene comprises 9 exons and encodes at least 3 different pre-mRNAs which contain unique exons 1. Splicing of variant 1 pre-mRNA generates the cytoplasmic secretory mRNA form (CLU-S) which includes the signal sequence coding region (SSCR). Alternative splicing of variant 1 pre-mRNA generates an mRNA that lacks exon 2 and the SSCR. Splicing of the other 2 pre-mRNAs gives rise to Variants 2 and 3. Figure adapted from Prochnow et al.[295].

CLU is expressed in many human cancers, including breast, bladder, colon, kidney and prostate[335,433–435]. CLU plays a significant role in the tumorigenesis and metastasis of several human cancers and is up regulated by many anti-cancer therapies to confer treatment resistance[335,436–438]. In prostate, CLU-S expression is very low in benign epithelial cells, but increases in prostate cancers with higher Gleason scores[435]. Furthermore, CLU-S expression has been shown to be significantly increased in prostate cancer cells following androgen deprivation therapy[439,440]. Overexpression of CLU-S in prostate cancer cells has also been demonstrated to protect these cells from chemotherapy-induced apoptosis, thus

aiding acquisition of a chemo-resistant phenotype[441]. Similarly, in breast, CLU expression is very low in normal epithelial cells, but is very high in breast cancer cells and is associated with metastatic progression[335]. Tamoxifen and cytotoxic treatments have been demonstrated to increase CLU expression in breast cancer cell lines which subsequently protects the cells from cell death[339]. Mechanisms by which CLU exerts its pro-survival activity are not fully elucidated. Proposed mechanisms include inhibition of the apoptotic protein Bax[344], enhancement of NF-κB transcriptional activity[349] and activation of the PI3K/AKT survival pathway[348].

It was hypothesised that antihormones induce up regulation of pro-survival genes early during response, allowing a cohort of cells to escape antihormone challenge and ultimately contribute to the emergence of resistant growth. The microarray work in Chapters 3 and 4 aimed to identify antihormone-induced pro-survival genes that may subsequently limit the efficacy of such agents and contribute towards the acquisition of resistance. Further study of strong candidates could prove significant in identifying novel therapeutic strategies to enhance antihormone response, as well as biomarkers representing drug outcome.

To this regard, Western blotting data indicated that CLU-S expression was up regulated by all three antihormone treatments in 4 ER+ cell lines encompassing HER2+ and HER2- disease (Chapter 4). Additionally, ontological investigations identified a breadth of literature exploring CLU expression in breast cancer where its increased expression has been associated with metastasis, cell survival and ultimately poor outcome[335,336]. Together, this suggests that CLU/CLU-S expression is rapidly induced in response to all three antihormone therapies in HER2+ and HER2- disease, potentially activating a common survival mechanism to promote the development of resistance. Indeed, initial microarray studies in cell models of acquired endocrine resistance identified increased CLU expression maintained through to the emergence of resistance to tamoxifen, fulvestrant and oestrogen deprivation.

In this Chapter, targeted CLU knockdown studies have thus been performed to aim to identify the role of CLU during antihormone-response and –resistance and to

determine whether its up regulation early during response contributes to the limited efficacy of these agents and subsequently promotes the development of resistance. Firstly, the log2 intensity plots, generated from the microarray data, of CLU expression in the antihormone-resistant cell models (i.e. TAMR and XR) were examined and subsequently verified by RT-PCR and Western blotting, to determine whether increased CLU/CLU-S expression was maintained through to emergence of resistance. Subsequently, CLU knockdown studies, via siRNA, were performed to determine whether CLU limits the growth inhibitory actions of antihormones during response and/or promotes the growth of antihormone-resistant cells.

6.2 Methods

6.2.1 Cell culture

Antihormone-treated MCF-7 and T47D cells were re-suspended in phenol-red-free RPMI medium supplemented with 5% FCS, penicillin-streptomycin (10 IU/ml to 10 μg/ml), fungizone (2.5 μg/ml) and glutamine (4 mM) and allowed to adhere overnight prior to the addition of antihormone, E2 and control (untreated medium) treatments, as described in Chapter 2, section 2.1.2.

The (short-term) TAMR, FASR, XR and T47D TAMR cell models and wild type control cells were cultured in phenol-red-free RPMI medium supplemented with 5% sFCS, penicillin-streptomycin (10 IU/ml to 10 μg/ml), fungizone (2.5 μg/ml), glutamine (4 mM) and respective antihormone treatment, as described in Chapter 2, section 2.1.2.

6.2.2 RT-PCR

Cells were prepared for RNA analysis as outlined in section 6.2.1. RT-PCR was performed, as described in section 2.4, to determine RNA expression of CLU. The CLU primers used were previously designed by Prochnow et al.[295]. The forward primer was complementary to exon 1a and the reverse primer complementary to exon 5 (Table 3). The nuclear and secretory isoforms of CLU exhibit similar mRNA sequences, with the exception of the former lacking exon 2; thus PCR resulted in the amplification of both isoforms, characterised by individual products of 271 bp and 400 bp, respectively. Densitometry analysis was performed and the raw

densitometry values of CLU were normalised to β-actin loading control. The data were analysed using GraphPad prism. An unpaired t-test or an ANOVA (with a Tukey's multiple comparisons post-hoc test) were used to compare the means. A p value <0.05 was considered statistically significant.

6.2.3 Western blotting

Cells were prepared for Western blotting as outlined in section 6.2.1. Twenty micrograms of protein was loaded and separated by SDS-PAGE and probed for secretory CLU antigen, as described in section 2.5. The secretory CLU antibody used within this project recognises the 60 kDa precursor and 40 kDa CLUα subunit. Densitometry analysis was performed and the raw densitometry values of CLU were normalised to β-actin loading control. The data were analysed using GraphPad prism. An unpaired t-test or an ANOVA (with a Tukey's multiple comparisons post-hoc test) were used to compare the means. A p value <0.05 was considered statistically significant.

6.2.4 CLU knockdown

To decipher the role of CLU during antihormone response and resistance, CLU knockdown studies were performed utilising siRNA as described in section 2.6.1. Briefly, cells were grown until approximately 60% confluency prior to the addition of the siRNA tranfection reagent mix. Cells were incubated for 4 days (unless sated otherwise) prior to RNA and protein lysis for subsequent RT-PCR and Western blot analysis (as described above). Since CLU-S is expressed at low levels in wild type MCF-7 and T47D cells, fulvestrant was added to the medium 48 hours post siRNA transfection to induce CLU-S expression.

6.2.5 Cell counting

Cell counting studies were performed to determine the effect of CLU knockdown on cell growth during antihormone response and resistance. Cells were transfected with CLU siRNA (as described above) in triplicate and incubated for 4 days prior to the measurement of cell number, as described in section 2.6.3.

6.2.6 Immunofluorescence

The cellular localisation of secretory CLU during antihormone response and resistance was examined by immunofluorescence studies as described in section

2.6.4. Briefly, cells were grown on glass coverslips, incubated with CLU primary antibody, followed by appropriate fluorphore-conjugated secondary antibody prior to examination on a fluorescent microscope.

6.2.7 Cellular fractionation

Nuclear and cytoplasmic fractions of MCF-7, TAMR and XR cells were prepared as described in section 2.5.2. The resultant protein were separated by SDS-PAGE as described above and probed for secretory CLU antigen, and the nuclear and cytoplasmic markers, SP-1 and Grb2, respectively.

6.3 Results

Initial microarray studies (Chapter 3) revealed increased CLU expression maintained through to the acquisition of resistance. Indeed, up regulation (fold change > 1.5) of CLU expression was demonstrated in TAMR and XR cells, with significant up regulation in the FASR cells versus MCF7 control cells (Chapter 3, Figure 18). Additionally, predominantly present detection calls were reported in the XR and FASR cell models, implying reliable gene expression, whereas absent calls were recorded in the TAMR and MCF7 control, suggesting very low gene expression (Chapter 3, Figure 18).

6.3.1 Verification of the microarray data by RT-PCR

As previously described, CLU has two main isoforms as a result of alternative splicing. The cytoplasmic secreted form promotes cell survival whereas the nuclear form is associated with cell death. Since this project is interested in the pro-survival role of CLU, PCR primers complementary to the DNA sequence of the pro-survival form were utilised. The PCR primers used were previously designed by Prochnow et al.[295], with the forward primer complementary to exon 1a and the reverse primer complementary to exon 5. However, since the nuclear and secretory isoforms exhibit similar mRNA sequences, with the exception of the former lacking exon 2, PCR resulted in the amplification of both forms, characterised by individual products of different base pair sizes.

The microarray expression profiles of CLU in TAMR and XR cell lines were verified by RT-PCR. To consider the heterogeneity of breast cancer, CLU-S expression was also examined by RT-PCR in T47D TAMR cells. This project eliminated FASR cells

from further study since we wished to focus on the first-line therapies (i.e. tamoxifen and AIs) and the resistance that develops from such agents. RT-PCR was performed on triplicate mRNA from wild type cells (i.e. MCF-7 and T47D) and TAMR, XR and T47D TAMR cells (cultured under the same conditions as those used to generate the samples for microarray gene expression profiling). In agreement with the microarray profile, CLU-S mRNA expression was significantly ($p < 0.01$) up regulated in the XR cell line compared to control (Figure 96B). However, in the TAMR cells, CLU-S expression was less than MCF-7 control (Figure 96A). In the T47D TAMR cell line, CLU-S expression was significantly ($p < 0.05$) increased versus control (Figure 96C). Interestingly, nuclear CLU mRNA was not detected by PCR in any of the three antihormone-resistant cell lines (Figure 96).

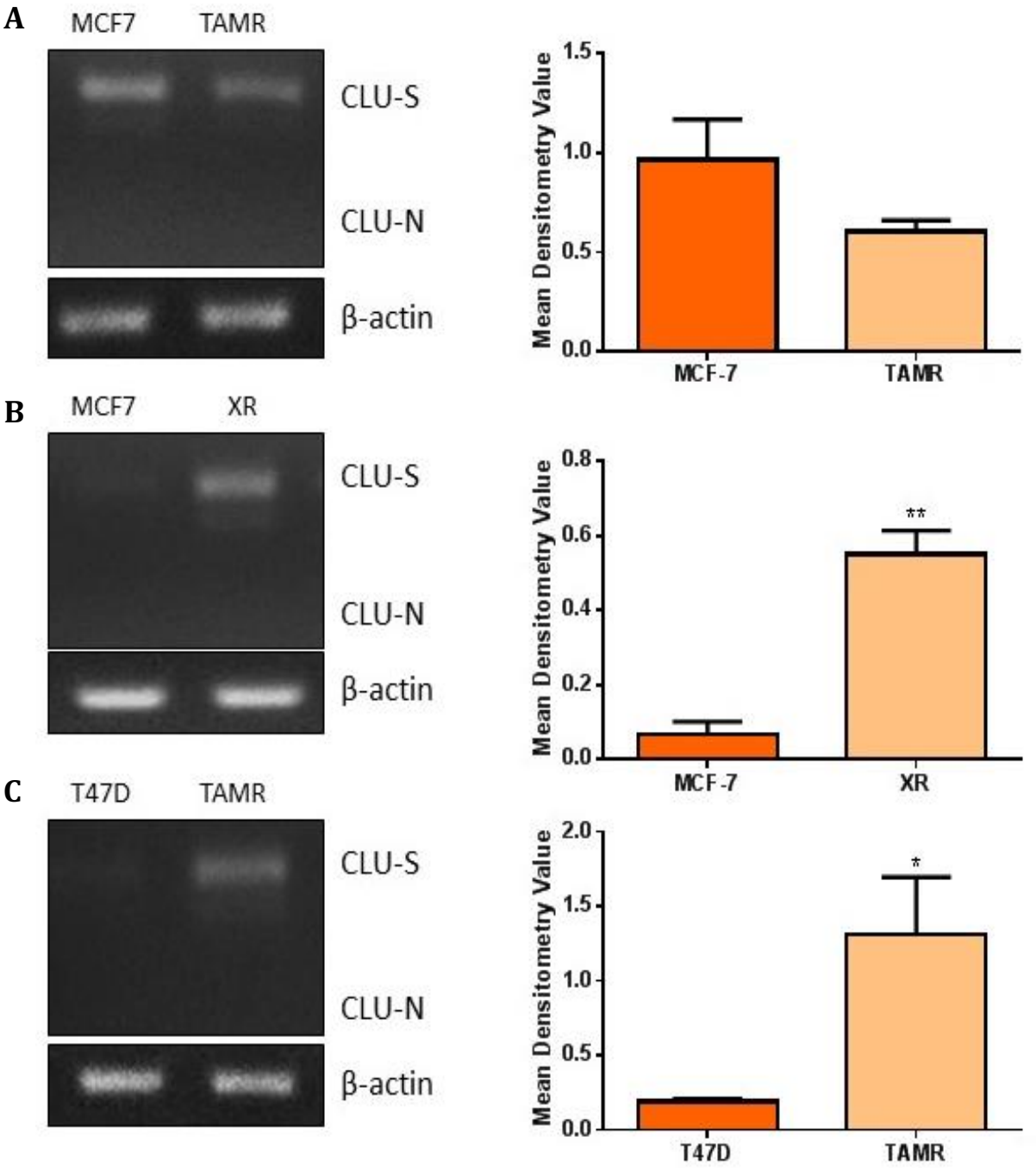

Figure 96 Representative PCR images from three independent experiments showing pro-survival CLU isoform (CLU-S) and pro-apoptotic nuclear CLU isoform (CLU-N) RNA expression and β-actin loading control in tamoxifen resistant (TAMR) (A) and oestrogen deprived-resistant (XR) (B) MCF-7 cells versus parental cells and TAMR T47D cells (C) versus parental cells. The corresponding β-actin normalised densitometry graphs showing CLU-S expression in the three cell lines is also shown, expressed as means ± SEM. The data were analysed by an unpaired T-test. * $p < 0.05$; ** $p < 0.01$

6.3.2 CLU-S protein expression in resistance

CLU-S expression was next examined at the protein level by Western blotting. Western blotting was performed on triplicate protein samples from wild type control and TAMR, XR and T47D TAMR cells (cultured under the same conditions as those used to generated the samples for microarray gene expression profiling and/or RT-PCR). As previously revealed in Chapter 3, CLU-S exists as a precursor and a mature form composed of α- and β-subunits. The secretory CLU antibody used within this project recognises the 60 kDa precursor and 40 kDa CLUα subunit.

In agreement with the previous microarray and PCR data, Western analysis revealed a significant ($p < 0.05$) increase in CLU-S precursor and a marked increase, although not significant, in CLUα expression in the XR cell line compared to control (Figure 97B). In the TAMR cell line, a small and non-significant increase in CLU-S precursor and CLUα protein expression was apparent versus control (Figure 97A). However, in comparison to the XR cell line, CLU-S precursor and CLUα expression was evidently weaker in the TAMR cells. In the T47D TAMR and control cells, CLU-S precursor protein expression was strong, whereas CLUα expression was markedly less, with similar expression levels in the control and resistant cells observed (Figure 97C).

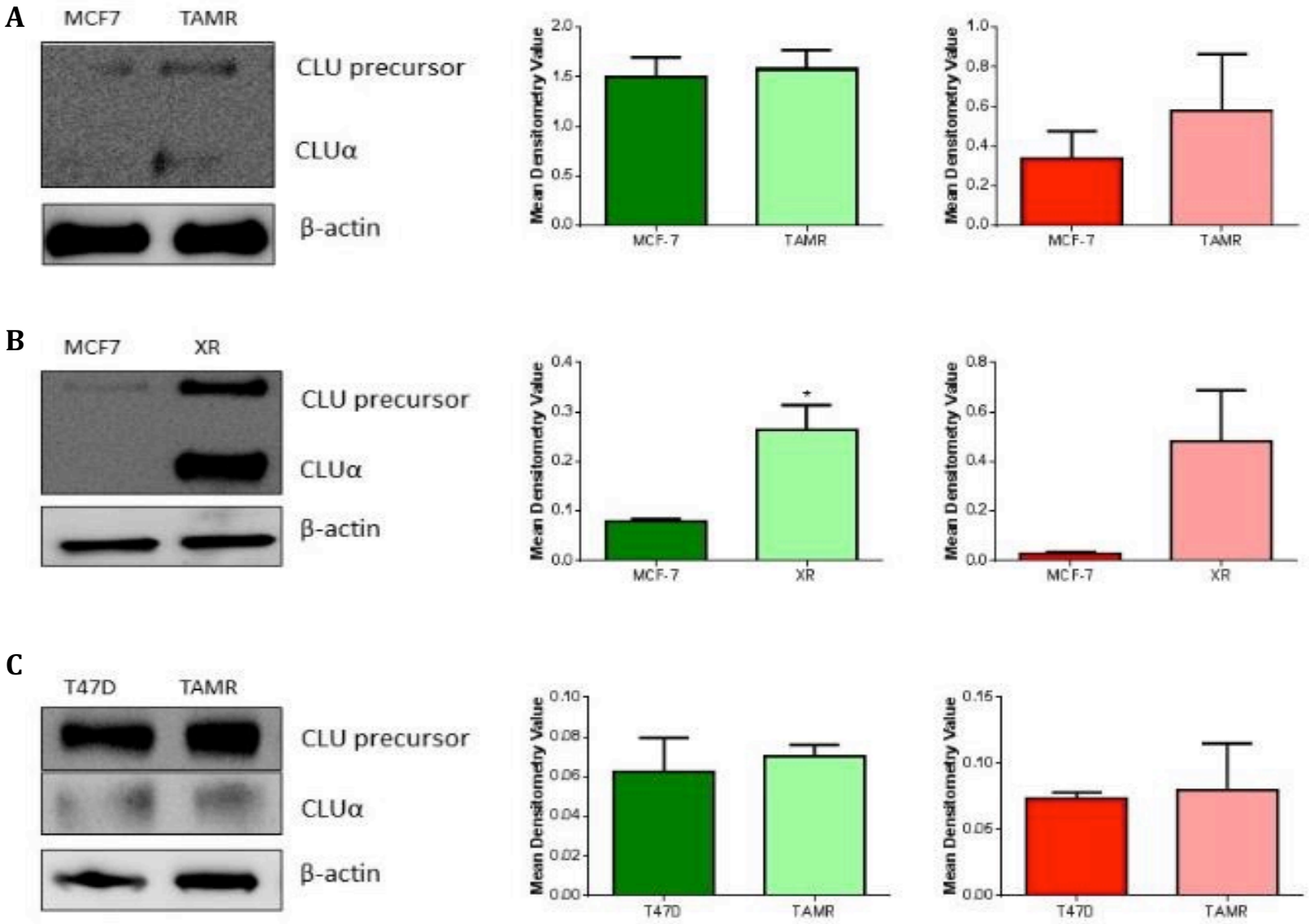

Figure 97 Representative Western blot images and corresponding β-actin normalised densitometry graphs from three independent experiments showing pro-survival CLU isoform precursor (green graphs) and CLUα (red graphs) protein expression in tamoxifen resistant (TAMR) (A) and oestrogen deprived-resistant (XR) (B) MCF-7 cells versus parental cells and TAMR T47D cells (C) versus parental cells. The results are expressed as means ± SEM. The data were analysed by an ANOVA and post-hoc Tukey's multiple comparisons test . * p <0.05.

6.3.3 CLU knockdown

Targeted CLU knockdown, via siRNA, was performed to investigate whether CLU-S promotes cell survival or proliferation during antihormone response and resistance and to determine whether such knockdown can enhance the growth inhibitory actions of antihormones during response and/or reverse antihormone-resistance. The CLU siRNA utilised comprised of a pool of 4 siRNA targeting different regions of the mRNA for optimal knockdown. Consequently, total CLU was targeted for knockdown as opposed to specific CLU-S knockdown. However, Prochnow et al. have shown that CLU-S represents the most abundant (> 99%) CLU form in several cell lines, including MCF-7 cells[295].

6.3.3.1 Antihormone response

Since CLU-S expression is very weak in wild type MCF-7 and T47D cells (as previously demonstrated by Western blotting in Chapter 4, Figure 49), CLU siRNA was combined with fulvestrant treatment to induce CLU-S expression to subsequently allow the effect of CLU knockdown to be examined. Consistent with BCL3 knockdown performed in Chapter 5, MCF-7 and T47D cells were incubated with CLU siRNA for 2 days prior to the addition of fulvestrant for a further 2 days.

The magnitude of CLU knockdown, specifically the CLU-S isoform, in fulvestrant-treated MCF-7 and T47D cells was examined at the mRNA and protein level. As demonstrated in Figure 98, 2 day fulvestrant treatment (depicted by the 'media' treatment arm) induced up regulation of CLU-S mRNA expression in MCF-7 and to a greater degree in T47D cells compared to untreated control. Similarly, lipid and control siRNA treatment combined at day 2 with fulvestrant for a further 48 hours induced similar CLU-S mRNA expression to fulvestrant alone ('media' arm) in the MCF-7 and T47D cells, indicating that the lipid and control siRNA had no effect on CLU-S expression. CLU siRNA treatment (comprised of 2 day CLU siRNA incubation prior to a further 2 days combined with fulvestrant treatment) successfully reduced CLU-S mRNA expression in the MCF-7 and T47D cell lines.

Disappointingly, due to problems and difficulties with Western blotting experiments, CLU-S knockdown in fulvestrant-treated MCF-7 and T47D cells could not be verified at the protein level.

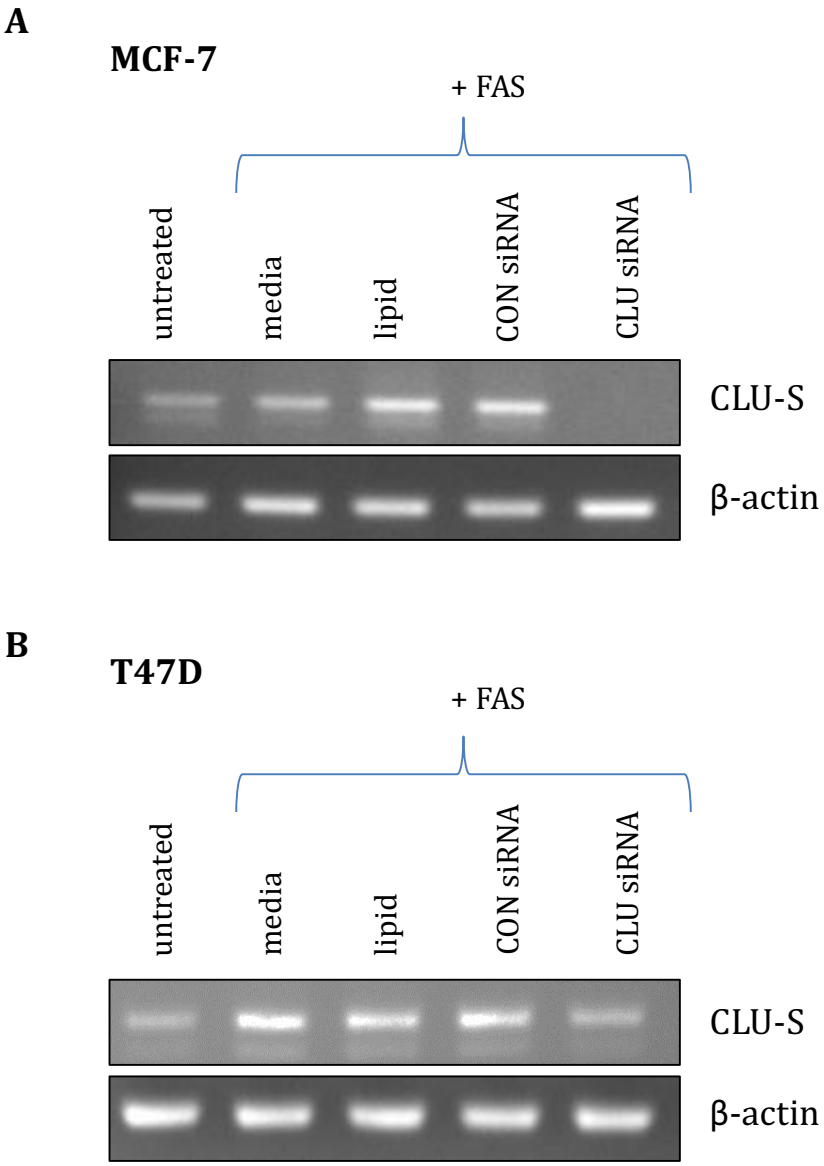

Figure 98 Representative PCR images from three independent experiments showing the mRNA expression of the pro-survival CLU isoform (CLU-S) and β-actin loading control in (A) MCF-7 and (B) T47D cells treated with media only, lipid only, unscrambled control small interfering RNA (CON siRNA) and CLU siRNA for 2 days prior to the addition of fulvestrant (FAS; 10^{-7} M) for a further 2 days. Untreated control is also shown.

6.3.3.2 Antihormone resistance

In contrast to wild type antihormone responsive MCF-7 and T47D cells, the antihormone-resistant cell models, particularly XR and T47D TAMR cells, constitutively express CLU-S with weaker protein expression detected in TAMR cells, as previously demonstrated in Figure 97. Therefore, CLU knockdown was simply induced via 4 day incubation with CLU siRNA. The magnitude of CLU-S knockdown was examined at the mRNA and protein level. At the messenger level, CLU-S expression in TAMR and XR cells was not affected by 4 day lipid and control siRNA incubations. However a small decrease in CLU-S expression was apparent in the control siRNA-treated T47D-TAMR cells compared to lipid and control which was mirrored by a decrease in actin expression (Figure 99). Four day CLU siRNA incubation induced down regulation of CLU-S mRNA expression in the three antihormone resistant cell models.

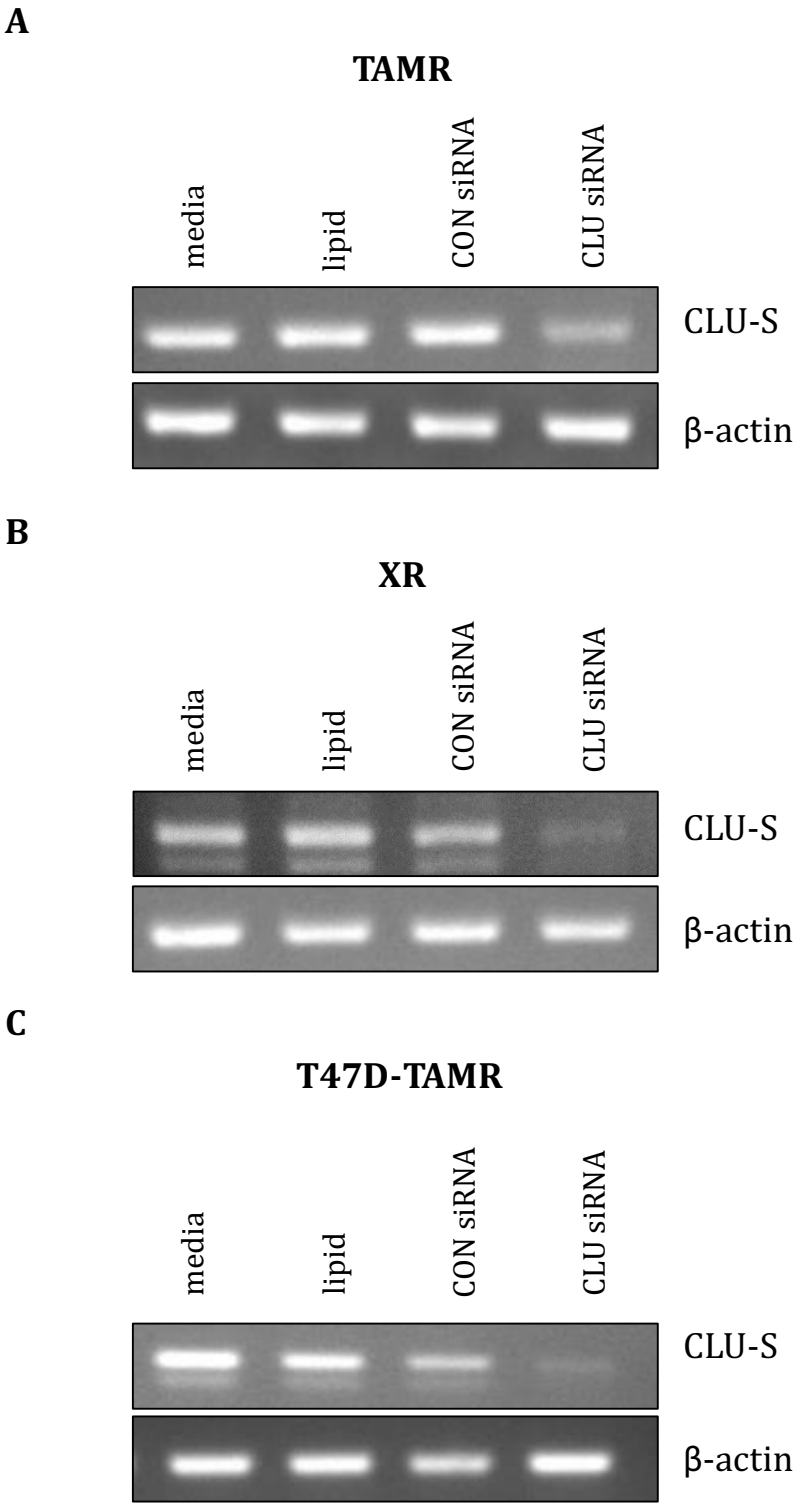

Figure 99 Representative PCR images from three independent experiments showing pro-survival secretory CLU (CLU-S) mRNA expression and β-actin loading control in (A) tamoxifen-resistant (TAMR) and (B) oestrogen deprivation-resistant (XR) cells derived from MCF-7 cells and (C) T47D-TAMR cells treated with media only, lipid only, unscrambled control small interfering RNA (CON siRNA) and CLU siRNA for 4 days.

At the protein level, lipid and control siRNA had no effect on CLUα expression in XR cells (Figure 100A). In agreement with the PCR data, 4 day incubation with CLU siRNA resulted in a substantial decrease in CLUα protein expression in XR cells. Interestingly, CLU-S precursor protein was not detected in XR cells irrespective of treatment. Similarly, in the T47D-TAMR cell line, lipid and control siRNA had no effect on the protein expression of CLU-S precursor and CLUα, whereas CLU siRNA resulted in a decrease in expression of both proteins compared to control (Figure 100B). Unfortunately, CLU-S expression could not be detected in the TAMR cell line (Figure 100A). This is unsurprising since CLU-S protein expression in these cells has been previously demonstrated to be very weak (Figure 97A).

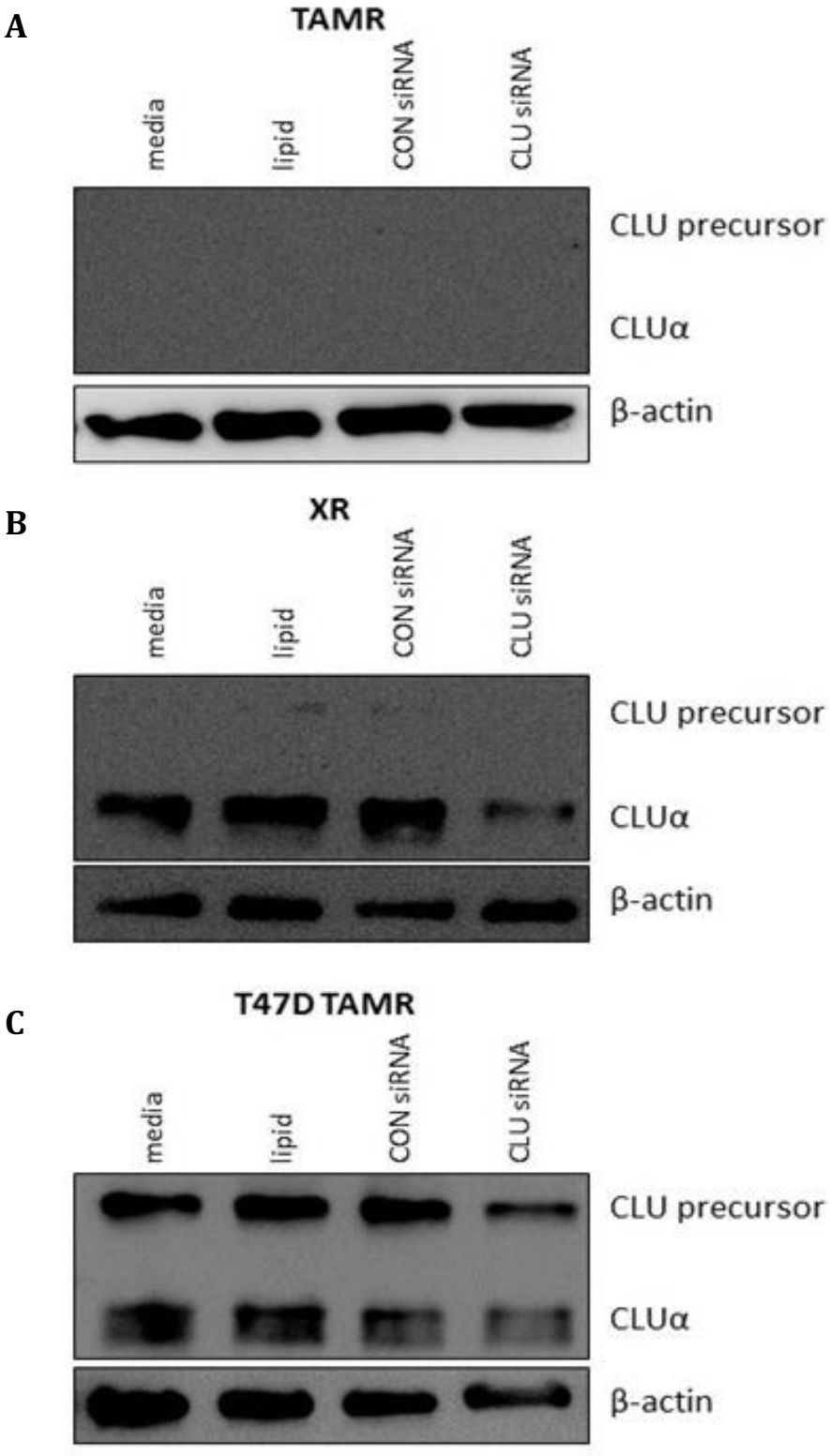

Figure 100 Representative Western blot images from three independent experiments showing pro-survival CLU isoform precursor and CLUα protein expression and β-actin loading control in (A) tamoxifen-resistant (TAMR) and (B) oestrogen deprivation-resistant (XR) cells derived from MCF-7 cells and (C) T47D-TAMR cells treated with media only, lipid only, unscrambled control small interfering RNA (CON siRNA) and CLU siRNA for 4 days.

6.3.4 Effect of CLU knockdown on cell growth during antihormone-response and –resistance

Following the establishment of substantial CLU-S knockdown in the antihormone-responsive and –resistant cell lines, cell counting experiments were next performed to determine whether CLU-S expression has any effect on cell growth. The rationale was that a decrease in cell number/cell growth mediated by CLU siRNA, suggests that CLU plays a role in promoting cell growth potentially via increasing cell proliferation or survival.

6.3.4.1 Antihormone response

As illustrated in Figure 101A, CLU knockdown (2 day CLU siRNA incubation followed by fulvestrant treatment for a further 2 days) reduced cell growth of fulvestrant-treated MCF-7 cells by approximately 20% compared to control. However, this reduction was not significant. Targeted CLU knockdown had no effect on the growth of fulvestrant-treated T47D cells (Figure 101B).

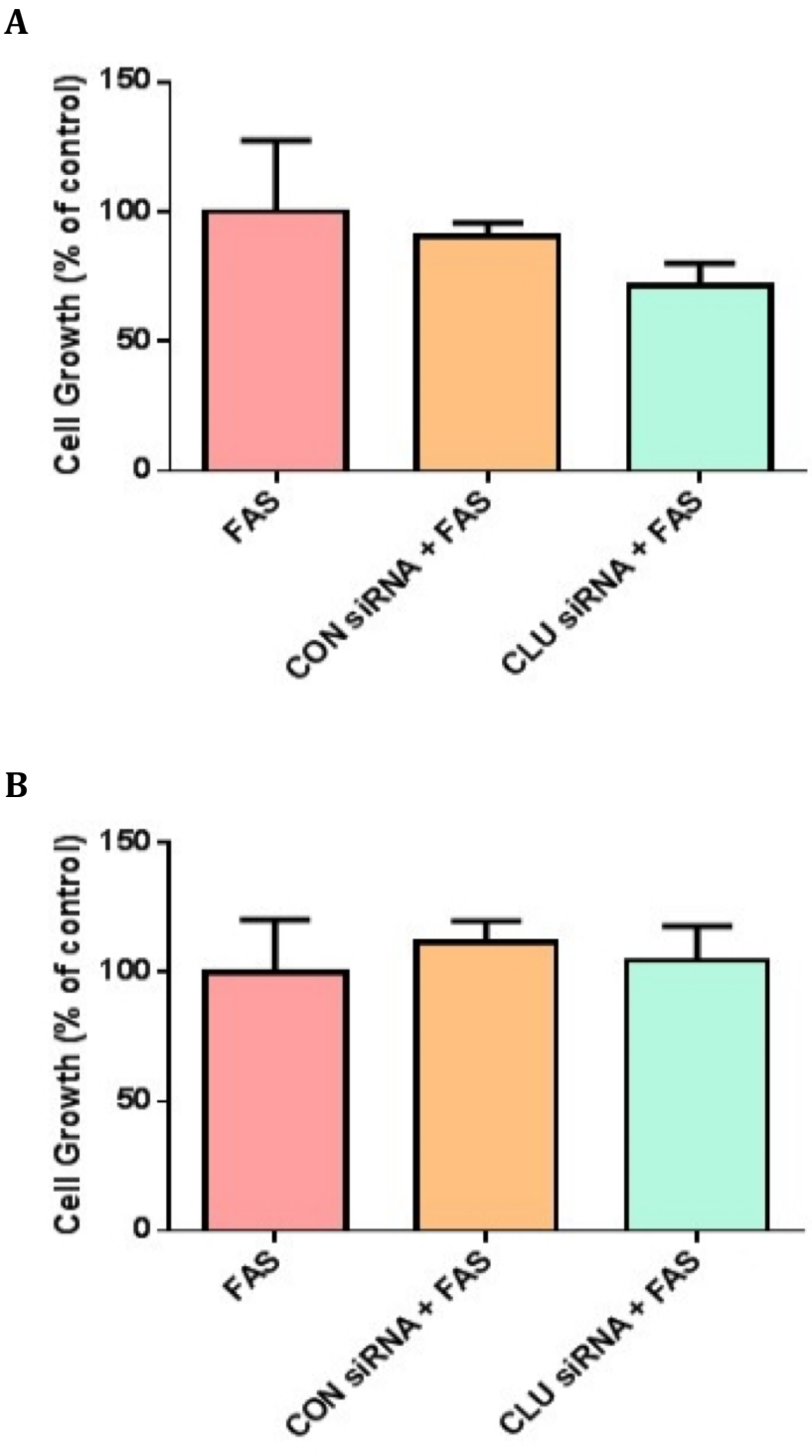

Figure 101 Effect of CLU knockdown (2 day CLU siRNA followed by 2 day fulvestrant (FAS; 10^{-7} M)) compared to control (CON siRNA; 2 day CON siRNA followed by 2 day FAS) and FAS alone on the growth of (A) MCF-7 and (B) T47D cells. The results are expressed as the means ± SEM of three independent experiments and presented as the % of the control. The data were analysed by an ANOVA and post-hoc Tukey's multiple comparisons test.

6.3.4.2 Antihormone resistance

During antihormone resistance, targeted down regulation of CLU using siRNA resulted in a small and non-significant decrease in TAMR cell growth (Figure 102A). However, CLU knockdown was without effect on the growth of XR and T47D-TAMR cells (Figure 102B and C).

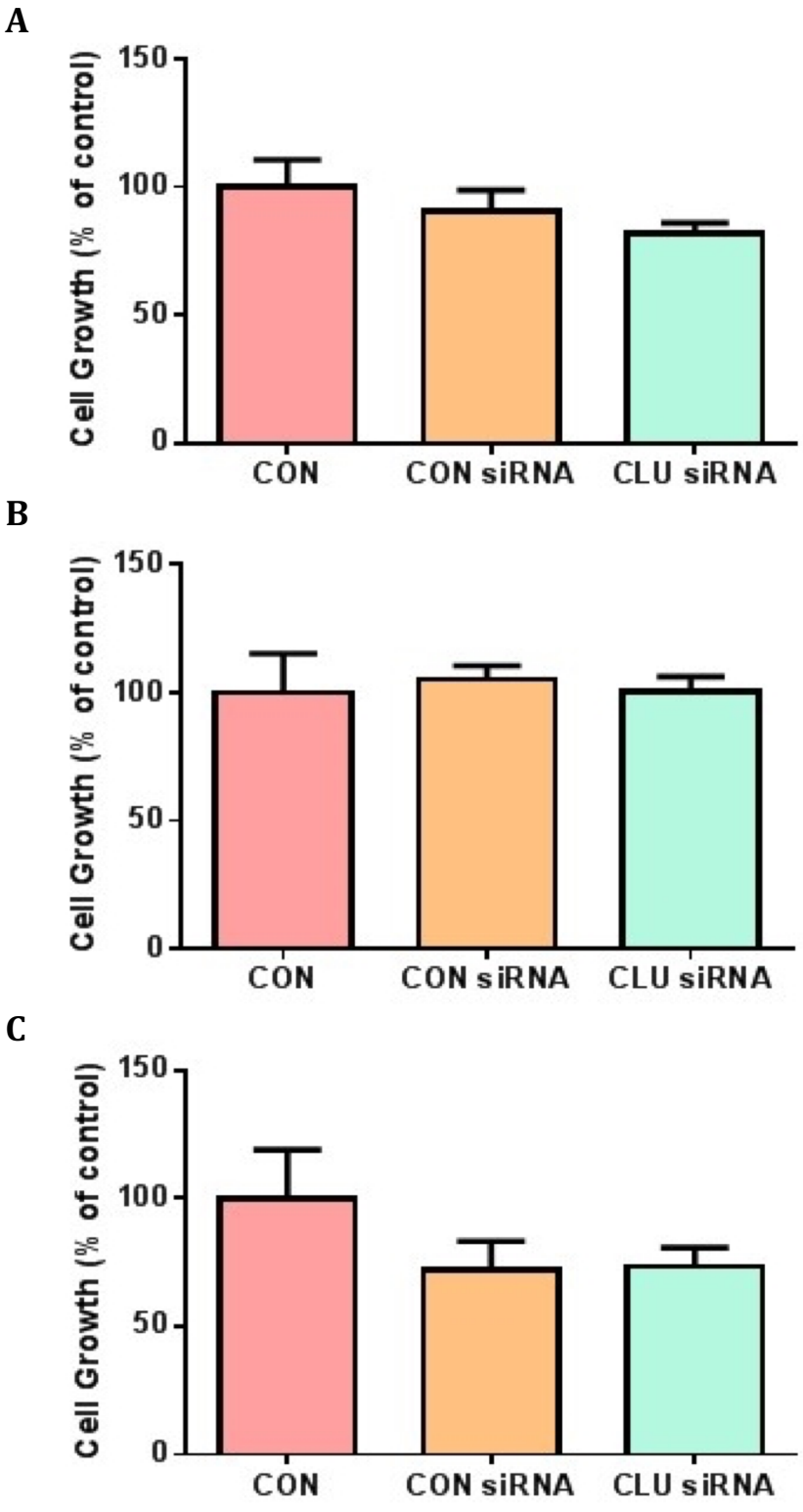

Figure 102 Effect of CLU knockdown (4 day CLU siRNA) compared to control (CON siRNA; 4 day CON siRNA) on the growth of (A) tamoxifen-resistant (TAMR; n=4) and (B) oestrogen deprivation-resistant (XR; n=3) cells derived from MCF-7 cells and (C) T47D-TAMR (n=2) cells. The results are expressed as the means ± SEM and presented as the % of the control. The TAMR and XR data were analysed by an ANOVA and post-hoc Tukey's multiple comparisons test.

6.3.5 Cellular localisation of CLU-S during antihormone-response and -resistance

6.3.5.1 Immunofluorescence

As previously described, CLU has two main isoforms, exhibiting functionally distinct activities. The nuclear isoform promotes cell death whereas the cytoplasmic secretory isoform promotes cell survival. Thus, cellular localisation studies, via immunofluorescence, were next performed to determine the cellular localisation of CLU-S during antihormone-response and –resistance.

Interestingly, during antihormone response in MCF-7 cells, immunofluorescence studies revealed relatively equal staining of CLU-S in the nucleus and cytoplasm (Figure 103). In agreement with previous PCR and Western blotting data, very little, if any, CLU-S was identified by immunofluorescence in untreated control and E2-treated MCF-7 cells (Figure 103).

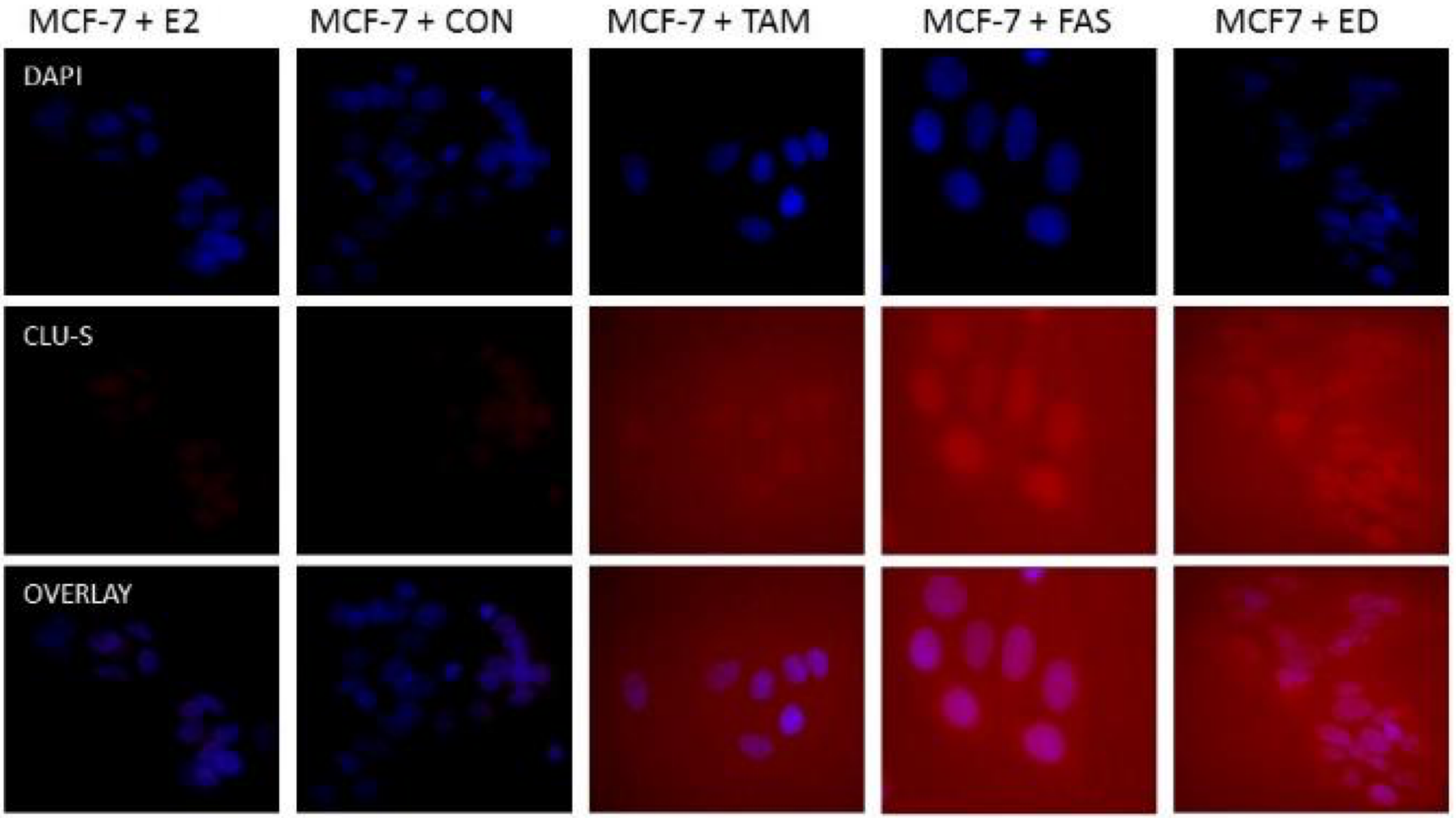

Figure 103 Immunofluorescence images of MCF-7 cells treated with oestradiol (E2; 10-9 M), untreated control (CON), tamoxifen (TAM; 10-7 M), fulvestrant (FAS; 10-7 M) and oestrogen deprivation (ED) for 7 days. Cells were stained with CLU-S/CLUα primary antibody, followed by staining with Alexa-fluor 594-conjugated secondary antibody (red) and counterstained with the nuclear dye DAPI (blue). Magnification: x63.

During antihormone resistance, a similar CLU-S cellular localisation profile was observed to antihormone response. Indeed, in the TAMR and XR cells, CLU-S was located both in the cytoplasm and nucleus (Figure 104). Interestingly, nuclear CLU-S appeared stronger, and cytoplasmic CLU-S appeared weaker, in the XR cells versus the TAMR cells.

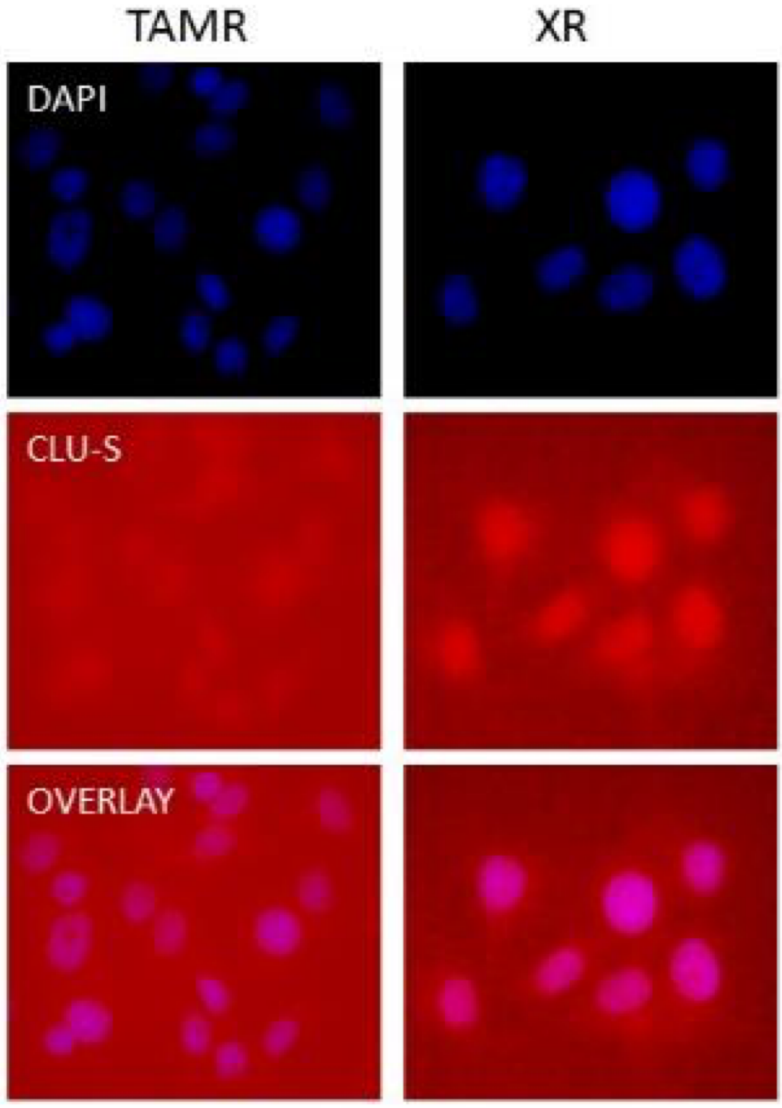

Figure 104 Immunofluorescence images of tamoxifen-resistant (TAMR) and oestrogen deprivation-resistant (XR) cells. Cells were stained with CLU-S/CLUα primary antibody followed by staining with Alexa-fluor 594-conjugated secondary antibody and counterstained with the nuclear dye DAPI (blue). Magnification: x63.

6.3.5.2 Cellular fractionation and subsequent Western blotting

CLU-S is a cytoplasmic secretory protein. However, immunofluorescence studies revealed equal expression of the protein in the nucleus and cytoplasm. Thus to verify this data, cellular fractionation and subsequent Western blotting studies were next performed in untreated MCF-7, TAMR and XR cells. In agreement with the immunofluorescence studies, very little CLU-S expression was detected in the untreated MCF-7 cells (Figure 105). Additionally, CLU-S expression was observed in the cytoplasm of TAMR and XR cells, however in contrast to the immunofluorescence data, very little CLU-S expression was apparent in the nucleus of such cells (Figure 105). The SP-1 nuclear transcription factor was used as a nuclear marker and as demonstrated in Figure 105 it was only expressed in the nucleus. However, although strongly expressed in the cytoplasm, some expression of the cytoplasmic marker, Grb2, was detected in the nucleus (Figure 105).

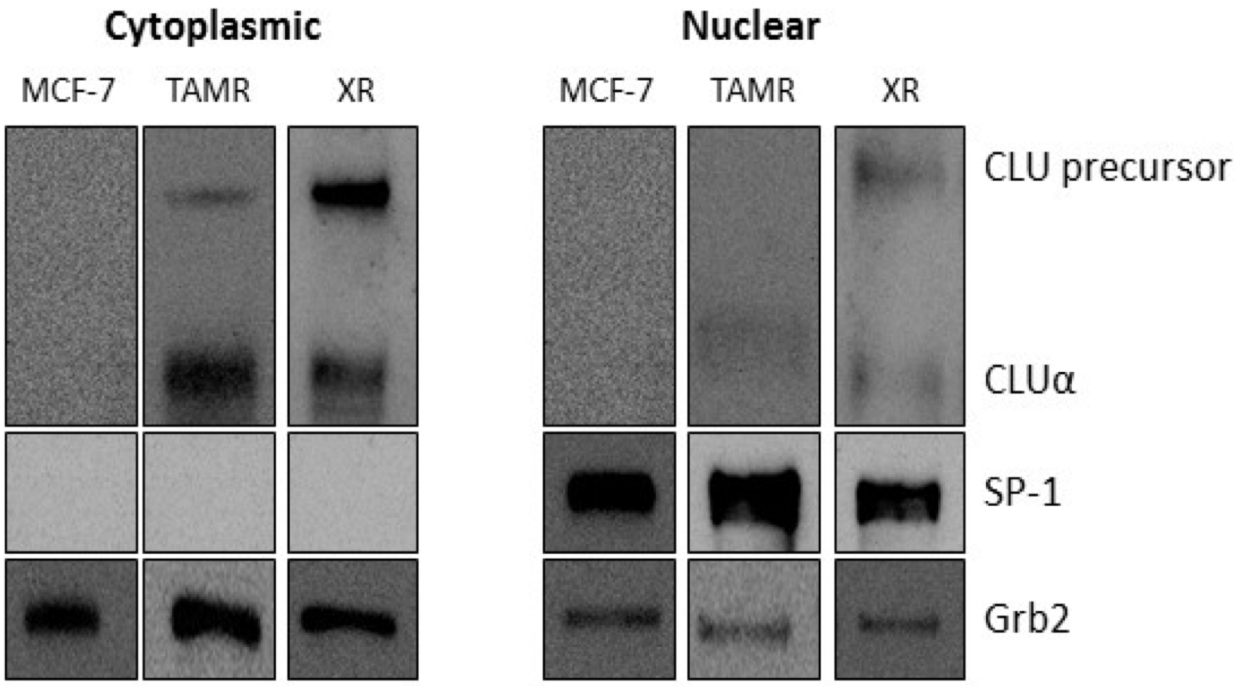

Figure 105 Representative Western blot images from three independent experiments showing pro-survival CLU isoform precursor and CLUα protein expression, SP-1 nuclear marker and Grb2 cytoplasmic marker in the cytoplasmic and nuclear fractions of untreated MCF-7, tamoxifen resistant (TAMR) and oestrogen deprivation resistant (XR) cells.

6.4 Discussion

Extensive microarray gene profiling, together with Western blotting, in Chapters 3 and 4 identified CLU as an antihormone-induced protein up regulated by all three antihormone treatments in four ER+ breast cancer cell lines, encompassing HER2+ and HER2- disease, with increased expression maintained through to the emergence of resistance. Thus, in this Chapter preliminary studies were performed to explore the hypothesis that CLU is a pro-survival gene, induced early during antihormone response and functions to allow a cohort of tumour cells to evade antihormone challenge, and subsequently contributes to the limited efficacy of these agents and ultimately the development of resistance.

CLU has been widely studied in breast cancer, where it has been demonstrated to promote cell survival, invasion and metastasis and ultimately contribute to poor patient survival[335,336]. However, the role of CLU during antihormone- response and -resistance remains largely unexplored. Initially, the expression of CLU in antihormone-resistant cell models was examined. The microarray gene expression profile of CLU in antihormone-resistant TAMR and XR cells was verified at the messenger and protein levels. However, in comparison to the microarray 'jetset' probe which was complementary to both nuclear and CLU-S isoforms, the PCR primers and CLU antibody were specific to the pro-survival CLU-S isoform. The CLU antibody recognised the CLUα chain together with the 60 kDa CLU precursor protein. In agreement with the microarray data, CLU-S mRNA and protein expression (CLUα and precursor) was increased in the XR cells versus control. Similarly, CLU-S protein expression (CLUα and precursor) in TAMR cells was up regulated versus control. Interestingly, CLU-S protein expression was markedly less in the TAMR cell line compared to the XR cells.

To consider the heterogeneity of breast cancer, CLU-S expression was also examined in a tamoxifen-resistant model derived from T47D cells. Similarly, CLU-S mRNA expression was increased in these resistant cells compared to control. However, at the protein level, relatively equal expression of the precursor, with a small increase in CLUα was apparent between the control and resistant cells. Interestingly, in contrast to the wild type MCF-7 cells, strong CLU precursor protein expression was apparent in the wild type T47D cells. Surprisingly, CLU

precursor protein was not apparent in untreated T47D cells cultured in FCS (as previously demonstrated in Chapter 4, Figure 50), but was apparent in untreated T47D cells cultured in sFCS. These differences are likely due to the growth factors present in FCS potentially cross-talking with the ER to promote CLU down regulation, which is not mediated in the presence of growth factor-depleted sFCS. In support of this, Chapter 4 previous revealed that CLU is ER regulated: E2 suppressed, and antihormones induced, CLU expression. Together, these studies demonstrate increased CLU-S expression in antihormone-resistant cells compared to parental control cells.

To our knowledge this is the first study to identify CLU expression in antihormone-resistant breast cancer cells. However, Toffanin et al. and Cappelletti et al. have reported increased CLU-S expression in antihormone-resistant T47D cells versus antihormone-sensitive MCF-7 cells[309,338]. Since 3 day tamoxifen and toremifene treatment led to an increase in T47D cell growth, the authors deemed the cell line antihormone resistant. However, this is in significant contrast to the literature, whereby T47D cells have been long established as antihormone sensitive. Indeed, E2 stimulates T47D cell proliferation which is inhibited by tamoxifen within 48 hours[405–407]. A clinical study examining the effects of toremifene in breast cancer patients prior to surgery revealed an association between increased CLU expression and poor antihormone response[309].

Following the identification of increased CLU-S expression in antihormone resistance, together with increased expression during antihormone response (as demonstrated in Chapters 3 and 4, Figure 38 and Figure 50), subsequent studies aimed to determine whether CLU-S expression contributed to the limited efficacy of antihormones and the consequent development of resistance. Transient CLU knockdown studies, utilising siRNA, were performed and the effect on growth of antihormone-treated and antihormone-resistant cells was examined. Since untreated MCF-7 and T47D cells express very little, if any, CLU-S, fulvestrant treatment was combined with siRNA to induce CLU-S expression to allow the effect of subsequent knockdown on cell growth to be determined. CLU knockdown was performed by incubating the cells for 2 days with siRNA prior to the addition of fulvestrant for a further 2 days. CLU-S knockdown was confirmed at the mRNA

level. Unfortunately, due to difficulties with Western blotting, CLU-S knockdown could not be verified at the protein level. Since this Western blot was performed towards the end of the project, it is possible that the CLU antibody may have lost its activity.

With regard to the antihormone-resistant cells, CLU-S is constitutively expressed, thus targeted gene knockdown was achieved by 4 day incubation with siRNA. CLU-S knockdown was confirmed at the messenger and protein levels of XR and T47D-TAMR cells, but could only be verified at the mRNA level in TAMR cells. This is not surprising, since protein expression of CLU-S was previously demonstrated to be very weak in this cell line compared to the other resistant cells. Importantly, CLU siRNA comprised of a pool of 4 siRNA complementary to different regions of the mRNA and therefore not specific to CLU-S. Since CLU-S and nuclear CLU have very similar mRNA sequences, apart from the latter lacking exon 2, it is strongly possible that this isoform was also targeted for knockdown. However, since CLU-S represents more than 99% of total CLU in MCF-7 cells[295], it is likely that down regulation of the nuclear isoform is insignificant.

Transient CLU knockdown resulted in a small decrease in fulvestrant-treated MCF-7 cell growth but was without effect on the growth of fulvestrant-treated T47D cells. This suggests that CLU/CLU-S may play a role in the limited efficacy of fulvestrant during antihormone response in MCF-7 cells and its targeting alongside antihormones may improve the growth inhibitory actions of these agents. The growth promoting role of CLU/CLU-S may be more enhanced following stable gene knockdown. However, CLU-S knockdown could not be verified at the protein level, as previously discussed. Therefore, it is possible that the magnitude of knockdown was greater in the MCF-7 cells versus the T47D cells, or perhaps the mRNA knockdown was not translated into knockdown at the protein level in the T47D cells. Alternatively, since more than 150 proteins are differentially expressed between both MCF-7 and T47D cells as previously discussed in Chapter 4[409], it is not surprising that CLU knockdown exerts different effects on the growth of both cell lines. Indeed, CLU may regulate the activity of a protein expressed only in the MCF-7 cells to promote cell growth, with such a protein mutated in T47D cells and therefore not regulated by CLU to promote cell growth. In agreement with these

findings, Redondo et al. have demonstrated a significant increase in cell death of tamoxifen-treated MCF-7 cells plus antisense CLU oligonucleotide versus tamoxifen treatment alone[339]. Similarly, down regulation of CLU-S via siRNA in tamoxifen-treated MCF-7 cells has been shown to promote a small decrease in cell growth[338].

Interestingly, CLU knockdown had no effect on the growth of antihormone-resistant cell models. This suggests that during response to fulvestrant, CLU transiently promotes the growth and/or survival of MCF-7 cells, possibly facilitating and allowing the re-organisation of cellular networks and the emergence of the dominant EGFR/HER2-driven MAPK and AKT signalling pathways to promote resistant cell growth. Toffanin et al. have reported a significant decrease in T47D (deemed antihormone-resistant, as previously discussed above) cell growth following CLU-S knockdown[338]. However, such effects were not significant in tamoxifen-treated T47D cells plus CLU-S knockdown, possibly due to tamoxifen-induced increased CLU-S expression in these cells. Interestingly, it was strongly apparent in Toffanin et al.'s study that down regulation of CLU-S in T47D cells promoted a greater effect on cell growth compared to knockdown of both the CLU-S and nuclear isoforms[338]. This suggests that the pro-apoptotic nuclear CLU form may play a role in T47D cells and may represent a larger percentage of total CLU present in this cell line compared to the <1% previously reported in MCF-7 cells[295]. Increased expression of pro-apoptotic nuclear CLU in T47D cells may have contributed to the lack of effect of CLU knockdown on the growth of T47D cells versus MCF-7 cells, since the nuclear isoform is likely to have been down regulated together with CLU-S. Thus, since this project is interested in the pro-survival role of CLU, further studies specifically down regulating the CLU-S isoform are necessary to precisely examine its role without contamination from the nuclear isoform. Such studies should include apoptosis assays and cell cycle analysis to determine whether CLU-S promotes cell survival (thus supporting the hypothesis that it is indeed a pro-survival gene) or cell proliferation during antihormone-response and –resistance.

Studies in triple negative breast cancer cell lines have reported a significant role for CLU-S in tumour growth and metastatic progression. Indeed, CLU-S was

demonstrated to promote cell survival via inhibiting apoptosis as well as increasing the ability of cells to survive the multiple stages of metastasis[337]. Similar roles of CLU-S may be identified in ER+ disease, or perhaps such unfavourable effects are confined to the more aggressive ER- phenotype. Interestingly, a strong link between HER2 signalling and CLU expression has been demonstrated in ER+/HER2+ BT474 breast cancer cells. Biroccio et al. demonstrated that trastuzumab treatment induces CLU protein expression in BT474 cells[408]. Furthermore, CLU inhibition increased the growth inhibitory action of trastuzumab together with increasing apoptosis, suggesting that CLU may exhibit a pro-survival role, induced by trastuzumab. Thus, it is plausible that antihormone-induced CLU-S expression may play a role in promoting cell survival which may be reversed by specific targeting of CLU-S alongside antihormone therapy. Similarly, in hormone-dependent prostate cancer, androgen withdrawal, chemotherapy and radiation therapy induce CLU-S expression, with such expression providing a protective role against apoptotic cell death and is therefore associated with disease progression[377,442,443]. Inhibition of CLU-S expression in prostate cancer cells enhances TNFα-mediated apoptosis[444], potentially identifying CLU-S as a valid target for new cancer treatment.

An antisense oligonucleotide blocking CLU-S mRNA, OGX-011, is currently in clinical development. In a Phase II trial of OGX-011 in combination with docetaxel in metastatic breast cancer, OGX-011 was well tolerated and decreased CLU levels, however the number of responses were limited and insufficient to meet the criteria for proceeding to the second stage of accrual[342]. This may be due in part to the limited sample size. In contrast, several trials have examined OGX-011 treatment in prostate cancer patients, with promising results. Indeed, in a Phase II trial of OGX-011 in combination with docetaxel and prednisone, in chemotherapy-naïve patients with metastatic castration-resistant prostate cancer (mCRPC), OGX-011 was well tolerated and markedly improved survival compared to docetaxel and prednisone alone (23.8 months versus 16.9 months)[382]. Similarly, in mCRPC patients progressing on first-line docetaxel, OGX-011 plus docetaxel (Phase II) was shown to be a feasible and safe second-line treatment, with

increased pain relief[445]. Subsequent Phase III trials evaluating OGX-011 in combination with chemotherapy in prostate cancer patients are underway.

Several studies have demonstrated potential mechanisms by which CLU promotes cell survival. For example, CLU has been reported to bind to the pro-apoptotic protein Bax, interfering with its activation and subsequently preventing downstream apoptosis[344]. Such an interaction between CLU and Bax, by co-immunoprecipitation, has been demonstrated in tamoxifen-treated MCF-7 cells[344]. Moreover, CLU has been shown to regulate NF-κB actions. In MCF-7 cells, overexpression of CLU-S has been demonstrated to promote NF-κB activation and transcription of downstream pro-survival genes, particularly BCL2, which subsequently prevents TNFα-induced apoptosis[446]. Targeted down regulation of the p65 subunit of NF-κB enhanced the sensitivity of CLU-S-overexpressing MCF-7 cells to TNFα-mediated apoptosis, confirming the significant role of p65/NF-κB in this pathway. Similarly, in prostate cancer cells, CLU-S has been reported to promote IκB degradation, thus allowing nuclear translocation of NF-κB and increasing transcription of genes implicated in cell survival and proliferation[349]. Another mechanism involved in CLU-S pro-survival activity is by modulating ERK1/2 activity[347]. ERK1/2 are members of the MAPK super family that mediate cell proliferation and survival and have been largely implicated in endocrine resistance[447–450]. In chemo resistant pancreatic cancer cells, CLU silencing via OGX-011 has been shown to re-sensitise the cells to chemotherapy via inhibition of chemotherapy-induced CLU-ERK1/2 activation[345]. Similarly in osteosarcoma cells, increased CLU-S expression has been reported to promote cell growth and increase chemo resistance via activation of ERK1/2 [347].

The functionally distinct CLU isoforms, involved in apoptosis and cell survival, are located in the nucleus and cytoplasm, respectively. Thus, to clarify the cellular localisation of CLU-S during antihormone-response and –resistance, immunofluorescence studies were performed. Unexpectedly, CLU-S (CLU precursor and CLUα) staining was identified equally in the cytoplasm and nucleus of MCF-7 cells treated with antihormones and in the TAMR and XR cell models. A major limitation of the fluorescence microscopy used in this project for distinguishing nuclear and cytoplasmic protein expression is the contribution of

signals from structures above and below the plane of focus as a result of illuminating the whole specimen[451] i.e. the fluorescent signal from the cytoplasm above and below the nucleus. Therefore, it is possible that the nuclear staining of CLU-S observed was indeed that from the cytoplasm. Possible means of circumventing this limitation are confocal microscopy and nuclear and cytoplasmic fractionation with subsequent Western blotting. The latter was next performed on untreated MCF-7, TAMR and XR cells to verify the cellular localisation of CLU-S. Interestingly in contrast to the immunofluorescence data, such studies revealed cytoplasmic expression of CLU-S (CLU precursor and CLUα) protein in TAMR and XR cells with very little expression observed in the nuclear extracts. Therefore, it is very likely that the above-mentioned limitation of the fluorescene microscopy contributed to the nuclear staining of CLU-S observed. Small levels of Grb2 protein, the cytoplasmic marker, were detected in the nuclear fractions, and thus the CLU-S apparent in the nuclear fraction, particularly in the XR cells, may reflect contamination from the cytoplasmic fraction proteins. Cellular fractionation studies are required to verify the localisation of CLU-S during antihormone-response. It is hypothesised that such studies would identify cytoplasmic expression of CLU-S.

Collectively, this Chapter has built on the data presented in Chapter 4, and demonstrated that antihormone-induced CLU-S expression is maintained through to the acquisiton of resistance. However, the role of CLU-S remains largely unexplored. Early induction of CLU-S was hypothesised to promote cell survival and consequently allow a cohort of cells to evade antihormone challenge, ultimately contributing to the emergence of resistant cell growth. CLU knockdown studies revealed a potential role for CLU in limiting the growth inhibitory actions of fulvestrant during antihormone-response in MCF-7 cells. Such effects were only transient and were not demonstrated during antihormone-resistance. Similarly, such effects were not demonstrated during antihormone-response or –resistance in the T47D cell line. However, since the CLU siRNA likely targeted both the pro-survival CLU-S and pro-apoptotic nuclear CLU isoforms, it is possible that downregulation of the latter obscured the growth inhibition induced by CLU-S knockdown. Additionally, T47D cells may express greater nuclear CLU to the

MCF-7 cells, potentially explaining the differences of CLU knockdown on fulvestrant-treated cell growth. Although cellular localisation studies via immunofluorescence identified equal nuclear and cytoplasmic expression of CLU-S (precursor and CLUα) in antihormone-treated and antihormone-resistant MCF-7 cells, subsequent cellular fraction and Western blotting, confirmed cytoplasmic expression of CLU-S protein during resistance. Further studies are necessary to confirm such localisation of the CLU-S protein during antihormone response.

It is unquestionable that further studies are required to precisely examine the role of the CLU-S isoform. Such studies include designing a siRNA specific to CLU-S, or more preferably inducing stable CLU-S gene knockdown. Additionally, cell cycle analysis and apoptosis assays could be performed to determine whether CLU-S is indeed a survival protein and/or promotes dysregulation of the cell cycle. Several studies have identified a role for CLU-S in activating NF-κB-mediated gene transcription and ERK1/2 signalling to promote cell survival and prolfieration. Thus, further studies could explore these potential cell survival pathways regulated by CLU-S. Such studies could include NF-κB reporter gene assays and examination of phosphorylated-ERK1/2 expression in CLU-S-knockdown cells. Since CLU-S is a secretory protein, its expression in the culture media should also be examined. Such studies may identify CLU-S as a therapeutic target in ER+ breast cancer to enhance endocrine response or reverse the resistant phenotype, or as a novel biomarker indicative of endocrine therapy outcome.

7 Conclusion and future studies

Although antihormones are the mainstay treatment for ER+ breast cancer and have contributed to a substantial decrease in mortality over recent decades, their growth inhibitory actions are compromised by the emergence of resistance. More than 40% of ER+ patients acquire resistance and virtually all advanced disease patients eventually relapse. In both instances, resistance is characterised by accelerated tumour growth and increased aggressive behaviour, together resulting in poorer patient outlook. Therefore, it is crucial to understand the complexities of the underlying mechanisms of resistant growth to provide novel therapeutic options for such patients and ultimately improvement in patient outcome.

Several mechanisms of endocrine resistance have been proposed. Of which, the most extensively studied is the alteration of ER expression and activity. Indeed, approximately 20% of antihormone-treated ER+ patients lose expression of the receptor and as such become insensitive to antihormone therapy[115,116]. The mechanisms involved in causing down-regulation or complete loss of the ER include hypermethylation of the ER promoter, MAPK-induced ER down regulation and microRNA-mediated ER down regulation[117,118,120,123]. ER activity is deregulated by a shift in the balance of coactivators and corepressors. Coactivators function to enhance ER-mediated gene transcription and overexpression of such proteins can directly influence the agonistic versus antagonistic activities of SERMs including tamoxifen, thus enhancing their agonistic activity, ultimately leading to resistance. Indeed, overexpression of the ER coactivator AIB1 is associated with increased relapse and death of tamoxifen-treated patients with HER3-overexpressing tumours[133,134].

Hyperactivation of growth factor signalling pathways has been heavily implicated in driving resistant cell growth. Increased expression of the RTKs EGFR, HER2 and IGF-1R have been demonstrated in endocrine-resistance cell lines and clinical samples[184–188]. Besides the capacity to promote cell growth in their own right, such signalling can also phosphorylate and subsequently activate the ER and its co-regulatory proteins, increasing the receptor transcriptional activity, ultimately promoting antihormone-resistant cell growth. Such signalling circumvents the

inhibitory effects of antihormones via bidirectional cross-talk and modulation of the ER to promote re-expression of oestrogen regulated genes in a ligand-independent manner and in the presence of antihormones[190,191]. Paradoxically, sustained hyperactivation of growth factor signalling has also been associated with reducing ER expression, and thus such cells do not respond to further antihormone therapy, indicating a loss of reliance on ER-mediated growth[121].

There is a large body of evidence implicating the role of antihormone-induced compensatory signalling as a mechanism of endocrine resistance. Surprisingly, upon E2 challenge the majority (70%) of oestrogen-regulated genes are repressed in ER+ breast cancer cells[38]. However, many of these oestrogen-suppressed genes are anti-proliferative and pro-apoptotic. The benefit of antihormone therapy therefore arises by counteracting these E2-induced repressive events, thus triggering re-expression of these negative regulators of cell proliferation[259]. Indeed, the main mechanism of action of antihormones is to inhibit cell proliferation and as such these agents are very anti-proliferative. However, antihormones are not particularly pro-apoptotic and are unable to promote significant levels of cell death[216]. The weak pro-apoptotic activity of antihormones may reflect a significant capacity for induction of pro-survival mechanisms by such agents during response. Such events may limit the anti-tumour activity of antihormones and provide a mechanism to aid cells to survive the initial impact of these agents and subsequently promote the emergence of resistant growth.

This inductive capacity of antihormones may be a double-edged sword, since more recent research has revealed that these agents can induce, and oestrogens suppress, genes involved in cell proliferation and survival[197,216,259]. One such gene that has been largely studied is the EGFR. Oestrogen suppresses EGFR at the transcriptional level in ER+ breast cancer cell models[260,261], and in turn, tamoxifen induces EGFR expression in ER+ MCF-7 cells during antihormone response, with such an effect observed from as early as one week of treatment[216]. EGFR-activated MAPK and AKT pathways cross-talk with, and phosphorylate, the ER to maintain transcriptional activation. Subsequent expression of the ER-regulated pro-survival gene BCL2 has been demonstrated, thus potentially allowing cells to escape growth

inhibition. As such, the anti-tumour activities of tamoxifen are incomplete, with only partial anti-proliferative effects and minimal induction of apoptosis demonstrated[216]. Following three months of tamoxifen treatment, increased EGFR expression is maintained in MCF-7 cells with substantial downstream kinase activity. Interestingly, these events parallel the emergence of tamoxifen resistance coincident with restoration of ER activity and expression of ER-regulated growth factor ligands, particularly the EGFR ligand amphiregulin[196]. Consequently, a self-propagating EGFR-driven autocrine growth-regulatory loop is generated in these cells, in which amphiregulin expression is induced by ligand-independent ER phosphorylation. Together, early tamoxifen-induced EGFR expression limits the anti-tumour response and provides protective mechanisms to a cohort of cells from which resistance subsequently emerges. In addition to EGFR, HER2 has also been established as oestrogen-suppressed and antihormone-induced in a panel of ER+ breast cancer cell lines[217]. Antihormones also induce expression of the pro-invasive genes, RhoE and δ-catenin, with expression maintained through to the acquisition of resistance, potentially contributing to the small antihormone-induced invasiveness observed in MCF-7 cells [304,305].

Despite considerable evidence implicating the role of antihormone-induced pro-proliferative genes contributing to the emergence of endocrine resistance, the role played by antihormone-induced pro-survival genes remains largely unexplored. Antihormones have been shown to promote activation of the pro-survival gene AKT in MCF-7 cells with such activation associated with decreased sensitivity of these cells to the growth inhibitory action of these agents [246,262–264]. This is complemented by studies of antihormone-treated tumour specimens which revealed a correlation between shorter disease free survival and activated AKT, supporting the link between the AKT pathway and antihormone failure[265]. Tamoxifen and oestrogen deprivation (mimicking AI therapy) treatments have also been shown to induce expression of the pro-survival gene BCL2, thus decreasing the anti-tumour responses to these agents[267,269]. More recently, increased expression of the pro-survival gene 14-3-3ζ has been associated with antihormone resistance. Down regulation of 14-3-3ζ in

endocrine-resistant cells led to the restoration of antihormone sensitivity, with parallel reduction in the expression of pro-proliferative and pro-survival genes[270].

Although these studies are limited, they reveal promising results for the role of antihormone-induced pro-survival genes in the development of endocrine resistance. Certainly, further studies are required to identify and characterise novel antihormone-induced pro-survival genes early during response that may limit the pro-apoptotic actions of antihormones and allow a cohort of cells to evade the growth inhibitory actions of these agents, resulting in anti-tumour response of finite duration and ultimately the emergence of resistant cell growth. Such findings may provide novel therapeutic strategies to delay, reverse or ultimately prevent the development of resistance. To this regard, this thesis has explored the role of antihormone-induced pro-survival genes in ER+ breast cancer cell lines, whose expression may contribute substantially to the emergence of resistance and investigated the potential of targeting such genes. The aims of this study were:

i) to identify novel pro-survival genes induced by currently-used endocrine therapies (tamoxifen, fulvestrant and oestrogen deprivation) via Affymetrix microarray gene expression profiling
ii) to determine whether the expression of such genes persist into the acquisition of resistance
iii) to determine whether such genes contribute to the limited efficacy of antihormones and subsequently the development of resistance.

Initially, a stringent filtering process was utilised to maximise the identification of the most robust antihormone-induced pro-survival genes (n=248; identified by ontology and website resources) via Affymetrix microarray gene expression profiling of ER+ MCF-7 cells following 10 day antihormone treatment (Chapter 3). The key filtering stages included:

- genes with a consistent expression profile observed for all of the gene probes representing that gene
- genes with a ‘marginal’ or ‘present’ detection call, signifying partial and reliable detection of gene expression, respectively, in at least one antihormone treatment and resistant cell line

- genes up regulated by antihormone treatment and maintained into the appropriate resistant setting (e.g. tamoxifen and TAMR)
- genes significantly ($p < 0.05$) induced by at least one antihormone treatment versus control
- genes induced by a fold change greater than 1.5 by at least one antihormone treatment versus control

Together, this stringent filtering process identified 14 genes significantly up regulated by at least one antihormone treatment during response, with expression maintained into antihormone resistance. Such genes included those involved in signal transduction (GABBR2, CXCR4, AKT1 and PSEN1) and the NF-κB cascade (BCL3 and ERC1) as well as chaperone proteins (BAG1 and CLU), the survivn co-factor HBXIP, the cell adhesion protein CTNND2, the caspase inhibitor BCL2L1; in addition to the nitric oxide generator DDAH2, the small leucine zipper protein TSC22D3 and IGFBP5 which regulates IGF activity.

It was hypothesised that these antihormone-induced genes may allow a cohort of cells to survive the growth-inhibitory actions of these agents early during response and subsequently contribute substantially to the emergence of resistance and ultimately poorer patient outcome. The majority of the microarray profiles of the 14 genes were successfully verified by RT-PCR, with the exception of BAG1, DDAH2 and HBXIP, which showed similar levels of RNA expression following E2-control and antihormone treatments. Additionally, RT-PCR verification of IGFBP5 continued to fail, with no mRNA expression detected. This was likely due to the PCR primers recognising an alternative region of mRNA to that recognised by the probes on the Affymetrix gene chip.

The genes of particular interest and therefore considered for further investigation were those significantly induced by all three antihormone treatments (i.e. tamoxifen, fulvestrant and oestrogen deprivation). The rationale was that further study of these genes may identify an antihormone-induced resistant mechanism common to three antihormone therapies used clinically. Such genes may ultimately provide a novel biomarker indicative of treatment response or a therapeutic target common to resistance to all three antihormones and thus offering a therapeutic

option to a significant cohort of breast cancer patients. These genes were: GABBR2, CTNND2, CLU, TSC22D3 and BCL3. The Affymetrix microarray profiles of these 5 genes in short-term antihormone-treated MCF-7 cells were verified at the mRNA and protein level by RT-PCR and Western blotting. However due to the lack of available antibodies, CTNND2 expression could not be verified at the protein level. Increased expression of these genes has been identified in several cancers, including breast, prostate and ovarian, and ontological investigation confirmed tumour-promoting functions[317,329,336,354,360]. However, very few studies have demonstrated their induction by antihormones in breast cancer and have explored their potential role in limiting antihormone-response and promoting the acquisition of resistance.

Breast cancer has been long established as a heterogeneous disease and it is becoming increasingly recognised that the use of the MCF-7 cell line to represent all ER+ breast cancer is insufficient. Genomic studies have established four major subtypes of breast cancer with each subtype exhibiting a disparate prognosis and treatment response partly due to inherent genetic differences between the subtypes[277,278]. These subtypes include luminal A (ER+/HER2-), luminal B (ER+/HER2+), basal (ER-/HER2-) and HER2 (ER-/HER2+).

To better reflect this heterogeneity, equivalent examination of GABBR2, CTNND2, CLU, TSC22D3 and BCL3 was performed during antihormone response in a panel of four ER+ breast cancer cell lines with differing HER2 status, thus encompassing luminal A and luminal B subtypes (Chapter 4). All three antihormone treatments induced increased mRNA and protein expression of these genes in ER+/HER2- MCF-7 and T47D and ER+/HER2+ BT474 and MDA-MB-361 cell lines, with the exception of GABBR2 in T47D cells. Additionally, as in Chapter 3, CTNND2 protein expression could not be detected. These key findings suggest that all three antihormones induce expression of common pro-survival genes in luminal A and luminal B subtypes. Furthermore, common resistant mechanisms may be induced by all three antihormone therapies in these breast cancer subtypes. Further study of the most robust candidate genes could prove significant in identifying biomarkers of limited response or targets for novel therapeutic strategies to enhance antihormone response and significantly delay, prevent or reverse the

development of resistance. The most promising genes (BCL3 and CLU) were subsequently taken forward for investigation.

BCL3 is a nuclear protein and belongs to the family of IκB proteins that function to inhibit the activity of NF-κB transcription factors[358]. In unstimulated cells, IκB proteins sequester NF-κB in the cytoplasm, preventing their nuclear translocation and downstream transcriptional activation of a large number of genes involved in cell survival and proliferation[358]. Upon stimulation via several stimuli, including growth factors, IκB is degraded by IκB kinase, thus allowing translocation of NF-κB dimers into the nucleus where they bind to DNA at specific NF-κB response elements to activate gene transcription[414,415]. The NF-κB family consists of five members: RelA, RelB and cRel proteins contain a transactivation domain at the C-terminus thus facilitating the recruitment and displacement of coativators and corepressors, respectively, necessary for transcriptional activation; however p50/NFKB1 and p52/NFKB2 proteins lack transactivation domains and thus such homodimers are inactive and unable to drive gene transcription[414]. BCL3 functions to provide transactivating domains to these otherwise inactive homodimers to activate transcription of cell growth and survival genes[372].

Antihormone-induced BCL3 protein expression in a panel of ER+ breast cancer cell lines was maintained through to the acquisition of resistance as demonstrated in short-term (i.e. 6 months) TAMR and XR cell models derived from MCF-7 cells and T47D TAMR cell models. Furthermore, BCL3 expression was maintained in long term (3 years) resistance (TAMR and XR) cell models derived from MCF-7, T47D, BT474 and MDA-MB-361 cells (Chapter 5). In support of these findings, a previous study has also demonstrated increased BCL3 expression in ER+, E2-independent MCF-7 cells versus the parental cell line[363]. Subsequent studies aimed to establish whether BCL3 expression correlated with, and ultimately contributed to, the limited efficacy of antihormones and the consequent development of resistance. However, in contrast to what was first hypothesised, a pro-survival role of BCL3 during antihormone response and resistance was not identified. This is in disagreement with the literature which supports a role for BCL3 in the survival of breast cancer cells. The mechanisms proposed by which BCL3 promotes cell survival in breast cancer cells include stabilisation of the anti-apoptotic protein

CtBP1 which represses the transcription of pro-apoptotic genes, as well as BCL3-mediated inhibition of the tumour suppressor gene, p53[367,368]. However, the survival role of BCL3 was assessed in this thesis by siRNA mediated BCL3 knockdown in antihormone responsive and resistant cells. It is possible that such transient knockdown is insufficient to promote significant apoptosis, which may be apparent with stable gene knockdown.

Interestingly, targeted down regulation of BCL3 by siRNA was associated with a substantial decrease in the growth of TAMR and to a lesser degree XR cells, but was without an effect on the growth of T47D-TAMR and antihormone-responsive cells. These findings suggest that BCL3 may play a role in promoting TAMR and XR cell growth with no such effect apparent in the T47D TAMR cells or during antihormone response. However, BCL3 knockdown could not be verified at the protein level in the T47D TAMR cells, potentially explaining why no effect on cell growth was observed. In contrast to these findings, BCL3 has previously been demonstrated to enhance the growth of MCF-7 cells *in vivo*[363]. However, there are significant experimental differences between these studies, likely contributing to the contrasting results. Indeed, Pratt et al.'s study utilised a stable BCL3 expressing system and was performed *in vivo* and therefore likely influenced by the stroma and tumour microenvironment. In contrast, in our study BCL3 expression was induced by fulvestrant treatment and cells were exposed to a transient increase in gene expression. It is possible that long term BCL3 expression contributes to the re-organisation of the cellular networks to promote cell growth which would not be possible following short term BCL3 exposure. Thus, it is feasible that with long-term BCL3 expression an increase in cell growth of antihormone-treated MCF-7 cells may be observed. Cell cycle studies were performed to investigate whether BCL3 promotes TAMR and XR cell growth via dysregulation of the cell cycle. However, such studies failed to identify such a role for BCL3. Unquestionably, stable BCL3 knockdown is required to more effectively examine the effects of BCL3 on cell survival, cell proliferation and the cell cycle.

The association between BCL3 and activation of NF-κB-mediated gene transcription was examined. Interestingly, p50/NFKB1 expression was observed in MCF-7 and T47D cells ± E2 and antihormone treatments, and also in the TAMR,

XR and T47D TAMR cell lines. However, p52/NFKB2 expression was not detected in antihormone-responsive or resistant cell lines. These findings suggest that p50/NFKB1 is expressed alongside BCL3 during antihormone response and in resistance, supporting the hypothesis that BCL3 co-activates p50/NFKB1 homodimers to promote transcription of target genes. In agreement with these findings, previous studies have demonstrated p50/NFKB1 expression in MCF-7 and T47D cells, in addition to tamoxifen resistant cells, but failed to identify p52/NFKB2 expression[358,360,423]. Immunofluorescence and immunoprecipitation studies revealed nuclear localisation and direct association of BCL3 and p50/NFKB1 in TAMR and XR cells thus suggesting that BCL3 co-activates p50/NFKB1 homodimers to promote NF-κB-mediated gene transcription and ultimately cell growth. Although immunoprecipitation studies revealed an association between both proteins in T47D TAMR cells, immunofluorescence studies demonstrated cytoplasmic expression of both proteins. Since p50/NFKB1 must be located in the nucleus to bind to DNA and activate gene transcription, it is unlikely that such an event was occurring in the T47D TAMR cells. This supports the absence of BCL3-mediated cell growth demonstrated in these cells, likely due to cytoplasmic localisation of BCL3 and p50/NFKB1 proteins, thus not activating NF-κB-mediated gene transcription and subsequent cell growth.

During antihormone response in MCF-7 cells, BCL3 was predominantly located in the nucleus and p50/NFKB1 was predominantly located in the cytoplasm and thus were not associated. This mirrors the cell growth studies which demonstrated that BCL3 had no effect on the growth of fulvestrant-treated MCF-7 cells. Surprisingly, both proteins were co-located in the nucleus of antihormone-treated T47D cells, however immunoprecipitation studies failed to identify a direct association between them. Additionally, cell growth studies demonstrated that BCL3 does not promote the growth of fulvestrant-treated T47D cells. Therefore it is likely that rather than co-activating p50/NFKB1 homodimers in fulvestrant-treated T47D cells, BCL3 functions to repress NF-κB activation by promoting the binding of inactive p50/NFKB1 homodimers to the κB sites on DNA, to prevent the binding of transactivating dimers[429,430].

Further studies, including a NF-κB reporter gene assay, are required to confirm p50/NFKB1 homodimer activation in TAMR and XR cells in addition to ChIP sequencing which would identify the potential pro-proliferative and pro-survival genes regulated by such transcriptional activation. Furthermore, examination of the other NF-κB subunits which contain a transactivation domain would confirm whether they are involved in the predicted NF-κB activity apparent in TAMR and XR cells.

The second antihormone-induced protein of interest, CLU, was studied in Chapter 6. CLU is a ubiquitously expression glycoprotein involved in several physiological processes important for tumorigenesis, including apoptosis and cell cycle regulation[371,431,432]. CLU exists as two main isoforms: nuclear CLU and cytoplasmic CLU-S. The former functions to promote cell death whereas the latter promotes cell survival. A previous study has demonstrated that CLU-S represents the most abundant isoform in MCF-7 cells, with approximately 0.01% represented by the nuclear isoform[295].

Increased CLU-S protein expression was demonstrated in TAMR, XR and T47D TAMR cells. Interestingly, CLU expression was associated with a small induction in fulvestrant-treated MCF-7 cell growth but was without effect on the growth of fulvestrant-treated T47D cells. However, due to difficulties with Western blotting, CLU-S knockdown was not confirmed at the protein levels in these cells. Therefore, it is possible that the conditions were not optimum for CLU-S knockdown in the T47D cells. In support of these findings, down regulation of CLU-S via siRNA in tamoxifen treated MCF-7 cells has been demonstrated to promote a small decrease in cell growth[338]. Additionally, in ER+/HER2+ BT474 cells, trastuzumab has been shown to increase CLU expression with an associated increase in cell survival[408]. However, CLU was without effect on the growth of our antihormone-resistant cells. This suggests that during antihormone-response CLU may transiently promote the growth and/or survival of MCF-7 cells, possibly promoting the reprogramming of intracellular signalling networks and the emergence of dominant EGFR/HER2-driven MAPK and AKT signalling pathways to promote resistant cell growth. Although CLU knockdown resulted in a substantial decrease in CLU-S expression, the CLU siRNA utilised was comprised of a pool of siRNA and thus not

specific to the CLU-S isoform. Therefore it is possible that nuclear CLU was also targeted for knockdown. However, as mentioned above, the majority of CLU present in MCF-7 cells is the secretory cytoplasmic isoform. Further studies, including specific CLU-S stable knockdown and cell survival assays are required to confirm whether this protein promotes cell survival, thus allowing cells to evade the growth inhibitory actions of antihormones and ultimately promote the emergence of antihormone-resistant cell growth.

Together, this thesis has demonstrated that antihormone-induced events, particularly the induction of pro-proliferative and pro-survival genes may be a mechanism involved in the emergence of endocrine resistance. Indeed, this study identified induction of CLU expression by short term antihormone treatment, with such induction potentially involved in promoting the growth of breast cancer cells during antihormone response, thus limiting the anti-tumour activities of these agents and possibly facilitating the re-organisation of cellular networks and the emergence of dominant MAPK and AKT signalling pathways to promote resistant cell growth. The potential growth-promoting role of CLU was transient, with such an effect not apparent in the endocrine resistant cell models. The second gene, BCL3, was also induced by short term antihormone treatment, however in contrast to CLU, BCL3 may play a role in promoting resistant cell growth but is without effect on the growth of cells during antihormone response. The role of BCL3 during response remains to be elucidated.

Although such inductive events are complex with multiple pathways induced by antihormones, as demonstrated by the several antihormone-induced genes identified in this study as well as the more established EGFR and HER2 proteins with subsequent activation of downstream MAPK and AKT pathways; this thesis has demonstrated that common genes can be up regulated by several antihormones in multiple cell types. Therefore, targeting these genes and treating resistant disease may be possible and an effective therapy, despite the complexity surrounding antihormone-induced events.

Although this thesis has identified a role for antihormone-induced BCL3 in promoting resistant cell growth and BCL3 appears a promising target for novel

therapies to decrease/prevent resistant cell growth, it is clear that antihormone-induced deregulation of single genes fails to fully explain the limited response to antihormones and subsequent development of resistance. Identification of the additional mechanisms contributing to limited endocrine response and resistance (perhaps involving antihormone-induction of the other genes identified in this thesis) may allow novel therapies to be devised targeting multiple pathways simultaneously to maximise therapeutic response to antihormones. From the findings of our study, it is possible that common pathways are activated by several antihormone therapies in multiple cell types and therefore targeting such pathways may be an effective therapy for several breast cancer subtypes treated with several antihormone therapies. The findings of this thesis further support the rationale for studying the inductive capacity of antihormones and in particular the induction of pro-survival and pro-proliferative genes as a mechanism of endocrine resistance.

Significantly, breast cancer is a highly heterogeneous disease and although this study utilised several cell lines, encompassing HER2+ and HER2- disease, equivalent investigations in additional cell lines to further reflect this heterogeneity are necessary. Additionally, the Breast Cancer Molecular Pharmacology Group have also developed (short-term) acquired tamoxifen- and fulvestrant-resistant cell models in BT474 and MDA-MB-361 cells, as well as the long-term resistant cell models briefly examined in Chapter 5. These models were not extensively studied in this thesis, but future work in such models may validate the findings presented here. Furthermore, although human breast cancer cell lines are powerful experimental tools, they do not take into account the tumour microenvironment, paracrine signalling and complex inter-relationships that exist between cells *in vivo*. Additionally, the ontology of some genes identified in this project suggested a greater role in the *in vivo* setting e.g. CXCR4. Therefore, it is unquestionable that further examination in *in vivo* models would prove beneficial and will also address characteristics unique to the *in vivo* setting (e.g. hypoxia and angiogenesis), which may contribute to limited antihormone responses. Over recent years unprecedented developments in cancer organoids as pre-clinical cancer models have been observed. Tumour-derived organoids are cultured in

vitro and maintain their genetic integrity over months in culture[452]. Organoids display hallmarks of the original tumour, including the 3 dimensional architecture and the ability to self-renew. Additionally, organoids recapitulate molecular features of the original tumour and can model clinically relevant drug responses[453,454]. Therefore, it is unquestionable that the establishment of breast cancer organoids will provide a powerful new tool for biomarker identification and drug development.

Ideally, to further verify the genes of interest as biomarkers or promoters of limited antihormone response, consecutive tumour samples at baseline and during neoadjuvant antihormone therapy are required. However, this would be a burden for the patient and is therefore almost impossible. Additionally, neoadjuvant therapy is usually short-term and therefore such studies would not address the long-term responses to a drug. To overcome these issues, non-invasive methods are required for monitoring tumour genomes and identifying biomarkers at various time points during the course of disease. To this end, circulating tumour cells and tumour DNA have been identified in the bloodstream which are shed from primary and metastatic tumours and are potential surrogates for the tumour itself[455]. Thus, analysis of such cells in the blood may provide a suitable non-invasive tool for examining sequential samples during therapy and obtaining genetic follow-up data that are urgently needed.

8 References

1. Cancer Research UK. Breast cancer. Available at http://www.cancerresearchuk.org. Accessed on 15th June 2015.

2. Travis, R. C. & Key, T. J. Oestrogen exposure and breast cancer risk. *Breast cancer Res.* **5,** 239–47 (2003).

3. Kaaks, R. *et al.* Postmenopausal serum androgens, oestrogens and breast cancer risk: the European prospective investigation into cancer and nutrition. *Endocr. Relat. Cancer* **12,** 1071–82 (2005).

4. Million Women Study Collaborators. Breast cancer and hormone-replacement therapy in the Million Women Study. *Lancet* **362,** 419–27 (2003).

5. Collaborative Group on Hormonal Factors in Breast Cancer. Breast cancer and hormone replacement therapy: collaborative reanalysis of data from 51 epidemiological studies of 52,705 women with breast cancer and 108,411 women without breast cancer. Collaborative Group on Hormonal Factors in Breast Cancer. *Lancet* **350,** 1047–59 (1997).

6. Collaborative Group on Hormonal Factors in Breast Cancer. Breast cancer and hormonal contraceptives: collaborative reanalysis of individual data on 53 297 women with breast cancer and 100 239 women without breast cancer from 54 epidemiological studies. *Lancet* **347,** 1713–27 (1996).

7. Collaborative Group on Hormonal Factors in Breast Cancer. Breast cancer and breastfeeding: collaborative reanalysis of individual data from 47 epidemiological studies in 30 countries, including 50302 women with breast cancer and 96973 women without the disease. *Lancet* **360,** 187–95 (2002).

8. Lichtenstein, P. *et al.* Environmental and Heritable Factors in the Causation of Cancer — Analyses of Cohorts of Twins from Sweden, Denmark, and Finland. *N. Engl. J. Med.* **343,** 78–85 (2000).

9. Pharoah, P. D., Day, N. E., Duffy, S., Easton, D. F. & Ponder, B. A. Family history

and the risk of breast cancer: a systematic review and meta-analysis. *Int. J. Cancer* **71,** 800–9 (1997).

10. Antoniou, A. *et al.* Average risks of breast and ovarian cancer associated with BRCA1 or BRCA2 mutations detected in case Series unselected for family history: a combined analysis of 22 studies. *Am. J. Hum. Genet.* **72,** 1117–30 (2003).

11. Siegel, R., Naishadham, D. & Jemal, A. Cancer statistics, 2013. *CA. Cancer J. Clin.* **63,** 11–30 (2013).

12. Antoniou, A. C. *et al.* Breast-cancer risk in families with mutations in PALB2. *N. Engl. J. Med.* **371,** 497–506 (2014).

13. Lee, A. V, Weng, C. N., Jackson, J. G. & Yee, D. Activation of estrogen receptor-mediated gene transcription by IGF-I in human breast cancer cells. *J. Endocrinol.* **152,** 39–47 (1997).

14. Hankinson, S. E., Colditz, G. A. & Willett, W. C. Towards an integrated model for breast cancer etiology: the lifelong interplay of genes, lifestyle, and hormones. *Breast Cancer Res.* **6,** 213–8 (2004).

15. Preston-Martin, S., Pike, M. C., Ross, R. K., Jones, P. A. & Henderson, B. E. Increased cell division as a cause of human cancer. *Cancer Res.* **50,** 7415–21 (1990).

16. Henry, J. A., Angus, B. & Horne, C. H. Oestrogen receptor and oestrogen regulated proteins in human breast cancer: a review. *Keio J. Med.* **38,** 241–61 (1989).

17. Love, R. R. & Philips, J. Oophorectomy for breast cancer: history revisited. *J. Natl. Cancer Inst.* **94,** 1433–4 (2002).

18. Beatson, G. On the treatment of inoperable cases of carcinoma of the mamma: suggestions for a new method of treatment, will illustrative cases. *Lancet* **148,** 162–165 (1896).

19. Ring, A. & Dowsett, M. Mechanisms of tamoxifen resistance. *Endocr. Relat.*

Cancer **11,** 643–58 (2004).

20. Green, S. *et al.* Human oestrogen receptor cDNA: sequence, expression and homology to v-erb-A. *Nature* **320,** 134–9 (1986).

21. McGuire, W. L. Current status of estrogen receptors in human breast cancer. *Cancer* **36,** 638–44 (1975).

22. Mosselman, S., Polman, J. & Dijkema, R. ER beta: identification and characterization of a novel human estrogen receptor. *FEBS Lett.* **392,** 49–53 (1996).

23. Kumar, V. *et al.* Functional domains of the human estrogen receptor. *Cell* **51,** 941–51 (1987).

24. Skafar, D. F. & Koide, S. Understanding the human estrogen receptor-alpha using targeted mutagenesis. *Mol. Cell. Endocrinol.* **246,** 83–90 (2006).

25. Hall, J. M. & McDonnell, D. P. The estrogen receptor beta-isoform (ERbeta) of the human estrogen receptor modulates ERalpha transcriptional activity and is a key regulator of the cellular response to estrogens and antiestrogens. *Endocrinology* **140,** 5566–78 (1999).

26. Kumar, R. *et al.* The dynamic structure of the estrogen receptor. *J. Amino Acids* **2011,** 812540 (2011).

27. Couse, J. F., Lindzey, J., Grandien, K., Gustafsson, J. A. & Korach, K. S. Tissue distribution and quantitative analysis of estrogen receptor-alpha (ERalpha) and estrogen receptor-beta (ERbeta) messenger ribonucleic acid in the wild-type and ERalpha-knockout mouse. *Endocrinology* **138,** 4613–21 (1997).

28. Kuiper, G. G. *et al.* Comparison of the ligand binding specificity and transcript tissue distribution of estrogen receptors alpha and beta. *Endocrinology* **138,** 863–70 (1997).

29. Speirs, V., Skliris, G. P., Burdall, S. E. & Carder, P. J. Distinct expression patterns of ER alpha and ER beta in normal human mammary gland. *J. Clin. Pathol.* **55,** 371–4 (2002).

30. Fuqua, S. A. W. *et al.* Estrogen Receptor {beta} Protein in Human Breast Cancer: Correlation with Clinical Tumor Parameters. *Cancer Res.* **63,** 2434–2439 (2003).

31. Jensen, E. V *et al.* Estrogen receptors and proliferation markers in primary and recurrent breast cancer. *Proc. Natl. Acad. Sci. U. S. A.* **98,** 15197–202 (2001).

32. Speirs, V., Malone, C., Walton, D. S., Kerin, M. J. & Atkin, S. L. Increased Expression of Estrogen Receptor {{beta}} mRNA in Tamoxifen-resistant Breast Cancer Patients. *Cancer Res.* **59,** 5421–5424 (1999).

33. Omoto, Y. *et al.* Clinical value of the wild-type estrogen receptor beta expression in breast cancer. *Cancer Lett.* **163,** 207–12 (2001).

34. Osborne, C. K., Schiff, R., Fuqua, S. A. W. & Shou, J. Estrogen Receptor: Current Understanding of Its Activation and Modulation. *Clin. Cancer Res.* **7,** 4338s–4342 (2001).

35. Pratt, W. B. & Toft, D. O. Steroid receptor interactions with heat shock protein and immunophilin chaperones. *Endocr. Rev.* **18,** 306–60 (1997).

36. Kumar, V. & Chambon, P. The estrogen receptor binds tightly to its responsive element as a ligand-induced homodimer. *Cell* **55,** 145–56 (1988).

37. Chen, D., Pace, P. E., Coombes, R. C. & Ali, S. Phosphorylation of human estrogen receptor alpha by protein kinase A regulates dimerization. *Mol. Cell. Biol.* **19,** 1002–15 (1999).

38. Frasor, J. *et al.* Profiling of estrogen up- and down-regulated gene expression in human breast cancer cells: insights into gene networks and pathways underlying estrogenic control of proliferation and cell phenotype. *Endocrinology* **144,** 4562–74 (2003).

39. Tzukerman, M. T. *et al.* Human estrogen receptor transactivational capacity is determined by both cellular and promoter context and mediated by two functionally distinct intramolecular regions. *Mol. Endocrinol.* **8,** 21–30 (1994).

40. Métivier, R., Penot, G., Flouriot, G. & Pakdel, F. Synergism Between ERα Transactivation Function 1 (AF-1) and AF-2 Mediated by Steroid Receptor Coactivator Protein-1: Requirement for the AF-1 α-Helical Core and for a Direct Interaction Between the N- and C-Terminal Domains. *Mol. Endocrinol.* **15,** 1953–1970 (2001).

41. Nichols, M., Rientjes, J. M. & Stewart, A. F. Different positioning of the ligand-binding domain helix 12 and the F domain of the estrogen receptor accounts for functional differences between agonists and antagonists. *EMBO J.* **17,** 765–73 (1998).

42. Renaud, J. P. *et al.* Crystal structure of the RAR-gamma ligand-binding domain bound to all-trans retinoic acid. *Nature* **378,** 681–9 (1995).

43. Brownell, J. E. & Allis, C. D. Special HATs for special occasions: linking histone acetylation to chromatin assembly and gene activation. *Curr. Opin. Genet. Dev.* **6,** 176–184 (1996).

44. Wolffe, A. P. & Pruss, D. Targeting Chromatin Disruption: Transcription Regulators that Acetylate Histones. *Cell* **84,** 817–819 (1996).

45. Wade, P. A. & Wolffe, A. P. Histone acetyltransferases in control. *Curr. Biol.* **7,** R82–4 (1997).

46. Oñate, S. A., Tsai, S. Y., Tsai, M. J. & O'Malley, B. W. Sequence and characterization of a coactivator for the steroid hormone receptor superfamily. *Science* **270,** 1354–7 (1995).

47. Hong, H., Kohli, K., Garabedian, M. J. & Stallcup, M. R. GRIP1, a transcriptional coactivator for the AF-2 transactivation domain of steroid, thyroid, retinoid, and vitamin D receptors. *Mol. Cell. Biol.* **17,** 2735–44 (1997).

48. Anzick, S. L. *et al.* AIB1, a steroid receptor coactivator amplified in breast and ovarian cancer. *Science* **277,** 965–8 (1997).

49. Dobrzycka, K. M., Townson, S. M., Jiang, S. & Oesterreich, S. Estrogen receptor corepressors -- a role in human breast cancer? *Endocr. Relat. Cancer* **10,** 517–36 (2003).

50. Chen, J. D. & Evans, R. M. A transcriptional co-repressor that interacts with nuclear hormone receptors. *Nature* **377,** 454–7 (1995).

51. Varlakhanova, N., Snyder, C., Jose, S., Hahm, J. B. & Privalsky, M. L. Estrogen receptors recruit SMRT and N-CoR corepressors through newly recognized contacts between the corepressor N terminus and the receptor DNA binding domain. *Mol. Cell. Biol.* **30,** 1434–45 (2010).

52. Schiff, R., Massarweh, S., Shou, J. & Osborne, C. K. Breast Cancer Endocrine Resistance: How Growth Factor Signaling and Estrogen Receptor Coregulators Modulate Response. *Clin. Cancer Res.* **9,** 447s–454 (2003).

53. Kato, S. *et al.* Activation of the Estrogen Receptor Through Phosphorylation by Mitogen-Activated Protein Kinase. *Science (80-.).* **270,** 1491–1494 (1995).

54. Arnold, S. F., Obourn, J. D., Jaffe, H. & Notides, A. C. Serine 167 is the major estradiol-induced phosphorylation site on the human estrogen receptor. *Mol. Endocrinol.* **8,** 1208–14 (1994).

55. Hall, J. M., Couse, J. F. & Korach, K. S. The Multifaceted Mechanisms of Estradiol and Estrogen Receptor Signaling. *J. Biol. Chem.* **276,** 36869–36872 (2001).

56. Duan, R., Porter, W. & Safe, S. Estrogen-Induced c- fos Protooncogene Expression in MCF-7 Human Breast Cancer Cells: Role of Estrogen Receptor Sp1 Complex Formation 1. *Endocrinology* **139,** 1981–1990 (1998).

57. Kushner, P. J. *et al.* Estrogen receptor pathways to AP-1. *J. Steroid Biochem. Mol. Biol.* **74,** 311–317 (2000).

58. Saville, B. Ligand-, Cell-, and Estrogen Receptor Subtype (alpha /beta)-dependent Activation at GC-rich (Sp1) Promoter Elements. *J. Biol. Chem.* **275,** 5379–5387 (2000).

59. Eeckhoute, J., Carroll, J. S., Geistlinger, T. R., Torres-Arzayus, M. I. & Brown, M. A cell-type-specific transcriptional network required for estrogen regulation of cyclin D1 and cell cycle progression in breast cancer. *Genes Dev.* **20,** 2513–

26 (2006).

60. Maor, S. *et al.* Estrogen receptor regulates insulin-like growth factor-I receptor gene expression in breast tumor cells: involvement of transcription factor Sp1. *J. Endocrinol.* **191,** 605–12 (2006).

61. Stein, B. & Yang, M. X. Repression of the interleukin-6 promoter by estrogen receptor is mediated by NF-kappa B and C/EBP beta. *Mol. Cell. Biol.* **15,** 4971–9 (1995).

62. Petz, L. N. & Nardulli, A. M. Sp1 binding sites and an estrogen response element half-site are involved in regulation of the human progesterone receptor A promoter. *Mol. Endocrinol.* **14,** 972–85 (2000).

63. Kahlert, S. *et al.* Estrogen receptor alpha rapidly activates the IGF-1 receptor pathway. *J. Biol. Chem.* **275,** 18447–53 (2000).

64. Razandi, M., Pedram, A., Park, S. T. & Levin, E. R. Proximal events in signaling by plasma membrane estrogen receptors. *J. Biol. Chem.* **278,** 2701–12 (2003).

65. Wong, C.-W., McNally, C., Nickbarg, E., Komm, B. S. & Cheskis, B. J. Estrogen receptor-interacting protein that modulates its nongenomic activity-crosstalk with Src/Erk phosphorylation cascade. *Proc. Natl. Acad. Sci. U. S. A.* **99,** 14783–8 (2002).

66. Björnström, L. & Sjöberg, M. Mechanisms of estrogen receptor signaling: convergence of genomic and nongenomic actions on target genes. *Mol. Endocrinol.* **19,** 833–42 (2005).

67. Björnström, L. & Sjöberg, M. Estrogen receptor-dependent activation of AP-1 via non-genomic signalling. *Nucl. Recept.* **2,** 3 (2004).

68. Dos Santos, E. G. *et al.* Rapid nongenomic E2 effects on p42/p44 MAPK, activator protein-1, and cAMP response element binding protein in rat white adipocytes. *Endocrinology* **143,** 930–40 (2002).

69. Harvey, J. M., Clark, G. M., Osborne, C. K. & Allred, D. C. Estrogen Receptor

Status by Immunohistochemistry Is Superior to the Ligand-Binding Assay for Predicting Response to Adjuvant Endocrine Therapy in Breast Cancer. *J. Clin. Oncol.* **17,** 1474– (1999).

70. Press, M. F. *et al.* Evaluation of HER-2/neu gene amplification and overexpression: comparison of frequently used assay methods in a molecularly characterized cohort of breast cancer specimens. *J. Clin. Oncol.* **20,** 3095–105 (2002).

71. Brufsky, A., Lembersky, B., Schiffman, K., Lieberman, G. & Paton, V. E. Hormone receptor status does not affect the clinical benefit of trastuzumab therapy for patients with metastatic breast cancer. *Clin. Breast Cancer* **6,** 247–52 (2005).

72. Spector, N. L. & Blackwell, K. L. Understanding the mechanisms behind trastuzumab therapy for human epidermal growth factor receptor 2-positive breast cancer. *J. Clin. Oncol.* **27,** 5838–47 (2009).

73. Jordan, V. C. *et al.* The St. Gallen Prize Lecture 2011: evolution of long-term adjuvant anti-hormone therapy: consequences and opportunities. *Breast* **20 Suppl 3,** S1–11 (2011).

74. Joensuu, H., Ejlertsen, B., Lønning, P. E. & Rutqvist, L.-E. Aromatase inhibitors in the treatment of early and advanced breast cancer. *Acta Oncol.* **44,** 23–31 (2005).

75. Olson, J. A. *et al.* Improved surgical outcomes for breast cancer patients receiving neoadjuvant aromatase inhibitor therapy: results from a multicenter phase II trial. *J. Am. Coll. Surg.* **208,** 906–14; discussion 915–6 (2009).

76. Brzozowski, A. M. *et al.* Molecular basis of agonism and antagonism in the oestrogen receptor. *Nature* **389,** 753–8 (1997).

77. Metzger, D., Losson, R., Bornert, J.-M., Lemoine, Y. & Chambon, P. Promoter specificity of the two transcriptional activation functions of the human oestrogen receptor in yeast. *Nucleic Acids Res.* **20,** 2813–2817 (1992).

78. Thomas, R. S., Sarwar, N., Phoenix, F., Coombes, R. C. & Ali, S. Phosphorylation at serines 104 and 106 by Erk1/2 MAPK is important for estrogen receptor-alpha activity. *J. Mol. Endocrinol.* **40,** 173–84 (2008).

79. Metzger, D., Clifford, J., Chiba, H. & Chambon, P. Conditional site-specific recombination in mammalian cells using a ligand-dependent chimeric Cre recombinase. *Proc. Natl. Acad. Sci. U. S. A.* **92,** 6991–5 (1995).

80. McDonnell, D. P., Clemm, D. L., Hermann, T., Goldman, M. E. & Pike, J. W. Analysis of estrogen receptor function in vitro reveals three distinct classes of antiestrogens. *Mol. Endocrinol.* **9,** 659–69 (1995).

81. Shang, Y. & Brown, M. Molecular determinants for the tissue specificity of SERMs. *Science* **295,** 2465–8 (2002).

82. Lavinsky, R. M. *et al.* Diverse signaling pathways modulate nuclear receptor recruitment of N-CoR and SMRT complexes. *Proc. Natl. Acad. Sci. U. S. A.* **95,** 2920–5 (1998).

83. Baum, M. *et al.* Anastrozole alone or in combination with tamoxifen versus tamoxifen alone for adjuvant treatment of postmenopausal women with early breast cancer: first results of the ATAC randomised trial. *Lancet (London, England)* **359,** 2131–9 (2002).

84. Michaud, L. B., Jones, K. L. & Buzdar, A. U. Combination endocrine therapy in the management of breast cancer. *Oncologist* **6,** 538–46 (2001).

85. Giordano, S. H. *et al.* Adjuvant systemic therapy for male breast carcinoma. *Cancer* **104,** 2359–64 (2005).

86. Davies, C. *et al.* Relevance of breast cancer hormone receptors and other factors to the efficacy of adjuvant tamoxifen: patient-level meta-analysis of randomised trials. *Lancet* **378,** 771–84 (2011).

87. Dowsett, M. *et al.* Meta-analysis of breast cancer outcomes in adjuvant trials of aromatase inhibitors versus tamoxifen. *J. Clin. Oncol.* **28,** 509–18 (2010).

88. Davies, C. *et al.* Long-term effects of continuing adjuvant tamoxifen to 10

years versus stopping at 5 years after diagnosis of oestrogen receptor-positive breast cancer: ATLAS, a randomised trial. *Lancet* **381,** 805–16 (2013).

89. Cuzick, J. *et al.* Selective oestrogen receptor modulators in prevention of breast cancer: an updated meta-analysis of individual participant data. *Lancet (London, England)* **381,** 1827–34 (2013).

90. Bulun, S. E., Price, T. M., Aitken, J., Mahendroo, M. S. & Simpson, E. R. A link between breast cancer and local estrogen biosynthesis suggested by quantification of breast adipose tissue aromatase cytochrome P450 transcripts using competitive polymerase chain reaction after reverse transcription. *J. Clin. Endocrinol. Metab.* **77,** 1622–8 (1993).

91. Geisler, J. *et al.* Influence of anastrozole (Arimidex), a selective, non-steroidal aromatase inhibitor, on in vivo aromatisation and plasma oestrogen levels in postmenopausal women with breast cancer. *Br. J. Cancer* **74,** 1286–91 (1996).

92. Johnston, S. R. D. & Dowsett, M. Aromatase inhibitors for breast cancer: lessons from the laboratory. *Nat. Rev. Cancer* **3,** 821–31 (2003).

93. Chumsri, S. Clinical utilities of aromatase inhibitors in breast cancer. *Int. J. Womens. Health* **7,** 493–9 (2015).

94. Cole, P. A. & Robinson, C. H. Mechanism and inhibition of cytochrome P-450 aromatase. *J. Med. Chem.* **33,** 2933–42 (1990).

95. Howell, A. *et al.* Results of the ATAC (Arimidex, Tamoxifen, Alone or in Combination) trial after completion of 5 years' adjuvant treatment for breast cancer. *Lancet* **365,** 60–2 (2005).

96. National Institute of Health and Care Excellence. Hormal therapies for the adjuvant treatment of early oestrogen-receptor-positive breast cancer. (2006). at <https://www.nice.org.uk/guidance/TA112/chapter/1-Guidance>

97. Fabian, C. J. The what, why and how of aromatase inhibitors: hormonal

agents for treatment and prevention of breast cancer. *Int. J. Clin. Pract.* **61,** 2051–63 (2007).

98. Wakeling, A. E., Dukes, M. & Bowler, J. A potent specific pure antiestrogen with clinical potential. *Cancer Res.* **51,** 3867–73 (1991).

99. Pike, A. C. *et al.* Structural insights into the mode of action of a pure antiestrogen. *Structure* **9,** 145–53 (2001).

100. Fawell, S. E. *et al.* Inhibition of estrogen receptor-DNA binding by the 'pure' antiestrogen ICI 164,384 appears to be mediated by impaired receptor dimerization. *Proc. Natl. Acad. Sci. U. S. A.* **87,** 6883–7 (1990).

101. Dauvois, S., White, R. & Parker, M. G. The antiestrogen ICI 182780 disrupts estrogen receptor nucleocytoplasmic shuttling. *J. Cell Sci.* **106 (Pt 4,** 1377–88 (1993).

102. Nicholson, R. I. *et al.* Responses to Pure Antiestrogens (ICI 164384, ICI182780) in Estrogen-Sensitive and-Resistant Experimental and Clinical Breast Cancer. *Ann. N. Y. Acad. Sci.* **761,** 148–163 (1995).

103. Long, X., Fan, M. & Nephew, K. P. Estrogen receptor-alpha-interacting cytokeratins potentiate the antiestrogenic activity of fulvestrant. *Cancer Biol. Ther.* **9,** 389–96 (2010).

104. Fan, M., Bigsby, R. M. & Nephew, K. P. The NEDD8 pathway is required for proteasome-mediated degradation of human estrogen receptor (ER)-alpha and essential for the antiproliferative activity of ICI 182,780 in ERalpha-positive breast cancer cells. *Mol. Endocrinol.* **17,** 356–65 (2003).

105. Osborne, C. K., Wakeling, A. & Nicholson, R. I. Fulvestrant: an oestrogen receptor antagonist with a novel mechanism of action. *Br. J. Cancer* **90 Suppl 1,** S2–6 (2004).

106. Howell, A. *et al.* Fulvestrant, formerly ICI 182,780, is as effective as anastrozole in postmenopausal women with advanced breast cancer progressing after prior endocrine treatment. *J. Clin. Oncol.* **20,** 3396–403 (2002).

107. Osborne, C. K. *et al.* Double-blind, randomized trial comparing the efficacy and tolerability of fulvestrant versus anastrozole in postmenopausal women with advanced breast cancer progressing on prior endocrine therapy: results of a North American trial. *J. Clin. Oncol.* **20,** 3386–95 (2002).

108. Howell, A. *et al.* Comparison of fulvestrant versus tamoxifen for the treatment of advanced breast cancer in postmenopausal women previously untreated with endocrine therapy: a multinational, double-blind, randomized trial. *J. Clin. Oncol.* **22,** 1605–13 (2004).

109. Di Leo, A. *et al.* Final overall survival: fulvestrant 500 mg vs 250 mg in the randomized CONFIRM trial. *J. Natl. Cancer Inst.* **106,** djt337 (2014).

110. Kuter, I. *et al.* Dose-dependent change in biomarkers during neoadjuvant endocrine therapy with fulvestrant: results from NEWEST, a randomized Phase II study. *Breast Cancer Res. Treat.* **133,** 237–46 (2012).

111. Robertson, J. F. R. *et al.* Activity of fulvestrant 500 mg versus anastrozole 1 mg as first-line treatment for advanced breast cancer: results from the FIRST study. *J. Clin. Oncol.* **27,** 4530–5 (2009).

112. Robertson, J. F. R. *et al.* Fulvestrant 500 mg versus anastrozole 1 mg for the first-line treatment of advanced breast cancer: follow-up analysis from the randomized 'FIRST' study. *Breast Cancer Res. Treat.* **136,** 503–11 (2012).

113. Bergh, J. *et al.* FACT: an open-label randomized phase III study of fulvestrant and anastrozole in combination compared with anastrozole alone as first-line therapy for patients with receptor-positive postmenopausal breast cancer. *J. Clin. Oncol.* **30,** 1919–25 (2012).

114. Mehta, R. S. *et al.* Combination Anastrozole and Fulvestrant in Metastatic Breast Cancer. *N. Engl. J. Med.* **367,** 435–444 (2012).

115. Gutierrez, M. C. *et al.* Molecular changes in tamoxifen-resistant breast cancer: relationship between estrogen receptor, HER-2, and p38 mitogen-activated protein kinase. *J. Clin. Oncol.* **23,** 2469–76 (2005).

116. Encarnación, C. A. *et al.* Measurement of steroid hormone receptors in breast

cancer patients on tamoxifen. *Breast Cancer Res. Treat.* **26,** 237–46 (1993).

117. Yan, L., Yang, X. & Davidson, N. E. Role of DNA Methylation and Histone Acetylation in Steroid Receptor Expression in Breast Cancer. *J. Mammary Gland Biol. Neoplasia* **6,** 183–192 (2001).

118. Iwase, H. *et al.* DNA methylation analysis at distal and proximal promoter regions of the oestrogen receptor gene in breast cancers. *Br. J. Cancer* **80,** 1982–6 (1999).

119. Ferguson, A. T., Lapidus, R. G., Baylin, S. B. & Davidson, N. E. Demethylation of the estrogen receptor gene in estrogen receptor-negative breast cancer cells can reactivate estrogen receptor gene expression. *Cancer Res.* **55,** 2279–83 (1995).

120. Oh, A. S. *et al.* Hyperactivation of MAPK induces loss of ERalpha expression in breast cancer cells. *Mol. Endocrinol.* **15,** 1344–59 (2001).

121. Holloway, J. N., Murthy, S. & El-Ashry, D. A cytoplasmic substrate of mitogen-activated protein kinase is responsible for estrogen receptor-alpha down-regulation in breast cancer cells: the role of nuclear factor-kappaB. *Mol. Endocrinol.* **18,** 1396–410 (2004).

122. He, L. & Hannon, G. J. MicroRNAs: small RNAs with a big role in gene regulation. *Nat. Rev. Genet.* **5,** 522–31 (2004).

123. Zhao, J.-J. *et al.* MicroRNA-221/222 negatively regulates estrogen receptor alpha and is associated with tamoxifen resistance in breast cancer. *J. Biol. Chem.* **283,** 31079–86 (2008).

124. Adams, B. D., Furneaux, H. & White, B. A. The micro-ribonucleic acid (miRNA) miR-206 targets the human estrogen receptor-alpha (ERalpha) and represses ERalpha messenger RNA and protein expression in breast cancer cell lines. *Mol. Endocrinol.* **21,** 1132–47 (2007).

125. Wang, Z. *et al.* Identification, cloning, and expression of human estrogen receptor-alpha36, a novel variant of human estrogen receptor-alpha66. *Biochem. Biophys. Res. Commun.* **336,** 1023–7 (2005).

126. Wang, Z. *et al.* A variant of estrogen receptor-{alpha}, hER-{alpha}36: transduction of estrogen- and antiestrogen-dependent membrane-initiated mitogenic signaling. *Proc. Natl. Acad. Sci. U. S. A.* **103,** 9063–8 (2006).

127. Shi, L. *et al.* Expression of ER-{alpha}36, a novel variant of estrogen receptor {alpha}, and resistance to tamoxifen treatment in breast cancer. *J. Clin. Oncol.* **27,** 3423–9 (2009).

128. Zhang, X. & Wang, Z.-Y. Estrogen receptor-α variant, ER-α36, is involved in tamoxifen resistance and estrogen hypersensitivity. *Endocrinology* **154,** 1990–8 (2013).

129. Kang, L., Guo, Y., Zhang, X., Meng, J. & Wang, Z.-Y. A positive cross-regulation of HER2 and ER-α36 controls ALDH1 positive breast cancer cells. *J. Steroid Biochem. Mol. Biol.* **127,** 262–8 (2011).

130. Zhang, X. T. *et al.* A positive feedback loop of ER-α36/EGFR promotes malignant growth of ER-negative breast cancer cells. *Oncogene* **30,** 770–80 (2011).

131. Yin, L. *et al.* Downregulation of ER-α36 expression sensitizes HER2 overexpressing breast cancer cells to tamoxifen. *Am. J. Cancer Res.* **5,** 530–44 (2015).

132. Murphy, L. C. *et al.* Altered Expression of Estrogen Receptor Coregulators during Human Breast Tumorigenesis. *Cancer Res.* **60,** 6266–6271 (2000).

133. Osborne, C. K. *et al.* Role of the estrogen receptor coactivator AIB1 (SRC-3) and HER-2/neu in tamoxifen resistance in breast cancer. *J. Natl. Cancer Inst.* **95,** 353–61 (2003).

134. Kirkegaard, T. *et al.* Amplified in breast cancer 1 in human epidermal growth factor receptor - positive tumors of tamoxifen-treated breast cancer patients. *Clin. Cancer Res.* **13,** 1405–11 (2007).

135. Font de Mora, J. & Brown, M. AIB1 Is a Conduit for Kinase-Mediated Growth Factor Signaling to the Estrogen Receptor. *Mol. Cell. Biol.* **20,** 5041–5047 (2000).

136. Kurebayashi, J. *et al.* Expression Levels of Estrogen Receptor-{{alpha}}, Estrogen Receptor-{beta}, Coactivators, and Corepressors in Breast Cancer. *Clin. Cancer Res.* **6,** 512–518 (2000).

137. Girault, I. *et al.* Expression analysis of estrogen receptor alpha coregulators in breast carcinoma: evidence that NCOR1 expression is predictive of the response to tamoxifen. *Clin. Cancer Res.* **9,** 1259–66 (2003).

138. Al-Hajj, M., Wicha, M. S., Benito-Hernandez, A., Morrison, S. J. & Clarke, M. F. Prospective identification of tumorigenic breast cancer cells. *Proc. Natl. Acad. Sci. U. S. A.* **100,** 3983–8 (2003).

139. Ginestier, C. *et al.* ALDH1 is a marker of normal and malignant human mammary stem cells and a predictor of poor clinical outcome. *Cell Stem Cell* **1,** 555–67 (2007).

140. Liu, S. *et al.* Breast cancer stem cells transition between epithelial and mesenchymal states reflective of their normal counterparts. *Stem cell reports* **2,** 78–91 (2014).

141. Moreno-Bueno, G., Portillo, F. & Cano, A. Transcriptional regulation of cell polarity in EMT and cancer. *Oncogene* **27,** 6958–69 (2008).

142. Gunasinghe, N. P. A. D., Wells, A., Thompson, E. W. & Hugo, H. J. Mesenchymal-epithelial transition (MET) as a mechanism for metastatic colonisation in breast cancer. *Cancer Metastasis Rev.* **31,** 469–78 (2012).

143. Abdullah, L. N. & Chow, E. K.-H. Mechanisms of chemoresistance in cancer stem cells. *Clin. Transl. Med.* **2,** 3 (2013).

144. Li, X. *et al.* Intrinsic Resistance of Tumorigenic Breast Cancer Cells to Chemotherapy. *JNCI J. Natl. Cancer Inst.* **100,** 672–679 (2008).

145. Zhang, M., Atkinson, R. L. & Rosen, J. M. Selective targeting of radiation-resistant tumor-initiating cells. *Proc. Natl. Acad. Sci. U. S. A.* **107,** 3522–7 (2010).

146. Creighton, C. J. *et al.* Residual breast cancers after conventional therapy

display mesenchymal as well as tumor-initiating features. *Proc. Natl. Acad. Sci. U. S. A.* **106,** 13820–5 (2009).

147. Shipitsin, M. *et al.* Molecular definition of breast tumor heterogeneity. *Cancer Cell* **11,** 259–73 (2007).

148. Harrison, H. *et al.* Oestrogen increases the activity of oestrogen receptor negative breast cancer stem cells through paracrine EGFR and Notch signalling. *Breast Cancer Res.* **15,** R21 (2013).

149. Asselin-Labat, M.-L. *et al.* Steroid hormone receptor status of mouse mammary stem cells. *J. Natl. Cancer Inst.* **98,** 1011–4 (2006).

150. Hebbard, L. *et al.* CD44 expression and regulation during mammary gland development and function. *J. Cell Sci.* **113 (Pt 1,** 2619–30 (2000).

151. Farnie, G. *et al.* Novel cell culture technique for primary ductal carcinoma in situ: role of Notch and epidermal growth factor receptor signaling pathways. *J. Natl. Cancer Inst.* **99,** 616–27 (2007).

152. O'Brien, C. S., Farnie, G., Howell, S. J. & Clarke, R. B. Breast cancer stem cells and their role in resistance to endocrine therapy. *Horm. Cancer* **2,** 91–103 (2011).

153. Liu, H. *et al.* Tamoxifen-resistant breast cancer cells possess cancer stem-like cell properties. *Chin. Med. J. (Engl).* **126,** 3030–4 (2013).

154. Raffo, D. *et al.* Tamoxifen selects for breast cancer cells with mammosphere forming capacity and increased growth rate. *Breast Cancer Res. Treat.* **142,** 537–48 (2013).

155. Karthik, G.-M. *et al.* mTOR inhibitors counteract tamoxifen-induced activation of breast cancer stem cells. *Cancer Lett.* **367,** 76–87 (2015).

156. Gil, E. M. C. Targeting the PI3K/AKT/mTOR pathway in estrogen receptor-positive breast cancer. *Cancer Treat. Rev.* **40,** 862–71 (2014).

157. Lundberg, A. S. & Weinberg, R. A. Control of the cell cycle and apoptosis. *Eur. J. Cancer* **35,** 1886–94 (1999).

158. Hwang, H. C. & Clurman, B. E. Cyclin E in normal and neoplastic cell cycles. *Oncogene* **24,** 2776–86 (2005).

159. Dubik, D., Dembinski, T. C. & Shiu, R. P. Stimulation of c-myc oncogene expression associated with estrogen-induced proliferation of human breast cancer cells. *Cancer Res.* **47,** 6517–21 (1987).

160. Dubik, D. & Shiu, R. P. Transcriptional regulation of c-myc oncogene expression by estrogen in hormone-responsive human breast cancer cells. *J. Biol. Chem.* **263,** 12705–8 (1988).

161. Musgrove, E. A., Lee, C. S., Buckley, M. F. & Sutherland, R. L. Cyclin D1 induction in breast cancer cells shortens G1 and is sufficient for cells arrested in G1 to complete the cell cycle. *Proc. Natl. Acad. Sci. U. S. A.* **91,** 8022–6 (1994).

162. Planas-Silva, M. D. & Weinberg, R. A. Estrogen-dependent cyclin E-cdk2 activation through p21 redistribution. *Mol. Cell. Biol.* **17,** 4059–69 (1997).

163. Prall, O. W., Sarcevic, B., Musgrove, E. A., Watts, C. K. & Sutherland, R. L. Estrogen-induced activation of Cdk4 and Cdk2 during G1-S phase progression is accompanied by increased cyclin D1 expression and decreased cyclin-dependent kinase inhibitor association with cyclin E-Cdk2. *J. Biol. Chem.* **272,** 10882–94 (1997).

164. Thiantanawat, A., Long, B. J. & Brodie, A. M. Signaling pathways of apoptosis activated by aromatase inhibitors and antiestrogens. *Cancer Res.* **63,** 8037–50 (2003).

165. Watts, C. K. *et al.* Antiestrogen inhibition of cell cycle progression in breast cancer cells in associated with inhibition of cyclin-dependent kinase activity and decreased retinoblastoma protein phosphorylation. *Mol. Endocrinol.* **9,** 1804–13 (1995).

166. Kilker, R. L., Hartl, M. W., Rutherford, T. M. & Planas-Silva, M. D. Cyclin D1 expression is dependent on estrogen receptor function in tamoxifen-resistant breast cancer cells. *J. Steroid Biochem. Mol. Biol.* **92,** 63–71 (2004).

167. Jeng, M. H. *et al.* Estrogen receptor expression and function in long-term estrogen-deprived human breast cancer cells. *Endocrinology* **139,** 4164–74 (1998).

168. Wilcken, N. R., Prall, O. W., Musgrove, E. A. & Sutherland, R. L. Inducible overexpression of cyclin D1 in breast cancer cells reverses the growth-inhibitory effects of antiestrogens. *Clin. Cancer Res.* **3,** 849–54 (1997).

169. Prall, O. W., Rogan, E. M., Musgrove, E. A., Watts, C. K. & Sutherland, R. L. c-Myc or cyclin D1 mimics estrogen effects on cyclin E-Cdk2 activation and cell cycle reentry. *Mol. Cell. Biol.* **18,** 4499–508 (1998).

170. Hodges, L. C. *et al.* Tamoxifen functions as a molecular agonist inducing cell cycle-associated genes in breast cancer cells. *Mol. Cancer Res.* **1,** 300–11 (2003).

171. Butt, A. J., McNeil, C. M., Musgrove, E. A. & Sutherland, R. L. Downstream targets of growth factor and oestrogen signalling and endocrine resistance: the potential roles of c-Myc, cyclin D1 and cyclin E. *Endocr. Relat. Cancer* **12 Suppl 1,** S47–59 (2005).

172. Dhillon, N. K. & Mudryj, M. Ectopic expression of cyclin E in estrogen responsive cells abrogates antiestrogen mediated growth arrest. *Oncogene* **21,** 4626–34 (2002).

173. Hui, R. *et al.* Constitutive overexpression of cyclin D1 but not cyclin E confers acute resistance to antiestrogens in T-47D breast cancer cells. *Cancer Res.* **62,** 6916–23 (2002).

174. Kenny, F. S. *et al.* Overexpression of cyclin D1 messenger RNA predicts for poor prognosis in estrogen receptor-positive breast cancer. *Clin. Cancer Res.* **5,** 2069–76 (1999).

175. Neuman, E. *et al.* Cyclin D1 stimulation of estrogen receptor transcriptional activity independent of cdk4. *Mol. Cell. Biol.* **17,** 5338–47 (1997).

176. Zwijsen, R. M. *et al.* CDK-independent activation of estrogen receptor by cyclin D1. *Cell* **88,** 405–15 (1997).

177. Ishii, Y., Waxman, S. & Germain, D. Tamoxifen stimulates the growth of cyclin D1-overexpressing breast cancer cells by promoting the activation of signal transducer and activator of transcription 3. *Cancer Res.* **68,** 852–60 (2008).

178. Finn, R. S. *et al.* PD 0332991, a selective cyclin D kinase 4/6 inhibitor, preferentially inhibits proliferation of luminal estrogen receptor-positive human breast cancer cell lines in vitro. *Breast Cancer Res.* **11,** R77 (2009).

179. Finn, R. *et al.* Phase I Study of PD 0332991, a Novel, Oral, Cyclin-D Kinase (CDK) 4/6 Inhibitor in Combination with Letrozole, for First-Line Treatment of Metastatic Post-Menopausal, Estrogen Receptor-Positive (ER+), Human Epidermal Growth Factor Receptor 2 (HER2)-Negati. *Cancer Res.* **69,** 5069–5069 (2009).

180. Finn, R. S. *et al.* The cyclin-dependent kinase 4/6 inhibitor palbociclib in combination with letrozole versus letrozole alone as first-line treatment of oestrogen receptor-positive, HER2-negative, advanced breast cancer (PALOMA-1/TRIO-18): a randomised phase 2 study. *Lancet Oncol.* **16,** 25–35 (2015).

181. US Food and Drug Administration. Palbociclib. (2015). at <www.fda.gov/Drugs/InformationOnDrugs/ApprovedDrugs/>

182. Johnston, S. R. *et al.* Changes in estrogen receptor, progesterone receptor, and pS2 expression in tamoxifen-resistant human breast cancer. *Cancer Res.* **55,** 3331–8 (1995).

183. Buzdar, A. & Howell, A. Advances in aromatase inhibition: clinical efficacy and tolerability in the treatment of breast cancer. *Clin. Cancer Res.* **7,** 2620–35 (2001).

184. McClelland, R. A. *et al.* Enhanced epidermal growth factor receptor signaling in MCF7 breast cancer cells after long-term culture in the presence of the pure antiestrogen ICI 182,780 (Faslodex). *Endocrinology* **142,** 2776–88 (2001).

185. Knowlden, J. M. *et al.* Elevated levels of epidermal growth factor receptor/c-

erbB2 heterodimers mediate an autocrine growth regulatory pathway in tamoxifen-resistant MCF-7 cells. *Endocrinology* **144,** 1032–44 (2003).

186. Gee, J. M. *et al.* Endocrine response and resistance in breast cancer: a role for the transcription factor Fos. *Int. J. Cancer* **84,** 54–61 (1999).

187. Nicholson, R. I. *et al.* Nonendocrine pathways and endocrine resistance: observations with antiestrogens and signal transduction inhibitors in combination. *Clin. Cancer Res.* **10,** 346S–54S (2004).

188. Stephen, R. L., Shaw, L. E., Larsen, C., Corcoran, D. & Darbre, P. D. Insulin-like growth factor receptor levels are regulated by cell density and by long term estrogen deprivation in MCF7 human breast cancer cells. *J. Biol. Chem.* **276,** 40080–6 (2001).

189. Joel, P. B. *et al.* pp90rsk1 regulates estrogen receptor-mediated transcription through phosphorylation of Ser-167. *Mol. Cell. Biol.* **18,** 1978–84 (1998).

190. Deblois, G. & Giguère, V. Ligand-independent coactivation of ERalpha AF-1 by steroid receptor RNA activator (SRA) via MAPK activation. *J. Steroid Biochem. Mol. Biol.* **85,** 123–31 (2003).

191. Lannigan, D. A. Estrogen receptor phosphorylation. *Steroids* **68,** 1–9 (2003).

192. Chan, C. M. W., Martin, L.-A., Johnston, S. R. D., Ali, S. & Dowsett, M. Molecular changes associated with the acquisition of oestrogen hypersensitivity in MCF-7 breast cancer cells on long-term oestrogen deprivation. *J. Steroid Biochem. Mol. Biol.* **81,** 333–41 (2002).

193. Vendrell, J. A. *et al.* Molecular changes associated with the agonist activity of hydroxy-tamoxifen and the hyper-response to estradiol in hydroxy-tamoxifen-resistant breast cancer cell lines. *Endocr. Relat. Cancer* **12,** 75–92 (2005).

194. Glaros, S., Atanaskova, N., Zhao, C., Skafar, D. F. & Reddy, K. B. Activation function-1 domain of estrogen receptor regulates the agonistic and antagonistic actions of tamoxifen. *Mol. Endocrinol.* **20,** 996–1008 (2006).

195. Shou, J. *et al.* Mechanisms of Tamoxifen Resistance: Increased Estrogen Receptor-HER2/neu Cross-Talk in ER/HER2-Positive Breast Cancer. *JNCI J. Natl. Cancer Inst.* **96,** 926–935 (2004).

196. Britton, D. J. *et al.* Bidirectional cross talk between ERalpha and EGFR signalling pathways regulates tamoxifen-resistant growth. *Breast Cancer Res. Treat.* **96,** 131–46 (2006).

197. Nicholson, R. I. *et al.* Growth factor signalling and resistance to selective oestrogen receptor modulators and pure anti-oestrogens: the use of anti-growth factor therapies to treat or delay endocrine resistance in breast cancer. *Endocr. Relat. Cancer* **12 Suppl 1,** S29–36 (2005).

198. Knowlden, J. M., Hutcheson, I. R., Barrow, D., Gee, J. M. W. & Nicholson, R. I. Insulin-like growth factor-I receptor signaling in tamoxifen-resistant breast cancer: a supporting role to the epidermal growth factor receptor. *Endocrinology* **146,** 4609–18 (2005).

199. Beenken, A. & Mohammadi, M. The FGF family: biology, pathophysiology and therapy. *Nat. Rev. Drug Discov.* **8,** 235–53 (2009).

200. Elbauomy, S. E. *et al.* FGFR1 amplification in breast carcinomas: a chromogenic in situ hybridisation analysis. *Breast Cancer Res.* **9,** R23 (2007).

201. Turner, N. *et al.* FGFR1 amplification drives endocrine therapy resistance and is a therapeutic target in breast cancer. *Cancer Res.* **70,** 2085–94 (2010).

202. Tomlinson, D. C., Knowles, M. A. & Speirs, V. Mechanisms of FGFR3 actions in endocrine resistant breast cancer. *Int. J. Cancer* **130,** 2857–66 (2012).

203. Meijer, D. *et al.* Fibroblast growth factor receptor 4 predicts failure on tamoxifen therapy in patients with recurrent breast cancer. *Endocr. Relat. Cancer* **15,** 101–11 (2008).

204. Ellis, M. J. *et al.* Letrozole is more effective neoadjuvant endocrine therapy than tamoxifen for ErbB-1- and/or ErbB-2-positive, estrogen receptor-positive primary breast cancer: evidence from a phase III randomized trial. *J. Clin. Oncol.* **19,** 3808–16 (2001).

205. Rasmussen, B. B. *et al.* Adjuvant letrozole versus tamoxifen according to centrally-assessed ERBB2 status for postmenopausal women with endocrine-responsive early breast cancer: supplementary results from the BIG 1-98 randomised trial. *Lancet Oncol.* **9,** 23–28 (2008).

206. Stoica, A., Saceda, M., Doraiswamy, V. L., Coleman, C. & Martin, M. B. Regulation of estrogen receptor-alpha gene expression by epidermal growth factor. *J. Endocrinol.* **165,** 371–8 (2000).

207. Liu, Y., el-Ashry, D., Chen, D., Ding, I. Y. & Kern, F. G. MCF-7 breast cancer cells overexpressing transfected c-erbB-2 have an in vitro growth advantage in estrogen-depleted conditions and reduced estrogen-dependence and tamoxifen-sensitivity in vivo. *Breast Cancer Res. Treat.* **34,** 97–117 (1995).

208. Pietras, R. J. *et al.* HER-2 tyrosine kinase pathway targets estrogen receptor and promotes hormone-independent growth in human breast cancer cells. *Oncogene* **10,** 2435–46 (1995).

209. El-Ashry, D., Miller, D. L., Kharbanda, S., Lippman, M. E. & Kern, F. G. Constitutive Raf-1 kinase activity in breast cancer cells induces both estrogen-independent growth and apoptosis. *Oncogene* **15,** 423–35 (1997).

210. Biswas, D. K., Cruz, A. P., Gansberger, E. & Pardee, A. B. Epidermal growth factor-induced nuclear factor kappa B activation: A major pathway of cell-cycle progression in estrogen-receptor negative breast cancer cells. *Proc. Natl. Acad. Sci. U. S. A.* **97,** 8542–7 (2000).

211. Biswas, D. K. *et al.* NF-kappa B activation in human breast cancer specimens and its role in cell proliferation and apoptosis. *Proc. Natl. Acad. Sci. U. S. A.* **101,** 10137–42 (2004).

212. deGraffenried, L. A. *et al.* NF-kappa B inhibition markedly enhances sensitivity of resistant breast cancer tumor cells to tamoxifen. *Ann. Oncol.* **15,** 885–90 (2004).

213. Zhou, Y., Eppenberger-Castori, S., Eppenberger, U. & Benz, C. C. The NFkappaB pathway and endocrine-resistant breast cancer. *Endocr. Relat.*

Cancer **12 Suppl 1,** S37–46 (2005).

214. Mawson, A. *et al.* Estrogen and insulin/IGF-1 cooperatively stimulate cell cycle progression in MCF-7 breast cancer cells through differential regulation of c-Myc and cyclin D1. *Mol. Cell. Endocrinol.* **229,** 161–73 (2005).

215. Zhang, X. *et al.* Mechanisms of Gefitinib-mediated reversal of tamoxifen resistance in MCF-7 breast cancer cells by inducing ERα re-expression. *Sci. Rep.* **5,** 7835 (2015).

216. Gee, J. M. W. *et al.* The antiepidermal growth factor receptor agent gefitinib (ZD1839/Iressa) improves antihormone response and prevents development of resistance in breast cancer in vitro. *Endocrinology* **144,** 5105–17 (2003).

217. Massarweh, S. *et al.* Tamoxifen resistance in breast tumors is driven by growth factor receptor signaling with repression of classic estrogen receptor genomic function. *Cancer Res.* **68,** 826–33 (2008).

218. Cristofanilli, M. *et al.* Phase II, randomized trial to compare anastrozole combined with gefitinib or placebo in postmenopausal women with hormone receptor-positive metastatic breast cancer. *Clin. Cancer Res.* **16,** 1904–14 (2010).

219. Osborne, C. K. *et al.* Gefitinib or placebo in combination with tamoxifen in patients with hormone receptor-positive metastatic breast cancer: a randomized phase II study. *Clin. Cancer Res.* **17,** 1147–59 (2011).

220. Kaufman, B. *et al.* Trastuzumab plus anastrozole versus anastrozole alone for the treatment of postmenopausal women with human epidermal growth factor receptor 2-positive, hormone receptor-positive metastatic breast cancer: results from the randomized phase III TAnDEM study. *J. Clin. Oncol.* **27,** 5529–37 (2009).

221. Marcom, P. K. *et al.* The combination of letrozole and trastuzumab as first or second-line biological therapy produces durable responses in a subset of HER2 positive and ER positive advanced breast cancers. *Breast Cancer Res.*

Treat. **102,** 43–9 (2007).

222. Jones, H. E. *et al.* Insulin-like growth factor-I receptor signalling and acquired resistance to gefitinib (ZD1839; Iressa) in human breast and prostate cancer cells. *Endocr. Relat. Cancer* **11,** 793–814 (2004).

223. Johnston, S. R. Combinations of endocrine and biological agents: present status of therapeutic and presurgical investigations. *Clin. Cancer Res.* **11,** 889s–99s (2005).

224. Baselga, J. Clinical trials of Herceptin(trastuzumab). *Eur. J. Cancer* **37 Suppl 1,** S18–24 (2001).

225. Lu, Y., Zi, X., Zhao, Y., Mascarenhas, D. & Pollak, M. Insulin-Like Growth Factor-I Receptor Signaling and Resistance to Trastuzumab (Herceptin). *JNCI J. Natl. Cancer Inst.* **93,** 1852–1857 (2001).

226. Sanabria-Figueroa, E. *et al.* Insulin-like growth factor-1 receptor signaling increases the invasive potential of human epidermal growth factor receptor 2-overexpressing breast cancer cells via Src-focal adhesion kinase and forkhead box protein M1. *Mol. Pharmacol.* **87,** 150–61 (2015).

227. Shaw, R. J. & Cantley, L. C. Ras, PI(3)K and mTOR signalling controls tumour cell growth. *Nature* **441,** 424–30 (2006).

228. Skolnik, E. Y. *et al.* Cloning of PI3 kinase-associated p85 utilizing a novel method for expression/cloning of target proteins for receptor tyrosine kinases. *Cell* **65,** 83–90 (1991).

229. Stephens, L. *et al.* A novel phosphoinositide 3 kinase activity in myeloid-derived cells is activated by G protein beta gamma subunits. *Cell* **77,** 83–93 (1994).

230. Downward, J. Mechanisms and consequences of activation of protein kinase B/Akt. *Curr. Opin. Cell Biol.* **10,** 262–267 (1998).

231. Alessi, D. R. *et al.* Characterization of a 3-phosphoinositide-dependent protein kinase which phosphorylates and activates protein kinase Bα. *Curr.*

Biol. **7,** 261–269 (1997).

232. Ma, X. M. & Blenis, J. Molecular mechanisms of mTOR-mediated translational control. *Nat. Rev. Mol. Cell Biol.* **10,** 307–18 (2009).

233. Hay, N. & Sonenberg, N. Upstream and downstream of mTOR. *Genes Dev.* **18,** 1926–45 (2004).

234. Mayo, L. D. & Donner, D. B. The PTEN, Mdm2, p53 tumor suppressor–oncoprotein network. *Trends Biochem. Sci.* **27,** 462–467 (2002).

235. Datta, S. R. *et al.* Akt Phosphorylation of BAD Couples Survival Signals to the Cell-Intrinsic Death Machinery. *Cell* **91,** 231–241 (1997).

236. Maehama, T. & Dixon, J. E. The tumor suppressor, PTEN/MMAC1, dephosphorylates the lipid second messenger, phosphatidylinositol 3,4,5-trisphosphate. *J. Biol. Chem.* **273,** 13375–8 (1998).

237. Gewinner, C. *et al.* Evidence that inositol polyphosphate 4-phosphatase type II is a tumor suppressor that inhibits PI3K signaling. *Cancer Cell* **16,** 115–25 (2009).

238. Dunlap, J. *et al.* Phosphatidylinositol-3-kinase and AKT1 mutations occur early in breast carcinoma. *Breast Cancer Res. Treat.* **120,** 409–18 (2010).

239. Stemke-Hale, K. *et al.* An integrative genomic and proteomic analysis of PIK3CA, PTEN, and AKT mutations in breast cancer. *Cancer Res.* **68,** 6084–91 (2008).

240. Ellis, M. J. *et al.* Phosphatidyl-inositol-3-kinase alpha catalytic subunit mutation and response to neoadjuvant endocrine therapy for estrogen receptor positive breast cancer. *Breast Cancer Res. Treat.* **119,** 379–90 (2010).

241. Maurer, M. *et al.* 3-Phosphoinositide-dependent kinase 1 potentiates upstream lesions on the phosphatidylinositol 3-kinase pathway in breast carcinoma. *Cancer Res.* **69,** 6299–306 (2009).

242. Shoman, N. *et al.* Reduced PTEN expression predicts relapse in patients with

breast carcinoma treated by tamoxifen. *Mod. Pathol.* **18,** 250–9 (2005).

243. Pérez-Tenorio, G. *et al.* PIK3CA mutations and PTEN loss correlate with similar prognostic factors and are not mutually exclusive in breast cancer. *Clin. Cancer Res.* **13,** 3577–84 (2007).

244. Gonzalez-Angulo, A. M. *et al.* PI3K pathway mutations and PTEN levels in primary and metastatic breast cancer. *Mol. Cancer Ther.* **10,** 1093–101 (2011).

245. Fedele, C. G. *et al.* Inositol polyphosphate 4-phosphatase II regulates PI3K/Akt signaling and is lost in human basal-like breast cancers. *Proc. Natl. Acad. Sci. U. S. A.* **107,** 22231–6 (2010).

246. Campbell, R. a *et al.* Phosphatidylinositol 3-kinase/AKT-mediated activation of estrogen receptor alpha: a new model for anti-estrogen resistance. *J. Biol. Chem.* **276,** 9817–24 (2001).

247. Fu, X. *et al.* Overcoming endocrine resistance due to reduced PTEN levels in estrogen receptor-positive breast cancer by co-targeting mammalian target of rapamycin, protein kinase B, or mitogen-activated protein kinase kinase. *Breast Cancer Res.* **16,** 430 (2014).

248. Creighton, C. J. *et al.* Proteomic and transcriptomic profiling reveals a link between the PI3K pathway and lower estrogen-receptor (ER) levels and activity in ER+ breast cancer. *Breast Cancer Res.* **12,** R40 (2010).

249. Beaver, J. A. & Park, B. H. The BOLERO-2 trial: the addition of everolimus to exemestane in the treatment of postmenopausal hormone receptor-positive advanced breast cancer. *Future Oncol.* **8,** 651–7 (2012).

250. Bates, N. P. & Hurst, H. C. An intron 1 enhancer element mediates oestrogen-induced suppression of ERBB2 expression. *Oncogene* **15,** 473–81 (1997).

251. Newman, S. P., Bates, N. P., Vernimmen, D., Parker, M. G. & Hurst, H. C. Cofactor competition between the ligand-bound oestrogen receptor and an intron 1 enhancer leads to oestrogen repression of ERBB2 expression in breast cancer. *Oncogene* **19,** 490–7 (2000).

252. Bosher, J. M., Totty, N. F., Hsuan, J. J., Williams, T. & Hurst, H. C. A family of AP-2 proteins regulates c-erbB-2 expression in mammary carcinoma. *Oncogene* **13,** 1701–7 (1996).

253. Stossi, F., Likhite, V. S., Katzenellenbogen, J. A. & Katzenellenbogen, B. S. Estrogen-occupied estrogen receptor represses cyclin G2 gene expression and recruits a repressor complex at the cyclin G2 promoter. *J. Biol. Chem.* **281,** 16272–8 (2006).

254. Oesterreich, S. *et al.* Estrogen-mediated Down-Regulation of E-cadherin in Breast Cancer Cells. *Cancer Res.* **63,** 5203–5208 (2003).

255. Rajendran, R. R. *et al.* Regulation of nuclear receptor transcriptional activity by a novel DEAD box RNA helicase (DP97). *J. Biol. Chem.* **278,** 4628–38 (2003).

256. Matsuda, T. Cross-talk between Transforming Growth Factor-beta and Estrogen Receptor Signaling through Smad3. *J. Biol. Chem.* **276,** 42908–42914 (2001).

257. Derynck, R., Akhurst, R. J. & Balmain, A. TGF-beta signaling in tumor suppression and cancer progression. *Nat. Genet.* **29,** 117–29 (2001).

258. Barcellos-Hoff, M. H. & Akhurst, R. J. Transforming growth factor-beta in breast cancer: too much, too late. *Breast Cancer Res.* **11,** 202 (2009).

259. Frasor, J. *et al.* Selective Estrogen Receptor Modulators : Discrimination of Agonistic versus Antagonistic Activities by Gene Expression Profiling in Breast Cancer Cells. *Cancer Res.* 1522–1533 (2004).

260. Yarden, R. I., Wilson, M. A. & Chrysogelos, S. A. Estrogen suppression of EGFR expression in breast cancer cells: a possible mechanism to modulate growth. *J. Cell. Biochem. Suppl.* **Suppl 36,** 232–46 (2001).

261. Wilson, M. A. & Chrysogelos, S. A. Identification and characterization of a negative regulatory element within the epidermal growth factor receptor gene first intron in hormone-dependent breast cancer cells. *J. Cell. Biochem.* **85,** 601–14 (2002).

262. Hutcheson, I. R. *et al.* Fulvestrant-induced expression of ErbB3 and ErbB4 receptors sensitizes oestrogen receptor-positive breast cancer cells to heregulin β1. *Breast Cancer Res.* **13,** R29 (2011).

263. Jordan, N. J., Gee, J. M. W., Barrow, D., Wakeling, A. E. & Nicholson, R. I. Increased constitutive activity of PKB/Akt in tamoxifen resistant breast cancer MCF-7 cells. *Breast Cancer Res. Treat.* **87,** 167–80 (2004).

264. Beeram, M. *et al.* Akt-induced endocrine therapy resistance is reversed by inhibition of mTOR signaling. *Ann. Oncol.* **18,** 1323–8 (2007).

265. Pérez-Tenorio, G. & Stål, O. Activation of AKT/PKB in breast cancer predicts a worse outcome among endocrine treated patients. *Br. J. Cancer* **86,** 540–5 (2002).

266. Martin, M. B. *et al.* A Role for Akt in Mediating the Estrogenic Functions of Epidermal Growth Factor and Insulin-Like Growth Factor I 1. *Endocrinology* **141,** 4503–4511 (2000).

267. Kumar, R., Mandal, M. & Lipton, A. Overexpression of HER2 modulates bcl-2, bcl-XL, and tamoxifen-induced apoptosis in human MCF-7 breast cancer cells. *Clin. Cancer Res.* 1215–1219 (1996).

268. Musgrove, E. A. & Sutherland, R. L. Biological determinants of endocrine resistance in breast cancer. *Nat. Rev. Cancer* **9,** 631–43 (2009).

269. Zhou, H., Zhang, Y., Fu, Y., Chan, L. & Lee, A. S. Novel mechanism of anti-apoptotic function of 78-kDa glucose-regulated protein (GRP78): endocrine resistance factor in breast cancer, through release of B-cell lymphoma 2 (BCL-2) from BCL-2-interacting killer (BIK). *J. Biol. Chem.* **286,** 25687–96 (2011).

270. Bergamaschi, A., Christensen, B. L. & Katzenellenbogen, B. S. Reversal of endocrine resistance in breast cancer: interrelationships among 14-3-3ζ, FOXM1, and a gene signature associated with mitosis. *Breast Cancer Res.* **13,** R70 (2011).

271. Shintani, T. & Klionsky, D. J. Autophagy in health and disease: a double-edged

sword. *Science* **306,** 990–5 (2004).

272. Codogno, P. & Meijer, A. J. Autophagy and signaling: their role in cell survival and cell death. *Cell Death Differ.* **12 Suppl 2,** 1509–18 (2005).

273. Lum, J. J., DeBerardinis, R. J. & Thompson, C. B. Autophagy in metazoans: cell survival in the land of plenty. *Nat. Rev. Mol. Cell Biol.* **6,** 439–48 (2005).

274. Ogier-Denis, E. & Codogno, P. Autophagy: a barrier or an adaptive response to cancer. *Biochim. Biophys. Acta* **1603,** 113–28 (2003).

275. Qadir, M. A. *et al.* Macroautophagy inhibition sensitizes tamoxifen-resistant breast cancer cells and enhances mitochondrial depolarization. *Breast Cancer Res. Treat.* **112,** 389–403 (2008).

276. Samaddar, J. S. *et al.* A role for macroautophagy in protection against 4-hydroxytamoxifen-induced cell death and the development of antiestrogen resistance. *Mol. Cancer Ther.* **7,** 2977–87 (2008).

277. Perou, C. M. *et al.* Molecular portraits of human breast tumours. *Nature* **406,** 747–52 (2000).

278. Sørlie, T. *et al.* Gene expression patterns of breast carcinomas distinguish tumor subclasses with clinical implications. *Proc. Natl. Acad. Sci. U. S. A.* **98,** 10869–74 (2001).

279. Parker, J. S. *et al.* Supervised risk predictor of breast cancer based on intrinsic subtypes. *J. Clin. Oncol.* **27,** 1160–7 (2009).

280. Sotiriou, C. & Pusztai, L. Gene-expression signatures in breast cancer. *N. Engl. J. Med.* **360,** 790–800 (2009).

281. Weigelt, B., Baehner, F. L. & Reis-Filho, J. S. The contribution of gene expression profiling to breast cancer classification, prognostication and prediction: a retrospective of the last decade. *J. Pathol.* **220,** 263–80 (2010).

282. Reis-Filho, J. S., Weigelt, B., Fumagalli, D. & Sotiriou, C. Molecular profiling: moving away from tumor philately. *Sci. Transl. Med.* **2,** 47ps43 (2010).

283. van 't Veer, L. J. *et al.* Gene expression profiling predicts clinical outcome of breast cancer. *Nature* **415,** 530–6 (2002).

284. van de Vijver, M. J. *et al.* A gene-expression signature as a predictor of survival in breast cancer. *N. Engl. J. Med.* **347,** 1999–2009 (2002).

285. Bueno-de-Mesquita, J. M. *et al.* Use of 70-gene signature to predict prognosis of patients with node-negative breast cancer: a prospective community-based feasibility study (RASTER). *Lancet. Oncol.* **8,** 1079–87 (2007).

286. Buyse, M. *et al.* Validation and clinical utility of a 70-gene prognostic signature for women with node-negative breast cancer. *J. Natl. Cancer Inst.* **98,** 1183–92 (2006).

287. Paik, S. *et al.* A multigene assay to predict recurrence of tamoxifen-treated, node-negative breast cancer. *N. Engl. J. Med.* **351,** 2817–26 (2004).

288. Neve, R. M. *et al.* A collection of breast cancer cell lines for the study of functionally distinct cancer subtypes. *Cancer Cell* **10,** 515–27 (2006).

289. Holliday, D. L. & Speirs, V. Choosing the right cell line for breast cancer research. *Breast Cancer Res.* **13,** 215 (2011).

290. Berthois, Y., Katzenellenbogen, J. A. & Katzenellenbogen, B. S. Phenol red in tissue culture media is a weak estrogen: implications concerning the study of estrogen-responsive cells in culture. *Proc. Natl. Acad. Sci. U. S. A.* **83,** 2496–500 (1986).

291. Bindal, R. D. & Katzenellenbogen, J. A. Bis(4-hydroxyphenyl)[2-(phenoxysulfonyl)phenyl]methane: isolation and structure elucidation of a novel estrogen from commercial preparations of phenol red (phenolsulfonphthalein). *J. Med. Chem.* **31,** 1978–83 (1988).

292. Staka, C. M. Acquired resistance to oestrogen deprivation: role for growth factor signalling kinases/oestrogen receptor cross-talk revealed in new MCF-7X model. *Endocr. Relat. Cancer* **12,** S85–S97 (2005).

293. Li, Q., Birkbak, N. J., Gyorffy, B., Szallasi, Z. & Eklund, A. C. Jetset: selecting the

optimal microarray probe set to represent a gene. *BMC Bioinformatics* **12,** 474 (2011).

294. McClintick, J. N. & Edenberg, H. J. Effects of filtering by Present call on analysis of microarray experiments. *BMC Bioinformatics* **7,** 49 (2006).

295. Prochnow, H. *et al.* Non-secreted clusterin isoforms are translated in rare amounts from distinct human mRNA variants and do not affect Bax-mediated apoptosis or the NF-κB signaling pathway. *PLoS One* **8,** e75303 (2013).

296. Kuriyama, K., Hirouchi, M. & Nakayasu, H. Structure and function of cerebral GABAA and GABAB receptors. *Neurosci. Res.* **17,** 91–9 (1993).

297. Rand, T. A., Ginalski, K., Grishin, N. V & Wang, X. Biochemical identification of Argonaute 2 as the sole protein required for RNA-induced silencing complex activity. *Proc. Natl. Acad. Sci. U. S. A.* **101,** 14385–9 (2004).

298. Matranga, C., Tomari, Y., Shin, C., Bartel, D. P. & Zamore, P. D. Passenger-strand cleavage facilitates assembly of siRNA into Ago2-containing RNAi enzyme complexes. *Cell* **123,** 607–20 (2005).

299. Ameres, S. L., Martinez, J. & Schroeder, R. Molecular basis for target RNA recognition and cleavage by human RISC. *Cell* **130,** 101–12 (2007).

300. Hutvágner, G. & Zamore, P. D. A microRNA in a multiple-turnover RNAi enzyme complex. *Science* **297,** 2056–60 (2002).

301. Bartlett, D. W. & Davis, M. E. Insights into the kinetics of siRNA-mediated gene silencing from live-cell and live-animal bioluminescent imaging. *Nucleic Acids Res.* **34,** 322–33 (2006).

302. Gee, J. M. W. *et al.* Antihormone induced compensatory signalling in breast cancer: an adverse event in the development of endocrine resistance. *Horm. Mol. Biol. Clin. Investig.* **5,** 67–77 (2011).

303. Gutierrez, M. C. *et al.* Molecular changes in tamoxifen-resistant breast cancer: relationship between estrogen receptor, HER-2, and p38 mitogen-

activated protein kinase. *J. Clin. Oncol.* **23,** 2469–76 (2005).

304. Gee, J. M. W. *et al.* Deciphering antihormone-induced compensatory mechanisms in breast cancer and their therapeutic implications. *Endocr. Relat. Cancer* **13 Suppl 1,** S77–88 (2006).

305. Borley, A. C. *et al.* Anti-oestrogens but not oestrogen deprivation promote cellular invasion in intercellular adhesion-deficient breast cancer cells. *Breast Cancer Res.* **10,** R103 (2008).

306. Jiang, Y. *et al.* Discovery of differentially expressed genes in human breast cancer using subtracted cDNA libraries and cDNA microarrays. *Oncogene* **21,** 2270–82 (2002).

307. Huang, E. *et al.* Gene expression predictors of breast cancer outcomes. *Lancet* **361,** 1590–6 (2003).

308. Zajchowski, D. A. *et al.* Identification of gene expression profiles that predict the aggressive behavior of breast cancer cells. *Cancer Res.* **61,** 5168–78 (2001).

309. Cappelletti, V. *et al.* Patterns and changes in gene expression following neo-adjuvant anti-estrogen treatment in estrogen receptor-positive breast cancer. *Endocr. Relat. Cancer* **15,** 439–49 (2008).

310. Shaw, V. The identification of anti-hormone induced genes as potential therapeutic targets in breast cancer. (Doctoral thesis; Cardiff University, 2007).

311. Osborne, C. K., Boldt, D. H., Clark, G. M. & Trent, J. M. Effects of tamoxifen on human breast cancer cell cycle kinetics: accumulation of cells in early G1 phase. *Cancer Res.* **43,** 3583–5 (1983).

312. Sutherland, R. L., Green, M. D., Hall, R. E., Reddel, R. R. & Taylor, I. W. Tamoxifen induces accumulation of MCF 7 human mammary carcinoma cells in the G0/G1 phase of the cell cycle. *Eur. J. Cancer Clin. Oncol.* **19,** 615–621 (1983).

313. Hur, J. *et al.* Regulation of Expression of BIK Proapoptotic Protein in Human Breast Cancer Cells: p53-Dependent Induction of BIK mRNA by Fulvestrant and Proteasomal Degradation of BIK Protein. *Cancer Res* **66,** 10153–61 (2006).

314. Hamelers, I. H., Van Schaik, R. F., Sussenbach, J. S. & Steenbergh, P. H. 17beta-Estradiol responsiveness of MCF-7 laboratory strains is dependent on an autocrine signal activating the IGF type I receptor. *Cancer Cell Int.* **3,** 10 (2003).

315. Tran, C. T. ., Leiper, J. M. & Vallance, P. The DDAH/ADMA/NOS pathway. *Atheroscler. Suppl.* **4,** 33–40 (2003).

316. Melegari, M., Scaglioni, P. P. & Wands, J. R. Cloning and Characterization of a Novel Hepatitis B Virus x Binding Protein That Inhibits Viral Replication. *J. Virol.* **72,** 1737–1743 (1998).

317. Jiang, X. *et al.* GABAB receptor complex as a potential target for tumor therapy. *J. Histochem. Cytochem.* **60,** 269–79 (2012).

318. Mazurkiewicz, M., Opolski, A., Wietrzyk, J., Radzikowski, C. & Kleinrok, Z. GABA level and GAD activity in human and mouse normal and neoplastic mammary gland. *J. Exp. Clin. Cancer Res.* **18,** 247–53 (1999).

319. Zhang, D. *et al.* GABAergic signaling facilitates breast cancer metastasis by promoting ERK1/2-dependent phosphorylation. *Cancer Lett.* **348,** 100–8 (2014).

320. Talvensaari-Mattila, A., Pääkkö, P. & Turpeenniemi-Hujanen, T. Matrix metalloproteinase-2 (MMP-2) is associated with survival in breast carcinoma. *Br. J. Cancer* **89,** 1270–5 (2003).

321. Maemura, K. *et al.* Gamma-amino-butyric acid immunoreactivity in intramucosal colonic tumors. *J. Gastroenterol. Hepatol.* **18,** 1089–94 (2003).

322. Matuszek, M., Jesipowicz, M. & Kleinrok, Z. GABA content and GAD activity in gastric cancer. *Med. Sci. Monit.* **7,** 377–81 (2001).

323. Roberts, S. S., Mendonça-Torres, M. C., Jensen, K., Francis, G. L. & Vasko, V. GABA receptor expression in benign and malignant thyroid tumors. *Pathol. Oncol. Res.* **15,** 645–50 (2009).

324. Nicholson-Guthrie, C. S., Guthrie, G. D., Sutton, G. P. & Baenziger, J. C. Urine GABA levels in ovarian cancer patients: elevated GABA in malignancy. *Cancer Lett.* **162,** 27–30 (2001).

325. Azuma, H. *et al.* Gamma-aminobutyric acid as a promoting factor of cancer metastasis; induction of matrix metalloproteinase production is potentially its underlying mechanism. *Cancer Res.* **63,** 8090–6 (2003).

326. Tu, H. *et al.* GABAB receptor activation protects neurons from apoptosis via IGF-1 receptor transactivation. *J. Neurosci.* **30,** 749–59 (2010).

327. Zhang, D., Zhang, J.-Y. & Wang, E.-H. δ-catenin promotes the malignant phenotype in breast cancer. *Tumour Biol.* **36,** 569–75 (2015).

328. Zhang, J.-Y. *et al.* δ-Catenin promotes malignant phenotype of non-small cell lung cancer by non-competitive binding to E-cadherin with p120ctn in cytoplasm. *J. Pathol.* **222,** n/a–n/a (2010).

329. Fang, Y., Li, Z., Wang, X. & Zhang, S. Expression and biological role of δ-catenin in human ovarian cancer. *J. Cancer Res. Clin. Oncol.* **138,** 1769–1776 (2012).

330. Lu, Q. *et al.* Increased expression of δ-catenin/neural plakophilin-related armadillo protein is associated with the down-regulation and redistribution of E-cadherin and p120ctn in human prostate cancer. *Hum. Pathol.* **36,** 1037–1048 (2005).

331. Zhang, J.-Y. *et al.* The expression of δ-catenin in esophageal squamous cell carcinoma and its correlations with prognosis of patients. *Hum. Pathol.* **45,** 2014–22 (2014).

332. Zeng, Y. *et al.* δ-Catenin promotes prostate cancer cell growth and progression by altering cell cycle and survival gene profiles. *Mol. Cancer* **8,** 19 (2009).

333. Kim, H. *et al.* δ-Catenin promotes E-cadherin processing and activates β-catenin-mediated signaling: implications on human prostate cancer progression. *Biochim. Biophys. Acta* **1822,** 509–21 (2012).

334. Rosenberg, M. E. & Silkensen, J. Clusterin: physiologic and pathophysiologic considerations. *Int. J. Biochem. Cell Biol.* **27,** 633–45 (1995).

335. Redondo, M. *et al.* Overexpression of clusterin in human breast carcinoma. *Am. J. Pathol.* **157,** 393–9 (2000).

336. Flanagan, L., Whyte, L., Chatterjee, N. & Tenniswood, M. Effects of clusterin over-expression on metastatic progression and therapy in breast cancer. *BMC Cancer* **10,** 107 (2010).

337. Niu, Z. *et al.* Small interfering RNA targeted to secretory clusterin blocks tumor growth, motility, and invasion in breast cancer. *Acta Biochim. Biophys. Sin. (Shanghai).* **44,** 991–8 (2012).

338. Toffanin, S. *et al.* Clusterin : A potential target for improving response to antiestrogens. *Int. J. Oncol.* **33,** 791–798 (2008).

339. Redondo, M. *et al.* Anticlusterin treatment of breast cancer cells increases the sensitivities of chemotherapy and tamoxifen and counteracts the inhibitory action of dexamethasone on chemotherapy-induced cytotoxicity. *Breast Cancer Res.* **9,** R86 (2007).

340. Miyake, H., Hara, I. & Gleave, M. E. Antisense oligodeoxynucleotide therapy targeting clusterin gene for prostate cancer: Vancouver experience from discovery to clinic. *Int. J. Urol.* **12,** 785–94 (2005).

341. Laskin, J. J. *et al.* Phase I/II trial of custirsen (OGX-011), an inhibitor of clusterin, in combination with a gemcitabine and platinum regimen in patients with previously untreated advanced non-small cell lung cancer. *J. Thorac. Oncol.* **7,** 579–86 (2012).

342. Chia, S. *et al.* Phase II trial of OGX-011 in combination with docetaxel in metastatic breast cancer. *Clin. Cancer Res.* **15,** 708–13 (2009).

343. Zielinski, R. & Chi, K. N. Custirsen (OGX-011): a second-generation antisense inhibitor of clusterin in development for the treatment of prostate cancer. *Future Oncol.* **8,** 1239–51 (2012).

344. Zhang, H. *et al.* Clusterin inhibits apoptosis by interacting with activated Bax. *Nat. Cell Biol.* **7,** 909–915 (2005).

345. Tang, Y., Liu, F., Zheng, C., Sun, S. & Jiang, Y. Knockdown of clusterin sensitizes pancreatic cancer cells to gemcitabine chemotherapy by ERK1/2 inactivation. *J. Exp. Clin. Cancer Res.* **31,** 73 (2012).

346. Chou, T.-Y. *et al.* Clusterin silencing in human lung adenocarcinoma cells induces a mesenchymal-to-epithelial transition through modulating the ERK/Slug pathway. *Cell. Signal.* **21,** 704–11 (2009).

347. Huang, H., Wang, L., Li, M., Wang, X. & Zhang, L. Secreted clusterin (sCLU) regulates cell proliferation and chemosensitivity to cisplatin by modulating ERK1/2 signals in human osteosarcoma cells. *World J. Surg. Oncol.* **12,** 255 (2014).

348. Ammar, H. & Closset, J. L. Clusterin activates survival through the phosphatidylinositol 3-kinase/Akt pathway. *J. Biol. Chem.* **283,** 12851–61 (2008).

349. Zoubeidi, A. *et al.* Clusterin facilitates COMMD1 and I-kappaB degradation to enhance NF-kappaB activity in prostate cancer cells. *Mol. Cancer Res.* **8,** 119–30 (2010).

350. Ayroldi, E. & Riccardi, C. Glucocorticoid-induced leucine zipper (GILZ): a new important mediator of glucocorticoid action. *FASEB J.* **23,** 3649–58 (2009).

351. Tynan, S. H., Lundeen, S. G. & Allan, G. F. Cell type-specific bidirectional regulation of the glucocorticoid-induced leucine zipper (GILZ) gene by estrogen. *J. Steroid Biochem. Mol. Biol.* **91,** 225–39 (2004).

352. Grugan, K. D., Ma, C., Singhal, S., Krett, N. L. & Rosen, S. T. Dual regulation of glucocorticoid-induced leucine zipper (GILZ) by the glucocorticoid receptor and the PI3-kinase/AKT pathways in multiple myeloma. *J. Steroid Biochem.*

Mol. Biol. **110,** 244–254 (2008).

353. Bachmann, P. S. *et al.* Divergent mechanisms of glucocorticoid resistance in experimental models of pediatric acute lymphoblastic leukemia. *Cancer Res.* **67,** 4482–90 (2007).

354. Redjimi, N. *et al.* Identification of glucocorticoid-induced leucine zipper as a key regulator of tumor cell proliferation in epithelial ovarian cancer. *Mol. Cancer* **8,** 83 (2009).

355. Espinasse, M.-A. *et al.* Glucocorticoid-Induced Leucine Zipper Is Expressed in Human Neutrophils and Promotes Apoptosis through Mcl-1 Down-Regulation. *J. Innate Immun.* (2015). doi:10.1159/000439052

356. Joha, S. *et al.* GILZ inhibits the mTORC2/AKT pathway in BCR-ABL+ cells. *Oncogene* **31,** 1419–1430 (2011).

357. D'Adamio, F. *et al.* A new dexamethasone-induced gene of the leucine zipper family protects T lymphocytes from TCR/CD3-activated cell death. *Immunity* **7,** 803–12 (1997).

358. Yde, C. W., Emdal, K. B., Guerra, B. & Lykkesfeldt, A. E. NFκB signaling is important for growth of antiestrogen resistant breast cancer cells. *Breast Cancer Res. Treat.* **135,** 67–78 (2012).

359. Maldonado, V. & Melendez-Zajgla, J. Role of Bcl-3 in solid tumors. *Mol. Cancer* **10,** 152 (2011).

360. Cogswell, P. C., Guttridge, D. C., Funkhouser, W. K. & Baldwin, a S. Selective activation of NF-kappa B subunits in human breast cancer: potential roles for NF-kappa B2/p52 and for Bcl-3. *Oncogene* **19,** 1123–31 (2000).

361. Westerheide, S. D., Mayo, M. W., Anest, V., Hanson, J. L. & Baldwin, A. S. The Putative Oncoprotein Bcl-3 Induces Cyclin D1 To Stimulate G 1 Transition. *Mol. Cell. Biol.* **21,** 8428–8436 (2001).

362. Wakefield, A. *et al.* Bcl3 selectively promotes metastasis of ERBB2-driven mammary tumors. *Cancer Res.* **73,** 745–55 (2013).

363. Pratt, M. A. C. *et al.* Estrogen Withdrawal-Induced NF- B Activity and Bcl-3 Expression in Breast Cancer Cells : Roles in Growth and Hormone Independence. **23,** 6887–6900 (2003).

364. Thornburg, N. J., Pathmanathan, R. & Raab-Traub, N. Activation of Nuclear Factor-{kappa}B p50 Homodimer/Bcl-3 Complexes in Nasopharyngeal Carcinoma. *Cancer Res.* **63,** 8293–8301 (2003).

365. Pallares, J. *et al.* Abnormalities in the NF-kappaB family and related proteins in endometrial carcinoma. *J. Pathol.* **204,** 569–77 (2004).

366. Puvvada, S. D. *et al.* NF-kB and Bcl-3 activation are prognostic in metastatic colorectal cancer. *Oncology* **78,** 181–8 (2010).

367. Kashatus, D., Cogswell, P. & Baldwin, A. S. Expression of the Bcl-3 proto-oncogene suppresses p53 activation. *Genes Dev.* **20,** 225–35 (2006).

368. Choi, H. J. *et al.* Bcl3-dependent stabilization of CtBP1 is crucial for the inhibition of apoptosis and tumor progression in breast cancer. *Biochem. Biophys. Res. Commun.* **400,** 396–402 (2010).

369. Yang, C. R. *et al.* Nuclear clusterin/XIP8, an x-ray-induced Ku70-binding protein that signals cell death. *Proc. Natl. Acad. Sci. U. S. A.* **97,** 5907–12 (2000).

370. Jones, S. E. & Jomary, C. Clusterin. *Int. J. Biochem. Cell Biol.* **34,** 427–31 (2002).

371. Trougakos, I. P. & Gonos, E. S. Clusterin/apolipoprotein J in human aging and cancer. *Int. J. Biochem. Cell Biol.* **34,** 1430–48 (2002).

372. Baeuerle, P. A. & Baltimore, D. NF-kappa B: ten years after. *Cell* **87,** 13–20 (1996).

373. Hinz, M. *et al.* NF-kappaB function in growth control: regulation of cyclin D1 expression and G0/G1-to-S-phase transition. *Mol. Cell. Biol.* **19,** 2690–8 (1999).

374. Na, S. Y. *et al.* Bcl3, an IkappaB protein, stimulates activating protein-1

transactivation and cellular proliferation. *J. Biol. Chem.* **274,** 28491–6 (1999).

375. Zhang, Q., Nottke, A. & Goodman, R. H. Homeodomain-interacting protein kinase-2 mediates CtBP phosphorylation and degradation in UV-triggered apoptosis. *Proc. Natl. Acad. Sci. U. S. A.* **102,** 2802–7 (2005).

376. Miyake, H., Hara, I., Kamidono, S. & Gleave, M. E. Synergistic chemsensitization and inhibition of tumor growth and metastasis by the antisense oligodeoxynucleotide targeting clusterin gene in a human bladder cancer model. *Clin. Cancer Res.* **7,** 4245–52 (2001).

377. Gleave, M. E. *et al.* Use of antisense oligonucleotides targeting the antiapoptotic gene, clusterin/testosterone-repressed prostate message 2, to enhance androgen sensitivity and chemosensitivity in prostate cancer. *Urology* **58,** 39–49 (2001).

378. O'Sullivan, J., Whyte, L., Drake, J. & Tenniswood, M. Alterations in the post-translational modification and intracellular trafficking of clusterin in MCF-7 cells during apoptosis. *Cell Death Differ.* **10,** 914–27 (2003).

379. Scaltriti, M., Santamaria, A., Paciucci, R. & Bettuzzi, S. Intracellular clusterin induces G2-M phase arrest and cell death in PC-3 prostate cancer cells1. *Cancer Res.* **64,** 6174–82 (2004).

380. Bi, J. *et al.* Overexpression of clusterin correlates with tumor progression, metastasis in gastric cancer: a study on tissue microarrays. *Neoplasma* **57,** 191–7 (2010).

381. Yang, G. F., Li, X. M. & Xie, D. Overexpression of clusterin in ovarian cancer is correlated with impaired survival. *Int. J. Gynecol. Cancer* **19,** 1342–6 (2009).

382. Chi, K. N. *et al.* Randomized phase II study of docetaxel and prednisone with or without OGX-011 in patients with metastatic castration-resistant prostate cancer. *J. Clin. Oncol.* **28,** 4247–54 (2010).

383. Mendes, O., Kim, H.-T., Lungu, G. & Stoica, G. MMP2 role in breast cancer brain metastasis development and its regulation by TIMP2 and ERK1/2. *Clin.*

Exp. Metastasis **24,** 341–51 (2007).

384. Schuller, H. M., Al-Wadei, H. A. N. & Majidi, M. GABAB receptor is a novel drug target for pancreatic cancer. *Cancer* **112,** 767–778 (2008).

385. Schuller, H. M., Al-Wadei, H. A. N. & Majidi, M. Gamma-aminobutyric acid, a potential tumor suppressor for small airway-derived lung adenocarcinoma. *Carcinogenesis* **29,** 1979–85 (2008).

386. Browne, B. C. *et al.* Inhibition of IGF1R activity enhances response to trastuzumab in HER-2-positive breast cancer cells. *Ann. Oncol.* **22,** 68–73 (2011).

387. Zapata, J. M. *et al.* Expression of multiple apoptosis-regulatory genes in human breast cancer cell lines and primary tumors. *Breast Cancer Res. Treat.* **47,** 129–40 (1998).

388. Olopade, O. I. *et al.* Overexpression of BCL-x protein in primary breast cancer is associated with high tumor grade and nodal metastases. *Cancer J. Sci. Am.* **3,** 230–7 (1997).

389. Tanaka, K. *et al.* Expression of survivin and Its Relationship to Loss of Apoptosis in Breast Carcinomas. *Clin. Cancer Res.* **6,** 127–134 (2000).

390. O'Driscoll, L. *et al.* Lack of prognostic significance of survivin, survivin-ΔEx3, survivin-2B, galectin-3, bag-1, bax-α and MRP-1 mRNAs in breast cancer. *Cancer Lett.* **201,** 225–236 (2003).

391. Marusawa, H. *et al.* HBXIP functions as a cofactor of survivin in apoptosis suppression. *EMBO J.* **22,** 2729–40 (2003).

392. Ayroldi, E. *et al.* Modulation of T-cell activation by the glucocorticoid-induced leucine zipper factor via inhibition of nuclear factor kappaB. *Blood* **98,** 743–53 (2001).

393. Ayroldi, E. *et al.* GILZ mediates the antiproliferative activity of glucocorticoids by negative regulation of Ras signaling. *J. Clin. Invest.* **117,** 1605–1615 (2007).

394. Ayroldi, E. *et al.* Glucocorticoid-induced leucine zipper inhibits the Raf-extracellular signal-regulated kinase pathway by binding to Raf-1. *Mol. Cell. Biol.* **22,** 7929–41 (2002).

395. Whirledge, S. & Cidlowski, J. a. Estradiol antagonism of glucocorticoid-induced GILZ expression in human uterine epithelial cells and murine uterus. *Endocrinology* **154,** 499–510 (2013).

396. Levenson, A. S. & Jordan, V. C. MCF-7: the first hormone-responsive breast cancer cell line. *Cancer Res.* **57,** 3071–8 (1997).

397. Osborne, C. K., Hobbs, K. & Clark, G. M. Effect of estrogens and antiestrogens on growth of human breast cancer cells in athymic nude mice. *Cancer Res.* **45,** 584–90 (1985).

398. Gottardis, M. M., Robinson, S. P. & Jordan, V. C. Estradiol-stimulated growth of MCF-7 tumors implanted in athymic mice: a model to study the tumoristatic action of tamoxifen. *J. Steroid Biochem.* **30,** 311–4 (1988).

399. Johnston, S. J. & Cheung, K. L. Fulvestrant - a novel endocrine therapy for breast cancer. *Curr. Med. Chem.* **17,** 902–14 (2010).

400. Robertson, J. F. R. *et al.* Fulvestrant versus anastrozole for the treatment of advanced breast carcinoma in postmenopausal women: a prospective combined analysis of two multicenter trials. *Cancer* **98,** 229–38 (2003).

401. Yersal, O. & Barutca, S. Biological subtypes of breast cancer: Prognostic and therapeutic implications. *World J. Clin. Oncol.* **5,** 412–24 (2014).

402. Creighton, C. J. The molecular profile of luminal B breast cancer. *Biologics* **6,** 289–97 (2012).

403. Dai, X. *et al.* Breast cancer intrinsic subtype classification, clinical use and future trends. *Am. J. Cancer Res.* **5,** 2929–43 (2015).

404. Rivenbark, A. G., O'Connor, S. M. & Coleman, W. B. Molecular and Cellular Heterogeneity in Breast Cancer: Challenges for Personalized Medicine. *Am. J. Pathol.* **183,** 1113–1124 (2013).

405. Lymperatou, D., Giannopoulou, E., Koutras, A. K. & Kalofonos, H. P. The exposure of breast cancer cells to fulvestrant and tamoxifen modulates cell migration differently. *Biomed Res. Int.* **2013,** 147514 (2013).

406. Chalbos, D., Vignon, F., Keydar, I. & Rochefort, H. Estrogens stimulate cell proliferation and induce secretory proteins in a human breast cancer cell line (T47D). *J. Clin. Endocrinol. Metab.* **55,** 276–83 (1982).

407. Sweeney, E. E., McDaniel, R. E., Maximov, P. Y., Fan, P. & Jordan, V. C. Models and mechanisms of acquired antihormone resistance in breast cancer: significant clinical progress despite limitations. *Horm. Mol. Biol. Clin. Investig.* **9,** 143–163 (2012).

408. Biroccio, A., D'Angelo, C., Jansen, B., Gleave, M. E. & Zupi, G. Antisense clusterin oligodeoxynucleotides increase the response ofHER-2 gene amplified breast cancer cells to Trastuzumab. *J. Cell. Physiol.* **204,** 463–469 (2005).

409. Aka, J. A., Adjo Aka, J. & Lin, S.-X. Comparison of functional proteomic analyses of human breast cancer cell lines T47D and MCF7. *PLoS One* **7,** e31532 (2012).

410. Mooney, L. M., Al-Sakkaf, K. A., Brown, B. L. & Dobson, P. R. M. Apoptotic mechanisms in T47D and MCF-7 human breast cancer cells. *Br. J. Cancer* **87,** 909–17 (2002).

411. Vojtěsek, B. & Lane, D. P. Regulation of p53 protein expression in human breast cancer cell lines. *J. Cell Sci.* **105 (Pt 3,** 607–12 (1993).

412. Shaw, V. E. E. *et al.* Identification of anti-hormone induced genes as potential therapeutic targets in breast cancer. *Cancer Res.* **65,** 874– (2005).

413. Oeckinghaus, A. & Ghosh, S. The NF-kappaB family of transcription factors and its regulation. *Cold Spring Harb. Perspect. Biol.* **1,** a000034 (2009).

414. Ghosh, S. & Karin, M. Missing pieces in the NF-kappaB puzzle. *Cell* **109 Suppl,** S81–96 (2002).

415. Hayden, M. S. & Ghosh, S. Signaling to NF-kappaB. *Genes Dev.* **18,** 2195–224 (2004).

416. Hatada, E. N. *et al.* The ankyrin repeat domains of the NF-kappa B precursor p105 and the protooncogene bcl-3 act as specific inhibitors of NF-kappa B DNA binding. *Proc. Natl. Acad. Sci.* **89,** 2489–2493 (1992).

417. Franzoso, G. *et al.* The oncoprotein Bcl-3 can facilitate NF-kappa B-mediated transactivation by removing inhibiting p50 homodimers from select kappa B sites. *EMBO J.* **12,** 3893–901 (1993).

418. Bours, V. *et al.* The oncoprotein Bcl-3 directly transactivates through kappa B motifs via association with DNA-binding p50B homodimers. *Cell* **72,** 729–39 (1993).

419. Fujita, T., Nolan, G. P., Liou, H. C., Scott, M. L. & Baltimore, D. The candidate proto-oncogene bcl-3 encodes a transcriptional coactivator that activates through NF-kappa B p50 homodimers. *Genes Dev.* **7,** 1354–1363 (1993).

420. Sutherland, R. L., Hall, R. E. & Taylor, I. W. Cell Proliferation Kinetics of MCF-7 Human Mammary Carcinoma Cells in Culture and Effects of Tamoxifen on Exponentially Growing and Plateau-Phase Cells. *Cancer Res.* **43,** 3998–4006 (1983).

421. Watanabe, N., Iwamura, T., Shinoda, T. & Fujita, T. Regulation of NFKB1 proteins by the candidate oncoprotein BCL-3: generation of NF-kappaB homodimers from the cytoplasmic pool of p50-p105 and nuclear translocation. *EMBO J.* **16,** 3609–20 (1997).

422. Bailey, S. T., Shin, H., Westerling, T., Liu, X. S. & Brown, M. Estrogen receptor prevents p53-dependent apoptosis in breast cancer. *Proc. Natl. Acad. Sci. U. S. A.* **109,** 18060–5 (2012).

423. Zhou, Y. *et al.* Activation of nuclear factor-kappaB (NFkappaB) identifies a high-risk subset of hormone-dependent breast cancers. *Int. J. Biochem. Cell Biol.* **37,** 1130–44 (2005).

424. Perkins, N. D. Integrating cell-signalling pathways with NF-kappaB and IKK

function. *Nat. Rev. Mol. Cell Biol.* **8,** 49–62 (2007).

425. Zhang, Q., Didonato, J. A., Karin, M. & McKeithan, T. W. BCL3 encodes a nuclear protein which can alter the subcellular location of NF-kappa B proteins. *Mol. Cell. Biol.* **14,** 3915–26 (1994).

426. Lin, L., DeMartino, G. N. & Greene, W. C. Cotranslational biogenesis of NF-kappaB p50 by the 26S proteasome. *Cell* **92,** 819–28 (1998).

427. Moorthy, A. K. *et al.* The 20S proteasome processes NF-kappaB1 p105 into p50 in a translation-independent manner. *EMBO J.* **25,** 1945–56 (2006).

428. Nakshatri, H., Bhat-Nakshatri, P., Martin, D. A., Goulet, R. J. & Sledge, G. W. Constitutive activation of NF-kappaB during progression of breast cancer to hormone-independent growth. *Mol. Cell. Biol.* **17,** 3629–39 (1997).

429. Carmody, R. J., Ruan, Q., Palmer, S., Hilliard, B. & Chen, Y. H. Negative regulation of toll-like receptor signaling by NF-kappaB p50 ubiquitination blockade. *Science* **317,** 675–8 (2007).

430. Wessells, J. *et al.* BCL-3 and NF-kappaB p50 attenuate lipopolysaccharide-induced inflammatory responses in macrophages. *J. Biol. Chem.* **279,** 49995–50003 (2004).

431. Trougakos, I. P., So, A., Jansen, B., Gleave, M. E. & Gonos, E. S. Silencing expression of the clusterin/apolipoprotein j gene in human cancer cells using small interfering RNA induces spontaneous apoptosis, reduced growth ability, and cell sensitization to genotoxic and oxidative stress. *Cancer Res.* **64,** 1834–42 (2004).

432. Pucci, S., Bonanno, E., Pichiorri, F., Angeloni, C. & Spagnoli, L. G. Modulation of different clusterin isoforms in human colon tumorigenesis. *Oncogene* **23,** 2298–304 (2004).

433. Kurahashi, T., Muramaki, M., Yamanaka, K., Hara, I. & Miyake, H. Expression of the secreted form of clusterin protein in renal cell carcinoma as a predictor of disease extension. *BJU Int.* **96,** 895–899 (2005).

434. Miyake, H., Gleave, M., Kamidono, S. & Hara, I. Overexpression of clusterin in transitional cell carcinoma of the bladder is related to disease progression and recurrence. *Urology* **59,** 150–4 (2002).

435. Steinberg, J. *et al.* Intracellular levels of SGP-2 (Clusterin) correlate with tumor grade in prostate cancer. *Clin. Cancer Res.* **3,** 1707–11 (1997).

436. Lau, S. H. *et al.* Clusterin plays an important role in hepatocellular carcinoma metastasis. *Oncogene* **25,** 1242–1250 (2006).

437. Zoubeidi, A., Chi, K. & Gleave, M. Targeting the cytoprotective chaperone, clusterin, for treatment of advanced cancer. *Clin. Cancer Res.* **16,** 1088–93 (2010).

438. Park, D. C. *et al.* Clusterin interacts with Paclitaxel and confer Paclitaxel resistance in ovarian cancer. *Neoplasia* **10,** 964–72 (2008).

439. July, L. V *et al.* Clusterin expression is significantly enhanced in prostate cancer cells following androgen withdrawal therapy. *Prostate* **50,** 179–88 (2002).

440. Zoubeidi, A., Chi, K. & Gleave, M. Targeting the cytoprotective chaperone, clusterin, for treatment of advanced cancer. *Clin. Cancer Res.* **16,** 1088–93 (2010).

441. Miyake, H., Nelson, C., Rennie, P. S. & Gleave, M. E. Acquisition of chemoresistant phenotype by overexpression of the antiapoptotic gene testosterone-repressed prostate message-2 in prostate cancer xenograft models. *Cancer Res.* **60,** 2547–54 (2000).

442. Zellweger, T. *et al.* Overexpression of the cytoprotective protein clusterin decreases radiosensitivity in the human LNCaP prostate tumour model. *BJU Int.* **92,** 463–469 (2003).

443. Miyake, H., Nelson, C., Rennie, P. S. & Gleave, M. E. Testosterone-repressed Prostate Message-2 Is an Antiapoptotic Gene Involved in Progression to Androgen Independence in Prostate Cancer. *Cancer Res.* **60,** 170–176 (2000).

444. Sensibar, J. A. *et al.* Prevention of Cell Death Induced by Tumor Necrosis Factor {alpha} in LNCaP Cells by Overexpression of Sulfated Glycoprotein-2 (Clusterin). *Cancer Res.* **55,** 2431–2437 (1995).

445. Saad, F. *et al.* Randomized phase II trial of Custirsen (OGX-011) in combination with docetaxel or mitoxantrone as second-line therapy in patients with metastatic castrate-resistant prostate cancer progressing after first-line docetaxel: CUOG trial P-06c. *Clin. Cancer Res.* **17,** 5765–73 (2011).

446. Wang, Y., Wang, X., Zhao, H., Liang, B. & Du, Q. Clusterin confers resistance to TNF-alpha-induced apoptosis in breast cancer cells through NF-kappaB activation and Bcl-2 overexpression. *J Chemother* **24,** 348–357 (2012).

447. Mebratu, Y. & Tesfaigzi, Y. How ERK1/2 activation controls cell proliferation and cell death: Is subcellular localization the answer? *Cell Cycle* **8,** 1168–75 (2009).

448. Coutts, A. S. & Murphy, L. C. Elevated mitogen-activated protein kinase activity in estrogen-nonresponsive human breast cancer cells. *Cancer Res.* **58,** 4071–4 (1998).

449. Shim, W. S. *et al.* Estradiol hypersensitivity and mitogen-activated protein kinase expression in long-term estrogen deprived human breast cancer cells in vivo. *Endocrinology* **141,** 396–405 (2000).

450. Gee, J. M., Robertson, J. F., Ellis, I. O. & Nicholson, R. I. Phosphorylation of ERK1/2 mitogen-activated protein kinase is associated with poor response to anti-hormonal therapy and decreased patient survival in clinical breast cancer. *Int. J. Cancer* **95,** 247–54 (2001).

451. White, J. G., Amos, W. B. & Fordham, M. An evaluation of confocal versus conventional imaging of biological structures by fluorescence light microscopy. *J. Cell Biol.* **105,** 41–8 (1987).

452. Huch, M. *et al.* Long-Term Culture of Genome-Stable Bipotent Stem Cells from Adult Human Liver. *Cell* **160,** 299–312 (2015).

453. Francies, H. E. & Garnett, M. J. What role could organoids play in the

personalization of cancer treatment? *Pharmacogenomics* **16,** 1523–6 (2015).

454. van de Wetering, M. *et al.* Prospective Derivation of a Living Organoid Biobank of Colorectal Cancer Patients. *Cell* **161,** 933–945 (2015).

455. Heitzer, E., Ulz, P. & Geigl, J. B. Circulating Tumor DNA as a Liquid Biopsy for Cancer. *Clin. Chem.* **61,** 112–23 (2015).

456. Fan, P., Maximov, P. Y., Curpan, R. F., Abderrahman, B. & Jordan, V. C. The molecular, cellular and clinical consequences of targeting the estrogen receptor following estrogen deprivation therapy. *Mol. Cell. Endocrinol.* (2015). doi:10.1016/j.mce.2015.06.004

457. Whitehead, K. A., Langer, R. & Anderson, D. G. Knocking down barriers: advances in siRNA delivery. *Nat. Rev. Drug Discov.* **8,** 129–38 (2009).

9 Appendices

Table 15 The list of pro-survival genes (n=248) examined by microarray gene expression profiling.

AATF	CD28	FGFR3	MAP3K2	NOTCH2	SERPINB2
AKT1	CD40LG	FGFR4	MAP3K3	NPM1	SERPINB9
AKT2	CD59	FLT1	MAP3K4	NRG2	SFRP1
AKT3	CDC123	FOXO1	MAP3K5	NTF3	SH3GLB1
ALOX12	CDC20	GABBR2	MAP3K6	OPA1	SHC1
ANXA1	CDC25A	GDNF	MAPK1	OR7A17	SKP2
API5	CDC25B	GLO1	MAPK14	PAK1	SNCA
ASCL1	CDC25C	GRB7	MAPK3	PAK7	SON
ATF5	CDC6	GSK3A	MAPK8	PAX7	SP1
AURKA	CDK1	GSK3B	MAPK8IP2	PEA15	SPHK1
AVEN	CDK10	GSTP1	MCL1	PELP1	SPP1
AZU1	CDK19	HAX1	MCM2	PIK3CA	SRC
BAG1	CDK4	HBXIP	MCM3	PIK3R1	STAMBP
BAG3	CDK6	HDAC1	MCM5	PIK3R2	STAT3
BAG4	CDK7	HIF1A	MKL1	PIM2	STK38
BCAR3	CEBPB	HIPK3	MMP1	POGK	TAX1BP1
BCL2	CFDP1	HMGB1	MMP13	POLA1	TBX3
BCL2A1	CFL1	HSP90B1	MMP14	POLB	TGFB1
BCL2L1	CFLAR	HSPA1A	MMP2	POSTN	TMX1
BCL2L10	CHUK	HSPA1B	MMP3	PRDX2	TNF
BCL2L2	CLU	HSPA5	MMP7	PRKAA1	TNFAIP3
BCL3	CPM	HSPA9	MMP9	PRKCZ	TNFAIP8
BDNF	CREBBP	HSPB1	MPO	PRLR	TNFRSF10D
BECN1	CRYAA	HTT	MTA1	PRMT1	TNFSF18
BFAR	CRYAB	IER3	MTA2	PRSS23	TPT1
BIRC2	CTCFL	IFI6	MTL5	PSEN1	TRIAP1
BIRC3	CTNND1	IGF1	MTOR	PTK6	TSC22D3
BIRC5	CTNND2	IGF1R	MYBL2	RAB30	TXN2
BIRC6	CXCR4	IGF2	MYC	RAC1	VEGFA
BIRC7	DAD1	IGFBP5	MYO18A	RAF1	VHL
BNIP1	DAXX	IKBKB	NAIP	RAN	WT1
BNIP2	DDAH2	IL10	NCOA1	RASA1	XIAP
BNIP3	DLC1	IL1A	NCOA2	RELA	YWHAZ
BRAF	EEF1A2	IL2	NCOA3	RND3	
BRE	ELK1	IRS1	NFKB1	RNF7	
BUB1	EP300	ITGB1	NFKB2	RPS6KA1	
CASP2	ERC1	KRAS	NME1	RPS6KA2	
CBX4	FAIM	KRT13	NME2	RPS6KA3	
CCL2	FAIM2	LOC441453	NME3	RPS6KA6	
CCNA2	FARP1	LTBP1	NME4	RTEL1	

CCND1	FAS	MALT1	NME5	RTN4
CCNE1	FGF17	MAP2K1	NME6	RXRA
CD27	FGFR1	MAP3K1	NOL3	SEMA4D

Table 16 List of 163 pro-survival genes up regulated by at least one antihormone treatment and in at least one antihormone–resistant cell line versus control.

AATF	CTCFL	MAP3K4	POLB
AKT1	CTNND2	MAP3K5	POSTN
AKT2	CXCR4	MAPK1	PRDX2
AKT3	DAD1	MAPK14	PRKAA1
ALOX12	DDAH2	MAPK3	PRKCZ
API5	DLC1	MAPK8	PRLR
ASCL1	EEF1A2	MAPK8IP2	PRMT1
ATF5	ELK1	MCL1	PSEN1
AURKA	ERC1	MCM3	RAB30
AVEN	FAIM	MCM5	RAF1
BAG1	FAIM2	MKL1	RAN
BAG3	FAS	MMP14	RELA
BAG4	FGFR1	MMP2	RNF7
BCAR3	FGFR3	MMP7	RPS6KA1
BCL2	FLT1	MMP9	RPS6KA6
BCL2L1	FOXO1	MPO	RTEL1
BCL2L10	GDNF	MTA2	SERPINB2
BCL2L2	GRB7	MTOR	SERPINB9
BCL3	GSK3A	MYO18A	SFRP1
BDNF	GSTP1	NCOA1	SKP2
BECN1	HAX1	NCOA2	SNCA
BIRC3	HBXIP	NFKB1	SON
BIRC5	HDAC1	NFKB2	SP1
BIRC6	HIPK3	NME1	SPHK1
BNIP1	HSP90B1	NME3	SPP1
BRE	HSPA1A	NME4	SRC
BUB1	HSPA9	NME5	STAMBP
CASP2	IER3	NME6	STAT3
CBX4	IGF1	NOL3	STK38
CCL2	IGF2	NOTCH2	TAX1BP1
CCNE1	IGFBP5	NRG2	TBX3
CD27	IKBKB	NTF3	TNF
CD28	IL10	OPA1	TNFRSF10D
CDC123	IL1A	OR7A17	TNFSF18
CDC25A	IL2	PAK1	TPT1
CDK10	ITGB1	PAK7	TRIAP1
CDK4	LTBP1	PAX7	TSC22D3
CDK6	MALT1	PEA15	TXN2
CFLAR	MAP2K1	PELP1	VHL
CLU	MAP3K3	PIK3R2	WT1
CPM		PIM2	XIAP

Table 17 List of the 92 genes identified with a detection call of marginal or present in at least one treatment and maintained into the appropriate resistant setting of MCF-7 cells.

AATF	ERC1	NME4
AKT1	FAS	NME6
AKT3	FGFR1	NOL3
API5	FGFR3	NOTCH2
ATF5	FOXO1	OPA1
AURKA	GABBR2	PEA15
AVEN	GRB7	PELP1
BAG1	GSK3A	PIK3R2
BCL2L1	HAX1	PIM2
BCL2L2	HBXIP	POLB
BCL3	HDAC1	POSTN
BECN1	HSPA1A	PRDX2
BIRC5	HSPA1B	PRKAA1
BNIP1	IGFBP5	PRKCZ
BRE	IKBKB	PRLR
CASP2	LTBP1	PRMT1
CBX4	MAP2K1	PSEN1
CCNE1	MAP3K3	RAF1
CDC123	MAPK1	RELA
CDK10	MAPK14	RNF7
CDK4	MAPK3	RPS6KA1
CFLAR	MAPK8IP2	RTEL1
CLU	MCL1	SFRP1
CPM	MCM3	SNCA
CTCFL	MCM5	SPHK1
CTNND2	MMP9	STAMBP
CXCR4	MYO18A	STAT3
DAD1	NFKB1	TAX1BP1
DDAH2	NFKB2	TRIAP1
ELK1	NME1	TSC22D3
	NME3	TXN2

Table 18 List of the 17 pro-survival genes significantly (p <0.05) induced by 10 day antihormone treatment compared to control.

AKT1	CXCR4	NME6
BAG1	DDAH2	PSEN1
BCL2L1	ERC1	STAMBP
BCL3	GABBR2	STAT3
CLU	HBXIP	TSC22D3
CTNND2	IGFBP5	